ISTITUTO VENETO
DI SCIENZE, LETTERE
ED ARTI

CORILA

SCIENTIFIC RESEARCH AND SAFEGUARDING OF VENICE

Corila Research Program 2001 results


ISTITUTO VENETO DI SCIENZE LETTERE ED ARTI
VENEZIA


CORILA

In this volume are collected the proceedings of the Annual General Meeting of Corila, held on 4-5th April 2002 at San Servolo, Venice.

ISTITUTO VENETO
DI SCIENZE, LETTERE
ED ARTI

CORILA

SCIENTIFIC RESEARCH AND SAFEGUARDING OF VENICE

Corila Research
Program 2001 results

Edit by
PIERPAOLO CAMPOSTRINI

VENEZIA - 2002

ISBN 88-88143-12-2

Corila - Venezia
30124 Venezia - Palazzo Loredan, Campo S. Stefano 2945
Tel. 0412407711 - Telefax 0415210598
ivsla@unive.it
www.istitutoveneto.it

30124 Venezia - Palazzo Franchetti, S. Marco 2847
Tel. +390412402511 - Telefax +390412402512
venezia@corila.it
www.corila.it

Stampa "La Garangola" Padova 2002

INDEX

AREA 3. ENVIRONMENTAL PROCESSES

RESEARCH LINE 3.1. Trends in global change processes

RESEARCH LINE 3.2. Hydrodynamics and morphology

RESEARCH LINE 3.3. Efficiency of lagoon metabolism

RESEARCH LINE 3.4. Chemical contamination

RESEARCH LINE 3.5. Quantity and quality of exchanges between lagoon and sea

RESEARCH LINE 3.6. Biodiversity in the Venice Lagoon

AMBITIOUS GOALS

PIERPAOLO CAMPOSTRINI
director of CORILA

I am particularly glad and honoured to introduce this volume, in which the efforts of the first year of CORILA's Research Programme are presented. The volume collects the memories presented in the First Annual Meeting of the CORILA's Research Programme, held in Venice, Isola di San Servolo, in the premises of the VIU-Venice International University, on 4-5 April 2002.

The aim of CORILA's Research Programme 2000-2004, made of four Areas (Economics, Architecture and Cultural Heritage, Environmental Processes, Data Management and Distribution) and ten Research Lines, is distinctly ambitious for several reasons, which will be outlined below.

First of all, Venice: *the destiny of this unique city has always received so much attention, especially after the large floods which occurred in 1966, given the enormous damage to humanity of its possible and definitive loss. The Italian Government, national and international organizations, both public and private, have raised and spent a huge amount of money on "saving" the cultural heritage of Venice. Many scientific and technical institutions have contributed to the production of millions of pages of reports, studies and plans.*

In this framework, can it be possible to discover and describe something really new and significant, as any scientific project aims to do? Moreover, will research results ever be considered useful by the Public Administrations entrusted with management of the lagoon and the city itself?

Secondly, the breadth of the Program is noteworthy. From Architecture to Economics, encompassing Biology, Chemistry, Physics, Engineering and much more. Which path could link such a heterogeneous group of disciplines and what kind of inter-disciplinary integration between them is really achievable?

Thirdly, the Program organization is characterised by complexity. The Call for Proposals leads to the selection of the best research projects. Today, the Program involves 70 different institutions, of which 18 from abroad, and over 300 researchers. Twenty-seven contract letters have been signed; every semester, the individual research groups submit administrative and scientific reports and receive the expense reimbursements. CORILA's core staff is in close contact with researcher groups to monitor and assist in achieving project goals. Will inevitable management issues overcome scientific quality? Will scientific results be deemed worth the money spent?

Last, but not least: in the light of recent history, the fragmented Italian scientific panorama, is it really possible to co-ordinate the number of research institutions participating, especially with regard to this delicate theme?

I cannot claim that this volume contains definitive answers to all of these questions, however its publication does represent a substantial step in the right direction. Despite all the difficulties, the more than 700 pages of this book are testimony to the enormous effort expended by our scientific community and are making us optimistic about the complete fulfilment of the goals.

The Call for Proposals issued in 2000 contained very specific questions to be addressed by the researches. They were important and difficult, being the distillation of discussions and interaction with national and local Public Administrations: the complexity of the issues at stake calls for further understanding, deeper knowledge and greater evidence, which gives rise to other questions, in an endless spiral.

However, environmental management issues cannot wait for complete elucidation of all Nature's secrets, and this is especially true in the case of the Lagoon of Venice: the very existence and state of the Venice lagoon is due more to human interventions during the past centuries, when scientific knowledge and monitoring capabilities were far more limited than at present. Current knowledge, in most cases, is sufficient to be able to decide appropriate management actions, but their effects must be monitored, in order to be able to make adjustments over time. Furthermore, there is now greater awareness that any single intervention should be considered in an integrated framework and that only a systemic approach is able to evaluate the correctness of actions on and in the environment.

We believe that the scientific community can play an essential role in the Venice Safeguarding, not only for its unique capability of answering to some particular issues, but also for the wider vision which is able to consider, developing sustainable, knowledge-based scenarios for the future.

CORILA's project is making a difference respect to previous research experiences, supporting a real co-ordination of the different research lines. The CORILA's Scientific Committee is performing a careful in itinere *evaluation of the research results and the CORILA's staff is working day-by-day jointly with the research groups, asking the researchers for adapting their usual way of working and sometimes also their language: they are experimenting more integration, more data sharing, more open discussions. Of course, the co-operation of any single researcher is essential and valuable. In fact, this way is more demanding, but it will produce, in medium terms, more satisfaction and superior scientific results.*

CORILA's research is specifically geared to better understand the functioning of the lagoon's systems, natural and man-made, both ecologically and in a socio-economic context, linking different disciplines and filling in the gaps in the existing knowledge, at least as regards the Administrations' most urgent needs.

The complete picture will appear at the end of the Research Project, in early 2004. What are presented here are preliminary results, in some cases waiting for corroboration or further elaborations. We have considered it important, however, to offer this publication to a wider scientific community, despite the provisional nature of some of the articles, in order to stimulate discussion, comments and suggestions, which might be useful to consider in the last part of the program.

More and updated information on the CORILA research activities can be browsed on the web site www.corila.it.

I must sincerely thank all the researchers, staff at CORILA and other collaborators involved in the work outlined in this publication, and especially the Istituto Veneto di Scienze, Arti e Lettere for their assistance in producing the volume and Dr. Cristina Zago for her tireless efforts in editing it.

AREA 1.
ECONOMICS

RESEARCH LINE 1.1.
Economic evaluation of environmental goods

NON-USE AND USE VALUES OF SANT'ERASMO: STATISTICAL SAMPLING AND MODELS

A. Alberini[1], A. Longo[2]
[1]*Dept. of Agricoltural and Resource Economics, University of Maryland, USA*
[2]*Dip. Scienze Economiche, Università Cà Foscari, Venezia*

Computing the monetary benefits ("valuation") of environmental policies, such as the public works concerning the island of Sant'Erasmo in the Lagoon of Venice, is important when one wants to compare different categories of benefits, and when one wants to compare the benefits of a policy with its costs. Valuation implies finding how much of one resource (e.g., income) one is willing to give up to obtain an improvement in, or avoid a degradation of, another (e.g., environmental quality).

Usually, one can infer how much individuals value a good by observing the amount of this good that is exchanged on the market and its price. However, most environmental resources, such as air or water quality, are typically not exchanged on regular markets, making it impossible to observe prices and quantities. To circumvent this problem, economists have resorted to special techniques for estimating the value of environmental quality changes. One such technique is the method of contingent valuation, which directly asks individuals how much they are prepared to pay for specified changes in environmental quality. Contingent valuation is, therefore, a stated preference method, in that it relies on individuals reporting what they would do under hypothetical circumstances. An alternative technique is the travel cost method, which estimates the demand for trips to a specific destination, and uses such demand to compute the welfare change associated with improvements in quality at the visited site. A discussion of the advantages and disadvantages of each of these approaches can be found in Freeman (1993).

This paper presents the survey questionnaire development work, the statistical sampling and the statistical modeling for a contingent valuation survey and a travel cost study aimed at estimating both non-use and recreational values of the island of Sant'Erasmo in the lagoon of Venice. To our kno-

wledge, this is the first study of non-market values of the lagoon of Venice.

We estimate the welfare change associated with the improvement in the environmental quality triggered by a project that aims at reducing erosion on the island of Sant'Erasmo and at enhancing the recreational aspects through the enlargement of the beach and the improvement of the accessibility to the island itself (Brochier et al., 2001).

The data for both the contingent valuation study and the travel cost model are collected through 2.000 telephone interviews sampling the population of the city center of Venice, of other cities located on the border of the lagoon and of other cities located far from the lagoon. We also chose to sample the population located far from the border of the lagoon because non-use value is, by definition, the value that people attach to a particular resource, independently by their actual or future use of that resource. It is possible, therefore, to find people located far from the lagoon that have a non-use value for the island of Sant'Erasmo. A second reason for studying the non-use value of people living far from the lagoon is to test the hypothesis that non-use values decrease with the distance from the good.

Moreover, an on site survey on 500 boaters and lagoon users will be implemented in order to obtain more precise information about the preferences of lagoon users.

A final mail survey on sport anglers collects data to get information on preferences about species, sites, season, timing of this particular group of users of the lagoon.

Four focus groups (two conducted in the city center of Venice and two in the mainland) were implemented in order to get sufficient information on the bid values for the contingent valuation survey and feedback on the questionnaire design. Optimal design criteria (Alberini, 1995a, 1995b) and appropriate sequential updating algorithms will be also used to determine the bid values.

The contingent valuation portion of the study applies the double bounded dichotomous choice approach asking people to report information about their WTP for a government program that will reduce erosion problems and improve environmental quality on and around the island of Sant'Erasmo.

To obtain estimates of mean and median WTP for the specified government program, we combine information from the responses to the initial and follow-up payment questions to form a lower bound and an upper bound for the interval around the respondent's WTP. To illustrate, if a respondent answers "yes" to €30 and "no" to the follow-up bid of €50, it is assumed that his or her unobserved WTP falls between €30 and €50.

Let WTPL be the lower bound and WTPH be the upper bound of the interval around the respondent's WTP. Assuming that WTP follows a distribution with cdf F(•;q), where q is a set of parameters, we will fit the log likelihood:

$$(1) \quad \text{In } L = \sum_{i=1}^{n} \ln[F(WTPH_i;\theta) - F(WTPL_i;\theta)]$$

If WTP is assumed to be following the log normal distribution, for example, log likelihood (1) specializes to:

$$(2) \quad \text{In } L = \sum_{i=1}^{n} \ln\left[\phi\left(\ln \frac{WTPH_i}{\sigma} - \frac{\mu}{\sigma}\right) - \phi\left(\ln \frac{WTPH_i}{\sigma} - \frac{\mu}{\sigma} - \phi\right)\right],$$

where μ and σ are the parameters of log WTP.

Mean and median WTP can be calculated using the properties of the distribution assumed for WTP. For example, if WTP is a log normal with parameters μ and σ, mean WTP is computed as exp. $(\mu+0.5\cdot\sigma^2)$and median WTP is exp(μ).

We will also examine the effect of covariates on WTP. If WTP follows the log normal distribution, log WTP = $x_i\beta+\varepsilon_i$, where x is a $1\times k$ vector and β is a $k\times 1$ vector of unknown coefficients. The log likelihood is:

$$(3) \quad \text{In } L = \sum_{i=1}^{n} \ln\left[\phi\left(\ln \frac{WTPH_i}{\sigma} - \frac{x_i\beta}{\sigma}\right) - \phi\left(\ln \frac{WTPH_i}{\sigma} - \frac{x_i\beta}{\sigma} - \phi\right)\right],$$

In addition to conventional analyses of WTP, we will also explore the potential for yea-saying and nay-saying behavior and we will attempt to identify respondents who misunderstood the scenario. We further test the hypothesis of no difference in WTP splitting the sample of observations between people living nearby the lagoon border, and those people living far from the lagoon.

The questionnaire also collects data to estimate a travel cost model of the lagoon of Venice (Random Utility Model), with particular regard to the island of Sant'Erasmo. We assume that trips are described by a Poisson distribution where the demand for trips to Sant'Erasmo is a linear function of the quality of the site, price per trip, and other characteristics of the respondent:

$$(4) \quad \Pr(y_1 = j) = \frac{e^{-\lambda_i}\cdot\lambda_i^{j}}{j!}, \quad j = 1,2,...$$

Where:

$$(5) \quad \lambda_i = \exp(\beta_0 + \beta 1\cdot p_i + x_i\beta 2),$$

where the intercept subsumes the effect of site quality, which does not vary across respondents, and x is a vector of individual characteristics of the respondent.

The questionnaire allows us to estimate the welfare change associated with the improvement of the site quality through the estimation of a second Poisson model (Fig. 1). In this way we compare data collected through revealed preferences method (the first Poisson model of trips made by the respondents in the last twelve months) with data collected through a stated preferences method (the second Poisson model of expected trips to Sant'Erasmo given the improvement on the site quality).

We impose restrictions on the coefficients of the revealed preference equation and the stated preference equation to test if they are identical. Moreover, we experiment with allowing for such sets of coefficients to be different, and we use a likelihood ratio test to test the null hypothesis that they are not different.

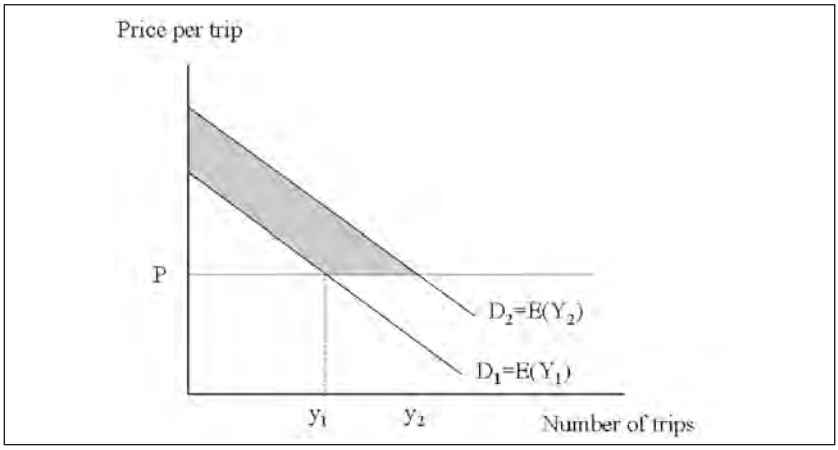

Fig. 1 – Demand curve for Sant'Erasmo.

Data collected with the on site questionnaire allow us to estimate the probability of participation. We will use probit models to estimate the probability of going to Sant'Erasmo before and after the site quality improvement.

Finally, the study will allow us to estimate the welfare change associated with the improvement in the environmental quality triggered by the project that aims at reducing erosion on the island of Sant'Erasmo. The welfare change will be measured summing the welfare change of both people who visited the island before the environmental improvement and

of those who did not visit the island before the environmental improvement, but decided to go there after the improvements.

The welfare change of those who visited the island before the environmental improvement can be measured by the area between the two demand curves, as shown in figure 1. In addition, we have to sum the welfare of those who never went to Sant'Erasmo before the environmental improvement, but decided to go after the environmental improvement. Formally it is given by:

$$(6) \quad \left(\int_{p_0}^{p(q_1)^*} E(y_2)dp - \int_{p_0}^{p(q_0)^*} E(y_1)dp\right)\cdot N_0 + \left(\int_{p_0}^{p(q_0)^*} E(y_3)dp\right)\cdot N_1$$

where N_0 is the number of people who go to Sant'Erasmo before the environmental improvement, N_1 is the number of people who decide to go to Sant'Erasmo only after the environmental improvement, $p(q_1)^*$ is the choke price of the demand curve after the environmental quality change for those who go to Sant'Erasmo before and after the environmental improvement, $p(q_0)^*$ is the choke price of the demand curve before the environmental change, $p(q_1|y_3)^*$ is the choke price of the demand curve for those who decide to go to Sant'Erasmo only after the environmental improvement.

Finally, data collected with the anglers survey will allow us to estimate a conditi o n al logit model of site choice, where the probability of selecting a specified site depends on site attributes. A travel cost model can be estimated for all trips to any site in the Lagoon, but not specifically for Sant'Erasmo. The travel cost model might be a Poisson equation:

$$(7) \quad E(Trips) = \exp(x_i \beta) = \lambda_i,$$

with the probability of j trips given by:

$$(8) \quad Prob\ (J_i = j_i) = \frac{\exp(-\lambda_i)\cdot\lambda_i^{ji}}{J_i!},\ ji = 0,\ 1,\ 2,\ \ldots$$

In addition to this first equation describing actual trips, it is possible to estimate an additional equation about hypothetical trips that would be undertaken at a different price level, or at a different level of the quality of the environment. The two equations can be combined and cross-equation restrictions can be imposed to improve the efficiency of the estimates.

References.

Alberini A., 1995a. Optimal Designs for Discrete Choice Contingent Valuation Surveys: Single-bound, Double-bound and Bivariate Models. *Journal of Environmental Economics and Management*, 28, 187-306.

Alberini A., 1995b. Efficiency v. Bias of Willingness-to-Pay Estimates: Bivariate and Interval Data Models. *Journal of Environmental Economics and Management*, 29, 169-180.

Brochier F., Giupponi C., Longo A., Rosato P., 2001. La Valutazione Economica degli Interventi di Salvaguardia della Laguna di Venezia: il Caso di S. Erasmo. Available at http://www.corila.it/Programma%20di%20Ricerca/Linee%20di%20ricerca/Linea_1_1/Linea_1_1_home.htm

Freeman M. A., III, 1993. The Measurement of Environmental and Resource Values: Theory and Methods. Resources for the Future, Washington DC, 516.

INDIVIDUAL TRAVEL COST METHOD AND FLOW FIXED COSTS

P. Rosato[1], E. Defrancesco[2]
[1]*Università di Trieste, Fondazione Eni Enrico Mattei*
[2]*Dip. Territorio e Sistemi Agroforestali, Università di Padova*

1. *Introduction.*

Travel cost method (TCM) has been developed by Clawson [1959], initially suggested by Hotelling [1949], in order to estimate social benefits from recreation in natural sites.

The method is based on the assumption that the recreational benefits in a specific site can be derived from the demand function, estimated observing users' behaviour, in relation to the costs sustained by them per number of visits. In other words, the classical model derived from economic theory of consumer behaviour postulates that a consumers' choice is based not only on price but on all sacrifices made to obtain the stream of benefits generated by a good or service. Obviously, if the paid price (p) is the only sacrifice made by consumer, the demand function for a good, with no substitutes, is $x = f(p)$, given his income and preferences.

However, the consumer often incurs other costs (c), in addition to the paid price, i.e. disbursements, travel expenses, time loss and stress from congestion and/or competition, e.g. crowded local markets. In this case, the demand function is the following: $x = f(p, c)$[1]. In other words, the price is an imperfect measure of the good's cost incurred by the purchaser. Under these conditions, the utility maximising consumer's behaviour should be reformulated in order to take into account such costs: given two goods or services (x_1, x_2), the prices (p_1, p_2), the access costs (c_1, c_2) and the income (R), the utility maximising choice of the consumer will be obtained as follows:

$$\begin{aligned} &\max\ U = u(x_1, x_2) \\ &\textit{subject to} \\ &(p_1 + c_1)x_1 + (p_2 + c_2)x_2 = R \end{aligned} \qquad [1]$$

[1] Suppliers often internalise the difficulties faced by consumers in founding a good into their pricing policies using price differentiation.

Now, assuming x_1 the aggregate of priced goods and services, x_2 the number of annual visits to a recreational site, negligible access costs to the market goods ($c_1=0$) and a free access to the recreational site ($p_2=0$), [1] can be written:

$$\begin{aligned} &\max\ U = u(x_1, x_2) \\ &\textit{subject to} \\ &p_1x_1 + c_2x_2 = R \end{aligned} \qquad [2]$$

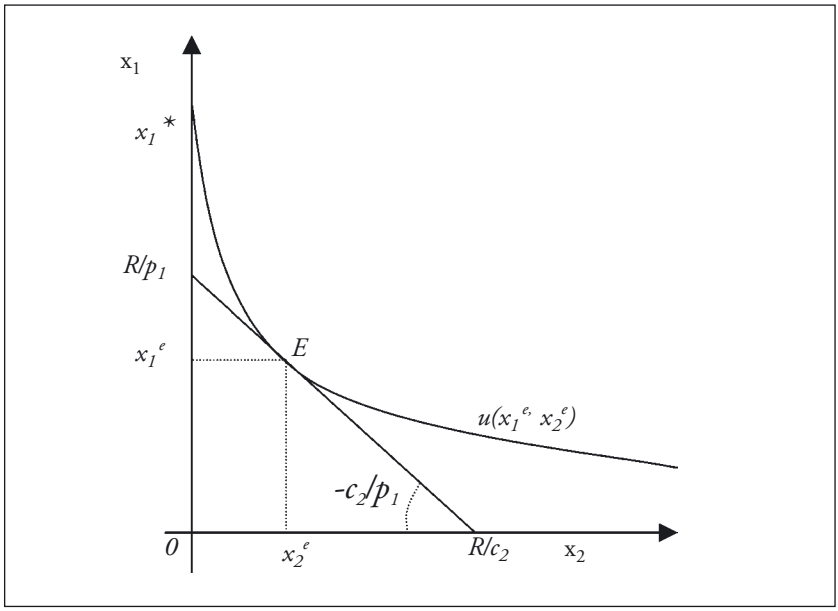

Fig. 1 – Utility maximization of a private and public recreational services user.

Under these conditions, the utility maximising behaviour of the consumer depends on:

a) his preferences [$u(x_1, x_2)$];

b) his budget (R);

c) the prices of the private goods and services (p_1);

d) the access cost to the recreational site (c_2).

Figure 1 shows the optimal choice between private goods and recreational activity, given the budget constraint: the point where the marginal rate of substitution is equal to the slope of the budget line and/or where the weighted marginal utility is equal $Um_1/p_1=Um_2/p_2$.

Figure 1 also highlights other important issues that will be useful later, when analysing the impact of different type of cost on consumers' optimal choice. First of all, the utility function shows that the user could renounce the recreational activity considered in the figure, allocating his budget only on x_1, while he could not set x_1 to zero (the utility function curve cuts only the Y-axis in x_1^*).

In other words, access to the recreational site could be considered if the income is over a specific threshold, once other needs[2] have been satisfied. With an increased income, the marginal rate of substitution grows and the optimal solution moves from the corner solution $[R/p_1]$, on the Y-axis, to point E[3]. TCM is based on the hypothesis that changes in the access costs to the recreational site (c_2) have the same effect as price variations: as the number of visits to a site decreases as the cost per visit increases. If the implicit assumptions in [2] are reasonable, then the demand function of the recreational site is $x^2 = f(c_2)$ and it can be estimated using the number of yearly visits and different costs per visit observed. There are two basic approaches to TCM: the Zonal approach (ZTCM) and the Individual approach (ITCM). The two approaches share the theoretical premises, but differ in the operational point of view. ZTCM takes into account the users frequency rate coming from different zones with increasing travel costs. ITCM, however, examines the behaviour of the single user in choosing the number of visits per time period, usually a year. The latter approach can be considered a refinement or a generalisation of ZTCM [Ward and Beal, 2000].

ITCM, developed by Brown and Nawas [1973] and Gum and Martin [1974], estimates the consumer surplus by analysing the individual visitors' behaviour and the cost sustained for the recreational activity. These observations are used to estimate the relation between the number of individual's visits in a stated time interval, usually a year, the cost per visit and socio-economic variables.

Figure 2 highlights the expected relation between the number of visits and cost per visit, given the other variables. It also shows that the number of visits decreases as the cost per visit increases. If we assume that all users have the same preferences and the same income, the number of visits are a function of the cost per visit:

$$x_2 = g(c_2) \qquad [3]$$

---

[2] In other words, consumer utility function is non-homothetic.

[3] Given that $u(x_1^e, x_2^e) = u(x_1^*, 0)$ and setting $R^* = p_1 x_1^*$, the willingness to accept a compensation (WTA) to renounce to x_2^e visits is WTA = $R^* - R$. In other words, WTA increases as marginal rate of substitution increases.

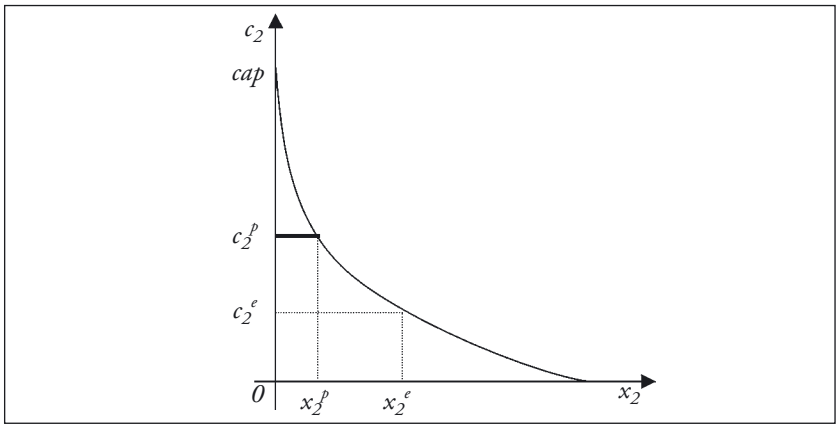

Fig. 2 – Individual's recreational demand function.

Therefore, if an individual incurs c_2^e per visit, it carries out x_2^e visits a year and if the cost per visit increases to c_2^p the number of visits will decrease to x_2^p. In other words, for a homogenous group of individuals[4], [3] shows the relationship between the number of visits and the cost per visit. The cost *cap* is the choke price: the cost per visit that sets the number of visits to zero. Equation [3] is the individual demand function for the recreational site use referred to an "average user". The annual user surplus can be easily obtained integrating the demand function from zero to the present number of yearly visits and subtracting the visits costs.

Figure 3 shows the user's behaviour with increasing additional costs per visit. Briefly, the additional cost (*ca*) modify the slope of budget line that gradually reduce the number of visits until the point in which, for the aggregate effect of the reducing of the marginal rate of substitution and the increasing of slope of the budget line, the optimal solution excludes the visit (x_2), and the entire budget is spent on x_1. The additional cost setting the visits to zero is *cap*, the choke price. Increasing the cost for visit to *cap*, the consumer's utility will be reduced to $u(R/p_1, 0)$. The demand function, subtracting the present travel cost, [$x_2=z(ca)$, $ca=\delta(x_2)$] is the curve *I* of figure 4.

[4] The function can also be estimated for non homogeneous sub-samples introducing among the independent variables income and socioeconomic variables expressing individual preferences [Hanley and Spash, 1993, p. 84].

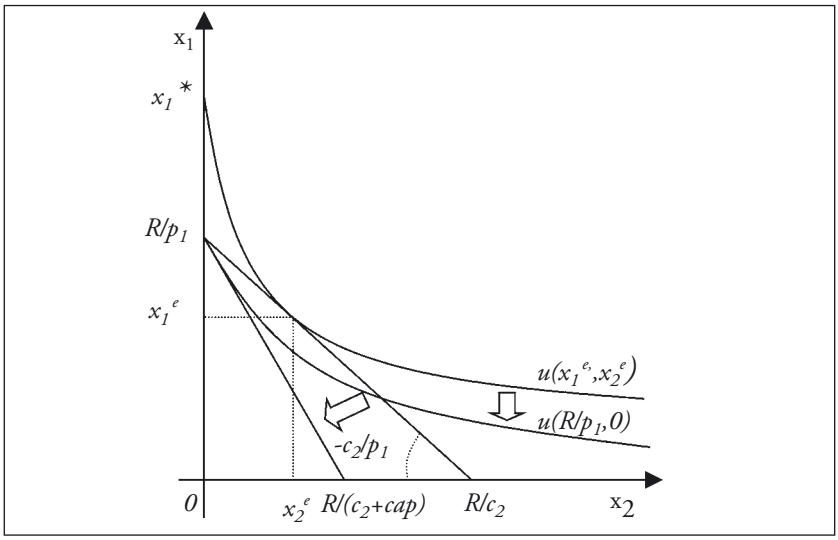

Fig. 3 – User's behaviour at increasing additional fees.

The aggregate demand function (*A*) [$x_2 = h(ca)$, $ca = \varphi(x_2)$] is obtained summing up the individual demands (*i*) at the different additional costs. It cuts the X-axis at the total present visits' numbers ($\Sigma_i x_{i2}^e$ and the Y-axis at the maximum additional cost incurred by the users. The recreational users' surplus is obtained taking the present value of the definite integral

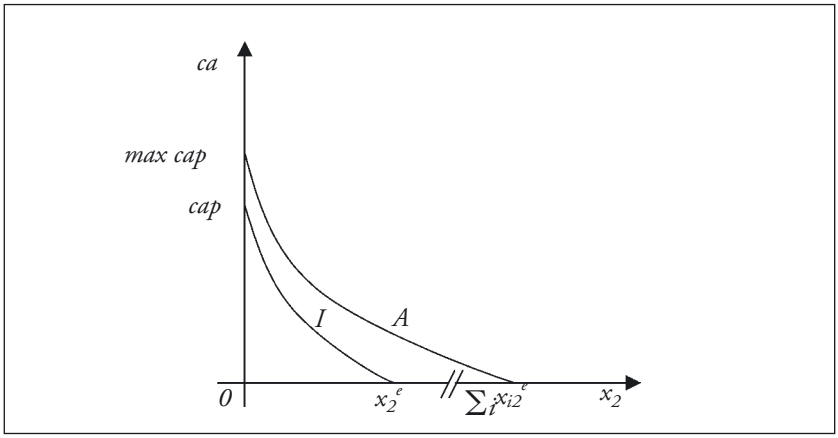

Fig. 4 – Individual's and aggregate recreational demand function.

of the aggregate demand function (*A*) from zero to total annual visits' number. That is:

$$S = \frac{\int_0^{\sum_i x_i^e 2} \varphi(x_2)\,dx_2}{r}$$

where *r* is an appropriate discount rate.

2. *Types of Cost and User's behaviour.*

The previous model shows that the aggregate recreational demand function is closely related to a "travel generator function" [3] that includes the costs perceived as relevant by the users in their decision-making process in establishing the number of annual visits. Some relevant costs for the decision-making process are often not measurable and/or subjective[5] [Randall, 1994; Common, Bull, Stoekl, 1999]. Usually, these costs are substituted with observable proxies. ITCM takes into account direct variable costs only (i.e. fuel, tolls, tickets, etc). On the other hand, the recreational use of natural resources often involves annual fixed costs, independent of the number of visits carried out. For example, with recreational fishing in open waters or sea, it is necessary to pay for an annual fishing licence and to incur boat-related annual expenses (i.e. laying-up, maintenance and assurance), generally independent from the annual number of visits. Such costs are irrecoverable in the short period (sunk costs), that is, on an infra-annual perspective, while, extending the analysis to a full annual perspective, they can be avoided, renouncing the recreational activity[6]. For example, the expenses in laying-up and for fishing licences, sunk costs already incurred, can be avoided the following year, renouncing the visits. With a longer time scale, the capital locked up in the boat is, at least partially, recoverable when selling it.

The literature on fixed costs and TCM is rather elusive. Some authors [Hanley and Spash, 1993, p. 88] argue that the welfare measures vary

[5] I.e. the problem of valuing travel time.

[6] The existence of fixed costs depends closely on the temporal interval considered [Tirole, 1991, p. 532]. I.e. the cost of a annual licence is fixed if an inferior interval to 12 months is considered; vice versa it is variable if the temporal horizon is extended to one year.

including the fixed costs or not and they suggest to exclude the fixed travel costs as "Individuals, maximising utility, are assumed to compare the marginal utility with the marginal costs of consumption". Likewise, Walsh [1986, p. 100] suggests considering the direct costs only since ".. the concept of fixed costs is not applicable to consumer decisions to take an additional trip to recreation site ". Ward and Beal [2000, p. 44], assert "TCM uses the cash costs directly incurred by visitors to travel to given the demand equation to that site". Ward and Beal [2000] argue, moreover, that the presence of high fixed costs related to specific equipment required for the recreational activity, reduces the price elasticity of the demand.

These assumptions seem reasonable when a) the amount of flow fixed costs is low in comparison to the variable costs, b) it is referred to multipurpose equipment or costs (i.e. car) and, above all, c) the analysis is closely of short period.

But are these assumptions reasonable in presence of relevant, specific annual fixed expenses and when the benefits' estimate are used to support medium-long run public decisions, i.e. a fee-policy? In our view, in these cases the opportunity cost of flow annual fixed expenses has to be taken into account, therefore conditioning the choices of the users on a full annual perspective. Indeed, a more accurate approximation to the decision making process faced by a recreational user is needed in order to forecast better the number of visits with additional entry fees. In the case of recreational fishing and/or boating, for example, the decision-making process faced annually from a user involves two sequential decisions:

a) '*Do I fish this year?'* (full annual perspective). This decision to sustain the annual fixed costs related to the recreational activity (i.e. payment of the licence, boat-related expenses), or to assign the saved money to other goods, or recreational activities. This decision depends on the comparison between a subjective, generally optimistic, forecast of the number of visits he will carry out during the year and a minimal threshold. In general, this estimate, carried out annually, can be considered analogous to that one operated preliminarily with the investment in the recreational activity related equipment, but it is supported by past experience, of the estimate of the number of annual visits, the variable costs and annual fixed expenses.
b) '*Do I fish today?'*, (infra annual perspective). After having incurred annual fixed expenses, the user decides on the number of visits to carry out on the base of the variable cost per visit. Obviously, the recreational demand function estimate, being based on the observed user's behaviour facing the direct variable travel cost, allows the modelling of the second

step of the decision-making process only. However, this two step annual decision-making process, already highlighted by other authors [Walsh, 1986]: a) justifies the assumption not to include the equipment depreciation fixed costs in the cost per visit, but b) suggests taking into account annual fixed expenses, giving important influence both on the choke price and on surplus estimates in an annual perspective. The influence of flow fixed expenses can be measured estimating the minimum number of visits per year that allows the individual to sustain them, thus '*to remain in play*'.

This issue suggests to redefine the utility maximising behaviour of a recreational user incurring both a variable cost per visit and also an annual fixed cost (c_o). Assuming R the available budget (net from the annual fixed expenses, already sustained), p_1 the price of the other goods and services (x_1) and c_2 the variable direct cost per visit (x_2), on a full annual (or inter-annual) perspective, the optimal choice can be obtained solving:

$$\begin{aligned} &\max\ U = u(x_1, x_2) \\ &\textit{subject to} \\ &p_1x_1 + c_2x_2 = R \quad \textit{if } x_2 > 0 \\ &p_1x_1 = R + c_0 \quad\ \ \textit{if } x_2 = 0 \end{aligned} \qquad [5]$$

The solution can be found comparing the utility $\left[u\left(\frac{R+c_o}{p_1},0\right)\right]$ reachable spending $R+c_o$ in x_1, with the utility $[u(x_1^o,x_2^o)]$ obtained spending actual income (R) on the combination between x_1 and x_2. The optimal solution depends on the parameters of [5]: the shape of the utility function, the ratio between prices and variable average cost per visit, the budget constraint line and the annual fixed cost.

The presence of a annual fixed expenses does not modify the slope of the budget line but it produces a similar effect to an income variation. If the demand of the recreational site is elastic in regards to the income, then budget variations will modify the marginal rate of substitution. In other words, a low budget will favour the corner solution allocating all the income on x_1. With the augmentation of income, the increase of the MRS favours intermediate solutions. It seems useful to thoroughly explore the equilibrium condition (indifference) between the recreational site use x_2 and the exclusive consumptions of x_1. Such condition can be obtained solving the following equation:

$$u(x_1^m,x_2^m) = u\left(\frac{R+c_o}{p_1},0\right) \qquad [6]$$

where x_1^m and x_2^m are the *optima* when the user accepts to incur annual direct fixed costs for recreational activity x_2 (fig. 5).

Assuming a convex utility function, monotonic and non-homothetic, a relevant annual fixed expense implies the existence of a minimum number of yearly visits per user x_2^m, generally greater than zero. In fact, starting from optimal point *M*, an increase of the cost of recreation (increase of the annual fixed cost and/or the variable cost per visit) will not set the visit to zero. In other words, as costs increase, the recreational demand function does not approach to zero but x_2^m.

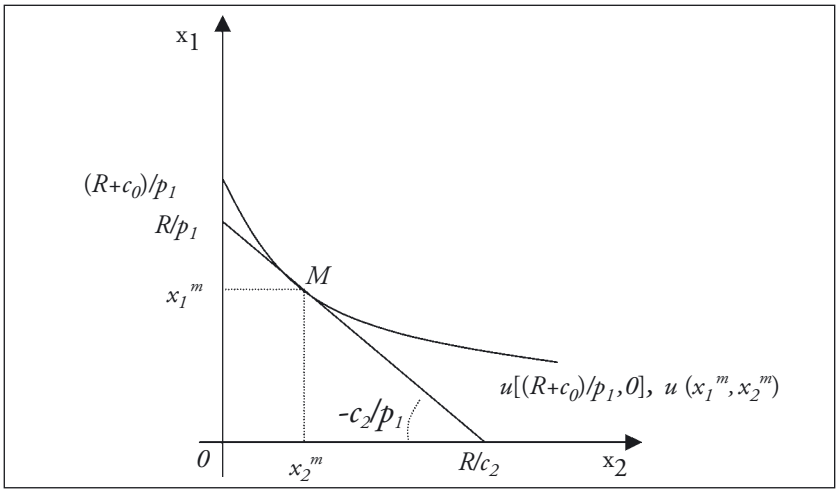

Fig. 5 – Utility maximization of a private and public recreational services user with annual direct fixed costs.

As a consequence, taking into account only the variable cost, we ignore the user's alternative of deciding every year, even with some rigidity due to an optimistic forecast of the number of visits, not to incur the annual fixed costs, freeing therefore an additional budget to be spent on other goods: in other words, it is assumed a decisional scenario, on an infra-annual base, more rigid than the real one.

3. *ITCM and Flow Fixed Costs.*

When the user decision-making process is similar to that outlined above, the ITCM has to take into account the alternative of not incurring the annual fixed expenses. Therefore, on a full annual base, the estimated num-

ber of yearly visits decrease with increasing entry fees, will be higher than the reduction predicted on an infra-annual base. Further additional unit cost increases ultimately reduce visits to a minimal value x_2^m greater than zero. The minimal yearly visits number can be obtained from the equation [6] taking into account its corresponding 'choke' price (point M, fig. 6).

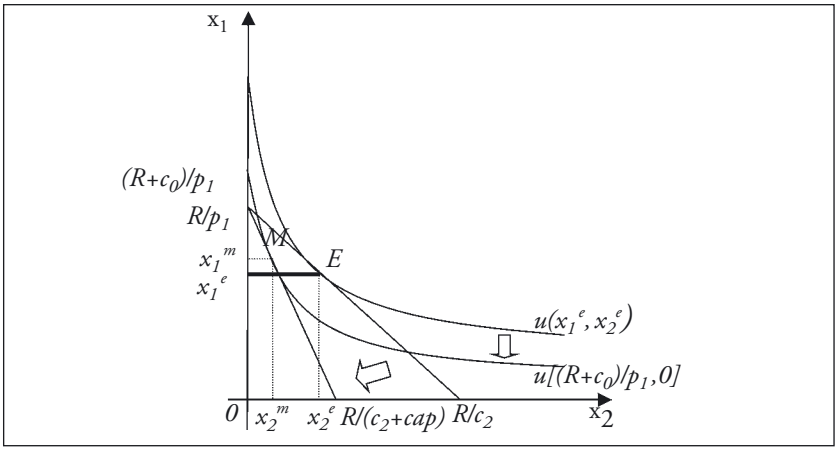

Fig. 6 – User's behaviour at increasing additional fees with annual direct fixed costs.

In this particular case, the so-called 'choke' price is not the price at which all visits cease on an infra-annual perspective, but the price at which the user decides to avoid annual fixed costs. As a result, the 'choke' price on an annual perspective is lower than one on an infra annual perspective, when periodic fixed costs are not involved (*cap**, fig. 7).

On an annual perspective, with relevant fixed costs, the individual's recreational demand function needs to be estimated using variable costs and the number of visits, based on observed data, per user. However, in order to avoid the overestimation of a recreational user's surplus the demand function has to be truncated to the minimal number of visits (x_2^m), justifying the annual fixed cost (fig. 7)[7].

Now we have to estimate x_2^m and/or *cap*. The minimal number of visits (x_2^m), is not observable, because it is evaluated by the user in phase (*a*) of his decision-making process, but it can be obtained from the equilibrium conditions of figure 6. Under this conditions, consumer surplus derived

[7] Ward and Beal [2000, p.151] suggest to add the average unit annual fixed cost per visit to unit variable cost in a ZTCM approach, in order to eliminate extremely high predictions from nearby zones of origin.

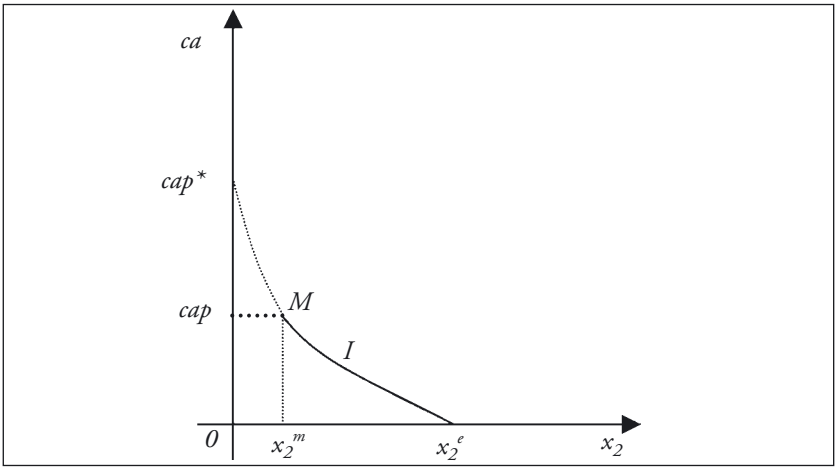

Fig. 7 – The individual's recreational demand function with annual fixed costs.

from allocating his entire budget ($R+c_o$) for the consumption of x_1, is equal to the surplus that he obtains in M; since:

$$x_1^m = \frac{R - cap\ x_2^m}{p_1} \qquad [6]$$

can be written as:

$$u\left(\frac{R+c_o}{p_1}\right) = u\left(\frac{R - cap\ x_2^m}{p_1},\ x_2^m\right) \qquad [7]$$

assuming a marginal consumer and placing:

$$p_1 = 1$$

$$cap = \delta(x_2^m)$$

$$u\left(x_2^m\right) = \int_0^{x_2^m} \delta(x_2)\,dx_2$$

we have:

$$u\left[C_0 + x_2^m \delta\left(x_2^m\right)\right] = C_0 + x_2^m \delta\left(x_2^m\right)$$

$$C_0 + x_2^m \delta\left(x_2^m\right) = \int_0^{x_2^m} \delta(x_2)\,dx_2 \qquad [8]$$

Solving [8] x_2^m can be obtained. Taking into account x_{i2}^m for every user i, based on his annual fixed expenses, the total recreational benefit of the site is:

$$S = \sum_i \frac{\int_0^{x_{i2}^e} \delta_i(x_2)dx_2 + \frac{\int_{x_{i2}^m}^{x_{i2}^e} \delta_i(x_2)dx_2}{r}}{1+r} \qquad [9]$$

We have to take into account x_2^m due to annual fixed costs sustained mainly when users are able to estimate with precision their future visits. On the other hand, x_2^m can be ignored when fixed costs do not influence the user decisions; in particular: a) when the fixed costs have been sustained a long time before the recreational activity, b) when the number of expected annual visits per user significantly differs from the real ones. In fact, as we said before, the investment in recreational equipment is based on an optimistic forecast of annual visits. By the way, usually, the best two days in a boat owners life is the day he buys the boat and the day he sells it to someone else.

4. *A numerical example.*

In order to verify the impact of the proposed method both on the reduction of the number of annual trips due to increasing fees and on welfare measures, a numerical example has been carried out, referring to recreational use of the Venice lagoon (boating and fishing). A detailed description of the collected data set can be found in a previous paper [Defrancesco, Rosato, 2000], showing the results of an on-site survey carried out during spring and summer 1999, aimed to estimate recreational benefits of the lagoon, using both contingent valuation and ITCM.

This exercise is based on an homogeneous sub-set of 129 recreational users, obtained selecting the visitors incurring high annual fixed expenses, paying an annual price to keep their boat in a marina. However, given the limited, non-random, sample size, our results have to be considered as an example and they can not be extended to the recreational users population of the lagoon.

ITCM has been based on the number of annual trips declared by those interviewed. The variable costs include: a) the direct variable cost

sustained by each user in order to reach the boarding point, off-site travel time valued in proportion of wage (6€ per hour), b) the cost of fuel for the boat, c) the cost for food and beverages, d) in the case of the fishermen, the cost of bait. The annual fixed cost takes into account the cost sustained in order to keep the boat in a marina, boat insurance and maintenance costs, and, if applicable, the annual cost of fishing license (tab. 1).

Tab. 1 - Descriptive Statistics on variables.

	Mean	**Standard Deviation**
Annual trips	26,8	5,8
Direct Variable Costs per Trip (€)	59,0	27,7
Annual Direct Fixed Expenses (€)	1071,0	592,9
Annual Income (.000€)	17,5	15,3

The estimated recreational demand function [3] predicts the individual annual trips as a linear function of the logarithm of variable costs per visit and income, closely fitting the data (adj R^2=53%).

Tab. 2 – The individual's recreational demand function coefficients.

		Coefficient	**Standard Error**
Constant	(c)	42,56	2,25
Ln(Direct Variable Cost per Visit)	(α)	-6,94	0,62
Ln(Annual Income)	(β)	4,44	0,50

The OLS estimated coefficients (tab. 2) differ significantly from zero (α=1%) and have the expected sign. In order to evaluate the individual recreational surplus the demand function, being asymptotic to the Y-axis, has been truncated to one visit [Ward and Beal, 2000], valuing the first trip on the base of its marginal benefit obtained solving the demand function for the cost that would produce one trip. On an infra annual perspective, the net recreational surplus of an user is equal to the difference between the total yearly surplus (the area under the demand function between one visit and the actual trips, plus the surplus related to the first trip) and the total variable cost sustained. The mean recreational sur-

plus per visit is equal to 611,80€, the standard deviation over the mean equals to 48% and the median value is 567,3€[8].

On the other hand, under a full annual perspective the behaviour of the lagoon recreational user is influenced by annual fixed expenses sustained for recreation, given his income. So, his unobservable x_2^m has to be estimated, imposing the equality [8]. In this specific case, [8] is:

$$c_o + x_2^m e^{\frac{x_2^m - (c+\beta \ln R)}{\alpha}} = 1 - \frac{(c+\beta \ln R)}{\alpha} + \int_1^{x_2^m} \left(e^{\frac{x_2 - (c+\beta \ln R)}{\alpha}} \right) dx_2 - ca x_2^m$$

where:
R = user income;
c_o = annual fixed costs;
ca = variable cost per visit.

In this case, the annual recreational surplus of the user is equal to the difference between the definite integral of the demand function from x_2^m to actual number of yearly trips, and the related total variable costs. In other words, if the agency managing the lagoon estimates the net recreational users' surplus in order to better define a fee policy, it has to take into account the surplus under a full annual perspective, estimated using x_2^m. By increasing entrance fees many users could decide to renounce a visit the lagoon, because of the relevant annual fixed cost which involves a number minimal of annual visits.

In this particular case, this adaptation of TCM highlights:

a) The individual minimal number of visits per year ranges between 2 and 12; the mean x_2^m is equal to 3,36 and standard deviation equals 1,22. The estimated coefficients of a regression model (tab. 3), expressing x_2^m as a function of logged income, logged variable cost and annual fixed costs (adj R^2=0,85), show that the minimal number of visits per user decrease with the increase of income and is positively related to the amount both of fixed and variable costs.

b) The number of visits carried out by all users decreases more rapidly on a full annual perspective, i.e. taking into account their behaviour facing annual fixed cost. In fact, figure 8 clearly highlights that, extending the analysis in the medium run, an annual additional fee higher than 500€ several results in users renouncing recreational activity, due to the num-

[8] The high mean value is due to the algebraic form of the demand function and, above all, to the particular sub-sample analysed.

Tab. 3 – The minimum annual number user's visits function.

	Coefficient	**Standard Error**
Constant	4,89	0,28
Annual Fixed Costs	0,002	0,00
Ln(Variable Unit Cost)	0,182	0,08
Ln(Annual Income)	-1,62	0,07

ber of yearly visits that would be less than the minimum justifying the annual fixed costs sustained. Therefore, the dotted line showing annual trips taking into account the annual fixed cost lies under the line of visits on a infra-annual perspective (based only on variable cost). Obviously, the distance between the lines increases as additional fees increase.

c) On a full annual perspective, the net mean surplus per visit is equal to 377,8€, the standard deviation over the mean equals 55% (median 352,1€). The unit mean surplus is, therefore, 38% less than the unit welfare estimate obtained applying the traditional TCM (infra-annual perspective). So, the exercise clearly highlights the impact of the varied estimation approaches on the lagoon's total recreational value (fig. 8).

5. *Concluding remarks.*

The aim of this paper is to propose a modified ITCM approach, taking into account flow fixed costs. A full annual perspective, in our view, when recreational users incur relevant annual direct fixed expenses, their behaviour could be influenced by them, on a full annual perspective. As a result, the agency managing a natural site for outdoor recreation should use caution when valuing recreational users surplus, which has to be estimated on a full annual perspective, mainly in order to define a proper fee policy. By ignoring flow fixed costs TCM, both surplus estimate and yearly number of visits at different additional fees could be overestimated. So, on a medium run perspective it could be useful to take into account the annual fixed expense which is directly connected to recreation. When flow fixed costs are relevant in respect to variable costs, the proposed approach works as it follows:

a) based on observable users' behaviour, the individual's recreational demand function, as usual, has to be estimated on actual yearly trips and related unit variable costs (infra annual perspective).

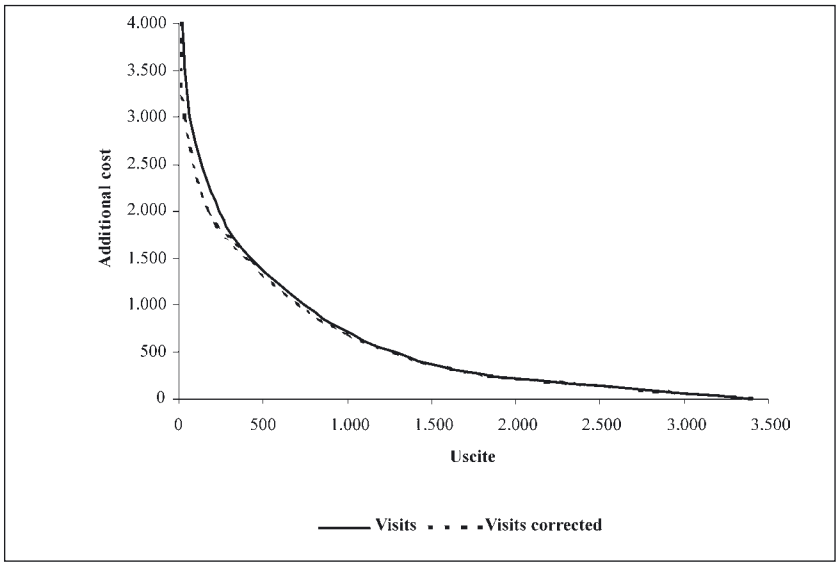

Fig. 8 – Number of total annual visits at increasing additional fees on an infra-annual perspective (traditional TCM) and taking into account yearly fixed expenses on a full annual perspective.

b) users face a full annual decision-making process, involving the amount of direct fixed expenses. This process is unfortunately unobservable. It could be valued by introducing the notion of the minimal number of annual visits (x_2^m) that justifies the annual fixed expenses incurred by the user;

c) using x_2^m the user behaviour can be described on a full annual perspective, taking into account a more precise estimate of the number of visits with different additional fees. Under a infra-annual perspective, i.e. ignoring x_2^m, both recreational surplus and the number of annual trips, at increasing additional fees, could be overestimated, in order to use them for medium-long run decision-making processes (i.e. fee policies). In actual fact, traditional TCM approach could produce questionable results, when annual direct fixed costs are relevant.

On the other hand, the minimal number of annual visits x_2^m closely depends on both the amount of the direct annual fixed expenses incurred by the user and the accuracy of the perceived fixed cost by him. In conclusion, further investigations are needed, in order to achieve a better definition of the types of cost really valued by the users in their decision-making process, when relevant annual fixed costs are incurred.

References.

Brown W.G., Nawas F., 1973. Impact of Aggregation on the Estimation of Outdoor Recreation Demand Functions. American Journal of Agricultural Economics, 55, 246-249.

Clawson M., 1959. Method for Measuring the Demand for, and Value of, Outdoor Recreation. Resources for the Future, 10, Washington D.C..

Clawson M., Knetsch J.L. (1966). Economics of Outdoor Recreation. The Johns Hopkins Press, Baltimore.

Common M., Bull T., Stoeckl N., 1999. The Travel Cost Method: an empirical investigation of Randall's Difficulty. The Australian Journal of Agricultural and Resource Economics, 43:4, 457-477.

Defrancesco E., Rosato P., 2000, Recreation Management in Venice Lagoon. FEEM, Nota di lavoro 65.2000, Venezia.

Gum R.L., Martin W.E., 1974. Problems an Solutions in Estimating the Demand for and Value of Rural Outdoor Recreation, America Journal of Agricultural Economics, 56, 558-566.

Hanley N., Spash C.L., 1993. Cost Benefit Analysis and the Environment. Edward Elgar, Aldershot.

Hotelling H., 1949, Letter, In An Economic Study of the Monetary Evaluation of Recreation in the National Parks, Washington D.C., National Park Service.

Nicholson W., 1995. Microeconomic Theory. Trydent Press, N.Y., 98-99.

Randall A., 1994. A Difficulty with the Travel Cost Method. Land Economics, 70-1, 88-96.

Tirole J., 1991. Teoria dell'organizzazione industriale. Hoepli, Milano.

Walsh R.G., 1986. Recreation Economic Decisions: Comparing Benefits and Costs. Venture Publishing, Inc. State College, Pennsylvania.

Ward F.A., Beal D., 2000. Valuing Nature with Travel Cost Method: A Manual. Edward Elgar, Northampton.

PSYCHOLOGICAL RESPONDING EFFECTS AND BIAS INTERPRETATION IN CVM STUDIES: AN INTRODUCTION REVIEW

V. ZANATTA
Dip. di Innovazione e Meccanica Gestionale, Università di Padova

1. *Introduction.*

This paper is focused on what a respondent may be thinking while answering a WTP question, and on the most relevant bias in CV studies deriving from psychological response effects in survey-based searches. The aim of the present analysis is reviewing some applications which could make able in controlling what CV really estimates. To start, it is important to gather some awareness in the process of economic thought (and not only of its product).

Some important studies of last decade demonstrated that the value assessed by CV can be sensitive to theoretically irrelevant factors and insensitive to theoretically relevant ones. For example, response modes, referred as different methods for eliciting preferences, can affect the results of CV (McFadden and Leonard, 1993; Swallow, Opaluch and Weaver, 1997; Blamey, Bennett and Morrison, 1999). Moreover, answers seem widely affected by respondents' moral satisfaction when they accept to pay for a symbolic amenity instead of for the specific level of provision described in the CV scenario (Kahneman and Knetsch, 1992; Brekke and Howarth, 2000). But where does such effects come from? What are psychological mechanisms these biases derive from? The present paper links some evidences from cognition process, decision making and answering formation, to some CVM common biases, as to introduce a theoretical and methodological basis for case study experiment.

2. *Preference formation process and survey response modes.*

Trough the last few decades, economists, sociologists and psychologist proposed different theories about how survey respondents sort their own individual preferences, and then answer questions. In fact, answers to

some questions are prone to a variety of well-documented response-effects, referred as differences in survey outcomes that reflect seemingly irrelevant procedural details (Tourangeau, Rips and Rasinski, 2000). These response effects may be due to problems in understanding the question, remembering relevant information, or other mental processes (Schuman and Kalton, 1985; Touregeau and Rasinsky, 1988). Krosnick has digressed a lot on most relevant form of response effects: moreover, he had the intuition that level of educational attainment could be a pervasive and systematic moderator of susceptibility to response effect in survey based studies (Narayan and Krosnick, 1996). On the contrary, better educated individuals, even if they grasp the general point of a question and are less easily affected by "emotionally colored" words, are more sensitive to precise verbal distinctions, where that is appropriate. The table 1 (Tab.1) reports a summary of response effects that can be considered relevant even in CV studies.

More generally, consolidated theories of the response process move from Cannell's Process Theory (Cannell, Miller and Oksenberg, 1981), to the Response Process Model formalized by Tourangeau, Rips and Rasinski (2000)[1]. In compliance to this last search, survey response process is divided in four main components: 1) comprehension of the item, 2) retrieval of relevant information, 3) use of that information to make required judgments, and 4) selection and reporting of an answer. Each of these components implies specific mental processes which can give rise to response effects: for example, respondents may misinterpret the question, forget crucial information, make erroneous inferences based on what they do retrieve, or express their answer into an inappropriate response category. If asked about a difficult or non-familiar topic, as environmental quality or supply could be, all effects can be emphasized. As in CVM the problem of accuracy in questionnaire answering is supposed to imply utility esteems, and finally evaluation of precise goods, decision making scholars tried to apply psychological cognition theory to improve interpretation of consumer behavior. As Hausman reports in its essay (Hausman, 1993), Fischoff explains people preferences construction by using two paradox extremes (Fishoff, 1991): 1) people have well-formed preferences about any relevant topic and can directly retrieve an appropriate response to an elicitation question; 2) people have well defined values only for very familiar topics, and must derive specific valuations for less familiar topic through some inferential process. If the first assumption

[1] See also Strack and Martin (1987).

Tab. 1 – Summary of response effects considered relevant in CV studies.

Type of Effect	**Definition**
Response order effects (Schwarz, Hippler, and Noelle-Neumann, 1991)	It is the effect related to the order in which response alternatives are presented to respondents.
Satisficing effect (Krosnick and Alwin, 1987)	It occurs when respondent shortcut the cognitive processes necessary for generating optimal answers, and report just what is supposed to be "right" for the interviewer
Acquiescence effect (Bachman and O'Malley, 1984)	It is the effect related to the tendencies of agree or disagree with any assertion, regardless of its content.
Middle alternative effects (not involving status quo options) (Krosnick, 1991)	It is the tendency to select a middle alternative option. Note: the proportion of respondents endorsing the middle option increases as a result of the cue in the question legitimating that response.
No opinion filter effects (Narayan and Krosnick, 1996).	Opinion filter effects; it is the effect from inclusion or omission of a "no-opinion" response options in questions*
Tone of wording effects (Krosnick 1991)	It is the effects related to how a word in the question "sounds"**
Balance effects (Converse and Presser, 1986)	A balanced question is one that does not increase the number of words devoted to articulating one of the opposing point of view about the item of the question itself.
Context effects (Schuman 1992)	It is the effect that is assessed by manipulating the order in which questions are asked.

* Experiments demonstrated that, although some people volunteered that they had no opinion when asked the question, many more selected that response when the "no opinion option" was offered explicitly in the question.

** Krosnick call it the Allow/Forbid Effect, as a typical example is the difference in results when the word "allow" is used instead that the word "forbid". Rationally, if the wording shift has no effect, the response proportions saying "no – do not allow" and "yes – forbid" should be equivalent.

would be true, potential CV biases could be overcome by methodological improvement in WTP elicitation methods, in compliance with Mitchell and Carson search (Mitchell and Carson, 1989). On the contrary, the second assumption leads to the conclusion that, in most cases, people must construct their responses at the time they are asked an elicitation question (Tversky et al.,1988). Obviously, it implies that this process of preferences sorting would be influenced by context factors, so that it couldn't be consistently represented as an expected utility calculation. Moreover, Schkade and Payne (1993) quoted many works of last two decades about human behavioral decision research, as they demonstrate that decision makers have not just formed preferences, but a repertoire of methods for identifying their preferences and developing their beliefs, deriving this multiple strategy both from experience and training[2]. In compliance to this, it can be also admitted that preferences would be typically constructed in condition of limited information processing capacity and inconsistency, i.e. the most natural attitude of human reasoning (Simon, 1955; March, 1958). It should be noted that this type of preference construction may involve CV studies, particularly in the case of nonuse values for unfamiliar goods (Gregory, Lichtenstein and Slovich, 1991). In fact, CV application needs appraisals of policy choices (and the related preliminary knowledge) and makes the value formulation problem more difficult than ordinary market decisions (Mitchell and Carson, 1993). In fact, first, individuals asked to express a WTP can base their own valuation not on the experience, as the information is simply provided by the hypothetical scenario described in the questionnaire (not tested in the real experience). Second, CV is usually applied to assess the monetary valuation of benefits from policy choices (for example, environmental policies) usually unfamiliar to the respondents. Third, there are relevant time constraints when CV questions are answered, rendering difficult all the four phases of Response Process described above.

[2] In Schkade and Payne (1993) a relevant observation can be found. Verbatim: "The economic model assumes that, although the assessed values may differ across people (because they have different utility functions) or across situations (some things are worth more than others), the process by which they reveal these preferences should be the same in all of these cases, namely, a maximization of expected utility. if different people use different strategies in different situations, these facts would be difficult to reconcile with the standard economic model".

3. *CVM and psychological-related biases.*

Observations reported above would lead to a long investigation on introduced items. But what is relevant here is focusing on some biases in CV studies, directly depending on psychological and cognitive aspects described, and that may occur while respondent create his/her preferences structure, in order to express his/her WTP.

3.1. *Information.*

Information biases may arise when complex information is communicated to the respondents. They are prevalently due to time constraints (in contingent market description, in questionnaire compilation, in preference creation for the commodity to be valued), but the real problem is related to the level of information to be provided in the survey instrument. Many authors (Fishhoff and Furby, 1988; Samples et al., 1986; Hanley et al., 1995) tried to give a straightforward solution, focusing an optimum level of information by which respondents are able to make a valid value formulation, without answering to a too long or incomprehensible survey. Moreover, individual cognitive process and preferences sorting in lack of adequate information can make unproductive CV assessment validity.

3.2. *Uncertainty and Ambivalence.*

Ready, Whitehead and Blomquist (1995), Wang (1997), Dubourg, Jones-Lee, and Loomes (1994,1997) each argued that respondents may not know their true WTP with precision, but may be able to place it within some range. Moreover, several authors (Walsh and Poe 1998; Gregory et al. 1995; Brown et al. 1996) have argued that discrepancies in estimating WTP from DC elicitation format and more continuous ones (Payment card, PC, for example) may originate in part from respondents uncertainty[3]. Recent studies tried to front this kind of bias through follow-up questions instrument, as reported in the table 2 (tab.2).

On the other hand, ambivalence is referred to as what respondents feel when he/she is forced to make difficult trade-offs between competing objectives (for example, environmental improving and a certain amount of money). Such ambivalence can lead to protest or non-responses, and the

[3] In fact, respondents to continuous methods questions report a value they have relatively high certainty they would pay, while DC respondents say "yes" to values they probably are unsure of.

Tab. 2 - Questions instrument.

Authors	**WTP elicitation format**	**Specifics**
Li and Mattsson (1995)	DC + follow up question: "How certain are you of your answer to the previous DC question?". Response scale from 0% certain to 100%	WTP distribution is estimated using probabilities given by the certainty responses.
Ready et al. (1995)	DC or Polychotomous Format (PF): a six-point scale graduated WTP elicitation format (from strongly oppose proposal to strongly support proposal). (two samples)	Comparison of DC and PF estimates.
Champ et al. (1997)	DC + follow up question "How certain are you that you would (would not) donate the requested amount?". Response scale from 0 (very uncertain) to 10 (very certain).	Comparison of hypothetical donations to a parallel sample actually donating money.
Swallow, Opaluch, and Weaver (2001)	DC + strength-of-preference indicators	Strength-of-preference indicators are modelled as quasi-cardinal measures using an ordered-response model
Ready, Navrud, and Dubourg (2001)	DC or PC + certainty follow up question (compared in two samples). Fixed certainty levels	Results given by DC and PC are made converged in case of a given specific certainty level (95% certain)

use of decision heuristics based on lexicographic preferences, or conservative feelings. As a consequence of ambivalence, it should be noted that the usual concept of indifference may not be appropriate for understanding how individual resolve trade-off conflicts (Opaluch and Sagerson, 1989). Opaluch and Sagerson consider ambivalence as the psychological concept

of "cognitive dissonance"[4], i.e. an "emotional state set up when two simultaneously held attitudes or cognitions are inconsistence, or when there is a conflict between belief and overt behavior"[5]. Moreover, ambivalence involves other biases reported in this paper (yea-saying).

3.3. *Acquiescence, "Yea-saying" and overestimation.*

A number of recent papers have provided some estimates of WTP derived in CV surveys exceeding those revealed in experimental or real-life markets. One possible explanation for the overestimation of values is the presence of yea-saying[6]. Among psychologists and sociologists, yea-saying in CV responses is known as acquiescence, and they define it as a tendency to agree with questions regardless of content (Bachman and O'Malley, 1984).

More generally, "yea saying" is the tendency to subordinate outcome-based or true economic preferences in favor of expressive motivations when responding to CVM questions. Expressive motivations may be either socially motivated[7] or internally motivated[8], and have largely been speculated in CVM studies by McFadden and Leonard (1993), Kanninen (1995), among the others. Recent studies demonstrated that yea-saying can be associated with anchoring bias[9] or may occur when cognitive process is weak because of insufficient information level. Moreover, it can be caused by the impossibility for the respondent to dissociate contingent

---

[4] Festinger, L. 1957. A Theory of Cognitive Dissonance. Stanford: Stanford University Press.

[5] Reber, A.S. 1985. The Penguin Dictionary of Psychology. London: Penguin Books.

[6] Cummings, Harrison, and Rutstrom (1995) found significantly higher proportions of "yes" responses in hypothetical DC questions than DC questions where payment was required. Early results of this type lead the NOAA expert panel on CVM to conclude that hypothetical markets tend to overstate WTP for private as well as public goods.

[7] It is where social pressure or desirability considerations motivate respondents to yea-saying (Mitchell and Carson, 1989).

[8] It is where respondents simply seek to express their attitudes and/or held values.

[9] Anchoring (referred as "starting point bias") occurs if stated WTP is based on both the true underlying WTP value and the starting point money amount (Whitehead, 2000).

WTP from inner attitudes or motivations. Regardless of the perspective we can adopt, the occurrence of "yea-saying" has led to searching for procedures minimizing the associated bias, as reported in the table 3 (tab.3).

Tab. 3 – Procedures minimizing the associated bias.

Authors	**WTP elicitation format**	**Specifics**
Stevens et al. (1991) Spash, and Hanley (1995)	DC + Follow-up questions instrument.	Follow-up questions are directed at identifying likely yea-sayers (post hoc approach). They can be rejected fro the sample.
Ready et al. (1995)	Polychotomous Format (PF): a six-point scale graduated WTP elicitation format (from strongly oppose proposal to strongly support proposal).	PF may allow respondents to limit ambivalence feeling and avoid direct yea-saying, but there is no place for uncertainty motivation (single normative dimension).
Blamey, Bennett, and Morrison (1999)	Dissonance Minimising Format (DM): a mixed yea (no) + motivation format.	DM may allow respondents to decouple the choice in term of WTP and attitude motivations, limiting yea-saying.

3.5. *Altruism, Embedding-Warmglow and non-use values measurement.*

The term "embedding" (Kahneman, 1986) refers to the situation where CV responses also reflect a purchase of moral satisfaction, i.e. a well-being associated with the act of contributing to good causes, originally not considered in the CV framework. The problem has been illustrated by a notorious experiment (Kahneman and Knetsch, 1992), and results showed that, in presence of different benefits from different environmental policies, respondents were willing to pay essentially the same amount for each policy[10] (as CV responses reflected not only the WTP for a certain envi-

[10] It happens because this moral satisfaction presents rapidly diminishing marginal utility with respect to the size of the gift, then we may expect that respondents will bid about the same for obtaining moral satisfaction (Nunes, 2000).

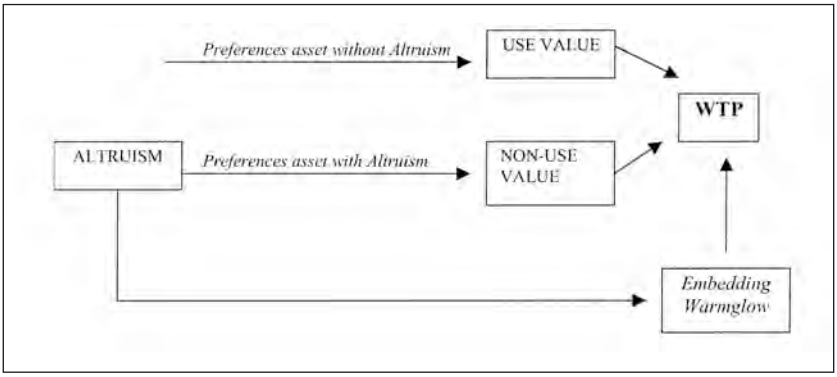

Fig. 1 – Consequence of altruism admittance in individual's preferences sorting.

ronmental good amount, but also an adding-up valuation hypothesis[11] or motivation hypothesis). Or, it can be said that "the sum of WTP responses for a group of public goods, when measured individually, may be larger than the WTP answers for the same group of public goods, because each WTP will contain a warmglow component" (Nunes, 2000). So, it can be said that CV responses also reflect a purchase of moral satisfaction , i.e. a well-being associated with the act of contributing to good causes, or the desire of the part of people to state their support for environmental issues (Diamond et al., 1993). According to Kahneman and Knetsch hypothesis, in this paper, we consider it as an issue related to consumer behavior and not a problem of survey design, as Mitchell and Carson argued (Mitchell and Carson, 1989). Therefore, altruism feelings are supposed to play a role in determining individual's utility function. Although supporting environmental protection for altruistic reasons is not inconsistent with the concept of maximization of utility (if the utility function is defined so that it implies the welfare of others[12]) , the discussion about non-use values[13] is here to be introduced, as it can be considered a direct consequence of altruism admittance in individual's preferences sorting (fig.1).

[11] The adding-up hypothesis (referred also as the Sub-Additivity effect) exists when respondents value differently a given set of public goods when valued individually then when valued aggregately (Hanemann, 1984).

[12] See Barro (1974).

[13] Non-use values include option value-the value of knowing that a resource is available for possible use in the future, existence value – the value of simply knowing that a resource exists, and bequest value – the value of leaving behind environmental resources for future generations (see Krutilla,1967).

In fact, Milgrom (1993) rose the question whether non-use values, as measured by survey instruments, are consistent with economic theory[14]. A number of CV studies noted that individuals may consider relevant bequest component when deciding WTP to provide for environment safeguard, probably in compliance with life expectancy consideration (Popp, 2001). If altruistic motives do exist for protecting the environment, CVM should take these motives into account. The table 4 (tab.4) reports some attempts to assess components of altruism and non-use values in demanding public goods.

4. *Concluding Remarks.*

The paper introduces some relevant and recent literature about how the cognition process and response making problems can influence survey results in CV based public goods appraisals. We hope the present analysis has been useful in supplying some baselines for understanding consumer's thought making, and in highlighting phases of WTP answering formation. Psychological biases involved in WTP choice (i.e. if marginal utility of a given environmental supply improvement can be paired to a money outlay one) are listed both from decision theory and applied economic points of view. Moreover, some searches from well-known scholars are quoted as methodological and practical improvements in CV response psycho-biases controlling. Evidently, a single CV study is inappropriate for facing all psychological biases reported in this paper. Therefore, we are going to introduce here two WP2 experiments aimed to awareness in WTP response measurement, particularly about non-use value expression. Tests are going to be led by two CV surveys administration, within the project of Economic Valuation of Benefits from Venice Lagoon Safeguard Intervention (CORILA, Research Line 1.1).

The first experiment involves a telephone survey about St. Erasmo island in the Venice Lagoon . By an hypothetical referendum to support (or not) an actual safeguard program now in progress on the island, the study wants to assess the WTP for environmental improvement deriving from the public works in issue. Using a split sample, some non-users of the Venice Lagoon will be demanded the WTP after having introduced a pre-

[14] Verbatim: "it would be necessary for respondent's individual existence values to reflect only their own personal economic motives and not altruistic motives, or a sense of duty, or moral obligation."

Tab. 4 – Attempts to assess components of altruism and non-use values in demanding public goods.

Authors	**Data Collecting**	**Altruism component estimation**
Deacon, and Shapiro* (1975)	Votes on two California environmental referenda	Regress voting results on personal characteristics (income, education, distance)
Holmes* (1990)	Votes on two California environmental referenda	Regress voting results on personal characteristics + some proxies for altruistic motives
Nunes (2000)	WTP on the protection of a Natural Area in Portugal	Using factor analysis**, individual warmglow motivation was transformed in a latent variable to be introduced in the multivariate regression of the WTP responses
Svedsater (2000)	Eexternal tests of part-whole effects and insensitivity to scope	Evaluation is made by four different measures or intensifiers of scope (i.e., absolute magnitudes, percentages, number of events, and verbal cues)
Popp (2001)	Phone Survey (by Washington Post) on WTP for cleaning up US air and water	Regress WTP on a function of individual specific socioeconomic variables. Test for altruism involves the relative weights placed on self-interest and altruism***

* The study was aimed to explore whether altruistic motives do influence the voting decisions. It was not a CV study, but it is reported here as a first attemp to regress altruistic (or self-interests) proxies in a decision model.

** Factor analysis can be considered a way to measure motivational factors. It is a data reduction technique used in empirical research in social sciences (for example, when comparing attributes of an objects group in terms of a variety of a priori chosen indicators, to determine which characteristics are the most important in classifying the objects). Psychologists and economists have used this technique as to study individual's perceiving different stimuli and categorize them into different response sets. See Thomson (1951), Rencher (1995).

*** The representation of the value function assumed here is:

$$NCOME_i + cEDUCATION_i + dLifeExpec_i + \varepsilon_i = \beta' S_i + dLifeExpec_i + \varepsilon_i$$

The systematic portion of the stochastic equation for WTP_i becomes a

liminary list of "Yea-reasons" and "No-reasons" to WTP question. Such a device (in the scenario description) would be able to add specific information about the island and the complex values involved, allowing a decision process that would be characterized by a certain degree of "awareness".

A second experiment is a method to impute use and non use components to the Total Economic Value that respondent is to appraise in the WTP response. This test involves a CV on-site survey turned to Venice Lagoon users, where individual WTP for environmental improvements derived from safeguard works in St. Erasmo Island are demanded. By such experiment we will try to estimate Use and Non Use (here referred as Bequest and Option) components of Total Economic Value (expressed by individual WTP). Value weights will be assessed using a Pair Comparison Approach (Analytic Hierarchy Process – AHP technique).

Experiments outputs and relative estimation results will be reported in next CORILA Working Papers.

---

non-linear function of $\beta'S_i$:

$$WTP_i=\alpha\ (\underset{r}{\beta'S_i})(1-e^{-rLifeExpeci})+(1-\alpha)(\underset{r}{\beta'S_i})+\varepsilon_i=v_i(x_i)+=\varepsilon_i$$

where α represents the unknown weight placed on self-interest, β is an unknown vector parameter and S_i is a socioeconomic data vector. r is the discount rate.

References.

Bachman J.G. and O'Malley P.M., 1984. Yea-Saying, Nay-Saying, and Going to Extremes: Black-White Differences in Response Styles. Public Opinion Quarterly 48: 491-509.

Barro R.J., 1974. Are Government Bonds Net Wealth. Journal of Political Economy 82 (6): 1095-1117.

Brown T.C., Champ P.A., Bishop R.C. and McCollum D.W., 1996. Which Response Format Reveals the Truth about Donations to a Public Good? Land Economics 72 (May): 152-66.

Cannel C., Miller P. and Oksenberg L., 1981. Research on interviewing techniques. In S. Leinhardt (ed.), Sociological Methodology 1981. 389-437. Jossey-Bass. San Francisco.

Champ P.A., Bishop R.C., Brown T.C. and McCollum D.W., 1997. Using Donation Mechanisms to Value Nonuse Benefits from Public Goods. Journal of Environmental Economics and Management 33 (June): 151-62.

Converse J.M. and Presser S., 1986. Survey Questions: Handcrafting the Standardized Questionnaire. Sage. Beverly Hills.

Diamond P.A., Hausman J.A., Leonard G.L. and Denning M.A., 1993. Does Contingent Valuation Measure Preferences? Experimental Evidence. in Hausman, J.A. ed. Contingent Valuation. A Critical Assessment. North-Holland, New York.

Dubourg W.R., Jones-Lee M.W and Loomes G., 1994. Imprecise Preferences and the WTP-WTA Disparity. Journal of Risk and Uncertainty 9 (Oct.): 115-33.

Fishhoff B. and Furby L., 1988. Measuring values: A conceptual framework for interpreting transactions with special reference to contingent valuation of visibility. Journal of Risk and Uncertainty 1: 147-184.

Fishhoff B., 1991. Value elicitation: Is there anything in there? American Psycholigist, vol. 46: 835-847.

Gregory R., Lichtenstein S., Brown T.C., Peterson G.L., Slovic P., 1995. How Precise are Monetary Representations of Environmental Improvements? Land Economics 71 (Nov.): 462-73.

Hanemann W.M., 1984. Welfare Evaluation in Contingent Valuation Experiments With Discrete Responses. American Journal of Agricultural Economics 66: 332-341.

Johnston R.J. and Swallow S.K., 1999. Asymmetries in Ordered Strength of Preference Models: Implications of Focus Shift for Discrete-Choice Preference Estimation. Land Economics 75 (May): 295-310.

Hanemann W.M., 1985. Some Issues in Continuous-and Discrete-Response Contingent Valuation. Northeastern Journal of Agricultural and Resource Economics 14 (1): 5-13.

Hanley N., Spash C.L. and Walter L., 1995. Problems in Valuing the Benefits of Biodiversity Protection, Environment and Resources Economics 5 (3): 249-272.

Kahneman D., 1986. Comments. In R.D. Cummings , D.S. Brookshire, and W.D. Schulze (eds.), Valuing Environmental Goods: An Assessment of the Contingent Valuation Method. Rowman&Allen: Totowa, NJ.

Kahneman D. and Knetsch J.L., 1992. Valuing public goods: The purchase of moral satisfaction. Journal of Environmental Economics and Management, 22, 57-70.

Kanninen B., 1995. Bias in Discrete Response Contingent Valuation. Journal of Environmental Economics and Management 28: 144-25.

Krosnick J. A. and Alwin D.F., 1987. An Evaluation of a Cognitive Theory of Response-Order Effects in Survey Measurment. Public Opinion Quarterly (51): 201-219.

Krosnick J.A., 1991. Response Strategies for Coping with the Cognitive Demands of Attitude Measures in Survey. Applied Cognitive Psychology, 5, 312-236.

Krosnick J.A. and Narayan S., 1996. Education Moderates some Response Effects in Attitiude Measurment. Public Opinion Quarterly (60): 58-88.

Li C. Z. and Mattsson L., 1995. Discrete Choice under Preference Uncertainty: An Improved Structural Model for Continget Valuation." Journal of Environmental Economics and Management 28 (Mar.): 256-69.

McFadden D. and Leonard G., 1993. Issues in the Contingent Valuation of Environmental Goods: Methodology for Data Collection and Analysis. in Hausman, J.A. ed. Contingent Valuation. A Critical Assessment. North-Holland, New York.

Milgrom P., 1993. Is Sympathy an Economic Value? Philosophy, Economics, and the Contingent Valuation Method. in Hausman, J.A. ed. Contingent Valuation. A Critical Assessment. North-Holland, New York.

Mitchell R.C. and R.T. Carson., 1989. Using Survey to Value Public Goods. The Contingent Valuation Method. Resources for the Future, Washington DC.

Mitchell R.C. and Carson R.T., 1993. The Issue of Scope in Contingent Valuation Studies. American Journal of Agricultural Economics vol. 75: 1263-1267.

Nunes P.A., 2000. Contingent Valuation of the Benefits of Natural Areas and its Warmglow Component. Ph. D. Thesis. Faculty of Economics and Business Administration, Department of Spatial Economics, Katholieke Universiteit, Leuven.

Opaluch J.J. and Segerson K., 1989. Rational Roots of 'Irrational' Behavior: New Theories of Economic Decision-Making. Northern Journal of Agricultural and Resource Economics 18 (Oct.): 81-95.

Popp D., 2001. Altruism and the Demand for Environmental Quality. Land Economics 77 (Aug.): 339-349.

Ready R.C., Whitehead J.C. and Blomquist G.C., 1995. Contingent Valuation When Respondents are Ambivalent. Journal of Environmental Economics and Management 29 (Sept.): 181-96.

Rencher A.C., 1995. Methods of Multivariate Analysis. Wiley. New York.

Samples K.C., Dixon J.A. and Gowen M.M., 1986. Information Disclosure and Endangered Species Valuation. Land Economics 62 (Mar.): 306-312.

Schuman H. and Kalton G., 1985. A Simple, General Purpose Display of Magnitude of Experiment Effect. In The Handbook of Social Psychology, ed. Gardner Lindzey and Eliot Aronson. Random House. New York.

Schuman H., 1992. Context Effects: State of the art /state of the past. in N. Schwarz and S. Sudman (eds.) Context Effects in social and psychological research. 35-47. Springer-Verlag. New York.

Schwarz N., Knauper B., Hippler H.J. and Noelle-Neumann E., 1991. A Cognitive model of Response-Order effects in Survey Measurement. in N. Schwarz and S. Sudman (eds.) Context Effects in social and psychological research. 187-201. Springer-Verlag. New York.

Spash C.L. and Hanley N., 1995. Preferences, Information, and Biodiversity Preservation. Ecological Economics 12:191-208.

Stevens T.H., Echeverria J., Glass R.J., Hager T. and More T.A., 1991. Measuring the Existence Value of Wildlife: What Do CVM Estimates Really Show? Land Economics 67 (Nov.): 390-400.

Svedsater H., 2000. Contingent Valuation of Global Environmental Resources: Test of Perfect and Regular Embedding. Journal of Economic Psychology 21 (6) 605-623.

Swallow S.K., Opaluch J.J. and Weaver T.F., 1997. Strength of Preference Indicators and an Ordered-Response Model for Ordinarily Dichotomous, Discrete Choice Data. http://www.soc.titech.ac.jp/titsoc/discuss/text/dp02-6.pdf

Thomson G.H., 1951. The Factorial Analysis of Human Ability, London University Press, London.

Tourangeau R., Rips L.J. and Rasinski K., 1988. Cognitive Processes Undelying Context Effects in Attitude Measurment. Psychological Bulletin 103: 299-314.

Tourangeau R., Rips L.J. and Rasinski, K., 2000. The Psychology of Survey Response. Cambridge University Press. Cambridge.

Tversky A., Sattath S. and Slovic P., 1988. Contingent weighting in judgment and choice. Psychological Review 95:371-384.

Wang H., 1997. Treatment of "Don't-Know" Responses in Contingent Valuation Surveys: A Random Valuation Model. Journal of Environmental Economics and Management 32 (Feb.): 219-32.

Welsh M.P. and Poe G.L., 1998. Elicitation Effects in Contingent Valuation: Comparisons to a Multiple Bounded Discrete Choice Approach. Journal of Environmental Economics and Management 36 (Sept.): 170-85.

Whitehead J.C., 2000. Anchoring and Shift in Multiple Bound Contingent Valuation. http://www.ecu.edu/econ/wp/00/ecu0004.pdf. http://cognet.mit.edu/MITECS/Entry/gilovich

THE ROLE OF LIABILITY, REGULATION AND ECONOMIC INCENTIVES IN BROWNFIELD REMEDIATION AND REDEVELOPMENT: EVIDENCE FROM SURVEYS OF DEVELOPERS IN EUROPE

A. Alberini[1], A. Longo[3], S. Tonin[2]
F. Trombetta[2], M. Turvani[2],

[1]*University of Maryland, USA*
[2]*Dipartimento di Pianificazione, IUAV, Venezia*
[3]*Dipartimento di Scienze Economiche, Università Cà Foscari, Venezia*

1. *Introduction.*

The industrial area of Porto Marghera near Venice has been subject to severe soil and ground water pollution for several decades caused by industrial plants located in the area. The recent cleanup process has brought a considerable interest in this area on the part of land users and developers who wish to exploit the area for commercial and/or industrial purposes.

This study examines the relative importance and efficiency of different market-based mechanisms and other incentives intended to promote the environmental remediation and reuse of "brownfields." Brownfields are "abandoned, idled or underused industrial and commercial properties where real or perceived contamination complicates expansion or redevelopment" (Simons, 1998).

Brownfield cleanup and reuse are attractive for many reasons. First, brownfield cleanup lowers the human health and ecological consequences of soil and water pollution at contaminated sites. Second, the reuse and redevelopment of brownfields helps stop the continued conversion of agricultural land and rural sites to urban uses and other development patterns that generate environmental problems, congestion and sprawl. Third, redeveloping abandoned industrial sites promotes economic growth in inner cities and is therefore a potentially important component of sustainable growth.

The promise of brownfield redevelopment for encouraging cleanup and helping to regenerate inner city areas has attracted considerable atten-

tion in federal, state, and local circles. In the US, it is generally argued that the 1980 Comprehensive Environmental Response, Compensation and Liability Act (CERCLA) has created disincentives to the redevelopment and reuse of potentially contaminated sites, as liability for the cost of cleanup has been construed to extend to lenders and landowners (Fogelman 1992). In an effort to mitigate these disincentives, the States have passed programs offering entrepreneurs and prospective redevelopers (a) reductions in regulatory burdens, (b) relief from liability for future cleanups and environmental damage once certain mitigation standards are met, and/or (c) financial support for regeneration of brownfields. By late 2000, forty-seven states had statutorily-defined or informal "voluntary cleanup programs" to promote reuse and cleanup of contaminated sites (Bartsch and Dorfman 2000; Meyer and VanLandingham 2000).

Similar initiatives are under consideration in several European countries. The current situation of the Porto Marghera area near Venice provides a suitable case study to test whether the implementation of different policy mechanisms, such as those currently used in Italy, but also those used in the US context, or in other EU countries, might enhance the attractiveness of contaminated sites to land users and developers.

Although economic inducements have been offered for decades to economic agents, little empirical evidence exists documenting the impact of (a), (b) and (c) on brownfield cleanup and investments. Our research attempts to fill this gap by uncovering the preferences of economic agents for the various economic tools available to promote cleanup and reuse of contaminated sites. In the Porto Marghera context it would be very useful for policymakers to know which policy mix and which economic tools are the most appropriate for redevelopment perspectives and cleaning up efforts, in order also to be able to attract a particular category of developers and land users.

We examine the value of the interventions from the perspective of the key actors involved—private developers. We use a conjoint choice experiment to study the responses of real estate developers engaged in infill (rebuilding on abandoned lands or utilizing underused sites in already urbanized areas) to different mixes of incentives. The goal of our surveys of developers is to find out what aspects of current brownfield policies are most appealing to developers, and what are the most cost-effective means of inducing more brownfield reclamation and redevelopment investment given those preferences. The sites and projects described to the partici-

pants in our surveys are abstract and do not refer to a particular locale, but we believe that the inference based on our surveys will be applicable to the case of the contaminated sites in Marghera.

2. *Structure of the Questionnaire.*

In our survey, we ask respondents recruited at the International Property Market Fair (MIPIM) held in Cannes, France, in March 2002, to tell us which they prefer between two alternative redevelopment projects, A and B, where each project is described by site attributes (e.g., location, previous use and contamination) and a policy mix.

The policy mix may include (a) liability reduction in the form of an assurance that the developer is not going to be held responsible for future cleanups; (b) regulatory relief in the form of a faster notice of approvals and/or less stringent cleanup standards depending on zoning or other land use restrictions; and (c) direct financial support in the form of tax credits, low-cost loans, grants, and assistance with environmental assessment at the site. These policies may affect different component of the costs and revenues associated with redeveloping the site. Liability relief, for example, reduces or eliminates the risk of future liability for cleanup costs, as long as the developer meets certain requirements. It may, in addition, help raise the revenue from the sale or rental of the site due to avoiding the stigma due to existing or suspected contamination.

3. *Statistical Model.*

To motivate the statistical analysis of the responses, we assume that respondents select the alternative with the highest indirect utility (profit). If indirect utility (profits) are a linear function of site attributes (**S**) and the policy mix:

$$(1) \qquad V_{ji}=\alpha_0+\mathbf{S}_{ji}+\alpha_1+\mathbf{L}_{ji}+\alpha_2+\mathbf{R}_{ji}\alpha_3+\mathbf{F}_{ji}+\alpha_4+\varepsilon_{ji}$$

where **L**, **R** and **F** are vectors of indicators and/or continuous variables capturing the extent of liability relief, regulatory relief and financial incentives, respectively, i denotes the individual and j the alternative, and if the error terms ε are independent and identically distributed and follow the type I extreme value distribution, the probability that alternative k is selected out of K alternatives is:

$$(2) \qquad \Pr(\text{resp.}i \text{ chooces } k)=\exp(\mathbf{w}_{ik}\alpha) \Big/ \sum_{j=1}^{k} \exp(\mathbf{w}_{ji}\alpha)$$

where **w** is a vector containing the alternative-specific attributes and α is the vector of coefficients in (1)[1]. Equation (2) is the contribution to the likelihood in a conditional logit model[2].

Once model (2) is estimated, rates of tradeoffs between any two attributes are the ratio of their associated a coefficients. The marginal value of each attribute is computed as the negative of the a coefficient on that attribute, divided by the coefficient of the "price" variable. We estimate the value of each policy package using the percentage of respondents that pick that policy over the "status quo" alternative in follow-up questions that ask respondent to indicate which they prefer, A, B or the "status quo".

Using the estimation results, we first determined what attributes actually matter to developers, a task we accomplished by performing statistical tests of significance of the associated coefficients. Next, we estimated the rate of tradeoff between attributes and the value of specific policy packages.

We are particularly interested in determining whether the attributes that are deemed attractive differ across developers, depending on their experience with brownfield sites. This can be accomplished by running conditional logit models that include the attributes interacted with a dummy variable indicating previous involvement in brownfield projects, or by separating the sample into two groups – brownfield-experienced and inexperienced developers – and running separate conditional logit

---

[1] The influence of firm- or individual-specific characteristics on the choice – such as the firm's profitability, its scale, and the size of the market that it operates in – can be captured only if individual or firm characteristics are interacted with alternative-specific characteristics and are included in w.

[2] Implicit in this model is the assumption of independence of irrelevant alternatives, which means that the ratio of the odds of selecting between any two alternatives is not altered by introducing a new alternative. This assumption is generally regarded as restrictive, and as making the model inadequate when two alternatives are perceived as close substitutes, so we will conduct formal statistical tests to see if it is violated, and will compare the results of conditional logit models with those of multinomial probit models, which relax this assumption. The basic model can be further amended to include random effects capturing unobserved individual factors that affect all responses to the conjoint choice tasks by the same individual.

models for these groups. Wald tests or likelihood ratio tests can be used to test the null hypothesis of no difference in the coefficients.

References.

Bartsch C. and Dorfman B., 2000: Brownfields "State of the States": An End-of-Session Review of Initiatives and Program Impacts in the 50 States. Washington, DC: Northeast-Midwest Institute.

Fogelman V.M., 1992: Hazardous Waste Cleanup, Liability, and Litigation: A Comprehensive Guide to Superfund Law. Westport, CT: Quorum.

Meyer P.B. and VanLandingham H.W., 2000: Reclamation and Economic Regeneration of Brownfields. (Reviews of Economic Development Literature and Practice No. 1). Washington, DC: U.S. Economic Development Administration.

Simons R.A., 1998: Turning Brownfields into Greenbacks. Washington, DC: Urban Land Institute.

COST AND BENEFIT ANALYSIS OF BROWNFIELD REMEDIATION AND REDEVELOPMENT

D. Patassini, M. Turvani and F. Trombetta
Dipartimento di Pianificazione, IUAV, Venezia

1. *Research Programme and Outcome.*

The aim of the research is a cost benefit assessment of brownfield remediation and redevelopment in the area of Porto Marghera (Venice, Italy). Three are the main goals:

1) a preliminary assessment of the legal framework for soil protection sectoral policies have to comply with;
2) case-studies focused on main actors fostering physical and functional transformation, brownfield remediation, redevelopment and creation of new market opportunities;
3) economic evaluation both of costs and benefits.

Among the different classes of benefits we concentrated mainly on those that accrue to real estate developers and are generated by remediation and redevelopment projects. Two main reasons account for this choice: firstly, developers are very crucial operators within remediation and redevelopment programmes in Marghera, acting as market makers. Were their contribution absent, any redevelopment would be hampered; secondly, developers dealing with large dismissed areas form a rather small and easily identifiable group. Furthermore, they have a clear view of locational attractiveness of the area as a whole and of local public policies as well. The economic evaluation of both location and public incentives have been studied by means of an ad-hoc sample survey which provides as main result a willingness to pay measure (WTP) for many site specific attributes and for an array of different public incentives.

Referring to cost analysis, a contextual knowledge support system has been designed. Relying on an extensive review of existing procedures, an original procedure has been implemented, connecting in a sequence various analytical and evaluation models, namely Electre, Giuditta, Rec and Aures, the combination of which suggested the acronym El.Gi.R.A.

Different scenarios for Porto Marghera are assumed as inputs to the procedure. These scenarios were derived from the last General Revision of the City Master Plan, the Voluntary Agreement on Chemical Plants at Marghera (Accordo di Programma), the preliminary studies for the new Master Plan of the area recently submitted to the local authorities (2002) as well as from other visions of certain interest held by different stakeholders. Each scenario defines a land use pattern consistent with the future envisaged for old industrial areas and for harbour's infrastructures development. There are many hypotheses currently being discussed: a new industrial zone fostering a radical greening in manufacturing mix; a science park; a 'fondaco' town, a sort of guest city (to host, among others, a master programme of tolerance and mutual understanding), a cultural exchange node, inspired by the role Venice has historically been playing in the Mediterranean civilization for many centuries. There are even other proposals at stake, more committed to the completion of environmental restoration of an area located between the lagoon and the old garden city. Each scenario involves specific land use patterns.

For a preliminary test of El.Gi.R.A. procedure, a zone called '43 hectares' has been selected. A number of remediation techniques (on site, off site and mixed) have been screened. Starting point has been the environmental matrix provided by the local soil quality information system (Sis) of the Municipality of Venice. The matrix provides a complete list of pollutants' concentrations as detected through samples' analysis conducted by private firms and public institutions during last years. Pollutants have then been grouped into classes, according to their chemical properties, to restrict the list of techniques locally feasible.

The assessment of selected remediation techniques has been carried out by means of a set of criteria related to technological, economical, social and environmental factors. For this purpose an Electre ranking procedure seems to be quite efficient. Besides, partial aggregation based on dominance test has been employed to carry out a scenario-led sensitivity analysis on weights vector, performances and thresholds. The output (i. e. the final pre-order or ranking) becomes the input for Giuditta, a well established procedure already used by public institutions (such as Province of Milano) which is mainly tailored to perform risk analysis. The results of this analysis are adjusted via interpolation with the help of cellular automata (Aures) in cases of low spatial density of the environmental matrix and then fed in Rec model. On its turn, Rec generates three normalized indexes of risk mitigation, environmental merit and overall financial costs. Rec produces also supplementary outputs that might be

used for a final evaluation such as risk differentials (before/after intervention), variation of pollutants' concentrations, and financial cost profiles for each option, where energy's and matter's consumptions have been duly included.

At the end of the procedure, effects on single spots or wider areas, can be aggregated by means of a second (and final) step of multicriteria analysis. Aures could be useful in modelling possible spatial diffusion patterns or spill-overs onto neighbouring areas. The complete procedure, already tested on a small number of contaminants, could provide potential investors in the area with basic information on the 'environmental remediation options'. El.Gi.R.A. could also foster further assessment of social and economic costs of cleaning processes.

2. *Research Phases.*

1. The first step of the research is considered a fundamental issue, as the legal system affects the profitability of remediation processes. Environmental pollution is mentioned in the economic literature as an instance of market failure. As a consequence governmental regulation becomes a central policy issue as it determines liabilities along with economic efficiency and effectiveness of intervention in multi-agent domains. Besides, the possibility of state failures should be taken in account while designing flexible and incremental policies along with consistent monitoring of effects and impacts. During this phase of the research laws of various countries have been analysed, in a comparative fashion, namely those of Usa, Germany, Netherlands and Italy. Following a 'law and economics' approach, legal and institutional structures have been linked with peculiar brownfield clean-up processes (Paper 2, Trombetta).

2. In the second step of the research, investors' choices and collective agents' behaviour during last years have been analysed, from the approval of 1995 Marghera Prg revision and through following interventions in the area (Paper 3, Trombetta and Turvani). The geographical information system available at the Municipality of Venice provides an environmental database for some 150 contaminants built up on a regular spatial grid which partially covers the 2000 hectares of the old industrial zone. In addition, the research group gathered many pieces of relevant information by cooperating with a joint-stock company, the Immobiliare Veneziana (Ive), that cleans up and re-sells areas on the market. Ive purchased two areas: Azotati and Complessi. Purchase contracts and remediation

projects have been carefully analysed. A focus group was held at Co.Ri.La. February 22nd 2002. The most important developers in the Venitian region were interviewed to elicit their preferences for different public incentives to foster remediation.

3. The role of location opportunities and incentive policies in enhancing clean-up can be considered the core issue of the research. As already mentioned above, a preliminary survey of literature on economic evaluation of remediation policies was conducted. The resulting paper (Paper 4, Tonin) shows to what extent the suitable economic evaluation methods are 'stated preferences' methods rather than 'revealed preferences' methods based on market prices' observation. The former are nowadays used in frontier research programmes as econometric models to evaluate environmental non market goods within advanced public decision processes based on empirical evidences. In this respect, a survey on location preferences and choices among contaminated and non-contaminated sites has been carried out in collaboration with Anna Alberini, University of Maryland. A sample of investors (out of some 17,000 real estate developers) has been ramdomly selected at the International Market of Real Estate (Imre) held in Cannes (France), March 2002. The Municipality of Venice and its Strategic Plan Office, exhibitors at Imre, created a conducive environment to carry on the survey with a 25-items questionnaire administered in person in three languages, English, Italian and French. Some 300 questionnaires have been collected and data have been processed by means of conditional logit statistical techniques. Preliminary results have been presented at Iaere Conference in Monterey (California), June 2002 (Paper 6, Alberini, Longo, Tonin, Trombetta, Turvani) whereas a final report will be ready by the end of current year (Paper 7). El.Gi.R.A. procedure is now being tested with environmental data from the '43 hectares' areas that were supplied by the Municipality of Venice.

GOVERNING ENVIRONMENTAL RESTORATION: INSTITUTIONS AND INDUSTRIAL SITES CLEAN-UPS

F. Trombetta and M. Turvani
Dipartimento di Pianificazione, IUAV, Venezia

1. *Introduction: the Brownfields Problem.*

Brownfields are defined by US Environmental Protection Agency as "abandoned, idled, or under-used industrial and commercial facilities where expansion or redevelopment is complicated by real or perceived environmental contamination".[1] The total surface of brownfields is a rough but significant indicator of the paramount scale of the problem. In the US 1.238 sites are in the National Priority List for remedial action and public financial support. A 1993 survey estimated over 100.000 non NPL sites, 40.000 of which needed attention. In 1995 the information system set up by federal law (CERCLIS) listed 39.692 sites, to be further investigated to assess contamination.

In the EU estimates of brownfields' extension (Giangrasso and Tassoni, 2001) are impressive: at the end of the eighties 150.000 sites resulted presumably polluted. Estimated cost of remediation for UE members is 1% of the internal GUP for most critical areas. In Italy 1995 data record more than 11.000 polluted sites with an associated cost of intervention estimated in more that 30.000 billion liras. Updated Italian figures calculate 260.000 ha polluted soil and 70.000 ha sea, more than 1% of the whole national territory.

Porto Marghera industrial area spreads over about 2000 hectares, mostly heavily polluted[2], but the Italian National Priority List completed in year 2001 defines a broader surface that needs further investigation: 3825 ha of land, and 2311 ha of lagoon. Aim of this paper is a tentative framework to design institutions to govern brownfields remediation.

---

[1] http://www.epa.gov./swerops/bf/glossary.htm.#brow

[2] For major details about pollution in the area browse http://www.ambiente.venezia.it/.

2. *The Standard Economic Approach to Brownfields: a Criticism.*

Brownfields flood local communities with externalities due to:

- negative effects on human health;
- negative impacts on other determinants of human welfare such as aesthetic values, urban congestion and degradation;
- ecosystemic damages induced by pollutants;
- perception of a subjective decrease in welfare of agents or of an increase in risk.

For analytical purposes we group these externalities into different classes according to the stakeholders they affect. The first group of externality on human heath can affect (i) workers on site and (ii) nearby inhabitants. The second group of externalities affects both (iii) inhabitants, probably on a wider scale than group (ii)[3], and tourists (iv)[4]. On eco-systemic externalities not much can be said as we still lack huge pieces of relevant information to assess pollution's impact on ecosystems (v) and their eventual rebounding on human heath (vi). Still a very strong case for precautionary behaviour emerges. The last group of externalities depends crucially on agents' perception. According to subjective views, real estate properties around brownfields can depreciate because of mere perceived pollution (vii) or workers may ask for a risk premium to work on sites that are considered polluted even though no real risk is undergone (viii). In these cases literature (Chan, 2001) refers to stigma placed on brownfields and surrounding properties.

Externalities affecting different stakeholders cannot be solved by the same instruments' mix. For example health damages generated by past exposures on workers cannot be internalized by higher safety standards and have to be compensated either by insurance repayment or by fines imposed via judicial settlement. In this paper we concentrate mainly on externalities of groups (ii) (iii) (iv) and (vii).

Externality is the core concept in environmental economics (Coase, 1960). Interpreted as market failures, externalities justify public agencies' intervention. Unfortunately state cannot redesign property rights (accurately, frequently and rapidly enough) to eliminate externalities. As Com-

---

[3] Except maybe for smoke releases that can travel long distances in the troposphere as acid rains prove, but this event has low probability in case of dismissed sites were chimneys are idle.

[4] This class of externalities might be particularly relevant in touristic district such as Venice is.

mons (1959) pointed out, property is not a relation between the owner and objects but a relation among actions affecting economic goods each individual is entitled to take. Pollution from industrial production is a creation of new and more complex non market relations affecting welfare of different classes of stakeholders. The pace of emergence of environmental negative externalities is very high because of swift technological change, scale of production, and ensuing societal evolution (Bresso 1993).

If no *una tantum* state intervention works, an alternative is "regulation" by norms that alter continuously markets' functioning, affecting relative prices at variable intensity. In this process the regulator interacts with markets, monitoring results and adjusting policies accordingly. Two are the main instruments for state regulation (Lèvêque, 1996): (1) economic instruments and incentives (taxes, subsidies, tradeable permits, deposit refund systems) and command and control regulation *stricto sensu* (emission standards, concentration limits, compulsory certification).

To produce optimal regulation, regulator must (a) possess and process all the relevant information for free and (b) act as benevolent maximizer of collective welfare (Dixit, 1996). No real regulator will ever meet these requirements: perfect knowledge about pollution does not exist and uncertainty about eco-system and health effects inevitably hampers both private negotiation and public intervention. But other problems derive from procedural nature of regulation: contrary to Baumol and Oates' (1971) claims, setting first environmental objectives in the political arena, and then choosing policy instrument overlooks the complexity and recurrent character of real decision making process in public agencies.

An institutional perspective on regulation suggests to frame both market and state failures within a holistic theoretical approach. Goals are not exogenous to feasible policy instruments. Regulation itself is an institution, a set of rules defining the game that agents are playing, both offering opportunities and imposing constraints. Different interests converge in regulatory processes: the theory of capture (Tirole, 1994) explains how the regulator may collude either with the regulated industry or with environmentalist associations, producing a different kind of regulation accordingly. As a result of this complex institutional evolution we observe nowadays hybrid forms of governance of environmental externalities such as co-regulation or self-regulation (Lèvêque, 1996), which are neither pure market nor pure state. Only by integrating all three possible types of intervention on environmental issues, one may add something to the positive and the normative theory of regulation.

3. *An Institutional Approach to Brownfield: from CAC to Cooperation.*

Regulation entails creation of: (a) new knowledge, (b) some consensus around controversial environmental issues, (c) new institutional structures and laws to address environmental issues (d) a monitoring system to evaluate the performance of the regulation itself and the possible rise of new externalities. Regulations based only on CAC show intrinsic weaknesses and liability norms are not sufficient to deal with the brownfield issue (Alberini, Austin 1997). Evolution towards cooperative governance of remediation issues is seen in a remediability perspective (Coase 1964), where institutions evolve in response to a perceived scope of improvement. The whole Law and Economics approach (Cooter *et* alii, 1999) shows that laws are no sufficient conditions for attainment of goals set by public agencies. Rational agents compare costs and benefits of compliance and decide to comply or not (Becker, 1964).

Western countries witnessed a shift towards alternative forms of governance, where responsible parties, land-owners and local collective agents cooperate: for example long term stewardship of contaminated sites in Usa, use of voluntary agreements (Amadei, Croci, Pesaro 1998) and introduction of risk-based criteria to choose remediation techniques in Italy (Decreto 471/99). Although Italy is a late-comer in soil remediation processes, compared to US, Holland and Germany, an even if each country has its specific legal system, there is a common pattern of evolution which stems from spill-over in the political debate and in the accumulation of knowledge.

4. *The Case of Marghera.*

Local remediation processes historically started with a rise in public perception of danger and consequent actions to promote state intervention. Legal action against managers and owners of Marghera chemical plants started very late in 1998. Common knowledge about the risks connected with high pollution in Marghera had been building up among local stakeholders at least since 1987 Enimont merger. Health-risks awareness seems to have developed following a peculiar pattern, similar to what happened in places such as Minamata, Japan. Workers at the plants and exposed daily to substances developed first a perception of health-risks. An informational role was played by isolated local healthcare practitioners but no restrictive approach of the local santitation authority as a whole was adopted until

much later. Trade unions never made a strong case against pollution, as their main concern has historically been placed onto job protection. Only in 1998 when Accordo per la Chimica a Marghera was signed at the national level, trade unions and firms agreed on the need of safer working environment, reconciling job protection and environmental care.

The legal suit was a rehearsal of what may happen if litigation remains the only governance mechanisms to deal with environmental externalities in Marghera. In hybrid forms of regulation, CAC with ensuing litigation risks is the stick and benefits from co-operative regulation are the carrot. Both privates and public agencies work to shape alternative governance structures for the transactions they are interested in. In Marghera stigma has always been very high and it hindered transactions of areas otherwise outstandingly well located. All site sales during last 7 years were fostered by public authorities. Two major sales of dismissed sites, for a total of 36 hectares, have been carried out by IVE Immobiliare Veneziana and a third area (10 hectares) was purchased by Vega Science Park (a Public Consortium), that rents spaces to high-tech firms.

Potential buyers in Marghera, attracted by the location of the site, consider environmental risk too high if no cooperation with public agents is offered. No market emerges in this situation, and no fiat state intervention can untangle the web of externalities. In Marghera there are no more than a dozen area sellers and even less developers. In this situation actual buyers develop specific competence and a competitive advantage in dealing with contaminated lands and acting repeatedly over time as developers in Marghera. The completion of a single transaction at a polluted site involves several steps, different forms of negotiation and quite complicated contracts. The design of such contracts involves trilateral negotiation among sellers that might be held responsible for pollution, several levels of local authorities and potential buyers: clean-up projects were provided by the buyer, IVE, paid for and submitted to local authority for approval by the seller. The whole process of approval at Municipality was speeded by the co-operative framework in which it took place.

"Accordo per la chimica", the voluntary agreement governing remedial and safety enhancing actions at the 800 hectares of still operating chemical facilities did so well as an instrument of co-regulation that a second step in that direction is now being taken: an integration to Accordo per la Chimica has just been signed by all public and private agents involved in the first round of cooperation and what is most relevant, a provision is made for other firms, external to the chemical area but operating at Marghera, to enter the process by adhering to the protocol.

References.

Alberini A. and Austin D.H., 1997. On and Off the Liability Bandwagon: Explaining State Adoptions of Strict Liability in Hazardous Waste Programs, Resources for the Future, Discussion Paper 98-08, Washington DC.

Amadei P., Croci E. and Pesaro G., 1998. Nuovi strumenti di politica ambientale. Gli accordi Volontari, FrancoAngeli, Milano.

Baumol W. J., Oates W. E., 1971. The Use of Standards and Prices for Protection of the Environment, in "Swedish Journal of Economics", vol. 73, 1.

Bresso M., 1993. Riflessioni su un quarto di secolo dell'economia dell'ambiente: strumenti di analisi e questioni teoriche aperte, in Musu I. (curatore) "Economia e Ambiente", Il Mulino, Bologna, p. 70.

Becker G.S., 1983. A Theory of Competition among Pressure Groups for Political Influence, Quarterly Journal of Economics, XCVIII, pp. 371-400

Chan N., 2001. Stigma and its Assessment Methods, Pacific Rim Real Estate Conference, Adelaide, Australia.

Coase R., 1960. The Problem of Social Costs, in "Journal of Law and Economics", n. 3, 1-44.

Coase R., 1964. The Regulated Industries: Discussion, in America Economic Review, vol. 54, May.

Commons J.R., 1959. Legal Foundations of Capitalism, The University of Wisconsin Press, Madison.

Dixit A.K., 1996. The Making of Economic Policy: a Transaction-Cost Politics Perspective, Mit Press, Cambridge, Massachusetts.

Giangrasso M., Tassoni E. Il programma nazionale di bonifica e ripristino ambientale dei siti inquinati, in "Ambiente e Sicurezza", n. 10, Aprile 2001, IlSole24Ore, Milano.

Lèvêque F., 1996. The Regulatory Game, in "Environmental Policy in Europe. Industry, Competition and the Policy Process", Lèvêque F., editor, Elgar, Cheltenham, UK.

Tirole J., 1994. The Internal Organization of Government, in "Oxford Economic Papers", 46, pp. 1-29.

CLEANUPS IN MARGHERA: INTERNATIONAL REGULATORY FRAMEWORK, NATIONAL LEGAL EVOLUTION, AND LOCAL EXPERIENCES

F. TROMBETTA
Dipartimento di Pianificazione, IUAV, Venezia

Aim of the paper is to reconstruct the normative framework investors and developers have to comply with when they carry out remediations at dismissed brownfields. Norms cannot be left out from a research programme dealing with costs and benefits of cleanups in Marghera because they impact strongly on the (i) necessity, (ii) economic feasibility, (iii) evaluation (Beinat 1997), and (iv) choice of particular remedial techniques and redevelopment process. The necessity of remediation depends clearly on soil quality but also crucially on statutory provision of the level of toxic releases' concentration that requires immediate remediation. The liability principle (a), assessing who is responsible for pollution and has to pay for it, and regulatory criteria (b), defining types of intervention allowed and preferred techniques of cleanup, impact on the overall cost-benefit ratio of each redevelopment process, fostering it or hampering it, depending on the final expected profit.

The focus of the research programme is on contaminated land in Marghera. Therefore the main accent is on Italian situation. Still the paper goes through a comparative survey of the legislation of different countries especially US, Holland and Germany. This turns out to be very useful because other countries started their regulation of soil contamination much earlier than Italy and have therefore gathered a great amount of experiences and data. Although different legal systems do not allow for institutional "photocopying" i.e. mechanical transfer of particular institutions across countries, useful insights can be drawn by problems faced by first-comers. When a particular liability principle, its related enforcement and incentive systems did not promote efficient remediation of polluted areas, we can learn very much by analysing what went wrong. Therefore the paper concentrates on main criticisms on CERCLA, the basic legal

reference for soil protection in US (Revesz and Stewart, 1995; Alberini and Austin, 1997).

Italy is a late-mover in the field of soil protection: the basic law was enacted in 1997, the so-called Decreto Ronchi which entails a series of other issues essentially on waste disposal. But this law was only a first move towards a feasible definition of the necessary framework for brownfields remediation. Limits for toxic compounds were regulated with a decree by Environment Ministry n° 471 issued in 1999. One of the major problem raised by Italian norms is the provision that local public authority has to pay for cleanup when no responsible parties can be found or when they refuse to comply. Unfortunately there are not enough funds to cope with the huge amounts of contamination present in Marghera and this led to a stalemate.

Nevertheless Venice Municipality has not remained inactive and tried to lure private capitals into redevelopment of Marghera (Drei, 2001). The way to do this has been found in more flexible provisions for cleanup. Nowadays it is possible to remediate a site below the multifunctionality level if it is demonstrated that it poses no risk to human health. Developers partially funded with public money also played an important role in this process. Under this respect Marghera represents an interesting workshop for new ideas both in institutional design and in new forms of cooperation among State, firms, local community and polity, ngo's and environmentalist associations. The voluntary agreement for Chemical Plants (Accordo di Programma) in Marghera in 1998 is shown to have introduced on local level solutions that have later on been adopted on a national level.

References.

Alberini A., Austin D.H., 1997. On and Off the Liability Bandwagon: Explaining State Adop-tions of Strict Liability in Hazardous Waste Programs, Resources for the Future, Discussion Paper 98-08, Washington DC.

Beinat E., 1997. Case study: expert based value function models for cleaning up a polluted site, in "Value Functions for Enviromental Management", by Beinat Euro, Kluwer Academic Publishers, Netherlands.

Drei Paolo, 2001. gennaio, Porto Marghera in "Venezia capace di futuro", A. Paolella e P. Perlasca, a cura di, allegato di "Attenzione".

Minsky M., 1989. La società della mente, Adelphi, Milano.

Revesz R.L., Stewart R.B., editors, 1995. Analyzing Superfund. Econonimcs, Science, and Law, Resources for the Future, Washington DC, USA.

A SURVEY OF LITERATURE ON ECONOMIC VALUATION METHODS TO ASSESS BROWNFIELD REDEVELOPMENT COSTS AND BENEFITS

S. TONIN
Dipartimento di Pianificazione, IUAV, Venezia

Acquiring, cleaning and redeveloping dismissed industrial facilities can be very expensive and requires more time than other real estate investment processes. In may cases private developers and investors are not willing to accept the risk of starting a project of redevelopment on contaminated sites. This is due to increasingly strict norms on environmental liabilities; in any case potential negative impacts of human health and losses of collective welfare of local communities due to brownfields lying idle, generate a strong demand for redevelopment and reuse.

But brownfield redevelopment projects are also a great opportunity to foster economic growth and sustainable urban development by increasing life standards, creating new jobs, recreational opportunities and raising environmental quality of public goods. Many abandoned facilities are located in industrial areas that are nowadays in very attractive locations due to expansion of cities and could therefore be used to increase the infrastructures' endowment and the production of services in large urban communities or to avoid further conversion of greenfields for productive activities.

This survey analyses briefly: (i) factors influencing economic evaluation of dismissed industrial sites such as the liability regime and longer times for approval of projects, (ii) pros and cons of redevelopment projects, (iii) increased difficulties in raising funds and financial assistance for the projects and higher uncertainty on final return on investment (iv) subjective perception of risk connected to dismissed sites even after cleanup has been completed i. e. stigma.

We then move to the different evaluation techniques of costs and benefits of remediation at contaminated sites. Traditional methods based on market prices are not suited in this case as we both lack data and the number of sales of dismissed industrial areas in Marghera is very

low. To cope with this problem literature has developed an array of non market methods such as contingent valuation, travel costs and conjoint analysis.

Hedonic Price Method is used to determine the influence of environmental contamination on real estate properties located near sources of pollution. Even though many efforts were devoted in literature to assess real estate values, there are few data on economic evaluation of redevelopment of dismissed and contaminated sites.

ECONOMIC VALUE ASSESSMENT OF ALTERNATIVE FISHING MANAGEMENT PRACTICES FOR THE VENICE LAGOON: A PROPOSAL FOR CONJOINT ANALYSIS

P. A.L.D. Nunes and P. Nijkamp
Dept. of Spatial Economics, Free University of Amsterdam

1. *Overview.*

An economic valuation exercise is anchored in the analysis of a change on the fishing management practices and not in the analysis a specific management practice. In other words, economists are able to assess the total economic value of the change of the current management practice to an alternative-fishing scenario. The economic valuation methodology that we suggest to apply is identified in the literature as conjoint analysis. This is characterized by the development of a survey narrative and monetary valuation mechanism that are characterized by presenting a set of two, or more, alternatives – interpreted in terms of a policy package – and ask the respondent to choose one from them. The valuation exercise is real: respondents need to make a choice about two policy packages, described in terms of different levels of provision among the set of fishing attributes under consideration. This gives to the researcher additional flexibility in the design of the policy packages since we have the freedom to set, alter, and combine different levels of attributes for each set of alternatives. In addition, conjoint analysis presents an important vantage to the well-know contingent valuation method since it allows not only for the total economic valuation of a change in the fishing management practice, but also capable of valuing (at the margin) each of the relevant attributes in analysis. The value assessment of each attribute requires the development and application of a model of individual consumer behavior. In the present study we explore the use of the random utility model.

2. *General model of individual choice behavior.*

2.1. *Random utility model formulation.*

Let G represent the set of fishing regime alternatives in the choice set, and S the set of vectors of measured attributes, that is the type of contract, the total area of the concession and the type of fishing technology. The choice for a fisherman can be defined as a draw from a multinomial[1] distribution with probabilities:

$$\text{Prob}\,(x \mid s, A) \quad \forall x \in \text{with } A \subseteq G \tag{1}$$

i.e. the probability of selecting fishing regime x, given the individual's s socio-economic characteristics and set of alternatives A, for each and every alternative contained in the set A. To operationalize the preceding condition, we establish an individual behavior rule, which maps each vector of observed attributes s and a possible alternative set A into a selected alternative of A. In other words, establish a model of individual behavior, interpreted as an analytical device, so as to represent the set of individual behavior rules relevant to all individuals who define the sampled population. We opt for a function that results from maximizing a specific utility function.

Let Uij be the utility of the ith alternative for the jth individual. Further assume each utility value can be partitioned into two components: a systematic component or representative utility', Vij, and a random component, eij the latter reflecting unobserved individual idiosyncrasies of tastes. The partitioning of the utility function is used for operational reasons when popu-lations of individuals are modeled. That is, one assumes that one part of utility is common to all individuals while the other is individual specific. This is a crucial assumption, implying that the existence of a significant element of the full attribute set is associated with homogeneous utility across the population under study. Formally we have:

$$U_{ij} = V_{ij} + \varepsilon_{ij} \tag{2}$$

and we assume that individuals will try to choose a fish regime alternative that yields them the highest utility. In other words, the individual j will choose alternative i if and only if:

[1] Multi-nomial refers to the existence of two or more possible outcomes.

$$U_{ij} > U_{hj} \quad \forall_i,\ h \in \text{A with } i \neq h \tag{3}$$

Combining equations 2 and 3, we have that a fish regime alternative i is chosen if and only if

$$\left(V_{ij}+\varepsilon_{ij}\right) > \left(V_{hj}+\varepsilon_{hj}\right), \text{ or } \left(V_{ij}-V_{hj}\right) > \left(\varepsilon_{hj}-\varepsilon_{ij}\right) \tag{4}$$

Since we can not observe $(\varepsilon_{hj}-\varepsilon_{ij})$, we can not assess exactly if $(V_{ij}-V_{hj}) > (\varepsilon_{hj}-\varepsilon_{ij})$. One can only make statements about choice outcomes up to a probability of occurrence. Thus, we need to calculate the probability that $(\varepsilon_{hj}-\varepsilon_{ij})$ will be less than $(V_{ij}-V_{hj})$:

$$\text{Prob}\left(x_{ij} | s_j, A\right) = \text{Prob}_{ij} = \text{Prob}\left[\left\{\varepsilon\left(s, x_h\right) - \varepsilon\left(s, x_i\right)\right\} < \left\{V\left(s, x_i\right) - V\left(s, x_i\right)\right\}\right] \forall_i,\ h \in \text{A} \tag{5}$$

also called random utility model (RUM): the probability that a randomly drawn individual from the sampled population, who can be described by attributes s and choice set *A*, will choose x_i equals the probability that the difference between the random utility of alternatives *i* and *h* is less than the difference between the systematic utility levels of alternatives *i* and *h* for all alternatives in the choice set. The analyst does not know the actual distribution of $(\varepsilon_{hj}-\varepsilon_{ij})$ across the population, but assumes that it is related to the choice probability according to a statistical distribution. Therefore, the next step is to specify a probability model for the observed data.

2.2. *Operationalizing the random utility model: the Logit choice model.*

There are many statistical distributions available, but the one used frequently used in discrete-choice modeling is the extreme-type I distribution, usually known as the Weibull distribution. Once chosen the family distribution, we will use it as the mechanism for translating the unobserved random index $(\varepsilon_{hj}-\varepsilon_{ij})$ into an operational component of the probability expression. This component, in turn, can be worked out so as to arrive at a choice model formulation in which the only unknowns are utility parameters with each attribute in the observed component of the random utility expression. In order to derived such a model formulation, we start with the definition of the Weibull distribution in terms of ehs:

$$\text{Prob}\ (\varepsilon_h \leqslant \varepsilon) = \exp\ (-\exp\text{-}\varepsilon) = e^{-e^{\varepsilon}} \tag{6}$$

In addition from equation 5, which defines consumer choice behavior, we have that:

$$\text{Prob}_{ij}=(\varepsilon_{hj}-\varepsilon_{ij})<(V_{ij}-V_{hj}) \quad \forall_i,\ h \in A \tag{7}$$

Rearranging equation 7, dropping the subscript j to avoid over-notation and assuming that $U_{ij} \neq U_{hj}$ we get:

$$\text{Prob}_i=\text{Prob}(\varepsilon_h<(\varepsilon_i+V_i-V_h)) \quad \forall_i,\ h \in A \tag{8}$$

Combining equation 6 and equation 8 we get:

$$\text{Prob}(\varepsilon_h<(\varepsilon_i+V_i-V_h))=\exp(-\exp-\varepsilon)=e^{-e^{\varepsilon}} \tag{9}$$

that is, the use of a parametric specification with the RUM allows us to obtain choice probabilities. Nevertheless, it is the use of a strict economic theoretic foundation that allows us to develop a simple operational model. We refer to the Independence-from-Irrelevant-Alternatives (IIA) choice axiom, which states that the probability of choosing one alternative over another is unaffected by the presence (or absence) of any additional alternatives in the choice set. This implies that the random elements in the utility are independent across alternatives and identically distributed: the probability of choosing alternative i can be written as the product of the *H-1* terms specified using equation 9 as follows for some given value of ε_i (say b)

$$\begin{aligned}&\text{Prob}_i=\text{Prob}(\varepsilon_h<(\varepsilon_i+V_i-V_h), \quad \forall_i,\ h \in A)=\exp\prod_{h=1}^{H}\exp(-\exp-[b-V_i-V_h])=\\&=\exp(-b)\exp\left[-\sum_{h=1}^{H}\exp-(b-V_i-V_h)\right]\end{aligned} \tag{10}$$

The probability of choosing a particular alternative i can be assessed by integrating the probability density function as expressed in equation 10 over all possible values of ε, i.e.

$$\begin{aligned}\text{Prob}_i&=\int_{b=-\infty}^{b=+\infty}\exp(-b)\exp\left[-\sum_{h=1}^{H}\exp-(b-V_i-V_h)\right]db\\&=\int_{b=-\infty}^{b=+\infty}\exp(-b)\exp\left\{-\exp(-b)\left[\sum_{h=1}^{H}\exp(V_h-V_i)\right]\right\}db\end{aligned} \tag{11}$$

To obtain the final result, let us apply a transformation of variables by replacing $\exp(-b)$ with z. The equation 11 can be rewritten in term of z as follows[2]:

[2] $\exp(-b)=z$ implies that $b=-\log z$, therefore we can replace db by $-\frac{1}{z}$. This in turn requires a change to the limits of integration.

$$\text{Prob}_i=\int_{\infty}^{0} z\exp\left[-za\left(-\frac{1}{z}\right)\right]dz=\int_{\infty}^{0}\exp\left[\left(-za\right)\right]dz \qquad (12)$$

with $a=\sum_{h=1}^{H}\exp(V_h-V_i)$. Since $\int\exp(-az)=\frac{\exp(-az)}{a}$ and that when $z=\infty$, $\exp(-\infty)=0$ and when $z=0$, $\exp(0)=1$ we have that $\text{Prob}_i=-\left[\frac{1}{a}(0-1)\right]=\frac{1}{a}$. Therefore, we can re-write Equation 12 as

$$\text{Prob}_i=\frac{1}{\sum_{h=1}^{H}\exp(V_h-V_i)} \qquad (13)$$

that defines the basic econometric specification consistent with the random utility model, and respective choice assumptions, and it is called the conditional Logit choice or Multinominal Logit (MNL) model. The task is now to estimate the utility parameters of the MNL model as described by Equation 13.

3. *Research goal: estimation of utility parameters.*

From the previous section, we have that the probability of an individual *j* to choose an alternative *i* can be written in the following closed-form MNL model. The first step in estimating the utility parameters refers to the specification of a functional form of the utility expression *V*(.), i.e. specify the relationship between the various attributes and observed consumer choices. In the present analysis, we work with a linear, additive form that maps the multidimensional X attribute vector into a unidimensional overall *V* utility (rating). Formally we have:

$$V_{ij}\left(=\sum_k \beta_{ik}X_{ikj}\right) \qquad (14)$$

The βs are utility parameters to be estimated: an estimate of β_{ik} is interpreted as estimate of the weight of the attribute *Xs* in the utility expression *Vi* of alternative *i*. Given estimates of the βs, an estimate of V_{ij} is computed by taking the bs and the *Xs* for individual *j* and alternative *h*. Utility parameters can be allowed to vary across the sampled observations: even though we define *V* as representative, because the levels of attribute contained in V_{ij} (see equation 14) vary across the *J* individuals. The next step to assess the *s* is to specify a statistical estimation technique. The approach that we use to

estimate the utility parameters of the closed-form MNL model is called Maximum Likelihood Estimation (MLE), i.e. that maximize the likelihood function of our random sample. In formal terms we have:

$$\underset{\beta}{MaxL}=\prod_{j=1}^{J}\prod_{h=1}^{H}\text{Prob}_{hi}^{dhj} \tag{15}$$

with d_{hj} defining a dummy variable such that $d_{hj}=1$ if alternative h is chosen and equal zero otherwise. Given, L in equation 15, the log-likelihood function L^* can be written as

$$\underset{\beta}{MaxL^*}=\sum_{j=1}^{J}\sum_{h=1}^{H} d_{hj}\log(\text{Prob}_{hi}) \tag{16}$$

Combining Equations 13-14 and 16 we have,

$$\underset{\beta}{MaxL^*}=\sum_{j=1}^{J}\sum_{h=1}^{H} d_{hj}\log\left(\frac{\sum_k \beta_{ik}X_{ikj}}{\sum \beta_{ik}X_{ikj}}\right) \tag{17}$$

The βs estimates are interpreted as a magnitude of the weight of the each attribute in the utility expression and this allows us to evaluate welfare changes associate associated to different levels of provision across the different attributes. The tasks that we face are to identify the relevant attributes and to specify levels of provision across the alternative attributes. The present valuation study takes into account four attributes: (a) the type of fishing contract, which is set at two different levels of provision, respectively *concessione individualle* and *concessione colectiva*; (b) the total fishing area of the concession, which varies across 3.5 and 10 ha and (c) the type of fishing technology, which is set a three systems including *rusca e reti fesse*, *manuale e reti fesse* and *vibrant* and the monetary value the fishing permit.

Therefore, the research objective is the estimation of:

$$\Delta\hat{V}=\hat{\beta}_0+\hat{\beta}_1X_1+\hat{\beta}_2X_2+\hat{\beta}_3X_3+\hat{\beta}_4X_4 \tag{18}$$

where X_1, X_2, X_3 and X_4 represent respectively the type of fishing contract, the total fishing area of the concession, the type of technology and the monetary value the fishing permit. In this context, for example, the ratio β_4/β_1 represents the marginal willingness to pay (expressed in monetary terms) for an additional ha of fishing.

References.

Jordan J.L., Hensher D.A. and J.D. Swaat (2000) Stated Choices Methods: Analysis and Applications, Cambridge University Press, UK.

EVALUATION OF ALTERNATIVE SCENARIOS FOR ALIEUTIC RESOURCES MANAGEMENT IN THE LAGOON OF VENICE

V. Boatto[1], L. Galletto[1], G. Orel[2], M. Pellizzato[1], L. Rossetto[1], A. Sfriso[3], S. Silvestri[1], A. Zentilin[2]
[1]*Dip. Territorio e Sistemi Agroforestali, Università di Padova*
[2]*Università di Trieste*
[3]*Dip. Scienze Ambientali, Università Cà Foscari, Venezia*

1. *Introduction.*

In the last years the fish industry in the lagoon of Venice has shown a gradual decline, which has been characterized either by the reduction in the number of fish belonging to typical Lagoon species (Fig. 1), or by the transition from multiple fishing methods to an activity which is based mostly on one species the bivalve *Tapes philippinarum*. The high spreading of this bivalve and its easy earnings are factors which have boosted

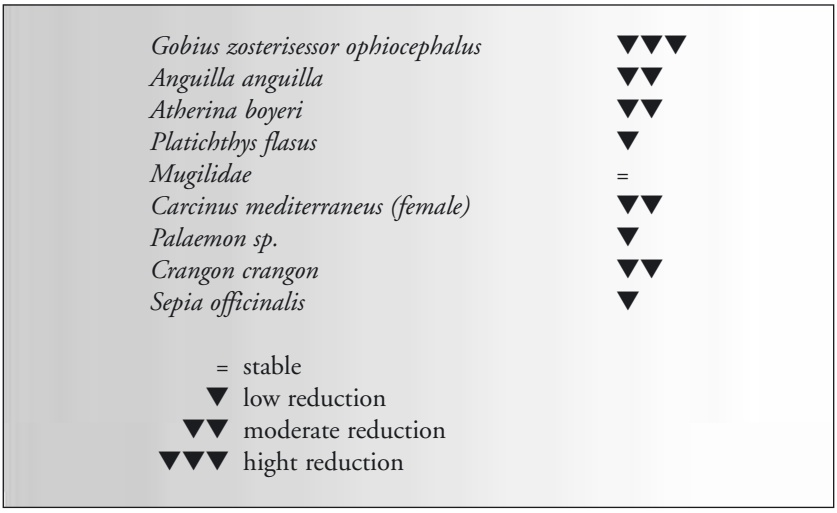

Fig. 1 – Quantity variations of the Lagoon fish production, based on market estimations (1990-2001) and on industry operators' evaluations.

its capture, at first realized by manual systems, which have been later refined in order to obtain higher yields. The mechanical impact of these tools (hydraulic dredge, vibrating rake, and "rusche") has had remarkable consequences on the environment: changes in the lagoon bottom morphology and composition, by modifying the texture and the webbing, suspending of remarkable sediment amounts, making the water turbid and, consequently, hindering the development of the plant population (ICRAM, 1994; Pranovi & Giovanardi, 1994; Sfriso, 2000).

Currently the production of clams, wrongly considered inexhaustible by the fishermen, is diminished of approximately 40%. According to economic data (Fig. 2) one finds a progressive gap between evolution of the production, which is decreasing and prices that show, on the contrary, an increasing trend. This fact happened especially at the end of year 2001, when prices have shown a great jump that does not seem due to an unexpected increase in the demand. The more likely reason of this fact (however deserving further deepening) seems to be related to the total reduction in product amount, which has been supplied at the market.

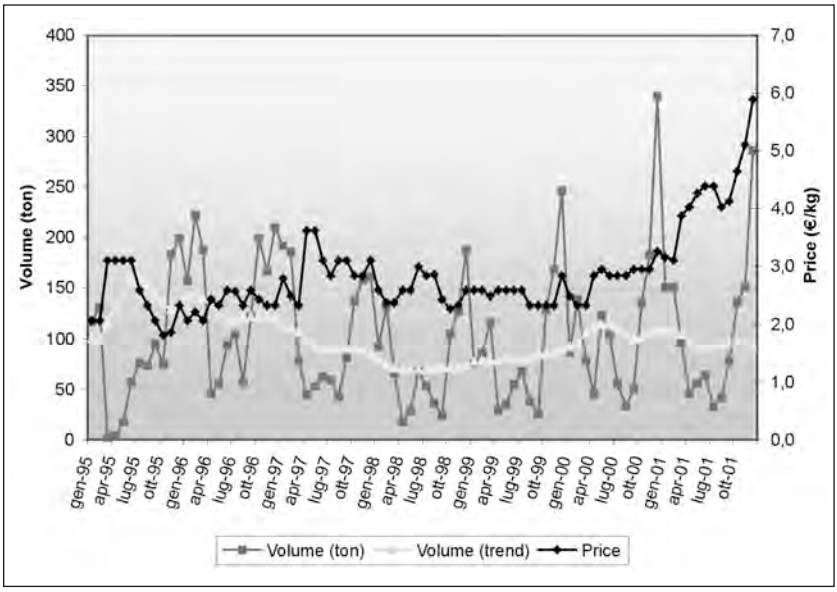

Fig. 2 – Monthly trend for *Tapes philippinarum's* total production (fishing and farming).

If this hypothesis were confirmed, the price increment should be caused by the stock depletion, as a consequence of deaths and of an excessive exploitation of the natural beds. About last year supply, considering the

available data, we can estimate a 25% contraction of the amount at the beginning of the year. Then, taking into account these data, it is likely to foresee that the lagoon fishing free access system should afford a deep crisis in the medium and long run and, hence, that it is necessary to make up an alternative management strategy for the alieutic resources, which makes the lagoon fishing a sustainable activity under different point views: environmental, biological, economic and social.

To pursue this goal, keeping into account the interventions which will impact the morphologic aspect of the Venice Lagoon, we have thought of analyzing three alternative solutions: the free access fishing (status quo); the traditional fishing and the restricted one. For each managerial alternative we have proceeded by estimating either its technical-productive and environmental results or their economic value for the enterprises and the whole Lagoon people community.

2. *Methodology.*

The starting point for the setting up of an operative plan is the exam of a descriptive model of the functioning on the lagoon ecosystem, which can be defined "paralic" model.

The "paralic" term drift from the Greek (para = close and halos = salt), and it designates habitats, which have or have had an unstable relationship with the sea.

The Mediterranean ponds, the lagoons in the northern Adriatic Sea, the Norwegian fjords, the Spanish "rias", the channels of the Istrian coast are all natural paralic aquatic habitats, while the salt fields, the ports are artificial paralic aquatic habitats. In these habitats, the more important biological parameters are distributed along a gradient of "confinement", which is defined as the time elapsing between two subsequent water changes in the same point of the lagoon basin. As far as you go away from the sea, the medium "confinement" increases, the species number lessens, the number of individual fish increases (and therefore the index of diversity diminishes), jointly with an increment of their size. Therefore, each species expresses its maximum biomass at a determined "confinement" degree. Hence, it is clear the technical-productive and economic meaning of this concept.

Local or general variations in the "confinement" degree modify these indexes and, likewise, modifications of these indexes are proves of changes in the "confinement" degree.

In general, it can be said that, as more confined is a lagoon zone, as more frequent are the dystrophic phenomena from which it is affected. These are the environmental basics which have been kept in mind in estimating in evaluating the change from fishing activity to a fish farming of the Manila clam, for their obvious impacts on the distribution of the permits, on the seeding optimization, on the growth rates increase, on the mortality rates, etc.

In the studies we have carried on, we could not avoid the appraisal either of the fishermen's preferences or a costs/benefits analysis. On this regard, we have found that conjoint analysis is most suitable key in order to appraise the fisherman behavior when he faces a departure from the quasi-free access current situation towards a more strict regulation, which is a system of negotiable permits. In other words, our proposal has been the estimation of the welfare changes connected with a departure from the current fishing system.

The methodology of contingent evaluation has been carried out in three phases:

1. Identification of factors, which can affect fishing activity: the fishing area size (hectares linked to the permit), the type of permit (on individual base or collective), the fishing system ("rusche", "rusche" and nets, vibrating rake) and the cost of the permit.

2. The previous information has been employed to set up a questionnaire in which each fisherman expresses his preference between two fishing alternatives. Each chosen alternative shows, therefore, the fisherman's willingness to pay (WTP) for a determined method of fishing regulation.

3. The appraisal procedure adopts a multinomial Logit model in which the probability that a person j chooses the alternative i instead of the alternative h, can be written as:

$$\Pr ob_{ij} = \frac{\exp(V_{ij})}{\sum_{h=1}^{H} \exp(V_{ij})}$$

In our study, the specification of the multinomial Logit model can be driven back to the estimation of the following expression:

$$\Delta \hat{V} = \hat{\beta} + \hat{\beta}_1 X_1 + \hat{\beta}_2 X_2 + \hat{\beta}_3 X_3 + \hat{\beta}_4 X_4$$

Where X1, X2, X3 and X4 are, subsequently, the fishing area, the type of permit, the fishing system and the price of the fishing permit which is

associated to the correspondent regulation formulated in the questionnaire.

This valuation method offers many advantages in comparison with the traditional methods of directed contingent valuation. In particular, it is possible not only to quantify the effects of a change in the fishing system, but also to estimate the marginal contribution of each important factor in the fishing activity. As an example, it is possible to determine the WTP for the permit of a further hectare of fish farming, or the WTP for an individual permit in comparison with the collective one and, moreover, the WTP for the traditional fishing system based on "rusche" dredge in comparison with the intensive one based on vibrating rake, etc.

3. *Results.*

3.1. *Aspects relating to the environmental impact.*

In order to deepen the knowledge on the impact of the Manila clam fishing activity, our survey is completed by a monitoring on the sedimentation flows, on the erosion/sedimentation processes and on the macroalgae and marine sea grass distribution in target areas close to the permit zones for the fishing activity and the farming of these bivalves.

Two different areas have been defined in all the basins of the Lagoon of Venice (North, Central and South): the former is affected by the clam fishing operations, the latter (the control station) is outside the direct interference of the sedimentation flows which are determined by these operations. We were not able to work within the fishing areas since the traps and the small poles of sedimentation were continuously taken away or moved. Consequently we worked close to fixed emplacements as wood poles and concrete poles used to indicate a pipeline, in order protect our survey instrumentation.

The results we have got let us point out the conclusion that the Manila clam fishing activity, particularly if it is carried on in a not restricted way, affects strongly the flows of sedimentation and the sediment fall back or removal from the Lagoon shoals. However, the results we have obtained in this survey show undeniably the need of allocating areas for the Manila clam controlled fishing as soon as possible, given that a controlled fishing system, as it already happens in some areas of the southern Lagoon, can remarkably reduce the environmental effects of the sedimentation flows. Moreover, as we expect, these results remark the role of the marine sea grass prairies, in contrasting the erosion phenomena in the zones close to those used for fishing.

In the northern and central Lagoon, where fishing is not restricted yet, the results show sedimentation flows meaningfully higher both near the boundaries of the fishing areas and in the control areas, especially if you look at the monthly variations. On the contrary, in the southern Lagoon, where some permit areas are already a reality and clams are seeded and harvested following a stated plan, the impact of the fishing activities declines remarkably around these areas and is practically absent on what relates to the erosion phenomena.

The marine sea grass, which can be found in the control areas of the central and southern Lagoon, show their importance in promoting the sedimentation processes and in contrasting the sediments loss also in areas which are affected by strong tide currents. In these zones we have discover a sinusoidal trend of the erosion/sedimentation processes, which is characterized by sedimentation when the leaf system is well developed (in spring and in autumn), and by erosion as more the leaf system is reduced (in summer and over all in winter). The macroalgae, instead, are absent or with negligible biomass.

3.2. *Fishing with traditional systems and tools.*

Survey on past fishing methods in the Lagoon of Venice has shown a great attention towards the type of instruments used for this activity, attention which is underlined by the definition of several regulations and the restrictions: nets were stamped and their length and mesh had to be equal to the deposited model, their mesh did not have to be too tight, too much small fish could not be fished, fishing with some tools was forbidden in certain periods of the year, etc..

Moreover there were institutions and boards which were devoted to the control, the management and the regulation of fishing and hunting, such as the Magistracy of the Justice, who supervised on all the professions, by establishing prices, measures and weights.

The professions were separated, and there was a corporation (in venetian language: “fraglia”) for each one, which had its own statutes (in venetian language: “mariegole”), or a group of fishermen, who owned a lagoon zone for fishing. The resources of each zone were allocated to the corporations and, within these, to each fisherman or group of fishermen. Until the end of the Second World War, motorboats, whose power was minimal, were mostly found at the fishing center of Chioggia, while the other centers employed mainly rowing and sailing boats. The main fishing systems were limited to the use of some trawl nets, fyke nets, gillnets, seine nets,

and other simple tools (Brunelli G. et al., 1940; Zolezzi G., 1944).

This type of instrumentation was a guarantee for keeping rather stable environmental conditions, and the lack of mechanized tools allowed minimal environmental impact.

About the clam fishing, there were two mainly known species: *Tapes decussatus* L., and *Scrobicularia plana* Da Costa. The fishing systems were exclusively manual and were based only on the use of rakes and triangular dredge made by iron and named "cassa", which were launched by hand.

Yields of a fishing activity carried on these bases were rather low (Tab. 1) and the fishermen looked forward more moderate revenues.

Tab. 1 – Fish production tons in the Lagoon of Venice in 1961 and in 1997; estimation of the production per operator for the main leading species and percentage reduction. The estimated fishermen number is equal to about 1.300 in 1961 and to about 900 in 1997.
Data: *Camera di Commercio, 1972; **C.V.N., 1997.

Main leading species fished in the lagoon of Venice	1961*		1997**		1961-1997
	tons	Kg per fisherman	tons	Kg per fisherman	Percentage reduction
Anguilla anguilla	197,7	15,2	6,3	7,0	53,9%
Gobius zosterisessor ophiocephalus	576,3	44,3	179,0	19,9	55,1%
Platichthys flesus	94,9	73,0	29,1	32,3	55,8%
Carcinus mediterraneus ♀	576,3	44,3	179,0	19,9	55,1%
Crangon crangon	339,9	261,5	32,9	36,6	86,0%

Going back to a type of traditional and low impact equipments would allow high advantages for the community and the environment, but it would be scarcely rewarding for the fishermen, given the biological depletion of the bottom, and it would repay neither the costs, nor the efforts applied to it. At present, this appears to be an attractive scenario, although with little application possibilities. The recovery of traditional methods could be applied in connection with fish-farming areas managed by a system of permits.

3.3. *Free access fishing system.*

The current phase of our research is the estimation parameters for the evaluation of the fishermen's WTP for the different fishing systems. At the same time, the surveys carried out through the questionnaires allow some important comments.

Many of the fishing enterprises, which operate currently in the Lagoon of Venice, have begun their activity recently (Fig. 3) 45% of them, in fact, have started after 1990, while only 9% declare they have been operating for more than forty years. The percentage of the opera-

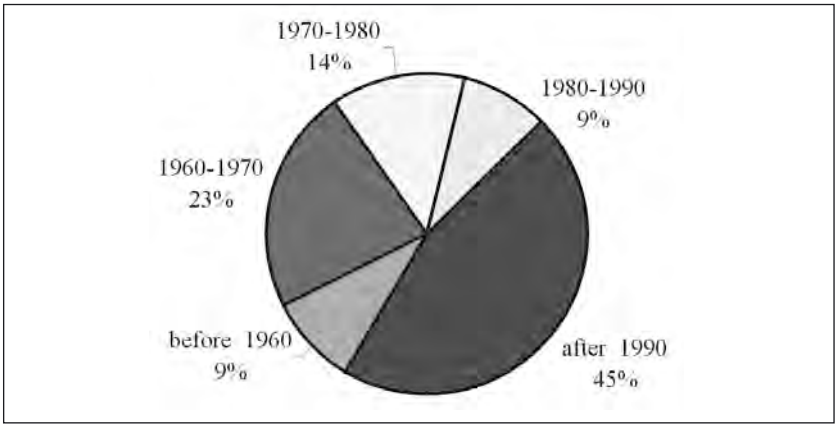

Fig. 3 – Operators in the fish industry: persentage groups year of activity beginning.

tors, which assert they have begun to fish between 1970 and 1980, is very low: 14%. This can be explained with a widespread exodus, which has characterized the fish industry, given the preference for other employment opportunities, as those which could be found in the manufacture industry. A low percentage of operators, 9%, marks also the following decade, from 1980 to 1990: in this years the lagoon production, becoming unstable for environmental reasons (dystrophic events, environmental crises, macroalgae proliferation, etc.), pushes the fishermen to choose the sea as the center of their own activity.

The operators' average educational level is rather high compared with the average of the people employed in the primary sector. In fact, only 25% declare that they have achieved an elementary education level, while, from the other side, 20% have achieved high school title. 55% of the fishermen have received training on fishing techniques directly from their relatives, while, the others have got their basic experience from persons working in the fish industry they knew. Only 5% assert they have undertaken formation courses.

The fishing enterprises are characterized by an extensive presence of collective units, moreover operators are engaged to a great extent in

associated participation structures, like cooperatives. Reasons for association are (Fig. 4): credit (53.3%) and technical (47.1) assistance, support in managing bureaucratic practices (66.7%) and fiscal and social security obligations (58.8%).

As far as the degree of diffusion of the fishing systems, the use of manual gears, as the "by hand" - in a tight meaning – fishing, the clams

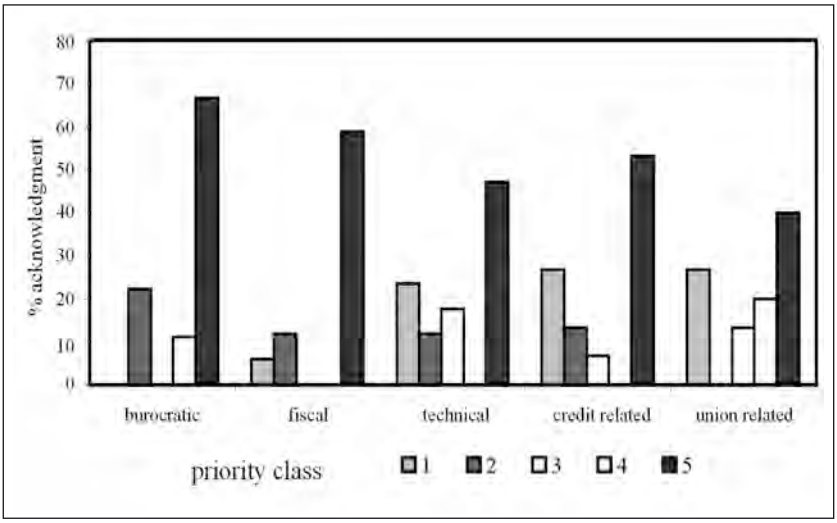

Fig. 4 – Degree of acknowledgement of the advantages given by the cooperative structure and related priority class.

manual rake fishing, jointly with the use of hangs (rods, reels, long lines, etc) is very low. It is substantially low also the use of seine nets, which are "often" utilized by a very small operators' percentage, namely 6 %. The most widespread gears are the "rusca" and the "vibrating" rakes, which are used for the clam fishing (Pellizzato & Giorgiutti, 1997). A medium level of spreading relates the trawl nets, fyke nets, gillnets, seine nets and traps (Fig. 5). Only 21% of the interviewed operators assert they possess structures or fixed equipments for the fishing activity, such as: "casoni" (warehouse for nets and other fishing tools), "buse" (for finfish fry storage), rafts (for mussels and clams selection and processing), etc. Two thirds of the interviewed operators declare they are supported by no structure for their working activity.

In the following lines we describe the main fishing systems and farming techniques, which you can find in the Lagoon of Venice.

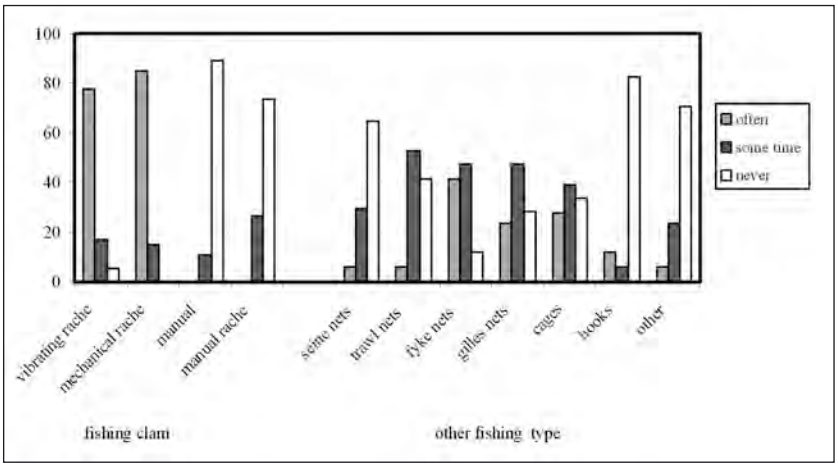

Fig. 5 – Frequency for use of the main fishing systems employed in the Lagoon of Venice.

3.3.1. *Finfish fry fishing.*

Currently finfish fry fishing activity engages a limited amount of operators, equal to approximately 30-40, who work less than three months per year. They use nets with thick meshes purposely made for the capture of the juvenile ones of gilthead sea bream, sea bass and gray mullets. A working day generally lasts at least 8 hours. Daily production of a company of fishermen, which is formed by 2-3 persons, is very variable: 1.000-30.000 finfish fry per day, with an average of approximately 3-4.000 heads per person per day (Franzoi & Pellizzato, 2002).

The species that are used in the Lagoon of Venice are: the gilthead sea bream (*Sparus aurata*), the sea bass (*Dicentrarchus labrax*) and the gray mullets (*Liza ramada* "botolo"; *L. aurata* "lotregano"; *L. saliens* "verzelata"; *Chelon labrosus* "bosega").

This type of fishing involves small companies, which are composed from 2 to 3 fishermen with motorboats and seine nets. The net is drawn by hand in the low bottom (inter-tidal and sub-tidal) zones and it is never lifted out off the water; the finfish fry are collected with a net and put in bushels filled with water which is frequently changed. The captured fish is amassed in pounds, called "buse di deposito". The starting date for this activity is fixed each year, but it happens often in the first half of March; the end usually falls within the first decade of May. In the last three years the fishing effort have been intense mostly in the gilthead sea finfish fry: on average 5 million of specimens per year have been captured, of which

2,3 million belong to the gilthead sea bream juveniles, 2,1 million of gray mullet juveniles and less than half million of sea bass juveniles (Franzoi & Pellizzato, 2002).

The utilization of the "valli da pesca" as areas of seeding and growth is a system of ecologically compatible exploitation (Ardizzone et al., 1988; Munford & Laffoley, 1994; Rossi et al., 1999; Barnabè-Quet, 2000), but which have to be managed and controlled (Rossi, 1981; Rossi et al., 1999; Cataudella et al., 1999), since the withdrawal of juvenile stages has, on the other hand, an impact negative on the fish resource. On this regard, parallel studies have evidenced the following needs: to establish a control which starts from the capture of the finfish fry and ends to its seeding in the "valle da pesca" (Franzoi & Pellizzato, 2002); to establish an activity beginning date which is based on the analysis of the environmental conditions and on directed sample observations on the finfish fry development stage, in order to safeguard those stages which are more premature and more vulnerable to the capture and transportation stresses (Rossi, 1981); to fix the end of the activity date in May in order not to interfere with the development of the nektonic species which need a lagoon reproduction (Franzoi et al., 1989); to reserve such activity to fishermen who possess adequate professional ability; to release into the sea e predetermined quota of grown up animals, in order to contribute to the maintenance of the parental stocks (Cataudella et al., 1999).

3.3.2. *Fixed nets fishing.*

This fish activity implies the control and the management of a wide lagoon space by a group of persons, while the phase of fish withdrawing requires usually the work of one fisherman alone; in this case average daily productivity is equal to approximately 2,5 kg/fyke net/day, and it reaches 5 kg/fyke net/day in the best conditions for operating. For this type of activity, are required 6-8 hours/day. There are two main fishing periods: from September to December and from March to July. The fyke nets emptied daily, product is gathered and nets are cleaned up. Working activity requires on average about 300 days per year, which are mostly utilized to put in order the equipments and to their maintenance and protection.

The composition analysis of a group of fyke nets, which were distributed in the total lagoon surface, has allowed to determine the basin production aptitude and to find out the typology of the fish product which is collected in the different lagoon areas and which on the whole comes

from the Lagoon of Venice. On the base of the collected data, which are backed and confirmed by a previous survey carried out from the Magistrate for Water Resources (C.V.N., 1999), we have characterized the Lagoon of Venice main production for the leading species: 36% of *Gobius zosterisessor ophiocephalus*, 20% of *Atherina boyeri*, 11% of *Sepia officinalis*, 8% of Mugilidae, 16% of *Carcinus mediterraneus*, 6% of *Palaemon sp./Crangon crangon,* the remaining 2% of *Platochthys flesus* and 1% consisting of other fish types (Fig. 6).

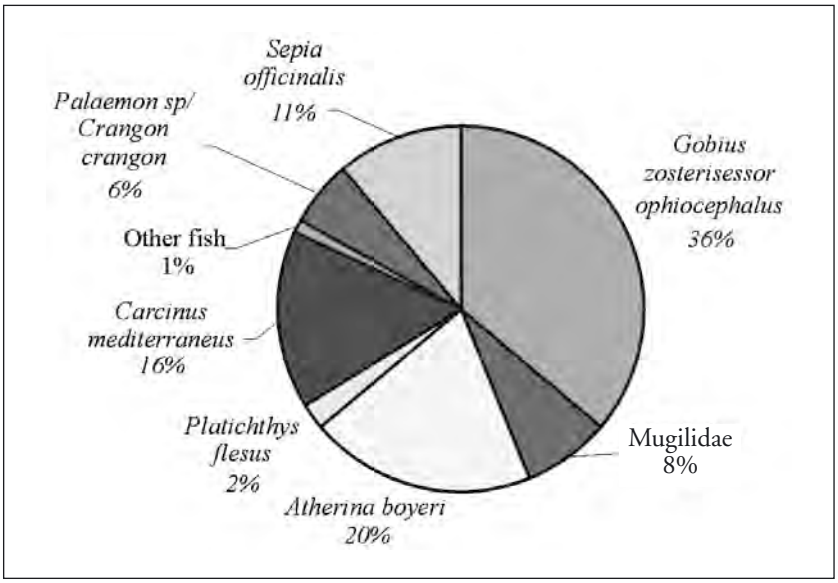

Fig. 6 – Production of the main leading fish species in the Lagoon of Venice.

Although it is somewhat difficult to attribute to each lagoon basin its productivity level, due to both the lagoon fish fauna mobility within the lagoon ecosystem and the interchanges that this system sets up with the sea, we have been able to determine the fish contribution of each single basin, as it is synthetically shown in Table 2.

3.3.3. *Mussel culture.*

The mussel culture in nursery-parks in the Lagoon of Venice regards approximately 42 hectares of the lagoon surface, which relate to an amount of 38 permits, and it is estimated to employ about 220 workers. Either environmental or bureaucratic problems have pushed most of the

Tab. 2 – Fishery contribution of the main lagoon fish species in each basin.

Species	Northern Lagoon	Central Lagoon	Southern Lagoon
Gobius zosterisessor ophiocephalus	15,0%	65,0%	30,0%
Atherina boyeri	28,5%	7,0%	24,0%
Platichthys flesus	5,0%	1,0%	0,0%
Mugilidae	12,0%	11,0%	1,6%
Carcinus mediterraneus (soft)	9,8%	8,6%	29,6%
Palaemon sp./Crangon crangon	6,1%	1,0%	9,6%
Sepia officinalis	22,0%	6,0%	4,0%
Other fish	1,6%	0,4%	1,2%

sector operators to establish new plantations in the sea (off-shore). Then an integrated management system has been created between the two production places, the lagoon and the sea, by improving – as an example – the lagoon production in the sea plantations, or utilizing the structures of one plantation for the seed harvest and then transferring it to another one etc. This sea-lagoon integrated system makes rather complex to determine how much product comes from the lagoon. Anyhow, we estimate that the clam lagoon annual production is about 4.000 tons, while the offshore plantations produce about 6-7.000 tons yearly.

Therefore, it appears that the lagoon mussel culture has remarkably reduced: in the 1993 an amount of 22.100 tons had been estimated, that is an amount which is five times greater than the current one. Causes of this production reduction can be related to several factors, one of them is the possible lessening of the nourishments in the Lagoon: this would have increased the duration of the productive cycle to 18 months, against the 9 months which are needed in the sea. Moreover the bureaucratic route to get a permit in the lagoon is much more complex than that one has to follow in order to start the same activity in the sea.

The mussel farming system in the Lagoon is the “French type” nursery-park.

The bottom heightening which this farming system implies, determines a gradual reduction of the length of the socks (“reste”) and a consequent reduction in the surface yield. Production is estimated to be about 80-100 kg per square meter in particularly favorable located nurseries. From an economic point of view, the mussels farming spreading to many other Italian locations and the growth the national production

(over 130.000 tins per year) have kept the average price of the product stable, therefore reducing the Veneto Region operators earnings.

3.3.4. *Clam fishing (Tapes philippinarum).*

The production has considerably varied in 2001 as compared to a 1997 survey (Provincia di Venezia, 2000), with a total losses estimation of approximately 40%.

This type of fishing implies and employment of 6-8 hours per day, for a fishing season of approximately 200 days per year. On average, each fisherman harvest about 150-200 kg of clams per day.

The main gears to be used in the clam fishing are the standard mechanical rake ("rusca") and the vibrating rake (Pellizzato & Giorgiutti, 1997). In the middle of 1998, about 600 boats, 5-6,5 m wide, were operative with the rusca in the Lagoon. They were propelled by a main 150/200 HP navigation engine and an auxiliary 15/25 HP engine. While fishing, the punts proceed at the speed of about 750 meters per hour (Provincia di Venezia, 2000) and are able to dig the sediment as far as 0,15 meters of depth, thanks to a metallic cutting edge in the lower side of the case, whose openness is approximately 1 meter wide. Vibrating rakes are equipped with a cage whose openness is approximately 2 meters wide, which is able to dig the sediment at about 0,1 meters of depth. The cage is equipped with an electrical shaker which, making it to jolt, allows the disintegration of the collected sediment and its leaching by the water that flows into the cage as it goes forward. This type of gear allows a daily average of 15 fishing actions, whose length is 100 meters. In January 1998, 84 vibrating rakes had been counted in the Venice Lagoon.

The ecosystem evolves towards a gradual fish resource depletion: estimated yields are approximately 15-20 g/sqm for the Northern Lagoon north, 20-30 g/sqm for the Central Lagoon, 25-35 g/sqm for the Southern Lagoon. Yield decreasing process is explained either with mortality phenomena which have taken place in August 2001, or with the fishing pressure increase, which has strengthened in the last years in conjunction with a free access modality of resources exploitation, and with lack of a regulation which sets up withdrawal limits.

3.4. *Restricted fishing.*

The proposed alternative model of fishing management introduces a more restrictive regulation as far as the clam way of fishing and it establis-

hes permits allocation for a certain amount of hectares of lagoon surface.

The most suitable solution seems to consist in a system of fishing areas, the surface of which to is equal to 3.000 hectares, to be designed respectively either to the seeding or to the growing phase and the following fishing. In such a way a triennial cycle of fish farming would be established, which would utilize only 9.000 lagoon hectares within a total surface of 30.000 hectares. The regulation would put into effect a restriction also on the fishing tools use; in particular the "rusca" (mechanical rake) would have to be replaced by the professional standard binder, the vibrating rakes would have to be discarded; only some units to use for collective services purpose would be kept. Anyhow, since the per capita income should be sustained to the medium levels, which have to be estimated before the regulation introduction, the tradable product density could be increased by means of seedings and/or reseedings.

This model presents many advantages: fishing would be set aside in zones which are approximately equivalent to one tenth of the current ones, bringing on a consequent environmental impact reduction, the recovery and the maintenance of traditional fishing ways would be guaranteed and, given that income would be guaranteed too (also by means of price control), the spasmodic race to the conquest of great fish mass, which has often had heavy consequences, would vanish.

The main question regards the collision with deeply rooted practices, which can be hardly eradicated, given that they assure high profits in the short run. Reconverting the job of many fishermen seems to be a particularly difficult task, in so far their social typology is scarcely inclined to modify their current way of working. Moreover they show a modest propensity to deal with the environmental problems and to reason within a frame of a medium-long term lasting sustainability, in a quite different way as compared with years ago, when the "Regole" closely controlled the fisherman's profession.

References.

Ardizzone G. D., Cataudella S. & Rossi R., 1988. Management of coastal lagoon fisheries and aquaculture in Italy. *FAO Fish. Tech. Pap.,* 293, 103 pp.

Barnabè G. & Barnabè-Quet R., 2000. *Ecology and Management of Coastal Waters: the Aquatic Environment.* Praxis Publishing Ltd, Chichester, Uk.

Brunelli G., 1940. La pesca nella laguna. In: Brunelli G., Magrini G., Milani L. e Orsi P., *La laguna di Venezia, III* (6), C. Ferrari, Venezia, 1-26.

Cataudella S., Franzoi P., Mazzola A. & Rossi R., 1999. Pesca del novellame da allevamento: valutazione di una attività e sue prospettive. In: *La pesca del novellame, Laguna, 6 (suppl)*, 129-135.

C.V.N., 1999. Monitoraggio delle attività di pesca artigianale e del pescato in laguna aperta. Accordo di Programma Magistrato alle Acque, Provincia di Venezia. Studio C.4.3. Relazione finale.

Franzoi P., Trisolini R., Carrieri A. & Rossi R., 1989. Caratteristiche ecologiche del popolamento ittico ripario della Sacca di Scardovari (Delta del Po). *Nova Thalassia*, 10, (suppl. 1), 399-405.

Franzoi P. & Pellizzato M., 2002. La pesca del pesce novello da semina in laguna di Venezia nel periodo 1999-2001. *Lavori Soc. Ven. Sc. Nat.* 27, 57-68.

ICRAM, 1994. Indagine preliminare sull'utilizzo della draga idraulica (turbosoffiante) per la pesca dei bivalvi in ambiente lagunare. *Quaderni* N. 7.

Munford J.G. & Laffoley D., 1994. *The management of lagoons to conserve their naturale heritage.* In: Falconer R. A. and Goodwin P. (Eds.), Wetland Management, Thomas Telford Services Ltd., London, 270-282.

Pellizzato M. & Giorgiutti E., 1997. *Attrezzi e sistemi di pesca nella provincia di Venezia.* Amministrazione Provinciale di Venezia, A.S.A.P., 190 pp.

Pranovi F. & Giovanardi O., 1994. The impact of hydraulic dredging for short-necked clams, *Tapes spp.,* on an infaunal community in the lagoon of Venice. *Sci. Mar.*, 58, 345-353 pp.

Provincia di Venezia, 2000. *Piano per la gestione delle risorse alieutiche delle lagune e della provincia di Venezia,* 102 pp.

Rossi R., 1981. La pesca del pesce novello da semina nell'area meridionale del Delta del Po. *Quad. Lab. Tecnol. Pesca,* 3, 23-36.

Rossi R., Franzoi P. & Cataudella S., 1999. Pesca del pesce novello per la vallicoltura: una esperienza nord-adriatica per la salvaguardia delle zone umide. In: *La pesca del novellame, Laguna, 6 (suppl.)*, 6-20.

Sfriso A., 2000. *Eutrofizzazione e inquinamento delle acque e dei sedimenti nella parte centrale della laguna di Venezia.* In: (CVN, MAV, LLPP, eds), Nuovi interventi per la Salvaguardia di Venezia, Venezia, 3 vol.

Zerbinato M., 1972. Camera di Commercio Industria Artigianato e Agricoltura Venezia. Relazione sull'andamento dei mercati ittici all'ingrosso di Venezia e Chioggia.

Zolezzi G., 1944. *La pesca nella provincia di Venezia, Boll. Pesca Idrobiol.* 231 pp.

AREA 2.
ARCHITECTURE AND CULTURAL HERITAGE

RESEARCH LINE 2.1.
Protection from high waters and architectural conservation

THE CATALOGUE OF THE EXTERNAL PLASTERS IN VENETIAN BUILDING

E. Danzi, M. Piana
Dip. Storia dell'Architettura, IUAV, Venezia

1. *The research and aims.*

The lagoon building culture has always entrusted precise duties of protection to the external coverings. The utmost slenderness of the venetian building walls, due to the search of the maximum lightness, has called for the assumption of any possible care for their protection: even a small decrease of their section could spark off serious phenomena of instability, with consequent dangerous disruptions. So, besides their undoubted aesthetic and formal value, the venetian finishes and plasters have always been applied on the external fronts also with the precise aim of avoiding the masonry decay: a sort of sacrifice surface with the task of assuming the decay due to the combination of weathering, saline aerosol and, at the building footing, capillarity with the consequent cycles of saline crystallization.

So far the studies concerning the plasters in the historical venetian building, mostly developed in the last twenty years, have only partially explained the technical and formal evolution of the external plasters over the centuries (Armani - Piana, 1982; 1984; 1985; Piana, 1988), and partially about their composition and decay (Biscontin - Piana - Riva, 1982; Charola - Laurenzi Tabasso - Lazzarini, 1985; Biscontin - Piana - Riva, 1986). Nevertheless at present it is still missing a quantitative information outlining the type, the stratification, the location in the city center and the present condition of the venetian plasters.

A huge amount of ancient coverings is still present on the external fronts of the city buildings: for example, there are several hundreds of plasters, generally frescoed in XIVth and XVth centuries, sometimes reduced in fragments, other times almost integrally preserved which every day, missing any

kind of information concerning their nature and value, run the risk of vanishing because of careless interventions of maintenance or restoration.

A sector of line 2.1 of the Corila research has been thus dedicated to a systematic survey and record of the historical external coverings of the city building. The recording of the plasters of the historical venetian centre, with data computerization, aims at collecting extensive informations about their nature and causes and types of their decay. This cataloguing is very demanding because of the large number of building (almost 15.000), but essential for any further investigation in this field. It will set up the base from which moving for the collected data processing, planned for the final phases of the research: this will allow to describe precisely the technical and formal evolution of the plasters, permitting a reconstruction of the city aspect over the centuries.

Moreover, the cataloguing will allow the carrying out of sampling of the most interesting plasters; the following chemical-physical analyses on the samples will aim to determine the specifications of composition and technologies used in the various categories of covering (*regalzieri* and medieval decorations, *marmorini* in one layer or with *cocciopesto* background layer, etc.). With the chemical-physical analyses, carried out on representative samples of each categories and datable for a certainty, it will be possible to set up a database which at the future time will be a reference for not otherwise datable plasters.

We will aim to evaluate, again through the chemical-physical analyses, the most significant interventions of consolidation, restoration and integration of plasters realized in the city in the last twenty years. These interventions, performed with different methods and materials, will be analysed, in the final fase of the research, to evaluate the efficacy of the adopted systems and the acceptability af the results under the architectonic and formal point of view.

Also in this case, the final target of this sector of the research is to provide methodological criteria which will be useful for guiding next interventions of conservation and restoration of the external coverings of lagoon building.

The cataloguing of venetian plasters, in the end, computerized and available for the public administration (Municipality and Monuments and Fine Arts Office), will become an instrument of great value, open to future updating and integration, immediately usable for the control, the protection management and the programming of the restoration interventions on the historical building heritage.

2. *The venetian plasters.*

The categories of historical plasters, singled out according to a classification by age and type, are the *stabiliture* (for example the *regalzieri*, the plasters with monochromatic painting, the plasters with decorated bands or outlining the openings, the *painting* layers applied on stone or masonry), the frescoes (figurative or not), the *marmorini* (in the version with one layer or on a layer of *cocciopesto* or sand, with white, pink or colored body, provided with in relief, colored, engraved bands and with underlined sharp edges), the common plasters (made of sand, brick or decorated). Also the plasters of XX and XXI centuries are classified, even if in a semplified way, together with other categories of covering: the stone coverings, the brickworks at sight, the removed coverings, and so on (Armani - Piana, 1984; 1985).

The *regalzieri*, the figurative frescoes and the *marmorini* are among the most interesting categories of plasters for their technological and formal qualities and for their importance and diffusion.

The *regalzier* is the kind of plaster most predominant on the medieval buildings: it vanished at the end of the XVth century, but very popular in the common building through all the Cinquecento (in the same centuries it spread in other zones of the peninsula and in large european areas); it is the reproduction of a dummy brickwork, frescoed on plaster made of one thin layer (Piana, 2000; Schuller, 2000; Wolters, 2000).

Fig. 1 - Venice, Santo Stefano Church: decoration reproducing a dummy brickwork, called as regalzier, on the right side of the building; XVth century.

Fig. 2 - Venice, San Luca, Palazzo Cavalli: fragment of red and white regalzier, end of XIVth century (?).

The white pointing weave is overlapping on a reddish background surface painted with large brushstrokes: these white painted pontings are often led by horizontal engravings, traced out with nails on the fresh plaster in harmony with the underlying true pointings.

The incongruity of an operation which methodically hides a true brickwork with an imitation one is only outward: this practice is justified by the will to standardize the color and design of the building surfaces. This was required by the marked variability of the medieval venetian brickworks, built with bricks of different tonality or size. The difference of size was due to the practice of using again material coming from demolished buildings or, because of the long time between the beginning and the end of a building, the contextual variation of the brick size.

Occasionally, in those parts of the brickworks subjected to smoothing, the *regalzier* was painted with oily binder paint, directly applied on the brick surface, as it was done on the external stone surfaces such as the famous case of Cà d'Oro or the bicoloured covering of Palazzo Ducale (Cecchetti, 1886; Boni, 1887; Piana, 2000; Schuller, 2000).

The imitating brickworks, widespread both in the civil building and in the religious one, were often matched with painted bands with phytomorphical, geometrical or marble like decorations (Bristot, 2000; Piana, 2000).

Fig. 3 - Venice, San Canciano, Palazzo Van Axel: band with phytomorphical decoration (XVth century).

Fig. 4 - Venice, San Luca, serial building: band with phytomorphical decoration (half XVIth century).

The figurative frescoes are less common, but very significant for the venetian history of art (Zanetti, 1760; Foscari, 1936; Wolters, 2000). It deals with decorations appeared in the Renaissance (the majority of them belongs to the XVIth century); nearly all the venetian painters of the Cinquecento practised their art on some urban fronts: from Giorgione and Titian to Veronese, Pordenone and Tintoretto. Beginning from the second half of the XVIth century, nevertheless, the gusto for the figurative decoration of the fronts declined, due to a general change of the cultural taste more than the reasons of decay due to the weathering (pointed out by Vasari in his *Vite*): the spirit of Counter-Reformation tended to attribute edifying duties to the scenes with human images, confining them in the churches and oratories.

The *marmorino*, in the end, defined *stucco, terrazzo* or *terrazzetto* in the documents of XVIth-XVIIIth centuries, is the most common and local type of plaster, still nowadays characterizing the city of Venice. The *marmorino*, composed of lime and fragments of Istria stone, was applied directly on the brickwork until the first decades of the XVIIth century, afterwards it was applied on a preparation layer made of *cocciopesto*.

Fig. 5 - Venice, San Severo, Palazzo Cavagnis: marmorino applied on a preparation layer made of cocciopesto (XVIIth century).

These coverings are characterized by the high accuracy of execution and the final treatments with linseed oil or soap and wax (Viola Zanini, 1629; Biscontin - Piana - Riva, 1982; Piana, 1984; Biscontin - Piana - Riva, 1986). The *marmorini* appeared in the city between Quattrocento e Cinquecento, in parallel with the propagation of the new architectural language; the reason of their quick diffusion and huge success in the next centuries must be identified in the capacity of the *terrazzetti* to evoke, sometimes to imitate strictly, the aspect and consistency of stone materials, in Venice expecially Istria stone, but we can find also colored *marmorini*, pinkish, yellowish or grey-cerulean (Piana, 1988; 1989).

Also great part of the "common" plasters, realized in the city in the XVIth-XIXth centuries with sands and *cocciopesto*, tried to imitate, in a poor way by executive expedients, the aspect of the more precious and expensive *marmorini*.

Bibliography.

Armani E., Piana M., 1982. *A Research programme on the Plaster of historical Buildings in Venice*, in: *Mortars, Cements and Grouts used in the Conservation of Historic Buildings*, atti del symposium ICCROM, Roma, pp. 385-400.

Armani E., Piana M., 1984. *Primo inventario degli intonaci e delle decorazioni esterne dell'architettura veneziana; indagine e classificazione degli intonaci colorati di una città che fu policroma*, in "Ricerche di Storia dell'Arte" n° 24, pp. 44-54.

Armani E., Piana M., 1985. *Le superfici esterne dell'architettura veneziana*, in: (a cura di Rotondi Terminiello G.) *Facciate dipinte, conservazione e restauro*, atti del convegno, Genova, pp. 75-78, figg. 101-103.

Biscontin G., Piana M., Riva G., 1982. *Research on Limes and Intonacoes of the historical Venetian architecture: Characterization on some Marmorino intonacoes from the 16th to the 17th century*, in: *Mortars, Cements and Grouts used in the Conservation of Historic Buildings*, atti del symposium ICCROM, Roma, pp. 359-371.

Biscontin G., Piana M., Riva G., 1986. *Aspetti e durabilità degli intonaci "marmorino" veneziani*, in: "Restauro e Città" 3/4, pp.117-126.

Boni G., 1883. *Il colore sui monumenti*, in: "Archivio Veneto", XIII, t. XXV, pp. 26-43.

Boni G., 1887. *La Cà d'Oro e le sue decorazioni policrome*, in: "Archivio Veneto" XXXIV, pp.115-132.

Bristot A., 2000. *Gli affreschi esterni di Santa Maria Gloriosa dei Frari*, in: (a cura di Valcanover F. e Wolfgang W.) *L'architettura gotica veneziana*, atti del convegno Istituto Veneto di Scienze, Lettere ed Arti, Venezia 2000, pp. 189-194.

Cecchetti B., 1886. *La Facciata della Cà d'Oro dello scalpello di Giovanni e Bartolomeo Buono*, in: "Archivio Veneto", XXXI, pp. 26-43.

Charola A., Laurenzi Tabasso M., Lazzarini L., 1985. *Caratteristiche chimico-petrografiche di intonaci veneziani del XIV-XX secolo*, in: atti del Convegno di Bressanone, *L'intonaco: storia, cultura e tecnologia*, Padova 1985, pp. 211-21.

Foscari L., 1936. *Affreschi esterni a Venezia*, Milano.

Piana M., 1984. *Una esperienza di restauro sugli intonaci veneziani*, in: "Bollettino d'Arte", Ministero per i Beni Culturali e Ambientali, 6, pp.103-106.

Piana M., 1988. *Gli intonaci Veneziani*, in *Primo corso di perfezionamento in restauro architettonico dell'Istituto Universitario di Architettura di Venezia*, Venezia, pp. 183-191.

Piana M., 1989. *Tecniche edificatorie cinquecentesche: tradizione e novità in Laguna, in: D'une ville à l'autre: structures matérielles et organisation de l'espace dans les villes européennes (XIII-XVI siécle)*, atti del convegno École Française de Rome, Roma, pp. 631-639.

Piana M., 2000. *Note sulle tecniche murarie dei primi secoli dell'architettura lagunare*, in: (a cura di Valcanover F. e Wolfgang W.) *L'architettura gotica veneziana*, atti del convegno Istituto Veneto di Scienze, Lettere ed Arti, Venezia, pp. 61-70.

Schuller M., 2000. *Le facciate dei palazzi medioevali di Venezia. Ricerche su singoli esempi architettonici*, in (a cura di Valcanover F. e Wolfgang W.) *L'architettura gotica veneziana*, atti del convegno Istituto Veneto di Scienze, Lettere ed Arti, Venezia, pp. 281-345.

Valcanover F., *Venezia e provincia*, in *Pittura murale esterna nel Veneto*, Bassano del grappa 1991.

Viola Zanini G., 1629. *Della Architettura, libri due*, I, XVI, Della prattica delle malte, Padova.

Wolters W., 2000. *Architektur und ornament. Venezianischer bauschmuck der renaissance*, München, pp. 73-97.

Zanetti A. M., 1760. *Varie pitture a fresco de' principali maestri veneziani*, Venezia.

THE PLASTERS DATA BASE

A. Ferrighi
Dip. Storia dell'Architettura,
IUAV, Venezia

1. *Introduction.*

The accurate knowledge of the historical plasters of the Venetian buildings is actually the basis for a successful preservation of them: in this specific case knowledge means the systematic collection and management of information, that is search, access and use. With a data system made on a local scale (GIS) you can perform all actions suited to an easy census. The outcoming system – still in course of testing and implementation – has the purpose of creating a geo-related data bank of the outer coatings of the city buildings, thus aiming at getting a quantitative and qualitative knowledge.

2. *Research scope.*

In the research all building organisms of Venice old town center are investigated with no exceptions and no time limits for the buildings. The importance and the features of each research item are taken from a registry data bank processed by Venice Municipality; the instrument they make use of is the "Centro Storico di Venezia" GIS. By means of *ad hoc* queries it has been devised to meet all the peculiar requirements of plasters classification. Two levels have been put together related to "Edificato" and to "Civici Centro Storico" in order to obtain all the coding systems needed for the item identification: each building is linked to its relevant street numbering. In addition to the data coming from the GIS, further data have been put in such as the univocal identification code (so called ID), obtained by putting together the quarter reference, the isle and the building number. Each architectonic unit is identified with a GIS item, represented through an accurate geographical position in the space and a series of features: the plasters data of the real building are collected and then transferred into specific categories of attributes.

3. *The plasters data bank "Plasters DB".*

For the plasters census different kinds of instruments have been provided for: besides the paper cards for the field survey, the computer card for implementation, up to the creation of an actual data bank (plasters DB). These cards have been carried out through accurate elaborations and trials which have produced such easy-to-use and reliable work tools.

3.1 *Survey cards.*

The complete drawing up of the paper cards has started off the survey campaign. The card is made up of two sheets: the former card or sheet, we call A for simpleness' sake, refers to all the data of the building and of the plasters in general which are present on the outer fronts; the latter, the card called B, is aimed at collecting the data referred only to historical inlayers plasters of peculiar importance, showing how different the investigation shall be for buildings with historical plasters.

Card A is filled in for all the buildings of the old town center, and for each card the data coming from GIS have been put in: in this way no misunderstandings can arise during the field survey, since card and architectonic unit match in one way. Not only the identification code, but also the whole toponymy related to the building (names of the road areas and street numbers) has been put in the card through different operations carried out on "Centro Storico di Venezia" GIS.

A small window has been devoted to the planimetry, in which the building is set in its context in order to recognize it more easily during surveys and write in the plasters codes of the fronts by hand. In order to display the plans to be entered into relevant field, the active layers in the GIS are referred to islands, canals, public areas, buildings and street numbers. To each of them a colour is given so that objects and spaces can be easily recognized.

An important remark shall be made for the the first data to fill in. Next to the data collector's name and to the date of the survey, three fields have been introduced with following wordings: surveyed AU, partially surveyed AU, not surveyable AU. For each architectonic cunit all outer fagades have to be examined, giving confirmation whether all fronts are visible; in this way it is possbile to take a census of all the plasters placed on the outer fronts: the survey of the AU is thus definitely carried out. In the opposite cases, that is if it is not possible to make a survey of one front at least or even of all fronts (because of scaffoldings for building works in

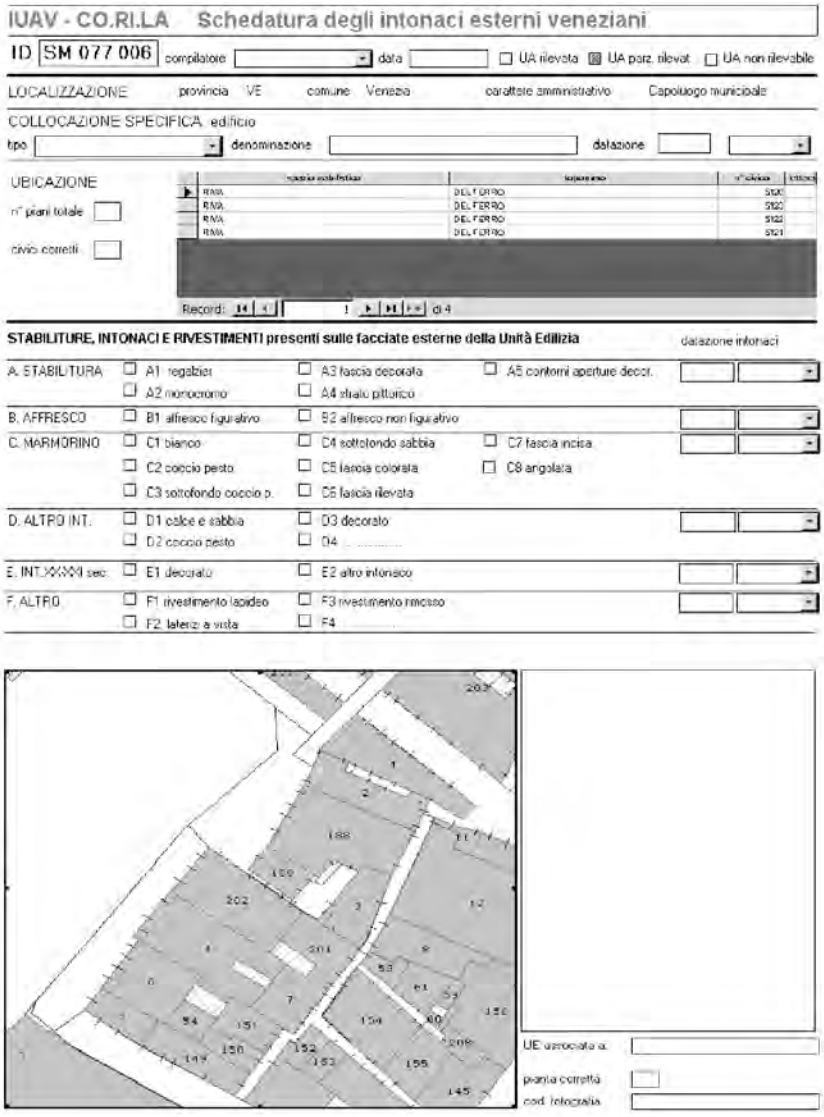

Fig. 1 - Card A. The figure shows the print of an architectonic unit card (AU) to be filled in. It refers to the AU n° 6 of the island 77 in S. Marco quarter, Riva del Ferro, ID Code SM077006. In the box below on the left side of the card you can see the map of the area all around the AU. It is used to enter the remarks of the codes of the plasters of the outer facades.

progress or because the front opens onto a private area), you have to choose between the two remaining possibilities.

To the census purposes, the most important section of Card A refers to the plasters section: by filling it in, it will be possible to determine which plasters have been surveyed and where they are. The plasters have been divided into categories, classified on their turn into types according to a chrono-typological rule.

Card B, the close examination card, is necessary to understand the features of the historical plasters through relevant stratigraphic ratios in a small but significant front portion. The card must clearly show the physical characteristics of the plaster on a macroscopic scale and the stratification of the different coatings (plasters carried out in different times: for instance, a recent cement plaster coat laid upon a XVIIth century lime and sand plaster coat). The description of coatings and layers starts from the layer adhering to the support (brickwork) up to the most external layer. Of both of them the class is recorded first, then for each class the type/types, and eventually they are described in detail in a free text. A further window has been introduced for the sketch of the front portion including the investigated item, in case it should not be possible to get a good picture.

Card B is designed to be "blank" , i.e. with no pre-compiled data in it, as it is not possible to know in advance which buildings with historical plasters will be object of a close investigation.

For the plasters of major interest, "representative" of relevant categories, a further card C will be used in addition to the mentioned second sheet, reporting the chemico-physical features, investigated and analyzed in the lab taking plaster samples.

3.2 *How the Plasters DB is organized.*

All the cards written up during the survey are entered in the new data bank (plasters DB), which is the result of several reworkings of the data base connected to "Centro Storico di Venezia" GIS, the structure of which has been designed by Ing. Stefania de Zorzi of CORILA.

To this purpose new tables have been created linked to one another through a ID_Edificio key (AU identification code) with a "one-to-many" relationship to the other cards specific for the plasters or the samples connected to it. This particular kind of link has become necessary as, though the AU remains the same, the plasters of that unit can be many. Branchings all depart from the main table "tbl_Edificio" containing the

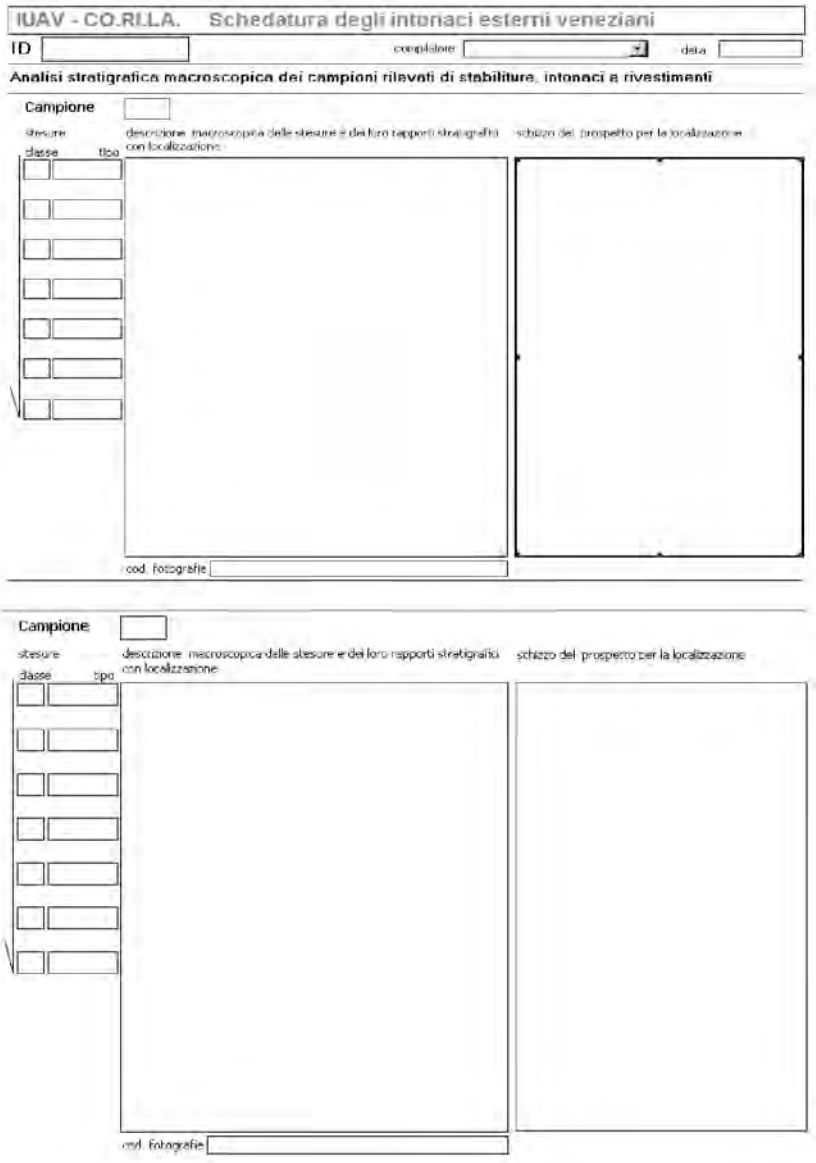

Fig. 2 - Card B. The figure shows a print of a "blank" Card B; for each sheet it is possible to put in the data of the two plaster samples. Each window has to be compiled by the field surveyor.

whole features of AU, ID, location, up to the building type, including the denomination specific to that AU. As already said, the other linked tables are referred to the plasters and plaster samples of that same AU, the dating of the major building or transformation phases of that AU ("Tbl_data_certa" / "Tbl_data_presunta"), the dating of the plasters ("Tbl_data_intonaco") and to the table for the input of AU pictures ("Tbl_data_edificio").

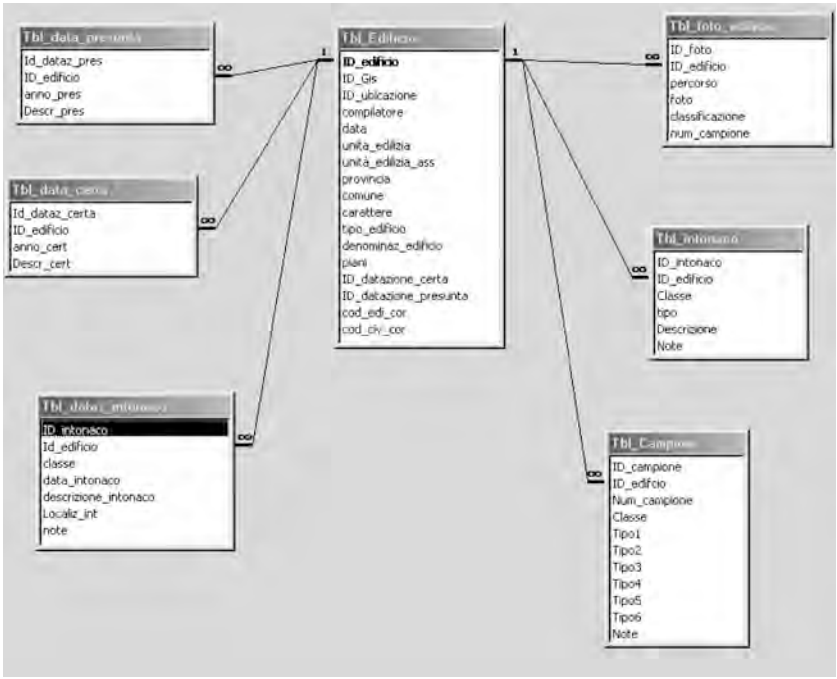

Fig. 3 - How the plasters DB is organized. The figure shows how the tables of the new data bank (plasters DB) are organized through their "One-to-many" relationships. The plasters, samples tables and so on are linked to the main table relative to the AU .

3.3 *Implementation cards.*

The data filled into the paper cards are transformed into alphanumeric data by inputting them into the DB through special frames written up with ACCESS software. The format of such frames, provided for the purpose of easing up the data input into tables, is different from the one of the tables used for the field survey. It has been necessary to design four frames

in total, with a specific layout each, for the respective information blocks to be put in. Inquiry occurs through links (connection keys): it is possible to skip form a frame to another within the same architectonic unit.

The frame "Dati generali" coincides with the first section of the paper card: it contains the general data block. The implementator puts the information into the check cells corresponding to the fields, moving forward simply with the TAB key (that is by pressing the TAB key of the keyboard); the check cells have been devised so as to prevent the input of any data different from the ones contained in the list of the controlled items.

Fig. 4 - General Data Frame. The frame for the input of the general data is made up on its turn of sub-frames relative to the tables for AU dating and locating.

Once the data input related to this section of the electronic card is over, it is possible to carry on the inquiry by pressing the two keys "Inserisci immagini" or "Inserisci data di nuovo edificio"; each of them implies most clear inquiry purposes. As clearly shown by its name, the latter key is necessary to skip to a new card: it is used in case data have been filled in relative to a building which is not possible to be surveyed, then no further data of that same building are available to be added. The inputting function of the former key occurs on the contrary as usual.

From the first frame it is possible to skip to the one used to input the pictures concerning both the building and the plaster samples: this frame is linked to a back up file for photos. The pictures are taken with digital cameras equipped with wide-angle and telephoto lens, saved in *.jpg format and named according to accurate rules in order to prevent any mismatching. Each picture file is named after the identification code of the related architectonic unit and has got an extension through which it is possible to specify both the kind of the picture (G for general, PM for intermediate detail or PP for detail) and the number of clicks for that unit. For instance: the file CS066032_01G.jpg corresponds to the general picture of unit 32 of the island 66 of the Castello quarter.

Fig. 5 - Photographic documentation frame.

By pressing the inquiry keys it is possible to skip to the third frame "Stabiliture, intonaci e rivestimenti presenti sulle facciate", corresponding with the second section of the paper card for which a particular accuracy is required as it concerns the input of the data related to the plasters on the outer building facades. Through the table linked to this frame it is possible to get the inquiries necessary for the data crossing; for instance, by making inquiries into these lists, you can get the figures corresponding to the "regalzien"$_c$ (a peculiar kind of surface finish), to the "Marmorini"

coats out of the total amount of the historical plasters. It is of course an elaborate frame made up of six sheets, each of them concerning a specific plaster class. Each sheet is compiled according the same method. On the page related to a kind of plaster two blank cells are present: the former contains the data of the plaster dating and some remarks; the latter the data of the different plaster kinds.

Fig. 6 - Frame of skim coats, plasters and coatings on the facades. Frame is open on page "E. XIXth-XXth cent. Plaster coat", where the file relative to "E2 altro intonaco", has been written up, that is to a recent cement-like plaster. As a matter of fact, in the dating frame, the filled in control cell refers to the end of XXth century.

Eventually it is the turn of the frame "Analisi stratigrafica macroscopica di stabiliture e intonaci dei campioni rilevati" only in case of samples of a historical plaster which is analysed in its stratigraphic ratios. This frame is made up of several sub-frames as well, each of them corresponds to a sample; the display mode has been devised in order to reproduce exactly the paper data. For the first sample the number 1 appears automatically and the sub-frame "Sample 1" will get filled in, then in sequence the category and the different types for each drawing up reporting location, features, and so on. On the right side of the sub-frame you can see the icon of the detail picture connected to the analysed sample.

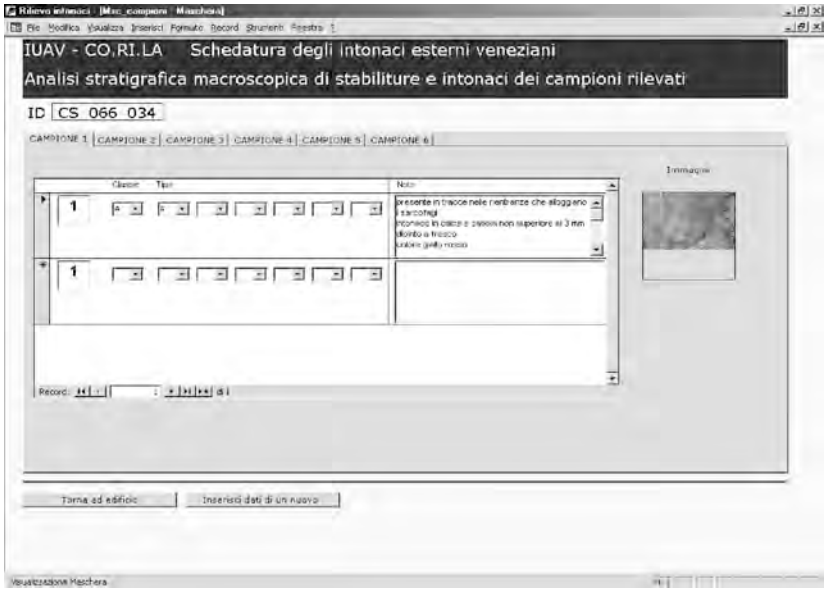

Fig. 7 - Frame for macroscopic stratigraphic analysis of skim coats and plasters of the surveyed samples. It is an actual case of filled in frame.

4. *Topic cards.*

Once survey and data transfer into Plasters DB are over, proper operations in the new data bank have allowed the "Centro Storico di Vennezia" GIS to be updated with all the features concerning the historical plasters.

Through the software Geomedia you can display the DB contents by inquiring the system at will and building up logical operations using the research terms; for instance it is possible to sort out only the AU with historical plasters, or you can learn which class of historical plaster belongs to that specific AU.

Topic cards are generated by this kind of research and data comparison and correspond to a sort of spatial representation of the plasters DB: it is possible to locate the AU and relevant different features on the territory through the levels linked to the attributes. The system flexibility allows to represent the data of the DB by colouring or halfton screening the GIS objects in a different way, thus making the contents of each table – containing only alphanumeric data – visible at once.

Fig. 8 - Mapping of the AU with historical plasters. In the map of the Isle of S. Maria Formosa the brick red underlines the AU which still show some historical plaster coats (XIVth– XIXth century), sometimes only traces of them. The remaining units in grey represent buildings with XXth and XXIth century plasters. Only 22% of the whole AU, already surveyed or partially surveyed, still show historical plasters.

5. *The first results.*

Of the whole Venice old town centre, this first survey campaign has allowed to analyse the Castello quarter. Out of the 25 Castello islands in this phase the inaccessible ones have been left out, such as the island of the dry docks within the *Arsenale* (Main Dockyard) and those where only recent architectonic units can be found, such as the Isle of S. Elena. The whole quarter includes 3.767 units (GIS item building); of 3.225 units out of them a census has been made according to the above described rules.

11% out of total amount of the recorded units have come out as not surveyable, 51% partially surveyable, that is it has not been possible to see a front at least, 38%, on the contrary, has been totally surveyed in all relevant outer fronts.

On the total amount of the both completely and partially surveyed units – which means 89% of the total AU – it has been possible to carry out all inquiries concerning the historical plasters. The major portion of

the historical plasters belongs to class "D. Altro intonaco", the common lime and sand (62%); only 10% belongs to class "A. stabilitura", finish coats such as *regalzier*, monocromo, and so on; only 1% belongs to class "B. Affresco", 27% belongs to class "C. Marmorino" .

These are figures arousing encouragement and concern at the same time: the data confirm that Venice is, among the big Italian old towns, the city which still has a remarkable number of historical plasters, certainly to a greater extent than other cities; on the other hand they also give evidence how far demolitions, restorations and rebuildings, often uncultured and pointlessly destructive, occurring more and more often, have really jeopardized one of the most interesting and peculiar finish examples of the lagoon architecture.

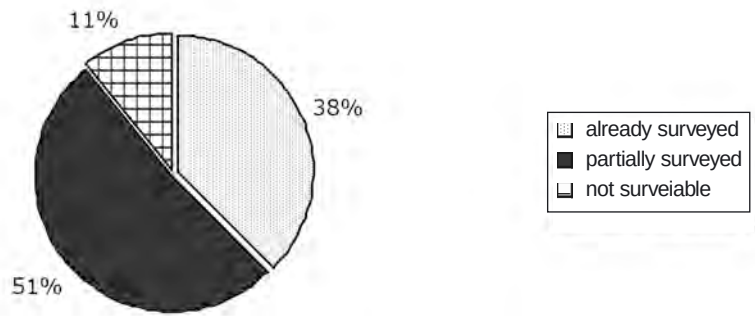

Fig. 9 - Diagram of surveyed AU's.

DATA-BASE "VENETIAN SKILLED WORKERS" (MAESTRANZE VENEZIANE) XVth-XVIIIth CENTURIES

S. FOSCHI, M. MORRESI
Dip. Storia dell'Architettura, IUAV, Venezia

This data-base arises from the necessity to know in a specific way not only the identity and the precise role of each master engaged in the various Venetian yards opened from the fifteenth to the late eighteenth century, but also the composition of the teams or workshops involved: this with the aim to specify their displacements or exchanges of professionalism and role among the different buildings.

The data-base intends to collect all the registered news concerning the skilled workers in action in Venice between XVth and XVIIIth centuries, coming from both printed or unpublished archives and publications.

Prof. Manuela Morresi is responsible for the ideation and scientific management of the project, Nexus – Sistemi Informatici SPA –Florence is in charge of the data-base programming in co-operation with Pierre Picotti, from the Office for bibliographic and documentary services of the IUAV.

Two different softwares, named EasyCat and EasyWeb, are programmed for the implementation on the Web of the collected data concerning the Venetian skilled workers.

EasyCat is the software used for the collection and the implementation of the data, while EasyWeb is the system for the use of the catalogue (or on-line catalogue), predisposed for the consultation on Internet of the data put in with EasyCat, at present in progress and soon consultable on the IUAV web-site, bibliographic and documentary services.

EasyCat, the program for data input, schedules the creation of three basic files: Skilled Worker-Records, Yard-Records and Presence-Records (figgs. 1, 2, 3).

During the implementation of the data it is possible to link the basic records: each Skilled worker-Record is linked to the necessary and relevant Yard-Record and Presence-Record, so that the name of the skilled worker is displayed together with all the information (dates, role, yard) which can be used to reconstruct his professional life (fig. 4).

From "Vedi Presenze" (see presences) it is possible to link to the list of the presences of the considered skilled worker in the various Venetian yards (figgs. 5, 6).

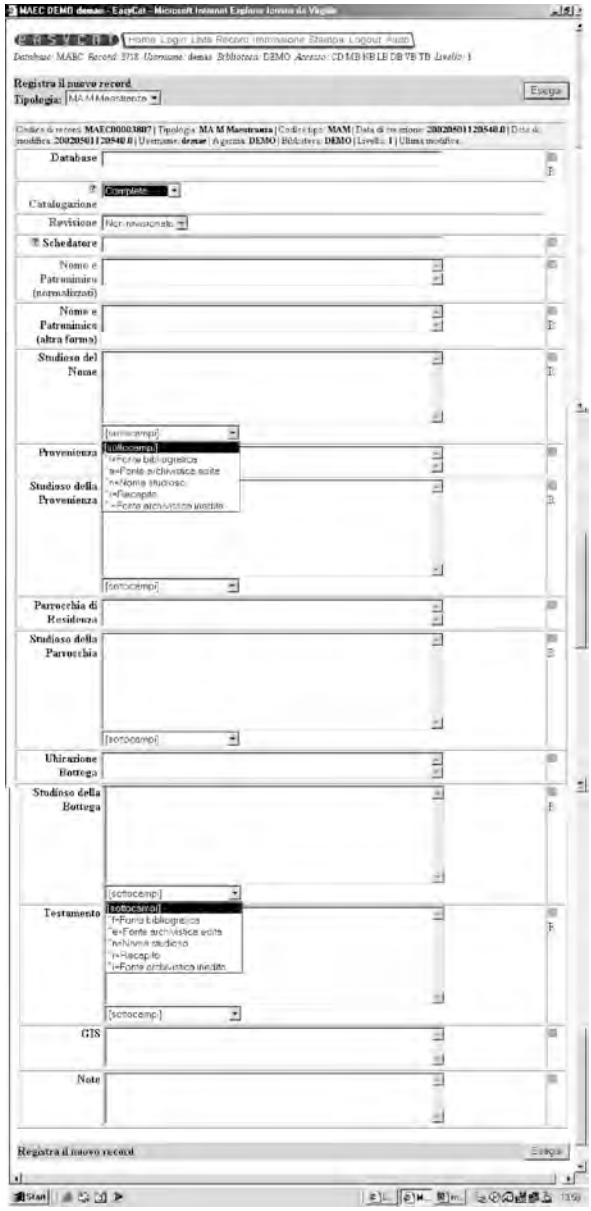

Fig. 1 - Example of Skilled Worker-Record. The input data in the fields and secondary fields give the information concerning the personal data of the skilled workers and the bibliographic references and archives (published or unpublished) concerning each reported information.

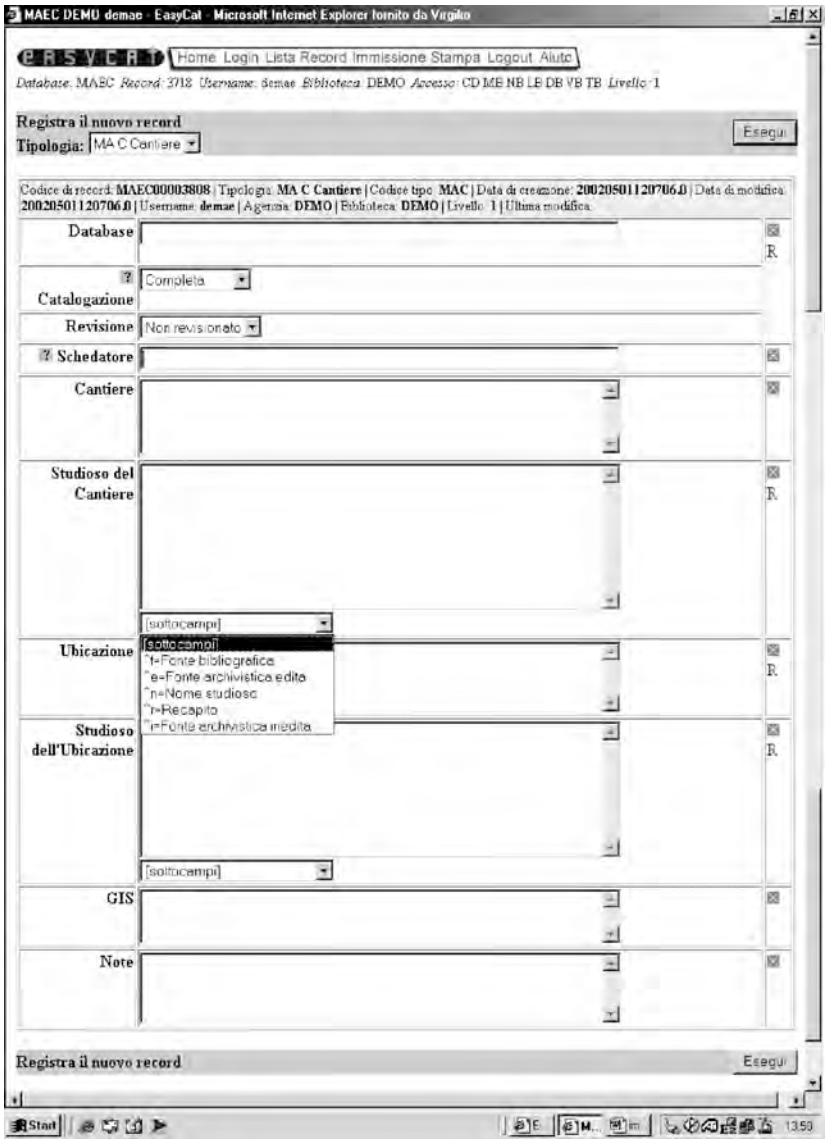

Fig. 2 - Example of Yard-Record. The input data in the fields and secondary fields give the information concerning a yard and the bibliographic references and archives (published or unpublished) concerning each reported information.

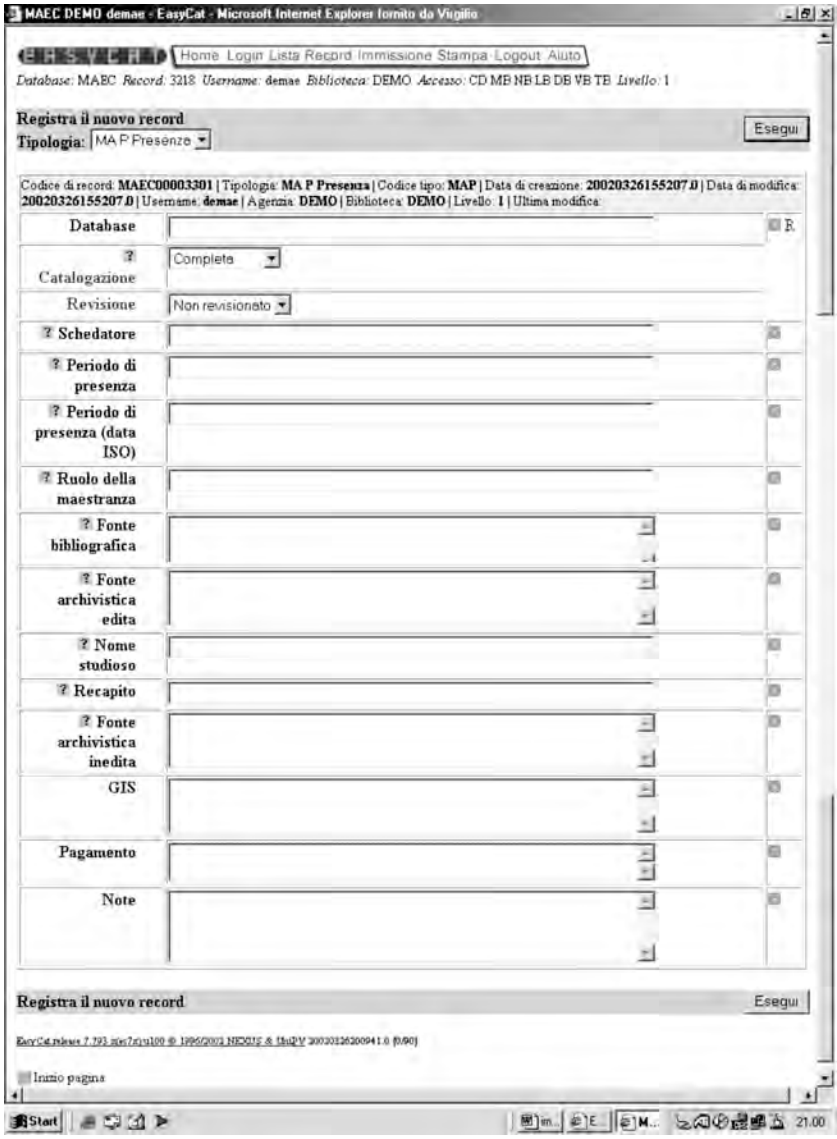

Fig. 3 - Example of Presence-Record. The input data in the fields and secondary fields give the information concerning the presence of the skilled workers in a yard and the bibliographic references and archives (published or unpublished) concerning each reported information.

Fig. 4 - Example of display of a record concerning a skilled worker. All the input data of the Skilled worker-Record are displayed and there are links to the presences in the various yards identified during the implementation of the data.

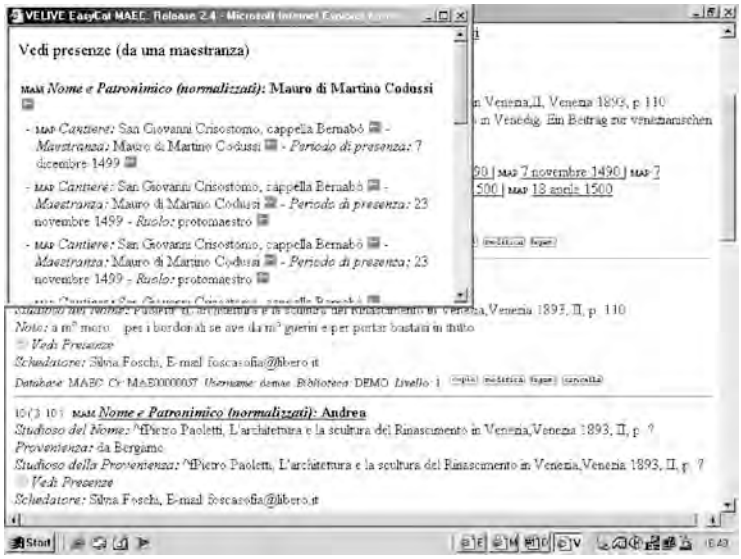

Fig. 5 - From the record of the skilled worker it is possible to link to the list of his presences in the various Venetian yards.

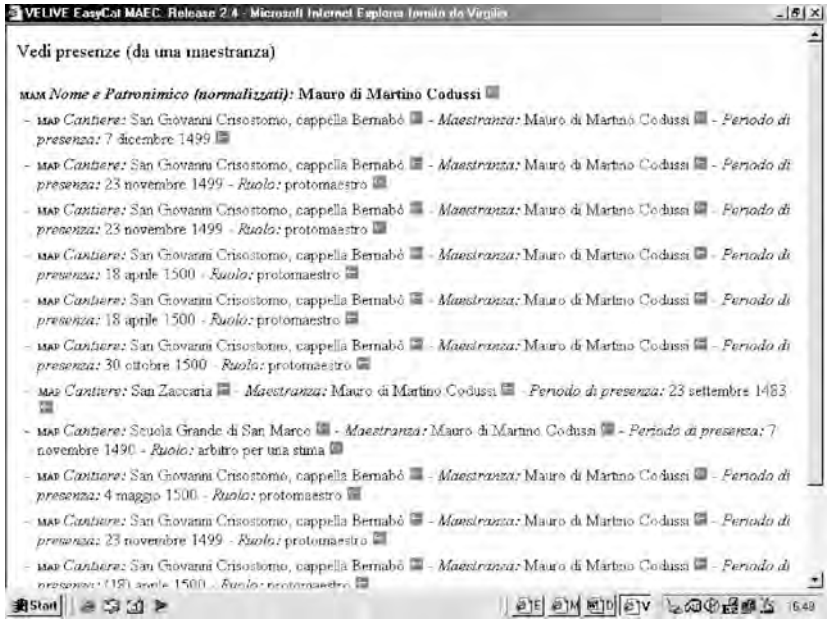

Fig. 6 - Presences of the considered skilled worker in the various Venetian yard.

From each of these "presenze" (presences) it is futher possible to link to three different kind of information: for example to the Yard-Record concerning San Giovanni Crisostomo (fig. 7).

From the "Vedi Presenze" (see presences) then it is possible to link to list of the skilled workers the work there (fig. 8), otherwise it is possible to link to the information concerning the who single presence of the considered skilled worker within that yard (fig. 9).

Finally, it is possible to link to the Skilled Worker-Record with all the input data concerning the considered skilled worker (fig. 10).

Further links, which is possible to create during the implementation of the data, will be able to give further information concerning the presence of collaborations within the same yard among various skilled workers.

In figure 10, the underlined dates further link to Presence-Records where the considered skilled worker works together with other people.

For example, on September 23rd 1483 Mauro Codussi works with Pietro Lombardo (fig. 11).

From this "Scheda-Presenza" (Presence-Record), where Pietro Lombardo is associated with Mauro Codussi, then you can link to the information of the "Scheda-Maestranza" (Skilled worker-Record) concerning Lombardo, in order to get all the personal data of Pietro Lombardo (fig. 12).

Fig. 7 - Record concerning a yard. Coming from the list of presences (fig.6) it is possible to link to the records with the complete information, in this case about the yard where the skilled worker has worked.

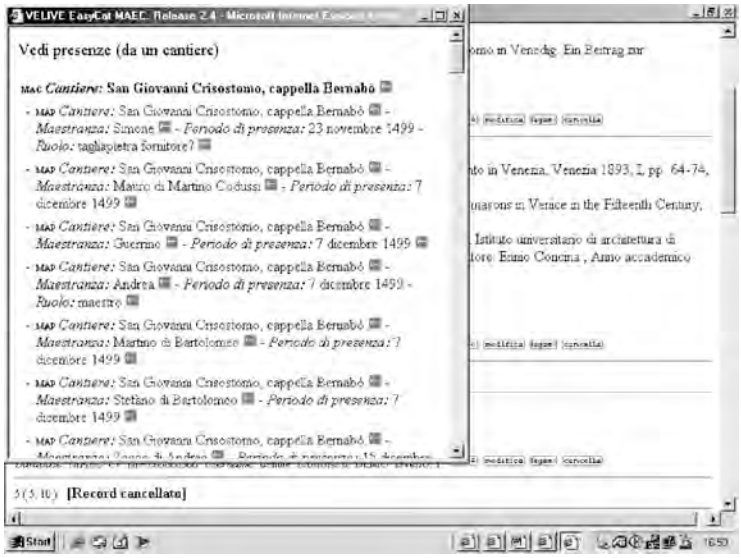

Fig. 8 - From the record concerning a yard (fig.7), it is possible to link to the list of the skilled workers that have worked there, with the dates of their presences.

Fig. 9 - From the list of presences (fig.6) it is possible to link to the record containing the complete information concerning the presence of the skilled worker in the yard.

Fig. 10 - From the list of presences (fig.6) you can finally link to the record containing the complete information concerning the skilled worker.

Fig. 11 - From a record concerning a skilled worker it is possible to link to the records with the information concerning the collaboration with other skilled worker. In this case it is displayed the record with the bibliographic information and archives concerning a document where both the names of Mauro Codussi and Pietro Lombardo appear.

Fig. 12 - Record concerning the skill worker Pietro Lombardo.

The specific links, which have been created during the implementation of the data among the collected information, allow multiple investigations which, only for convenience of communication, we could classify as “primary” kind and “secondary” kind.

An investigation of “primary” kind is the one that, raising a query to the system about the name of a yard allows, to know all the skilled workers that have worked there and, accordingly, all the related information (as role, dates, amounts paid, wills and so on) (figgs. 13, 14).

Another investigation of “primary” kind is the one that, raising a query to the system about the name of a skilled worker, allows to know all the yards where he has worked and, accordingly, all the related information (roles, dates and so on) (fig. 15).

And, again, from this record it is possible to link to the list of the presences of the skilled worker in the Venetian yards (fig. 16), otherwise to the collaborations with other skilled workers (fig. 17).

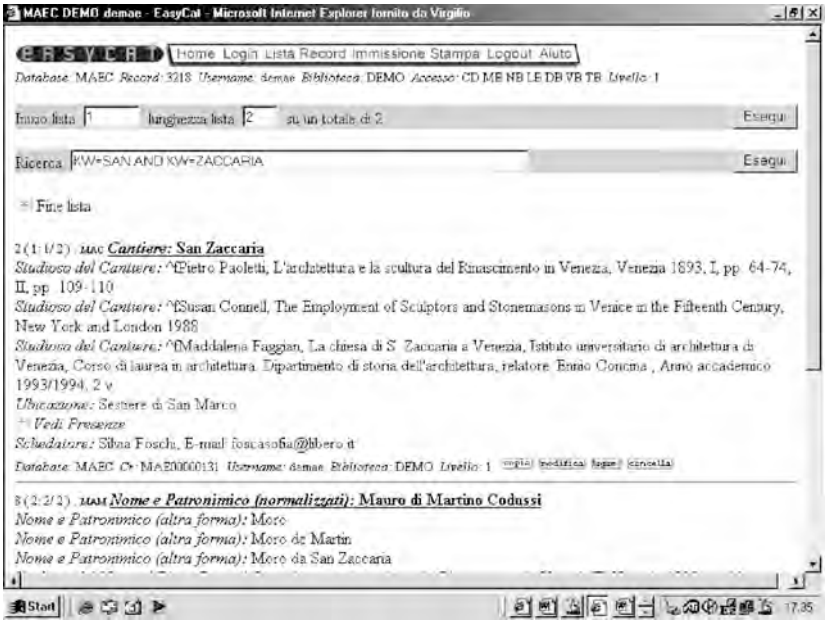

Fig. 13 - Record concerning the yard of San Zaccaria. Example of search done raising a query to the system about a specific yard. All the input data in the related Yard-Record are displayed and it is possible to link to the skilled workers and the related presences detected during the implementation of the data.

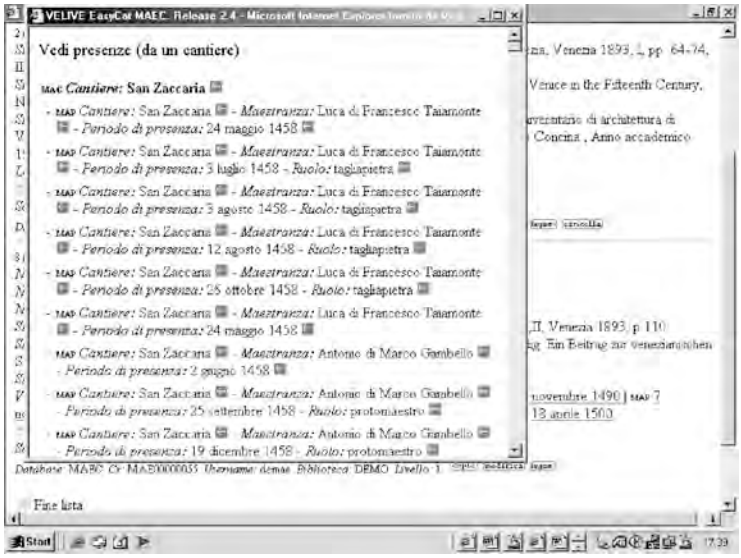

Fig. 14 - Display of the list of skilled workers working in the yard and related dates.

Fig. 15 - Record concerning the skilled worker Giovanni Buora. Example of search done raising a query to the system about a specific skilled worker. All the input data in the related Skilled Worker-Record are displayed and it is possible to link to the yards and the related presences detected during the implementation of the data.

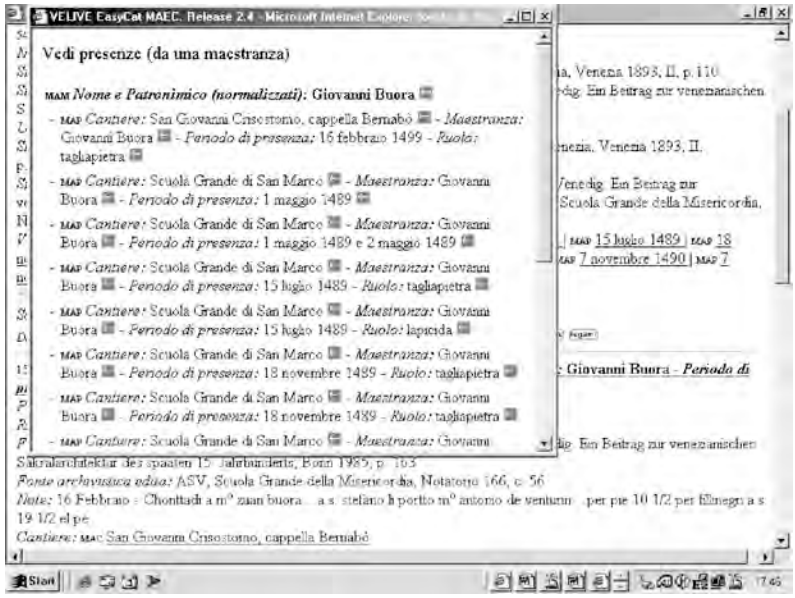

Fig. 16 - List of the presences of the skilled worker in the Venetian yards.

Fig. 17 - Collaborations with other skilled workers.

Investigations of "secondary" kind will be possible raising a query to the system about the contents of each field or more fields combined with each other.

In EasyWeb, thus, along with the search by lists and fields, shown above, a free search will be possible, raising queries to the system with the necessary flexibility to respond to the requirements of the expert who will use this instrument.

The following one is an example of search by fields, where the system has been interrogated about the provenance, in this case about the skilled workers coming from Bergamo (the result is here displayed using EasyWeb) (fig. 18). The result will display the records concerning the filed skilled workers coming from Bergamo (fig. 19).

In conclusion, starting from any "branch" of the "tree" formed by the Skilled Workers/Yards/Presences-Records, all the existing "branches", that are all the input data, will be accessible on the Web (in some cases, agreed upon with the experts who give the transcription of the archives, the unpublished classification will be hidden and then not available on line.)

For the examples used in this demonstration, we have chosen well-known authors and the incompleteness of the related input data is due to the current state of work in progress of the system.

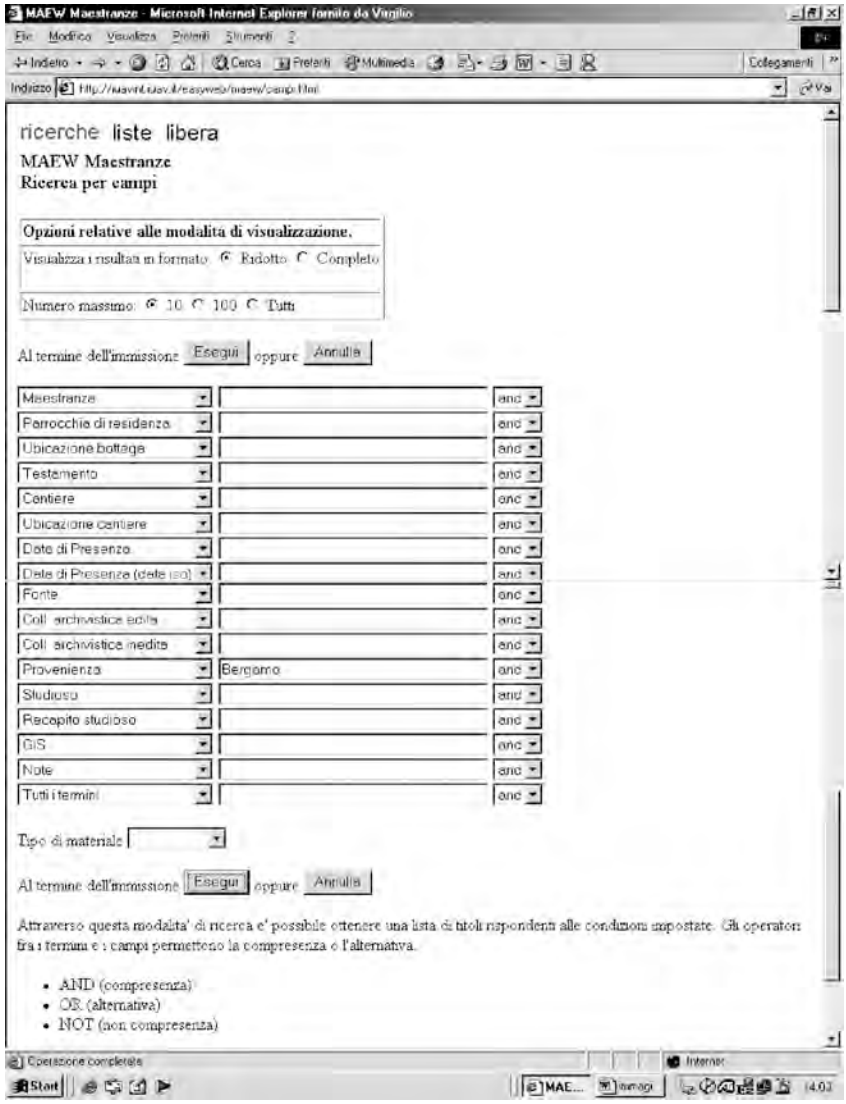

Fig. 18 - Example of search by fields possible with EasyWeb. In this case the system has been interrogated about the content of the single field "provenienza" (provenance).

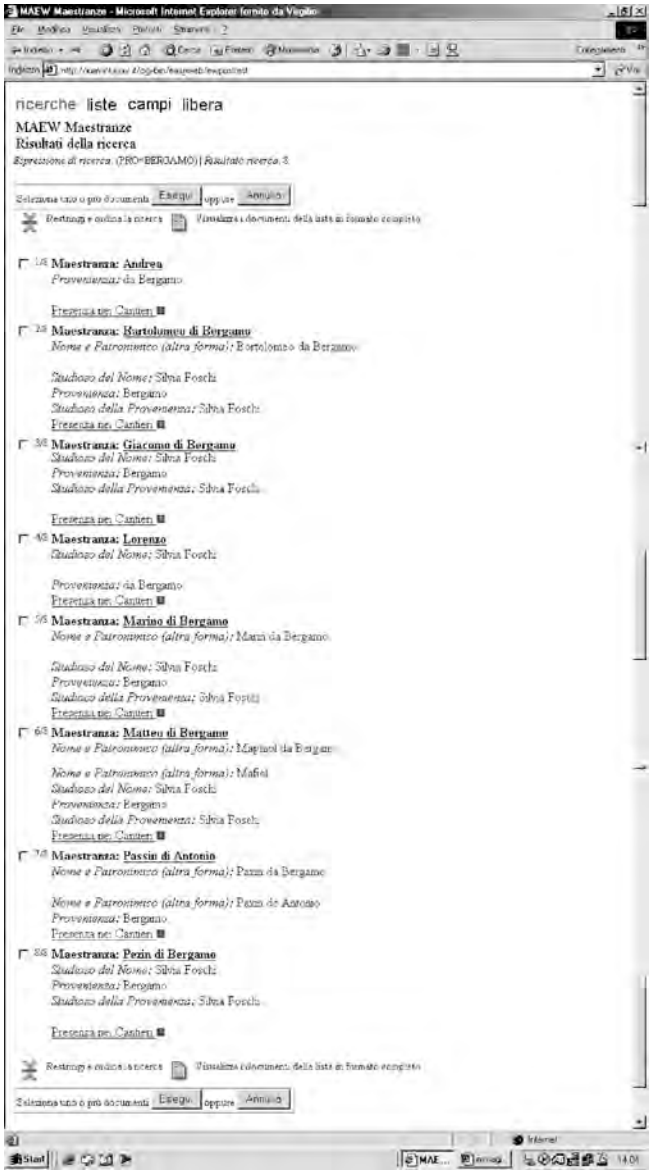

Fig. 19 - Display of the search by fields. In this case the list of the skilled workers coming from Bergamo is displayed. From each of those records, here displayed in small size, it is possible to link to the related records with the information in full size.

THE LAGOON BUILDING AND WATER

P. FACCIO
Dip. Storia dell'Architettura, IUAV, Venezia

The scope of our research is that of studying the relationship between water – by which we mean resurfacing humidity or recurrent flooding tide – and the possible alterated behaviour of the historical structures.

In this first research stage the wall faces are privileged as a structural element, in particular the relationships which might arise between the parameters characteristic of water and salts content and the mechanic features of the walls, giving also indication on the effectiveness of restoration techniques.

For a historical assessment of the phenomenon, it is really fundamental to carry out an archive research on the techniques and the instruments used to monitor and if possible restrain the consequences of the problem.

The research, carried out in kind cooperation with the Monuments and Fine Arts Venice Office, has made it possible to identify a series of architectural items showing the interventions having the purpose referred to before.

Two corrective measures have emerged from the study, the former consisting in techniques making use of accumulation tanks, the latter consisting in several treatments of the wall faces to settle the problem of resurfacing humidity and, in some cases, the consequent desalting of walls.

The solution of the problem concerning recurrent water at flood level is remitted to measures consisting in raising the level of treading floors or using accumulation tanks.

In this last case we make use of accumulation tanks with flexible couplings or tanks with flapped walls and support micropiles. In some cases it is possible to find tanks used as bentonite insulators. In the analysed buildings the mentioned techniques can be found in Duomo of S. Donato on the Isle of Murano, in the Cotton Mill of S. Marta and in the Scuola dei Crociferi.

The solution attempted to settle the problem of water resurfacing in the walls caused by capillarity turns out to be particularly significant and has been applied mainly in the second research stage.

The analysis of the interventions has allowed us to determine actions closely affecting the walls: they describe the attempt of acting on the material chemically or physically or in alternative they illustrate measures which rather drain contact water by means of a canal system.

The concept of barrier against capillary water resurfacing can be generally described using following typologies:

Physical barrier – consisting in inserting water-proof sheets to the basis of the affected walls and replacing the employed plasters with other specific macroporous ones capable of blocking the humidity flow.

Chemical barrier – consisting in boring through the walls horizontally and injecting special resins into the holes which hinder adhesion of water molecules; eventually everything is coated with a macroporous plaster.

Electrosmosis – consisting in creating a magnetic field between wall and land by means of a series of electrodes which repel water with the same polarities as the existing one.

The problem of the barrier against water resurfacing in the analysed cases is faced at the beginning through two techniques which can be defined of a mechanical nature: the cut by inserting a lead plate or in alternative the replacement of the lower part of the wall portions applying the unstitching-stitching technique, widely used in the State Archives.

In some cases the unstitching-stitching solution has been combined with the insertion of the wall-cutting plate and can be observed in the Church of S. Nicolò dei Mendicoli – one of the building belonging to our study cases – and in many walls in Venice.

In the course of years mechanical cutting undergoes some changes, as materials different from lead are used, such as plates made of synthetic materials.

The high disturbing effect of the cutting devices forces the technique to be modified in order to minimize the mechanical impact as much as possible. The methods referred to belong to the range of the chemical cuts or barriers, consisting in inserting resins up to a saturation point - natural seal or at low pressure – into one or two wall bands. This kind of intervention prevents capillary water resurfacing by filling up the pores of the component materials.

The use of resin injection up to a saturation point comes out to be particularly difficult in case of highly disordered walls, as many walls in Venice really are, and for this reason it is not so common.

In the last years those techniques have been preferred which do not foresee any insertion of insulating material into the walls, on the contrary they use electrosmosis. Interventions implying this measure can be found, in the range of our study cases, in Ca' Pesaro and in Palazzo Grimani in S. Maria Formosa.

All the mentioned techniques deal with the problem of the capillary water resurfacing with variable success percentages. Anyway the major result is mainly represented by the role played by salts content in the walls once dehumidification is complete.

This is one of the biggest problems to face as it does persist even once the barrier has been made, a problem which seems to be connected to the physical-mechanical behaviour of the historical wall.

The problem of salts content in dehumidified walls can be solved using desalting techniques by washing - Roperies of Arsenale – and using macroporous plaster coats in combination with dehumidification itself.

The variable permanence of the salts content represents one of the major questions, and the research will go on inquiring on this topic.

This brief report has been put in relation to the current scientific documentation, in particular to the studies aiming at proving possible relationships between humidity percentage and strength features on the one hand and salts content and strength features on the other hand.

As a matter of fact researches show how difficult it is to establish a definite correlation among the events which are mainly described in qualitative terms.

In the light of what has been written, a research methodology has been determined by which it is possible to describe the arousing problems thoroughly. To this purpose it is fundamental to fix a real study case which allows a direct testing on the features describing the phenomenon, in particular investigation procedures through standard cards for data summary.

Palazzo Gussoni in Venice has been sorted out as a reference study case: it is a building overlooking Canal Grande and is now undergoing a restoration intervention.

The palace shows serious problems resulting form resurfacing humidity, in particular in the walls of the through-hall on the ground floor.

A testing campaign has been planned to assess the humidity content in the main walls and relevant quantity and type of salts.

The weight analysis has been selected to assess humidity content, the chemico-physical analysis of samples for quantity/typology of salts.

Testing has been organized sorting out some wall portions, characteristic for their location and typology.

Sample-taking has been carried out at several depth levels in the walls in order to underline some possible gradients and how big the influence of the exposure to the air is, also depending on position.

The first sample-taking corresponds to an average surface depth from 0 to 5 cm, the second from 10 to 15 cm, the third one from 30 to 35 cm.

Besides sampling at different depth levels, sampling at different heights has been carried out in that same place, both to establish the resurfacing height and the rotting phenomena which might occur in the wooden structure of the floors.

The samplings heights are at approx. 100 cm from floor level and correspond with the points where beams rest on the walls.

Results have been processed with standard cards through which it is possible to display and compare them in reference to sample-taking points.

The test results on humidity content give a general indication of a rather homogeneous distribution at the lowest deep level, with a slight reduction in the wall sample towards rio Noal. A significant gradient has been generally measured at the height of the floor shutter, reaching its peak value in depth, probably because of the effect of exposure to the air in relation to the soaking cycles.

The salts contains mainly chlorides, nitrates, sulfates and occasionally oxalates. The presence of nitrates is probably due to the remarkable pollution caused by drain town waters into Canal Grande.

Collection and processing of data have made it possible to carry on the research.

The core of the research progress is definitely the testing practice, aiming in particular at verifying two major hypotheses.

The first one refers to the option of mechanical cut using lead barriers to settle the problem of capillary resurfacing. Later on some desalting techniques of walls will be defined, and reports will be made of them, not only on how they are performed, but also as far as the definition of all specifications items is concerned.

The second research phase will make it possible to keep under control – in the medium-long term – the interventions results on dehumidification and salts content quantification interventions and the relationship to be established to the mechanical values describing the strength of the concerned wall.

This is a most significant aspect as it will let us track - as times goes by - the progress of the behaviour of the wall masses treated with physical parameters resulting directly from tests carried out on the field.

The aim will be then that of providing a correlation between historical walls strength values in situ, in variable humidity conditions and salts contents.

To this purpose a stratigraphic analysis has been carried out on photo orthoplanes of the walls of the through-hall on the ground floor, identifying W.S.U. or portions of homogeneous walls.

The described walls will be examined in order to give a physical description of the blocks and of the bonding agent. For the blocks a sclerometric campaign will be performed and an investigation on mortars in parallel.

Once the strengths arrangement curve will be defined, some very small core samples will be taken from some blocks. They will be tested anhydrous and water saturated in order to define possible strengths variations.

A second testing campaign will give reports on salts and humidity contents – with the same test procedures as the first campaign – in the sample parting walls which have been submitted to the scheduled desalting interventions.

Fig. 1 - Plan showing buildings location.

S. NICOLÒ' DEI MENDICOLI:	WALL CUT (THE OLDEST EXAMPLE OF EMPLOYMENT OF THIS TECHNIQUE)
PALAZZO GRIMANI ON S. M. FORMOSA	TESTS PERFORMED WITH ELETCTROSMOSIS
ROPERIES OF ARSENALE	DESALTING THROUGH WASHING
LIVING BUILDING IN S. GIOBBE	ELECTROSMOSIS
DUOOE OF S. DONATO ON MURANO	TANK WITH FLAPPED WALLS AND SUPPORT MICROPILES
STATE ARCHIVES OF VENICE	ROOMS OF THE SUMMER DINING-HALL: TANK WITH FLEXIBLE COUPLINGS ALONG WITH TANK WITH BENTONITE INSULTAOR FOR THE FORMER KITCHEN-ROOMS
COTTON MILL S. MARTA	TANK WITH FLAPPED WALLS AND SUPPORT MICROPILES
SCHOOL OF THE CROCIFERI	TANK WITH FLEXIBLE COU-PLINGS
CRYPT OF S. MARCO AND NARTECE	FIRST HISTORICAL INTERVENTIONS (LATE XIX CENTURY)
CA' PESARO	WATER DRAINAGE AND ELECTRO-SMOSIS TESTS
CA' TRON	DRAINAGES
S. ANTONIN	DRAINAGES
S. ROCCO	NOT SPECIFIED INTERVENTION
STATE ARCHIVES	COMPLETE STITCHING – UN-STITCHING
CHIESA DEI MIRACOLI	WALL CUT AND EMPLOYMENT OF POLYESTER RESINS
7 CHIMNEYPOTS HOUSE	DETACHMENT AND EMPLOYMENT OF DEHUMIDIFYING MACROPOROUS PLASTERS
PALAZZO LABIA	NOT SPECIFIED INTERVENTION

Fig. 2 - Table listing the investigated cases and relevant applied technique.

Fig. 3 - Palazzo Gussoni.

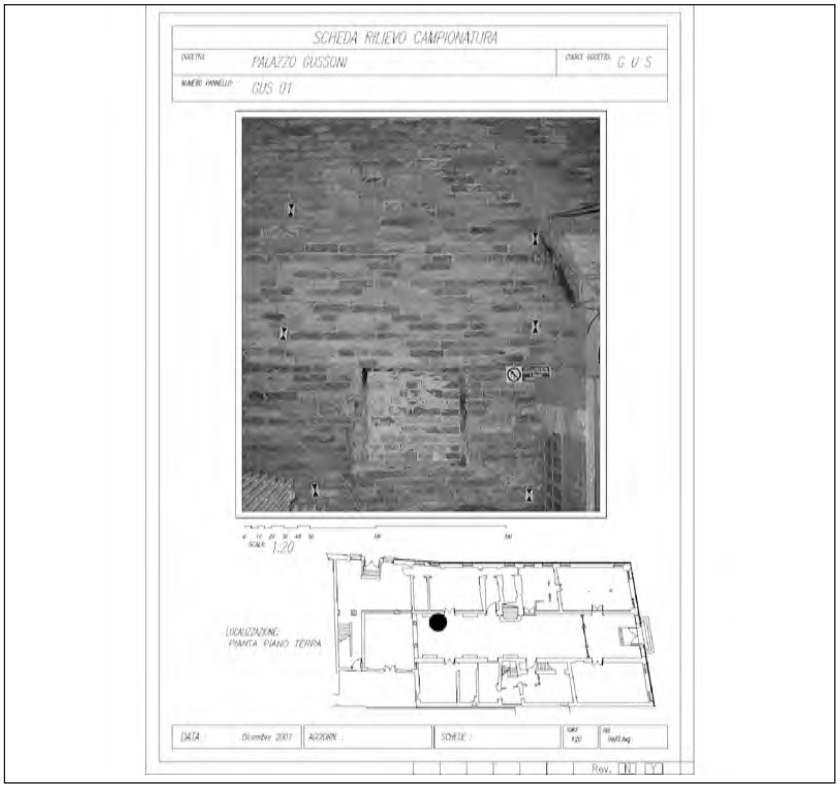

Fig. 4 - Picture of details of the through-hall walls.

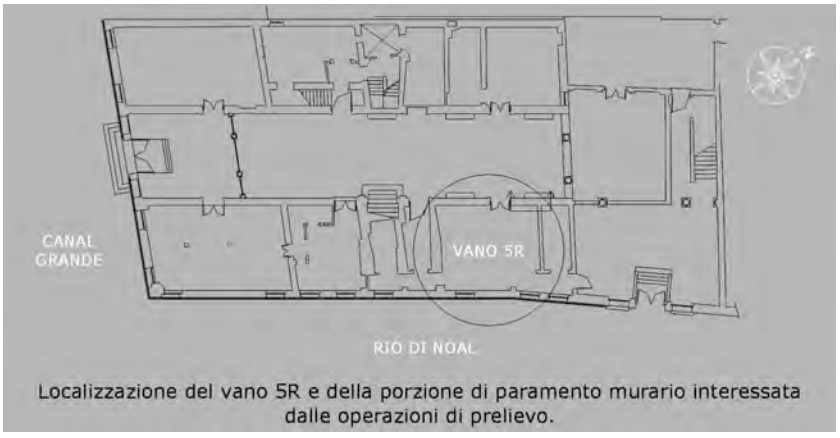

Fig. 5 - Map of the sample-taking positions.

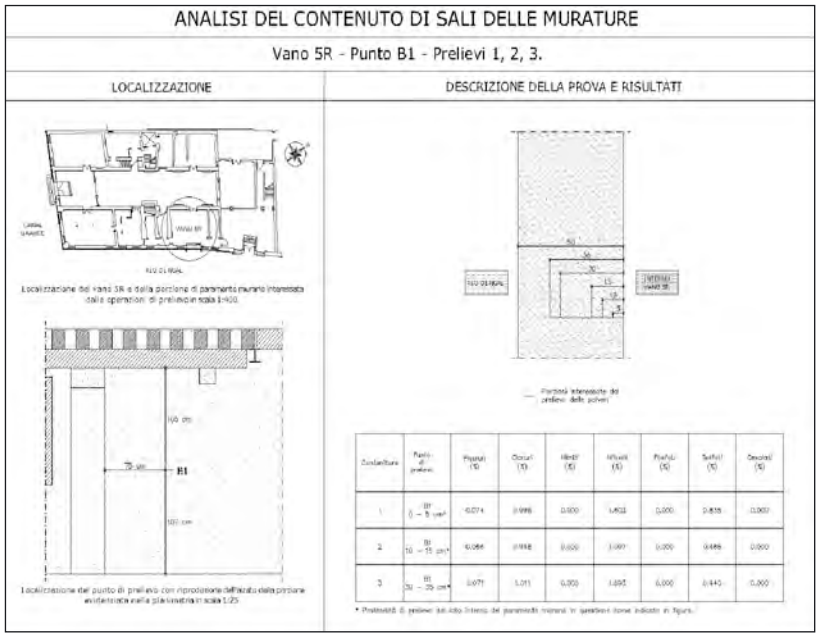

Fig. 6 - Standard Card containing data.

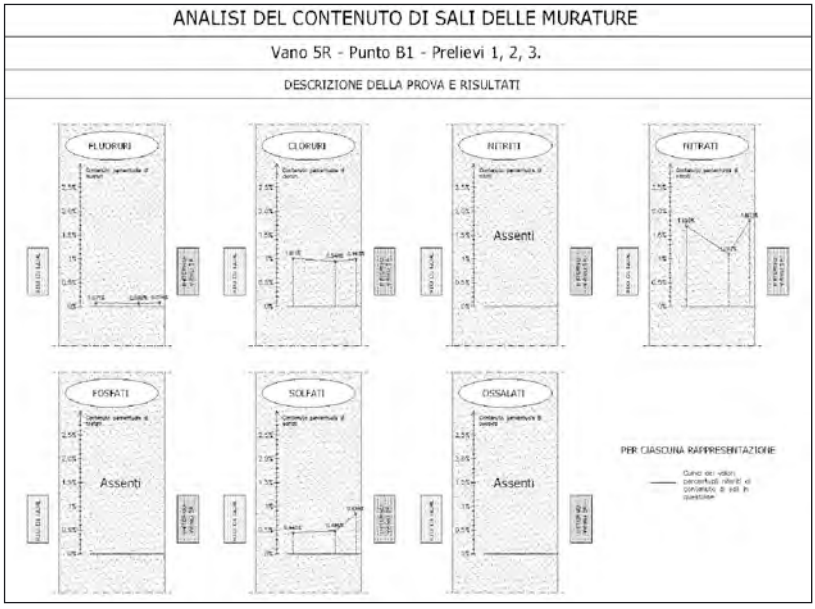

Fig. 7 - Lab card on salts content.

AREA 3.
ENVIRONMENTAL PROCESSES

RESEARCH LINE 3.1.
Trends in global change processes

INFLUENCE OF HEAT FLUX FORCING ON THE VERTICAL CIRCULATION IN NORTHERN-CENTRAL ADRIATIC SEA

A. Bergamasco[1], V. Filipetto[1], A. Tomasin[2], S. Carniel[1]
[1]*Istituto per lo Studio della Dinamica delle Grandi Masse, CNR, Venezia*
[2]*Dip. di Matematica Applicata, Università Cà Foscari, Venezia*

Abstract.

The thermoaline circulation of the central-north Adriatic basin is investigated by means of a 3D numerical model. Three different runs, where the surface heat fluxes annual average are respectively negative, slightly positive and slightly negative are performed.

Results confirm that surface heat fluxes alone can start and trigger the general circulation in the basin, both vertical and horizontal: when the heat fluxes have negative annual budget (meaning that, on average, the basin loses heat to the atmosphere) an horizontal cyclonic surface circulation is generated with a northward flow along the eastern coast and a southward return current system along the western one; while from the vertical point of view an antiestuarine circulation is established. A similar circulation pattern is present if the heat fluxes have a slightly negative annual budget and the residence time becomes minimum.

If the annual balance is positive the surface circulation switches from cyclonic to anticyclonic and the vertical circulation switches from antiesturine to estuarine.

A modification in the heat fluxes budget is strictly connected with a change in the turnover time of the water column in the Jabuka Pit.

1. *Introduction.*

Periodic cycles related to climatic fluctuations interested the Earth in the historical time. In the last decades important climatic changes (IPCC, 2001) due both to natural changes and to the human activities seem to be

occurring even if it is important to assess and quantify these phenomena and their consequences over a wide environment spatial and temporal scale despite the uncertainty to individualise long-term tendencies given by systematic error and natural climatic variability.

Actual climate changes, like atmospheric and marine warming, concern global, regional and local scales. In fact the warming tendency observed is also related to thermal forcing change, due to the interactions between the atmosphere and ocean and the coupled system is not well understood.

The main objective of this work is focused on the formation and evolution of the vertical thermoaline circulation in the Adriatic Sea under different heat fluxes forcing. Other driving circulation forcings, like Bora and Scirocco wind and rivers discharge are at the moment not included in order to concentrate to the heat flux forcing sensitive to the variation of the climatic variability. The rivers influence, though important for water cycle, is subordinate to thermic one and winds and their variations give contributions on shorter temporal scale.

The description of the model and the three numerical experiments

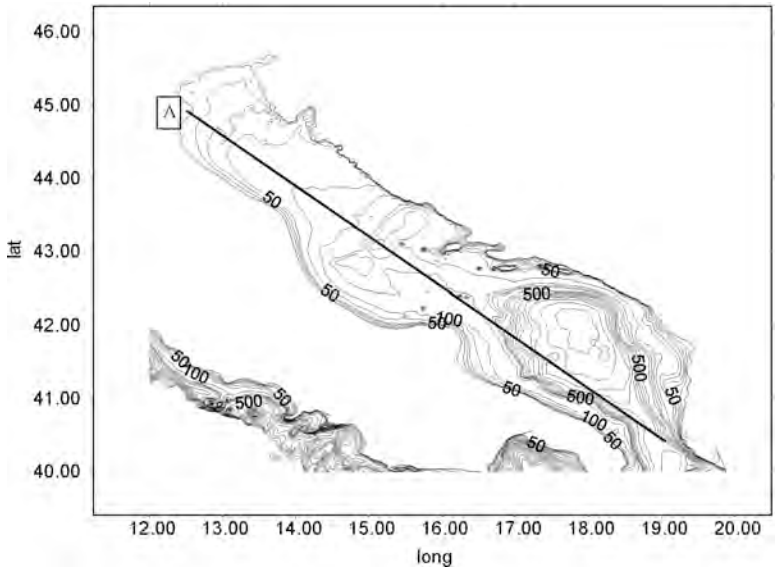

Fig. 1a. Bathymetry of the Adriatic Sea. The continuous line and letter A represent the transect along the main axis of the basin.

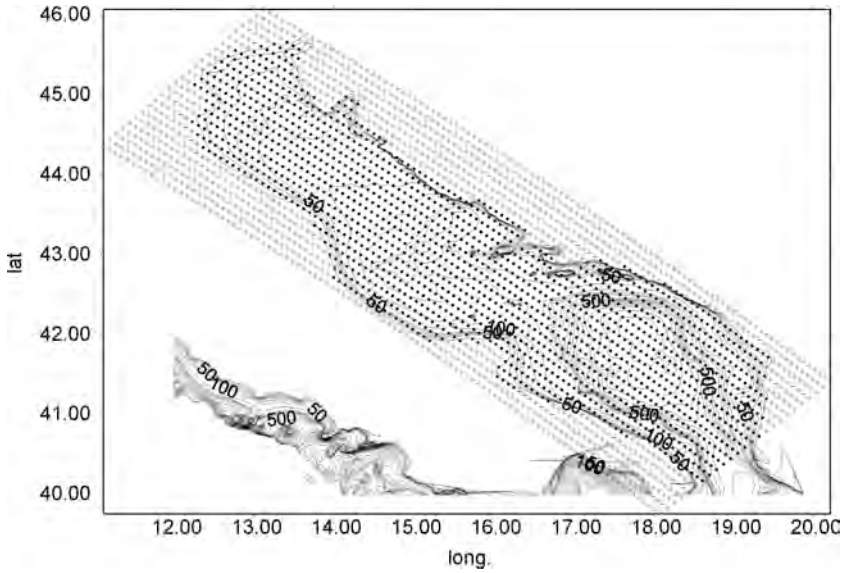

Fig. 1b. Grid used on the model. The points indicate the sea grid point, while the crosses represent the land point.

carried out are presented in Section2; the results and discussions are given in Section 3, finally the conclusions are presented in Section 4.

2. *Model description and numerical experiments.*

The numerical model used in this work is the Princeton Ocean Model (POM) in the 1997 version (Mellor, 1998). It is a three dimensional free surface model for an incompressible, Boussinesq and hydrostatic fluid resolving nonlinear and time dependent primitive equation; it reproduces the velocity field and the surface sea elevation providing the space-time evolution of temperature and salinity. The turbolence closure scheme proposed by Mellor and Yamada (1982) is adopted for the parameterisation of vertical mixing.

It resolves the vertical dimension using the sigma coordinates system to describe in detail basins with significant topographical variability.

In this work it has been implemented for the Adriatic Sea; its bathymetry, is computed averaging and smoothing (Shapiro, 1970) original data from Naval Oceanographic Database (Fig. 1a).

The grid, composed by 25x100 points and 47° degree rotated to the parallel axis (Fig. 1b), has a coarse horizontal resolution (10.5 km in the transverse direction and 7.7 km in the axial one) and a relatively high resolution in vertical: 35 sigma levels are used with a logarithmic distribution at the surface and bottom layers, in order to point out the deep water formation processes, and the dense water dispersion more properly. Thus the resolution spans from centimetres to hundreds metres.

Along the open boundary, located at the Otranto Strait, the M_2 component (28.9841 degree/h) of the sea level elevation is imposed (Polli, 1960), with 7.2 cm amplitude (we decide to use this value in agreement with tide-gauge measurements in Otranto relative to 1997), in order to have perpetual cycle.

A radiation condition is applied for temperature and salinity fields with a relaxation coefficient equal 0.1. That is means a temporal connection between the internal solution and the border of about 2 hours.

This allows the system to evolve inside the domain and radiate outside through the boundary both temperature and salinity values.

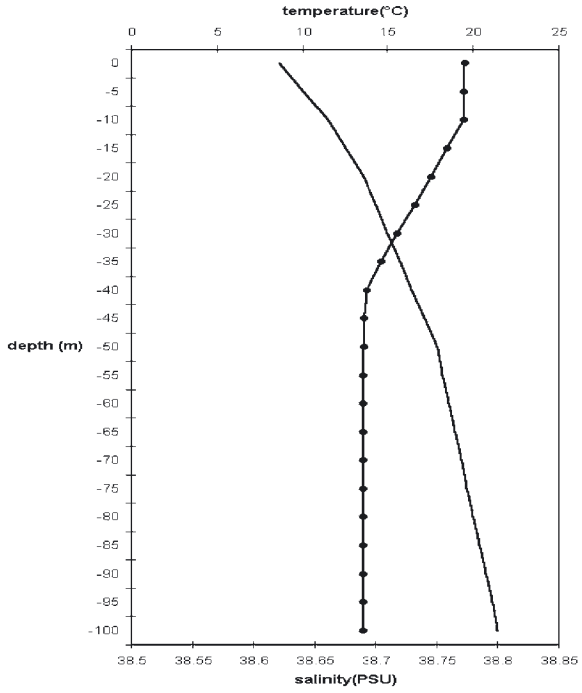

Fig. 2. Initial temperature and salinity profiles used in the model.

2.1 *Initial conditions and phisical forcings.*

The model is initialized with horizontally uniform temperature and salinity profiles. Vertically it is assumed a stratification similar to an autumn situation with a thermocline set at a depth between 20 and 30 m (similar to the case of Bergamasco and Gacic, 1995). Initial temperature-salinity profiles are shown in Fig. 2.

The basin is first spin up only with M_2 tide imposed at the open boundary for geostrophic adjustment of the domain, then the perpetual year using heat fluxes forcing is computed.

The heat fluxes are imposed in the northern/central Adriatic Sea with the maximum intensity at the centre on the northern basin, idealizing a spatial distribution derived from the climatology of May (Artegiani et al., 2002). This simulates a winter cooling and a spring-summer heating. The values, changing on a monthly base, are different in each experiments. In all the runs there is a seasonal cycle with a maximum heat loss in January-February and a maximum heat gain in June-July. The values and the seasonal cycle are in agreement with studies made by Stravisi and Crisciani (1986), Picco (1991), Artegiani et al. (2002).

Other forcings like wind stress and river runoff are neglected for the objective of this work. The numerical integration is carried out for at least five years.

2.2 *Numerical experiments.*

Three numerical experiments are carried out. Three different idealized annual variations are selected, but in all cases the fluxes represent realistic value with seasonal variability. The configurations adopted are, in fact, consistent with both the domain natural variability and the possible climatic changes trend. In Run 1, called "central Run", the maximum cooling of 100 W/m^2 is reached on January and February, while the maximum heating of 50 W/m^2 is reached on June (see Table 1). The annual heat budget is negative –21.6 W/m^2, as estimated for the actual Adriatic Sea from several authors (Artegiani et al. 1997a; Picco, 1991). In Run 2, called "Warming Run", the annual heat balance is slightly positive, +8.3 W/m^2. All the fluxes are shifted toward positive values and the winter heat balance is smaller than the spring one. In Run 3, defined as "Tropicalization Run", the winter fluxes are the same of Run 1, but the spring fluxes are higher (see Table 1); the annual heat budget is slightly negative –7.5 W/m^2. Fluxes change their values the first day of each month.

Table 1 - Monthly surface heat flux components. All units are in W/m2.

Month	Sep.	Oct.	Nov.	Dec.	Jan.	Feb.	Mar.	Apr.	May.	Jun.	July	Aug	annual average
1^ Run	-20	-40	-60	-80	-100	-100	0	20	30	50	40	0	21.6
2^ Run	10	-10	-30	-50	-70	-70	30	50	60	80	70	30	+8.3
3^ Run	-20	-40	-60	-80	-100	-100	10	40	60	100	80	20	-7.5

3. *Results and discussion.*

The average kinetic energy trend is computed for the northern and central basin, due to the open boundary condition imposed, the fluxes in fact force the system in these two regions . In Run 1 the kinetic energy increases for three years showing an evolution, after which the system reaches a quasi steady condition. In Run 3 in two years the average kinetic energy reaches a steady state. The average kinetic energy of the first year is similar to that of Run 1, then during the following years it decreases because of the different fluxes.

In Run 2 there is a transient behaviour during the first three years; this is also visible in the average kinetic energy trend is variable for three years, when a steady state is reached. It is interesting to note a phase-difference of kinetic energy between Run 1, Run 3 and Run 2. In the Run 1 and Run 3, whit negative annual heat fluxes balance, the kinetic energy is maximum in summer, while in Run 2, when the annual heat fluxes budget is positive, the maximum of kinetic energy is reached in winter (Fig. 3).

3.1 *Horizontal and vertical circulation.*

In Run 1 cyclonic circulation is generated characterized by two main gyres situated over the southern deep basin and the central one, having a mean surface velocity (i.e. at the first sigma level) between 0.12-0.16 m/s. A northward flow along the eastern coast and a southward current along the western one describe a cyclonic circulation also in the shallow northern region (Fig. 4) as described by Orlic et al.,1992; Artegiani et al. 1997a,b. A general circulation with similar features is observed in the Run 3, even if with a less intense velocity field.

An anticyclonic circulation is established in the Run 2, as is evident in Fig. 5, with a mean surface velocity one order of magnitude less then in Run 1 (0.03-0.04 m/s).

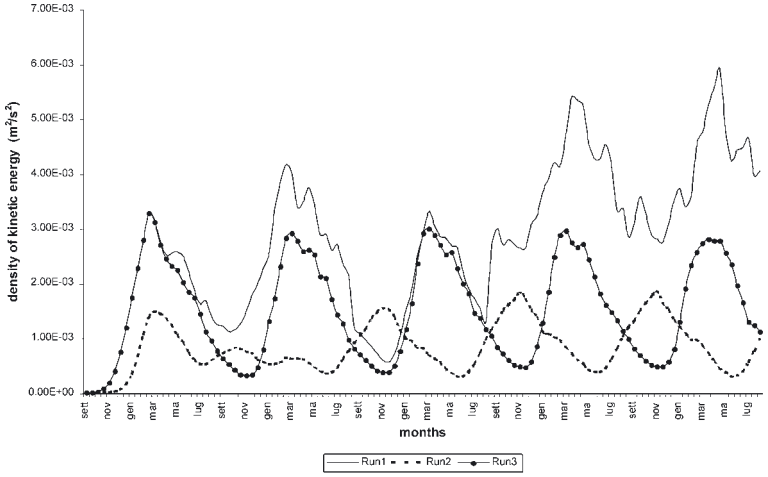

Fig. 3. Kinetic energy density trend. The values are express per unit of mass and per sea grid point (m2/s2). In the Run1 the values are higher and increase every year. In Run2 a steady state condition is reached in 3 year, while in Run3 a steady condition is reached in 2 years.

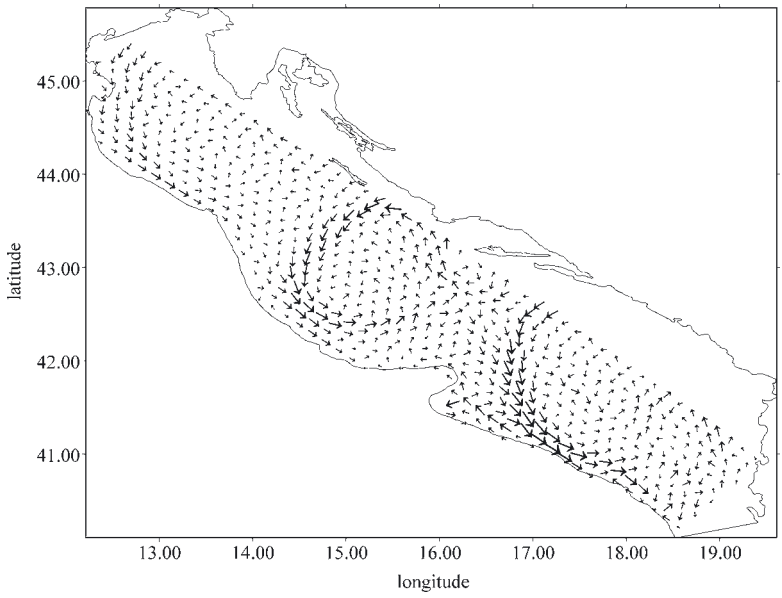

Fig. 4 Cyclonic circulation pattern at the surface. It is a average of the surface velocity relative to the last 15 days of January.

Vertically, Run 1, called "central Run" generates an antiestuarine cell. The colder and denser water, produced in the northern region, flows southward in deep layers, while the warmer and lighter water flows northward superficially. As expected, a dense water formation process is developed in wintertime, mostly during January and February, more pronounced every year. Density transects along the main axis of the basin show that in autumn the thermocline is broken and the mixing, consequence of cooling, homogenizes the entire water column in the northern region. In this area the strong winter cooling imposed originates a dense water formation as shown by the outcropping of isopycnals. This event becomes more evident during winters, leading to water masses more and more dense from year to year (Malanotte-Rizzoli, 1994). Summer heating stops the process and restores the stratification. Water formed in winter flows southward sinking off the Jabuka pit.

Run 2 provides a completely different situation as the summer heating is more important then the winter cooling. The vertical circulation established is now estuarine, the water flows northward on the bottom and southward on the surface layer, and an anticyclonic horizontal circulation is generated. Only during the first winter there is a dense water formation on the northern basin, due to the initial conditions imposed, then the summer strong heating heats the water in this shallower region, forming lighter water. The stratification produced remains stable even during following winters.

The general behaviour of Run 3 is similar to that of Run 1. Again the winter cooling determines homogenization and bottom water formation, but a stronger summer heating cause a more intense flushing of the northern region, a southward "sliding" of the new water formed, a much efficient turnover of the Jabuka pit and the dense water spreading in the southern basin. Therefore in this case the quantity of dense water does not increase during the simulation as in Run 1, as well as the kinetic energy that remains almost equal to the first year value as shown in Fig. 3.

For the three experiments volume of dense water formed and present in Jabuka Pit is estimated, computed as a fraction of the Jabuka pit volume and it is shown in Fig. 6. In Run 1 the amount of dense water with the density anomaly of 29.3 kg/m^3 increases every year and in three years the Jabuka pit is filled with this water mass. This result is in good agreement with the results provided by a stochastic forecasting model of the slime blooms in the Northern Adriatic sea developed in 1990 (Tomasino, 1996). It is interesting to note that probably there is a volume of dense water related to hydrodynamic stability of the water column, equal to 1/5

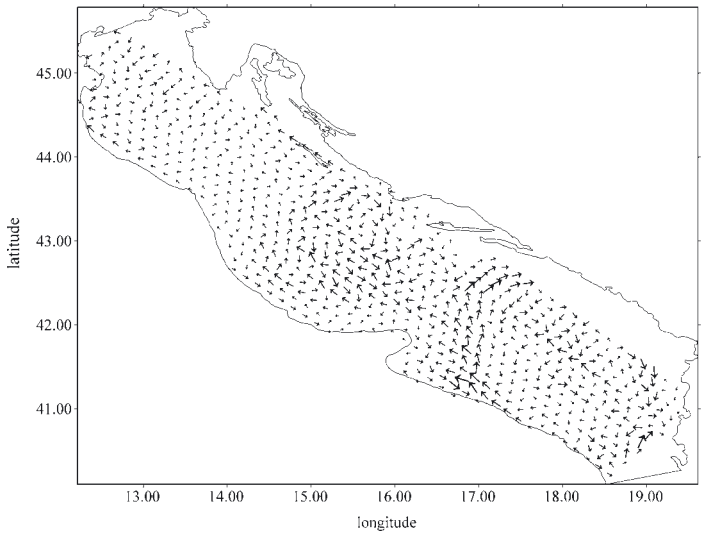

Fig. 5 Anticyclonic circulation pattern at the surface. It is a average of the surface velocity relative to the last 15 days of January.

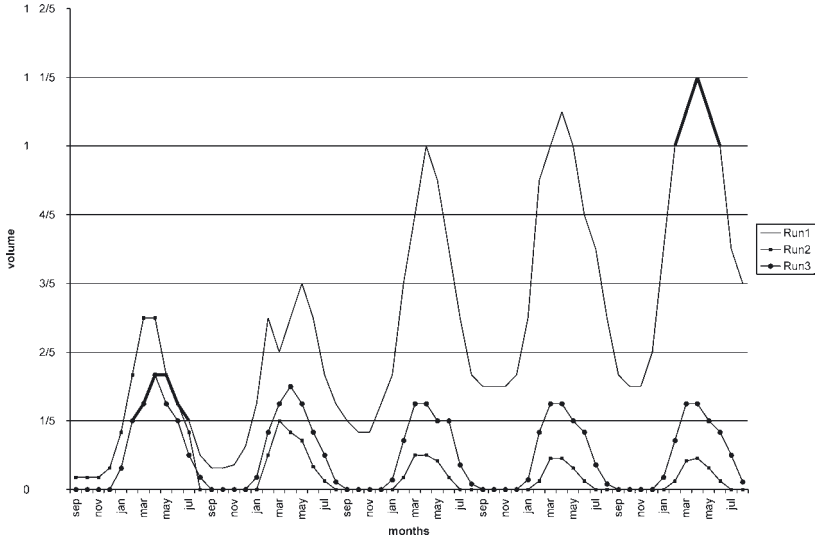

Fig. 6. Evolution of the volume of dense water formed and volume of the pit ratio in the three Runs. The continuous thick line represent the volume produced in the first year and exported in the fifth year, in Run1. For Run1 and Run3 is presented the density anomaly of 29.3 kg/m3, for Run 2 the density anomaly of 29.1 kg/m3.

of the all volume of the pit. The remaining amount of dense water present in the pit and produced in the first year can be compared to the volume exported during the fifth year, as it is shown in the Fig. 6. This estimation means that with these heat fluxes most of the dense water stored needs at least 5 years to leave the pit.

In Run 2 the water masses volume with density of 29.1 kg/m^3 decreases rapidly after the first year, the pit is not filled up with dense water and a steady state condition is reached after three years. In Run 3, in five years, no evident changes occur on the volume of dense water (density 29.3 kg/m^3) on the Jabuka pit and in two years the system goes toward a steady state. The filling of the pit is not reached even if, as observed in the Run 1, the volume of dense water is always greater then 1/5 of the volume of the pit, meaning that the water flushing with this surface heat fluxes is more efficient and a more quantity of water is "drained".

3.2 *Turnover of the Jabuka pit.*

The residence time of bottom water in the Jabuka pit and the flushing of the northern region are strongly influenced by the heat fluxes imposed. The turnover times of the water column are very different in three experiments and the results are not counter-intuitive.

In Run 1 the strong winter cooling (annual heat balance <0) produces a large amount of dense water (Hendershott and Malanotte-Rizzoli, 1976) while the summer heating is not enough to generate a strong circulation able to completely drain the remaining water stored on the bottom of the pit. In this condition every year a new and denser water it would be required to allow the turnover of the pit. As expected Run 2 residence time gets also larger, even if it is because no significant dense water formation occurs.

On the other hand it is interesting to note that in Run 3, when the annual heat fluxes balance is negative but near zero, the dense water residence time in Jabuka pit is minimum and therefore the water exchange rate is higher then in the other two experiments. This means that a more efficient flushing, with respect to Run 1, is induced by the high summer heating, and the dense water produced in wintertime flows away from the Jabuka pit more rapidly. The dense water formed upon the shelf and driven to the pit has a shorter turnover time in this experiment, so it is not stored up for long time and the renewal is faster then in the other experiments.

4. *Conclusion.*

The work is focused on the Northern Adriatic Sea vertical thermoaline circulation and the horizontal general circulation induced only by a forcing mechanism, the heat fluxes between the sea and the atmosphere.

Three numerical experiments, examining the generation and evolution of the thermoaline circulation and of the turnover time in the Mid-Adriatic pit induced by different heat fluxes evolutions, have been carried out. Despite relying on a relatively idealised, even though realistic, flux behaviour and coarse resolution, the results are interesting to study the actual velocity field and a possible one considering future climatic changes.

Surface heat fluxes having negative annual budget, -21.6 W/m^2 (Run 1), imposed perpetually every year, are able to start a dense water formation process, an antiestuarine circulation and a long turnover time of the Jabuka pit. The fluxes can represent a situation similar to a cold year (in agreement with estimation made by some authors, Artegiani et al.,1997a; May,1982; Maggiore et al, 1998).

If the annual heat fluxes are slightly positive, +8.3 W/m^2 (Run 2), a possible situation in warm years (as it seems to be the trend for the future years, IPCC 2001), there is not evidence of dense water formation. The vertical circulation established is estuarine, while the horizontal one is anticyclonic. A strong vertical stratification exists during the all year because the winter cooling event is not sufficient to generate dense water and to induce the vertical mixing.

In this way the northern Adriatic flushing occurs from the intermediate or bottom layers and the water column under the thermocline can not to be ventilated; consequently some deep zones can remain isolated.

In the third experiment the annual heat fluxes budget is slightly negative, -7.5 W/m^2 (Run 3), thermoaline circulation is antiestuarine, but in this case there is almost a balance between dense water formed in wintertime and summer flushing, in a way that the Jabuka pit turnover time diminishes.

This experiment can be considered a transient phase representing an intermediate situation between the two previous ones; it could be the more sensitive condition to a minimum fluxes variation able to switch from an antiestuarine to an estuarine circulation in relation to a natural interannual variability. It can be seen also as a possible situation establishing with accentuated oscillation on the “tropic line”.

The heat fluxes interannual variation can involve an oscillation in the northern-central Adriatic Sea between the situation observed in Run 1

and Run 3, thus a shifting between some year of a dense water formation and others characterized by a more efficient flushing.

The results of this work pointed out that the heat fluxes alone can generate a general circulation, both horizontal and vertical, similar to that experimentally observed one. This raises interesting questions about the mean wind field effect on the basin circulation, that could be more important in modulating rather then generating currents features and have much more influence in short time scale.

On the other hands it could be possible that on long time scale heat fluxes changes could influence the general circulation more than the wind.

The fluctuation between colder (annual heat balance <<0) and warmer (annual heat balance near 0) years are of primary importance for the climatic state maybe stable, for the turnover of the pit and for the system efficiency of flushing the northern semienclosed basin. This fluctuation in fact allows the system to evolve without an increment of energy, necessary, on the contrary, with a sequence of cold years that would lead to a more and more stratified conditions.

References.

Artegiani A., Salusti E., 1987. Fields observations of the flow of dense water on the bottom of the Adriatic Sea during the winter of 1981. Oceanologica Acta, Vol. 10, No. 4, 387-391.

Artegiani A., Bregant D., Paschini E., Pinardi N., Raichic F., Russo A., 1997a. The Adriatic Sea General Circulation. Part I: Air-Sea Interactions and Water Mass Structure. Journal of Physical Oceanography, 27, 1492-1514.

Artegiani A., Bregant D., Paschini E., Pinardi N., Raichic F., Russo A., 1997b. The Adriatic Sea General Circulation. Part II: Baroclinic Circulation Structure. Journal of Physical Oceanography, 27, 1515-1532.

Artegiani A., Cushman-Roisin B., Gacic M., Poulain P.M., 2002. Physical Oceanography of the Adriatic Sea. Past, present, future. Kluwer Academic Publishers, pp 246.

Bergamasco A., Malanotte-Rizzoli P., 1989. Modellistica del Nord Adriatico. Numero Speciale del Bollettino di Oceanologia Teorica ed Applicata, 295-302.

Bergamasco A., Gacic M., 1995. Baroclinic Response of the Adriatic Sea to an Episode of Bora Wind. Journal of Physical Oceanography, 26, 1354-1369.

Bergamasco A., Oguz T., Malanotte-Rizzoli P., 1999. Modeling dense water mass formation and winter circulation in the northern and central Adriatic Sea. Journal of Marine Systems, 20, 279-300.

Bunker A.F., Charnock H., Goldsmith R.A., 1982. A note on the heat balance of the Mediterranean and Red Seas. Supplement to Journal of Marine Research, 40, 73-84.

Franco P., Jeftic L., Malanotte-Rizzoli P., Michelato A., Orlic M., 1982. Descriptive model of the Northern Adriatic. Oceanologica Acta, Vol. 5, No. 3, 379-389.

Gacic M., Marullo S., Santoleri R., Bergamasco A., 1997. Analysis of the seasonal and interannual variability of the sea surface temperature field in the Adriatic Sea from AVHRR data (1984-1992). Journal of Geophisycal Research, 102, 22937-22946.

Hendershott M.C., Rizzoli P., 1976. The winter circulation of the Adriatic Sea. Deep-Sea Research, 23, 353-373.

Hopkins T.S., 1978. Physical Processes in Mediterranean Estuaries. In: Transport processes in estuarine environments, Seventh Bell W. Baruch Institute for Marine Biology and Coastal Research Symposium, Georgetown, South Carolina, May 1976, B. Kjerfve (ed.), 269-310.

Hopkins T.S., Kinder C., Pariente R., 1998a. Description of the Northern Adriatic circulation as computed from ELNA hydrography. In: Ecosystems Research Report, the Adriatic Sea, EU/Environment Series, Brussels.

Hopkins T.S., Kinder C., Pariente R., 1998b. Water-mass modification in the Northern Adriatic, a preliminary assessment from the ELNA data set. In: Ecosystems Research Report, the Adriatic Sea, EU/Environment Series, Brussels.

IPCC, 2001. Climate Change 2000. The Science of Climate Change. Contribution of working group I to the third assessment report of the Intergovernmental Panel on Climate Change. Cambridge University press, Cambridge.

Maggiore A., Zavatarelli M., Angelucci M.G., Pinardi N., 1998. Surface heat and water fluxes in the Adriatic Sea: seasonal and interannual variability. Physics and Chemestry of the Earth, Vol. 23, Issue 5-6, pp 561-567.

Malanotte-Rizzoli P., 1994. The Northern Adriatic Sea as a prototype of convection and water mass formation on the continental shelf. The general ciculation of the ocean. Istituto Veneto di Scienze, Lettere ed arti, Venice 1994, pp. 268-287.

Manca B., Giorgetti A., 1998. Thermohaline properties and circulation patterns in the southern Adriatic Sea from May 1995 to February 1996. Atti del XII° Congresso dell'Associazione Italiana di Oceanologia e Limnologia, II, 399-414.

May P.W., 1982. Climatological flux estimates in the Mediterranean Sea: Part I. Wind and wind stresses. NORDA Rep. 54, NSTL, MS 39529.

Mellor G.L., 1998. User guide for a three dimensional, primitive equation, numerical model. Progress in Atmosphere and Ocean Science, Princeton University, pp. 41, http://www.aos.princeton.edu/WWWPUBLIC/htdocs.pom.

Mellor G.L., Yamada T., 1982. Development of a turbolence closure model for geophysical fluid problems. Reviews of Geophysics and Space Physics, 20, 851-875.

Orlic M., Gacic M., La Violette P.E., 1992. The currents and circulation of the Adriatic Sea. Oceanologica Acta, Vol. 15, No. 2, 109-124.

Picco P., 1991. Evaporation and Heat Exchanges between the Sea and the Atmosphere in the Gulf of Trieste during 1988. Il Nuovo Cimento, Vol. 14C, No. 4, 335-345.

Polli S., 1960. La Propagazione delle maree nell'Adriatico. Atti del IX° Convegno dell'Associazione Geofisica Italiana, Roma, 20-21 Novembre 1959.

Shapiro R., 1970. Smoothing, filtering and boundary effects, Rev. Geophys. Space Phys., 8, 359-387.

Stravisi F., Crisciani F., 1986. Estimation of surface heat and buoyancy fluxes in the Gulf of Trieste by means of bulk formulas. Boll. Ocean. Teor. Appl., Vol. IV, No. 1, 55-61.

Tomasino M., 1996. Is it feasible to predict s"slime blooms" or "mucilage" in the Northern Adriatic Sea? Ecol. Modelling, 84, 189-198.

Tsimplis M.N., Baker T.F., 2000. Sea level drop in the Mediterranean Sea: An indicator of deep water salinity and temperature changes?. Geophysical Research Letters, Vol. 27, No. 12, 1731-1734.

Umgiesser G., Carniel S., On the numerical behaviour of a general lagrangian module for oceanic applications. CNR-ISDGM, Technical Report, 2002 (in preparation).

Weaver A.J., Hughes T.M.C., 1992. Stability and variability of the thermohaline circulation and its link to climate. Review Article in Trends in Physical Oceanography. Council of Scientific Research Integration, Research Trends Series, Trivandrum, India, 1-56.

BOX MODELING OF THE EASTERN MEDITERRANEAN SEA

Y. ASHKENAZY and P. H. STONE
Department of Earth Atmosphere and Planetary Sciences, Massachusetts Institute of Technology, Cambridge, MA 02139

Abstract.

The thermohaline circulation, i.e., the combined heat-salinity driven deep ocean circulation, plays an important role in understanding climate dynamics and climate instability. Recently, a new source of deep water formation in the Eastern Mediterranean was found in the southern part of the Aegean sea. Till then, the only source of deep water formation in the Eastern Mediterranean was in the Adriatic sea; the rate of the deep water formation of the new Aegean source is three times larger then the Adriatic source. We develop a simple 3 box-model to study the stability of the thermohaline circulation of the Eastern Mediterranean sea. The 3 boxes represent the Adriatic sea, Aegean sea, and the Ionian sea. The boxes exchange heat and salinity and may be described by a set of nonlinear differential equations. We analytically analyze these equations and find that the system may have one, two, or four stable flux states. We also find that under certain perturbations (e.g., extreme change in precipitation or/and temperature) the system can form a new state similar to the new one with the Aegean water source. We study the stability of the four stable states and give their basins of attraction.

1. *Introduction.*

Recent observations of a major increase in the amount of bottom water formation and discharge from the Aegean Sea [Roether, 1996] raise the possibility that the circulations in the Eastern Mediterranean are unstable and subject to sudden changes. The idea that density-driven circulations in the ocean could under a given set of boundary conditions display more than one equilibrium state, and therefore have a behavior like that recently observed in the Aegean, was first put forth by Stommel [Stommel, 1961]. He

illustrated the behavior with a very simple two-box model of the thermohaline circulation. The two equilibrium states that he found in his simple box model have since been found in simulations of the North Atlantic thermohaline circulation with the most sophisticated coupled atmosphere-ocean general circulation models [e.g., Manabe and Stouffer, 1988]. These recent results lend considerable credibility to Stommel's box model. However, there is nothing in his model that limits its applicability to large-scale circulations in the North Atlantic – indeed in his paper he even suggested that it might be relevant to the Mediterranean. In this project we apply the same basic ideas as Stommel's to develop a box model of the Eastern Mediterranean, and explore what the possible multiple equilibrium states are, and what their stability characteristics might be.

2. *Three box model of the Eastern Mediterranean Sea.*

The major change in the deep water formation in the Eastern Mediterranean Sea occurred, basically, in the vicinity of the Adriatic-Aegean-Ionian seas. Hydrographic surveys since early last century [Nielsen, 1912] indicated that the dominant source region for deep water over the entire eastern Mediterranean was the Adriatic sea. Water outflowing from the Adriatic were deposited in the bottom of the Ionian Sea [Schlitzer, 1991]; then they spread southward and eastward [Malanotte-Rizzoli, 1988, and Wüst, 1991]. The deep water over-turning time was approximately 100 years with an average formation rate of $0.3Sv = 0.3 \times 10^6 m^3 s^{-1}$ [Roether, 1991]. An additional, much more dominant, source of deep water was found in a hydrographic survey during 1995 [Roether, 1996]. The new source is located in the southern part of the Aegean sea and has an average outflow rate of about $1Sv$.

We represent the Adriatic sea (Ad), the Ionian sea (IS), and the Aegean sea (Ag), by three boxes, a, b, and c respectively. All three boxes are forced by surface fluxes of heat and moisture and the boxes are assumed to be well mixed, so that their states can be described by a single temperature and salinity for each box. The flux between Box *a* and Box *b* is q_1 (representing Ionian-Adriatic flux) and the flux between Box *c* and Box *b* is q_2 (representing the Ionian-Aegean flux); see Fig. 1. The boxes "interact" through "pipes" with the fluxes q_1 and q_2.

The circulations between the boxes are assumed to be proportional to the density gradients between the boxes, and with this parameterization the state of the system can be described by conservation equations for

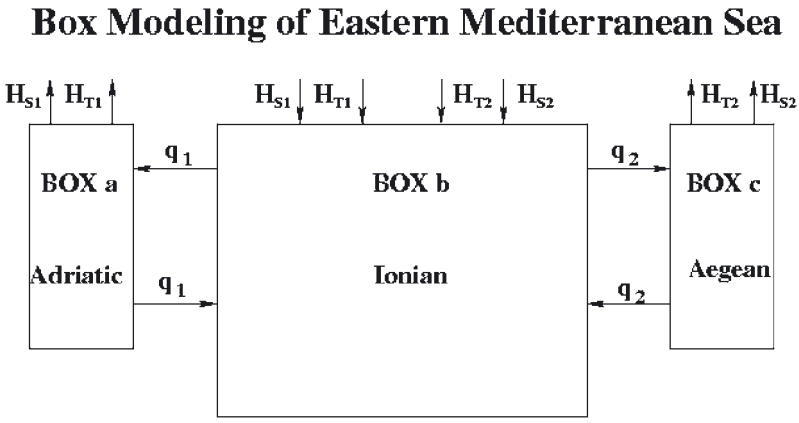

Fig. 1: Illustration of the 3-box model of the Eastern Mediterranean Sea.

heat and salinity for each box, giving a total of six equations for the temperatures and salinities of the three boxes. The equations are nonlinear because of the nonlinear advection of heat and salinity between the boxes, and this nonlinearity gives rise to the possibility of multiple equilibrium states. In our first analysis of this model, we have made the simplifying assumption that the temperatures of the boxes are fixed, i.e., that the temperatures are very strongly tied down by interaction with the atmosphere. This leaves us with three equations for the salinities.

The volume fluxes between the boxes are proportional to the density gradients between the boxes,

$$\begin{aligned} q_1 &= k^1[\alpha(T_b - T_a) - \beta(S_b - S_a)], \\ q_2 &= k^2[\alpha(T_b - T_c) - \beta(S_b - S_c)], \end{aligned} \tag{1}$$

where $T_{a,\,b,\,c}$ are the temperature of the boxes, $S_{a,\,b,\,c}$ are the salinity of the boxes, α and β are the thermal and haline expansion coefficients, and $k_{1,\,2}$ are the flux constants. The surface virtual salinity fluxes are H_{s_1} and H_{s_2}. We define the following variables and constants: $T_1 \equiv T_b - T_a$, $T_2 \equiv T_b - T_c$=const, $S_1 \equiv S_b - S_a$, $S_2 \equiv S_b - S_c$, $h_{s_1} \equiv H_{s_1} V_a$ and $h_{s_2} \equiv H_{s_2} V_c$. Following [Stommel, 1961 and Stone, 1997] the salt equations can be written as,

$$\begin{aligned}
\frac{\partial S_a}{\partial t} &= -\frac{h_{S_1}}{V_a} - \frac{|q_1|}{V_a}(S_a - S_b), \\
\frac{\partial S_c}{\partial t} &= -\frac{h_{S_2}}{V_c} - \frac{|q_2|}{V_c}(S_c - S_b), \\
\frac{\partial S_b}{\partial t} &= \frac{h_{S_1}}{V_b} + \frac{h_{S_2}}{V_b} - \frac{|q_1|}{V_b}(S_b - S_a) - \frac{|q_2|}{V_b}(S_b - S_c).
\end{aligned} \tag{2}$$

These equations basically describe the amount of salt entering/leaving the boxes through the pipes plus the contribution of the virtual salinity fluxes. After subtracting the first two equations from the third equation the system is reduced to two equations,

$$\begin{aligned}
\frac{\partial S_1}{\partial t} &= h_{S_1}\left(\frac{1}{V_a} + \frac{1}{V_b}\right) + \frac{h_{S_2}}{V_b} - \left(\frac{1}{V_a} + \frac{1}{V_b}\right)|q_1| S_1 - \frac{|q_2|}{V_b} S_2, \\
\frac{\partial S_2}{\partial t} &= \frac{h_{S_1}}{V_b} + h_{S_2}\left(\frac{1}{V_c} + \frac{1}{V_b}\right) - \frac{|q_1|}{V_b} S_1 - \left(\frac{1}{V_c} + \frac{1}{V_b}\right)|q_2| S_2.
\end{aligned} \tag{3}$$

Using Eqs. (1), the circulation flux equations can be written as,

$$\begin{aligned}
-\frac{1}{k_1\beta}\frac{\partial q_1}{\partial t} &= h_{S_1}\left(\frac{1}{V_a} + \frac{1}{V_b}\right) + \frac{h_{S_2}}{V_b} - \left(\frac{1}{V_a} + \frac{1}{V_b}\right)|q_1|\left(-\frac{q_1}{k_1\beta} + \frac{\alpha}{\beta}T_1\right) - \frac{|q_2|}{V_b}\left(-\frac{q_2}{k_2\beta} + \frac{\alpha}{\beta}T_2\right), \\
-\frac{1}{k_2\beta}\frac{\partial q_2}{\partial t} &= \frac{h_{S_1}}{V_b} + h_{S_2}\left(\frac{1}{V_c} + \frac{1}{V_b}\right) - \frac{|q_1|}{V_b}\left(-\frac{q_1}{k_1\beta} + \frac{\alpha}{\beta}T_1\right) - \left(\frac{1}{V_c} + \frac{1}{V_b}\right)|q_2|\left(-\frac{q_2}{k_2\beta} + \frac{\alpha}{\beta}T_2\right)
\end{aligned} \tag{4}$$

To obtain the fixed points of the system we set the left hand side to zero. It is easy to show, either by direct calculation or by comparing the volume terms, that the equations that satisfy these conditions are,

$$\begin{aligned}
|q_1|\left(\frac{\alpha}{\beta}T_1 - \frac{q_1}{k_1\beta}\right) = h_{S_1} &\Rightarrow |q_1|(q_1 - k_1\alpha T_1) + k_1\beta h_{S_1} = 0, \\
|q_2|\left(\frac{\alpha}{\beta}T_2 - \frac{q_2}{k_2\beta}\right) = h_{S_2} &\Rightarrow |q_2|(q_2 - k_2\alpha T_2) + k_2\beta h_{S_2} = 0.
\end{aligned} \tag{5}$$

These are two independent equations and each has either one or three solutions. It follows that the equilibrium states of the Adriatic and Aegean seas (boxes *a* and *c*) interact independently with the Ionian sea (box *b*), and in fact in equilibrium the model decouples into two separate two-box models, each identical to the original Stommel two-box model. Thus, for example, there might be two possible stable states for the Aegean, one with strong bottom water formation, and one without. This is indeed reminiscent of the change in behavior of the Aegean from the 1980s to the 1990s.

For $q_1>0$ there are two solutions,

$$q_1^{1,2} = \frac{k_1\alpha T_1 \pm \sqrt{(k_1\alpha T_1)^2 - 4k_1\beta h_{S_1}}}{2}, \tag{6}$$

if

$$(k_1\alpha T_1)^2 > 4k_1\beta h_{S_1}. \tag{7}$$

For $q_1<0$, there is one negative solution,

$$q_1^3 = \frac{k_1\alpha T_1 - \sqrt{(k_1\alpha T_1)^2 + 4k_1\beta h_{S_1}}}{2} \tag{8}$$

Similar solutions exist for q_2. The $q^3_{1,2}$ solution is the salt dominant flux solution while $q^1_{1,2}$ is the temperature dominant solution. $q^1_{1,2}$ corresponds to sinking in boxes *a* and *c* while $q^3_{1,2}$ corresponds to sinking in box *b*. Like in Stommel's model $q^2_{1,2}$ is an unstable solution.

All together there are either one, three, or nine fixed points; i.e., (q_1^3, q_2^3), (q_1^3, $q_2^{1,2,3}$) or ($q_1^{1,2,3}$, q_2^3), and ($q_1^{1,2,3}$, $q_2^{1,2,3}$), respectively. For the nine fixed points case, it is possible to show that (i) four of these fixed points are stable, i.e., ($q_1^{1,3}$, $q_2^{1,3}$), (ii) four are semistable (saddle points), i.e., (q_1^2, $q_2^{1,3}$) and ($q_1^{1,3}$, q_2^2), and (iii) one is unstable, i.e., (q_1^2, q_2^2). In addition, there are no spiral modes in the system – there are only simple damping or simple repelling of these fixed points.

Although the fixed points of Eqs. (4) are independent of each other their stabilities depend on each other. To study the basin of attractions of the stable fixed points we first set dq_1/dt (or dq_2/dt) to zero and then find the dependence of q_1 on q_2 (or vice versa). The "stability lines" are the lines for which q_1 (or q_2) is minimal or maximal. In Fig. 2 we present two

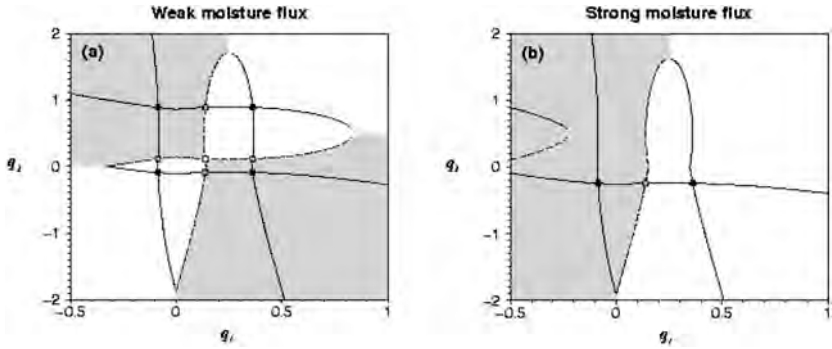

Fig. 2 - (a) The basins of attraction of the 4 stable states (indicated by black circles). The gray circles indicate the semi-stable states and the white circle indicates the unstable state. The solid lines indicate the minima lines while the dashed lines indicate the maxima lines. This case resembles the case of weak moisture flux forcing for which there are 4 stable states. The volumes of the boxes are: va=0,5, vb=10, and vc=1, in arbitrary units. (b) Same as (a) but for strong moisture flux forcing. Here there are just two stable states (units are non-dimensional).

examples of the fixed points with their basin of attraction. Figure 2a shows the situation when the moisture flux forcing is weak (small h_{s_i}) for which there are 9 fixed points. Figure. 2b shows the situation when the moisture flux forcing is strong (large h_{s_i}) for which there are 3 fixed points. In both cases the moisture flux forcing in the Aegean is assumed to be stronger than in the Adriatic. We have also assumed that the volume of the Ionian is ten times larger than the volume of the Aegean, which is twice larger than the volume of the Adriatic. These ratios are approximately realistic, and illustrate some of the possible ways in which the basins can interact. In Fig. 2a (weak moisture flux) the four heavy dots indicate the stable equilibria of the system. One has strong bottom water formation in both the Adriatic and the Aegean; one has no bottom water formation in either (actually there is a slightly negative amount of bottom water formation in this state); and the other two have strong bottom water formation in one of the seas, but not the other. The shading indicates the attractor basin for each equilibrium. In the case with strong moisture flux forcing (Fig. 2b), two of the stable equilibria have disappeared, and two remain. In one there is strong bottom water formation only in the Adriatic, and in the other there is no strong bottom water formation in either basin. In effect, the stronger moisture forcing of the Aegean has, in this case, eliminated the states with strong bottom water formation in

the Aegean. Fig. 2b may represent the situation before 1990 where the Adriatic was the only source of deep water formation, while Fig. 2a may represent the situation after 1990 with two sources of deep water, the Adriatic and the Aegean.

3. *Preliminary results.*

The parameter values used in our model our given in the Table. The Ionian sea basin is taken to be between 15.5E-23E and 30N-40.5N, the Aegean basin between 23E-27E and 35N-41.5N, and Adriatic basin between 12E-20E 42N-46N and 15E-20E 40.5N-42N. Virtual salinity fluxes, H_{s_1} and H_{s_2}, were approximated using the annual average evaporation minus precipitation, E-P, over the different basins with the depth D the different boxes,

$$H_s = S_0(P-E)/\mathrm{D} \tag{9}$$

The precipitation also includes the water runoff of the main rivers. The most critical parameters are k_1 and k_2. We approximate k_1 and k_2 using the surface temperature and salinity in Eq. (1) and comparing it to the reported fluxes of $0.3Sv$ for the Adriatic and $1Sv$ for the Aegean. We note however that we used the annual average of the surface temperature and salinity prior to 1990 and thus the approximation of k_2 may not be accurate. Under the current setting, the Aegean constant k_2 is about 3 times larger than the Adriatic constant k_1.

We find, under the current setting that there are 4 possible stable states,

$$\begin{aligned}
&(q_1, q_2)=(0.7Sv, 0.8Sv),\\
&(q_1, q_2)=(0.7Sv, -0.0008Sv),\\
&(q_1, q_2)=(-0.00007Sv, 0.8Sv),\\
&(q_1, q_2)=(-0.00007Sv, -0.0008Sv),
\end{aligned} \tag{10}$$

The salinity dominant circulations are very small, practically zero. The first possibility represents qualitatively the current thermohaline circulation while the second possibility represents qualitatively the thermohaline circulation prior to 1987 (for which the only source of deep water was the Adriatic).

Since the salinity dominant parts of the above fixed points are very small, the corresponding basins of attraction are small. I.e., only a small perturbation is needed to switch from the second state to the first state,

but a much larger perturbation is needed to switch from the first possibility to the second or the third. Thus, according to our model the current thermohaline circulation is more stable than the thermohaline circulation prior to 1987. On the other hand, if the moisture flux into either the Adriatic or the Aegean becomes strong, the system may be reduced to have just two stable states as illustrated in Fig. 2.

It is clear however that the Adriatic deep water formation of q_1=0.7 is more than twice larger than the observed value of 0.3*Sv*. This is likely due in part to the simplicity of our model and in part due to inaccurate estimation of the model's parameters. Although the Aegean flux of q_2=0.8*Sv* is close to the measured flux of 1*Sv* we regard this value as speculative since we estimate k_2 using the surface temperature and salinity gradients prior to 1990. Then we assume that the same gradients exist after 1990 and used these values to estimate k_2 from Eq. (1).

4. *Summary.*

We model the recent change the in deep water formation of the eastern Mediterranean using a 3 box model. The boxes represent the Adriatic, Ionian, and Aegean seas. The equations governing the dynamics are nonlinear and may have four stable states. Transitions from one configuration of single source of deep water in the Adriatic to two sources of deep water in the Adriatic and the Aegean seas may occur when the moisture forcing is weakened. For strong enough moisture flux forcing, the system may return to the single source state. Plugging in the approximated parameters we find that the model's Adriatic source is 0.7Sv which is twice larger than the observed flux of 0.3Sv. The model's Aegean flux is approximated to be 0.8Sv. We use data prior to 1990 to estimate the model's parameters for which the Aegean source of deep water wasn't formed yet, and thus the model's flux for the Aegean sea is speculative. We hope to estimate the model's parameters from data post 1990 which will enable us to more reliably estimate the bottom water formation in the Aegean sea.

In the current model we assumed that the temperature of the different boxes is fixed. This simplification enables us to find, analytically, the steady states of the system, as well as, their stability. In the future we plan to study a more complex version of the model with variable temperature, which may improve our understanding of the thermohaline circulation in the Eastern Mediterranean.

Table 1 - The parameters for the 3-box model.

parameter	short description	value
V_a	volume of Adriatic sea	27,600 km^3
V_b	volume of Ionian sea	640,000 km^3
V_c	volume of Aegean sea	61,600 km^3
k_1	flux constant between Adriatic and Ionian sea	$1.9\times10^9 m^3 s^{-1}$
k_2	flux constant between Aegean and Ionian sea	$5.34\times10^9 m^3 s^{-1}$
α	thermal expansion coefficient	$1.5\times10^{-4}(°C)^{-1}$
β	haline expansion coefficient	$8\times10^{-4}(psu)^{-1}$
T_1	temperature gradient between Adriatic and Ionian sea	2.55°C
T_2	temperature gradient between Aegean and Ionian sea	1°C
H_{s_1}	virtual salinity flux from Adriatic to Ionian sea	$1.16\times10^{-12} s^{-1}$
H_{s_2}	virtual salinity flux from Aegean to Ionian sea	$-2.41\times10^{-12} s^{-1}$
S_0	standard (Mediterranean) sea water salinity	38 *psu*

References.

Malanotte-Rizzoli P. and Hecht A., 1988. Large-scale properties of the eastern Mediterranean - a review. Oceanol. Acta , 323-335.

Manabe S. and Stouffer R.J., 1988. Two stable equilibria of a coupled ocean-atmosphere model. J. Climate , 841-866.

Nielsen J.N., 1912. Rep. Dan. Oceanogr. Hydrography of the Mediterranean and adjacent waters. In: Report of the Danish Oceanographic Expedition 1908-1910 to the Mediterranean and Adjacent Waters , 72-191.

Roether W. and Schlitzer R., 1991. Eastern Mediterranean deep water renewal on the basis of chlorofluoromethans and tritium. Dyn. Atmos. Oceans , 333-354.

Roether W., et al., 1996. Recent changes in eastern Mediterranean deep waters. Science , 333-335.

Schlitzer R., et al., 1991. Chlorofluoromethane and oxygen in the Eastern Mediterranean. Deep-Sea Research , 1531-1551.

Stommel H., 1961. Thermohaline convection with two stable regimes of flow. Tellus, 224-230.

Stone P.H., 1997. Global scale climate processes and climate sensitivity. In: Environmental Dynamics Series.V: Hydrometeorology and Climatology (M.Marani and R.Rigon, eds., Istituto Veneto di Scienze, Lettere ed Arti, Venice), 47-84.

Wüst G., 1961. On the vertical circulation of the Mediterranean Sea. J. Geophys. Res., 3261-3271.

LONG-TERM CLIMATE VARIABILITY OVER THE CENTRAL EUROPE

V. Defendi, G. Taroni, A. Bergamasco
Istituto per lo Studio della Dinamica delle Grandi Masse, CNR, Venezia

Abstract.

The Central Europe climate variability is here investigated through four long-term time series of pressure and temperature corresponding to four locations: Milan and Padua in Italy, Stockholm and Uppsala in Sweden. The performed statistical analysis (elementary statistics and trend analysis) is a useful instrument for trying to understand how the system works in this case on regional scale. On a local scale some inferences about the influence of the considered meteorological parameters on the mean sea level at Venice and Trieste are presented.

A first attempt of correlating the Central Europe climate and the North Atlantic Oscillation is based on the construction of a regional index obtained by the available pressure time series and then compared with the well known NAO index.

The use of climatic indexes is a way of studying the dynamical interconnections linking processes taking place in different parts of the system, but reducing the complexity of the climate system that is characterized by many components and governed by only partially known physical processes.

1. *Introduction.*

The Earth's climate has always been changing on different timescales and is governed by many factors interconnected by complex and not well understood physical processes.

The important point is to identify which factors matter most and when they come into play. The fact that a small perturbation of the system may produce effects elsewhere requires to understand the nature of the feedback processes. These chain reactions can induce different

responses on different scales to any perturbation, such as sudden switches between several states or reversals from a positive stimulus to a negative reaction (Burroughs 2001).

A useful starting point for studying the various climatic components and their interactions on different scales is to establish statistical rules about their behaviour, obtaining a phenomenological model of the climate system. This kind of analysis requires long time series in order to reduce the uncertainties about the probability of occurrence of certain outcomes, to estimate the frequency of extreme events and to understand how the system works.

No general consensus exists about the consequences of a climatic change due to the lack of data (the availability of observations is limited to only a few world areas, the atmospheric data are in general more abundant than the oceanic ones and the ignorance of the importance of the ocean/atmosphere coupled system), the climate drift and the discordant results obtained by simulations with different climate models, the difficulty to separate natural variability from anthropogenic impacts and to estimate the response time of the system to modifications (Khandekar 2000, Crowley 2000, Jones et al. 2001). Moreover, the probability of modifications in the climatic influence of a phenomenon is an issue over long periods of time, in particular for locations distant from the centres responsible for generating the phenomenon.

Due to these uncertainties, the problem can be faced by analysing long-term series. In particular, air temperature and air pressure values are fundamental meteorological and climatological parameters, because they influence climate on local, regional and global scales, conditioning human activities and human life in general.

The principal aim of this work is to investigate the climate variability on regional scale (Central Europe) and trying to see this variability in the context of a global scale.

2. *Time series analysis.*

The choice of using atmospheric data for assessing any variability associable with possible climate change is a good starting point. In particular, temperature and pressure have a key role in regulating the hydrological cycle, the heat and air transports on Earth, citing only some processes.

The time series used in this work are relative to the four locations (Fig. 1) listed below:

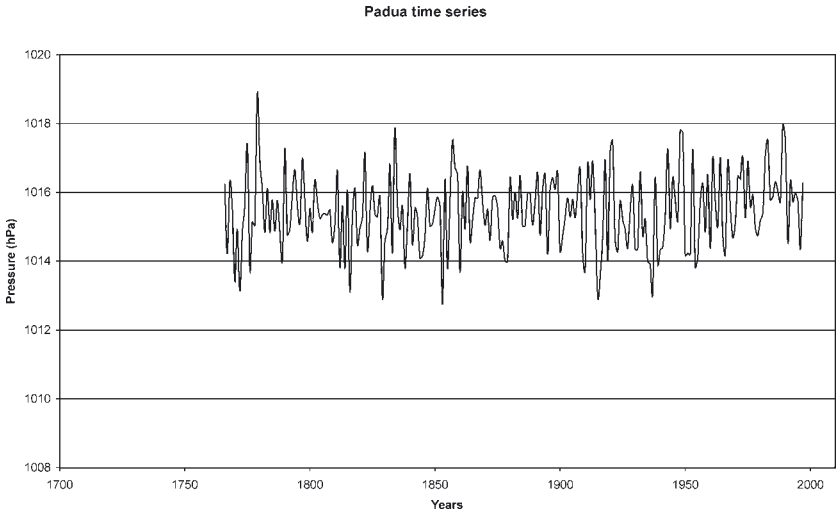
Padua time series
Pressure (hPa)
1020
1018
1016
1014
1012
1010
1008
1700
1750
1800
1850
1900
1950
2000
Years

(a)

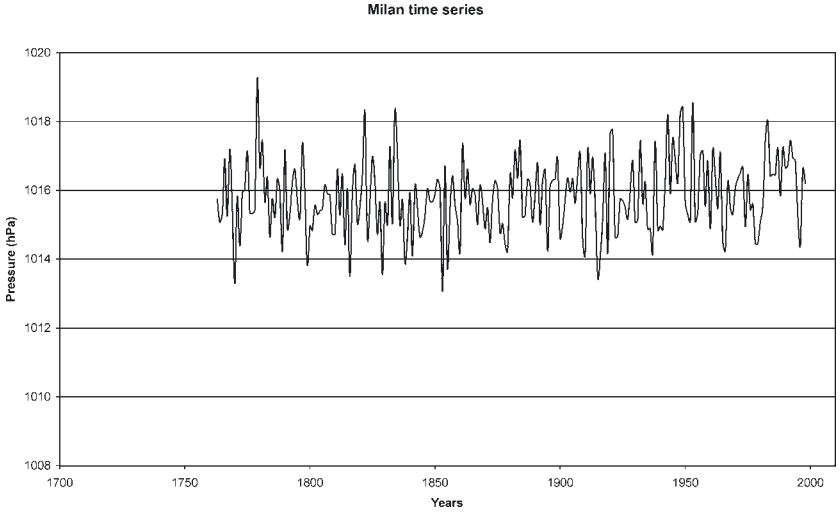
Milan time series
Pressure (hPa)
1020
1018
1016
1014
1012
1010
1008
1700
1750
1800
1850
1900
1950
2000
Years

(b)

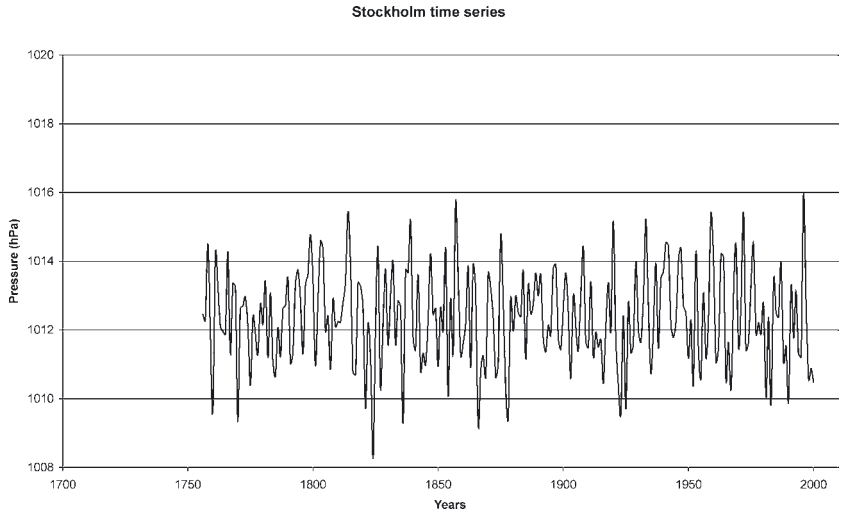

(c)

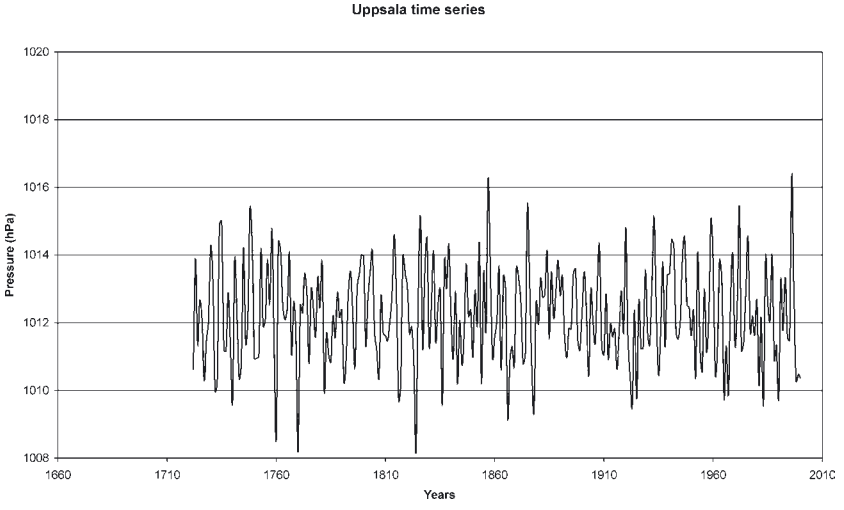

(d)

Fig. 1 - Pressure time series: (a) Padua, (b) Milan, (c) Stockholm and (d) Uppsala.

- Padua (Italy):
  Lat: 45.25°N
  Lon: 11.53°E
  Time length: 1766-1997
- Milan (Italy):
  Lat: 45.28°N
  Lon: 9.12°E
  Time length: 1763-1998
- Stockholm (Sweden):
  Lat: 59.20°N
  Lon: 18.03°E
  Time length: 1756-2000
- Uppsala (Sweden):
  Lat: 59.52°N
  Lon: 17.38°E
  Time length: 1722-2000

First a classical statistical analysis is performed on the yearly averages obtained by the daily temperature and pressure values.

The second issue is of identifying significant trends in the data for interpreting current events and deciding whether the observed features are an expression of the natural climatic variability or an evidence of a climatic change. This analysis is focussed on testing the hypothesis of presence of an annual trend in pressure both locally (considering the single stations) and regionally (considering the "near" stations), but some considerations on temperature are also reported for completeness.

The elementary statistics for pressure and temperature are summarised respectively in Table 1 and 2. In particular, the two indexes, b1 and b2, indicate if the data distribution is nearly normal. In fact, the standardized asymmetry coefficient, b_1, gives the degree of asymmetry of the data histogram, while the standardized kurtosis coefficient, b2, expresses the flattening or the sharpening of the data histogram as regards the normal distribution. The test of normality is obtained by the standardization of b1 and b2. Under this hypothesis the sum of the squares of b1 and b2 is approximately distributed as a chi-square function with two degrees of freedom. By this consideration the hypothesis of normal distribution of the data is accepted with a 5% level of significance, if the sum mentioned above is lower than or equal to 6.

In order to explain some relations in the dataset examined, we present in Table 1 and 2 some elementary but indicative statistics related to the annual trend of the observed phenomena.

The P-value (indicated by asterisks in the tables) tests the statistical significance of the correlations, expressed by r, between pressure (or temperature) and the sampling year: P-values < 0.05 indicate statistically significant non-zero correlations at the 95% confidence level.

As it can be seen, Table 1 does not show variability in the pressure mean value, the pressure minimum and maximum of the geographically "near" stations. The correlation coefficient between pressure and sampling year has a 2.5% level of significance only for the Milan time series.

Table 1. Statistics for the pressure time series. N = number of observations, m = mean, s = standard deviation, pmin = pressure minimum, pmax = pressure maximum, b1 = standardized asymmetry coefficient, b2 = standardized kurtosis coefficient, r = correlation coefficient between pressure and sampling year, (*) = P-value of 2.5%.

	PADUA	**MILAN**	**STOCKHOLM**	**UPPSALA**
N	223	236	245	279
μ	1015.4	1015.8	1012.3	1012.2
S	1.16	1.07	1.39	1.45
pmin	1012.8	1013.1	1008.3	1008.2
pmax	1018.9	1019.3	1015.9	1016.4
b1	-2.84	1.35	0.10	0.40
b2	8.23	0.26	-0.65	-0.53
r (p, year)	0.10	0.15 (*)	-0.013	-0.005

As regards temperature (Table 2) the evidence of a positive trend indicated by the positive correlation coefficient between temperature and sampling year is clear. This is confirmed by the estimated mean surface temperature of about 0.32°C (0.16°C per decade) for the recent 20-year period (1978-1997) (Khandekar 2000). According to Camuffo and Sturaro (This volume) this trend is accompanied by an increase in the frequency of the hottest days compared to the frequency of the coldest ones.

The stronger correlations (5% level of significance) correspond to the Padua and Milan stations.

The values of b1 and b2 for Padua and Milan seem to reject the hypothesis of normal distribution for temperature, but the presence of an annual trend and of possible autocorrelations in the two time series could invalidate this result.

Table 2. Statistics for the temperature time series. N = number of observations, μ = mean, s = standard deviation, Tmin = temperature minimum, Tmax = temperature maximum, b1 = standardized asymmetry coefficient, b2 = standardized kurtosis coefficient, r = correlation coefficient between temperature and sampling year, (*) = P-value of 2.5%, (**) = P-value of 5%.

	PADUA	**MILAN**	**STOCKHOLM**	**UPPSALA**
N	223	236	245	278
μ	13.0	12.8	5.8	5.2
s	0.62	0.61	0.95	0.99
Tmin	10.1	11.3	3.2	2.5
Tmax	14.5	14.7	7.9	7.8
b1	-3.53 (*)	-0.012	0.09	0.16
b2	4.08(**)	0.04	-1.23	-0.88
r (T, year)	0.24 (**)	0.3 (**)	0.14 (*)	0.14 (*)

2.1 *Trend analysis.*

In order to test the existence of trend in the pressure time series, from 1750 to 1992, of Padua and Milan, two alternative hypotheses H_0 (absence of trend) and H_1 (presence of an annual positive trend) must be considered. The choice of H_1 is based on the considerations reported in Pirazzoli and Tomasin (1999) about an increase of the atmospheric pressure on the region of the Northern Adriatic in the last decades.

The strength of the linear relationship between the two variables considered (Padua pressure and Milan pressure) is measured by the Bravais-Pearson coefficient that shows a strong correlation characterized by a 1‰ level of significance.

A simple method for estimating the existence of a linear trend in the pressure series, h(t), derives from the correlation coefficient, r, between h(t) and the sampling year (t=1,T).

If ρ is the "true" correlation coefficient, the random sample variable, Z, is described by the transformation $z=\sqrt{(T-3)}\log((1+r)/(1-r))/2$ and is distributed asymptotically according to the normal law of mean equal to $\log((1+\rho)/(1-\rho))/2$ and unitary variance.

A strong correlation (P-value = 1‰) is present between sampling year and pressure at Padua and Milan, so the effect due to correlation has to be removed from the z statistics for identifying the annual trend. In this case, it is not possible to use a simple statistical test based on the sum of

the two sample values and the method of non-parametric combination for dependent tests (Pesarin 2001) is applied. The theory of the combined tests allows giving a synthetic and statistically correct judgement on the overall significance of the presence or absence of trend, eliminating the problem of the interdependence between the two stations.

The independence of pressure and sampling year is accepted for the Padua station and rejected for the Milan station. The opportune combination of the two statistics gives a result with a level of significance of about 5% (P-value = 4.8%).

2.2 *Autocorrelation analysis.*

Our model is based on the assumption that there is a correlation between sampling year and pressure (or temperature). For validating this model, the errors or residuals, represented by the differences between the observed pressures and the computed ones, must be considered. These errors, ε, must be independent, with zero mean, normally distributed and characterized by the same variability. If the correlation coefficient, r, is significant and the errors respect the conditions above listed, the linear model is accepted. In particular, the independence of the errors is tested computing the autocorrelations: the errors are independent if they are no autocorrelated. The search of absence of autocorrelation makes sense if the time series do not present any dependence with the sampling year t. In fact, the existence of a monotone trend involves strong and significant autocorrelations. The hypothesis of absence of autocorrelation in the pressure time series verifies if the succession h(t) is linearly independent from h(t+k) with k=1, L (L<T). The autocorrelation of k order, r(k), is defined by the Bravais-Pearson correlation coefficient between h(t) and h(t+k) with k=1, L.

The tests more frequently used are based on the sample autocorrelations and in particular the test of Ljung-Box (Piccolo 1984), here chosen for its efficiency and simpleness, is function (opportunely weighed sum of squares) of the first n sample r (k) autocorrelations.

For the application of the Ljung-Box criterion it is necessary to remove the linear trend with the sampling year from the original time series. Another approach uses the Helmert transforms (Nenna 1984, Carbognin & Taroni 1996a, 1996b) which may test the normal distribution of the residuals from the linear regression.

The Ljung test applied to the residuals e(h(t)) verifies the absence of autocorrelation. The presence of significant autocorrelations in the resi-

dual series points out that the linear model only partially explains the interest phenomenon. In this case, it is necessary to use other methods that consider the autocorrelations still present, improving the data adjustment. In fact, the same correlation coefficient between observations and sampling year may lose its efficiency, even if it is an unbiased and consistent estimator.

The removal of autocorrelations in the residuals is carried out recursively through the Durbin method (1960).

The results of the Ljung-Box test show that the autocorrelations of the residuals of the linear regression are significant for the Padua (P-value = 0.0043, level of significance = 5%) and the Milan (P-value = 0.045, level of significance = 2.5%) temperature time series. The autocorrelations for Uppsala and Stockholm are not significant at the 5% level.

The residuals of the regression for the pressure time series are never significant at the 5% level.

The absence of autocorrelations in the residuals indicates the rightness of the model of linear interpolation in describing the computed annual trend.

For the Padua station, the correlation coefficient between temperature and sampling year changes from 0.326 to 0.256 (P-value $\leqslant$ 0.001), eliminating the first autocorrelation. In the case of Milan r changes from 0.246 to 0.210.

The decrease of r is more sensible for the Padua station, which shows stronger autocorrelations for residuals according to the Ljung test.

The presented analysis is based on the elementary autocorrelations. In fact, the study of the best fit is not yet finished and it will be later performed with refined instruments.

2.3 *Pressure and mean sea level at Venice and Trieste.*

Above we have focussed on the Padua and Milan time series. The influence area of these stations justifies this interest, in particular for what concerns Padua that may be considered representative of the Venetian meteorological situation. In this context, it is important to make some considerations about the influence of the meteorological parameters on the sea level.

Table 3 shows the Bravais-Pearson correlation coefficient between the Padua pressures and the mareographic levels at Trieste and Venice from 1896 to 1994, limiting our attention to the Northern Adriatic. A partial correlation coefficient, obtained removing from the data the time trend

Table 3 - Correlations and partial correlations (in Italics) between pressure at Padua and mean sea level at Trieste and Venice. The two asterisks indicate a level of significance of 1%.

	Trieste mean sea level	**Venice mean sea level**
Padua pressure	-0.38 (P-value = 0**) *-0.75 (P-value = 0**)*	-0.12 (P-value = 0.24) *-0.66 (P-value = 0**)*

effect that moves both pressure and mean sea level in the same positive direction, is also computed.

The correlations between the mean sea level of Trieste and the Padua pressure time series is significant at the 1% level and negative, meaning that a decrease of pressure corresponds to an increase of the mean sea level.

Regarding these simple correlation coefficients, Venice does not show the same P-value of Trieste and this result seems to be contradicting if the nearness of the two stations is considered.

The partial correlation coefficients are both negatively correlated and statistically significant.

A global judgement about the presence or absence of a linear dependence can be obtained combining these results using the Pesarin method (2001). The two alternative hypotheses are H_0 (absence of correlations between the two mareographic stations and the pressure and temperature values considered for Padua) and H_1 (presence of negative trend). Table 4 summarizes the combination of the correlations between the mean sea level of Trieste and Venice.

The overall mean sea level seems strictly linked to the Padua temperature, while the mean sea level of Venice and Trieste is strictly correlated to the Padua pressure.

Table 4 - Correlations between pressure, temperature and combined (Venice + Trieste) mean sea level.

	Mean sea level (Venice + Trieste)
Padua pressure	P (Trieste) = 8.33e-5 P (Venice) = 0.12 P (Venice + Trieste) = 0.003
Padua temperature	P (Trieste) = 0.06 P (Venice) = 0.016 P (Venice + Trieste) = 0.03

These results seem to point out that pressure mostly influences the dynamical behaviour of the mean sea level. Camuffo and Sturaro (2002) show, using instrumental records of sea level at Venice (1872-2000), that it is present a continuous relative sea level rise from 1872 to 1960s, followed by a stop in this trend. The combined effect of subsidence and sea level results in a 31 cm rise. One of the possible reasons for explaining this changing trend is the forcing due to pressure and in particular its local rise (Pirazzoli & Tomasin 1999). This aspect is particularly important for Venice, subject to the phenomenon of flood tides or *acqua alta*.

3. *Climatic indexes.*

The search for teleconnections has to consider the different scales involved in the climate system and their interactions, so our inferences about the Central Europe climate have to be fitted in a global context. For doing this it is necessary to reduce the complexity of the system decreasing the number of degrees of freedom. The climate system, in fact, is characterized by a natural variability ruled by cycles with specific frequencies and by an induced variability and it is very difficult to discriminate between these two aspects of the problem. Moreover, the estimate of the impact of human activities is still affected by a high uncertainty. In this context, the use of climatic indexes allows simplifying the system and describing quantitatively the preferential modes of variability and the involved dynamical processes.

Based on the definition found in literature of the North Atlantic Oscillation (NAO) index (Hurrell 1995, Hurrell & van Loon 1997), we have created a regional index for quantifying the Central Europe climatic variability. This index, IS, is computed as follows:

$$IS=\left(\frac{P_1-MP_1}{STD_1}\right)-\left(\frac{P_2-MP_2}{STD_1}\right)$$

where
P_1= Milan (or Padua) pressure
MP_1= long-term mean of Milan (or Padua) pressure
STD_1= long-term standard deviation of Milan (or Padua) pressure
P_2= Stockholm (or Uppsala) pressure
MP_2= long-term mean of Stockholm (or Uppsala) pressure
STD_2= long-term standard deviation of Stockholm (or Uppsala) pressure

The long-term mean and standard deviation are computed considering the complete time series length (231 years) relative to their overlapping period.

The indifferent use of the two Italian and the two Swedish stations is justified by the significance of the estimated correlations reported in Table 5.

Table 5 - Correlations between sampling year and pressure stations and between pressure stations computed for the overlapping period (231 years). The P-values are indicated in brackets and the bold ones represent P-values < 0.05.

	Year	**Milan**	**Padua**	**Stockholm**	**Uppsala**
Year		0.13	0.08	0.009	-0.002
		(**0.05**)	(0.24)	(0.89)	(0.97)
Milan			0.82	0.13	0.14
			(**0.0**)	(0.054)	(**0.036**)
Padua				0.07	0.065
				(0.33)	(0.34)
Stockholm					0.95
					(**0.0**)

As it can be seen, the pairs of variables, Milan and Padua pressure and Stockholm and Uppsala pressure, have P-values < 0.05, meaning statistically significant non zero correlations at the 95% confidence level. This result is evident if we consider that these stations are representative of the same geographical region.

The Padua/Stockholm index is compared as an exemplification with the NAO index (Fig. 2), which is responsible of the climate variability in the Northern Atlantic (Hurrell & van Loon 1997, Marshall et al. 2001) and strongly influences the European climate.

The choice of Padua and Stockholm rather than another pair of stations makes sense if we remember the considerations about Table V. Moreover, the Padua station is the nearest one to the Venetian area.

The comparison between the two series is relative to the overlapping period (from 1865 to 1996) as to which the two indexes are standardized.

The plot shows a correlation in the alternation of positive (index > 0) and negative (index < 0) phases, so the trend is very similar. The main differences regard the higher values of the NAO index and the more frequent oscillations of our index. According to our opinion, this is due to the different spatial scale. In fact, the two stations we have used are characterized by a lower distance between them than the two stations (one in the Azores and the other in Island) used for computing the NAO index.

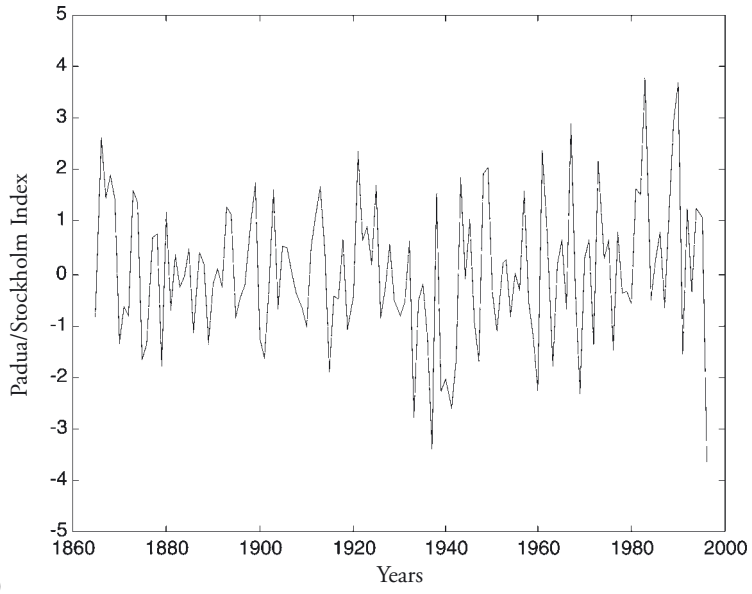

(a)

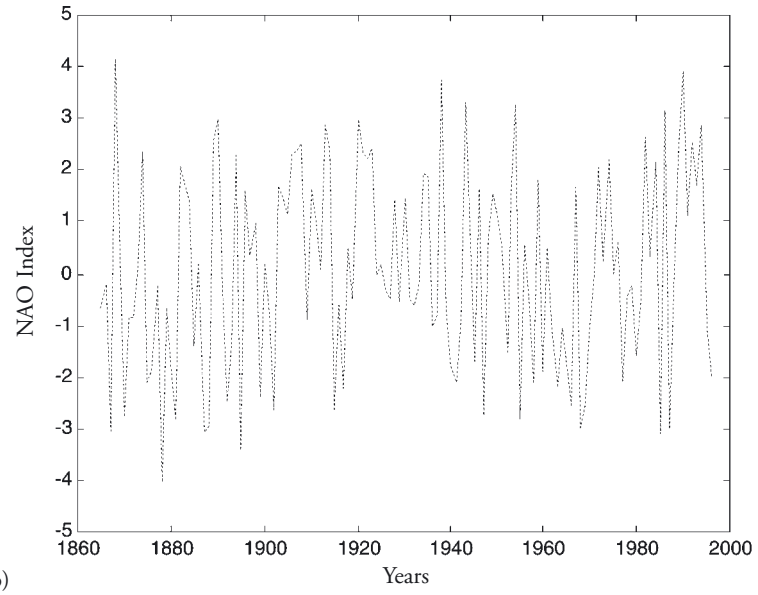

(b)

Fig. 2 - (a) Padua/Stockholm index and (b) NAO index.

It is interesting to underline that the correlations are always significant at the 95% level, positive and practically very similar. In fact, the correlation between Padua/Stockholm (or Padua/Uppsala) and NAO is 0.34, between Milan/Stockholm (or Milan/Uppsala) and NAO is 0.38.

This kind of elaboration represents the first step in evaluating the response of the climate system to an initial stimulus on different spatial and temporal scales.

4. *Concluding remarks.*

In this work we have used a statistical approach in analysing the available long-term time series for reducing the complexity of the climate system establishing statistical rules about the behaviour of its component. Dealing with climate studies, one of the main problems is that much of the variance of the examined data is the product of the natural variability of the system. Moreover, the influence of extreme events may be high on short-term temporal scale. A useful way for extracting information from a time series is the search for any significant linear trend in the considered data. The computation of the correlation coefficient, r, is a simple method for exploring the existence of a link and the presence of a possible trend between two variables. The interpretation of this coefficient is critical, because the level of significance is important, but not sufficient. In fact, the ratio, equal to $(1-r^2)$, between the variance computed by the model and the variance of the observations must be estimated.

In this context, the results about the positive trend between the NAO index and our index are highly significant, but in terms of the variance we can only say that the linear trend explain 10% of the time series variance, while the remaining 90% is due to other causes.

These considerations are not simple philosophical speculations, but they underline the difficulty of establishing the causes of climate variability and the importance of understanding the processes at work and the possible teleconnections due to the interactions on different scales. Much work has to be done in order to reduce the uncertainties in climate studies and to improve the understanding of the system.

References.

Burroughs W.J., 2001. Climate change: a multidisciplinary approach, First edition. Cambridge University Press, pp. 291.

Camuffo D. & Sturaro G., 2002. Use of proxy-documentary and instrumental data to assess the risk factors leading to sea flooding in Venice. Global and Planetary Change (in press).

Carbognin L. & Taroni G., 1996a. Eustatismo a Venezia e Trieste nell'ultimo secolo. Istituto Veneto di Scienze, Lettere ed Arti, CLIV, 281-298.

Carbognin L. & Taroni G., 1996b. Linearità tra due variabili: piezometria e subsidenza nell'area veneziana. Istituto Veneto di Scienze, Lettere ed Arti, CLIV, 33-52.

Crowley T.J., 2000. Causes of climate change over the past 1000 years. Science, 289, 270-277.

Durbin J., 1960. The Fitting of Time Series Model. Revue de l'Institut International de Statistique, 28, 233-244.

Hurrell J.W., 1995. Decadal trends in the North Atlantic Oscillation and relationships to regional temperature and precipitation. Science, 269, 676-679.

Hurrell J.W. & van Loon H., 1997. Decadal variations in climate associated with the North Atlantic Oscillation. Climatic Change, 36, 301-326.

Jones P.D., Osborn T.J. & Briffa K.R., 2001. The evolution of climate over the last millennium. Science, 292, 662-667.

Khandekar M.L., 2000. Uncertainties in greenhouse gas induced climate change. Report prepared for Science and Technology Branch, Alberta Environment, ISBN 0-7785-1015-4, Edmonton, Alberta.

Marshall J., Kushnir Y., Battisti D., Chang P., Czaja A., Dickson R., Hurrell J., McCartney M., Saravanan R. & Visbeck M., 2001. North Atlantic climate variability: phenomena, impacts and mechanisms. International Journal of Climatology, 21, 1863-1898.

Nenna E., 1984. Estensioni della trasformata di Helmert al caso della regressione lineare semplice. Statistica, 1, 79-86.

Pesarin F., 2001. Multivariate permutation tests with applications in biostatistics, First edition. John Wiley & Sons, pp. 432.

Piccolo D. & Vitale C., 1984. Metodi statistici per l'analisi economica. Bologna: Il mulino, pp. 747.

Piccolo D., 1998. Statistica. Bologna: Il mulino, pp. 964.

Pirazzoli P.A. & Tomasin A., 1999. L'evoluzione recente delle cause meteorologiche dell'acqua alta. Istituto Veneto di Lettere, Scienze ed Arti, CLVII, 317-344.

VENICE IN THE CONTEXT OF EUROPEAN-SCALE CLIMATE CHANGES WITH SPECIAL REFERENCE TO THE 'ACQUA ALTA' PHENOMENON

D. Camuffo, G. Sturaro
Istituto di Scienze dell'Atmosfera e del Clima, CNR, Padova

Abstract.

Due to its geographical position, and because it was built at sea level, Venice is extremely sensitive to climate changes and, in the future, risks being submerged as a consequence of the expansion of oceanic water in response to global warming.

The climate changes of the Venetian area are investigated by making use of eight highly reliable European series, covering a very long time interval, nearly three centuries. These are daily pressure and temperature series derived from the EC funded project IMPROVE: Padova (It., 1725-present), Milan (It., 1763-present), Central Belgium (Be., 1767-present, temperature only), Uppsala (Se., 1722-present), Stockholm (Se., 1756-present), San Fernando/Cadiz (Es., 1776-present), St Petersburg, Russia (1743-present) and Central England (UK., 1772-present). An important aspect in the analysis is the high (daily) resolution of the series, which allows more insight into past variability by looking at the frequency of extreme events. An analysis of the distribution of extreme events across Europe has shown that recent warming is characterised by an increase in frequency of the hottest days, in association with a decrease in frequency of the coldest.

A key problem for Venice is the increasing frequency of sea surges flooding the city (locally named *acqua alta*) that has reached an unsustainable level. After careful examination of both proxy documentary and instrumental data, it has been possible to reconstruct the extreme weather conditions and natural hazards which have taken place in the last two millennia, with particular reference to surges. An accurate series of the flood surges has been obtained combining instrumental observations (1872-2000) with documentary data for the previous period. The period of minimum solar activity of Spörer (1416-1534) was anomalous for surges. Not only have meteorologically perturbed periods been identified, but also the

effects of the accelerated subsidence of the city and of certain works undertaken in the lagoon that varied the exchanges between the sea and the lagoon. The impact of subsidence and of the modified dynamical exchanges of the lagoon on the change in flooding frequency have been established. During the instrumental period the tide gauge measured a 31-cm rise. The frequency of surges has dramatically increased since the 1960s, reaching about two flooding events per year, the greatest value since 792 AD.

Keywords: global warming, Venice, sea surges, sea level rise, extreme events.

1. *Introduction: Storm surges flooding Venice.*

Venice provides an interesting example of a well-documented close interaction between man and the environment, showing how the combination of proxy-documentary and instrumental data can be usefully employed to study the past as a key to interpret the present.

Due to its geographical position, and because it was built close to sea level, Venice is extremely sensitive to climate changes and could, in the future, risk being submerged as a consequence of the response of oceanic water expansion to global warming (Pirazzoli, 1989). This delicate position has been accentuated by human intervention that has caused land subsidence following the extraction of underground water for industrial activities and the excavation of canals which have changed the hydrological regime of the Lagoon, favouring the entrance of sea water. However, it should be noted that the Mediterranean, mainly a closed basin strongly influenced by the local climate, responds in a peculiar way to global warming, different from the expected ocean expansion.

Venice is exposed to flood tides, locally called *acqua alta* (literally, high water) that are generated by a number of factors: (i) a pressure pattern with a low on the western or central Mediterranean. This low generates two winds: a Sirocco wind, which drags water from SE along the Adriatic Sea and a Bora wind in the Venice area, which drags water from NE; (ii) the so-called barometric effect, which raises the sea level where the atmospheric pressure is lower; (iii) the rapid change in atmospheric pressure, which generates a free oscillation in the Adriatic sea (*seiche*); (iv) the luni-solar astronomical forces, which are stronger in syzygy, i.e. when Earth, Sun and Moon are in conjunction with each other. The first factor is the most dominant.

Under the pressure of these extreme flood events, the key problems concerning Venice are: (i) the expected sea level rise; (ii) the sinking of the ground, due to the extraction of water from subsoil in addition to natu-

ral factors, e.g. tectonic movements, soil compaction and sediment load; and (iii) the exchanges between sea and lagoon waters (UNESCO, 1969; Giordani Soika and Meneghini, 1970; Frassetto, 1971; Pirazzoli, 1977; Tomasin and Frassetto, 1979; Carbognin et al., 1984). The sea-lagoon exchanges have recently been modified in several ways, in particular by deepening three channels connecting the lagoon with the sea and by excavating new channels for the passage of large vessels. The main modification of the sea-lagoon equilibrium occurred in the period 1963-75, when the Malamocco channel was opened. Other works concerned the transformation of marshes into terrain for the growing industrial area (Miozzi, 1969; Rosa Salva, 1974; Pirazzoli, 1982; Archivio di Stato, 1983; Favero et al., 1988). The surges that flood Venice, not only provoke damage to population and goods, but also impregnate walls with sea salt, which over a short period of time destroys mortar, marble, limestone, brick and other building materials. Indeed, while in past centuries flood surges were rare, they have become more and more frequent.

Regular instrumental records of the sea level with floating mechanical tide gauge started in 1871. The tide gauge was displaced in 1906 and 1923 within the city centre. In modern times, several tide gauges have been installed showing that the relative sea level response of early instrumental positions were homogeneous with the present location (Pirazzoli, 1989). The measurements show that in the period 1872-2000 the combined effect of the subsiding soil and rising sea level had a relative rise of 31 cm (Fig. 1). A continuous relative rise is evident from 1872 to the 1960s (average rise rate: 2.6 mm yr^{-1}); after that the sea level seems to have ceased to rise (relative sea level rise after 1970 is 0.7 mm yr-1). A number of reasons can be invoked to explain this change in trend. The first is that the rate change occurred in correspondence with a special law regulating the extraction of underground water in the Industrial Area, thus stopping subsidence. This would have been positive news for Venice, but considered alone it seems in contradiction with much evidence of sea level rise prior to the industrial activity, which became important after World War II. Other three reasons are of meteorological nature. The first is a reduction of the precipitation in the Mediterranean basin (Piervitali et al., 1998). The second is the increased number of clear days in the last 50 years over the Mediterranean basin (Piervitali et al., 1997). During clear days, the higher sea surface temperature and the increased intensity of the coastal breezes have proven to be correlated with a higher evaporation rate (Colacino and Dell'Osso, 1977). The third factor is a local rise of the atmospheric pressure (of the order of 1 hPa) which has been noticed in a number of stations (Pirazzoli and Tomasin, 1999; Cocheo and

Camuffo, 2002). In any case, all of these meteorological factors are of ephemeral nature and may disappear sooner or later. In addition, it can be noted that the Mediterranean sea is connected with the Atlantic Ocean through the narrow Gibraltar Strait that limits the water exchange. For this reason a certain lowering of the sea level in the Mediterranean decoupled from the ocean level rise is possible, but only to a limited extent.

At present, the sea level in Venice seems to fluctuate around the same or a slightly variable value, but a significant change in trend has not yet

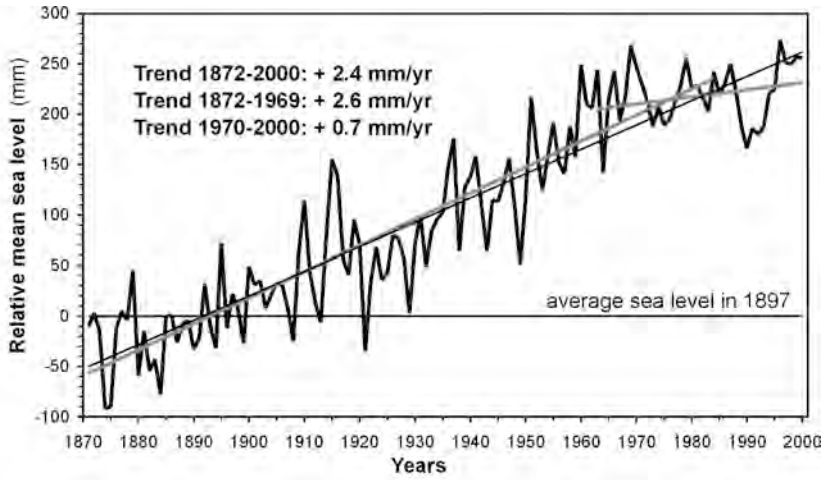

Fig. 1 - Instrumental record of relative sea level at Venice. Regular measurements started in 1872; 'zero' is the average level in 1897. In recent decades, due to extensive data scattering, the trend-line analysis does not support the hypothesis that the sea level has become stationary. Trend values are reported for different periods.

been established. In fact, the whole series can be subdivided into periods in which one factor or another has been dominant. Depending on the choice of the subdivisions and hypothesis made, slightly different values of relative sea level rise can be obtained. The whole instrumental period 1872-2000 will be used in this study to determine the main trend. This choice is also subjective, but it has the advantage of using the most complete documentation available today. In this paper an estimation of the frequency of surges in the period before the instrumental record, i.e. prior to Present Day Warming, will be made.

2. *The long series of the flood surges at Venice.*

The long series of flood surges from documentary sources (792-1867 AD) and tide-gauge records (1872-2000) has been revised and updated (Camuffo, 1993; Enzi and Camuffo, 1995; Camuffo and Sturaro, 2002) and it was possible to establish links between trends, natural forcing and anthropogenic factors. Secondary flooding at successive tidal oscillations may follow a flood surge. As in the above studies, the number of surges has been defined by counting the meteorological events that have triggered one or more flooding tides, i.e. surges occurring repeatedly within a few days were counted as one. In order to point out anomalous periods with different frequencies of sea storm occurrence, the series has been firstly filtered with the cosine-like Hamming-Tuckey (HT) filter (Vinnichenko et al, 1973; Wei, 1990) and then expressed as cumulative frequency distribution (CFD).

HT groups together and smoothes scattered data identifying periods of scarce or intense flooding activity, allowing a comparison between them (Fig. 2). As a preliminary test with the maximum entropy analysis

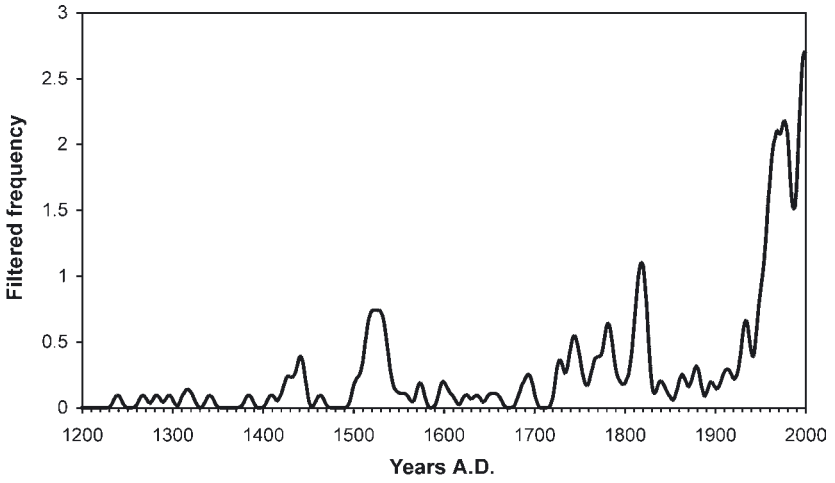

Fig. 2 - Frequency distribution of flooding surges in the documentary (1200 – 1871) and instrumental (1872-today) periods. The data have been handled with the Hamming-Tuckey filter with 19-yr window and 2-yr step. In order to show the present-day situation and to avoid the filter truncation at 9.5 yr before present, the data 1991-2000 have been repeated for 2001-2010, assuming unchanged conditions.

(MESA; Priestley, 1981) revealed a minor recurrence, with an 18.6-yr period (i.e. the lunar nutation period), the HT filtering window was chosen equal to 19 yr to avoid spurious oscillations generated by the filter.

The frequency of flood surges increased slightly during the Wolf Minimum of solar activity (1282-1342). In the period which culminated in 1424, 1433 and 1442, an exceptional combination of the attractive luni-solar forces caused an increase in the frequency of exceptional tides. In fact, the Moon in perigee was coincident with its maximum declination and the Sun and Moon were both at their greatest declination (Lamb, 1972). With the exception of this period, the astronomic component is of minor relevance when compared with the meteorological forcing. The next maximum in flooding surges occurred in the first half of the 16th century (1500-1540), during the Spörer minimum of solar activity (1416-1534); another maximum took place between 1730-1830. It is not possible to assess whether or not solar activity affected the atmospheric circulation (Eddy, 1977) by generating an anomalous occurrence of the Sirocco wind and surges during the Spörer minimum, because nothing similar was found during the other periods of reduced solar activity, i.e. the Oort Minimum (1010-1090) or the Maunder Minimum

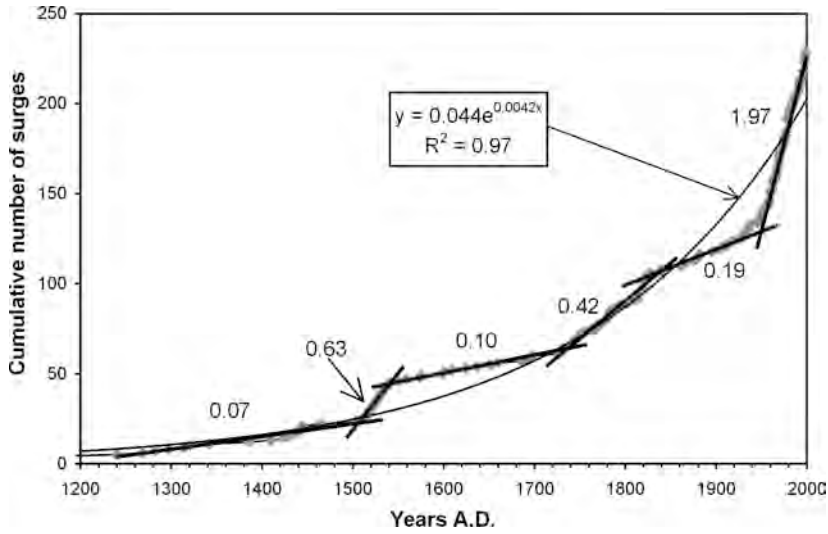

Fig. 3 - Cumulative Frequency Distribution of the flooding surges in the documentary (792 – 1871) and instrumental (1872-today) periods. Bold numbers give the number of surges per year in the different time periods. An exponential trend (maximum likelihood) is fitted through the data.

(1645-1714). Finally, an impressive increase in flooding frequency was found in recent times.

CFD does not introduce distortions in data and is appropriate to estimate the flooding frequency from the curve slope, thus showing changes in trend (Fig. 3). The main trend of CFD is exponential (correlation coefficient, r^2=0.97), which is expected in a regime of continuous relative sea level rise. Upon the general exponential trend, fluctuations are present. To aid the interpretation of these fluctuations, linear trends were calculated as a first order approximation of the number of surges per year in every given time period. CFD shows that flooding frequency was very low (i.e. <0.10 surges yr^{-1}) until 1740, excluding the Spörer period 1500-1540 (0.63 surges yr^{-1}) that in Italy had several kinds of meteorological anomalies (Camuffo and Enzi, 1995).In the most recent times, (1965-2000) the frequency has notably increased to almost two flooding surges per year (1.97 surges yr^{-1}).

In order to investigate whether a recent change in the flooding regime has occurred, the recent period has been analysed in detail (Fig. 4). The

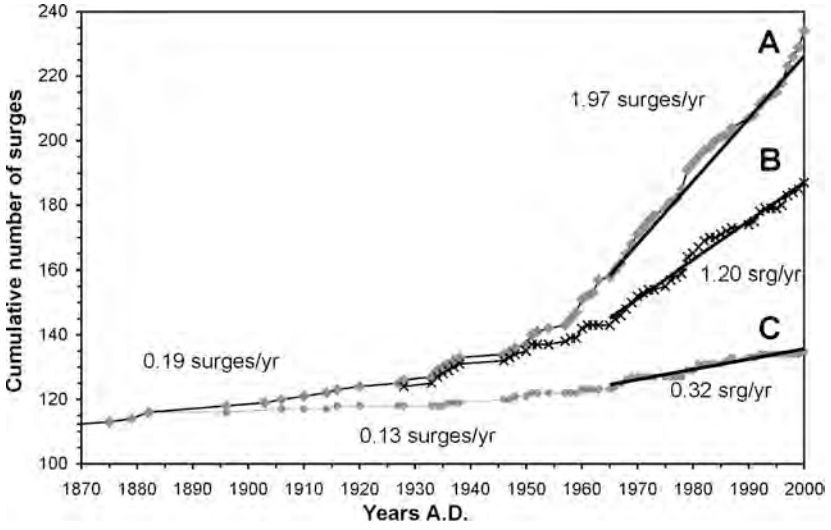

Fig. 4 - The same as in Figure 3 but for the recent period (1870-2000). The line A (1.97 surges yr-1) represents the observed data; B (1.20 surges yr-1) is the calculated number of flooding events in the absence of the subsidence which occurred between 1925 and 1965 (10 cm); C (0.13 surges yr-1 in the period 1872-1925 and 0.32 surges yr-1 after 1965) is the calculated number of flooding events in the absence of the average subsidence since 1872 (2.4 mm yr-1).

figure shows two regimes: the first one, for the period 1830-1930 characterised by the flooding rate of 0.19 surges yr^{-1}, and the second (1965-2000) with a rate of 1.97 surges yr^{-1}. The exact transition between the two regimes is unclear and seems affected by anomalous factors that have altered the situation. Looking at the works in the lagoon (Pirazzoli, 1982), disturbing factors are possibly linked to the deepening of the Lido channel and its inlet (1928-30) up to the level of -11 m. The main works which characterised the second regime were the excavation of the main channel from the Malamocco inlet to the Industrial Area (1963-1969) which reached -15 m in depth. However, at the same time the uncontrolled extraction of underground water for industrial use in the immediate hinterland caused a further subsidence of the terrain that in the period 1925-65 was estimated to be 10 cm, by making reference between the sea level in Venice and in Trieste, which lies 200 km East of Venice (Carbognin et al., 1976).

The surge frequency in the period 1960-2000 is affected by the combined effect of static and dynamic factors, i.e. the lower level of the city (subsidence) and the increased exchanges between sea and lagoon. However, it is possible to attempt a distinction between the relative weights of these two contributions. Under the hypothesis of only 10 cm subsidence, curve B of Figure 4 was drawn. The curve was calculated as follows: (i) from 1925 to 1965, the subsidence was considered to occur linearly up to 10 cm and was subtracted from the observed relative sea level; (ii) after 1965 the total value (10 cm) was subtracted from the sea level. The result, curve B, shows how many flooding surges would have occurred in the absence of such a 10-cm subsidence, i.e. 1.2 surges yr^{-1} (r^2=0.98).

Under this hypothesis the effect of the subsidence alone has contributed by 1.97-1.20=0.77 surges yr^{-1}. Under the same hypothesis and the additional hypothesis that the meteorological factors have not changed in the last 70 years, the dynamic effect can be estimated. The dynamic effect is 1.97-0.77-0.19=1.01 surges yr^{-1}, obtained by subtracting from the present-day regime both the subsidence contribution and the regular regime prior to 1930.

However, if one considers that the overall rate of relative sea level rise since 1872 is 2.4 mm yr^{-1} (Fig. 1) and this value is progressively subtracted from the observed sea level, the curve C is obtained. Curve C, which represents the situation in the absence of the static effect, is characterised by a very low frequency (0.13 surges yr^{-1}; r^2=0.99) until 1965 and has an increased rate (0.32 surges yr^{-1}; r^2=0.94) for the present period. In the case of an unchanged meteorological regime, an estimate of the dynamic effect is given by the difference 0.32-0.13=0.19 surges yr^{-1}. The latter estimate seems more realistic than the above 1.01 surges yr^{-1}, because it takes into

consideration the change in relative sea level over a much longer period and is less affected by temporary fluctuations of the system. From this analysis it is evident that the subsidence and the dynamic effect have both contributed to the increased occurrence of flood surges in Venice, the former accounting for some 90% of the increase.

3. *Climate changes at European scale.*

One and a half centuries have passed since the end of the Little Ice Age. Nevertheless, we are presently witnessing an uninterrupted global temperature rise. The most frequent questions are:

(1) Is this warming part of a natural (and unexpectedly extensive) climate change? When, and at what unknown level, will this warming stop?

(2) Has the natural warming already come to an end and is the present temperature rise only an effect of air pollution? How far can we risk continuing to pollute the atmosphere?

(3) Are we witnessing the combined effect of both natural and uncontrolled anthropogenic changes? What are the relative weights of the two contributions?

Models seem to confirm the last hypothesis of a combined effect of natural variability and increased radiative forcing due to air pollution, but much work is still needed to clarify mechanisms and to discover the exact weights of the two contributions. Sound, long-term instrumental data are especially needed to reach a precise understanding of the present situation, to pose the scientific problem in correct terms and to set-up and to test models. In fact, knowing the past is the key to interpreting the present and forecasting the future.

This was the rationale on which the recent EU research project "Improved understanding of past climatic variability from early daily European instrumental sources" (IMPROVE) has been developed with the funding of the European Commission, DG XII.

Within the project seven daily pressure and temperature series were produced, i.e. Padova (It., 1725-present), Milan (It., 1763-present), Central Belgium (Be., 1767-present, temperature only), Uppsala (Se., 1722-present), Stockholm (Se., 1756-present), San Fernando/Cadiz (Es., 1776-present) and St Petersburg, Russia (1743-present). These series have been augmented with newly-produced series (Central England, UK., 1772-present). These series are especially useful to characterise climate variability and determine teleconnection behaviour across Europe: high-

frequency temperature variability; seasonal temperature extremes; recurrence intervals; growing seasons.

An important aspect is the high (daily) resolution of the series, which allows more insight into past variability, as monthly averages smooth out and mask many important climatic features. Also, in analysing and correcting errors and inhomogeneities in the long series, metadata have been considered as important as data. Metadata are fundamental not only to correct, make homogeneous and interpret data, but also to distinguish apparent climatic changes, due to variations in observational methodology, from real climatic changes. This not only helped to produce more accurate series, but also clarified the question of the quality of the existing ones. In actual fact, the long series are affected by a huge number of problems, and not only casual reading errors. Reading errors are mainly randomly distributed and they disappear when the averages of many series are calculated. The real problem is the presence of systematic errors that vary in the course of time, the changes in measuring style due to national or international regulations or the simple evolution of technology, that affected the observations in the same way and simultaneously in all sites. All homogeneity assessment techniques would perform poorly if all station time series were affected similarly by common factors, and changes in measuring style cannot be assessed with statistical analysis, but only with historical research of all the metadata.

At present, attention is being mainly devoted to forecasting future scenarios. To this aim, the quality of data is essential and a number of subjective and relatively objective criteria exist for testing monthly data and sources of inhomogeneity (e.g. Jones et al., 1999). However, the evaluation of the data quality, as deduced from the statistical analysis of the data, appears more optimistic than the error deduced by looking at the instruments capability and the field practice. For instance, in general a first contribution ±0.2°C corresponds to the accuracy of standard thermometers (WMO, 1983) but the overall error in the field is greater. In the sunny countries, the largest error is reached on clear, calm days, when the screen may over-heat by +2.5°C and on clear nights when it may under-cool by -0.5°C. The correction based on metadata describing observational errors and problems requires a long and unrewarding work to improve the quality of long series. One of the aims of IMPROVE is to encourage critical revision and improvement of the quality of existing series, while providing, at the same time, examples of typical errors to be removed and identifying the procedures needed to amend them.

The actual warming rate has been proven to be at such a slow rate that

temperature changes, over years (i.e. 0.006°C/yr) and even decades (i.e. 0.06°C/decade), are in most cases smaller than the instrumental resolution and can hardly be directly detected. This occurs especially with temperature averages, for which the climate signal is often below the noise and/or the instrumental limit. However, looking at the frequency distribution of extreme events, things appear differently. Extreme events depart so much from the average, that they can be easily detected, and in computing their signal to noise ratio the observational error becomes less relevant. IMPROVE has clearly demonstrated that this approach is very promising.

For the above reasons these long series are very useful in interpreting the climate variations that affected and are affecting the Venice area in the last three centuries. The series now available from IMPROVE and especially the Padova series will be analysed to understand the climate changes that may have significant impact for Venice and its lagoon system.

First results showed that the recent warming is characterised by an increase in frequency of the hottest days, in association with a decrease in frequency of the coldest. Also, there is a local rise of the atmospheric pressure (of the order of 1 hPa) which has been noticed in a number of stations (Pirazzoli and Tomasin, 1999; Cocheo and Camuffo, 2002). The rise can be interpreted in terms of a real change in the climate of the northern Adriatic region, which is associated with less frequent invasions of air from the north-east, especially the cold Bora wind. Under this point of view, the pure barometric effect is modest i.e. 1 hPa pressure rise explains 10 mm decrease in sea level. However, it is associated with the greater advantage of having no sea water dragged by the Bora wind that might temporarily reach a contribution of the order of half a meter (Giordani Soika and Meneghini, 1970). The decrease in Bora events is paralleled by a decrease in the number of events of strong Sirocco over the Adriatic (Piervitali et al., 1997). However, although both winds have nearly halved the frequency of their gale events in the last 50 years, the frequency of flooding surges in Venice has doubled in the same period. Thus, a positive meteorological forcing is not able to compensate the other effects contributing to Venice *acqua alta.*

4. *Conclusions.*

The long history of flood surges at Venice has shown an alternation of 'regular' periods with one or two surges per decade, and anomalous periods with an increased flooding rate. The main anomalous periods

were, in the past, the Spörer minimum of solar activity (1500-1540) and recently after 1965.

In the course of the centuries the Venetian Authorities intervened continually to protect the city against a rise in sea level, for example by diverting rivers outside of the lagoon, building improved dams, controlling channel depth, and raising the level of the lowest part of the town by building new pavements over the early ones. In general, these protective measures gave satisfactory results and the flooding threat was substantially controlled. In effect, it changed from the early value at the origin of the city of about one flooding surge every two decades to about two surges per decade prior to 1930, as a result of the progressive natural sinking of the city. Although the flooding caused a number of unpleasant consequences (e.g. making the water in collecting wells bitter; increasing the putrefaction rate of corpses buried in churches with the consequential unpleasant smell; damage to merchandise) they were considered acceptable at that rate.

The analysis of this long series clearly shows that the problem has changed and has become dramatic since the middle of the past century when the works undertaken were not to protect the city, but to develop new trade routes that became unsustainable for the city. The excavation of new deep channels (chiefly the so-called '*canale dei Petroli*' 1963-69) for the passage of oil ships gave a negative contribution of 10% or more. The excessive extraction of underground water also contributed negatively, especially in the period 1930-1965. Fortunately, the pumping was regulated before worsening too much the situation, possibly leading to a small rebound. However, the natural subsidence is still active and constitutes a risk factor as well as sea level rising due to global warming. The decrease in strong Bora and Sirocco events measured in the Adriatic in the last 50 years, is not able to counterbalance the effects on the *acqua alta* phenomenon due to RSL rise.

The problem is what to do now. The sea level had been increasing until the 1960s and although it seems to fluctuate now around the same or a slightly variable value, scattered data make it difficult to assess whether or not any change in trend is real. In any case, mitigating measures are urgently needed. One possibility is to leave lagoon inlets open at all times, while reducing channel depth to limit the height of the surge, as well as raising the floor level in the lowest parts of the city, thus returning to an acceptable flooding rate, e.g. prior to 1900. However, although this rate might be considered acceptable, it is no longer sustainable because of the irreversible damage caused by sea salt to historical buildings. When

the buildings absorb sea water, the NaCl migrates for capillary rise inside brick, mortar, marble and other stone types. When later NaCl undergoes dissolution and recrystallisation cycles, it exerts mechanical stress inside the pores which in a short time disrupts the building materials (Camuffo, 1998). In order to protect the buildings against this irreversible form of decay, Venetians built their buildings with a basement in Istria Stone, which is a limestone of a very low porosity, in order to stop the capillary rise from the canals or the soil. Originally, the basement's height was of a sufficient level. At present, after the combined effect of subsidence and sea level rise, it is totally inadequate to protect buildings against the capillary rise and most of the buildings are exposed to new irreparable damage at each flooding. The problem of Venice can only be managed by stopping the entrance of sea water during flooding surges, e.g. by activating mobile gates at each occurrence.

Acknowledgements: Special thanks are due to Dr Luigi Alberotanza, director of CNR-ISDGM, Venice, for having facilitated this study especially by supplying the sailing facilities for the inspection and measurement of the sites, Dr Laura Carbognin and Dr Alberto Tomasin for the supply of useful data, and Dr Silvia Enzi for the archive documentation. The study is supported by CORILA. We acknowledge the use of long series from the EU-funded project IMPROVE.

References.

Archivio di Stato, 1983. *Laguna, lidi, fiumi - Cinque secoli di gestione delle acque, Helvetia*, Venice, 152 pp.

Camuffo D., 1993. Analysis of the Sea Surges at Venice from A.D. 782 to 1990, *Theoretical and Applied Climatology*, 47, 1-14.

Camuffo D., 1998. *Microclimate for Cultural Heritage*. Developments in Atmospheric Science 23, Elsevier, Amsterdam, 415 pp.

Camuffo D., 2001. *Canaletto's paintings open a new window on the relative sea level rise in Venice*. Journal of Cultural Heritage, 4, 227-281

Camuffo D. and Bernardi A., 1981. *A comparison of the Evaporation Rate over the Mainland with that over the Sea*. Il Nuovo Cimento, 4C, 635-646.

Camuffo D. and Enzi S., 1992. *Critical Analysis of Archive Sources for Historical Climatology of Northern Italy*, pp. 65-74 in: B. Frenzel (ed.): "European Climate Reconstructed from Historical Documents: Methods and Results", Paleoclimate Research, Special Issue 7, Fischer Verlag, Stuttgart.

Camuffo D. and Enzi S., 1995. *Climatic features during the Sporer and Maunder Minima*, pp. 105-124 in B. Frenzel (ed.) Solar output and climate during the Holocene, Fischer Verlag, Stuttgart.

Camuffo D. and Sturaro G., 2002. Use of proxy-documentary and instrumental data to assess the risk factors leading to sea flooding in Venice, Global & Planetary Change, in press.

Carbognin L., Gatto P., Mozzi G., Gambolati G., Ricceri G., 1976. *New trend in the subsidence of Venice*. IAHS, 121, 65-81.

Carbognin L., Gatto P., Mozzi G., Gambolati G., Ricceri G., 1984. Case History no 9.3. Venice, Italy, pp. 161-174 in Poland, J.F. (ed.) *Guidebook to Studies of Land Subsidence Due to Ground-Water Withdrawal, International Hydrological Programme*, Working Group 8.4, UNESCO, Paris.

Cocheo C. and Camuffo D., 2002. *Corrections of systematic errors and data homogenisation in the Padova series* (1725 – today). Climatic Change, 53 (1-3), 77-100.

Colacino M. and Dell'Osso L., 1977. *Monthly mean evaporation over the Mediterranean sea, Archiv fur Meteorologie Geophysik und Bioklimatologie*, 26A, 283-293.

Eddy J.A., 1977. Climate and the changing Sun. Climatic Change, 1, 173-190.

Enzi S. and Camuffo D., 1995. *Documentary Sources of Sea Surges in Venice from A.D. 787 to 1867*. Natural Hazards, 12, 225-287.

Favero V., Parolini R. and Scattolin M., 1988. *Morfologia storica della Laguna di Venezia. Arsenale ed. Venice.*

Frassetto R., 1971. *The subsidence and storm surge effects in Venice. Consiglio Nazionale delle Ricerche*, ISDGM, Tech. Report No. 54, Venice, 11 pp.

Giordani Soika A. and Meneghini D., 1970. *Di alcune modificazioni del clima di Venezia nell'ultimo trentennio – ripercussioni sul fenomeno dell'acqua alta, Bollettino del Museo Civico di Storia Naturale di Venezia*, 20/21, 13-26.

Jones P.D., New M., Parker D.E., Martin S. and Rigor I.G., 1999. Surface Air Temperature and Its Changes over the Past 150 Years. *Reviews of Geophysics*, 37:2, 173-199.

Lamb H.H., 1972. *Climate: present, past and future*, Vol.1., Methuen, London, 613 pp.

Miozzi E., 1969. *Venezia nei Secoli*, vol. I-IV, Ed. Libeccio, Venice.

Oppolzer T.R., 1887. *Canon der Finsternisse,* Karl Gerold's Sohn, translated by O. Gingerich (1962): *Canon of Eclipses*, Dover Publication, New York.

Piervitali E., Colacino M., Conte M., 1997. Signals of climatic change in the central-western Mediterranean basin, *Theoretical and Applied Climatology*, 58, pp. 211-219.

Piervitali E., Colacino M., Conte M., 1998. Rainfall over the Central-Western Mediterranean basin in the period 1951-1995. Part I: precipitation trends, *Nuovo Cimento* 21C, 3, pp. 331-344.

Pirazzoli P.A., 1977. Le acque alte a Venezia e le loro cause, pp. 29-35 in *Atti dei Convegni 1977*, Scuola Grande di San Teodoro, Associazione Civica Venezia Serenissima, Venice.

Pirazzoli P.A., 1982. Influences des traveaux récents et des périodicités astronomiques sur l' '*acqua alta*' à Venise: la réponse des marégraphes. *Oceanologica Acta*, special issue SCOR/IABO/UNESCO, pp. 177-184

Pirazzoli P.A., 1989. "Effetto serra" e livello marino: quali prospettive per Venezia? *Ateneo Veneto* 176, 7-30.

Pirazzoli P.A. and Tomasin A., 1999. L'evoluzione recente delle cause meteorologiche dell'"acqua alta". *Istituto Veneto di Lettere Scienze e Arti*, CLVII, 317-344.

Priestley M.B., 1981. *Spectral Analysis and Time Series*, Academic Press, London, 890 pp.

Rosa Salva P., 1974. Trasformazioni ambientali ed alterazioni nella laguna veneta, *Urbanistica*, 62, 5-44.

Rusconi, A., 1983. *Il Comune Marino a Venezia: ricerche e ipotesi sulle sue variazioni altimetriche e sui fenomeni naturali che le determinano*. Min. Lavori Pubblici, Ufficio Idrografico Magistrato alle Acque, Pubbl. No 157, Venice.

Tomasin A. and Frassetto R., 1979. Cyclogenesis and forecast of dramatic water elevations in Venice, pp. 427-438, in Nihoul, J.C.J. (ed.) *Marine Forecasting*, Elsevier, Amsterdam.

UNESCO, 1969. *Rapporto su Venezia*, Mondadori, Milan, 348 pp.

Vinnichenko N.K., Pinus N.Z., Shmeter S.M. and Shur G.N., 1973. *Turbulence in the free atmosphere*, Consultant Bureau, New York, 263 pp.

Wei A.M., 1990. *Time series analysis*, Addison-Wesley, Edwood City, 478 pp.

WMO (World Meteorological Organisation), 1983: *Guide to meteorological instruments and methods of observation*. WMO Report No.8, Geneva.

THE PO RIVER FLOW: LAST 200 YEARS TREND, CONSIDERATIONS AND FUTURE TENDENCIES

M. Tomasino, P. Traverso, D. Zanchettin
Dipartimento di Scienze Ambientali, Università Cà Foscari, Venezia

Summary.

Time-series analysis of hydrological data can help us to understand the present and to identify tendencies. This becomes even more important when we deal with extreme hydrological events, to understand if they are natural critical or antrophic-induced events (greenhouse effect, etc.). From the discharges' analysis of the Po river's data, it emerges that we are approaching the peak of a cycle's change and that we are moving (for natural causes, the sun) towards a colder cycle.

1. *Preface.*

In the last years discussion about Earth heating caused by greenhouse gases has intensified, but while the majority of scientists has lined up with IPCC indications and media have amplified catastrophic forecast sceneries, the number of scientists who don't believe these facts will be fulfilled (at least not this century), is increasing.

The actual situation is well known: polar and alpine glaciers retire, marine levels rise, air temperatures are always higher, especially in their minimum values.

All these facts are indubitable, but it's neglected to say that all these phenomena are cyclic: glaciers retire and then advance, sea levels rise and then lower, temperatures increase and then fall, and this happens from time immemorial. Now a question rises spontaneously: if these cycles really exist, how can we define in which cycle's point we are now? An answer can be given analysing hydrological data series, but not only, as we'll see forward.

Analysis of the past allows us to individuate the most probable cycles, to understand some links between hydrometeorological parameters in

order to define the most probable forcing between the examined variables, making it possible to establish or thereabouts the position where we are actually, and then to forecast future tendencies.

This way, it's clear that we suppose that the future follows, at least in portion, past courses.

2. *Po river discharges data and their forecast.*

Analysing the Po river discharges data at Pontelagoscuro, the last section not influenced by the sea, it has been recently demonstrated [Tomasino, Dalla Valle, 2000] that discharges, strictly connected to the integral of the rain over the entire Po basin, follow and are modulated by solar cycles. The conclusions of the quoted work are: Po discharges follow cycles with a mean width of about 20 years (almost double the eleven-years solar cycle) and widths between 10 and 35 years (see Fig. 1).

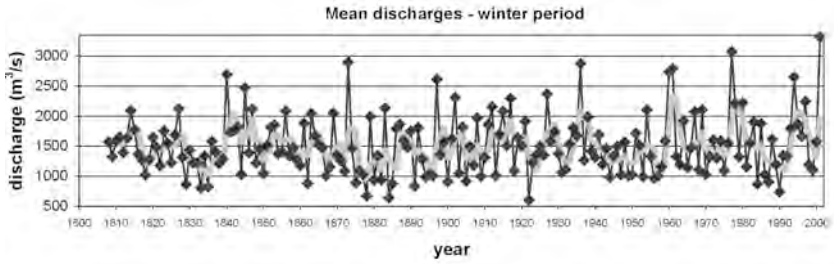

Fig. 1 – Po river discharges at Pontelagoscuro time-series for october – march period from 1818 to 2000 with three years filter (not centered).

Hydrological cycles were discovered first by Bacone in the 17th century and then by Brückner in the end of 19th century, but the solar forcing couldn't be individuated.

In order to use this argument to forecast, we need to integrate hydrological and meteorological knowledge with astronomical knowledge about solar cycles, and this is not easy as a consolidated theory about the sun still doesn't exist; in spite of this, in a recent work [Landscheidt, 1999], analysing solar cycles' series it has been forecasted that after the actual 23rd solar cycle four or five cycles will follow with weak sunspots' intensity, and that the minimum in solar activity will be around 2026.

It's well known that in the past the sun went through low activity periods, less known is that we can forecast when this is going to happen.

From data analysis we are able to individuate three minimum points of solar activity, indicated as Wolf, Spörer and Maunder, corresponding to minimums in aurora borealis' frequencies and sediment 14C contents. It's also pointed out that it's very important to consider the special phases of eleven-years solar cycle and the torque connected with irregular sun motion around the mass centre of the solar system [Landscheidt, 1988].

These phases are characterized by accumulations of energetic solar eruptions (flares, coronal mass ejections and eruptive prominences) that seem to have an impact on atmospheric weather and Earth's climate, through cosmic ray's regular effects on clouds and changes on circulation in stratosphere and troposphere. This way, from the results of spectral analysis over the Po river discharges time-series data, the existence of the effects of mentioned cycle on Po discharges has been verified [Landscheidt, 2000]. It's possible to calculate the solar torque's cycle for the future, and by its trend (see Fig. 2) we can get indications about discharges data, because it allows us to know in advance sudden changes: defining the probable temporal around of system's critical points let us apply chaos theory's techniques to forecast. This way we were able to predict the wet period of the end of the 2000 and of the first 2001 months with an anticipation of about 9 months (the article was published in June 2000). The possibility of such an event was not marked out by seasonal models of European Centre for Weather Forecast of Reading (Molteni, personal communication, 2001).

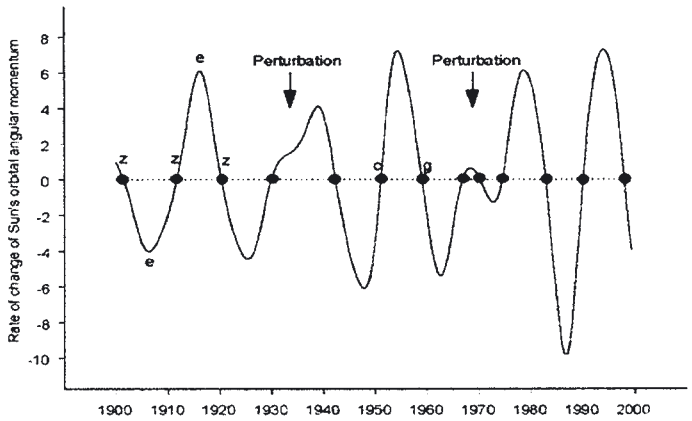

Fig. 2 – Solar torque trend with indication of characteristic points (from Landscheidt, 2001).

It's wrong to think that forecasts are easy and obvious, because if it's true that solar eruptions are predicted inside a very probable time around, the effects on Earth are more or less intense according to the position of Earth compared to the sun, and to the conditions of the interplanetary space that surrounds the Earth.

However, it has to be pointed out that climatic changes are not connected with a maximum in sunspots' activity, but with other phases of solar activity's cycle.

Nature often repeats trends and connects functions in different scales. This is a fundamental argument for them who deal with seasonal forecasting: if we are able to define the phases, these can be seen as fractals, each one with autosimilarity characteristics (rise and reduction). So, looking at Fig. 3, we can deduce that higher discharges' periods correspond to full triangles and lower discharges' periods to blank triangles. As said above, since the solar torque cycle is predicted with a good reliability, we are able to individuate in advance singular maximum and minimum points (or at least their around) and with the analysis of the cycle (ie: if we are in rise or reduction phase), using highest frequency harmonics, estimate future discharges' tendencies. These estimates are made of mean annual or seasonal (six months) values.

This kind of probable indications are useful to water reservoirs' administrators who can then optimise the management of resources either during wet periods when floods are more probable or during dry periods.

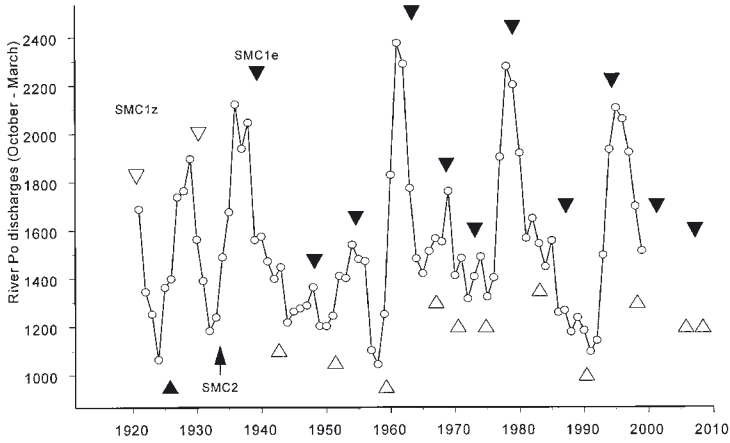

Fig. 3 – Po river discharges at Pontelagoscuro filter trend for october – march period from 1818 to 2000 with the indication of fractals obtained by the study of characteristic points of solar torque (from Landscheidt, 2000).

3. *The Po river discharges, mucilages and their forecast.*

It was discovered that, with the object of preventing (bathing, state of the sea, etc.), the knowledge of the minimum points of the Po river discharges is essential to know in advance the Adriatic Sea's conditions in late spring – summer. We remember that since 1990 a forecasting system of chance of mucilages' appearance in Northern Adriatic, based on the studies of the Po river discharges' trend, is available. After ten years of full agreement between forecast and natural evidences, the work [Tomasino, 1996] starts now to obtain agreements in Italian scientific community circle.

What is sure is that analysing the Po river discharges' data for the October – March period with a three year filter, we are able every year in April, on the basis of the tendencies, to make very reliable previsions on the possibility or not of the mucilages' appearance in Northern Adriatic for the late spring – summer.

In Fig. 4, that shows the model return's graph, look at the point corresponding to year 2000. This point shows the exit from winter of the Po river – Northern Adriatic system for the year 2000. The consequent forecast was: ' during the year 2000 it's highly probable mucilages' appearance', and in fact the function value fell in the proximity of an unchaining threshold individuated in the above mentioned work [Tomasino, 1996]. The forecast, discussed in the spring in a seminary at Dipartimento di Scienze Ambientali of University of Venice, has actually come true. It was also easy to forecast, when new 2001 values were available, that 'mucilages would not appear in 2001', as the function had risen to maximum values. One more time the forecast has come true.

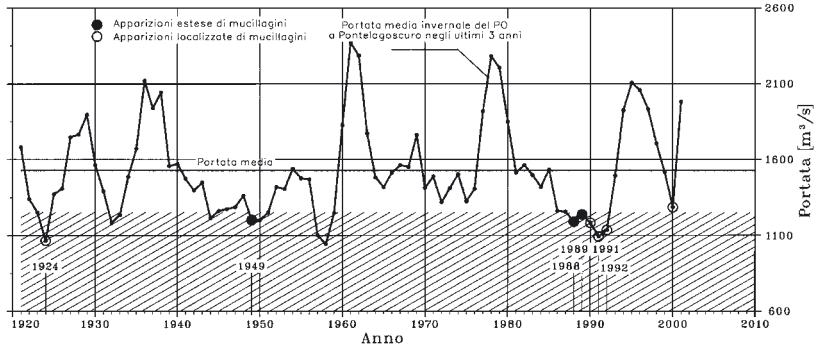

Fig. 4 – Po river discharges at Pontelagoscuro filter trend for october – march period from 1818 to 2000 with the indication of mucilages appearance in Northern Adriatic. The sketched area indicates the high risk of mucilages' appearance area.

It's worth to remember that mucilages are usually present in Northern Adriatic and are an endemic problem, which means that they can appear more than once in a year time, but in small quantity and in little areas. This is mainly due to the scarce depth of the sea and to the consequent high use of nutrients during sunny weather by both the water column and the bottom. Deficient rivers' discharges, with scarce contribution of nutrients to the sea, and sequent little floods in the late spring – summer period, are enough that not predicted events, as the one in 1997, happen.

The episode mentioned is emblematic: analysing the mean Po river discharges for the year 1997, we understand that two months of very low discharges (the April – May discharges approached the absolute minimum points in the observation period – see Fig. 5) are enough to send the system in crisis by cause of the nutrients deficit turned up during late spring fitoplancton bloom.

Contribution of new waters relatively more abundant and their restriction in the superficial layer due to the presence of the thermal picnoclino already established and to the sequent stop of general circulation in Northern Adriatic, fired the phenomenon. This eventuality had already been predicted: the 1997 episode is the demonstration of the theory '15 days stop of the circulation due to stable sunny weather is enough to let mucilages appear', pointed out in Tomasino's work of 1996.

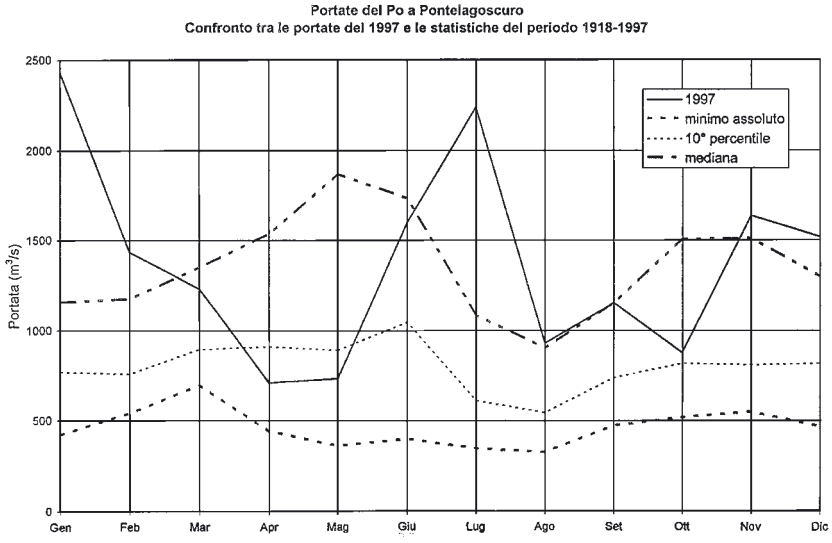

Fig. 5 – Po river monthly discharges at Pontelagoscuro for the year 1997.

4. *The Po river discharges and climatic future.*

Going back to the Po river hydrological data time-series, it has been pointed out that it is possible to individuate their cycles using innovative techniques and confirming the results with objective analysis as spectral analysis, and that these cycles are strictly connected with solar cycles but not with a maximum of solar activity (in fact they seem to follow well the trend of solar torque). This allows us to know in advance when hydrological extremes as floods and drought happen.

Hydrological extremes, just because of this connection with the sun, should not been attributed only to greenhouse effect , as the majority of scientists thinks.

Analysing the investigations about the paleoclima in Italy [Camuffo, Enzi, 1995] [Piervitali, Colacino, 2000], it's pointed out that in minimum solar activity periods, as the ones named Spörer (1416 – 1534), Wolf (1282 – 1342) and Maunder (1645 – 1715), many climatic anomalies and natural calamities happen, even if sometimes with a reduced intensity.

An important result from the analysis is that extreme events during these periods are many more than the ones happened during mean or high solar activity periods.

The analysis of the paleoclima is therefore useful to understand qualitative interconnections but also to get quantitative informations: these periods' extremes are in fact comparable to actual extremes; a proof of this statement is that we have to go back to 1705 in Maunder period in order to find in Piemonte floods comparable to the floods of 1994 and 2000 [Crosio, Ferrarotti, 1996].

Concluding, in analogy with the past, we can say that if we are approaching a solar minimum we must expect high hydrological extremes for the near future and maybe, the hydrological extremes of these last years already point at this important change of climatic cycle many scientists can't or don't want to read.

The hypothesis that we are entering in a new big humid-wet cycle therefore seems justified and probable.

Bibliography.

Camuffo D., Enzi S., 1995. "Climatic features during the Spörer and Maunder Minima". Solar output and the climate during the Olocene, ESF Project, pag. 105-124.

Crosio F., Ferrarotti B., 1996. "Trino gli anni del diluvio". Ed. Studi Trinesi 13.

Landscheidt T., 1988. "Solar rotation, impulses of the torque in the sun's motion and climatic variation". Climatic Change 12, 265-295.

Landscheidt T., 1999. "Extrema in sunspot cycle linked to sun's motion". Solar Physics 189, 413-424.

Landscheidt T., 2000. "River Po discharges and cycles of solar activity". Hydrological Sciences Journal 45, 491-493.

Piervitali E., Colacino M., 2000. "Evidence of drought in the western Sicily during the period 1565-1915 from liturgical offices". Climatic Change 24, 1-15.

Tomasino M., 1996. "Is it feasible to predict slime blooms or mucilage in the Northern Adriatic See?". Ecological Modelling 84, 189-198.

Tomasino M., Dalla Valle F., 2000. "Natural climatic changes and solar cycles: an analysis of hydrological time series". Hydrological Sciences Journal 45 (3), 477-489.

SUBSIDENCE DUE TO PEAT SOIL LOSS IN THE ZENNARE BASIN (ITALY): DESIGN AND SET-UP OF THE FIELD EXPERIMENT

A. Fornasiero[1], G. Gambolati[1], M. Putti[1]
P. Teatini[1], S. Ferraris[2], A. Pitacco[3]
F. Rizzetto[4], L. Tosi[4], M. Bonardi[4], P. Gatti[4]
[1]*Dip. di Metodi e Modelli Matematici per le Scienze Applicate, Università di Padova*
[2]*Dip. di Economia e Ingegneria Agraria, Forestale e Ambientale, Università di Torino*
[3]*Dip. Agronomia Ambientale e Produzioni Vegetali, Università di Padova*
[4]*Istituto per lo Studio della Dinamica delle Grandi Masse, CNR, Venezia*

Abstract.

The Zennare Basin has been selected to represent the peat soil agricultural farmland of the south catchment of the Lagoon of Venice. The area was reclaimed during the 1930's and at present lies almost entirely below mean sea level (down to – 4 m a.s.l.). The extensive land subsidence that occurred since reclamation is primarily caused by the loss of sediment mass due to oxidation of the organic soil component, with consequential CO_2 gas release into the atmosphere. Because the process is essentially controlled by soil temperature and moisture, a field experiment has been designed and implemented for the determination of the relationships that control the CO_2 fluxes from the soil and the land sinking rates.

1. *Introduction.*

In the U.S. system of soil taxonomy, organic soils (or histosols) are formally defined as soils having more than 50% organic matter in the upper 80 cm [Soil Survey Staff, 1975] and commonly termed "peats". According to this definition, peat soils in Italy cover about 1200 km^2 [Andriesse, 1988]. A significant fraction of this extent is located in the low-lying

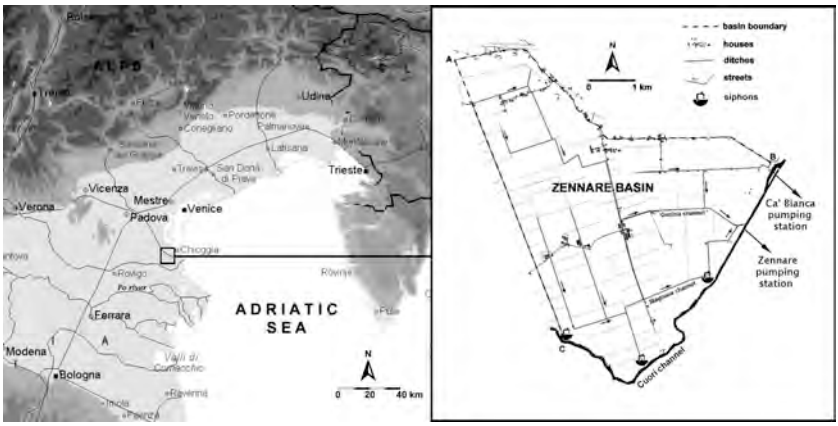

Fig. 1 – (a) Map of the Eastern Po plain with the location of Zennare Basin. (b) Schematic representation of the Zennare Basin with the location of the principal drainage network and hydraulic structures.

coastal areas of the Eastern Po river plain (Fig. 1a) and are originated from wetland reclamation during the last few centuries.

Land subsidence is the most commonly observed response of histosols to drainage for agricultural purposes. Worldwide subsidence rates in drained peaty areas vary from less than 1 cm/year to more than 10 cm/year. The oldest records of land subsidence are from the polders of the Western Netherlands, reclaimed in a period between the 9th and the 13th centuries, which subsided by only 1.5-2 m in about 800 - 1000 years (approximately 1.7 mm/year) [Nieuwenhuis and Schokking, 1997]. In the Everglades of Florida the arable organic soils experienced an average subsidence rate of 2.5 cm/year between 1924 and 1978 [Ingebritsen et al., 1999] and the histosols of the Sacramento-San Joaquin delta in California settled at a rate of up to 8 cm/year between 1922 and 1950 [Rojstaczer and Deverel, 1995]. Records of land subsidence in Malaysia reveal that the subsidence rates decreased from 12 cm/year over the period 1960 - 1974 to 6.4 cm/year in the following 14 years and to 2 cm/year thereafter [Wösten et al., 1997].

Under drainage, at least five sources of organic soil subsidence have been recognized [Stephens et al., 1984]: shrinkage due to desiccation, consolidation, wind and water erosion, burning, and biochemical oxidation. The latter has been found to be the dominant cause of land subsidence in temperate and tropical peat soils [Andriesse, 1988; Deverel and Rojstaczer, 1996]. Under natural waterlogged conditions, the soil is anaerobic (oxygen-poor) and organic carbon accumulates faster than it

can decompose. Drainage for agricultural purposes leads to aerobic (oxygen-rich) conditions and the microbial activity oxidizes the carbon in the peat soil causing carbon loss in the form of gaseous CO_2 flux from the soil to the atmosphere. Since drainage must be regularly adapted to new levels for the rooting system requirements of the cultivated species, the loss in soil substance of drained histosols is irreversible and permanent until the peat deposit ultimately disappears (Fig. 2).

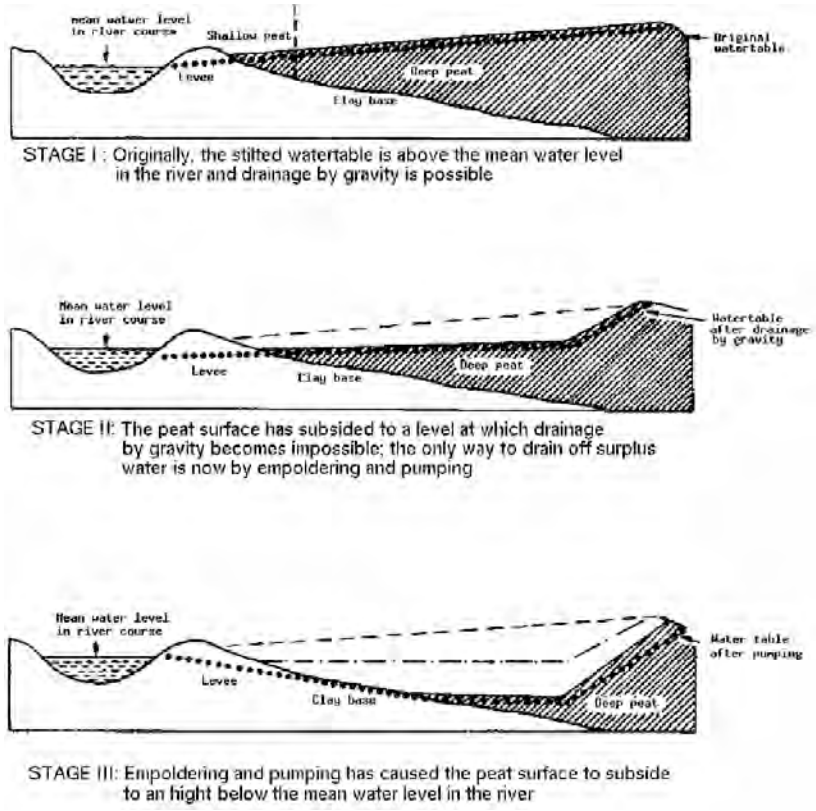

Fig. 2 – Possible stages in peat subsidence after drainage.

Experimental field [Deverel and Rojstaczer, 1996; Clair at al., 2002] and laboratory [Moore and Dalva, 1997] studies have demonstrated that the rate of CO_2 production from organic soils, and hence of related land sinking, primarily depends on peat composition and two hydrologic variables: soil temperature and moisture. Soil microbial activity generally doubles for each 10°C increase in temperature above 5°C and it has been

established that in general CO_2 fluxes are much influenced by the depth of drainage, the higher the water table the lower the soil loss.

Agricultural lands located in the south-eastern part of the Veneto Region are characterized by the presence of soils with high organic content. Their drainage started soon after the reclamation and caused an adverse effect on the stability of those areas, with large subsidence rates that lead the zone to lie almost entirely below mean sea level (down to –4 m a.s.l.). Land settlement of several tens of centimeters recorded up to now and subsidence that will likely occur in the years to come constitute a serious problem for a sustainable development of this area in the near future. Pumping of agricultural drainage into waterways will become more and more expensive, with the reclamation authorities that in some cases may be forced to lower the pumping station elevation. Also saltwater intrusion from the adjacent Adriatic Sea, at present localized over a few zones, could become a widespread phenomenon to take care of.

In 2001 a research project (VOSS – Venice Organic Soil Subsidence) was initiated to study the process. The end goal is the development of a modeling tool for the prediction of this type of land subsidence to be effectively used in the agricultural practices and management strategies for the farmland south of the Venice Lagoon. The model development and validation are supported by extensive laboratory and field experiments in a hydrologically closed basin, the Zennare Basin, selected in the area of interest. At the moment of writing the project focused the two main issues: (1) hydrogeological characterization of the basin and (2) design and implementation of a field experiment for the determination of the most important parameters to be used in the modeling effort. This paper is mainly concerned with the description of the second issue.

After a brief description of the main hydro-geologic features of the study basin and an account of the observed land subsidence, the design of the field experiment and its implementation are presented and discussed.

2. *The Study Site.*

The Zennare Basin (45° 10' E and 12° 9' N) is an area of about 23 km^2 located right south of the Venice Lagoon, approximately 10 km from the Adriatic Sea (Fig. 1b). The basin was occupied in the 19th century by swamps and was reclaimed about 70 years ago. At present it lies almost entirely below mean sea level, mostly between -2 and -4 m, except for a small part in its northern part [Fig. 2, Rizzetto et al., this issue], and is almost completely dedicated to cereal growing.

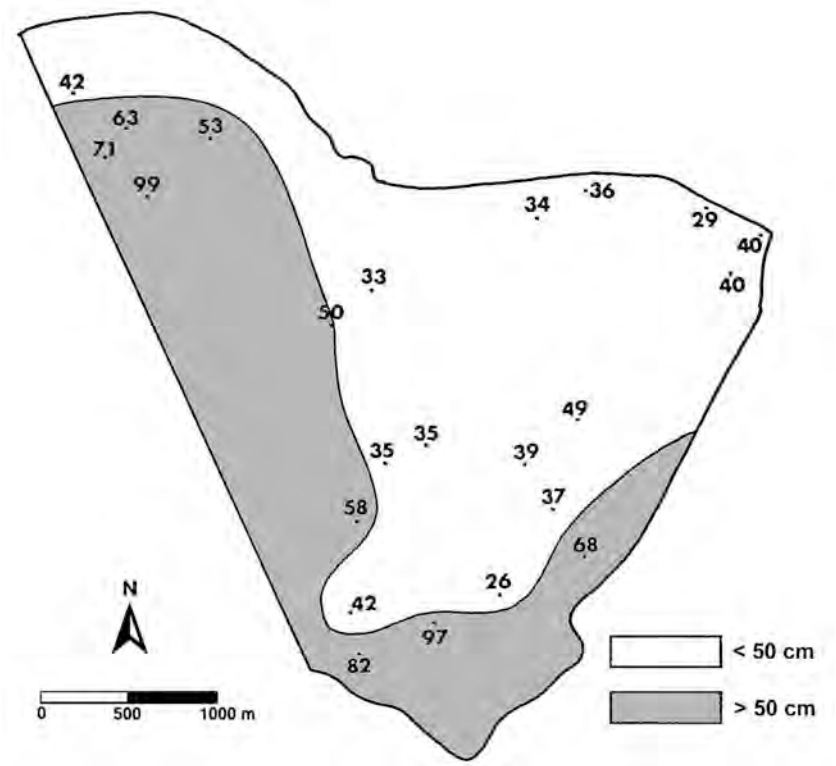

Fig. 3 – Estimate of land subsidence within the Zennare Basin between 1965 and 1983 (after Consorzio di Bonifica Adige-Bacchiglione [1996]).

Although an ad hoc monitoring campaign has never been made, the present critical ground elevation is due to land subsidence primarily caused by organic soil oxidation. An accurate measurement of the histosols sinking rates within the area is not available. However, land settlements ranging between 30 and 100 cm have been estimated between 1965 and 1983 by the reclamation authority [Consorzio di Bonifica Adige-Bacchiglione, 1996] with the aid of elevation maps of the area (Fig. 3). The average subsiding rate of 2.8 cm/year thus obtained provides an overall settlement of about 1.5 m over the last fifty years, that match pretty well with the protrusion of old hydraulic structures located within the basin and funded on the mineral soils underlying the outcropping peat layer (Figs. 4, 5). The fact that the loss of mass from peat soils might be the major subsidence process affecting this area is somehow confirmed by

Fig. 4 – Effects of land subsidence in the Zennare Basin: an old abandoned weir originally constructed to close a drainage ditch completely protruded above the ground level. A qualitative position of the ditch section in the original configuration is sketched.

Fig. 5 – The effect of land subsidence in the Zennare Basin: an old masonry culvert presently above the water level and substituted by two lower concrete drainpipes, the higher of which already unusable. A qualitative position of the ditch section in the original configuration is sketched.

the significantly smaller displacement rates (less than 1 cm/year) measured by high precision leveling surveys since the end of the 19th century by IGM (Military Geographic Institute) and CNR (National Research Council) along a leveling line adjacent to the study basin and running along the embankments of the Venice Lagoon margin where oxidation of organic soils is precluded [Tosi et al., 2000].

From the lithologic point of view, boreholes drilled down to –15 m from the ground surface [Gatti et al., this issue], geophysical investigations [Francese et al., this issue], field surveys, and aerial photograph interpretation [Rizzetto et al., this issue] carried out during the first year of the project have allowed the identification of the main geologic features of the area. A top peat layer between 1 and 1.5 m thick is nowadays uniformly present in the southern and central parts of the basin and is underlain by an alternation of sandy, silty, and clayey deposits with a few thin (few centimeters) intervening peat layers. The mineral sediments outcrop in the northern basin and constitute an almost impermeable aquiclude for the organic layer. The upper 40 cm of peat soil consists of ploughed and oxidized organic matter below which a fibrous peat usually with well-preserved fibres of *Phragmite australis* in growing position is found [Gatti et al., this issue]. The peat deposit is intersected by two paleo-river bed systems and a few small paleo-channels [Rizzetto et al., this issue; Francese et al., this issue].

The basin is hydrologically well defined (Fig. 1b). It is bounded southeastward by the embankment of the Cuori channel (B-C alignment, Fig. 1b) with water level as regulated by the Ca' Bianca pumping station (Fig. 1b), ranging between 1 and 1.25 m below m.s.l.. Hence the channel water level is always at least 2 m above the surrounding cultivated plain. An impermeable boundary is represented northward by the bank of the provincial road n. 7 “Rebosola” running about 2 m above the ground elevation (A-B, Fig. 1b). The study area is limited at the west border by a ditch (C-A, Fig. 1b) directly connected to the Cuori channel through a siphon operated by the reclamation authority.

The drainage network is made from a small number of channels approximately 5 m large and 1.5 m deep connected to a fine system of small ditches that subdivide the basin into rectangular fields of about 30-50 × 200-500 m and control the depth of the water table. Two major waterways, the Magnana and the Gorizia channels, convey the drainage water to the Zennare pumping station that discharge the water into the Cuori channel. The lowering of the water level at the pumping station entry from 1930 also provides an estimate of land subsidence in agreement with the other available information.

3. *Experimental Methods.*

The Zennare Basin has been instrumented at the end of 2001 – beginning of 2002 in order to measure the hydrological and meteorological parameters on which peat oxidation depends and to record the land subsidence rate. A number of test sites have been established in order to perform an accurate global hydrological balance of the basin, based on the *a priori* knowledge that water outflow is concentrated at the Zennare pumping station and water recharge occurs as rainfall, concentrated sinks through three siphons located along the Cuori channel embankment (Fig. 1b) and distributed infiltration through the same bank.

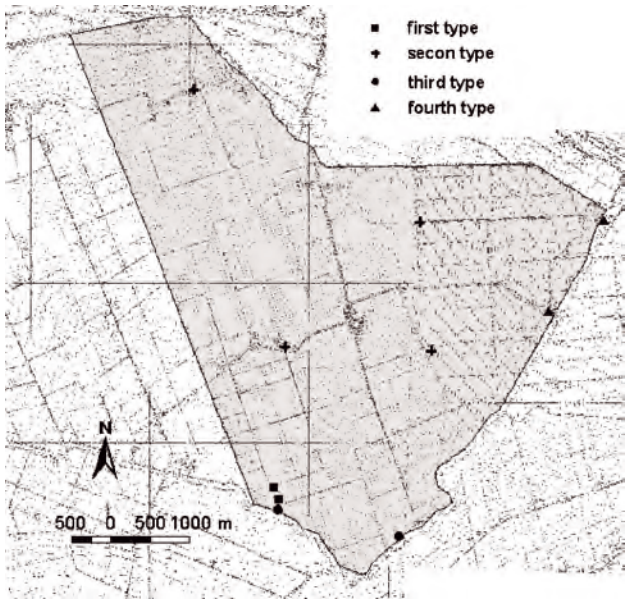

Fig. 6 – Location of the monitoring sites within the Zennare Basin.

Three types of monitoring sites have been planned and installed within the basin. Two principal test sites ("first type", Fig. 6) with an areal extent of 100 m^2, 200 m apart from each other, are established in the southern tip of the basin. Each site is permanently equipped with the following instruments (Fig. 7): *i*) a tilting bucket pluviometer with a sensitivity of 0.2 mm; *ii*) a non-directional anemometer with an accuracy of 0.25 m/s; *iii*) two piezometers, one located within the test site and the other close to the adjacent ditch, made from 3 m long PVC pipe of 2

inches diameter and instrumented with a pressure transducer characterized by a measuring range of 0 – 300 mbar and an accuracy of ±0.5 %FS; *iv*) five tensiometers to measure the capillary pressure, inserted 45° sloped so that the ceramic cups are located along the same vertical line with a 15 cm depth interval down to 75 cm (Fig. 8); the measurement range of the electronic pressure sensor is 0 – -950 mbar with an accuracy of ±0.5 %FS; *v*) five three-wire time domain reflectometry (TDR) 15 cm long probes for soil moisture content inserted horizontally along the same vertical and at the same depth as the tensiometers (Fig. 9); and *vi*) four soil temperature sensors at 1, 5, 15, and 30 cm depths with a measurement range between -15°C and 50°C (Fig. 9), plus one other 1 m deep sensor in the southern site. As suggested by Deverel and Rojstaczer [1996], ground surface displacement at each site is monitored by three displacement transducers characterized by a measurement range of 0 – 25 mm and an accuracy of ±0.5 %FS. The transducer body is attached at one end to a steel tripod anchored on three piles set into the ground to a depth of 11-12 m where an over-consolidated layer is located. The other end is connected to the land surface through a 0.5 cm thick, 10×10 cm aluminum plate resting on the soil (Fig. 10). The triangular steel structure, with sides of approximately 2 m, has been designed so to be as light as possible but with a negligible deformation compared to the expected subsidence rate when loaded with the force exerted by the displacement transducers (2.5 kg each) and by a 40°C thermal excursion.

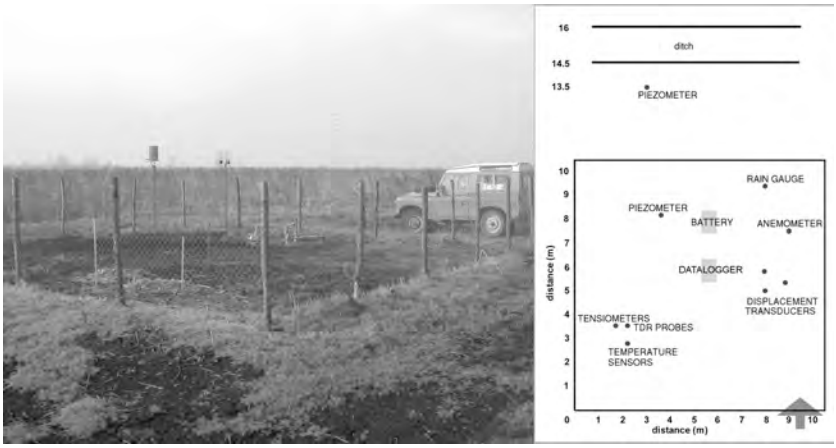

Fig. 7 – A principal test site established in the Zennare Basin with a schematic illustration of the instrument distribution.

Fig. 8 – Tensiometer location within a test site.

Except for the TDR probes, all sensors are connected to a datalogger (TER GEOLOG) with the electric power supplied by a single 12 volts rechargeable battery with an electrical capacity of 260 Ah that ensures about 1 month of continuous functioning at a hourly sampling rate. TDR probes will be connected in a near future through a multiplexer to an independent acquisition system. To avoid vandalisms and thefts, all the electric connections are sealed underground, with the datalogger and the battery buried inside waterproof IP68 cases. Since cultivation practices affect the soil peat structure and its characteristics in relation to the water-oxygen fluxes, the soil around the displacement transducers, the tensiometers and the TDR probes is managed so as to reproduce the actual conditions of the cultivated fields. At the end of the site installation a system of boardwalks is established to allow access without disturbing the soil surface.

Four other monitoring sites ("second type", Fig. 6) are installed in the basin, also outside the zone characterized by the presence of outcropping organic soils, with the aim at providing useful information on the basin hydrological balance. In each station a rain gauge and a piezometer of the same type as those used in the principal sites are installed and connected to a small datalogger (TER AC420). The energy is supplied by a small 12

volts 12 Ah rechargeable battery lasting a couple of weeks, depending on rainfall intensity. The electric wires and the datalogger are buried into the ground.

Fig. 9 – TDR probes (upper) and temperature sensors (lower) soon after their establishment.

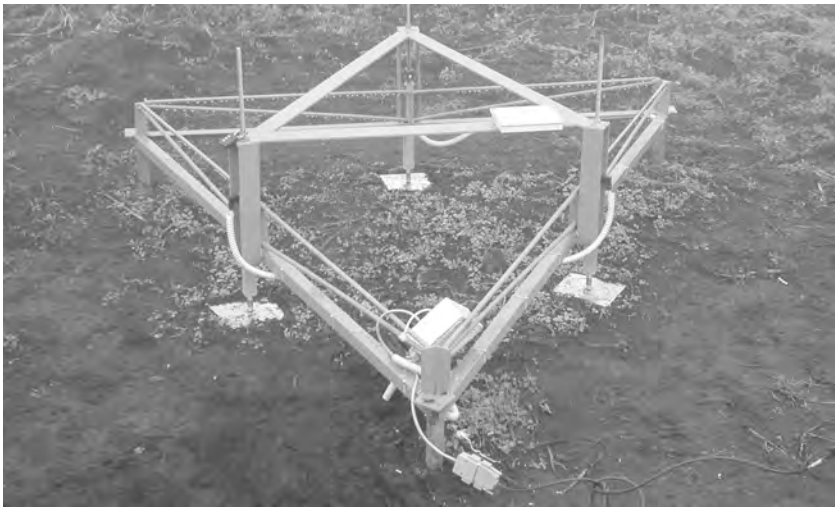

Fig. 10 – Steel tripod constructed to continuously monitor the ground elevation changes in the test field.

A third type of surveying site (Fig. 6) is established at two locations at the base of the Cuori channel embankment where a 2 m deep well is equipped with a water level transducer, whose housing contains the pressure sensor, the datalogger, and the battery. The measurement of the aquifer water table depth and channel water level fluctuations, together with the embankment geometry, will be used for the estimation of the distributed recharge through the channel levee.

Finally, two other monitoring sites, managed directly by the reclamation authority, are located at the Zennare and Ca' Bianca pumping stations where rainfall and water levels at the inlet and outlet of the pumping system are continuously measured ("fourth type", Fig. 6).

Two independent approaches to quantify CO_2 peat – atmosphere exchange rates are planned to be used during the research project: *i*) a chamber method and *ii*) a micrometeorological technique. Chamber methods are pointwise monitoring tools that measure changes in the gas concentration within a bottomless container placed on the ground surface. The non-steady-state (NSS) chamber method [Hutchinson and Livinston, 2001] will be used to estimate the CO_2 flux, as emitted from the soil, using the rate of CO_2 concentration increase. A rigid stainless steel chamber with a planar 50×50 cm dimension and a 25 cm height has been constructed by Geotea S.r.l. and Pergeo S.r.l.. The chamber is equipped with a barometric pressure transducer to check and compensate for the air pressure difference within and outside the chamber, an infrared gas analyzer, and a sampling port to collect air samples for later analyses by a portable gas chromatograph. To reduce soil disturbance related to chamber insertion, a collar connecting the chamber to the soil is located few centimeters below the ground surface. One collar will be permanently installed in one of the principal test site, while a second one will be moved around the basin to control and possibly estimate the spatial variability of CO_2 fluxes.

At a larger scale (on the order of few thousands of m^2) a micrometeorological technique, known as the eddy covariance technique [Moncrieff et al., 1997], is planned for use. This is based on the simultaneous high-frequency (10-20 Hz) measurement at about 1 m above the ground surface of the wind components by a three-dimensional ultrasonic anemometer and CO_2 concentration by an infrared analyzer (Fig. 11). The micrometeorological measurements will be carried out in a central basin position where a clear, flat fetch of several hundreds of meters is available to the north-east, the most frequent wind direction.

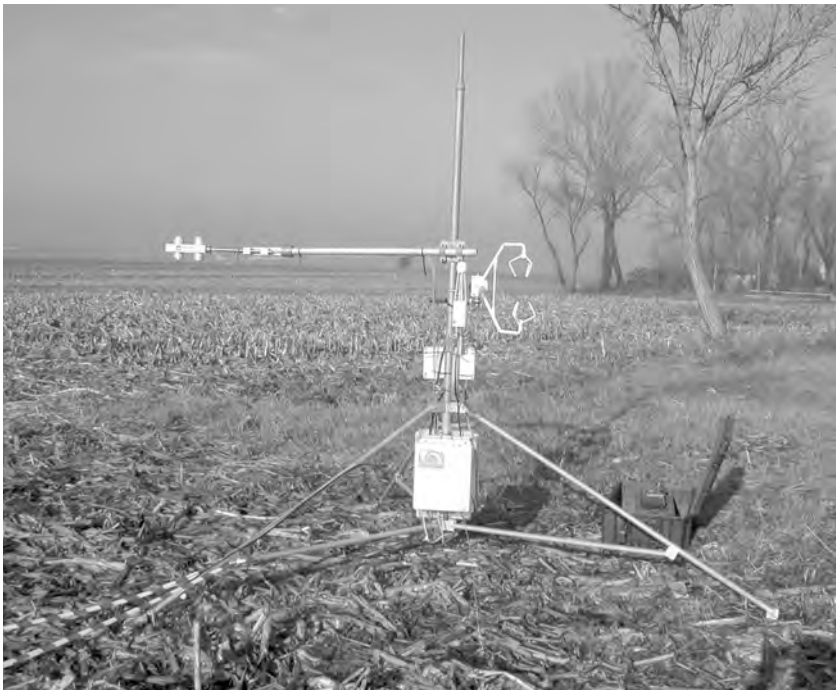

Fig. 11 – The micrometeorological instrumentation for the eddy covariance measurement during a first application period in the Zennare Basin.

5. *Conclusions.*

The Zennare Basin has been equipped in order to monitor the process of land subsidence caused by biochemical oxidation of organic soils. A number of sensors continuously record rainfall, wind speed, soil temperature and moisture, capillary pressure, and water table depth at different locations within the basin. An *ad hoc* extensometric apparatus has been designed and set up to directly measure the peat surface displacements. The CO_2 fluxes are designed to be recorded in a near feature over two distinct spatial scales, from chambers ($\approx$0.3 m^2) to patch ($\approx$1000 m^2).

The field experiment has been designed with a redundant number of sensors for each instrument type to avoid gaps in the data. Moreover, the high variability of rainfall characterizing the summer season has suggested the use of several pluviometers.

Acknowledgments.

This work has been funded by Co.Ri.La., Consorzio Venezia Nuova – Sistema Informativo, and Consorzio di Bonifica Adige – Bacchiglione. The authors gratefully acknowledge the assistance in the field provided by the personnel of the Consorzio di Bonifica Adige – Bacchiglione, particularly by Massimo Barbetta and Gianpaolo Minorello. The owners of the land where the sites are located are also acknowledged: Azienda Agricola Della Rocca, Adriano Baretta, Anna Gallimberti, Luigino Guzzo, and Silvio Viale.

References.

Andriesse J. P., 1988. Nature and management of tropical peat soils. FAO Soils Bulletin 59.

Clair T. A., Arp P., Moore T. R., Dalva M., Meng F.-R., 2002. Gaseous carbon dioxide and methane, as well as dissolved organic carbon losses from a small temperate wetland under a changing climate. Environ. Poll. 116, 143-148.

Consorzio di Bonifica Adige-Bacchiglione, 1996. Studio del fenomeno della subsidenza nei bacini Orientale, Zennare, Punta Gorzone e Foresto Centrale, ricadenti nel comprensorio consorziale. Technical Report, 37 pp.

Deverel S.J., Rojstaczer S., 1996. Subsidence of agricultural lands in the Sacramento – San Joaquin Delta, California: role of aqueous and gaseous carbon fluxes. Water Resour. Res. 32, 2359-2367.

Francese R., et al., this issue. Geophysical investigations within the Zennare Basin (Venice).

Gatti P., et al., this issue. The peat deposit of the subsiding Zennare Basin, south of the Venice Lagoon, Italy: geotechnical classification and preliminary mineralogical characterization.

Ingebritsen S.E., McVoy C., Glaz B., Park W., 1999. Florida Everglades: subsidence threatens agriculture and complicates ecosystem restoration. In: Galloway, D., et al. (Ed.), Land subsidence in the United States, U.S. Geological Survey, Circular 1182, 95-106.

Hutchinson G. L., Livingston G. P., 2001. Vents and seals in non-steady-state chambers for measuring gas exchange between soil and the atmosphere. Eur. J. Soil Sci. 52, 675-682.

Moore T. R., Dalva M., 1997. Methane and carbon dioxide exchange potentials of peat soils in aerobic and anaerobic laboratory incubations. Soil Biol. Biochem. 29, 1157-1164.

Moncrieff J. B., et al., 1997. A system to measure surface fluxes of momentum, sensible heat, water vapour and carbon dioxide. J. Hydrol. 188-189, 589-611.

Nieuwenhuis H. S., Schokking F., 1997. Land subsidence in drained peat areas of the Province of Friseland, The Netherlands. Q. J. Eng. Geol. 30, 37-48.
Rizzetto F., et al., this issue. Geomorphological evolution of the south catchment of the Venice Lagoon (Italy): the Zennare Basin.
Rojstaczer S., Deverel S.J., 1995. Land subsidence in drained histosols and highly organic mineral soils of California. Soil Sci. Soc. Am. J. 59, 1162-1167.
Soil Survey Staff, 1975. Soil Taxonomy - a comprehensive system. U.S.D.A.
Stephens J.C., Allen L. H., Chen E., 1984. Organic soil subsidence. In: Holzer, T. L. (Ed.), Man-induced Land Subsidence, Geological Society of America, Reviews in Engineering Geology, v. 6, 107-122.
Tosi L., Carbognin L., Teatini P., Rosselli R., Gasparetto Stori G., 2000. The ISES Project subsidence monitoring of the catchment basin south of the Venice Lagoon (Italy). In: Carbognin, L., et al. (Ed.), Land Subsidence, Proc. of the 6th Int. Symp. on Land Subsidence, La Garangola Publ., Padova (Italy), Vol. II, 113-126.
Wösten J.H.M., Ismail A.B., van Wijk A.L.M., 1997. Peat subsidence and its practical implications: a case study in Malaysia. Geoderma 78, 25-36.

GEOMORPHOLOGICAL EVOLUTION OF THE SOUTHERN CATCHMENT OF THE VENICE LAGOON (ITALY): THE ZENNARE BASIN

F. Rizzetto[1], L. Tosi[1], M. Bonardi[1], P. Gatti[1], A. Fornasiero[2], G. Gambolati[2], M. Putti[2], P. Teatini[2]

[1]*Istituto per lo Studio della Dinamica delle Grandi Masse, CNR, Venezia*

[2]*Dip. Metodi e Modelli Matematici per le Scienze Applicate, Università di Padova*

Abstract.

The investigated area is the Zennare Basin, located in the southern catchment of the Venice Lagoon (Italy). This zone was completely reclaimed in the 1930's for agricultural purposes. The Zennare Basin is a subsiding basin that lies down to 4 m below sea level, characterized by the presence of bogs with peat layers generally less than 2 m thick providing evidence of ancient swamps. Within the VOSS Project (Venice Organic Soil Subsidence) a detailed geomorphological study of the Zennare Basin was carried out using data derived from aerial photographic interpretation, field surveys, stratigraphic analyses of the deposits and altimetrical investigations.

The sedimentological and geomorphological studies allowed the reconstruction of the main geological features of the basin, i.e. paleo-river beds, which constitute part of the input to the land subsidence simulation model.

1. *Introduction.*

The Zennare Basin is located in the coastal plain south of the Venice Lagoon, between the Brenta and Adige rivers (Fig. 1). Since the XIX century, several reclamation works were carried out to improve land use of the territory which was previously characterized by marshes and swamps. Nowadays as the ground surface of the Zennare Basin lies down to about 4 m below mean sea level, reflooding is avoided by

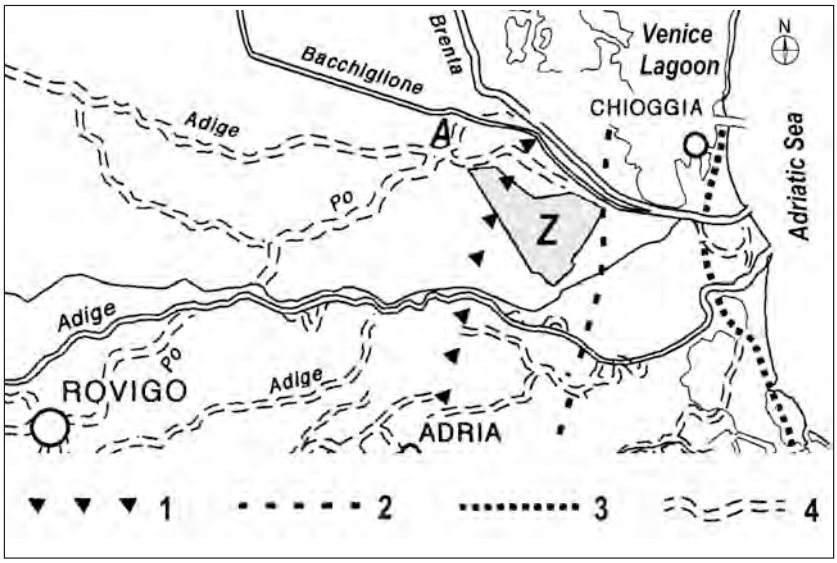

Fig. 1 – Location of the Zennare Basin (Z), in the coastal plain south of the Venice Lagoon. Conca d'Albero (A); coastline position around: 1) 5-6,000 years B.P., 2) 4,500 years B.P., 3) 500 years B.P.; 4) main paleo-river beds (modified after Bondesan et al. [2001]).

water-pumping stations; nevertheless, many works have to be continuously carried out to maintain the efficiency of the network of drainage canals and to mitigate the damages caused by land subsidence.

Geomorphological investigations and sedimentological and stratigraphical characterization of the basin are part of the VOSS Project (Venice Organic Soil Subsidence), aimed at studying the land subsidence process with the aid of field analyses and a mathematical model.

The high subsidence rate of the basin (up to 2 cm/year) [Fornasiero et al., this issue] is mainly due to the oxidation of the soils rich in organic matter, whereas natural compaction gives only a secondary contribution (about 2 mm/year) [Gambolati and Teatini, 1998].

The oxidation of the peat soil causes the CO_2 emission into the atmosphere with consequent loss of organic matter and lowering of the ground surface. This process is induced by the intensive agricultural practices and the drainage needed to maintain the water table 50-100 cm below the ground surface.

2. *Materials and methods.*

General information about the geology and geomorphology of the area between the Brenta and Adige rivers are reported in Favero and Serandrei Barbero [1978] and Provincia di Venezia [1994]. Nevertheless a more detailed investigation at the scale of the Zennare Basin is required to meet the goal of the VOSS research project.

The results were obtained with the aid of a multidisciplinary investigation, which includes studies on historical and present maps, aerial photographic interpretations, field surveys, sedimentological and stratigraphical analyses of the deposits and altimetrical data processing.

The 1962 and 1990 series of aerial photographs were used for a preliminary interpretation of the morphological setting of the Zennare Basin with the superficial landforms and deposits reported in topographic maps on a 1:5,000 scale.

Sediment samples were taken from new cores and trenches and studied in order to determine the lithological characteristics and the depositional environment. In particular several drillings, made with a handboring equipment, were carried out to better define the lithological boundaries preliminarily recognized by aerial photographic interpretations.

Three lithological classes were used to map the outcropping deposits: sand, silt and peat. Each class represents the prevailing lithology of the first meter of depth. Small amounts of clay sediments were not mapped because they were found only in much restricted areas, so they were included into the class of the silt.

3. *The altimetrical analysis of the Zennare Basin.*

The altimetrical analysis of the Zennare Basin was carried out to highlight the differences in altitude with the purpose to better define landforms pointed out by the aerial photographic interpretations and to recognize new morphological features. A basic topographic map on a 1:5,000 scale was used to construct a DEM (Digital Elevation Model) of the area with a 0.5 m vertical resolution (Fig. 2).

The altimetrical study shows that the basin lies completely below mean sea level with the lowest areas located in the southern part. These depressions are indicated in the geomorphological map with

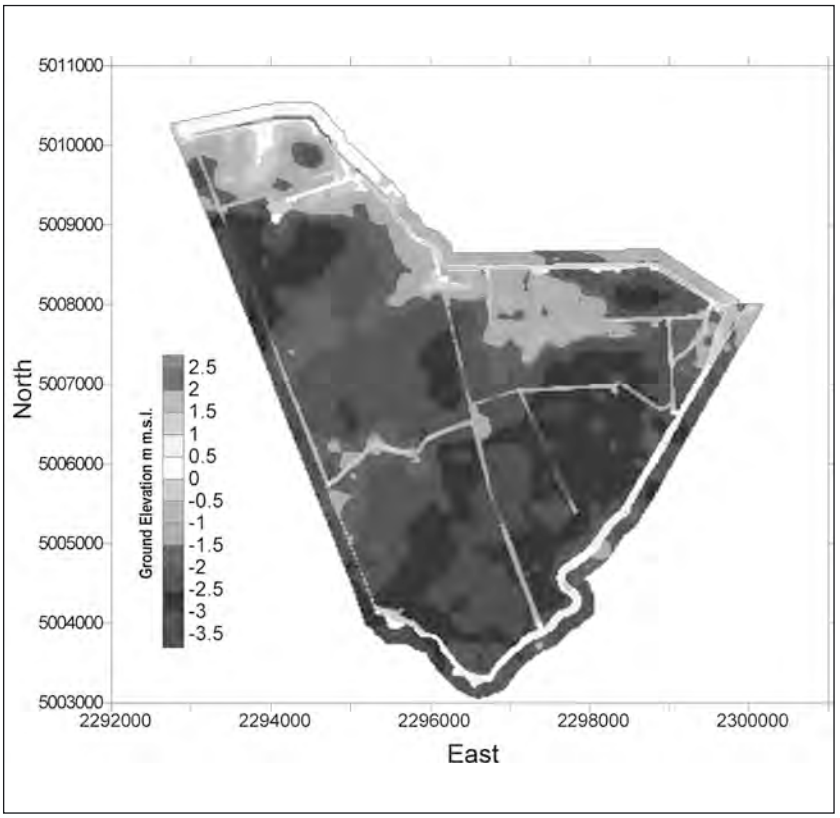

Fig. 2 – DEM of the Zennare Basin obtained from a topographic map on a 1:5,000 scale.

green lines and are generally related to peaty soils. The most elevated areas correspond to ancient silty-sand fluvial ridges, clearly recognizable in the map.

4. *The geomorphological map of the Zennare Basin.*

The geomorphological map provided in Figure 3 represents a summary of the knowledge obtained from the multidisciplinary investigations performed in the study. The legend is shown in Figure 4. The original map was made on a scale of 1:5,000 and for the present paper some enlargements are required to appreciate the details.

Fig. 3 – Geomorphological map of the Zennare Basin.

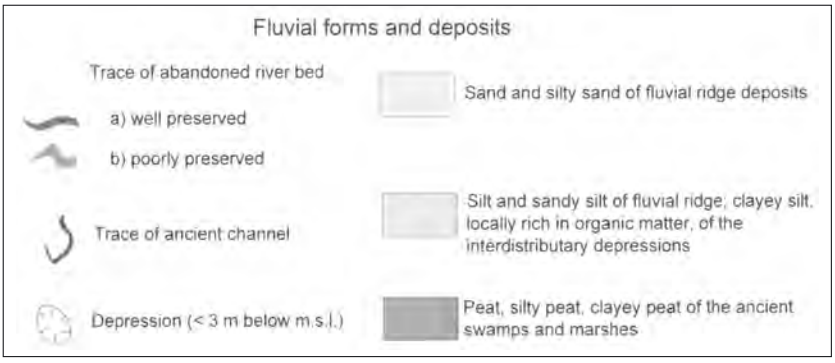

Fig. 4 – Legend of the geomorphological map.

The contents of the geomorphological map are morphographic, morphometric, morphogenetic and lithological data. Morphographic data are landforms, such as paleo-river beds and ancient channels. Two different colors indicate the paleo-river beds: red for the well preserved and pink for the poorly preserved. Ancient channels are colored in brown. Morphometric data are the depressions between 3 and 4 m below sea level, indicated with green hachure contour lines. Morphogenetic data are the depositional environments referred to the landforms, i.e. fluvial, deltaic, marshy. Finally, lithological data are the grain size and texture of sediments.

Several traces of paleo-river beds with the main direction toward the southern Venice Lagoon margin were found. Two paleo-river systems, probably related to the ancient Adige river, cross the central part of the

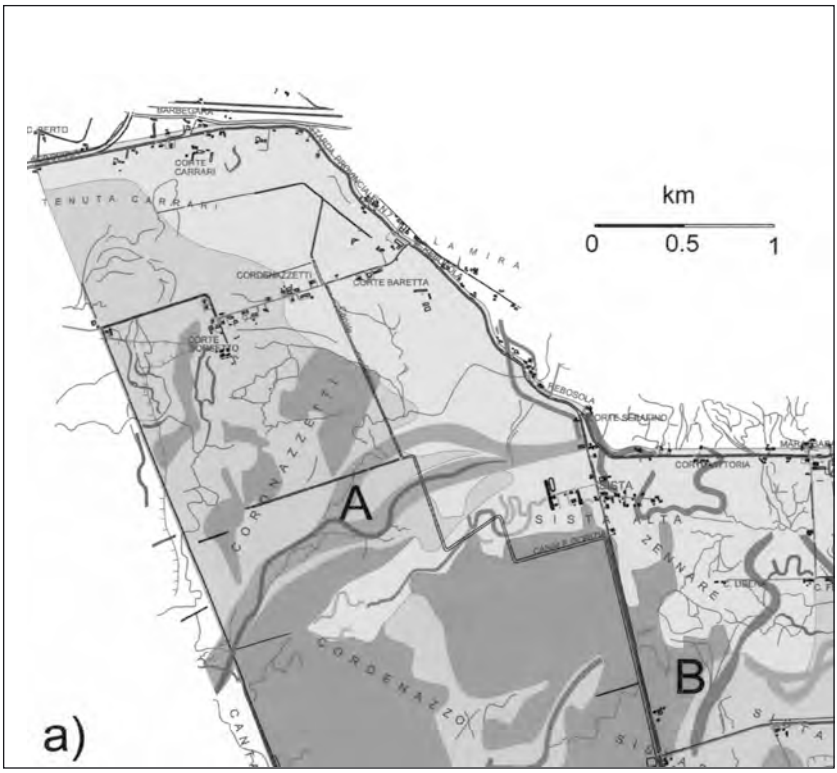

Fig. 5 –Details of the north-western part of the geomorphological map.

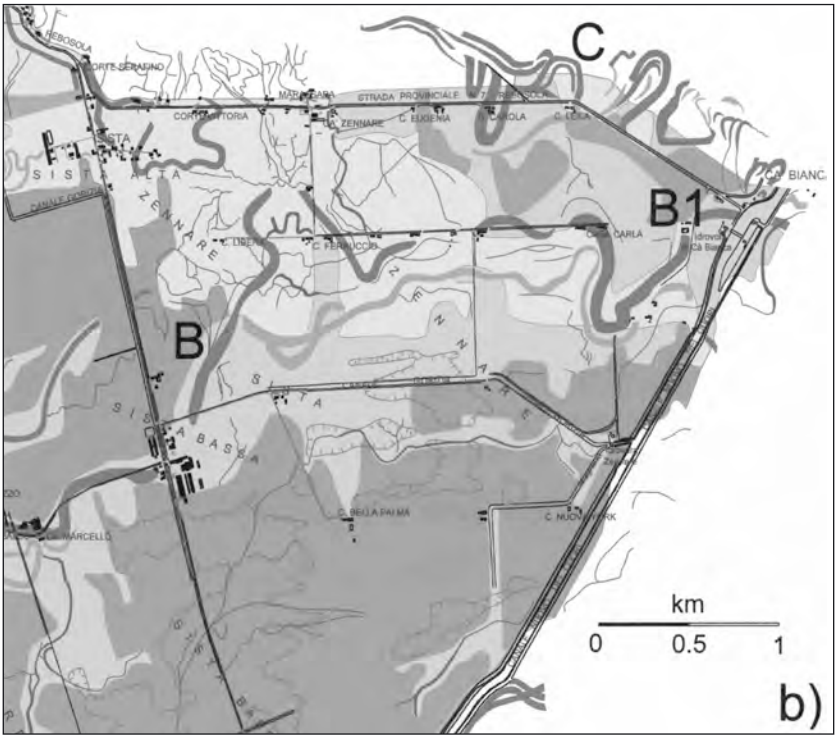

Fig. 6 –Details of the eastern part of the geomorphological map.

Zennare Basin along a SW-NE direction: while the northern trace (A) (Fig. 5) disappears next to Sista Alta, the southern one (B) (Fig. 6), whose direction goes from Motta Molara to Ca Bianca, along the Cordenazzo, Sista Bassa and Ca' Zennare alignment, is easily recognizable.

An evidence of a partial southern paleo-river bed is an ancient street built on its relict fluvial ridge, slightly elevated above the surrounding swamp areas. It is reported in the "Carta del Regno Lombardo-Veneto" (Fig. 7a), in the "Carta Idrografica Stradale Amministrativa Consorziale della Provincia di Padova" (Fig. 7b) and in the "Carta della Deputazione Provinciale di Padova" (Fig. 7c), respectively dated 1833, 1862 and 1882. However, no trace of this street can be found in the 1896 I.G.M.I. (Istituto Geografico Militare Italiano) map (Fig. 7d).

In the north-eastern part of the Zennare Basin, there is evidence of the Brentone Vecchio (B1) (see Fig. 6), i.e. the ancient southernmost

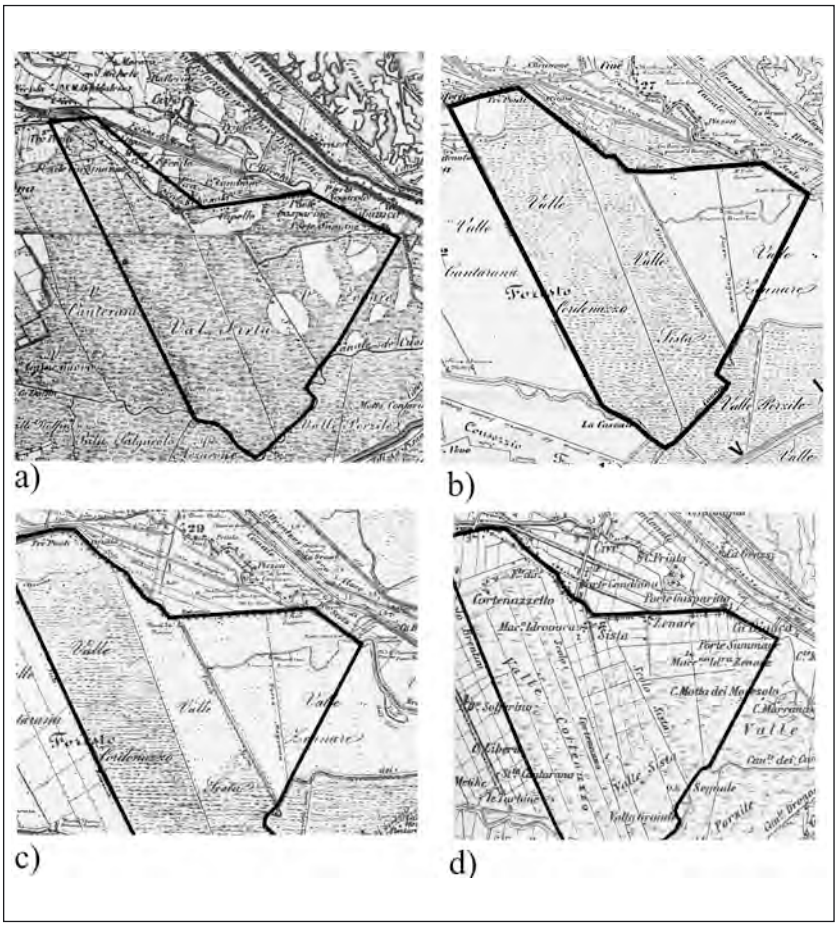

Fig. 7 – Historical maps: a) Carta del Regno Lombardo-Veneto (1833), b) Carta Idrografica Stradale Amministrativa Consorziale della Provincia di Padova (1862), c) Carta della Deputazione Provinciale di Padova (1882), d) 1896 I.G.M.I. map. a, c, d after Zunica [1981] and b after Provincia di Padova [1862].

path of the Brenta and Bacchiglione river systems [Favero and Serandrei Barbero, 1978]. The old course of the Canale dei Cuori is shown by the traces of its meanders, which intersect the new canal (Canale Nuovo dei Cuori) built at the end of the XIX century (Fig. 8).

The northernmost ancient branch of the Po River, which dates back to the Bronze Age, crossed Agna, Cona and Conca d'Albero

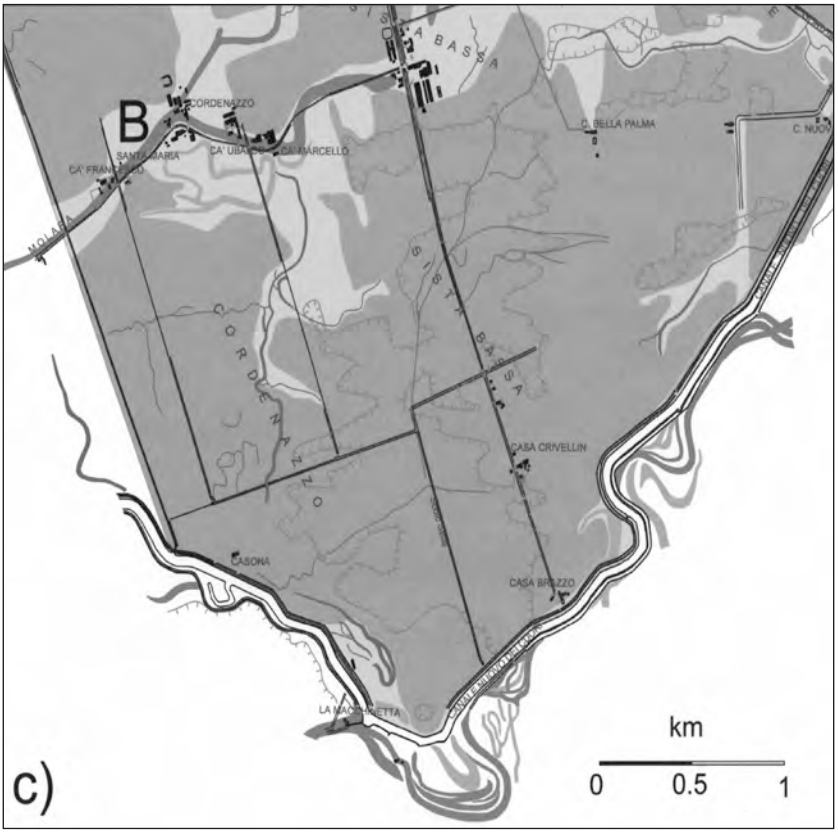

Fig. 8 –Details of the southern part of the geomorphological map.

[Castiglioni, 1978] heading towards Chioggia. An evidence could be the meanders located WNW of Ca Bianca (C) (Fig. 6). Next to Conca d'Albero a paleo-course of the Adige river flowed into this branch of the Po (Fig. 1). This information indicates complex relationships among the ancient flow directions of the Po, Adige, Brenta and Bacchiglione rivers which exist in this coastal plain area. Further analyses, such as mineralogical and radiocarbon dating, are needed for a complete reconstruction of the corresponding paleo-courses.

Finally, detailed investigations on several narrow channels which were frequently branched (drawn with brown color), indicate that the majority of them are related to the earliest reclamation works.

5. *Holocene evolution of the Zennare Basin and its surrounding area.*

Favero and Serandrei Barbero [1978] have identified the position reached by the inner coastline during the Flandrian transgression, 5-6,000 years B.P., just in the north-western part of the Zennare Basin (Fig. 1). Even if the transgression crossed the basin, no trace of marine-lagoon environments was found in the outcropping sediments, whereas they clearly appear from cores at a depth of 2-3 m below ground surface. These deposits were buried by intensive fluvial sediment supplies which caused the rapid eastward progradation of the coastline.

Evidence of beach ridges is recognizable about 1-2 km east of the Zennare Basin from aerial photographs and field surveys (Fig. 1). The coastline reached this area about 4,500 years B.P. [Bondesan et al., 2001] and stationed here for a longer time than in the inner position. Subsequent fluvial depositional events filled up the back barrier lagoon and the surrounding swamps and caused a new eastward migration of the coastline.

The analysis of several historical land use maps shows the environmental transformations of this land during the last two centuries. The 1833 map (see Fig. 7a) indicates the predominance of swamps and marshlands. Only in correspondence of the fluvial ridges located in the north-eastern part there are small drained sites used for agricultural activity or urban area. The first water pumping station and a few elemental canals are reported in the 1862 map (see Fig. 7b), whereas the first network of drainage channels appears in the 1896 map (see Fig. 7d).

At present, fluvial and deltaic sedimentations constitute the outcropping deposits: in particular sandy and silty soils characterize remnants of ancient fluvial ridges, whereas clayey silts, often rich in organic matter, fill the interdistributary lowland; bogs with peat layers, up to 2 m thick, occur in the reclaimed marsh areas.

6. *Concluding remarks.*

The present analysis points out the morphological and sedimentological characteristics of the Zennare Basin. Several paleo-river beds and remnants of natural channels and reclamation canals were identified using aerial photographs and field surveys. These features, together

with the landforms and the characteristics of superficial deposits were reported in the geomorphological map which constitutes the geological input to the mathematical model for the simulation of the land subsidence process.

In addition, new data and investigations allowed a better understanding of the evolutionary process occurred in the study area from the Flandrian marine transgression to the historical land reclamations. The results show a complex relationship among the various fluvial sediment sources, i.e. the Po, Adige, Bacchiglione and Brenta rivers that flowed into the lagoon and the Adriatic Sea, crossing the Zennare Basin in different times and following different directions.

Acknowledgements.

This study was financially supported by Co.Ri.La. with the contributions of Consorzio di Bonifica Adige-Bacchiglione, Servizio Informativo of the Magistrato alle Acque per la Laguna di Venezia, A.T.A. and TE.MA companies. Authors acknowledge Ufficio Difesa del Suolo of the Provincia di Venezia, ARPAV, and ISES Project for made available part of the material used for the study and Dr Laura Carbognin for the revision of the manuscript.

References.

Castiglioni G. B., 1978. Il ramo più settentrionale del Po nell'antichità. Atti e Mem. Acc. Patav. SS. LL. AA. Vol. 90 Parte 3, 157-164.

Bondesan M., Elmi C. & Marocco R., with a contribution by Favero V., 2001. Forme e depositi di origine litoranea e lagunare. In: Castiglioni, G. B. & Pellegrini, G. B. (Eds.), Note illustrative della Carta Geomorfologica della Pianura Padana. Suppl. Geogr. Fis. Dinam. Quat. 4, 105-118.

Favero V. & Serandrei Barbero R., 1978. La sedimentazione olocenica nella piana costiera tra Brenta ed Adige. Mem. Soc. Geol. It. 19, 337-343.

Fornasiero A., et al., this issue. Subsidence due to peat soil loss in the Zennare Basin (Italy): design and set-up of the field experiment.

Gambolati G., Teatini P., 1998. Numerical analysis of land subsidence due to natural compaction of the Upper Adriatic Sea basin. In: Gambolati, G., (Ed.), CENAS, Coastline Evolution of the Upper Adriatic Sea due to Sea Level Rise and Natural and Anthropic Land Subsidence, Kluwer Academic Publ., 103-132.

Provincia di Padova, 1862. Carta Idrografica Stradale Amministrativa Consorziale.

Provincia di Venezia, 1994. Studio geoambientale e geopedologico del territorio provinciale di Venezia, parte meridionale. Servizi Grafici Editoriali, Padova.

Zunica M. (Ed.), 1981. Il territorio della Brenta. Cleup, Padova.

GEOPHYSICAL INVESTIGATION WITHIN THE ZENNARE BASIN (VENICE)

R. Francese[1], A. Galgaro[1], E. Farinatti[2]
M. Putti[3], P. Teatini[3], F. Rizzetto[4], L. Tosi[4]
[1]*Dip. Geologia, Paleontologia e Geofisica, Università di Padova*
[2]*A.T.A. Studio Associato di Geologia Tecnica e Geofisica, Rovigo*
[3]*Dip. Metodi e Modelli Matematici per le Scienze Applicate Università di Padova*
[4]*Istituto per lo Studio della Dinamica delle Grandi Masse, CNR, Venezia*

Abstract.

A multi-technique geophysical investigation is performed to map the shallow depositional units in the Zennare peat basin nearby the Venetian Lagoon. The detection and resolution capabilities of Earth Resistivity Tomography, Refraction Seismic, and Ground Probing Radar are compared in a small test area within the basin, where also additional stratigraphic point information is available. The results obtained with the different methods prove comparable, and the integration of these distinct geophysical responses allows for a more precise identification of the subsurface structure. The Ground Probing Radar survey, because of its cost-effectiveness, has been extended to the entire basin. Some coherent noise patterns, associated with the frozen ground surface, required a specific processing sequence to enhance the radar record quality. The radar images outline the main shallow discontinuities of the basin related to the different depositional framework, allowing for a detailed reconstruction of peat layers as well as of a series of sand-silty paleo-channels distributed within the area. Borehole and remote sensing data are used to calibrate the geophysical interpretation.

1. *Introduction.*

A geophysical investigation with various techniques was recently carried out in a peatland area of the Zennare Basin in the vicinity of the Venice Lagoon (Fig. 1). This investigation is part of a research project

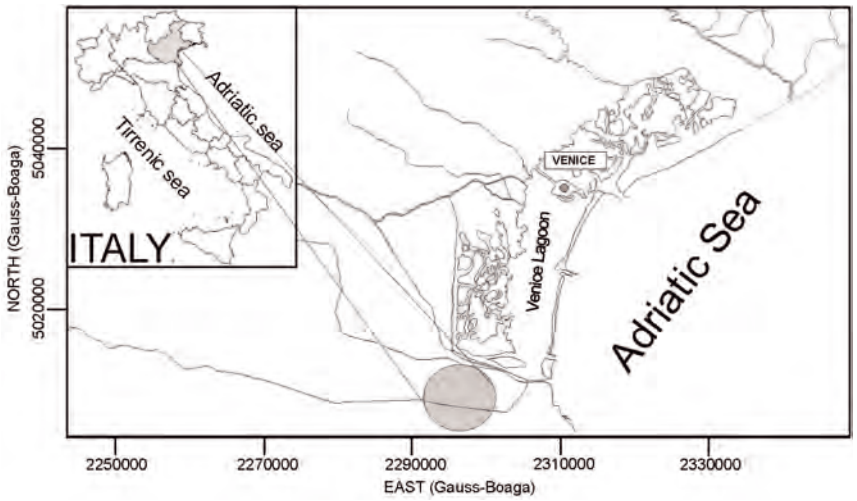

Fig. 1 - Geographical location map of the investigated area.

aimed to model the volume reduction of some shallow organic depositional units due to the aerobic peat oxidation [Nieuwenhuis and Schokking, 1997]. The target of the surveys was to map geometry and stratigraphy of the uppermost sandy and peaty layers [Hanninen, 1992; Saarenketo et al., 1992] and to assess the potentials of a multi-technique geophysical approach that make use of Refraction Seismic, ERT (Earth Resistivity Tomography) and GPR (Ground Probing Radar).

The above techniques are sensitive to variation of acoustic impedance, electrical and electro-magnetical suscettivity, respectively, and are characterized by different degrees of resolution, but all are able to detect the near-surface peaty and sandy bodies. Because of their capability of mapping moisture, mineralogical and textural changes, ERT and GPR were highly successful in detecting the peat-clay or peat-sand interface [Ulriksen, 1982].

On the basis of a field test GPR was selected as the most adequate technique to carry out the entire geophysical investigation. The GPR images clearly outlined the spatial distribution of the peat bodies. The initial data analysis was based on a series of stratigraphic boreholes, and the final interpretation has been controlled by means of aerophotographycal remote sensing [Rizzetto et al., this issue].

2. *General Settings.*

The Zennare Basin is an area of approximately 23 km^2 located south of the Venice Lagoon, about 10 km from the Adriatic Sea. The basin was reclaimed about 70 years ago and presently lies almost entirely below the mean sea level, mostly between -2 and -4 m [Rizzetto et al., this issue]. The land use is completely devoted to agriculture.

The near surface stratigraphy in this area is mainly made of peat, silt, and sand. The peat deposits are located in the central and southern portion of the basin, while silt and sand terrains outcrop in the northern area [Rizzetto et al., this issue]. A number of paleo-channels with width ranging from some meters to few tens of meters cross the silt and peat deposits.

The depth of the water table is approximately 0.5-1 m, varying only slightly with the ground elevation and seasonal changes, and is controlled by pumping stations. The shallow aquifers of the central and northern parts of the basin are generally characterized by a salt contamination due to sea water intrusion from the nearby lagoon and the Adriatic Sea. The contamination is increased by the sea water that, flowing into the watercourse mouths up to 10 km landward, is dispersed from the river beds frequently laying at a level higher than the surrounding land.

The transition zone between the fresh and the brackish water is located about 4 - 8 m below the ground surface. In the southern part of the Zennare Basin, where the main bog is located, a thick and almost continuous clay layer is present below the outcropping peat unit, precluding the organic soil to be contaminated (personal communication of the Scientific Coordinators of the ISES Project).

3. *Data acquisition and processing.*

ERT survey was carried out using two different spreads: a 155-m "Wenner" profile and a 45-m "Dipole-Dipole" profile. The first profile (5-m electrode spacing) targeted the deeper layers while the second one (3-m electrode spacing) was aimed to obtain an accurate map of the near surface formations. The resistivity pseudosections were inverted to true resistivity sections using an iterative algorithm.

Refraction Seismic was used to achieve a deeper understanding of the shallow stratigraphy. Two 12-channel profiles with 3 m geophone spacing were spread in the field. GRM (Generalized Reciprocal Method) analysis was used to process the data and obtain a near-surface velocity section.

Both the ERT and the seismic profiles were acquired in the southern part of the Zennare Basin where the peat layers are thicker (Fig. 2).

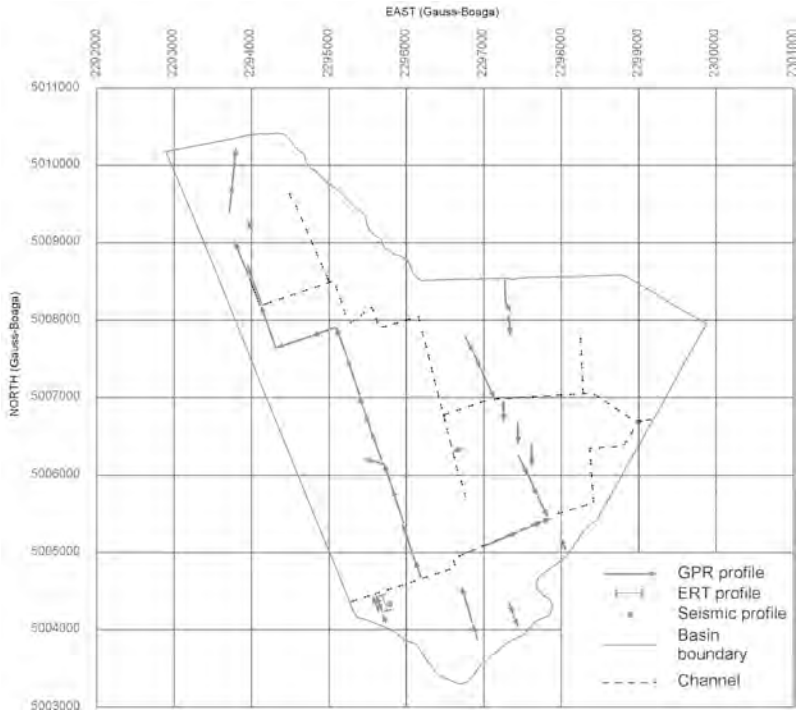

Fig. 2 - Field layout of the geophysical profiles.

The GPR survey was extended to the entire Zennare Basin because of its cost-effectiveness and resolution capabilities. The investigation was carried out with a GSSI SIR-2 system in bi-static configuration, with a constant offset of 0.4 m, using two 500-MHz antennas. The basin was explored with two N-S 2-km long profiles and a series of short E-W sections (Fig. 2).

Data acquisition faced a major inconvenient because of the frozen surface during the field operations. In some area the electro-magnetic energy propagated into the ground was trapped in the frozen layer and generated ringing and reverberative patterns in the radargrams.

Radar data have been processed using the CWP-SU rel.3.4. software package running under a SPARC architecture. Two different processing

sequences (according to the geographical position of the profiles) were devised to increase the radar signal quality [Annan, 1996]. The sequence for the sand and silt deposit was quite straightforward: raw data were converted from GSSI SIR-2 into the CWP-SU internal format. Furthermore, major processing steps were zero-offset correction, DC component removal, band pass filtering, horizontal filtering, and amplitude recovery. A running average filter (Daniels, 1996) was applied to the data to correct for DC component. The band pass gate was centered on the antenna natural frequency. A statistical analysis of signal-free traces permitted the estimation of the amplitude decay function that allowed a time-dependent amplitude recovery gain. The low-reflectivity peat deposits required further processing steps to enhance the weak response from the bottom of the peat layer. A velocity filter and a predictive deconvolution were both applied to the data to remove some coherent noise patterns and sharpen the boundary response.

The time section was transposed into depth using a relative dielectric constant equal to 40 in the peat layers and 10 in the sand-silty layers. These values were obtained from averaged field data obtained at borehole locations.

4. *Results and discussion.*

The Wenner resistivity profile shows a fairly conductive and discontinuous top layer with a thickness ranging from 3 to 4 m and a resistivity of 10÷20 ohm·m. Many lateral and vertical variations in resistivity are visible in the section. The clayey deeper layers are even more conductive. The dipole-dipole profile shows a more detailed spatial distribution of the underground resistivity (Fig. 3).

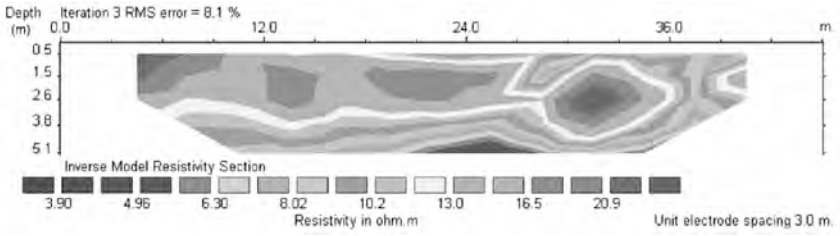

Fig. 3 - ERT inverted resistivity profile.

In particular, the top peaty layer 1.5 m thick exhibits resistivity values ranging from 7.0 to 10.0 ohm·m in the central and left portions of the profile. Resistivity values are higher in the shallower unsaturated zone (above the water table) and lower in the deeper zone (fresh water saturated area). The highly conductive layer (less than 8.0 ohm·m) at the bottom of the ERT "Dipole-Dipole" profile is the response of a clayey horizon. A sand-filled paleo-channel, 6.0 m wide, with resistivity values ranging from 12.0 to 30.0 ohm·m is clearly visible in the right portion of the profile.

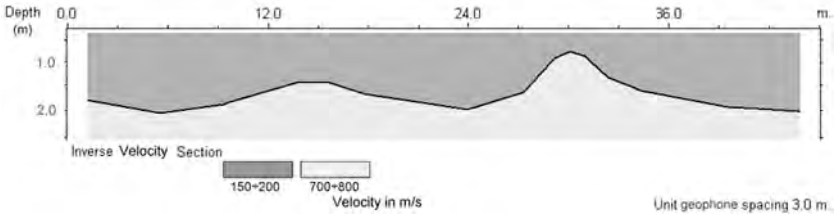

Fig. 4 - Refraction seismic profile.

The seismic section (Fig. 4) was laid out practically coincident with the ERT "Dipole-Dipole" profile. The results evidenced a 200 m/s low velocity layer with a thickness ranging from 1 to 2 m. A deeper layer characterized by a strong increase of P-wave velocity, up to 700-800 m/s, is probably related to a sudden change in lithology. This variation marks the transition to inorganic deposits.

The radar images proved to be very sensitive to small lithological changes. Particularly sand and silt deposits exhibit peculiar electromagnetic responses. Data recorded in the southern part of the basin (Fig. 5) indicates at least three different reflectors. The deepest reflector, visible at about 1.5 m depth, was interpreted as the bottom of the peat layer lying on the clayey-silt deposits. A second reflector occurs within the peat layer at about 1.0 m depth. The uppermost reflector, located about 0.5-0.7 m deep, is the image of the water table. Small variations in the water table depths are probably related to ground surface irregularities.

Some profiles performed in the central part of the basin exhibit the response of the infilling sequences of major sandy paleo-channels. The radar scan of a paleo-channel structure is clearly visible in Fig. 6. The bottom of the channel is evidenced by a series of diffraction patterns due to textural and lithological changes at the contact between the infilling sand deposits and the underlying silt layers. Some east prograding clino-forms are reco-

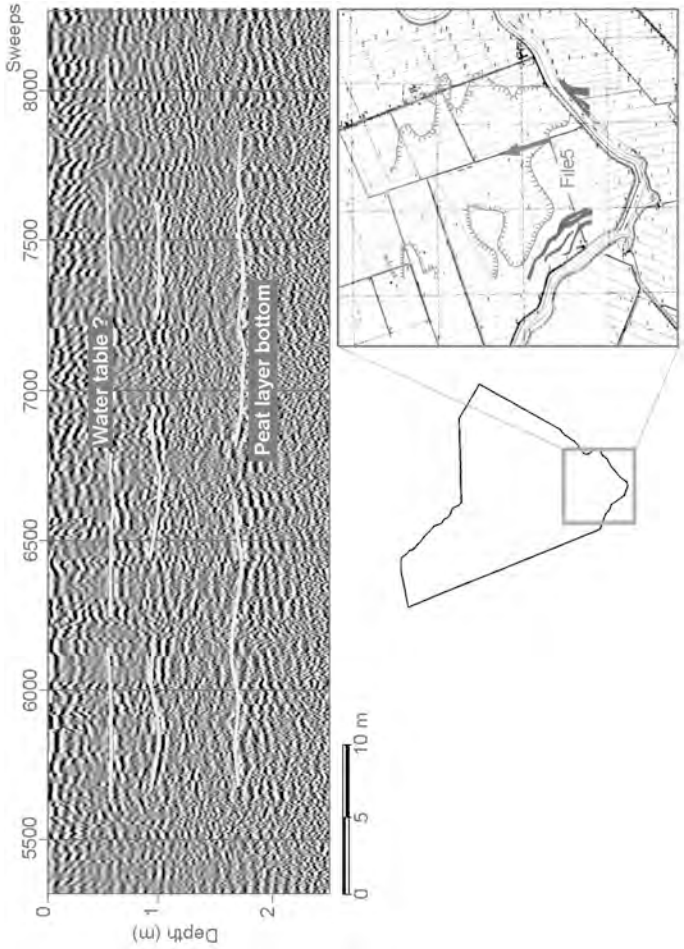

Fig. 5 - Example of the GPR profile in the southern part of the Zennare Basin.

gnizable within the channel infilling sequence. The geomorphological map of the area (in the right side of the figure) supports this interpretation.

An initial analysis of the raw data collected in the northern part of the basin indicates the presence of narrow channel structures (Fig. 7) within the first two meters of depth. The geomorphological map of the area evidences some small channels nearby the radar profile. These sharp shallow patterns are interpreted as ancient canals related to the reclamation started in the 19th century.

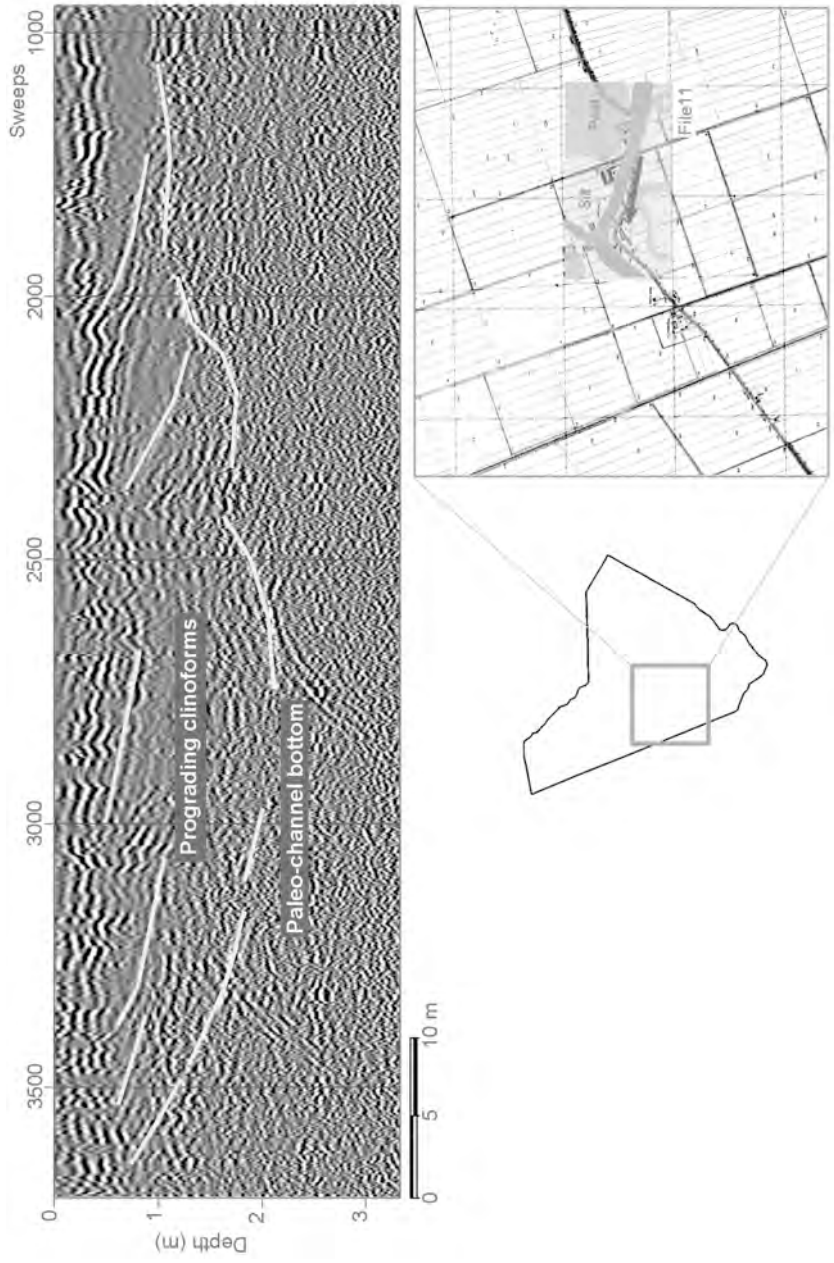

Fig. 6 - Example of the GPR profile in the central part of the Zennare Basin.

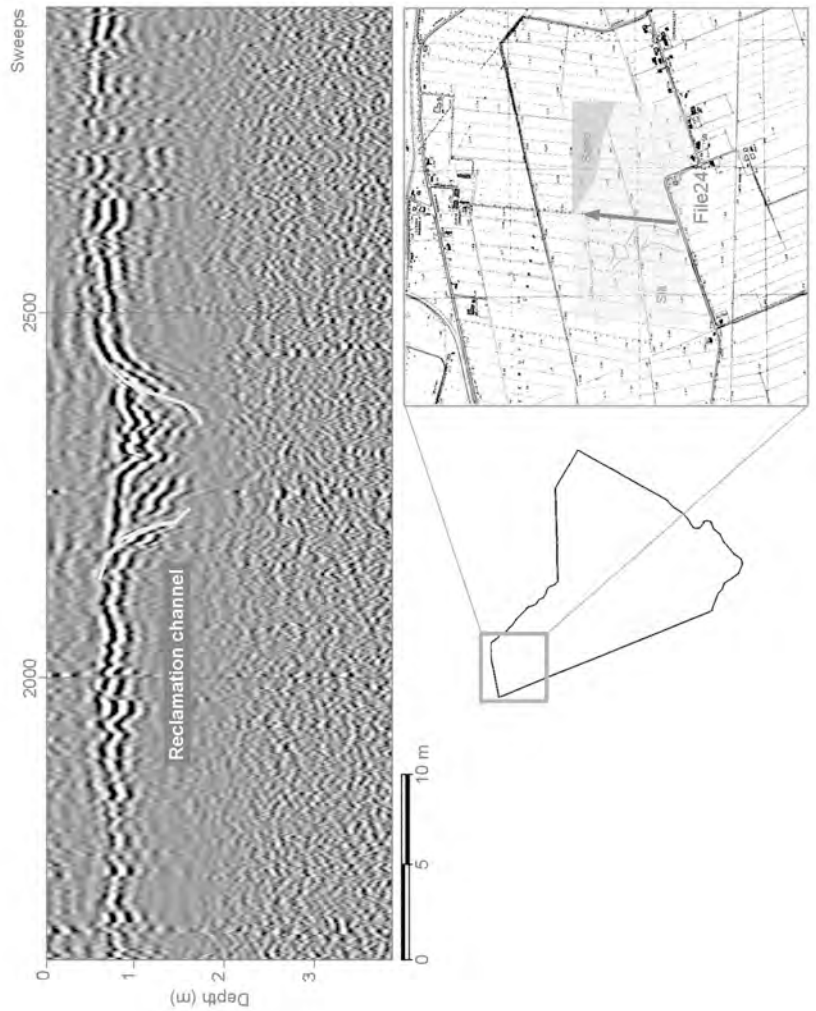

Fig. 7 - Example of the GPR profile in the northern part of the Zennare Basin.

5. *Conclusions.*

A high-resolution geophysical investigation successfully imaged the distribution and thickness of the peat in the uppermost depositional layers within the Zennare Basin. The different physico-chemical and textural properties of sand, silt, clay, and peat lithologies generated distinct geophysical responses.

Three different techniques were tested in the field before carrying out the exploration survey. ERT and refraction seismic provided comparable results in terms of lithology detection and mapping capability.

The GPR provided a much higher resolution with a reduced logistical effort. Because of these accomplishments the radar technique was extended for the survey of the entire basin. Specific processing sequences were tested to enhance the radar images. A multi-step routine was used to enhance the quality of the data degraded by the low reflectivity of the peat deposits.

Analysis and interpretation of the radar images allowed a detailed reconstruction of the fresh water table, peat layer boundaries, and sand and silt filled paleo-channels. The initial interpretation of the geophysical response was supported by remote sensing analysis and borehole data collected in various locations within the peaty basin. The ringing character of some radar profiles due to the frozen surface made their interpretation somewhat difficult when nearby borehole calibration was not available.

The integrated interpretation of the field data measured in the test area proved to be the most efficient approach to outline the framework of the near-surface stratigraphy within these depositional contexts.

Acknowledgments.

This work has been funded by Consorzio Venezia Nuova – Sistema Informativo and Co.Ri.La., that we gratefully thanks for the support.

References.

Annan A.P., 1996. Trasmission dispersion and GPR. J. Environ. Eng. Geophys 0, 125-136.

Daniels D.,J., 1996. Surface Penetrating Radar. Institution of Electrical Engineers (IEE), London, UK, 300 pp.

Rizzetto F., et al., this issue. Geomorphological evolution of the southern catchment of the Venice Lagoon (Italy): the Zennare Basin.

Hanninen P., 1992. Application of Ground Penetrating Radar techniques to peatland investigations. In: Fourth Int. Conf. on Ground Penetrating Radar, Rovaniemi, Finlan, Geol. Survey of Finland, Special Paper 16, 217-221.

Nieuwenhuis H.S., Schokking, F., 1997. Land subsidence in drained peat areas of the Province of Friseland, The Netherlands. Q. J. Eng. Geol. 30, 37-48.

Ulriksen P., 1982. Application of impulse radar to civil engineering. Doctoral Thesis, Lund University of Technology, Lund, 175 p.

Saarenketo T., Hietala, K., Salmi, T., 1992. GPR application in geotechnical investigations of peat for road survey purposes. In: Fourth Int. Conf. on Ground Penetrating Radar, Rovaniemi, Finlan, Geol. Survey of Finland, Special Paper 16, 293.

THE PEAT DEPOSIT OF THE SUBSIDING ZENNARE BASIN, SOUTH OF THE VENICE LAGOON, ITALY: GEOTECHNICAL CLASSIFICATION AND PRELIMINARY MINERALOGICAL CHARACTERIZATION

P. Gatti[1], M. Bonardi[1], L. Tosi[1], F. Rizzetto[1], A. Fornasiero[2], G. Gambolati[2], M. Putti[2], P. Teatini[2]
[1]*Istituto per lo Studio della Dinamica delle Grandi Masse, CNR, Venezia*
[2]*Dip. di Metodi e Modelli Matematici per le Scienze Applicate, Università di Padova*

1. *Abstract.*

This study is part of the VOSS Project (Venice Organic Soil Subsidence) and deals with the geotechnical classification and a preliminary mineralogical characterization of peat soils of the experimental site in the Zennare Basin. The scope is to better understand the correlation between peat oxidation and loss in ground elevation.

For the geotechnical characterization a visual classification and the von Post classification were used. A preliminary mineralogical characterization was done using an Environmental Scanning Electron Microscope (ESEM).

The peat in the experimental site is formed by vegetal deposits and can be distinguished in two levels: a completely decomposed amorphous granular top level and a slightly decomposed fibrous bottom level with a higher organic content. The limit between the two levels corresponds to the depth to which the plough furrows.

2. *Introduction.*

This study investigates the following: a) water content in peat layers, b) mineralization grade, c) type of minerals and their distribution, d) mineral zonations, e) structure of the organic components in the Zennare Basin.

Because of the high organic and moisture content in the soil, ad hoc analytical techniques and instrumentations had to be used. Textural, geochemical and mineralogical analyses of few peat samples have been obtained using an Environmental Scanning Electron Microscope (ESEM) equipped with an Energy Dispersive Spectrometer (EDS).

Furthermore, a geotechnical classification of the organic soil is proposed using different in situ and laboratory methods based on basic geotechnical properties such as structure, water content, ignition loss, humification grade.

3. *Geological-stratigraphycal setting.*

The analyzed peaty soil has been collected from one site in the Zennare Basin, a 23 Km^2 area which is part of the south catchment of the Venice Lagoon between the Adige and Bacchiglione rivers (Favero, Serandrei Barbero, 1978). At present the area is covered by alluvial sediments where sandy and silty soils represent the remnants of ancient fluvial ridges and peaty soils the interdistributary lowlands characterized by the presence of marshes and swamps. In the second half of the 19th century reclamation works started for agricultural activities. The area was completely reclaimed in the first half of the 20th century. Soil ploughing enhanced the oxidation of the peaty soil with consequent formation and emission of carbon dioxide, mass loss, and subsidence.

The outcropping peat deposit extends for many square kilometres with a thickness of 1-2 metres. It derives from the accumulation of reeds (*Phragmites australis*) living in wetlands before the reclamation. *Cupressus sempervirens, Sambucus nigra, Salix, Eriophorum* and *Carex* constitute the actual natural vegetation in addition to corn, the most important crop in the area.

According to the "Treatment of Organic Soils in the U.S.D.A. 7th Approximation Soil Classification", the Zennare Basin soil is a *Histosol* (order soil number 10). It is defined as *soil with organic matter that does not contain mineral layers in the upper 40 cm.*

An experimental site has been selected within the study area to collect the samples for geotechnical and mineralogical analyses. The results show that there are two major levels of the same original peat (Tab. 1): the top layer, between 0 and 40 cm deep, is constituted by oxidized soil ploughed due to agricultural activities; the underlying layer between 40 and 100 cm deep, is constituted by fibrous peat with well-preserved fibres, in growing

position between 50 and 90 cm deep. Furthermore, at a depth ranging between 100 to 110 cm there is a transition layer of clayey peat, and between 110 and 145 cm a clay unit with spread vegetable remains. Finally, between 145 and 200 cm of depth, a layer of gray silty medium sand is observed. Samples of the two peaty layers were collected by digging a 2 meters-deep trench and horizontally inserting a 15-cm diameter plastic tube. The G1 sample was cored at a depth of 22.5-37.5 cm, and the G2 at a depth of 92.5-107.5 cm. The water table depth ranges between 40 and 70 cm and is controlled by pumping stations.

4. *Historical data of reclamation.*

The study basin is the result of very deep transformations (Benincasa, 2001) caused by human intervention to reclaim large cultivable areas from marshes and swamps (Fig.1).

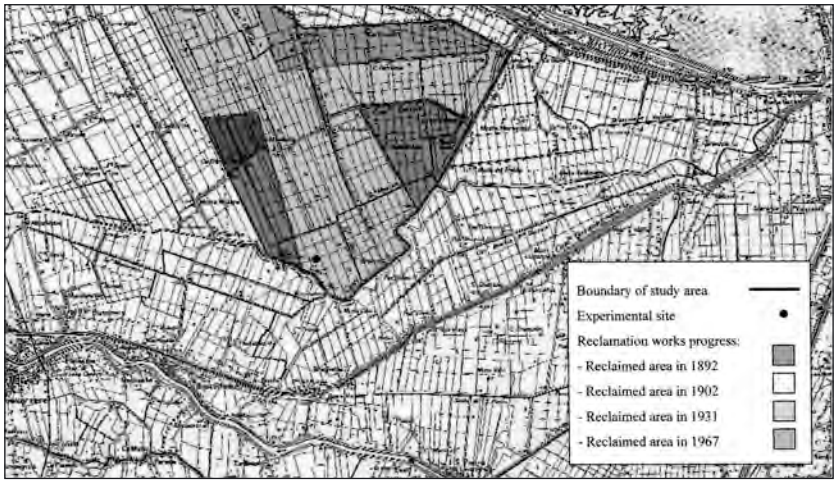

Fig. 1 - Historical reclamation data.

In 1833 (map of the Regno Lombardo Veneto, scale 1:86400, 1833) the area appeared as a bog including Valle Cordonazzo in the west, Valle Sista in the center and Valle Zenare in the east.

In 1892 (map I.G.M. - Brenta (F°. 65; IV SE), scale 1:25000) only the northern part started to be reclaimed.

In 1902 (map I.G.M.- Brenta (F°. 65; IV SE), scale 1:25000) most of

Tab. 1 - Description of the trench stratigraphy.

	Samples	depth, cm	Description
	G1 S2	0 - 40	*Black amorphous granular* peat with numerous remains of little brown roots, leaves, seeds and light olive green woody reed fragments. Size of fragments is from 1 mm to some centimeters. Small roots give some cohesion to the soil by keeping the grains of peat together. Slight smell.
		40 - 50	*Brown fibrous peat*, very moist, with a rather compact structure, prevalently consisting of light olive green soaked reeds, randomly arranged. Reeds are up to 3 cm long and 1 cm wide. Presence of several roots from 1 mm to some centimeters long. Slight smell.
		50 - 80	*Brown fibrous peat*, very moist, with a compact structure, prevalently consisting of light olive green intact soaked reeds, in growing position. Reeds are more than 10 cm long and some cm wide. Very strong smell.
	S5	80 - 90	*Brown fibrous peat*, more compact than the previous one and with abundant brownish dark gray clayey matrix. Reeds remains prevail over clayey components and have the same features as the previous ones. Very strong smell.
	G1	90 – 100	*Brownish gray fibrous peat*, very compact and with an increasing quantity of brownish medium gray clayey matrix. Reed remains prevail over clayey components and are arranged in horizontal layers. Very strong smell.
	S6	100 – 110	*Grayish-brown fibrous clayey peat*, very compact. The clayey component increases up to 50%. Reed remains are arranged in horizontal layers. Very strong smell.
	S8	110 – 145	*Light blue-grayish clay*, very compact with spread remains of dark brown-blackish roots and brownish green reeds. Strong smell.
		145 – 200	*Gray silty medium sand* with a lot of mica. Rare vegetal remains. No smell.

the study area started to be reclaimed except for the southern part of Valle Cordenazzo in the west as well as the southern part of Valle Zenare in the east.

In 1931 (map I.G.M. - Brenta (F°. 65; IV SE), scale 1:25000) only the northern part of Valle Cordenazzo was still wet.

In 1967 (map I.G.M. - Civè (F°. 65; IV SE), scale 1:25000) the overall study area has been reclaimed.

Interview to some local people has revealed that, farmers had to ameliorate a few areas of the basin for agricultural use due to acidity and salinity of soil even if no trace of salty environment was found by experimental studies. Up to the 1980's, they used to spread lime over these areas to reduce the acidity and to flood these fields with fresh water to reduce the salinity. They tried to cultivate crops different from corn, such as soybean, but return was not high enough.

5. *Visual Classification.*

A visual *in situ* classification (Muskeg Engineering Handbook, 1969) is fundamental to describe the peat state because some characteristics, i.e., the colour, can change rapidly on exposure to air as result of oxidation; within an hour the peat is coloured with a uniform dark brown or black.

Very high quality samples have been accurately collected for laboratory tests without disturbing the soil structure or changing the moisture content. The samples have been taken horizontally to avoid sediment compression and have been kept in a humidity and temperature controlled room.

To a visual analyses (Tab. 2), G1 sample structure appears amorphous granular and G2 structure appears fibrous. This is confirmed by the scanning electron microscope observation. The highly humified fibres have been totally reduced by agricultural machines.

While G1 contains just rare few millimetres fibres represented by little roots, G2 consists almost exclusively of reeds in growing position. Because of the nature of the reed stems, the remains are well-preserved and keep the peat very compact.

G1 sample is not too wet to the touch while G2 is.

The colour is black for G1 because of the oxidisation due to agricultural use of the soil. G2 sample is generally brown but reeds are greenish yellow because they are less decomposed than the matrix due to their siliceous content.

Due to the presence of H_2S, smell is very slight for G1 and very strong for G2 because anacronyc decomposition is proceeding.

Tab. 2 - Visual classification table.

sample name	**G1 (depth: 22.5-37.5 cm)**	**G2 (depth: 92.5-107.5 cm)**
sample dimension	L = 16 cm; Ø = 15 cm	L = 24.5 cm; Ø = 15 cm
sample direction	horizontal	horizontal
sample quality	Q5	Q5
peat structure	granular position and woody fibres	fibrous with reeds in growing
water content	not too wet	very wet
colour	black freshly exhumed reeds	brown with greenish yellow
smell	very slight	very strong

6. *Geotechnical Classification.*

6.1. *von Post Classification (1922).*

A common classification scheme used in Europe (Tab. 3) is that proposed by von Post (1922) based on a simple squeeze test for assessing the degree of humification on a scale from 1 to 10 (H_1 being the least humified). In addition to humification (H_n), the predominant plant is noted together with wetness (B), fine fibres (F), coarse fibres (R), wood and shrub remnants (V), organic content (N), smell (A), plasticity (P) and pH (Muskeg engineering handbook, 1969).

This is a simple and highly informative system which has the advantage of requiring only close scrutiny of the peat. It attempts to describe peat and its structure in quantitative terms and to provide the means with which to correlate the types of peat with their physical, chemical, and structural properties.

Another classification system "Treatment of Organic Soils in the U.S.D.A. 7th Approximation Soil Classification" is used to complete the von Post classification.

The botanical composition represents the principal vegetal component. It is not possible to identify it for the G1 sample because it is macroscopically invisible. G2 sample peat appears to consist mainly of the com-

mon reeds, Phragmites (symbol: Ph), a plant which is tolerant of brackish conditions (Hobbs, 1986). It is 1-4 m tall and it grows in up to 2 m deep water. It usually forms a densely packed closed reed swamp community. By preventing water circulation the clay and silt deposition is encouraged; the rich mineral nutrients and concomitant breakdown and humification of the newly dead plant detrital fragments produce a luxuriant emergent growth. Reeds are well preserved and in growing position because they are not oxidized and acid conditions have prevented the production of detrital mud. The basal reed peat is, however, more divided and reeds are in a horizontal position.

The degree of humification relates to the degree of biochemical decomposition of original plant components. This is a visual/manual method: a representative sample is picked by hand and squeezed firmly. A considerable difference appears between G1 and G2 samples with respect to the degree of humification: the highest grade (H_{10}) is evident for the first sample composed of little oxidized detrital fragments, while a very low grade (H_3) is present for the second sample composed of well preserved non-oxidized fibres. The G2 sample presents an H_3 degree as a general property but an H_2 degree is attributable to stronger parts of the reeds like stems.

For the "Treatment of Organic Soils in the U.S.D.A. 7th Approximation Soil Classification" the G1 sample represents a Histosol (organic soil) as order and Saprist (humification about H_9 to H_{10}) as sub-order; G2 represents a Histosol as order and Fibrist (humification about H_1 to H_5) as sub-order.

The water content of peat is estimated on a scale from 1 (dry) to 5 (very high, greater than 2000%), designated B_1 to B_5. It was calculated using ASTM Designation D 2974-87 test method: "Standard Test Methods for Moisture of Peat and Other Organic Soils". G1 sample presents a moisture content of 95% identified as B_2 degree ($w<500\%$) and G2 sample presents 629% that corresponds to B_3 degree ($500\% < w<1000\%$).

Fine fibres are defined as less than 1 mm long. The content is graded on a scale from 0 to 3. G1 sample has a low visible content of fine fibre (F_1) while G2 has a moderate content (F_2). Coarse fibres are defined as more than 1 mm long. The content is graded on a scale from 0 to 3. G1 sample presents only visible fine fibers and no coarse ones (R_0); G2 total fiber content is mostly constituted by coarse fibres (R_3: high content).

Macroscopic wood content is graded on a scale from 0 to 3. G1 sample does not present it (W_0: no content), while G2 has a moderate con-

tent (W_2) if we consider reed stems as "woody" because of their strong siliceous composition.

Organic matter content (Andreiko et al., 1983) is calculated by subtracting percent ash content from one hundred determined by ASTM Designation D 2974-87 test method: "Standard Test Methods for Ash of Peat and Other Organic Soils" (Annual book of ASTM standards, 1996). G1 sample presents a 49% of organic matter; it corresponds to the N_2 class (40 %< N<60%). For G2 the organic content is 73% that corresponds to N_3 (60 %< N<80%). The smell, which is an indication of fermentation under anaerobic conditions, is graded on a scale from 0 to 3 in the von Post classification. It is very slight (A_1) for G1 and very strong (A_3) for the G2 sample. This is due to the differing degree of decomposition of the two peaty samples.

Regarding the plasticity index, if it is impossible to determine its value the sample is classified as P_0, if it is possible it is P_1. The Zennare Basin peats are classified as P_1.

The pH is evalueted by using ASTM Designation 2976-71: "Standard Test Method for pH of Peat Materials". G1 and G2 samples have the same pH=5 that in the von Post classification corresponds to index pHL. This acid reaction can be caused by the presence of carbon dioxide and humic acid arising from peat decay.

6.2. *ASTM Classification (1992): Standard Classification of Peat Samples by Laboratory Testing.*

ASTM classification (Tab. 4) is under the jurisdiction of the American Society for Testing and Materials Committee and has been approved by agencies of the American Department of Defence (Annual book of ASTM standards, 1996).

Comments regarding moisture, ash, organic matter content, degree of humification and pH are in the von Post classification paragraph.

Fiber content is determined using the standard test method D 1997-91 that covers the laboratory determination of the fiber content of peaty samples by dry mass. The description of the term "fiber" used in this method is fundamental: *a fragment or a piece of plant tissue that retains a recognisable cellular structure and is large enough to be retained on a 100-mesh sieve (openings 150 μm). Plant materials larger than 20 mm in smallest dimension are not considered fibers.*

G1 sample has a fiber content of 44 % and it is classified as hemic

Tab. 3 - von Post classification table.

sample name	**G1 (depth: 22.5-37.5 cm)**	**G2 (depth: 92.5-107.5 cm)**
botanical composition	---	Ph (Phragmites australis)
H: degree of humification or decomposition *	H_{10}: completely de-composed peat containing no discernible plant tissues. When squeezed, all of the peat releases through the fingers as a uniform dark paste.	H_3: Slightly decomposed peat that when squeezed, releases turbid brown water, but in which no amorphous peat passes between the fingers. Plant remains are still relatively intact. H_2 (for stronger part of reeds): almost completely undecomposed peat that, when squeezed, releases yellowish water. Plant remains are still relatively intact. No amorphous material present.
B: moisture content *	B_2: w<500%	B_3: 500%<w<1000%
F: fine fibres content (Ø <1 mm)	F_1: low content	F_2: moderate content
R: coarse fibres content (Ø >1 mm)	R_0: no content	R_3: high content
W: woody fibres content	W_0: no content	W_2: moderate content
N: organic matter content *	N_2: 40%<N<60%	N_3: 60%<N<80%
A: smell	A_1: very slight	A_3: very strong
P: plasticity	P_1: it's possible to determi-nate the plastic limit test	P_1: it's possible to deter-minate the plastic limit test
pH *	pH_L: pH<7	pH_L: pH<7

(fiber content between 33% and 67%). G2 sample results in a fiber content of 30% and it is classified as sapric (fiber content < 33%). Therefore, due to the definition of "fiber", G2 appears to be less fibrous than G1 only because it is composed almost exclusively by more than 2 mm long and wide coarse fibers (Gatti, 1997).

*determined by ASTM test.

Tab. 4 – ASTM classification table for the peat samples collected in the Zennare Basin.

sample	**G1 (depth: 22.5-37.5 cm)**	**G2 (depth: 92.5-107.5 cm)**
moisture content (85°C) (standard test method: D 2974-87)	95%	629%
ash content (440°C) (standard test method: D 2974-87)	51%	27%
organic matter content (440°C) (standard test method: D 2974-87)	49%	73%
fibre content (150 _m<fibre<20 mm) (standard test method: D 1997-91)	44% *(Hemic)	30% **(Sapric)
degree of humification (standard test method: D 5715-95)	H10	H3
pH (standard test method: D 2976-71)	5	5

7. *Geotechnical characteristics of peat of the experimental site within the Zennare Basin.*

The peat bulk density (Tab. 5) is very low. It is related to the organic content and influenced by the degree of saturation or gas content emitted by the humification process. Peats are generally under-saturated and are buoyant under water due to the presence of gas. G1 sample presents a bulk density (mass of oven dry soil per unit volume) equal to 0.302 g/cm^3 while G2 sample has a bulk density equal to 0.253 g/cm^3 due to its larger organic content and its decomposition in act (Landva, 1983).

* in the G1 sample there is no fibres >2mm.
** almost 70 % of the G2 sample is composed by fibres >2mm.

Water content of fibrous peat is almost five times higher than that of the amorphous peat, while the organic content is almost double. In general, the greater the organic content the greater the water content. The difference, however, is also due to the higher degree of decomposition of amorphous peat with respect to the fibrous peat. In fact, fibrous peat (low humification) has a higher total water content than the granular-amorphous peat (high humification). The amount of intracellular water generally exceeds the interparticle water in fibrous peat and the proportion declines with the increase in humification as the cellular structure is destroyed (Landva and Pheeney, 1980). The organic content has a considerable effect on the physical and mechanical properties of peat. In general, the greater the organic content the greater the void ratio and the compressibility of the peat.

The specific gravity of the solids (ratio between specific weight of solids and specific weight of water) in peat is usually between 1.1 and 2.5 but more frequently between 1.4 and 1.6. It is measured by using Kerosene with a known specific gravity. G1 specific gravity is 1.670 for G1 and 1.449 for G2, due to the higher fibre content of this latter.

Peat fibrous nature makes the consistency of limits test difficult. They can usually be carried out only if the von Post humification exceeds the H3 degree. It is important to realise that limit measurement requires to destroy not only the fabric and structure sample, as in a clay soil, but partly decomposed fibres are themselves broken down into very fine detritus, each particle being surrounded by a powerful adsorption complex. Consequently, the tested material bears little relation to the material sampled, except in the case of much humified peat, as the G1 sample, in which breakdown has been virtually completed in the mire. The forcible reduction leads to a very high liquid limit for peat in comparison with clay, due to its low specific gravity and high cation exchange; the higher the cation exchange ability, the stronger the adsorption complex and the greater the interparticle adherence. The observed decline in the liquid limit with increased humification is the evidence of the weakening of the adsorption complex, presumably due to the decomposers. G1 sample, which has a high degree of humification, has a resulting liquid limit of 142, almost four times less than the G2 sample liquid limit of 524. Therefore, the fibrous state would be expected to have a higher liquid limit than the amorphous state.

Plasticity index results from the difference between liquid limit and plasticity limit. It is 41 for sample G1 and 161 for sample G2. The numerical value of the plastic limit, however, appears to be of little interest as no corre-

lation has so far been found between the plasticity index and other properties. This is presumably because the plastic limit is associated with strength, a property that can be highly erratic in peat that is highly frictional.

Tab. 5 - Geotechnical characteristics of the Zennare Basin peat.

sample	depth cm	γ g/cm^3	w %	O_C %	G_S	LL %	PL %	PI 150 to 20 mm, %	pH	fibres from	fibres >20mm %
G1	22.5-37.5	0.302	95	49	1.670	142	101	41	5	44	0
G2	92.5-107.5	0.253	629	73	1.449	524	363	161	5	30	≈70

TABLE LEGEND
γ: Bulk Density
w: Moisture Content
O_C: Organic Matter Content
G_S: Specific Gravity of Soil Solids
LL: Liquid Limit
LP: Plasticity Limit
PI: Plasticity Index

8. *Analyses of peat using ESEM.*

ESEM (Environmental Scanning Electron Microscope) is a new type of scanning electron microscope, which allows the examination of specimens in the presence of gases without preparation. As a result, it is possible to identify vegetal structures which would be stressed by sample drying (Cohen, 1983). This is fundamental to a detailed examination of the fabric and structure of peat which is characterized principally by water content and porosity (presence of voids).

While ESEM identifies morphology of crystals and vegetal structures an EDX (Energy Dispersive X-ray) system is useful to recognize the mineral composition.

Tab. 6 – Description of samples used for ESEM analyses.

Depth, cm	Stratigraphy description	Sample
0-50	Amorphous granular peat	S2, 29-30 cm
50-100	Fibrous peat	S5, 83-84cm
100-110	Fibrous clayey peat	S6, 107-108 cm
110-120	Light blue grayish clay	S8, 119-120 cm

These systems have been used to analyze four samples (S2, S5, S6, and S8) selected as representative of the four layers, which characterize the first 120 cm-stratigraphy of the experimental site in the Zennare Basin (Tab. 6).

Figure 2 shows the results of ESEM analyses.

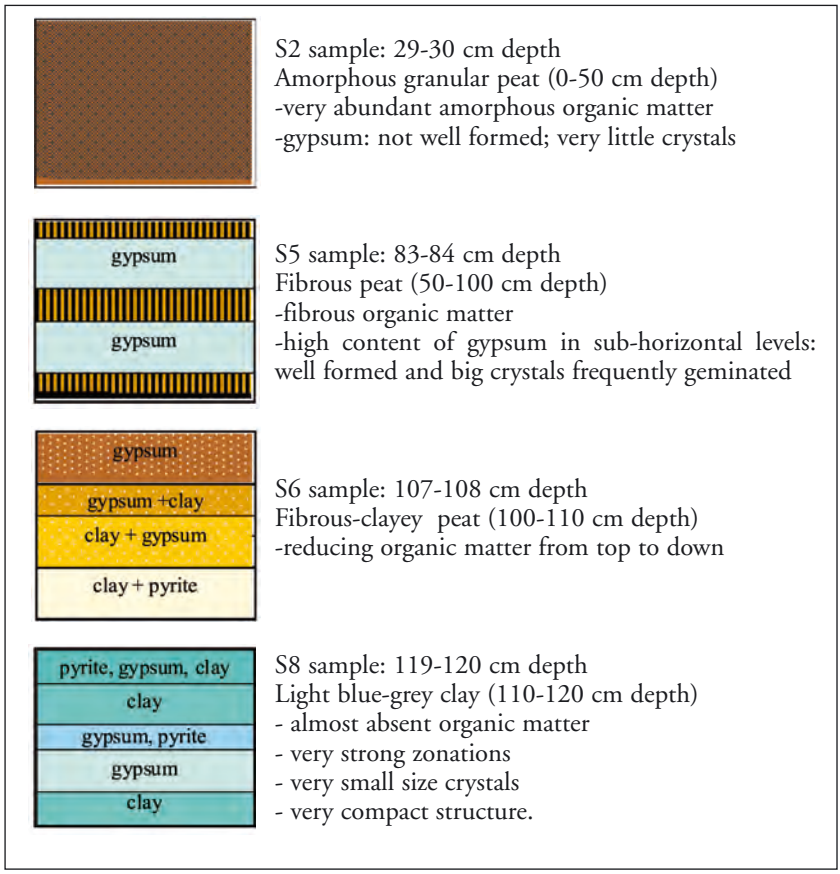

Fig. 2 – Mineral zonation of the four samples analyzed by ESEM.

The ploughed peat is very homogeneous and has a compact structure with pores smaller than the other peat levels due to lower decomposition gas content. The underlying peat level presents a strong zonation concerning the presence, size and shape of gypsum (Fig. 3).

The graph in figure 4 shows the general trend of main elements analyzed by he ESEM. The gypsum trend follows that of the organic matter while clay minerals and pyrite have an opposite behavior. The high gypsum content is probably due to the agricultural practice to spread lime on the fields to diminish the acidity of the soil in act until 1980's.

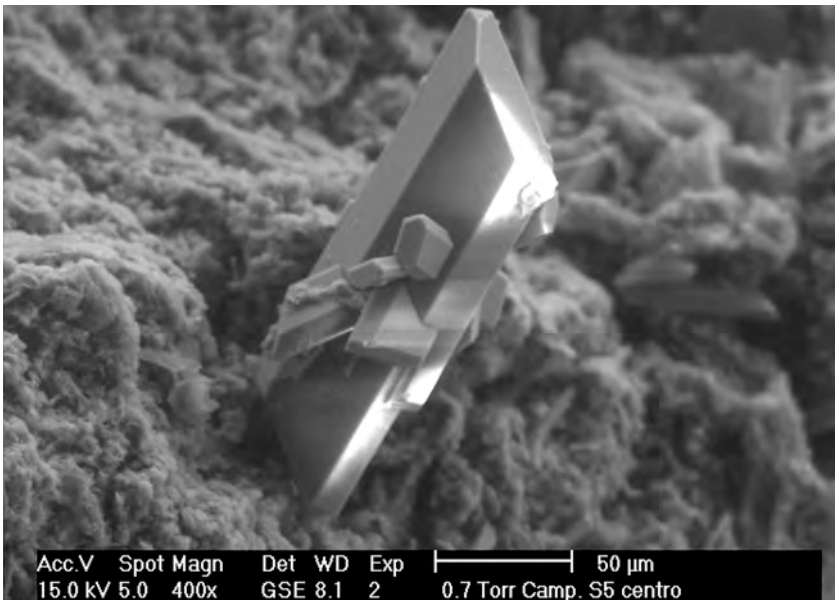

Fig. 3 – ESEM image of gypsum from S5 sample.

Figure 5 shows the results of some chemical analyses regarding the presence of sulphate, sulphide and total sulphur. Their trends are very similar: the content is very high in the fibrous peat level where there is a high gypsum content too.

9. *Conclusion.*

The peat deposit in the Zennare Basin can be divided into two levels (here referred to as top and bottom layers) based on their texture. The limit between them is defined by the depth to which the plough furrows (40-50 cm deep).

The top level consists of decomposed, oxidized homogeneous amorphous granular peat. It has lower liquid limit and water content and

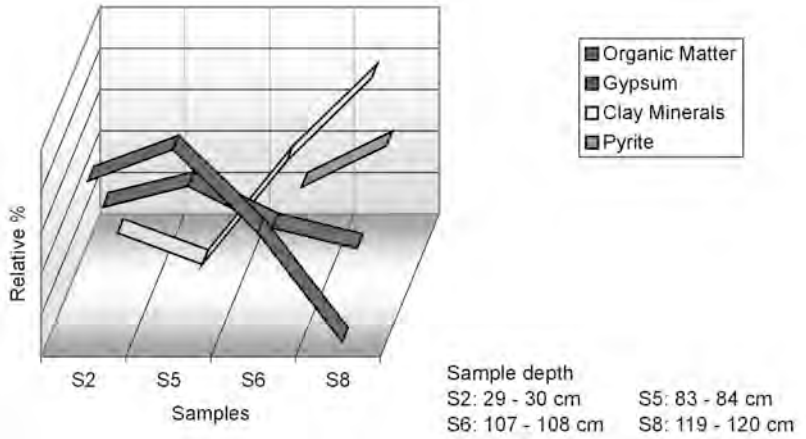

Fig. 4 - General trend of main ESEM analyzed elements from S2, S5, S6, S8 samples.

higher bulk density than the underlying peat level lying below it due to lower organic content. The top level has a higher specific gravity due to lower fiber content. The chemical analyses show that the top peat unit is characterized by a rich phosphorous content with elements suitable for agricultural practices, and the ESEM observation does not show any zonation. Moreover the structure appears more compact and with smal-

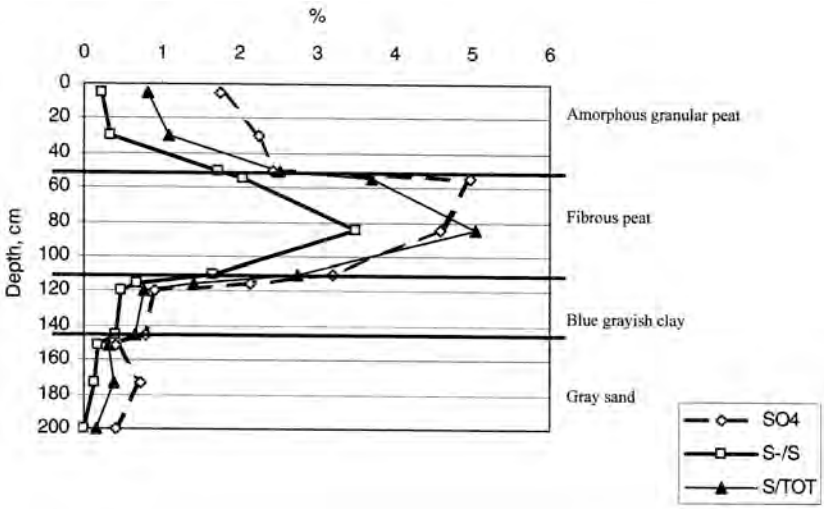

Fig. 5 - Sulphate, Sulphide and total sulphur content versus depth.

ler pores than that of the other level due to a lower content of decomposition gas.

The bottom level, which is not ploughed, is constituted by generally slightly decomposed fibrous peat with the presence of several almost completely undecomposed reed remains. It is very rich in sulphur because it is still decomposing. It has a very low bulk density because of the gas content emitted by the humification process in act. Fibers are still recognizable; the water content and the liquid limit are almost five times higher than the overlying ploughed peat and there is a higher organic content. Furthermore, the high liquid limit depends on the weakening of the adsorption complex due to the decomposition. The high water content occurs because the level is below the water table and because it contains a considerable amount of intracellular water inside the undecomposed fibers.

The bright colours and high content of undecomposed organic matter indicates that this level is poorly oxidized. ESEM observations show that the bottom level is well zoned with the presence of big crystals of gypsum, because the mineral growth is not disturbed. Porosity is very high and fibers are easily recognizable.

Acknowledgement.

This work was carried out with the financial support of Co.Ri.La. in the framework of Co.Ri.La. Project – Targeted Subproject 3.1.

We thank Dr. Biol. Francesco Scarton of SELC, Mestre, Venezia for information concerning the plant classification and habitat.

We thank Dr. Geol. Francesco Benincasa for historical information.

We thank Mr. Gianni Marocco, Mr. Giuseppe Paganini and Mr. Gobbo for the assistance during the field work and information on the past and present agricultural practices.

References.

Andreiko M.J., et al., 1983. Comparison of ashing techniques for determination of the inorganic content of peats. In: Testing of Peats and Organic Soils, ASTM STP 820, P.M. Jarret (Ed.) American Society for Testing and Materials, 5-20.

Annual book of ASTM standards, 1996, Section 4, vol.04.08 Soil and Rock (I).

- Standard Classification of peat samples by laboratory testing. D 4427-92, 634-635.
- Standard Test Method for laboratory determination of the fibre content of peat samples by dry mass. D 1997-91, 163-164.
- Standard test method for pH of peat materials. D 2976-71 (Reapproved 1990), 283-284.
- Standard test method for moisture, ash, and organic matter of peat and other organic soils. D 2974-87 (Reapproved 1995), 280-281.

Benincasa F., 2001. Esame della cartografia storica della parte meridionale della provincia di Venezia compresa tra Civè e il Canale dei Cuori. Evoluzione storica dei terreni appartenenti all'azienda agricola Gallimberti (Chioggia, Venezia). Provincia di Venezia.

Cohen A.D., 1983. Obtaining more precise descriptions of peats by use of oriented microtone sections. Testing of Peats and Organic Soils.

Favero V., Serandrei Barbero R., 1978. La sedimentazione olocenica nella piana costiera tra Brenta e Adige. Mem. Soc. Geol. It., 19, 337-343, 2 ff.

Gatti P., 1997. Torba di Loreo. Studio sperimentale. M.Sc. Thesis, University of Padova, Italy.

Hobbes N.B., 1986. Mire morphology and the properties and behavior of some British and foreign peats. Quarterly Journal of Engineering Geology 19, 7-80.

Landva A.O., Pheeney P.E., 1980. Peat fabric and structure. Canadian Geotechnical Journal, 3, 416-435.

Landva A.O. et al., 1983. Geotechnical classification of peats and organic soils. In: Testing of Peats and Organic Soils, ASTM STP 820, P.M. Jarret (Ed.), American Society for Testing and Materials, 37-51.

Muskeg Engineering Handbook 1969. Muskeg Subcommittee at NRC Associate Committee on Geotechnical Research, I.C. Mac Farlane, Ed., University of Toronto Press.

RESEARCH LINE 3.2.
Hydrodynamics and morphology

SUSPENDED SEDIMENTS CONCENTRATION IN THE SHOALS OF A TIDAL LAGOON

L. Dal Monte and G. Di Silvio
Dipartimento di Ingegneria Idraulica, Marittima, Ambientale e Geotecnica, Università di Padova

Abstract.

In this research we derive an expression for the "representative concentration" of suspended sediments in the shoals, affected by the interaction between the most relevant hydrodynamic and morphodynamic mechanisms at work in a lagoon. "The representative concentration" in a location of the lagoon is defined as the long-term averaged value of the instantaneous concentration.

The instantaneous concentration is computed with a monomial transport formula (Engelund and Hansen type) where the bottom velocity is proportional to the height of significant wave. Using a monomial expression that approximates the Bretschneider formula, the height of the significant wave is related to the length of the fetch and the wind velocity. By introducing some approximations of the usual formulas and some hypothesis on the statistical distribution of the wind and of the fetch, an expression is obtained for the local concentration averaged over the year and over the wind directions.

The equilibrium conditions should lead to an almost uniform distribution of the suspended sediments concentration over the lagoonal basin. This circumstance suggests new areas of future work based on the correlation between morphometric characteristics of the shoals and the marshes of a tidal lagoon.

1. *Introduction.*

The concept of a representative concentration of suspended sediments in a lagoon has been utilized by the researchers for developing more or less detailed long-term morphological model. Although any "concentration model" is necessarily based on a number of empirical assumptions, these should retain their physical meaning.

Because of the different importance of the physical agents in the lagoonal basin, a distinction has to be made on the different components of the sediments concentration in the various compartments. In particular, the concentration in the sea depends on the material picked up from the littoral bottom by the sea waves and transported by tidal and littoral currents. In the channels sediment stirring is due to the tidal currents and, according to the usual transport equations (Engelund and Hansen, Ackers and White), concentration increases with the n-th power (n=4-6) of the flow velocity. Thus the channel concentration is directly proportional to the n-th power of the tidal prism and inversely proportional to the n-th power of the channel cross-section. In the shallows, by contrast, tidal currents are generally weak and sediment stirring is almost exclusively produced during the storms by the alternate wave action near to the bottom. In this case, according to the same formulae, concentration increases with the local wave height and is just inversely proportional to the shoal depth. The wave height in its turn depends on the wind velocity and the length of effective fetch.

The sediments in the shoals are subject to both the tidal currents and the wave action. The former ones exchange the material between the channels and the shoals, the latter causes the re-suspension of the material. Moreover, the marshes tend to capture the sediments transported by the tidal currents. Finally, the interaction between marshes and shoals depends on the number of the shoals in the basin which also influences the length of effective fetch. In conclusion, the "representative concentration" in the system are controlled by the lagoon's morphology and climate.

Our research work is based on the analysis of the duration curve of wind records measured in Lido Airport (in the period 1951-1977) and on the planimetric and batimetric data collected in 1990 in the lagoon of Venice. As in equilibrium conditions time- and space-averaged concentration of suspended sediments in channels and shoals should also be uniform, we expect that this would reflect in a relationship between the morphometric characteristics of the system.

2. *Instantaneous concentration in the shoals.*

Let us consider a monomial transport formula (Engelund and Hansen type) and let us call qs the instantaneous volumetric discharge of sediments per unit width produced by the wave and v the water velocity near the bottom.

One finds:

$$q_s \propto v^n \qquad n \cong 5 \div 6 \tag{1}$$

The velocity near the bottom v in shallow water can be expressed as:

$$v = \frac{1}{2}\sqrt{\frac{g}{h}} H_w \tag{2}$$

and the average transport instantaneous concentration in the water column as:

$$c = \frac{q_s}{q} \propto \frac{v^n}{v\,h} = k \frac{H_w^{n-1}}{h^{\left(\frac{n-1}{2}+1\right)}} \tag{3}$$

where q is the instantaneous water discharge per unit width, h the local depth and H_w the height of the significant wave. The coefficient k depends in principle on the local grainsize distribution of the bottom and, possibly, on the bottom protection by vegetation, but it can roughly be assumed as a constant for a given lagoon.

The significant height H_w of the wave produced by the wind in shallow water can be computed by the formula of Bretschneider:

$$\frac{H_w g}{u_A^2} = 0.283\, tgh\left[0.53\left(\frac{gh_s}{u_A^2}\right)^{3/4}\right] tgh\left\{\frac{0.00565\left(\frac{gF_e}{u_A^2}\right)^{1/2}}{tgh\left[0.53\left(\frac{gh_s}{u_A^2}\right)^{3/4}\right]}\right\} \tag{4}$$

where u_A is the wind velocity, h_s the uniform water depth along the fetch and F_e the fetch length.

We want to approximate eq.(4) with a monomial formula of the type:

$$H_w = k_1 \cdot F_e^{\alpha} \cdot h_s^{\beta} \cdot u_A^{\gamma} \tag{5}$$

Although the exponents α, β, γ and the coefficient k_1 depend in general on the local conditions, they are reasonably constant within a limited

range of F_e, h_s and u_A (F_e=1000÷5000 m, h_s=0.5÷2.0 m, u_A=15÷25 m/s).

By a comparison between the Bretschneider formula (eq. 4) and the monomial approximation (eq.5), we find the following acceptable values:

$$\alpha=0.32 \qquad \beta=0.50 \qquad \gamma=1.45 \qquad k_1=3.2\ 10^{-3} \tag{6}$$

The vertically averaged concentration in the water column produced by a wind having a sufficient duration can be approximately computed by combining eqs.(3) and (5).

With the values (eq. 6) n=5, α=1/3, β=1/2 and γ=3/2, one finds:

$$c = k\ \frac{h_s^2\ F_e^{4/3}\ u_A^6}{h^3} \tag{7}$$

For a given location in the lagoon, the quantities h_s and F_e depend on the wind direction α, while the wind velocity depends on both α and t. Eq.(7) holds if the wave does not break, i.e. if the wave height provided by eq.(5) is less than about 0.78 h.

3. *Annually averaged magnitude of the wind for a given direction.*

The duration curve of the wind's intensity and direction can be expressed as:

$$u_A(\alpha,t) \cong u_{A0}(\alpha) e^{-\gamma(\alpha)\frac{t}{\Delta T_a}} \tag{8}$$

where $u_{A0}(\alpha)$ is the annual maximum velocity of the wind in the direction α; t is the duration of the wind blowing in the sector ($\alpha\pm\Delta\alpha/2$) with a velocity larger than u_A; ΔT_a is the total duration of the wind blowing in the sector ($\alpha\pm\Delta\alpha$); $\gamma(\alpha)$ is an "index of wind variability".

The "index of dominance" for a given angle α is defined as the density of duration ($dT_a/d\alpha$), scaled to the ratio ($T_a/2\pi$):

$$r(\alpha) = \frac{dT_a}{d\alpha}\frac{2\pi}{T_a} = \frac{\Delta T_a}{\Delta\alpha}\frac{2\pi}{T_a} \tag{9}$$

Both indexes $\gamma(\alpha)$ and $r(\alpha)$ can be obtained from the measured duration curves of the wind.

From eq.(8) one can write:

$$\ln\frac{u_A(\alpha,t)}{u_{A0}(\alpha)} = -\gamma(\alpha)\frac{t}{\Delta T_a} \tag{10}$$

In figure 1, for instance, it is plotted the straight line (eq. 10) that interpolates the wind velocities within the sector (30°±5°), recorded at the Lido Airport in Venice. Eq. (10) provides the values of $u_{A0}(\alpha) = 14.8$ *m/s*, while the index of dominance $r(\alpha)$ is directly provided by the wind records (for α=30° it is $r(\alpha)$=2.86).

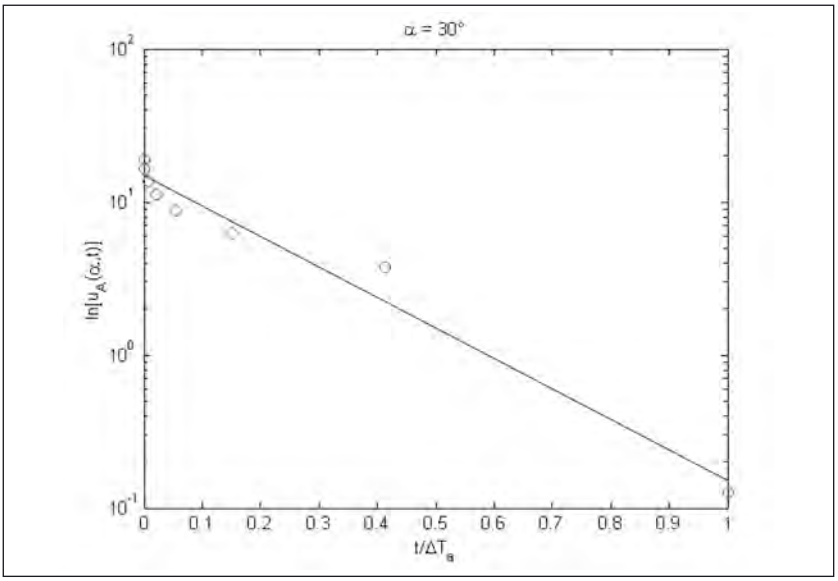

Fig. 1- Straight line (eq. 10) that interpolates the wind velocities within the sector (30°±5°).

Note that when the $r(\alpha)=const=1$, the wind prevails uniformly all over the directions. In any case the average value of $r(\alpha)$

$$\bar{r} = \int_0^{2\pi} \frac{r(\alpha)}{2\pi} d\alpha \qquad (11)$$

should be 1. If $r(\alpha) \rightarrow$) for a certain value of α, it should be zero for any other value of α. This is the case of a wind that blows only from a direction.

By contrast, when $r(\alpha) \rightarrow 1$ and $\gamma(\alpha) \rightarrow 0$, the wind blows with a constant intensity $u_A(\alpha)$ from all directions.

In figures 2a, 2b, 2c and 2d, the polar graphs of $\gamma(\alpha)$, $u_{A0}(\alpha)$, $r(\alpha)$ and $W(\alpha)$, are reported for all the wind directions. The quantity $W(\alpha)$ (annually averaged magnitude of the wind blowing in the direction a) represents the overall effect of the wind during the year as far as the con-

centration in the water column is concerned. The value of $W(\alpha)$ is obtained by averaging over the year the expression of $u_A^6(\alpha, t)$ appearing in eq.(7). From eqs.(8) and (9) one finds:

$$W(\alpha) = \frac{1}{T_a}\int_{T_a} u_A^6(\alpha,t)dt = \frac{u_{A0}^6(\alpha)}{6\gamma(\alpha)}\left[1-e^{-\gamma(\alpha)}\right] \cong \frac{u_{A0}^6(\alpha)}{6\gamma(\alpha)} \quad (12)$$

From the figures.2a, 2b, 2c and 2d one can observe that the largest values of $W(\alpha)$ pertain to the North-Eastern winds (called "bora") which are both the most intense (high u_{A0}) and persistent (large $r(\alpha)$).

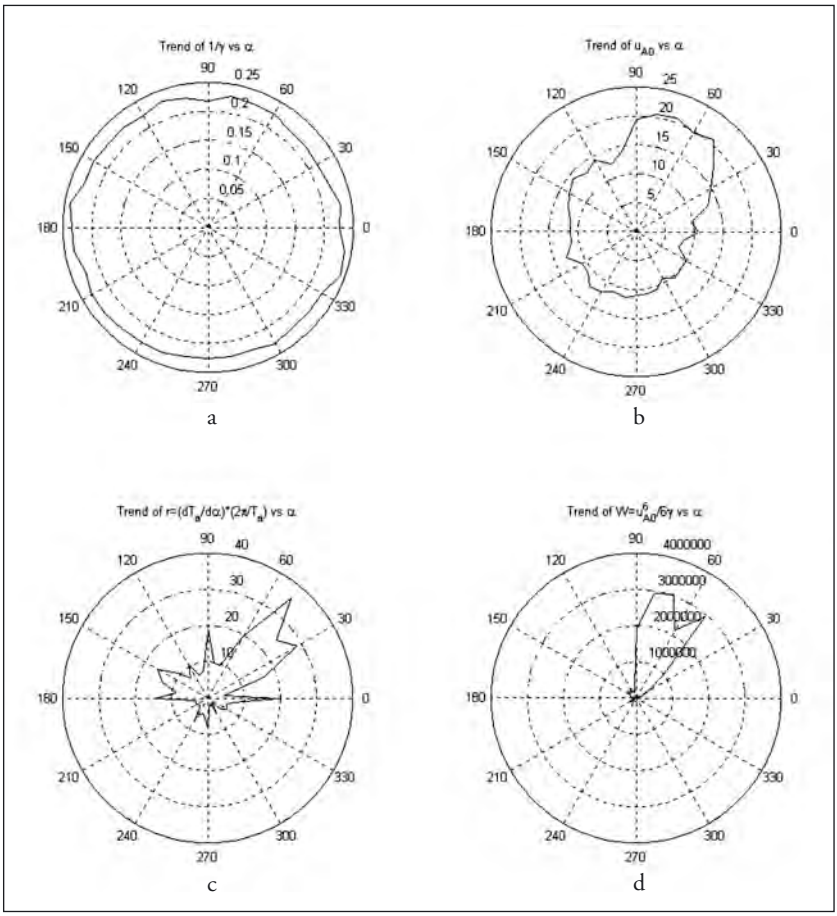

Fig. 2a, 2b, 2c and 2d - Polar graphs of g(a), uA0(a), r(a) and W(a), reported for all the wind directions.

4. *Annually averaged water depth in the shoals and marshes of a lagoon.*

The local water depth *h(t)* in the shoals is variable during the tidal cycle and during the year. If one assumes a linear distribution of the water level around the mean sea level during each tidal cycle and a linear duration curve of the range during the year, one can define for each location of the lagoon the averaged depth

$$h_e(P) = \frac{1}{T}\int_{year} h(t)dt = \frac{1}{4}\frac{a_m}{2}\left(1+\frac{z}{a_m/2}\right)^2 \qquad (13)$$

The value of h_e results to be a function of the local position of the bottom, z, below the mean sea level and of the tidal range a_m.

From eq. (13) one finds different values of h_e depending on the range of variation of z :

$$h_e(P) = z \qquad z \le -\frac{a_m}{2} \qquad (14)$$

$$h_e(P) = \frac{1}{4}\frac{a_m}{2}\left(1+\frac{z}{a_m/2}\right)^2 \qquad -\frac{a_m}{2} \le z \le \frac{a_m}{2} \qquad (15)$$

$$h_e(P) = 0 \qquad z \ge \frac{a_m}{2} \qquad (16)$$

5. *Local instantaneous concentration and annually averaged concentration.*

Let us consider the average transport instantaneous concentration in the water column (eq. 7).

By putting:

$$k_h(P,\alpha) = \frac{h_s(P,\alpha)}{h_e(P)} \qquad (17)$$

one obtains local instantaneous concentration:

$$c(P,\alpha,t) = k\frac{\left(k_1^4 k_h^2(P,\alpha)\cdot F_e^{4/3}(\alpha)\cdot u_A^6(\alpha,t)\right)}{h_e(P)} \qquad (18)$$

For a given location P and direction α, eq. (18) holds if the wave develops along the entire length of the fetch without breaking. This occurs

when the wave height $H_W(P, \alpha, t)$, given by eq. (5) using the values found for α, β, γ and k_1 (eq. 6), is smaller than 0.78 $h_e(P)$, namely when the wind velocity is not too large:

$$u_A^{3/2} \le \frac{0.78 \cdot h_e^{1/2}(P)}{k_1 \cdot k_h^{1/2}(P,\alpha) \cdot F_e^{1/3}(\alpha)} \tag{19}$$

When the wind velocity is larger than expressed by eq. (19), the wave height progressively increases along the fetch's length and breaks before reaching the location P. Since the shoals are relatively uniform in depth, we may assume that, as the fetch further increases, a continuous breaking ("spilling") takes place in such a way that the wave height remains constant and controlled by the local depth. In this case the local instantaneous concentration is given by eq. (7) where one puts $H_W(P, \alpha, t)=0.78h_e(P)$:

$$c(P,\alpha,t) = k \cdot (0.78)^4 \cdot h_e(P) \tag{20}$$

Eq. (20) holds when the wind velocity is larger than expressed by eq. (19). For a given location P and wind direction α, the duration of breaking conditions is obtained by putting $t=\Delta T_b$ in eq. (19) and in eq. (8). One finds:

$$\frac{\Delta T_b}{\Delta T_a} = \frac{1}{6\gamma(\alpha)} \cdot \ln x_1(P,\alpha) \tag{21}$$

where

$$x_1(P,\alpha) = \frac{k_1 u_{A0}^6(\alpha) \cdot F_e^{4/3}(\alpha) \cdot k_h(P,\alpha)}{(0.78)^4 \cdot h_e^2(P)} \tag{22}$$

is a kind of "breaking frequency index" characteristic of a given location and wind direction.

The annually averaged concentration for a certain location $\tilde{c}(P, \alpha)$ is computed with the assumption that wind intensity and tidal oscillation are mutually independent. From eqs. (7) and (8) one finds the following expression:

$$\tilde{c}(P,\alpha) = \frac{1}{T} \int_{year} c(\alpha,t)dt = k \frac{h_s^2(\alpha) F_e^{4/3}(\alpha,t) u_{A0}^6(\alpha,t)}{h_e^3(P)} \tag{23}$$

where $u^6_{A0}(\alpha,t)$ is the wind magnitude given in eq. (12) and $F_e(\alpha,t)$ is the active fetch.

Eq.(23) provides the time-averaged concentration in the water column for a given location, should the wind exclusively blow in the

direction α. The actual annually averaged concentration in this location is given by averaging eq.(23) over all the wind directions (2π), namely

$$C(P) = \int_0^{2\pi} \frac{\tilde{c}(P,\alpha)}{2\pi} d\alpha \tag{24}$$

6. *Active fetch in a given location.*

The active fetch to be put in eq.(23) for computing the concentration can be either the "real" fetch F_e (when no breaking occurs) or the fetch at the breaking point F_b, if breaking takes place. The different value of the duration of time T_b for which P is subject to breaking condition defines different situations. Therefore, the breaking point is characterised by a certain breaking fetch F_b and a duration T_b.

These values can be computed with the hypothesis that continuos breaking (spilling) takes place in the surf zone, in such a way that wave's height (i.e. concentration, if $h_s \cong$cost) remains constant and equal to the wave's height at the breaking point. These two values, F_b and T_b, at the breaking point are found by substituting the two conditions $F_e=F_b$ and in eqs. (5) and (6):

$$F_b^{4/3}(P,\alpha) = \frac{0.78^4 h_e^2(P)}{k_1^4 u_A^6(\alpha) k_h^2} \tag{25}$$

$$T_b(P,\alpha) = \frac{\Delta T_a}{6\gamma} \ln\left[\frac{F_e^{4/3}(P,\alpha) k_1^4 u_A^6(\alpha) k_h^2}{0.78^4 h_e^2(P)}\right] \tag{26}$$

When $\frac{T_b}{\Delta T_a} \geq 0$, with reference to the duration curve, the occasional breaking is defined by the following:

$$F = \begin{cases} F_e(\alpha) & for \quad \frac{T_b}{\Delta T_a} \leq \frac{t}{\Delta T_a} \leq 1 \quad (no\ breaking) \\ F_b(\alpha) & for \quad 0 \leq t \leq \frac{T_b}{\Delta T_a} \qquad (breaking) \end{cases} \tag{27}$$

When $\frac{T_b}{\Delta T_a} \geq 0$, the situation of never breaking occurs. Finally, when there is a permanent breaking.

7. *Concentration as a function of the breaking frequency index.*

The breaking frequency index is given in eq. (22) and depends on the direction a of the wind. Depending on the value of x1(P,a) one can distinguish three different breaking conditions with a certain expression of the concentration:

1. $0 \le x_1 \le 1$ $\qquad c((P,\alpha,t) = k\dfrac{\left(k_1^4 k_h^2(P,\alpha)\cdot F_e^{4/3}(\alpha)\cdot u_A^6(\alpha,t)\right)}{h_e(P)}$

(never breaking)

2. $1 \le x_1 \le e^{6\gamma}$ $\qquad c((P,\alpha,t) = k\dfrac{\left(k_1^4 k_h^2(P,\alpha)\cdot F_e^{4/3}(\alpha)\cdot u_A^6(\alpha,t)\right)}{h_e(P)}$

(occasional breaking)

3. $e^{6\gamma} \le x_1 \le$ $\qquad c(P,\alpha,t) = k\cdot(0.78)^4\cdot h_e(P)$

(permanent breaking)

Occasional breaking is the most interesting breaking condition we can analyse as we know the two different expressions of the concentration in both breaking and no breaking cases. One can evaluate the time averaged concentration in a given location subject to occasional breaking by averaging the instantaneous concentration when breaking and no breaking occur:

$$\tilde{c}(P,\alpha) = \frac{1}{\Delta T_a}\left(\int_0^{T_b} c\,dt + \int_{T_b}^{\Delta T_a} c\,dt\right) = \frac{0.78^4\ k\ h_e(P)}{6\gamma(\alpha)}\{1 + \ln(x_1) \qquad (28)$$

The concentration computed with eq. (28) is referred to a certain location P of the lagoon and a particular direction α of the wind. Moreover, it depends on the breaking frequency index $x_1(P, \alpha)$. For these reasons we choose to analyse $x_1(P, \alpha)$ and its statistical meaning with reference to the statistical distribution of the wind's velocity $u_{A0}(\alpha)$ and the statistics of the effective fetch $F_e(\alpha)$.

Firstly, we simplify eq. (22) introducing a new coefficient X defined as:

$$X = U\cdot F \qquad \begin{cases} U = u_{A0}^6 \\ F = F_e^{4/3} \end{cases} \qquad (29)$$

Our aim is now to analyse the Cumulative Distribution Function of the coefficient *X*:

$$CDF_X(x) = \Pr[X \le x] = \int_{U_{\min}}^{U_{ma}} \Pr[uF \le x \,|\, U = u] pdf_U(u) du = \\ = \int_{U_{\min}}^{U_{ma}} CDF_F(x/u) pdf_U(u) du \tag{30}$$

where $pdf_U(u)$ represents the Probability Density Function of the coefficient *U*. Eq. (30) can be solved only through the statistical analysis of the wind velocity $u_{A0}(\alpha)$ and the length of the fetch $F_e(\alpha)$, both dependent on the direction α.

The probability distribution of the wind velocity can be analysed looking at the data recorded in Lido Airport. We choose the maximum wind velocity $u_{A0}(\alpha)$ characteristic of each sector $\Delta\alpha = 10°$. Figure 3 shows that these velocities can be interpolated with an exponential expression:

$$\frac{u_{A0}}{u_{A0,\min}} = e^{\rho \frac{\beta}{2\pi}} \tag{31}$$

where ρ and β are the statistical characteristics of the wind velocity.

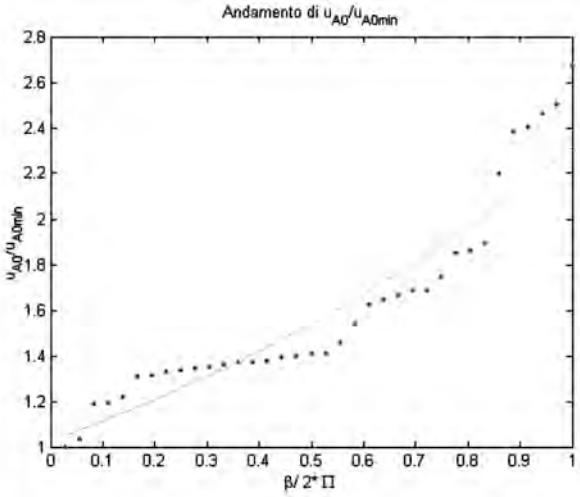

Fig. 3 - Interpolation of the ratio ($u_{A0}/u_{A0,\,min}$) with the exponential equation (31).

From eq. (31) it is now possible to define the Cumulative Distribution Function and Probability Density Function of the wind velocity $u_{A0}(\alpha)$:

$$\begin{cases} CDF_{u_{A0}}(u) = \Pr[u_{A0} \le u] = \dfrac{1}{\rho} \ln\left(\dfrac{u}{u_{A0}}\right) \\ pdf_{u_{A0}}(u) = \dfrac{d}{du} CDF_{u_{A0}}(u) = \dfrac{1}{u\rho} \end{cases} \tag{32}$$

The probability distribution of the fetch can be found only by computing the real values of the effective fetch for every location P of the lagoon and for every direction α.

The evaluation of the effective fetch is based on the analysis of the batimetric data collected in the lagoon of Venice in 1990. For each location P and for each sector $\Delta\alpha = 10°$, a special Matlab program computes the minimum distance between the point P and a point in that sector which is higher than the mean sea level. When the real effective fetches are computed, one can interpolate them with an exponential expression (figure 4):

$$\frac{F_e}{F_{e,\min}} = e^{\varphi \frac{\beta_{Fe}}{2\pi}} \tag{33}$$

where φ and β_{Fe} are the statistical characteristics of the effective fetch.

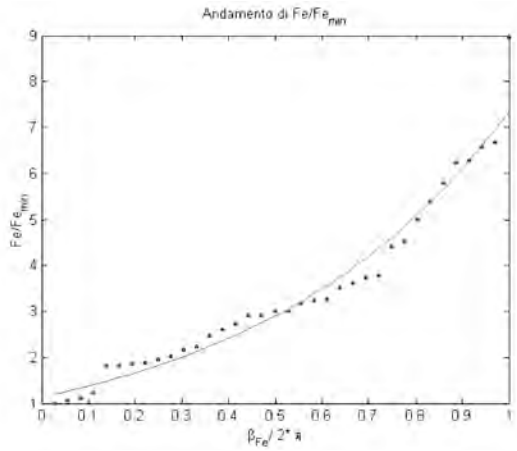

Fig. 4 - Interpolation of the ratio ($F_e / F_{e,\,min}$) with the exponential equation (33).

From this eq. (33) one can find the probability distribution of effective fetch:

$$\begin{cases} CDF_{F_e}(f) = \Pr[F_e \le f] = \dfrac{1}{\varphi}\ln\left(\dfrac{f}{F_{e,\min}}\right) \\ pdf_{F_e}(f) = \dfrac{d}{du}CDF_{F_e}(f) = \dfrac{1}{f\varphi} \end{cases}$$

8 *Conclusions.*

From this study we obtain an expression of the annually averaged concentration in a point of the lagoon P, as a function of the wind direction α, provided by eq. (28).

Eq. (28) shows that this concentration depends on a breaking frequency index $x_1(P, \alpha)$ which variation determines three different breaking conditions. Therefore, the expression of the suspended sediments concentration is based on the statistical distribution of the breaking frequency index.

This is carried on by the introduction of the coefficient X, which depends on the probability distribution of the wind's velocity and the effective fetch:

$$CDF_X(x) = \frac{1}{\rho}\ln\left(\max\left\{x/(U_{\min}F_{\max),1}\right\}\right) + \\ + \frac{\left[\ln\left(\dfrac{x}{\max\{x/F_{\max}, U_{\min}\}F_{\min}}\right)\right]^2 - \left[\ln\left(\dfrac{x}{\min\{x/F_{\min}, U_{\max}\}F_{\min}}\right)\right]^2}{2\rho\varphi} \qquad (33)$$

The solution of eq. (34) depends on a previous definition of the values of the effective fetches over the entire lagoonal basin.

After the computation of the fetch for every point of the lagoon, their statistical distribution can also be related with the morphodynamic characteristics of the basin itself and the presence of shoals nearby.

The actual annually averaged concentration over the lagoonal basin (eq. 24) is given by averaging eq.(28) over all the wind directions (2π). We expect that the results will show that, in equilibrium conditions, this concentration $C(P)$ of suspended sediments in the shoals is almost uni-

form. This could probably affect the relationship between the morphological characteristics of shoals and marshes.

Bibliography.

Di Silvio G., 1989. Modelling for the Morphological Evolution of Tidal Lagoons and their Equilibrium Configuration, *Proc. IAHR, 23rd Congress*, Ottawa, August 21-25, p. C-169.

Di Silvio G., Gambolati G., 1990. Two-dimensional model of the long-term morphological evolution of tidal lagoons, *VIII International Conference on Computational Methods in Water Resources*, Venice, June 11-15.

Di Silvio G., Teatini P., 1992. Conterminazione Lagunare, *Istituto Veneto di Scienza, Lettere ed Arti, VII*, Venezia,

Di Silvio G., Padovan A., 1998. Interaction between marshes, channels and shoals in a tidal lagoon investigated by a 2-D morphological model, *3rd International Conference on Hydroscience and Engineering*, Cottbus / Berlin, Germany, August 31- September 3.

Lapin L.L., 1983. Probability and Statistics for Modern Engineering, *Brooks / Cole Publishing Company*.

Luculano G., 1991. Introduzione alla Probabilità e alla Statistica, *Pitagora Editrice Bologna*.

Van Rjin L. C., 1993. Principle of Sediment Transport in Rivers, Estuaries and Coastal Seas, *Aqua Publications*.

SOME PORE PRESSURE MEASUREMENTS AT THE MARSH OF S. FELICE IN THE VENICE LAGOON

P. Simonini and S. Cola
Dipartimento Ingegneria Idraulica, Marittima, Ambientale e Geotecnica, Università di Padova

Abstract.

This paper presents some preliminary results of a geotechnical investigation concerning the evaluation of soil profile, grain size distribution, porosity and horizontal/vertical permeability along with some verticals in the S. Felice marsh of the Venice lagoon. In addition, some results of in-situ pore pressure measurements in the marsh soils as a consequence of the tidal range are shown and discussed.

1. *Introduction.*

Geotechnical studies on the shallowest soil deposits of the Venice lagoon, up to a few meters below ground level, are relatively unusual. Geotechnical research is usually concerned with the characterisation of deeper soils and is directly related to building foundations and other civil engineering works [e.g. Simonini & Cola, 2000].

However, geotechnical research on the shallowest deposits of wetlands and marshes could be of great interest for the analysis and the modelling of some of the relevant processes occurring in the lagoon, such as the evolution of the stability of the marsh boundaries or the erosion of the channel banks and/or the upper crust of the marsh. To this purpose it is necessary to develop a suitable constitutive model for these soils that would be capable of predicting their drained/undrained response under different conditions.

A new preliminary geotechnical investigation was therefore undertaken as a first-step characterisation of the soils within some marshes in the north-eastern lagoon area. The results of this investigation should act as a guide to plan a second-step study, which would be mostly concerned with the mechanical behaviour of the soils.

The investigation commenced at the S. Felice marsh where a basic classification of soils, together with in-situ and laboratory tests, was performed. In particular, with the specific aim of measuring the hydraulic response of the soils, permeability in both the vertical and the horizontal direction on a small and large scale was measured in the marsh soils. In addition, the pore pressure evolution in the marsh, as a consequence of the tidal range, was also measured. This paper presents and discusses the preliminary results of the investigation carried out so far at the S. Felice marsh.

2. *Brief remarks on the properties of the Venice Lagoon Soils.*

The shallowest deposits, from ground level to depths of a few metres, were formed during the Holocene period, when the lagoon reached the present form as a consequence of the last marine ingression. Marshes and wetlands originated from these soils. From below the Holocenic sediments to depths of 50-60 metres below mean sea level (m.s.l.) deeper formations of the lagoon were formed throughout the last glacial period, the Würm, of the Pleistocene period, when the rivers transported material from the nearby Alpine ice fields.

The main feature of Holocenic and Würmian sediments in the Venice lagoon is the presence of a predominant silt fraction, which is a product of alteration and crushing of original calcareous-siliceous sands. The silt is never pure but always combined with clay and/or sand, forming, apparently without any regular trend in depth and site, a chaotic and erratic interbedding of different sediments.

It is important to point out that the predominance of the silt fraction influences significantly the overall mechanical response of these soils. Even though the soils appear as cohesive materials their behaviour can be generally described, in the range of stresses of engineering interest, in terms of mechanical (i.e. frictional) rather than of electro-chemical (i.e. cohesive) interaction among the soil particles, with the exception of a very few cases of more plastic clays [Cola & Simonini, 2002].

Note also that the above geotechnical characteristics are typical of the sediments in the entire lagoon area and also of the bordering mainland.

3. *Geotechnical investigation at the S. Felice marsh.*

The S. Felice marsh is located, along with the S. Felice channel, in front of the Treporti Village and near the Lido inlet. This is a lagoon area

where the marshes are significantly subjected to most of the typical relevant environmental actions – i.e. tidal flow, wave impact, wind, sedimentation, erosion, evaporation, vegetation influence etc. - effecting a continuous evolution of their morphology.

The geotechnical investigations were concentrated in two test verticals referred to as SF1 and SF2. Undisturbed sampling, using a Shelby sampler, was carried out from ground level to depths of 120 and 90 cm respectively. On the same verticals, preliminary measurements of soil permeability were performed at various depths using a falling head test. In addition some infiltration tests were carried out on the marsh soils as described in the following sections.

3.1. *Soil profile and basic information.*

On the samples taken from the boreholes SF1 and SF2, the grain size distribution, Atterberg limits (LL and LP), natural water content (ω_o), organic content (O_C), specific weight (γ_s), in-situ void ratio (e_o) were determined with the aim of reconstructing profiles of these properties as precisely as possible.

Grain size distribution was evaluated by using both sedimentation analysis and laser light-scattering technique, the latter undertaken at the CNR (National Research Centre) at Pisa. Since this second method requires a much smaller quantity of soil (1g of material each test) it was used tentatively as an alternative tool to carefully analyse the interbedding of lagoon deposits. Some differences were observed between results of the two methods especially when evaluating the diameters of the greatest and smallest particles, but a properly calibrated laser technique would probably be a more suitable method to reconstruct the grain-size distribution at a centimetric scale.

Figures 1 and 2 depict soil profiles and all the basic indexes of the soils at SF1 and SF2. The second column reports relevant information concerning grain size distribution, such as the diameters D_{60}, D_{50} and D_{10}, whereas the third column shows Atterber limits and natural water content. Organic content, together with the in-situ void ratio, are reported in the final columns.

Features to note from Figures 1 and 2 are:

- The predominance of a silty fraction can be clearly appreciated at the two test sites. The percentage of silt always exceeds 55% of the whole grain size distribution, thus confirming the similarity of the nature of these sediments to those typical of the lagoon area at greater depths.

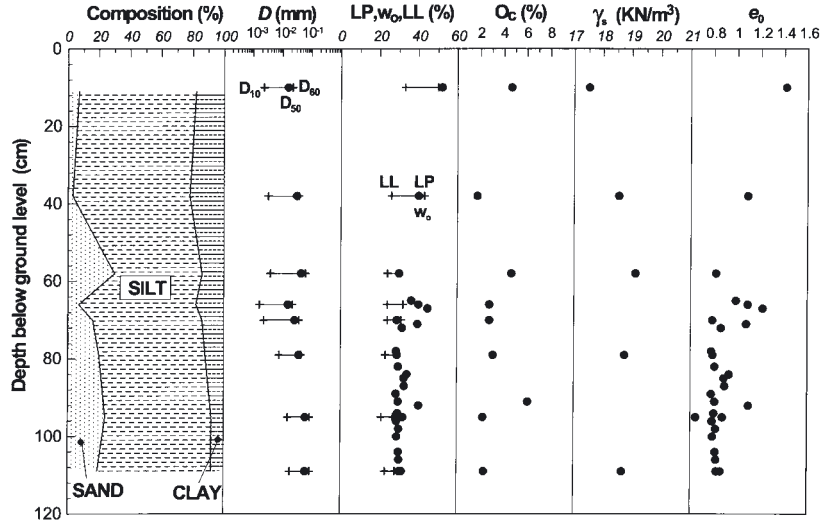

Fig. 1 - Soil profile and basic information at SF1.

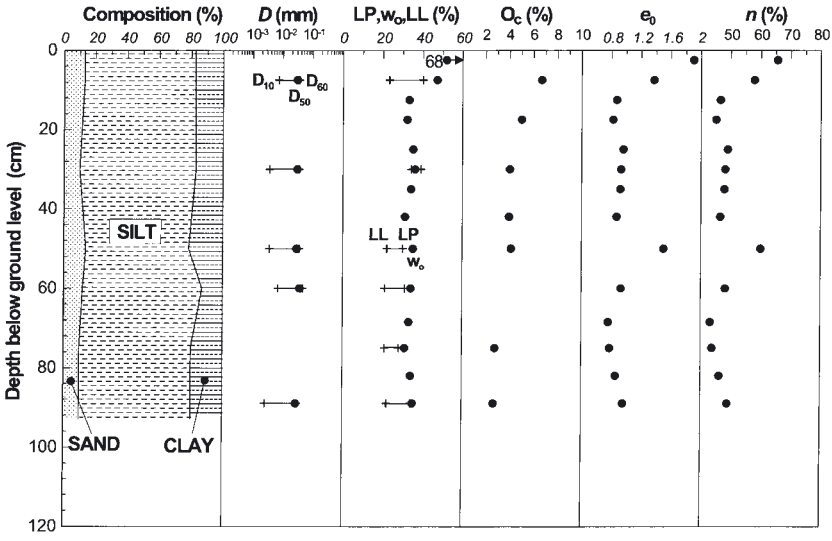

Fig. 2 - Soil profile and basic information at SF2.

Note the presence of a sandy lamination at a depth of 0.6 m at SF1;

- For both sites the Atterberg limits are characterised by average values of the liquid limit LL and plasticity index PI=LL-LP equal to 34 and 9% respectively. These soils can be therefore classified as ML of the USCS classification system and are slightly more silty than other typical lagoon cohesive soils;
- The soils are generally characterised by low activity A=PI/CF (CF = clay fraction = percentage of soil with grain-size less the 0.002 mm): the majority of the samples fall in the range 0.25<A<0.75 and some organic samples just below the ground crust show activity A >0.75;
- The organic content is generally small and increases slightly towards the ground surface, where the mineralisation process is still occurring;
- The in-situ void ratio eo lies in the range between 0.7 and 1.0. Some higher values are determined on samples of the ground crust and on samples with organic inclusions (i.e. at 94 cm at SF1).

3.2. *Soil permeability*

The investigation, carried out with falling head tests both in situ and in the laboratory, was aimed to evaluate the anisotropic permeability tensor, that is

$$\mathbf{k}= \begin{vmatrix} k_h & 0 & 0 \\ 0 & k_h & 0 \\ 0 & 0 & k_v \end{vmatrix}$$

where, k_h and k_v are respectively the horizontal and vertical permeability.

In situ permeability measurements were performed using a standpipe piezometer, provided at the tip with a toroidal porous-stone filter with 20 mm external diameter. The piezometer was first driven down to the selected depth, where the fully saturated soil condition could be hypothesized. The permeability was then calculated by applying the Darcy law to the measurement of water outflow induced by an applied hydraulic head of 1.0 m. Due to the shape of the standpipe and the filter it was presumed that the permeability could be related to a water flow occurring prevalently in horizontal direction.

Laboratory permeability measurements were carried out by using the oedometric cell as the falling head permeameter. The specimens of 20 mm height and 50 mm diameter were trimmed from the original soil core in both the vertical and horizontal direction in order to analyse the hydraulic anisotropy. In this case, much larger hydraulic gradients with respect to those used with the in-situ tests were applied to the soil specimen.

Figure 3 summarizes and compares the results of the above determinations. The site permeability lies approximately in the range of 10^{-8} and $5*10^{-8}$ m/s with some higher values corresponding to the sandy lamination. Laboratory measurements show a slightly higher trend with an anisotropy ratio oscillating between 1 and 21.6. This extremely high value is probably due to some sandy laminations included in the horizontal specimen, which provides less resistance to the induced water flow. Reasonable anisotropic ratios for homogeneous samples are in the range 1-4.

Vertical permeability measurements were also executed using an infiltrometer with diameters ranging from 120 to 292 mm, located in several zones of the marsh. In order to take into account the different vegetation conditions typical zones were selected as a function of the type of vegetation, namely salicornia and limonium. Table 1 present all the measurements carried out to date.

It is interesting to note that the smallest values were measured in a bare zone, characterised by the absence of any vegetation. Much higher values were estimated in green zones, where the presence of roots may probably explain the noticeable speeding up of the vertical seepage.

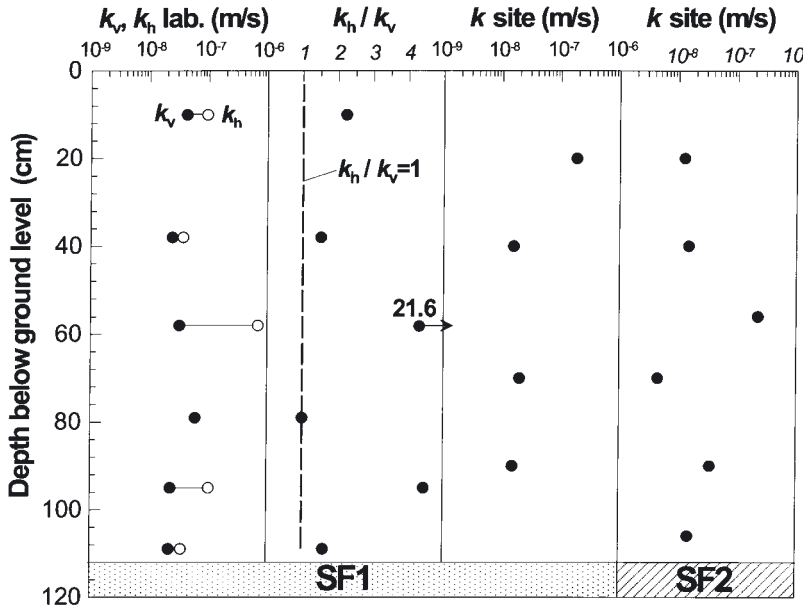

Fig. 3 - Permeability measured at SF1 and SF2.

4. *Pore pressure measurements and undrained soil response.*

Figure 4 sketches a schematic layout of the pore pressure measurement system installed in the S. Felice marsh, near to the SF2 vertical borehole. The pore pressure was monitored on two levels (0.56 m and 1.06 m depth) of each borehole. The verticals were horizontally spaced 3 m from each other and 3 m from the marsh border.

Standpipe piezometers were provided by a special pore pressure transducer equipped with a remote recording system and were powered by batteries. The recording time-step was programmed directly in-situ, using a portable computer and an optical interface. An additional pore pressure transducer measured the tidal range in the nearby channel.

Water pressure oscillations were continuously measured in the four piezometers and in the channel from 7 to 21 March 2002: all the measurements were then referred to the mean marsh level, at +0.30 m above m.s.l. Note that this seasonal period was characterized by small temperature variations and extremely low water evapotranspiration, as a consequence of the absence of any significant sun radiation and vegetation dormancy.

Figure 5 shows the tidal range: the water table in the channel exceeds the marsh surface during the sigize tide, when the ground was completely submerged by a water height of about 15 cm.

Figures 6a, b, and c compare the piezometric level measured at the four points with that in the channel. Several features can be noted:

- Significant damping and delay of the pore water response occurs especially for the decreasing tide;
- Pore pressure is always positive only below depths of about -0.30 m below mean marsh level, even though the tide approaches –0.80 m. Above -0.30 m, the pressure oscillates from positive to negative values;

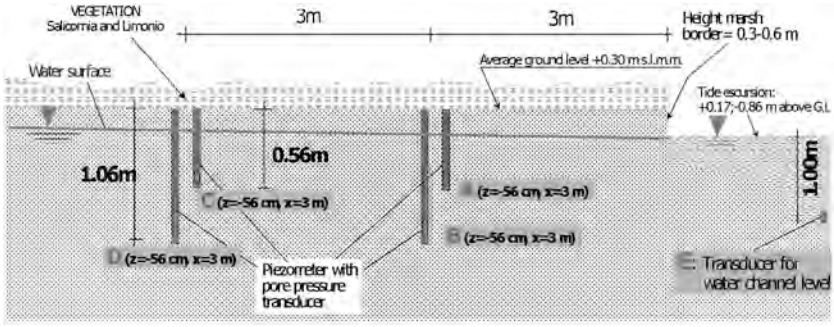

Fig. 4 - Layout of pore pressure measurement system.

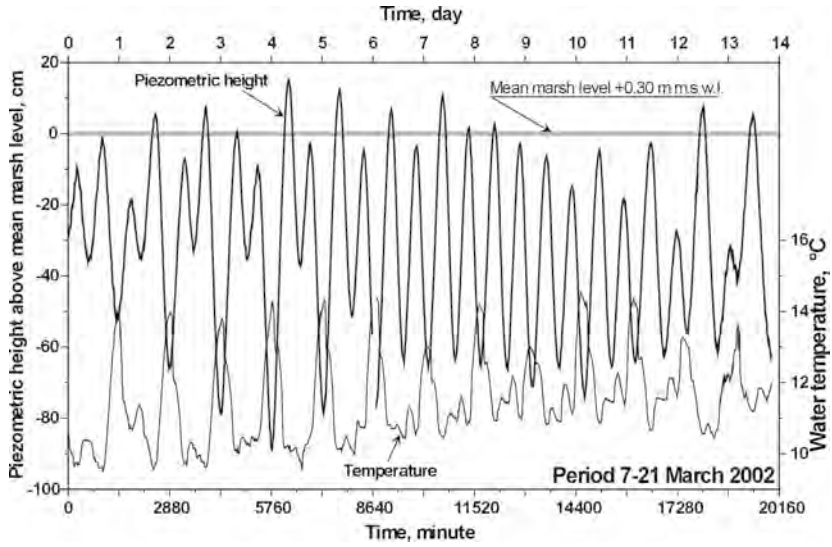

Fig. 5 - Tide level and temperature excursions in the period 7-21 March 2002.

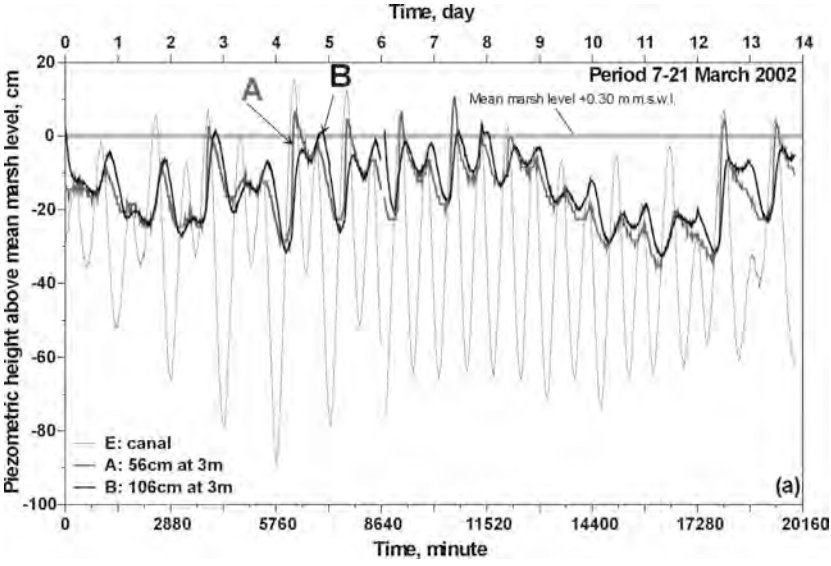

Fig. 6a

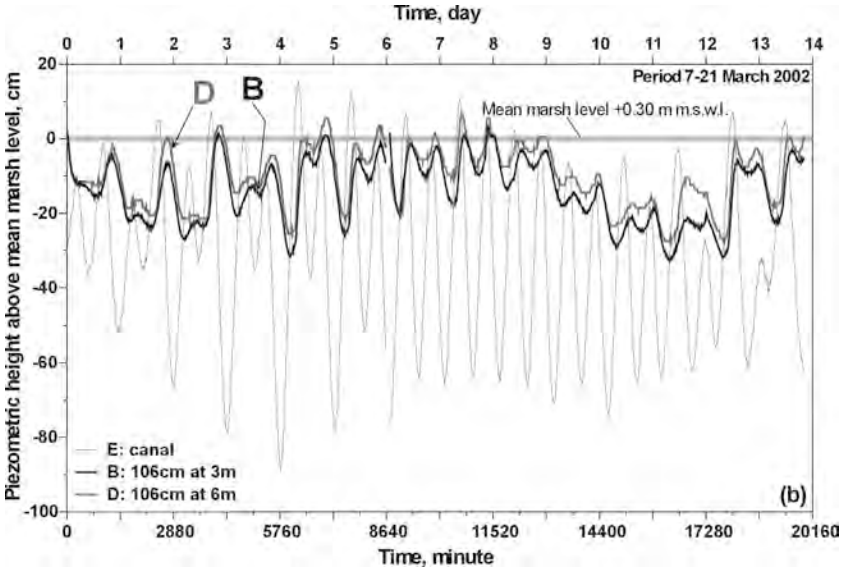

Fig. 6b

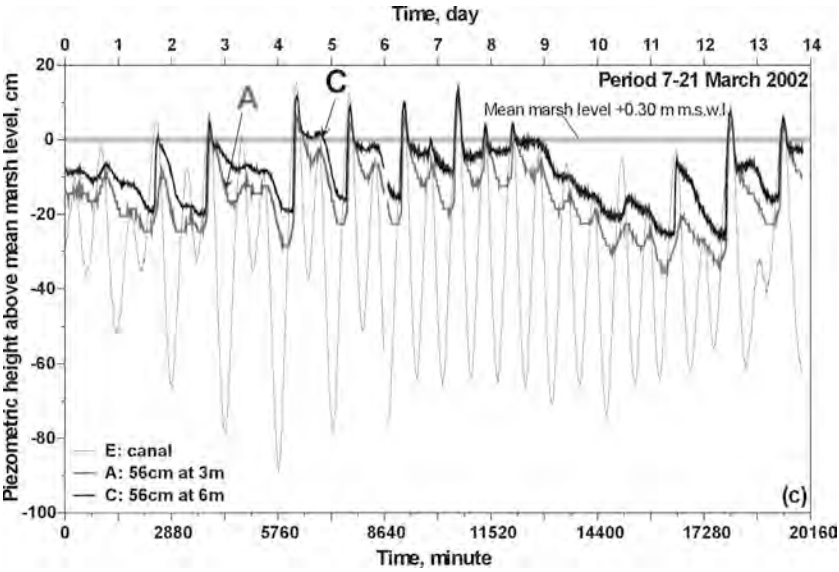

Fig. - 6a, b, c. Pore pressure evolution as a consequence of the tidal range in the period 7-21 March 2002.

- Full soil saturation occurs only when the marsh is flooded: in this case the immediate response of pore pressure transducers indicates that a fully coupled behaviour with no significant damping was reached in the porous medium;
- The effect of low permeability together with the pore pressure trends measured in the ground may support the hypothesis of fully undrained soil behaviour, characterised by the absence of any groundwater flow in the marsh ground;
- Significant hydraulic gradients and associated seepage forces can be hypothesised to act on the soil skeleton only within a thin layer along the marsh boundaries.

5. *Conclusions.*

From the site and laboratory investigations carried out so far on two vertical boreholes in the S. Felice marsh the following main preliminary conclusions can be drawn.

The soil forming the upper 1.20 m of the marsh is entirely composed of silt combined with clay and/or sand with low organic content, the latter increasing towards the marsh surface. These materials, when homogenous, are characterised by a low permeability with an anisotropy ratio, as measured in the laboratory, varying between 1 and 4.

The effect of the low permeability together with the pore pressure trends measured in the ground could support the tentative hypothesis of undrained soil behaviour with the absence of any significant groundwater flow.

The presence of a nearly saturated zone where the pore pressure oscillates from positive to negative values, as a consequence of the tidal excursion, was observed in a shallow layer with a thickness of about 0.3 m. No influence of tide was measured below 0.3 m. This thickness is of course a function of the degree of evapotranspiration, which was extremely low in the period 7-21 March 2002. Fully saturated conditions occurred when the marsh was entirely flooded: in this case, the immediate pore pressure response suggests the presence of a fully coupled behaviour with no significant water pressure damping in the porous medium.

These above hypotheses should be however corroborated by further investigations to be carried out in other periods of the year.

Table 1. Permeability measured with in-situ infiltrometer.

Type of vegetation	**Permeability (m/s)**	**Comments**
No vegetation	$3.7\ 10^{-8}$	Outcrop level
Salicornia	$3.9\ 10^{-7}$	Average marsh level
Salicornia	$1.2\ 10^{-7}$	Average marsh level
Salicornia	$1.8\ 10^{-6}$	Average marsh level
Salicornia	$3.4\ 10^{-6}$	Average marsh level
Limonium	$1.0\ 10^{-6}$	Meander border

References.

Cola S. & Simonini P., 2002. Mechanical behaviour of Venice lagoon silts as a function of their grading characteristics. Canadian Geotechnical Journal, Vol. No. 6.

Simonini P. & Cola S., 2000. Use of piezocone to predict maximum stiffness of Venetian soils. Journal of Geotechnical and Geoenvironmental Engineering, ASCE, Vol. 126, No. 4, pp. 378-382.

COMPARING MORPHODYNAMICS OF THE LAGOON OF VENICE AND SOME ESTUARIES OF THE NETHERLANDS

H. DE VRIEND[1] and G. DI SILVIO[2]
[1]*Delft University of Technology, Faculty of Civil Engineering and Geoscience, Netherland*
[2]*Dipartimento di Ingegneria Idraulica, Marittima, Ambientale e Geotecnica, Università di Padova*

Morphodynamics of tidal lagoons is controlled by several forcing factors. While tidal currents are the dominant factor in the channels, waves are definitely important both on the shoals inside the lagoon and on the seaside near the inlet. In these zones, in fact, tidal currents are generally too weak for entraining the sediments from the bottom, although currents are responsible for the transport of the particles put in suspension by the waves. In some cases (e.g. the lagoon of Venice before the river diversion between the XIV and XVI centuries) also the fluvial input is a substantial component of the sediment budget. Finally, soil subsidence and rising of the sea level (eustatism) also play a fundamental role in the balance, as well as the compaction rate on vegetated marshes.

For the lagoon of Venice none of these factors can be neglected, although each of them can be more or less important in other estuaries. Indeed the variety of estuarine landscapes displayed at the edge of an alluvial plain (estuaries proper, deltas, lagoons, sounds, etc.), can probably be explained in terms of relative importance of these factors.

Comparing the relative importance of forcing factors, however, is not trivial. A number of flow- and transport-models are available for describing, at the time scale of a single event, the detailed effects of each factor. In some cases the models are extremely sophisticated and able to explain very complex morphological features. Yet implementing all these models together for predicting their combined effects at the historical scale (years, decades or centuries) is virtually impossible. The difficulty depends, among others, on the time-depending boundary conditions that should be prescribed step-by-step in the correct coupled way.

An alternative approach is represented by *long-term conceptual models* which account for all the factors mentioned above, somehow averaged over a significant period of time (say, one year). A reasonable definition of the time-averaged quantities is crucial. A conceptual model of this type has been proposed, based on the *long-term transport concentration* prevailing in any location of the lagoon and on a simple *dispersion-convection flow* for assessing the long-term water and sediment fluxes.

The conceptual model is able to describe the altimetric (and, up to a point, the planimetric) evolution of an estuary under action of the forcing factors. In stationary conditions, the model indicates that the quasi-equilibrium configuration of estuarine landscape depends on a limited number of parameters which include all these factors.

As for any conceptual model, this approach requires the determination of a few *calibration parameters* to be evaluated against field data. Calibration and verification of the model can be carried out either by comparing the historical evolution of a given lagoon (this is under way with the lagoon of Venice from 1810 to the present), or by comparing quasi-equilibrium configurations of different estuarine systems. For this purpose, the forcing factors in two Dutch estuaries (Wadden sea and Schelde) are being collected and compared with the corresponding factors in the lagoon of Venice. On the same time the morphological configuration of the three estuaries will be analized.

A critical discussion of the validity and limitation of the model for different estuaries will be reported in the paper.

MODELING THE BOTTOM STRESS DISTRIBUTION IN THE VENICE LAGOON

G. Umgiesser, M. Sclavo, S. Carniel
Istituto per lo Studio della Dinamica delle Grandi Masse, CNR, Venezia

1. *Introduction.*

The Venice Lagoon is a complex system and increasing pollution problems and silting-up of interior channels are threatening its unique appearance and environment. For instance, particulate matter loadings, originating also from human wastes, have increased the channels' natural tendency to accumulate sediments. This brings as a consequence a modification in the tidal propagation within the lagoon channels and an increased possibility of releasing toxic substances during resuspension periods. Moreover, severe problems have to be addressed when, after channels dredging, sediments need to be properly disposed.

In order to preserve the delicate lagoon ecosystem, therefore, a modeling apporach combining the hydrodynamic behaviour of the Venice Lagoon and the sediment distribution to better understand the relation between them is highly desiderable.

As a preliminary step towards this direction, we present here a coupled hydrodynamic-wave model, reproducing the circulation of the Venice Lagoon and the effects that winds may have on the wave-currents interactions. Particularly, the study is focused on the determination of the bottom stress values, the main forcing for erosion and deposition processes. Sensitivity tests adopting only currents and wind at different speeds and directions have been performed and results are presented and discussed.

2. *The hydrodynamic model.*

The hydrodynamic model used is the two-dimensional finite elements numerical model developed at ISDGM during the 90's [Umgiesser and Bergamasco, 1993] successfully tested in other circulation applications

[Bergamasco and Umgiesser, 2000; Zampato and Umgiesser, 2000; Umgiesser, 2000] and coupled to a simple deposition model as well [Bergamasco et al., 2001]. The numerical model provides as results the prognostic values of sea surface elevation and of the vertically integrated velocities. The main structure of the code solves the shallow water equations in the hydrostatic approximation expressed by the well known equation set:

$$\frac{\partial \eta}{\partial t} + \frac{\partial U}{\partial x} + \frac{\partial V}{\partial y} = 0 \tag{1}$$

$$\frac{\partial U}{\partial t} - fV + gH\frac{\partial \eta}{\partial x} + RU + X = 0 \tag{2}$$

$$\frac{\partial V}{\partial t} + fU + gH\frac{d\eta}{dy} + RV + Y = 0 \tag{3}$$

where $H=h+\eta$ is the total depth of the water column (with h depth of the water column and η the sea surface elevation), f the Coriolis parameter, t the time, g the gravity acceleration, R the friction coefficient and X and Y contain all other terms, such as wind stress or non linear terms.

In the above written equations, the vertical integrated velocities (total transports) are given by $U=\int udz$ and $V=\int vdz$, where u and v are the velocities along x and y direction.

The friction coefficient is given by $R=C_D u/H$, where C_D is the drag coefficient that depends on the bed roughness length (see later). Therefore a quadratic friction law has been used.

These equations are integrated in time by a semi-implicit algorithm. In this procedure the unknown transports from the momentum equation are substituted into the continuity equation resulting only in a linear system to be solved for the water levels. With the knowledge of the new water levels the unknown transports may be solved for explicitly.

The spatial discretization of the equations is done on a triangular finite element grid. These linear finite elements give enough flexibility to describe the complex geometry and bathymetry of the Venice Lagoon. On this grid the water levels are described by linear form functions and defined on the nodes (intersections) of the grid. On the other hand, the velocities are described by constant form functions over one element, which corresponds to the definition of the velocities on the center of the elements.

This "staggered" approach of defining the various variables and unknowns is well known from the finite difference technique and allows for propagation properties that conserve energy and mass. The same is also valid in this case for the finite elements.

Moreover, as the average depth of the Venice Lagoon is about 1 meter and in some regions the tidal amplitude may be greater than the water column, a drying algorithm is implemented [Zampato and Umgiesser, 2000]. The shallow water flats during a tidal cycle are sometimes covered with water, and sometimes are dry: during the dry period these elements are taken out of the algebraic system and are later added again, once the surrounding water level is higher than the water inside the dry element. The specific implementation done here conserves the mass in each element.

3. *The wave model.*

The SWAN model is an advanced third generation model, specifically developed for shallow waters. There is full consideration of all the dominant physical processes that control the evolution of the wave field. A description of the model is given by Booij et al. (1999) and Ris et al. (1999).

In SWAN the waves are described with the two-dimensional wave action density spectrum $N(\sigma, \theta)$ rather than the energy density spectrum $E(\sigma, \theta)$ since in the presence of currents, action density is conserved whereas energy density is not. The independent variables are the relative frequency σ (as observed in a frame of reference moving with the action propagation velocity) and the wave direction θ (the direction normal to the wave crest of each spectral component). The action density is equal to the energy density divided by the relative frequency: $N(\sigma, \theta)=E(\sigma, \theta)$.

The evolution of the wave spectrum is described by the spectral action balance equation which for Cartesian coordinates is:

$$\frac{\partial}{\partial t}N + \frac{\partial}{\partial x}c_x N + \frac{\partial}{\partial y}c_y N + \frac{\partial}{\partial \sigma}c_\sigma N + \frac{\partial}{\partial \Theta}c_\theta N = \frac{S}{\sigma} \qquad (4)$$

The first term in the left-hand side of this equation represents the local rate of change of action density in time, the second and third term represent propagation of action in geographical space (with propagation velocities c_x and c_y in x – and y – space, respectively). The fourth term repre-

sents shifting of the relative frequency due to variations in depths and currents (with propagation velocity c_σ in σ – space). The fifth term represents depth-induced and current-induced refraction (with propagation velocity c_σ in σ - space). The expressions for these propagation speeds are taken from linear wave theory. The term S(=s(σ, θ)) at the right hand side of the action balance equation is the source term in terms of energy density representing the effects of generation, dissipation and non-linear wave-wave interactions.

4. *Bottom stress computation.*

The bottom stress is the main forcing factor for erosion and deposition processes. Both current and wave action contribute to the bottom stress and the wave-current interactions enhance these values. In the particular lagoon environments the two contributions are crucial for a correct assessment of the bottom stress.

The bottom stress due to currents only has been computed using the formula [Burchard et al., 1999]:

$$\tau_c = \rho c_D U_c^2 \tag{5}$$

In (5), U_c is the current velocity, $C_D = k^2 / \left[\ln^2\left(\frac{z_o + 0{,}5h}{z_o}\right)\right]$ where C_D is the drag coefficient, k the von Karman constant (0.40), h the water depth, ρ the water density and z_o the bed roughness length.

The bed shear stress due to wave only has been calculated following Soulsby (1997):

$$\tau_w = \frac{1}{2}\rho f_w U_w^2 \tag{6}$$

with $f_w = 1.39 \left(\frac{z_o}{A}\right)$ expressing the friction factor, $A = U_w T_p / 2\pi$ where T_p is the wave peak period and U_w is the maximum bottom velocity from SWAN. For consistency, the value adopted for the bottom roughness in the wave model is the same used by the hydrodynamical one, that is $5 \cdot 10^{-4}$ m.

To compute the non linear wave-current enhancement to the mean bottom stress tm, various models could be used [e.g. Grant and Madsen,

1979 and 1982]. In this paper we adopted the following empirical formulation of Soulsby (1997), that is easier to implement and gives, according to the author, comparable results:

$$\tau_m = \tau_c \left[1 + 1.2 \left(\frac{\tau_m}{\tau_c + \tau_w} \right)^{3.2} \right] \tag{7}$$

The maximum shear stress, due to the combination of waves and currents, has been computed taking into account also the non linear interactions:

$$\tau_{\max} = [(\tau_m + \tau_w \cos\Theta)^2 + (\tau_w \sin\Theta)^2]^{0,5} \tag{8}$$

with Θ representing the angle between current and waves (see Figure 3 for reference).

5. *The model setup and simulations.*

The hydrodynamic model has been applied to the Venice lagoon with a grid consisting of 4359 nodes and 7845 elements (see figure 1). The resolution is variable from about 1 km in the shallow parts far from the inlets down to about 50 meters in the small channels that run in the lagoon. The model is run with a 5 minute time step until a steady state has been reached.

The model can be used in a 2- and 3- dimensional version and has already been applied in various case studies in the lagoon. Here the 2-D version is used, since we are focusing only on the basic processes that regulate the bottom stress experienced by the water body. In case the sediment transport will be added, clearly the 3-D version has to be applied.

The model has been forced by semidiurnal tides and by two different wind regimes, constant in time and space: Scirocco, blowing from S-E, and Bora, blowing from N-E, winds had idealized but realistic magnitudes, respectively of 10 and 15 m/s. At the model open boundaries, that is in the proximity of the three inlets directly communicating with the Adriatic Sea, the sea surface elevations are prescribed using a semidiurnal tide having 40 cm of amplitude.

In the proposed tests, 25 frequencies and 24 uniformly distributed directions have been considered in the SWAN model. The frequencies are geometrically distributed with $f_{n+1} = 1.1\, f_n$ and $f_0 = 0.05$ Hz. The model has

Fig. 1 - Finite element grid of the Venice lagoon adopted by the hydrodynamical model.

been run in stationary mode, i.e. given the input wave conditions at the outer border of the grid, the model iterates till when equilibrium conditions have been reached. Given the limited extension of the Venice lagoon area and the consequent limited time required for the wave energy to move from one end to the other, this is perfectly consistent with a sound representation of the physical truth.

The SWAN computational grid used for the tests (represented in Figure 2) had a resolution of 100x100 m, and 305x421 grid points.

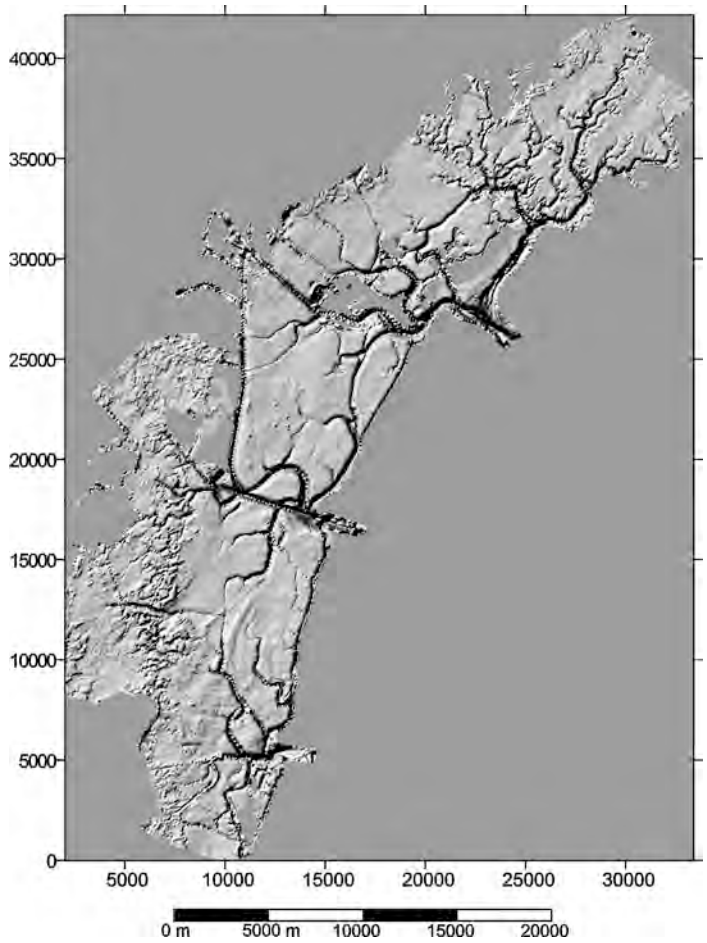

Fig. 2 - Bathymetry of the Venice lagoon used by the wave model.

Even if the hydrodynamic model is a finite element one, the wave model has been run on a regular 100 meter grid. Therefore, for consistency, all results have been interpolated to the regular grid used by the wave model. All final computations, such as wave current interactions, have been performed on this regular grid and the relative strength of the bottom stress have been compared.

In order to investigate the relative weight of the afore mentioned contributions, we have devised different scenarios as explained in the next chapter.

6. *Results.*

During a tidal cycle the bottom stress distribution due to currents only appears to be non negligible only during maximum flood or ebb tide. (Following pictures refer to the latter situation). Values appear to be higher in correspondance of deeper channels, those hydrodynamically more active. The situation does not change significantly when the wind forcing is switched on, except that now the values at the inlet is increased and some shallow areas are showing some evidence of increased stress. As an example, we present here results of a Scirocco wind forced situation (Figure 4) where the bottom stress is computed only from currents as expressed by equation (5).

Figure 5 presents the bottom stress using formula (6), i.e., taking into account only the wave contribution. The scale presents a maximum value of 2 N/m2 as this value is considered strong enough to mobilize the cohesive sediments for the Venice lagoon [Amos, pers. comm.]

Comparing figures 4 and 5, the bottom stress induced only by currents is maximum along the deepest channels, i.e., where the hydrodynamic is more active. In the case where only waves have been taken into account, the channels show very low values, reflecting the fact that in deep region wave effects are negligible. On the other hand, the shallower parts exhibit values of up to 1.2 N/m2. Therefore, generally speaking, the two pictures are in a way complementary: where wave effects are higher, current effects are weaker.

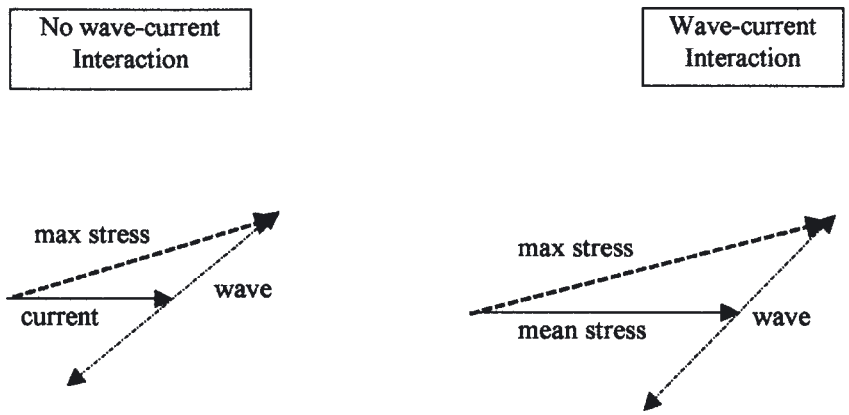

Fig. 3 - Graphical representation of the computation of the maximum shear stress, due to the combination of waves and currents.

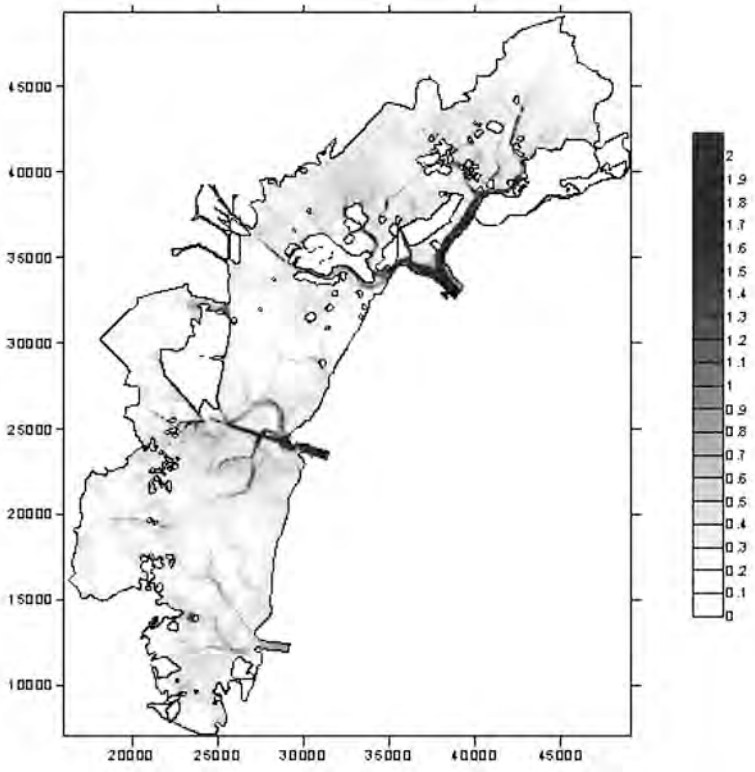

Fig. 4 - Bottom shear stress (N/m2) induced by currents only during a Scirocco event.

The non-linear effects of the combination wave-currents have been investigated using the formula (7) for the mean shear stress. Results show an enhancement of more than 100% in the shallow areas where currents are less important than the wave action. In these areas it is therefore very important to include also the combined effect of currents and waves. On the other hand in the deep channels the wave current enhancement is rather low. Both findings can be deduced by equation (7) that shows that the enhancement effect is strongest in areas of high wave action.

Figure 6 presents the total stress due to waves and currents, computed using the formulation (8), during a case of a Bora event. The picture reflects a high value of stress in the whole area. Clearly, during strong Bora wind events it can be expected that much of the lagoon basin will be in erosion and the concentration of the sediments in the water column will be high everywhere.

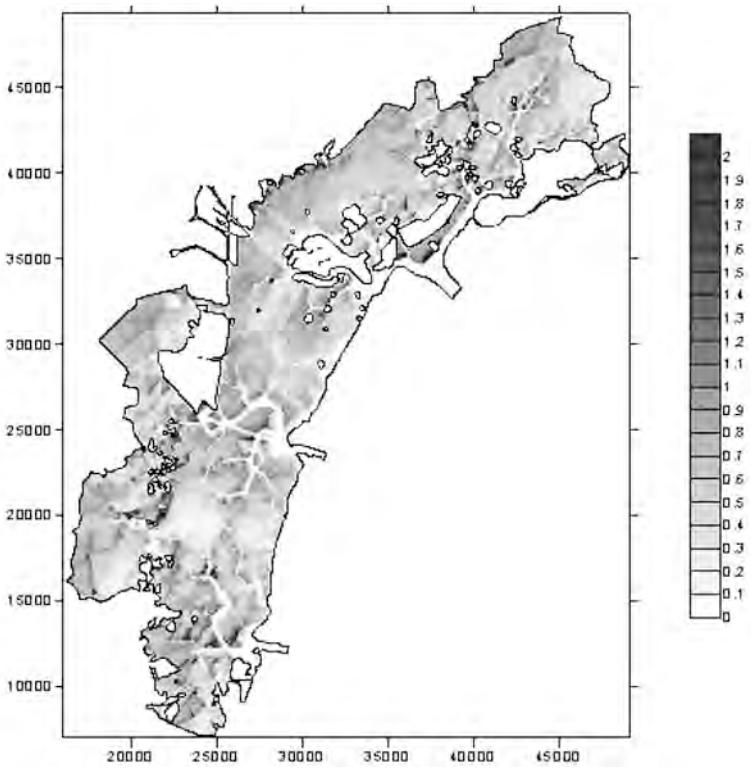

Fig. 5 - Bottom shear stress (N/m2) induced by waves only during a Scirocco event.

Note that in the Lido inlet bottom stress is lower when compared to Scirocco situation. This is due to the fact that there are two mechanisms for water exchange working against each other. This is particularly evident on this inlet, as the Bora wind induces high residual inflow through it, balancing partly the outflowing tidal ebb current [Cucco and Umgiesser, 2002].

7. *Conclusions.*

This paper deals with the computation of bottom stress in the Venice lagoon. Due to the very shallow nature of the lagoon it has been seen that the waves will be a major contributor to the total stress that is controlling

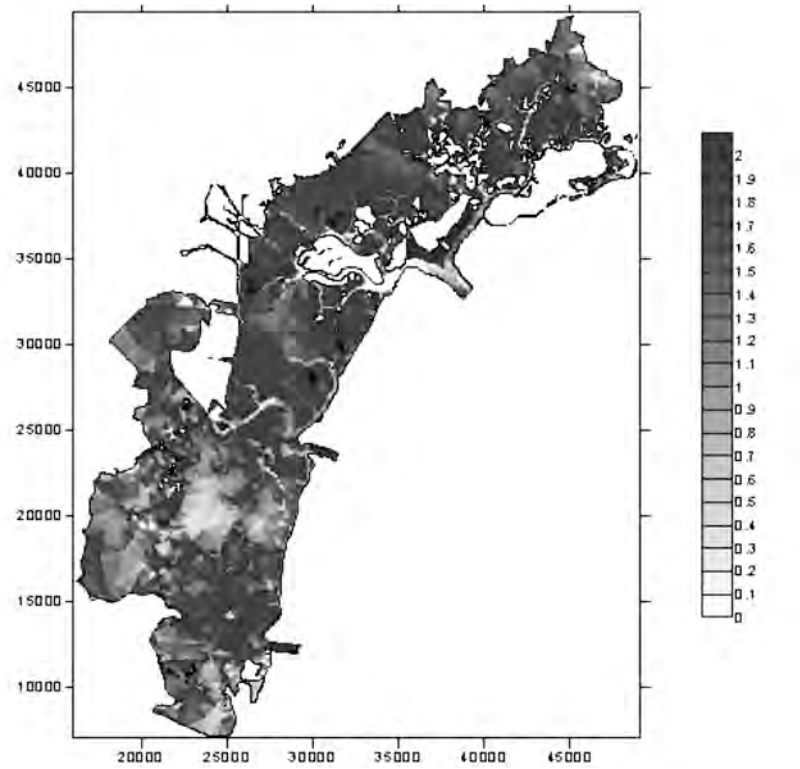

Fig. 6 - Total stress due to wave and currents, computed using the formulation (8), during a Bora event.

the erosion and deposition mechanisms at the sediment water interface. It is therefore necessary to have a valid tool that allows the computation of the wave climate in the lagoon.

The absolute values of the bottom stress must still be treated with some care. Clearly it depends through equation (5) and (6) on the bed roughness length z_0. In the case of the waves this means that by doubling its value the bottom stress due to waves will increase by a factor of 40%. In the case of the stress due to currents the picture is a little bit more difficult since by changing z_0 also the current speed will change and the effects on the bottom stress should be less strong.

It is therefore clear that a detailed calibration must be carried out by varying the roughness length in a way that is compatible with the bottom type in the lagoon. Once this has been done the computed bottom stress

can be used with models describing the sediment dynamics (erosion and deposition) to compute the sediment transport in the lagoon of Venice.

Acknowledgements.

The work has been partially funded by Co.Ri.La. Project, Linea 3.2 ("Hydrodynamics and Morphology of the Venice Lagoon"). The authors are grateful to Dr. C. Amos for the useful discussions.

References.

Bergamasco A., Carniel S. and Umgiesser G., 2001. A simple hydrodynamic-deposition coupled model of the lagoon of Venice. *Biol. Mar. Med.*, 8(1), pp. 300-308.

Bergamasco A. and Umgiesser G., 2000. Un modello ad alta risoluzione per la simulazione barotropica della Laguna di Venezia. In: *La ricerca Scientifica per Venezia: Il Progetto Sistema Lagunare Veneziano*. Vol. II - Tomo I, Metodologie di sperimentazione e di rilevamento - Studio dei Processi, Istituto Veneto di Scienze, Lettere ed Arti Ed., p.721-734 (in italian, ISBN 88-86166-82-6)

Booij N., Ris R.C. and Holthuijsen L.H., 1999. A third-generation wave model for coastal regions, Part I, Model description and validation. *J.Geoph.Research*, 104, C4, pp 7649-7666.

Burchard H., Bolding K., Villareal M.R., 1999. GOTM – a general ocean turbulence model. Theory, applications and test cases, *Tech. Rep. EUR 18745 EN*, European Commission.

Cucco A. and Umgiesser G., 2002. Modeling the water exchanges between the Venice lagoon and the Adriatic Sea. This issue.

Grant W.D. and Madsen O.S., 1979. Combined wave and current interaction with a rough bottom. *J.Geoph.Research*, 84, C4, pp 1797-1808.

Grant W.D. and MadsenO.S., 1982. Moveable bed roughness in unsteady oscillatory flow. *J.Geoph.Research*, 84, C1, pp 469-481.

Ris R.C., Booij N., Holthuijsen L.H., 1999. A third-generation wave model for coastal regions, Part II, Verification, *J.Geoph.Research*, 104, C4, pp 7667-7681.

Soulsby R., 1997. *Dynamics of marine sands. A manual for practical applications*. Thomas Telford Ed., 248 pp.

Umgiesser G., 2000. Modeling residual currents in the Venice Lagoon. In: *Interactions between Estuaries, Coastal Seas and Shelf Seas*, Ed. T. Yanagi, TERRAPUB Ed., pp. 107-124.

Umgiesser G. and Bergamasco A., 1993. A staggered grid finite element model of the Venice Lagoon. In: Finite Elements in Fluid, K. Morgan, E. Ofiate, J. Periaux and O.C. Zienkiewicz (eds), Pineridge Press.

Zampato L. and Umgiesser G., 2000. Hydrodynamic modeling in the channel network of Venice. *Il Nuovo Cimento*, Vol 23 C, N. 3, pp. 263-284.

MORPHODYNAMICS PROCESSES IN THE LAGOON OF VENICE: THE SCANELLO SALT MARSH AREA

M. Bonardi[1], A. Cucco[1], L. Schiozzi[1],
L. Tosi[1], R. Sitran[2] and I. Scroccaro[1]
[1]*Istituto per lo Studio della Dinamica delle Grandi Masse, CNR, Venezia*
[2]*Istituto per l'Ambiente Marino Costiero, Messina*

Abstract.

Geomorpholgical variations have been naturally occurring in the Lagoon of Venice since its formation. In recent times, however, complex morphodynamic changes, caused by natural processes and by the direct or indirect impact of man activities have been recognised. Moreover, there remains a lack of knowledge concerning sediment erosion, re-suspension, transport and sedimentation, sea-lagoon balance and the role played by the hydrodynamics.

A detailed study of the Scanello salt marsh area, in the Northern part of the Venice Lagoon, was carried out, in order to better understand the erosion-transport-sedimentation processes and the hydrodynamics interaction. Understanding the role that the hydrodynamics plays in the erosion, transportation and deposition of sediments in this test area, is essential to the understanding the morphological variations, that are presently occurring in the Venice Lagoon and morphological and environmental restorations required.

A 2D hydrodynamic finite element model was used to provide the circulation field of the entire Venice basin. Results obtained by different simulations allowed the investigation of the main hydrodynamic features of the Scanello area.

Key-words: Hydrodynamics, Morphology, Erosion, Transport, Sedimentation.

1. *Introduction.*

Geomorphological variations have been naturally occurring in the Lagoon of Venice since its formation. In recent times, however, complex morphodynamic changes, caused by natural processes and by the direct or indirect impact of anthropic activities have been recognised. Consequently, an effective management of the Venice basin requires an in depth understanding of physical and geomorphological processes, which present a huge complexity. Despite numerous debates over the past few years, there remains a lack of knowledge concerning sediment erosion, resuspension, transport and sedimentation, sea-lagoon balance and the role played by the hydrodynamics.

The Venice Lagoon, with a surface area of about 550 km^2 and an average water depth of about 0.6 m (Cossu & de Fraja Frangipane, 1985), is Italy's largest lagoon. It is connected to the Adriatic Sea through three inlets (Lido, Malamocco and Chioggia), which guarantee the water exchange with the sea. The primeval lagoon reached approximately its present position 6,000 years ago, even if it was smaller than the present one and the flowing out of its waters was possible through eight sea openings against the three it has now (Carbognin et al., 1984). The lagoon morphology, consisting of shallows, mud flats, salt marshes, islands and a thick network of channels, was subjected to the great mutability of those factors which had generated and developed the morphology throughout the ages. Among these, the activity of the main lagoon tributaries (Adige, Bacchiglione, Brenta, Sile and Piave) was determinant and threatened to make it a marshland. Together with the increase in the depth of the lagoon due to subsidence and eustatic rise, human activities have now inverted the lagoon's natural tendency to silt up and have triggered off the opposite process, transforming it slowly into a sea environment.

We report the results of a detailed study of three salt marshes, called BV (*Barena Vecchia*), BN (*Barena Nuova*) and BNW (*Barena Nord Ovest*), of the Scanello area (fig. 1), carried out in order to better understand the erosion-transport-sedimentation processes and the hydrodynamics interactions. In fact understanding the role that hydrodynamics plays in erosion, transportation and deposition of sediments in this test area is essential to understanding the morphological variations, that are presently occurring in the Venice Lagoon.

In order to integrate physical, chemical, sedimentological, mineralogical and micropalaeontological data already investigated in the past and to evaluate the long-term evolutional trends of the whole lagoonal basin 53 bottom sediment samples and 26 sediment cores were collected in the

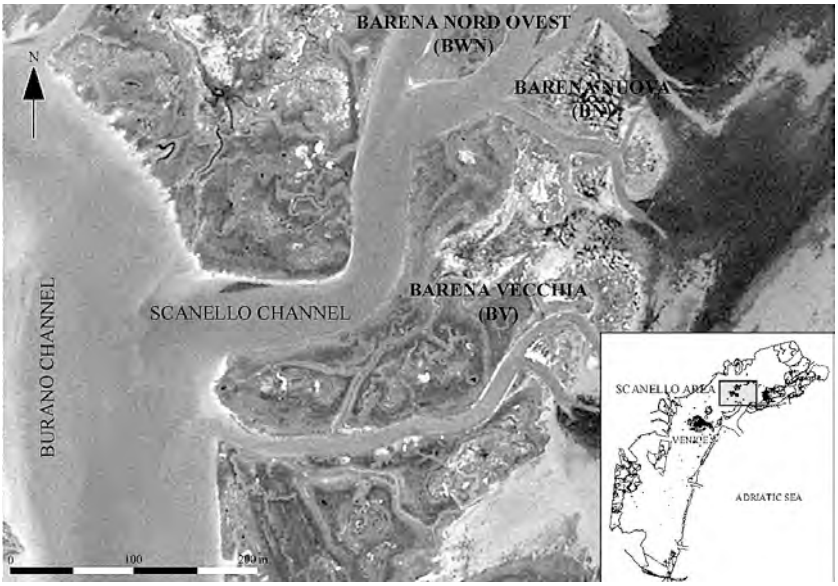

Fig. 1 - Study area.

entire Lagoon of Venice. In the framework of this general study the area of Scanello, located in the Northern basin of the Lagoon of Venice, South East of the Island of Burano (fig. 1), has been chosen as a representative site. In fact previous studies (Bonardi et al., 1997; Bonardi, 1998; Bonardi et al., 1999) highlighted the palaeoenvironmental evolution of the area, known for the presence, at different depths, of archaeological remains dating back to Roman times. The investigation of these salt marshes environments has, therefore, allowed the quantification of the mean sea level variations, related to global changes. Furthermore a detailed topographic study of two salt marshes of the area (Bonardi, 1998) was carried out in order to better understand the recent scale erosional and depositional trends.

2. *Results and discussion.*

2.1 *Hydrodynamic modeling.*

The tidal currents, in particular for the marshy area of Scanello, have been investigated by mathematical modelling. A 2D hydrodynamic finite element model, developed at CNR-ISDGM in Venice (Umgiesser &

Bergamasco, 1993; 1995), has been used to study the circulation pattern of this area.

2.1.1 *The model.*

The hydrodynamic model used is a two-dimensional finite element model. The finite element method gives the possibility to follow the morphology and the bathymetry of the area and to represent with a higher resolution the zones where hydrodynamic activity is more interesting. The numerical computation has been carried out on a spatial domain that represents the entire Venice lagoon through a finite element grid.

The grid for the Venice lagoon has been constructed manually and part of the Scanello area has been created with an automatic mesh generator. The grid contains 8072 nodes and 15672 triangular elements. A higher grid resolution has been imposed inside the area of Scanello in order to obtain more information about the circulation of water. The grid is shown in figure 2 and the zoom for the Scanello area is presented in figure 3. The bathymetric data necessary for the hydrodynamic model have been provided by CORILA.

Fig. 2 - Finite element grid of the Venice lagoon.

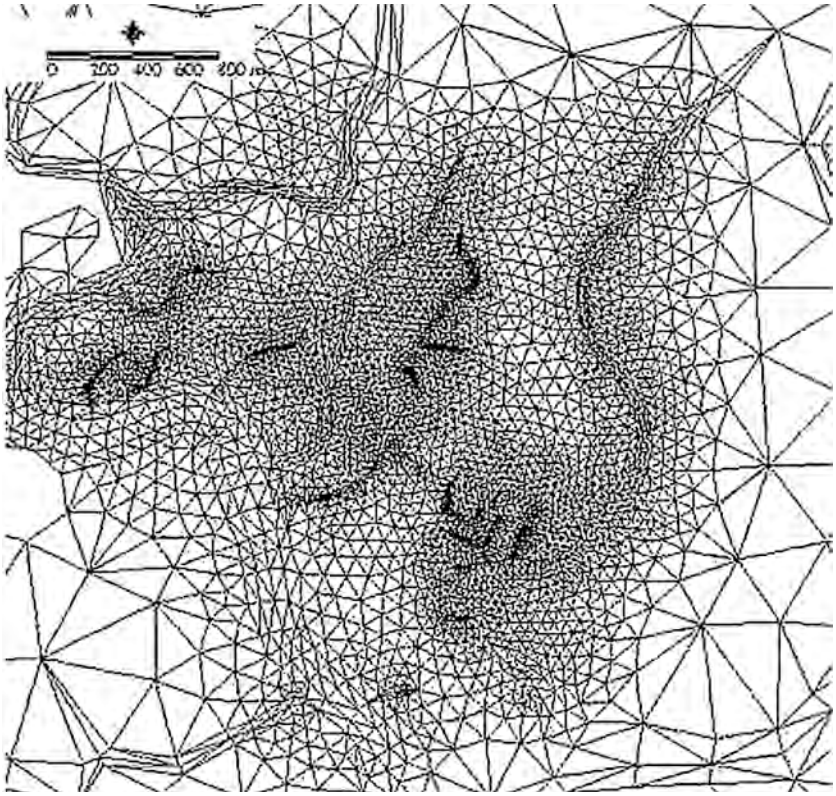

Fig. 3 - Zoom of the Scanello marshy area.

The model considers as open boundaries the three inlets of Lido, Malamocco and Chioggia, elsewhere as closed boundary the whole perimeter of the Venice lagoon.

The model uses finite elements for spatial integration and a semi-implicit algorithm for integration in time. The terms treated implicitly are the water levels, the friction term in the momentum equation and the divergence term in the continuity equation, all other terms are treated explicitly. The model resolves the vertically integrated shallow water equations in their formulations with levels and transports:

$$\frac{\partial J}{\partial t} - fV + gH\frac{\partial \zeta}{\partial \chi} + RV + X = 0$$

$$\frac{\partial V}{\partial t} + fU + gH\frac{\partial \zeta}{\partial y} + RU + Y = 0$$

$$\frac{\partial \zeta}{\partial t} + \frac{\partial U}{\partial x} + \frac{\partial V}{\partial y} = 0$$

where ς is the water level, U and V the vertically-integrated velocities (total or barotropic transports), g is the gravitational acceleration, $H=h+\varsigma$ the total water depth, h the undisturbed water depth, t the time and R the friction coefficient. The terms X and Y contain all other terms like the wind stress, the nonlinear terms and those that need not to be treated implicitly in the time discretization.

The following provides a description of the simulations and results.

2.1.2 *Simulation and results.*

The model has been calibrated using the sea level data measured by fourteen tide gauges located inside the lagoon. The parameter to be varied was the bottom friction (Strickler coefficient).

Different values of bottom friction were assigned to channels and shallow water zones, because of the different morphology and bottom vegetation. The calibrated model reproduces quite faithfully the tidal oscillation in most part of the lagoon.

Simulations have been carried out with a time step of 300 seconds and have been extended to one full year (2001). At the three inlets of the lagoon the same tidal forcing has been imposed. The tidal wave prescribed at the open boundaries is complete of all principal tidal components (M_2, S_2, N_2, K_2, K_1, O_1 and P_1). Other types of forcings have been neglected. The river runoff and the wind forcing have not been taken into account for the time being. A spin up time of one day has been always used for the simulations. Spring and neap tide events have been simulated. The results obtained concerns the main hydrodynamic features of Scanello marshy area.

The tidal circulation has been investigated. The instantaneous circulation in this area is completely driven by the inflowing and outflowing of water through the three main channels of Gaggian, Burano and Della Dolce. The channel of Scanello plays a marginal role in the hydrodynamics of the system because of its smaller section. The magnitude of the

current inside this channel reaches the maximum value at the beginning and decreases towards the end. During ebb flow (Fig. 4) the velocity rises up to the maximum value of 0.36 m/s. However, during the flood flow, the maximum current velocity reaches the lower intensity of 0.32 m/s.

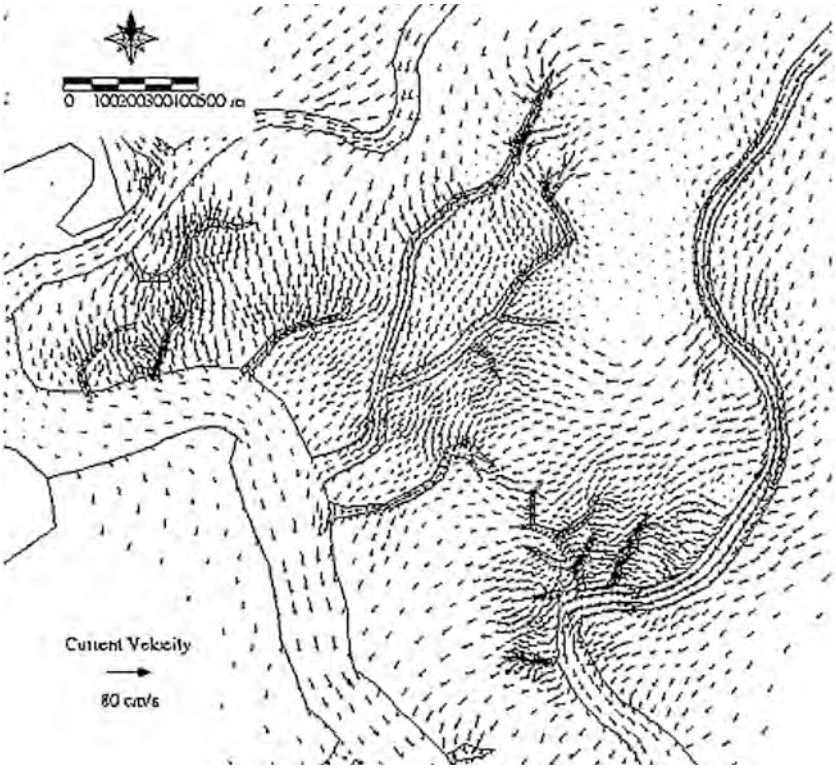

Fig. 4 - Instantaneous circulation pattern of Scanello area observed during ebb tidal cycle.

The residual currents inside this channel are weak: less than 0.01 m/s. The current pattern is entirely caused by non linear topographic effects, especially due to the bottom friction. The magnitude of the residual velocity is an order less then the instantaneous velocity one. The dominant direction is toward the beginning of the channel and it is parallel to its major axis. Similar behaviour of the current velocity has been observed inside the deepest channels where the residual circulation is dominated by ebb tide. Otherwise in the surroundings, where the average depth is less than 0.5 m, residual current magnitude is greater and it reaches values of

0.03 m/s. In these areas the residual circulation is still driven by ebb tidal forcing and the velocity is directed toward the Treporti channel.

More information about the circulation of water in this area will come from further analysis, which will consider both wind and tidal forcing.

2.2 *Geomorphological features.*

Previous studies (Bonardi, 1998) have revealed the evolutive trend of two of the salt marshes, called BV (*Barena Vecchia*) e BN (*Barena Nuova*), under study. Comparing historical topographic maps from 1931 to 1986 and air photos taken in 1961, 1968, 1987 and 1996, it has been possible to evaluate the spatial variations of the salt marshes. In a time span of about 70 years a maximum withdrawing of 58 m of the edge lining the Burano Channel of *Barena Vecchia* was observed (fig. 5, tab.1), whereas a maximum accretion of 80 m of the mud flat facing the northestern edge of *Barena Nuova* was deducted (tab. 1). Table 1 indicates how sedimentation rates are apparently higher than erosional ones; the comparison, however, is purely speculative because it is not possible to directly compare the amount of eroded and deposited sediments if their thickness and spatial distributions were not previously quantified.

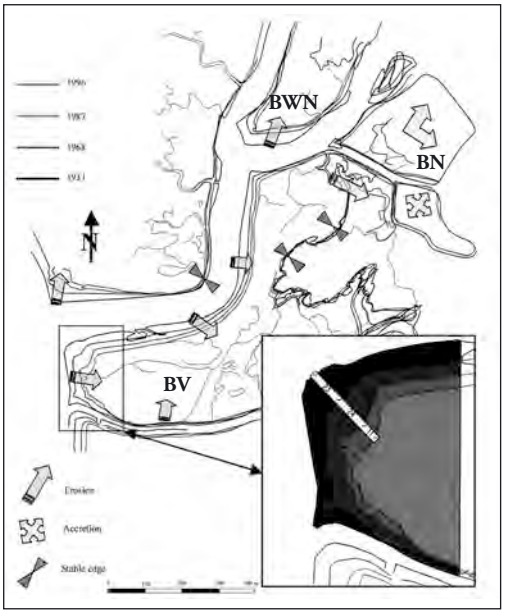

Fig. 5 - Comparison of *Barena Vecchia* (BV), *Barena Nuova* (BN) and *Barena Nord Ovest* (BWN) edges between 1931 and 1996.

Tab. 1 - Erosion rates at *Barena Vecchia* (BV) between 1931 and 1996 and accretion rates at *Barena Nuova* (BN) between 1931 and 1996.

Time span	Maximum surface reduction at Barena Vecchia (BV) (m)	Erosion rates (m/year)
1931-1968	23	0.6
1968-1987	24	1.3
1987-1996	11	1.2
1931-1999	*58*	

Time span	Maximum surface accretion at Barena Nuova (BN) (m)	Accretion rates (m/year)
1931-1968	0	0
1968-1987	56	2.9
1987-1996	24	2.7
1931-1996	*80*	

Furthermore, a series of GPS (Global Positioning System) surveys, conducted for 18 months between 1996 and 1997 and referred to the air photos taken in 1987, has led to the annual quantification of erosional processes (4m/year) occurring along the edges of *Barena Vecchia* and of the area extension of the salt marsh-mud flat limit and the consequent increasing of the salt marsh accompanied by the formation of tidal creeks, the so-called ghebi, at *Barena Nuova* (fig. 6). On the basis of textural and mineralogical analyses performed on the sediments from some cores taken in the Scanello area (Bonardi, 1998) we can suppose that the clayey silts eroded at the edge of *Barena Vecchia* settle down at the mud flat facing Barena Nuova concurring to expand its surface area.

In the framework of the morphological recovery activities of salt marshes performed by the Italian Ministry of Public Works, Water Authority of Venice by way of its concessionary Consorzio Venezia Nuova, the edges of the Barena Vecchia salt marsh have been marked out with containing piling. Therefore, during the topographic survey performed in 2000 the reconstructed edges of Barena Vecchia were mapped; the restored southwestern limits of the salt marsh actually lie approximately along the ones surveyed in 1996. Since salt marshes encourage water exchange, attenuate wave motion and limit the dispersion of sediment in the lagoon and the loss of sediment to sea, the topographic sur-

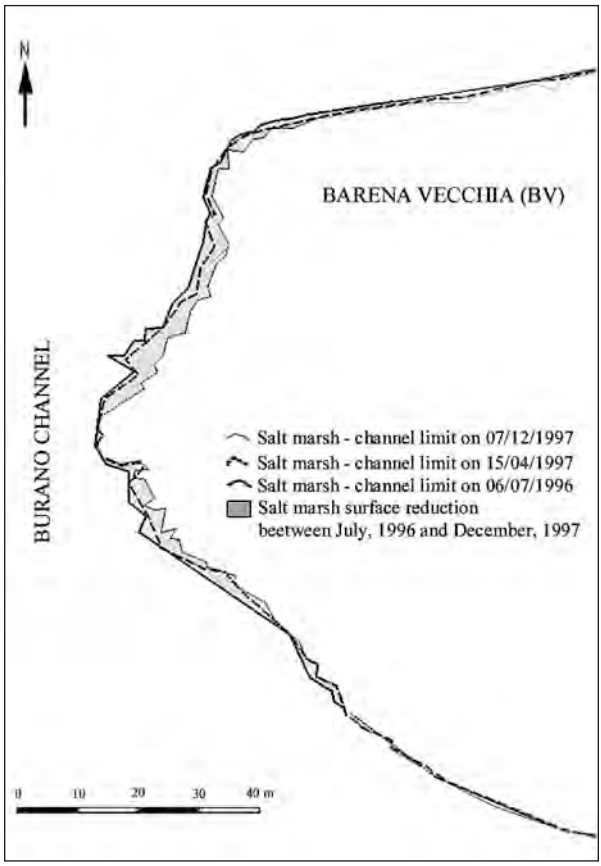

Fig. 6 - Comparison of *Barena Vecchia* (BV) edges between July, 1996 and December 1997.

vey was extended also to Barena Nord Ovest, in order to find out if these restoration activities could interfere with the natural morphological trends of the adjacent mud flats and salt marshes.

In 2002, a new series of GPS measures was so performed only at *Barena Nuova* and *Barena Nord Ovest* (fig. 7). *Barena Nuova* shows a general surface reduction even though it is very limited and meanly quantified in 0.50 m in the two years considered time span. A maximum shifting back of about 2 m was observed at the southwestern corner and in correspondence of the main tidal creeks. Nevertheless, it is important to note that between 2000 and 2002 at the salt marsh edge retreat there was a contemporaneous increase in its altitude, which varies between a mini-

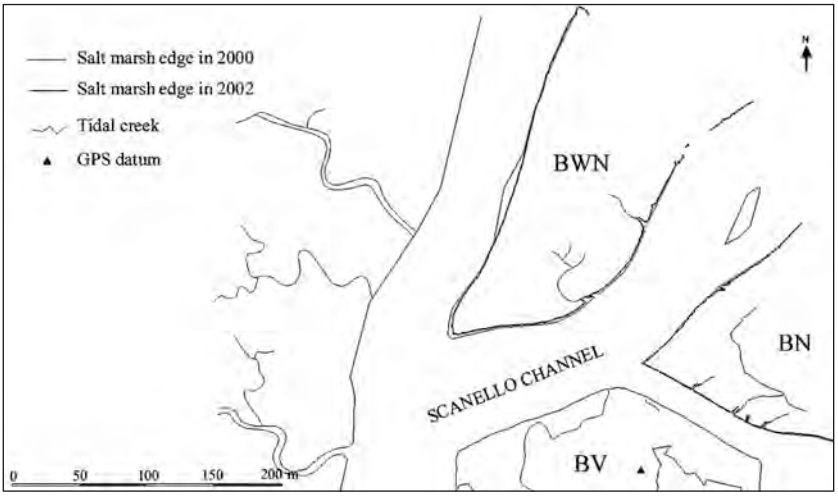

Fig. 7 - Comparison of *Barena Nuova* (BN) and Barena Nord Ovest (BWN) edges between 2000 and 2002.

mum of about 2 mm to a maximum of about 2 cm, and deepening of the tidal creeks. *Barena Nord Ovest* also suffers a general surface reduction, but it is greater than the one observed at *Barena Nuova*. In fact it retreated about 3.75 m at its southwestern corner and more than 7 m along Scanello Channel (fig. 7); however, a slight accretion of about 1 m was observed along the northwestern edge facing Scanello Channel. Even though altitude measures were not performed in 2000, it appears that a tidal creeks deepening is actually taking place on the edge facing *Barena Nuova* of this salt marsh.

Therefore, the 2002 topographic survey supported our hypothesis on sediment erosion, i.e. eroded sediments from *Barena Vecchia* deposit in the mud flat facing *Barena Nuova* and *Barena Nord Ovest*. In fact, after the recovering activities carried out at *Barena Vecchia* the adjacent salt marshes have shown a progressive, even if slight, surface reduction. In any case, the altitude increase and the tidal creeks deepening both indicate that the salt marshes under investigation are becoming more stable. The altitude elevation reflects a depositional trend governed by the tidal regime, which favour the transport and settling of the sediments transported as suspended load. Further, the tidal creeks deepening could be connected to the actual local hydrodynamics which feels the effects of an improvement in water exchange linked to the restoration of *Barena Vecchia*.

3. *Conclusions.*

The study of the salt marshes of the Scanello area, chosen as a representative site in the Lagoon of Venice, has permitted to integrate the data which has been collected in previous research projects in order to evaluate the current geomorphological changes and hydrodynamics interactions.

The topographic surveys, which have been conducted since 1996, and their comparison with historical topographic maps from 1931 to 1986, as well as air photos taken in 1961, 1968, 1987 and 1996, have permitted to evaluate the medium and short term erosional and depositional trends of the salt marshes under investigation. The use of hydrodinamic modeling has given an effort to understand the role that the hydrodynamics plays in the erosion, transportation and deposition of sediments in this test area.

These first results on the actual morphological evolution of the area also contribute to a better understanding of the other studies, in part already carried out, which evaluate the depositional palaeoenvironments.

The medium and short term erosional and depositional trends seem to be strongly connected to local hydrodinamics. In fact, it has been pointed out that the sediments, eroded at *Barena Vecchia* before its restoration, settled down at *Barena Nuova* and *Barena Nord Ovest*. Even if the wave motion produced by motor boats along Scanello Channel could be considered the most disintegrating agent on the edges of *Barena Vecchia*, it seems plausible that local hydrodynamics favour the transport of the eroded sediments northwards as well as their deposition. Actually *Barena Nuova* and *Barena Nord Ovest* suffer a slight surface reduction which can be correlated to the lack of supply of the sediments coming from *Barena Vecchia*. Nevertheless, local hydrodinamic features appear to be fundamental in explaining their increase in altitude and the tidal creeks deepening, considered as the signals of the morphological stabilisation of the salt marshes under study.

Acknowledgement.

This work has been funded through the CORILA Project 3.2 "Hydrodynamics and Morphology of the Venice Lagoon". The authors wish to thank Morgan S.r.l., in the person of Marco Giada, as partner in this research project.

References.

Bonardi M., Canal E., Cavazzoni S., Serandrei Barbero R., Tosi L., 1997. Sedimentological, archaeological and historical evidences of paleoclimatic changes during the Holocene in the Lagoon of Venice (Italy). World Resource Review, 9(4), 435-446.

Bonardi M., 1998. Studio dei processi evolutivi di alcune barene della Laguna di Venezia (Bacino Nord) in relazione alle variazioni del livello marino. Rapporto Finale, Consorzio Venezia Nuova, pp.65.

Bonardi M., Canal E., Cavazzoni S., Serandrei Barbero R., Tosi L., Enzi S., 1999. Impact of paleoclimatic fluctuations on depositional environments and human habitats in the Lagoon of Venice (Italy).

Carbognin L., Gatto P., Marabini F., 1984. The city and the Lagoon of Venice. A guidebook on the environment and land subsidence. In: Proceedings of the Third International Symposium on Land Subsidence, Venice (Italy), 1-36.

Cossu R., de Fraja Frangipane E., 1985. Stato delle conoscenze sull'inquinamento della Laguna di Venezia. Consorzio Venezia Nuova, Servizio Informativo, 4 volumes.

Umgiesser G. & Bergamasco A., 1993. A staggered grid finite element model of the Venice Lagoon. In: K. Morgan, E. Ofiate, J. Periaux, Zienkiewicz, O.C. (eds), Finite Elements in Fluids. Pineridge Press.

Umgiesser G. & Bergamasco A., 1995. Outline of a Primitive Equation Finite Element Model. Rapporto e Studi, vol. XII, pp. 291-320, Istituto Veneto di Scienze, Lettere ed Arti, Venice, Italy.

SEDIMENTATION MECHANISMS IN NORTHERN VENICE LAGOON

C.L. AMOS[1], G. UMGIESSER[2], M. BONARDI[2] and S. CAPPUCCI[1]
[1]*Southampton Oceanography Centre Empress Dock, Southampton Hampshire, UK*
[2]*Ist. per lo Studio della Dinamica delle Grandi Masse, CNR, Venezia*

1. *Introduction and background.*

1.1 *The nature of the Venice problem.*

There are no problems with natural change, merely our interpretation of the impact on us of changes in time which are both inevitable and essential to long-term stability. Likewise, there are no problems in Venice Lagoon that are not human-induced and measured in terms of human impact. This impact has been very large and is manifested by the interaction between the natural environment within Venice Lagoon and human development over 1300 years to produce the shifting balance between encroachment of the sea or the land about the City of Venice. Concerns over this balance are best described in the three quotes given below:

"*Le barene, che rimangano sommerse durante le alte maree, hanno assolto da sempre a una funzione di serbatoio regulatore, assorbendo l'eccedenza delle acque. Il loro progettato interramento per guadagnare spazio alla zona industriale viene considerato da molti tecnici la minaccia forse piu grave alla salvezza di Venezia*" (Montanelli et al. 1970).

"*Lo spazio lagunare, tra terra e mare, s'e andato formando e qualificando nei millenni: esso e dovuto all'instabile equilibrio dei rapporti tra fiumi, laguna e mare…. La laguna insomma e uno spazio naturale e tuttavia mantenuto e programmato dall'uomo*" (Zampetti, 1976).

"*Resta dunque aperto e sospeso un problema concettuale e operativo, tipico del restauro scientificamente intenso, progettuale nel senso piu moderno, di aperta dialettica tra conservazione e restauro del manufatto e conservazione dell'ambiente e del paesaggio lagunare, di cui il manufatto e parte determinante ed ineliminabile*" (Grillo, 1989).

The quotations above show that as early as 1970, there were great concerns about the loss of tidal flats which bordered the inner parts of Venice Lagoon. Three areas off Mestre were sequestered for industrial development to be serviced by the artificial Malamocco canal which bisects Venice Lagoon; this was done without consideration of the impact on Venice. Furthermore, large tracts of tidal flat in the western and northern lagoon were taken up for "*Pesca arginata*" fish farming such that by 1968 more than 50% of the natural lagoon had been destroyed. In total, over 160 km^2 of the lagoon has been reclaimed, thus reducing the lagoon by 25% of its original size.

The bed of Venice Lagoon is the substrate upon which biodiversity is dependent. The food chain is founded upon primary production taking place within the dwindling tidal flats. The marshes (*le barene*) and mudflats (*le paludi*) provide essential habitats for feeding fish, invertebrates and plants which govern the well-being of the lagoon. These habitats are under threat of being lost entirely from the lagoon. Present rates of loss are 1 km^2/year. Pollutants (industrial and domestic) have been freely discharged into the lagoon in the past (Zampetti, 1976). The tidal flats sequester these pollutants which become released to the water column when the flats are eroded. Within 40 years the tidal flats within Venice Lagoon may no longer exist, and the productivity will consequently fall as will the water quality. Tidal flushing is central to the well-being of the lagoon. This flushing is expressed as the ratio of the tidal prism (P) to lagoonal volume (V); as V increases through erosion, so the efficiency of the tides to remove pollutants decreases. Yet, the northern lagoon is enjoying growth in the tidal flats (Cappucci, 2002). Palude della Centrega has steadily grown while the southern and central parts have scoured and deepened. Recent estimates of the sediment budget of the lagoon suggest that there is a net loss of material to the open sea via the three entrances (Chioggia, Malamocco and Lido). If this is true, then why is there accumulation in the north? and perhaps more importantly, what are the factors which influence this growth? The input of sediment to the northern region is small and confined to a seasonal discharge of the river Sile (Carbognin and Cecconi, 1997). Thus the balance (budget) of materials is governed by the throughput within the main tidal channels which feed the northern flats. Furthermore, the trapping efficiency of the tidal flats (sensu Schubel and Carter, 1984) must be high or else they would suffer the same fate as their southern counterparts. The trapping efficiency depends in part on the type of estuarine circulation: salt wedge types weakly export; partially-mixed types import; homogeneous types strongly export. However, other factors are important such that:

"*There is a need for theoretical developments and scientific numerical modeling of some of the mode complex defining equations. There is a corresponding need for field observations aimed at understanding specific processes such as bottom source conditions and tidal transport*"(Officer, 1981).

The above statement is relevant to Venice Lagoon. In this study, we propose to examine the balance of sediment within the main channel (Scanello) which feeds an actively accreting tidal flat (Palude della Centrega) in an attempt to understand why this region is accreting and which factors are important in this accretion, and to update the defining equation governing the sediment budget.

The strategy used herein is three-fold. It assumes that the general mapping of the region has been undertaken and that a good account of the bathymetry, surficial geology, habitat distribution, and sediment distribution is known (Figure 1). Only once this has been completed can one move forward with well-formulated and relevant hypotheses. These are then evaluated through strategic sampling followed by in situ instrumentation. The work described herein is largely within the last of these three activities.

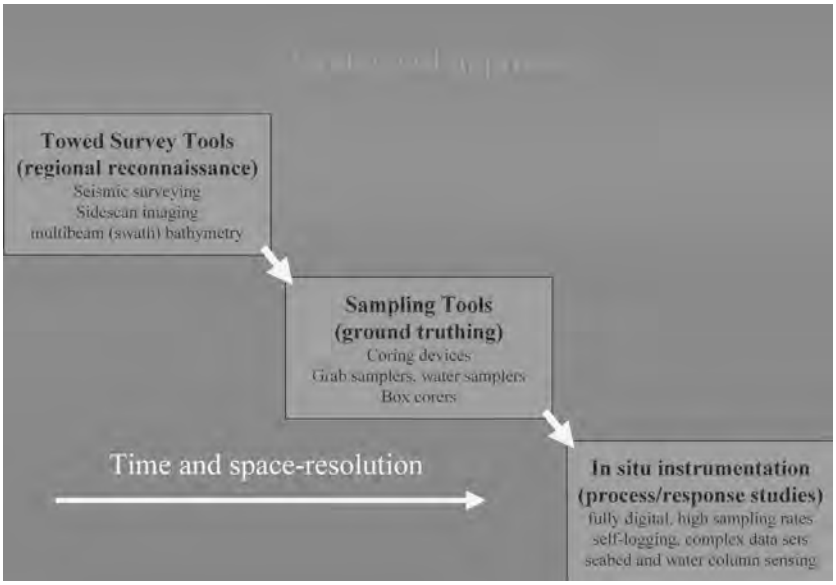

Fig. 1

1.2. *The environmental context of the study region and relevant background information.*

The balance in sedimentation was strongly influenced in the last 600 years by river diversion, by channelisation, by land reclamation (including the barene on which Venice sits); by dredging of the canals; and by stabilization of the barrier island system which protects the lagoon from the destructive waves of the northern Adriatic which are formed when the Scirocco wind blows. Initial sensitivity analyses using a very simple box model of Palude della Centrega suggest that the evolution of the flats (trapping efficiency) is controlled by the balance between wave erosion during Bora events and tidal sedimentation during fine weather (Cappucci, 2002). This balance is strongly affected by (1) turbidity of the waters flooding the tidal flats, (2) by seagrass density which suppresses wave action and tidal flow (Thompson et al. in press), and (3) biostabilization due to microphytobenthos which enhances stability.

The tidal flats are largely supplied by material transported in the tidal channel (Scanello canal). The filtering efficiency (F) of the tidal flats is defined as $F = [1 - \frac{M_{loss}}{M_{total}}]$, where M_{loss} is the mean seaward flux of material, and M_{total} is the total flux through Venice Lagoon (including all sour-

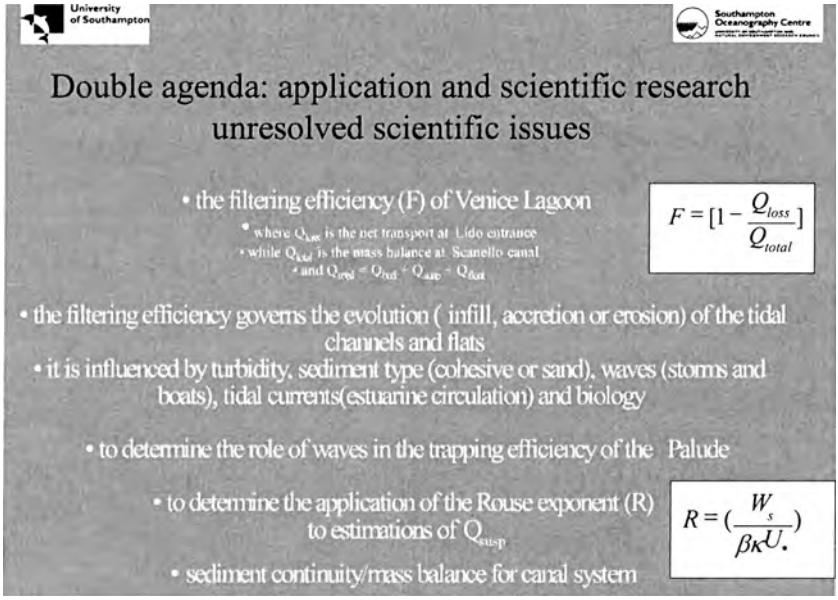

Fig. 2

ces Q_{total} , Figure 2). M_{total} is composed of three main components: Q_{bed} (the bedload), Q_{susp} (the suspended load) and Q_{float} (the floating load). Scanello canal is of particular interest due to clear evidence of resuspension during flood tides, and the phenomenon of floating aggregates on the ebb tide seen during the F-ECTS study (Amos, *et al.*, 2000). The aggregates are held buoyant by gas bubbles which may be the result of photosynthesis on the wide tidal flats seen landward or may be due to eutrophication due to hypersalinity caused by evaporation (Life-Barene, pers. comm., 2001). One of the objectives will be to examine this mechanism as a means of sediment export. We hypothesise that the aggregates are lifted off the tidal flats during tidal inundation and exported with the ebbing flow thus complicating evaluation of M_{loss}. The aggregates are not longer visible on the subsequent flood, so what has become of the aggregates? We will attempt to answer this question in this study and determine M_{total} and M_{loss} for the survey duration.

Instrumentation required to monitor each component of the sediment budget is shown schematically in Figure 3 which shows the sediment mass balance equation and the major boundary conditions to this mass balance. The first term is monitored by in situ benthic landers (e.g. AQUILA, STA-

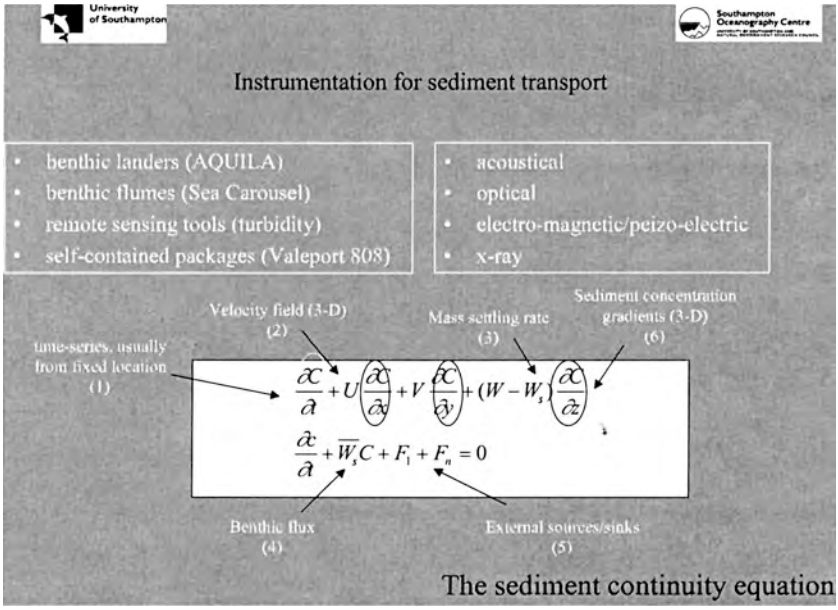

Fig. 3

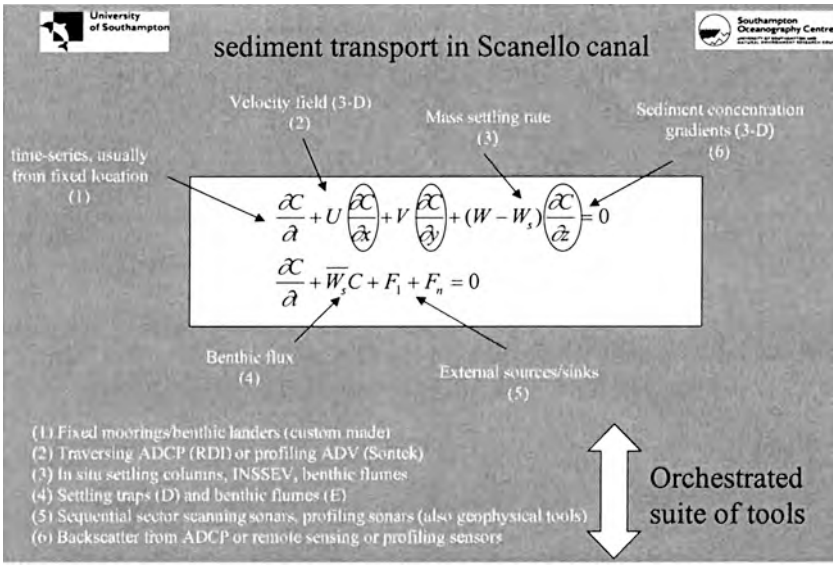

Fig. 4

BLE), the 3-D velocity field is measured using ADCP, spatial gradients in turbidity or is derived through numerical modeling (Umgiesser, 2000) (C) are determined by sampling and remote sensing. The major open boundary is the benthic flux which is best determined using benthic flumes such as Sea Carousel, while the external sources (rivers and open sea) remain to be solved. Thus an orchestrated suite of tools are required to be adopted together in order to close the mass balance of sediment in Venice Lagoon. A proposed suite of tools is shown schematically in Figure 4.

From an applied standpoint, it is the change in elevation (h) of the tidal flats that must be determined. This is defined as the difference in deposition (D) and erosion (E) which is equal to the benthic flux (W_sC) per unit time, per unit area, and by the divergence in the horizontal sediment transport rate ∇g_s (see Figure 5). Notice that sediment porosity is an important parameter to define, yet evidence from Venice Lagoon suggests much higher densities of recently-deposited sediments than are found in other estuaries.

We also know that even in regions dominated by fine-grained sediments there is a large bedload component. Flindt et al. (1997) have discovered large quantities of macrophytes (*Ulva rigida* and *Chaetomorpha aerea*) moving throughout Venice lagoon close to the bed at current

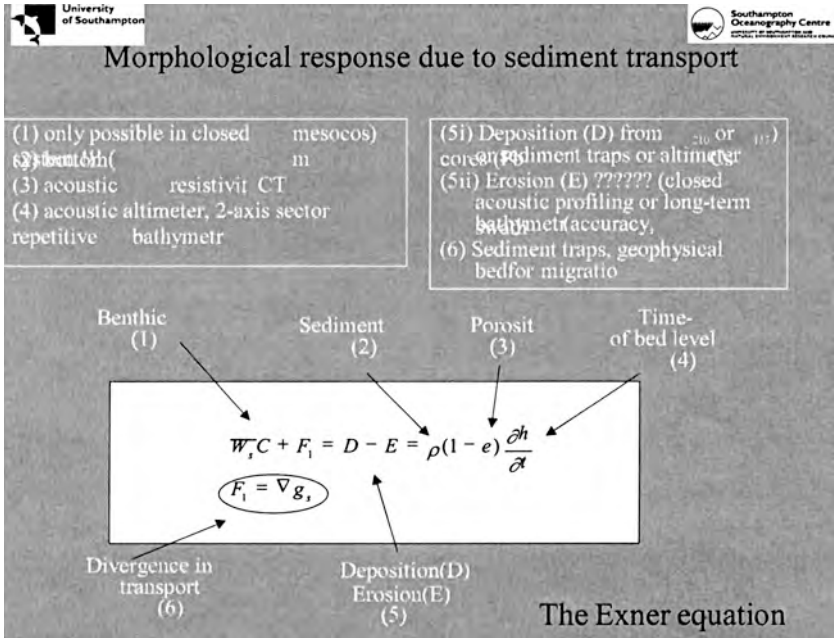

Fig. 5

speeds as low as 0.02 m/s ! Furthermore, Sea Carousel deployments showed bedload transport of rip-up clasts during bed erosion; this component is largely unquantified yet contributes to the evolution of the tidal flats (in the form of submerged beach development). As well, it enhances erosion through the action of the ballistic momentum flux, also known as the solid-transmitted stress (Amos, Sutherland *et al.*, 2000). The model of SEDTRANS has included this component of the stress in the estimation of the total bed shear stress. Laboratory simulations of this effect have been made by Levy (2000) and Flindt *et al.* (2000) who show that the threshold of erosion is governed by the onset of motion of the macrophytes (0.02 m/s) and not by the bed properties, and that erosion rates can be 1-2 orders of magnitude greater than that due to the fluid-transmitted stress (Amos, *et al.* 2000; Thompson et al. in press).

The effect of waves and wave resuspension in Venice is central to understanding tidal flat evolution. Work by Williams *et al.* (in press) show that energy spectra under waves are very similar to those of unidirectional flows measured within the benthic boundary layer. Also, energy dissipation in the inertial sub-range falls off as the Kolmogoroff scale of $f^{5/3}$

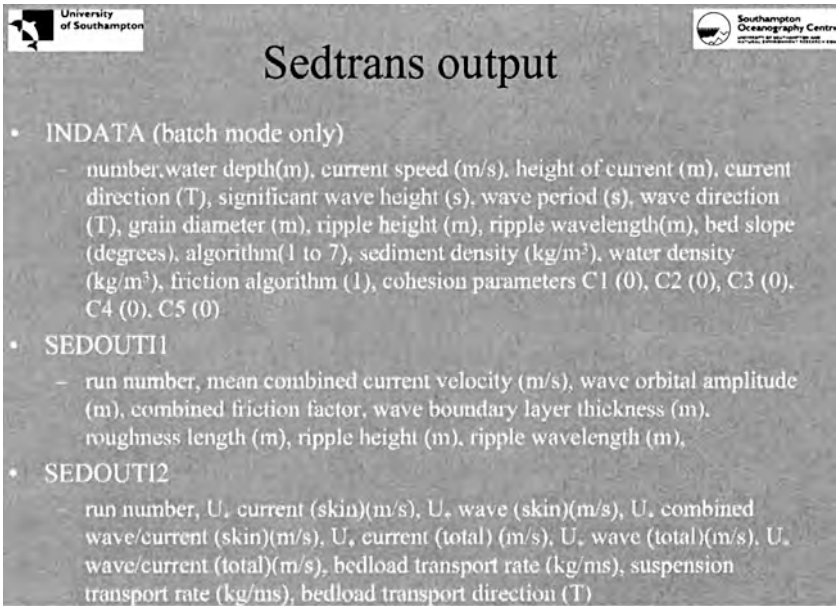

Fig. 6

which suggests a wave bed shear stress may be estimated. The waves in Venice Lagoon are complex to model because waves are not simple Airy types and possess neither clearly-defined crestlines nor simple propagation directions. As is not the waves that influence the bed, but pressure fluctuation induced by the waves, high-frequency (4 Hz) flow measurements made under varying wave climates (including ship passage) will help to provide an understanding of (1) the bed shear stress induced by waves, and (2) the contribution of this stress to resuspension.

All data will be combined within SEDTRANS which is presently being coupled with the 2-D hydrodynamic model of Venice Lagoon of Umgiesser (2000). The input and output parameters of SEDTRANS are shown in Figure 6. In particular, the cohesion parameters (C1 to C5) have been the subject of study under the F-ECTS programme and form the basis of Amos et al. (in review).

The main scientific objectives of the study of tidal flat stability undertaken herein are:

- to determine the mass balance of sediment across the mouth of Scanello canal (situated in the northern lagoon) over a 2-week period, and to determine which factors, other than tidal asymmetry, control this mass

balance; in particular we will monitor and quantify the mass transport of floating aggregates, and attempt to determine this contribution to the sediment mass balance; this will be carried out using a traversing ADCP to map the 3-D distribution of currents and turbidity within the canal.

- to determine the bedload transport rate and direction as a function of flow conditions, and the relative contribution of bedload to the sediment mass balance. To determine the organic/inorganic components to bedload, and the range of flow conditions under which each component is mobile. Finally, to determine the contribution of bedload to resuspension (scouring and stability) of Scanello canal and the application of the Roussian relation $(\frac{W_s}{\beta\kappa U})$ to concentration gradients ()

  under waves and currents; this will be carried out by deploying an ultrasonic sector-scanning sonar a strategic points within the canal on a fixed tripod for (1) time-series analysis of the canal bed, and (2) to profile laterally the passage of material as bedload and the vertical distribution of this material (the flux curtain principle).
- to determine the energy spectrum of nearbed flows under (1) pure tidal conditions, (2) tidal currents and natural waves, and (3) pure wave motion within Scanello with a view to examining the possibility of defining the wave contribution to the Reynolds stress, turbulent kinetic energy, and energy dissipation within the benthic boundary layer. Thereafter, to attempt to correlate these stress calculations to turbidity measurements; this will be achieved using the self-logging EM flow meters which will burst sample throughout the water column at 4 Hz for 5 minutes each 60 minutes;
- to examine tidal front dynamics with reference to the Treporti/Burano confluence in order to define the scouring potential of these fronts; and
- to determine the role of submerged beaches in the protection of tidal flats from wave erosion.

1.3 *The background of fine-grained sediment transport relevant to this study.*

The transfer functions which link hydrodynamic processes with sedimentation response are well know for sand (> 63 microns), but virtually unknown for fine-grained sediments (< 63 microns) which characterise Venice Lagoon. The reason for this is that (1) they are dependent on the bio-chemical character of the material which control flocculation, cohesion and adhesion, and (2) on the depositional history (consolidation, biostabilization, gas formation, bioturbation, etc.) which controls the

shear strength, bulk density and fabric of the bed. These factors are site specific. Thus results from laboratory experiments on abiotic material, or taken from other estuaries cannot be applied directly to Venice Lagoon. Furthermore, existing numerical simulations of the sedimentation process of fine-grained sediment are over-simplistic and miss the fundamental mechanisms of sedimentation which govern long-term evolution. Amongst these omissions are:

- The time/depth dependency of the erosion threshold and friction angle
- The time/concentration dependency of the deposition threshold
- The time dependency on erosion rate
- The concept of degree of retention as a function of flow rate and turbulence
- The impact of the solid-transmitted stress through bedload transport
- The impact of suspended load on fluid-transmitted stress reduction
- The relationship between bed shear stress and bed roughness, and the time-variation due to bursting and sweeping phenomena
- The time-scale of flocculation/aggregation and impact on particle settling rate
- The resuspension of aggregates during storms and the mapping of density/settling rate as a function of storm intensity
- The interaction of waves and currents within the benthic boundary layer
- The impact on second-order waves (cnoidal/solitary) on sediment transport and resuspension
- The in situ pore pressure build-up under waves and the potential for liquefaction
- The application of the Rouse profile to wave-dominant conditions
- The effects of buoyancy on the mean sediment flux

The list is not exhaustive, but provides insight into the depth of ignorance over the fundamental factors influencing mudflat evolution. A review of the detailed objectives of the first field campaign (August, 2001) is given in Figure 7. Below is a brief account of some of the results obtained within this survey. A series of reports as well as the raw data have been compiled on a series of CD-roms available through CORILA.

2. *Results.*

The survey of August, 2001 concentrated on the region from the Lido entrance to Burano which is located within northern Venice Lagoon. As stated above, four major activities were undertaken which include (1) a survey of the mass transport of sand within the Lido entrance; (2) tidal front analysis and resulting bed scour off Treporti; (3) evaluation of the

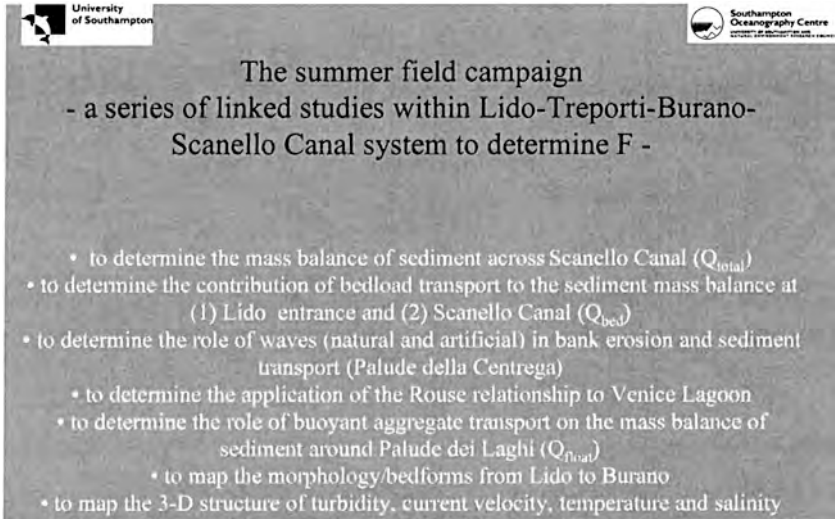

Fig. 7

dynamics of submerged beaches discovered off Treporti; and the sediment mass balance in the Scanello-Burano canal system (see Figure 8). The study involved a regional survey of the Treporti-S. Felice-Burano-Scanello canal system. These data are strongly linked to measures of sedimentation underway by Cappucci (2002) since 1998 on Palude della Cona. Reports

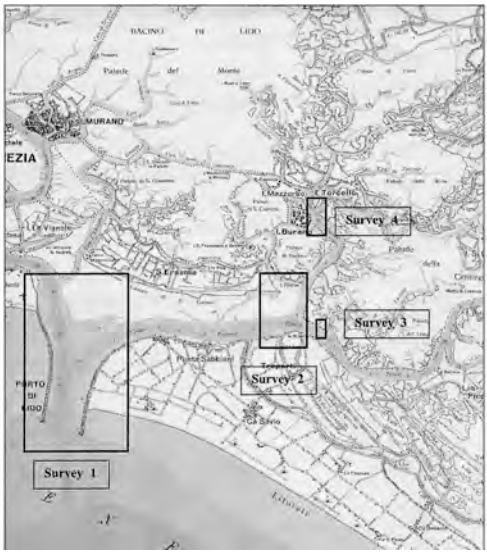

Fig. 8

on these four surveys are found in Chick (2002), Reed (2001), Tremblay (2002), and Munford (2002) respectively.

2.1 *Initial results of the tidal front survey.*

A bathymetric survey of the scour off Treporti was undertaken and water depths in excess of 20 m were found. This scour was associated with a tidal front that appears periodically at the confluence of the ebbing water masses of Burano and S. Felice canals off Treporti. The development of the front has been monitored in detail by Reed (2001) using a traversing ADCP, and several points of conclusion were made. Several examples of the ADCP profiles are shown in Figure 9 which shows the strength of back-scatter within the water column (a measure of particulate matter). The profiles are from north to south off Treporti and show the development of the tidal front. Figure 9A was taken close to high water; ebbing had begun in Burano canal whilst the waters were still flooding S. Felice. The tidal front of these two water masses is clear in Figure 9B and extends from the sea surface to the bed in the shoal region between the two canals. As well, a second from can be seen developing close to the margin off Treporti. Perhaps of more importance, is the development of a strong front in centre channel. Suspension either side of the front is evident (high back-scatter close to the bed) during early ebb in Figure 9C within the scour hole. Thus frontal dynamics appear important in the morphological evolution of the bed of Venice Lagoon.

A calibration of turbidity to ADCP back-scatter was attempted but showed considerable scatter in results. A summery of the data is given in Table 1. The reason for the scatter is simply the fact that the majority of material in suspension was organic matter.

Strong residual currents were found within the Treporti-Burano canal system. These residuals have a profound affect on the mass balance of sediment within Venice Lagoon. A summary of the mass transport of water in the survey area is given in Table 2. Notice that S. Felice shows a net inflow of 2.6 x 107 m^3 on the flood, but a net ebb of only 1.7 x 107 m^3 showing residual mass movement of over 10 million m^3 towards the northern lagoon each tide (Reed, 2001).

2.2 *Initial results of the submerged beach survey.*

A series of submerged beaches were discovered during the summer field campaign around the margins of Palude della Centrega. These beaches were particularly well developed in the region east of the confluence

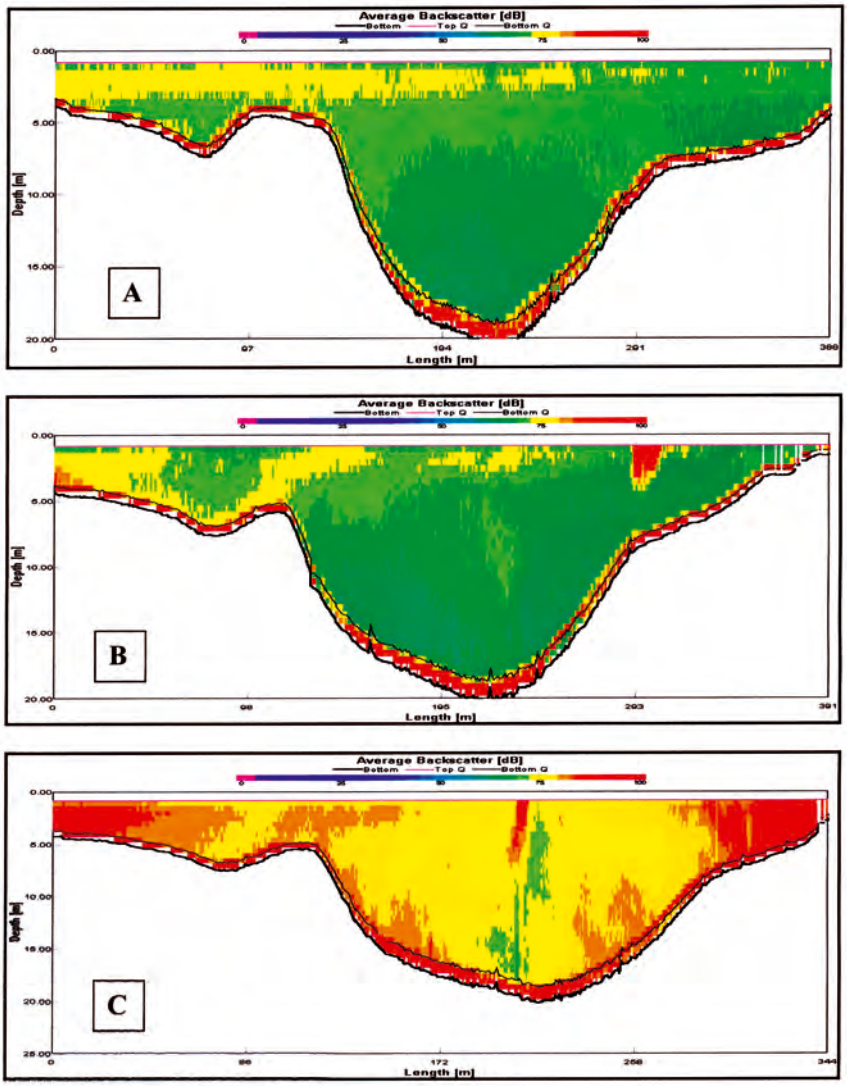

Fig. 9

of the Treporti and Burano canals. The beaches were composed entirely of fine sand were perched on the eroded shoulder of the Pallude. A schematic of the submerged beach and the equipment used to study its dynamics is shown in Figure 10. The mean grain size of the sand was order 125 microns and appeared to decrease in size with water depth. Wave suspen-

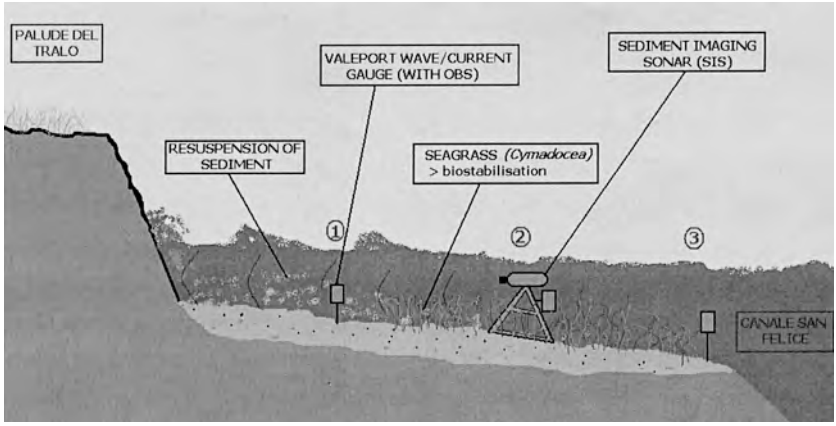

Fig. 10

sion of the sand was visible close to the palude cliff, whilst the seagrass *Cymadocea nodosi* was present in the deeper parts. Three Valeport 808 sensors (current velocity, pressure, and turbidity) were underdeployed across the transect to monitor the passage of waves, the magnitude of the

Table 1 - Concentrations of Suspended Sediment and Backscatter.

Transect no.	Canal	Acoustic Backscatter level (dB)	Total Backscatter Concentration g/m^3	Suspended Sediment Concentration g/m^3	Transect no.	Canal	Acoustic Backscatter level (dB)	Total Backscatter Concentration g/m^3	Suspended Sediment Concentration g/m^3
2	Burano (i)	70	182.74	125.63	30	Burano (i)	74	112.39	71.52
4	Burano (ii)	65	138.86	87.60	32	Burano (ii)	73	108.04	67.17
6	Burano (i)	69	111.22	80.74	34	Burano (i)	76	160.47	97.65
8	Burano (ii)	74	144.39	92.29	34	Burano (i)	81	130.65	77.55
10	Burano (i)	68	177.72	111.05	36	Burano (ii)	70	158.12	97.65
10	Burano (i)	72	169.18	113.90	36	Burano (ii)	74	120.60	71.52
12	Burano (ii)	65	130.65	80.40	40	Burano (ii)	68	141.54	89.28
12	Burano (ii)	69	164.32	115.74	42	Burano (i)	72	154.44	96.98
14	Burano (i)	72	171.19	121.10	44	Burano (ii)	80	158.29	106.03
16	Burano (ii)	82	159.96	112.56	46	Burano (i)	80	138.52	91.12
18	Burano (i)	78	149.58	94.97	46	Burano (i)	88	176.04	113.57
20	Burano (ii)	82	162.98	99.66	48	Burano (ii)	80	154.44	100.00
22	Burano (i)	77	183.41	122.78	48	Burano (ii)	85	189.28	128.81
22	Burano (i)	81	196.81	133.00	50	Burano (i)	82	184.42	130.32
24	Burano (ii)	80	150.75	68.68	52	Burano (ii)	82	147.57	91.46
24	Burano (ii)	86	201.84	131.15	52	Burano (ii)	86	147.23	94.30
26	Burano (i)	80	204.85	144.22	54	Burano (i)	83	142.38	82.08
28	Burano (ii)	83	139.53	82.24					

Table 2 - Levels of Q averaged throughout the tidal cycle

Treporti (C)		Centre of Intersection		San Felice (A)		Burano (A)	
Start time	Q Discharge (M^3/s)	Start time	Q Disharge (M^3/s)	Start time	Q Disharge ((M^3/s)	Start time	Q Disharge (M^3/s)
06:16	1692.57	06:20	1222.47	06:45	1248.47	07:03	581.58
07:26	2001.02	07:30	1513.23	07:33	1367.01	07:47	540.35
08:09	2041.09	08:12	1625.06	08:15	1505.7	08:28	486
09:08	1833.27	09:13	1401.43	09:16	1337.05	09:30	328.92
10:12	1255.55	10:15	1112.01	10:22	979.32	10:44	-1.55
11:06	501.31	11:12	513.88	11:15	436.43	11:42	-242.78
12:09	-986.96	12:13	-763.41	12:18	-665.04	12:38	-406.96
13:12	-1790.88	13:15	-1440.6	13:19	-1225.71	13:34	-496.93
14:10	-1495.24	14:14	-1295.35	14:18	-1121.26	14:47	-252.74
15:09	-1254.96	15:12	-1053.44	15:15	-931.51	15:36	-130.91
16:16	-494.12	16:19	-494.53	16:23	-444.25	16:38	177.53
17:07	856.18	17:11	583.43	17:14	591.45	17:27	607.2
Approx.	1400	Approx.	900	Approx.	900	Approx.	600
Σ of Flood Q	11580.99	Σ of Flood Q	8871.51	Σ of Flood Q	8365.43	Σ of Flood Q	3321.58
Ave.Σ of Flood Q	1447.62375	Ave.Σ of Flood Q	1108.93875	Ave.Σ of Flood Q	1045.67875	Ave.Σ of Flood Q	415.1975
Σ of Ebb Q	-6022.16	Σ of Ebb Q	-5047.33	Σ of Ebb Q	-4387.77	Σ of Ebb Q	-1110.01
Ave.Σ of Ebb Q	-1204.432	Ave.Σ of Ebb Q	-1009.466	Ave.Σ of Ebb Q	-877.554	Ave.Σ of Ebb Q	-222.002
Total discharge Q through flood (m^3)	3.65E+07	Total discharge Q through flood (m^3)	2.79E+07	Total discharge Q through flood (m^3)	2.64E+07	Total discharge Q through flood (m^3)	1.05E+07
Total discharge Q through ebb (m^3)	-2.38E+07	Total discharge Q through ebb (m^3)	-2.00E+07	Total discharge Q through ebb (m^3)	-1.74E+07	Total discharge Q through ebb (m^3)	-4.40E+06

tidal flows and the general turbidity of the water masses. As well, a Sediment Imaging System (SIS) was deployed at the outer limit looking landwards. The SIS logged the backscatter within the water column continuously through two days of surveying. An example of a scan is shown in Figure 11. The figure shows the shoaling bed of the submerged beach and the less well defined water surface. Unfortunately, the sea state was calm and so very little resuspension was evident in the data. Consequently, this survey will be repeated during February, 2003.

2.3 *Initial results of sand transport and bedforms in Lido inlet.*

A sidescan mosaic of the outer part of Lido canal was undertaken in asssociation with a series of ADCP profiles across the inner part of the Lido entrance (San Nicolo to Punta Sabbioni). The sidescan survey sho-

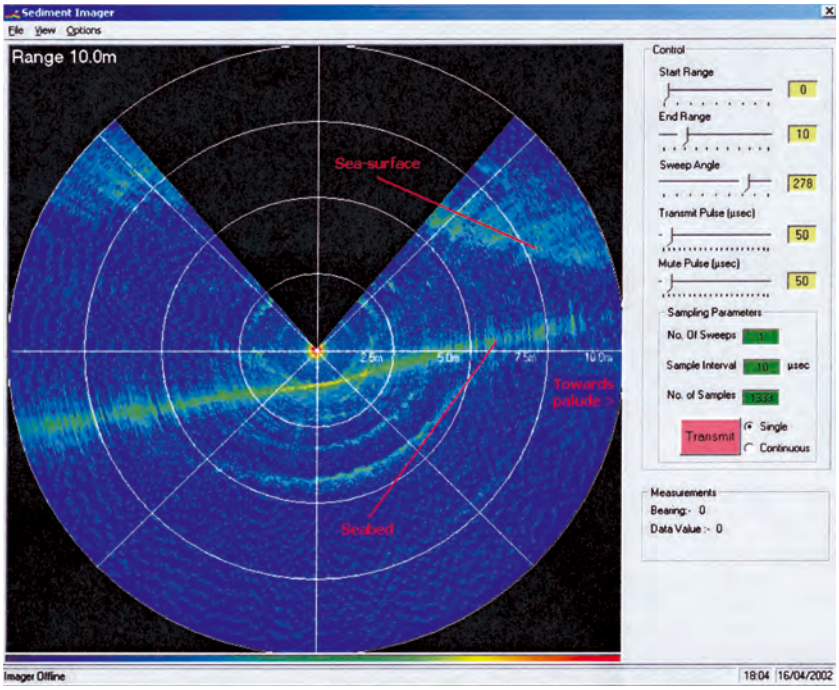
Sediment Imager
File View Options
Range 10.0m
Sea-surface
Seabed
Towards palude >
Control
Start Range
End Range
Sweep Angle
Transmit Pulse (usec)
Mute Pulse (usec)
Sampling Parameters
No. Of Sweeps
Sample Interval
No. of Samples
Transmit
Single
Continuous
Measurements
Bearing:- 0
Data Value :- 0
Imager Offline
18:04 16/04/2002

Fig. 11

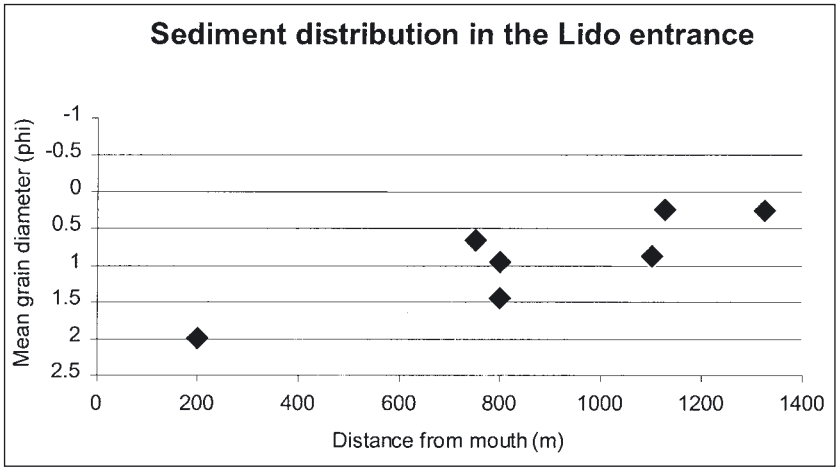
Sediment distribution in the Lido entrance
Mean grain diameter (phi)
-1
-0.5
0
0.5
1
1.5
2
2.5
0
200
400
600
800
1000
1200
1400
Distance from mouth (m)

Fig. 12

wed a dynamic seabed composed of asymmetric megaripples (oriented towards the land), sand ribbons, and regions of shelly gravel. Bottom samples were also collected in order to calibrate the sidescan sonograms. The size analysis of these sands are shown in Figure 12. A decrease in grain size is evident with distance into the Lagoon. The current data from the ADCP survey was used as input to SEDTRANS in order to evaluate the potential sand transport rates at the time. A strong import was apparent in the results which was greatest along the northern margin and least along the southern margin.

Acknowedgments.

This study has been supported by funds from CORILA under the project Hydrodynamics and morphology of the Venice Lagoon (3.2). We thank C. Cottrill, D. Brown and D. Paphitis (Southampton University) for their efforts in the field.

References.

Amos C.L., Sutherland T.F. et al., 2000. Corrosion of a remoulded cohesive bed by saltating littorinid shells. Continental Shelf Research 20: 1291-1315.

Amos C.L. et al., 2000. The Venice Lagoon Study (F-ECTS) Field Results - February, 1999. Geological Survey of Canada open File Report 3904.

Amos C.L., Cappucci S., Bergamasco A., Umgiesser G., Bonardi M., Cloutier D., Flindt M., De Nat L. and Cristante S., in review. The stability of tidal flats in Venice Lagoon - the results of two in situ benthic annular flumes. Journal of Marine Systems.

Cappucci S., 2002. Sedimentation processes on a tidal flat in Venice Lagoon. Unpublished PhD. University of Southampton, UK., 173p.

Carbognin L. and Cecconi G., 1997. The Lagoon of Venice, Environmental Problems and Remedial Measures. Meeting on Environmental Sedimentology, Venice: 71p.

Chick C., 2002. The distribution of bedforms in Lido inlet Lagoon and sand transport rates, Venice Lagoon. Unpublished B.Sc. Thesis, University of Southampton, UK., 88p.

Flindt M. et al., 1997. Loss, growth and transport dynamics of Chaetomorpha aerea and Ulva rigida in the Lagoon of Venice during an early summer field campaign. Ecological Modelling 102: 133-141.

Grillo S. 1989. Venezia, Le Difese a Mare. Publ. Arsinale Editrice, Venice: 253p.
Holloway, P., 1981. Longitudinal mixing in the upper reaches of the Bay of Fundy. Estuarine, Coastal and Shelf Science 13: 495-515.
Levy A., 2000. The effects of the macrophytes on bed stability. Unpublished M.Sc. Thesis, Acadia University, Canada.
Montanelli I., Samona G. and Valcanover F., 1970. Venezia, Caduta e Salvezza. Publ. Sansoni Nuovi Spa: 28p.
Munford G., 2002. The role of submerged beaches in the salt marsh protection in Venice Lagoon. Unpublished B.Sc. Thesis, University of Southampton, UK., 63p.
Schubel J.R. and Carter H.H., 1984. The estuary as a filter for fine-grained suspended sediment. In The Estuary as a Filter (V.S. Kennedy, ed). Publ. Academic Press: 81-105.
Reed P., 2001. An ADCP survey of a tidal front in northern Venice Lagoon. Unpublished M.Sc. Thesis. University of Southampton, UK.,39p.
Thompson C., Amos C.L., Lecouturier M. and Jones T.E.R., in review. A new method to determine drag coefficient over naturally roughened beds. Journal Geophysical Research.
Tremblay G., 2002. Dynamique sedimentaire du Canale Burano, Lagune de Venise. Unpublished B.Sc. Thesis, University of Quebec a Rimouski, Canada, 24p.
Umgiesser G., 2000. Modeling residual currents in the Venice Lagoon. In. Interactions between Estuaries, Coastal Seas and Shelf Seas. T. Yanagi (ed), Terra Scientific Publishing Company, Tokyo, 107-124.
Williams J.J., Bell P.S., Humphrey J.D., Hardcastle P.J. and Thorne P.D., in press. New approach to measurement of sediment processes in a tidal inlet. Continental Shelf Research.
Zampetti P., 1976. Il Problema di Venezia. Publ. Sansoni Nuova SpA: 157p.

A CRITICAL EVALUATION OF HEAVY METALS CONTAMINATION OF VENICE LAGOON BOTTOM SEDIMENTS

L. Schiozzi[1], M. Bonardi[1], A. Basu[2]
[1]*Istituto per lo Studio della Dinamica delle Grandi Masse, CNR, Venezia,*
[2]*Indiana University, Bloomington, USA,*

Abstract.

Although several studies have been conducted on the trace metals distribution of bottom sediments of the Lagoon of Venice, they were neither coordinated nor did they follow similar methodologies for sampling and analysis. Hardly any quantitative consideration was given to textural and compositional characteristics of the sediments before reporting geochemical data and evaluating their significance. Comparison of published data of heavy metal content in bottom sediments of the Lagoon of Venice is therefore, very often, impossible.

Key words.

Lagoon of Venice, northern lagoon basin, bottom sediments, trace elements, geochemical data set.

1. *Introduction.*

The majority of laws regulating pollution establish (state) that a substance, and therefore sediment, is "toxic and hazardous" when the sum of each toxic element with respect to the maximum allowed value identifies the different degrees of alteration. Without considering whatsoever the validity of a given critical value, or maximum allowable concentration provided for by law, the importance of being able to distinguish conditions of technical genetic changes from natural changes in a geo-environ-

mental context and below a certain acceptable concentration should be emphasized. That is, changes connected to source areas that have been modified in some way due to the presence of naturally high concentrations of one or more trace elements.

Assessing the degree of sediment contamination, therefore, depends on the choice of suitable natural, geochemical background values. For the Venice Lagoon these are especially difficult to define since its morphological and geological configuration result extremely detailed. Modifications to the basin occurred in the course of time were also due to human activities centered there. Moreover, though since the seventies different studies by different authors have been made, both the researcher and the legislator find themselves in difficulty because the various datasets of available information are hard to compare. Accurate detailed descriptions are often missing on the sampling site, sampling methods, analytical methods and instruments used, concentration determinations of major elements and especially the characteristic texture and composition of analyzed sediments as summarized in Table 1. As a matter of fact the grain-size and mineralogy of sediment are absolute parameters, if one wants to estimate the possible presence of contaminated elements and particularly heavy metals. In fact, the latter can vary by some orders of magnitude depending on the nature of the rock source, action of atmospheric factors, and transport and erosion processes (Loring & Rantala, 1992).

In Table 2 a series of possible allowable concentrations is given.

To show how values of some heavy metal concentrations in bottom sediments are difficult to compare, we give as an example, the comparison made between concentrations of Fe, Cr, Co, Ni, Cu, Zn, and Pb in sediment samples from the north lagoon basin collected by Donazzolo between 1976 and 1979 (Donazzolo et al., 1984) and those, still unpublished, of the samples taken in 1996 by Basu and Bonardi.

2. *Materials and methods.*

In 1996, 30 bottom samples were collected with a Van Veen grab; each sample is representative of the first 20 cm of collected sediment. Textural, mineralogical and geochemical analyses were carried out on each sample. The sandy fraction (2 mm - 62.5 mm), previously separated from the > 2mm fraction, was analyzed by sieving, while pelite was analyzed by photosedigraph analysis (Fritsch, Analysette 20). Semi-quantitative mineralogical analyses were carried out on a fraction < 62.5 mm using the x-ray

Table 1 - Geochemical studies on sediments from the Lagoon of Venice.

Author, year	Location	Sediment type	Leaching technique	Analytical instrument used	Grain-size	Mineralogy	Major elements	Other analyses
Donazzolo et al., 1982	Northern Basin	Core sediments	HNO_3 8N	AAS	% Pelite	No	Fe	^{210}PB, ^{226}Pb
Barillari et al., 1982	Petta di Bo' S. Angelo della Polvere	Bottom sediments	HF HNO_3, $HClO_4$	AAS	Detailed	Carbonates	%	TOC
Donazzolo et al. 1984	Whole Lagoon	Bottom sediments	HNO_3 8N	AAS	Bibliographic data	No	Fe	No
Pavoni et al., 1987	Central Basin	Core sediments	HNO_3 8N	AAS	No	No	Fe	TOC, N, P, Eh, pH
Campanaro et al., 1987	Valle di Brenta	Bottom sediments	Three extractions: a. HCl 1N; b. HNO_3; c. HF HNO_3, $HClO_4$	AAS	No	No	No	Chlorinated hydrocarbons
Menegazzo Vitturi et al. 1987	Central Basin	Sub-superficial sediments	HF, HNO_3, H_2SO_4	AAS	No	No	Al, Fe, Ca, Mg, Na, K	TOC, P
Bernardi et al., 1988	Palude della Cona	Bottom sediments	HCl 1N	PIXE	No	No	No	No
Pavoni et al., 1988	Whole Lagoon *(Donazzolo et al., 1984)*	Bottom sediments	HNO_3 8N	AAS	No	No	Fe	No
Bastianini et al., 1989	Industrial Zone Northern Basin	Core sediments	No	XRF	No	No	Mg, Al, Si, S, Cl, K, Ca, Ti	TOC, ^{210}Pb, ^{137}Cs
Zonta et al., 1994	Palude della Cona	Bottom sediments	Two extractions: a. HCl 1N; b. HNO_3	AAS	Detailed	No	Fe	SEM
Basa & Molinaroli, 1994	Whole Lagoon *(Donazzolo et al., 1984)*	Bottom sediments	HNO_3 8N	AAS	No	No	Fe	No
Sfriso et al., 1995	Alberoni Sacca Sessola S. Giuliano	Bottom sediments	HF and aqua regia in teflon bombs	AAS	No	No	Fe	KPH_2 phytoaromahum
Frignani et al., 1997	Northern Basin Central Basin	Core sediments	No	XRF	% Sand, silt, clay	Silicates, Calcite, Dolomite	Al, Fe, Ca, Mg, Si	^{210}Pb, ^{137}Cs
Perin et al., 1997	Central Basin	Bottom sediments	Sequential extractions (5 steps)	AAS	% Sand, pelite	Complete (XRD)	Fe	No
Cochran et al., 1998	Campalto S. Erasmo S. Felice	Core sediments	No	XRF	No	No	No	^{210}Pb
Ministero dei Lavori Pubblici, Magistrato alle Acque, Consorzio Venezia Nuova, 1999	Whole Lagoon *(Donazzolo et al., 1984)*	Bottom sediments, Core sediments	CVN, IRSA-CNR, US EPA certified methodologies		%, > 2mm, sand, pelite	No	No	TOC, Physical features, Hydrocarbons, PCB, IPA, PCDD

powder diffraction on a Philips PW 1800/10 diffractometer, following standard procedures (Biscaye, 1965; Wilson, 1987). Geochemical analyses were performed on fractions < 2 mm, by total acid digestion with a mixture of hydrofluoric, nitric, and perchloric acid; samples were treated after a series of controlled drying was done to desiccate them and then diluted with hydrochloric acid. The solutions obtained were analyzed by means of a PerkinElmer Optima 3000 ICP Optical Emission Spectrometer.

3. *Results and Discussion.*

Lacking information, as we have seen, on the texture and composition of sediments in a large part of the series given in the literature, it was believed that a preliminary comparison could be made only on material belonging to sediment families of similar origin (after Brambati, 1968). Therefore, it was decided to consider only the bottom samples coming from the north lagoon basin, since this area is that which is texturally more homogeneous, showing average pelite content higher than 70%, inside the whole Venice lagoon system (Barillari, 1978; Barillari, 1981; Ministero dei Lavori Pubblici, Magistrato alle Acque through its concessionary

Table 2 - Examples of possible background concentrations.

Fe	Mn	Cr	Ni	Cu	Zn	Pb	Cd	As	Hg	
Prater & Anderson, 1977 Unpolluted sediments										
< 17000		< 25	< 20	< 25	< 90	< 40			< 0.1	
Chesler & Voutsinou, 1981 Unpolluted sediments										
	754	26	38	9,5	21	20				
Voutsinou-Taliadouri, 1995 Unpolluted sediments										
	170-980	14-180	12-207	3-35	17-72	5-32				
Whitehead et al., 1984 Background concentration values for Mediterranean Sea sediments										
7.1 ± 3.4 (%)	370 ± 330	16 ± 13		19 ± 10	63 ± 43	26 ± 23	0.13 ± 0.13			
Selli et al., 1977 Adriatic Sea sediments										
		44,8	49,8	25,1	88,7	32	0,7		0,3	
Donazzolo et al., 1982 Lagoon of Venice sediments										
7500		21	20	15	49	23	1,2		0,1	
Donazzolo et al., 1987 Lagoon of Venice sediments										
20000		20	20	20	70	25	1,0		0,1	
Ministero dei Lavori Pubblici, Magistrato alle Acque di Venezia through its Concessionary Consorzio Venezia Nuova (Jobstruibizer), 1999										
		63 / 106	28 / 49	29 / 75	121 / 615	68 / 91				1
		37 / 90	20 / 34	14 / 30	45 / 84	20 / 40				2
		47 / 124	25 / 62	24 / 69	55 / 161	30 / 50				3
Lagoon of Venice - Classification of dredged material for reuse as landfill in the lagoon following Protocol 8/4/93										
		20	45	40	200	45	1		0,5	4
		100	50	50	400	100	5		2	5
		500	150	400	3000	500	20		10	6
Ministero dei Lavori Pubblici, Magistrato alle Acque di Venezia through its Concessionary Consorzio Venezia Nuova, 1999 - Bottom sediments										
		37 ± 15	24 ± 24	18 ± 9	60 ± 35	28 ± 12			0.8 ± 0.6	7
		35 ±11	19 ± 5	25 ± 15	143 ± 129	40 ± 21			1.2 ± 0.7	8
		42 ± 14	23 ± 10	18 ± 16	80 ± 78	37 ± 30			0.44 ± 0.17	9
		59 ±14	31 ± 10	111 ± 108	469 ± 412	169 ± 175			7.0 ± 9.1	10
		41 ± 16	22 ± 7	20 ± 9	76 ± 41	33 ± 14			0.62 ± 0.25	11
Ministero dei Lavori Pubblici, Magistrato alle Acque di Venezia through its Concessionary Consorzio Venezia Nuova, 1999 - Lagoon of Venice core sediments										
		26,1	15,9	15,6	48,1	23,0	0,59		0,7	12
		32,6	17,6	18,5	72,1	28,8	0,54		0,8	13
		30,1	19,1	17,1	56,4	24,4	0,63		0,7	14
		32,5	19,4	13,1	42,6	21,3	0,56		0,1	15
		51,1	27,3	19,4	83,3	32,5	0,50		0,5	16
		53,9	27,6	20,8	92,5	33,4	0,63		0,5	
		55,3	27,6	17,3	60	29,6	0,50		0,4	
		50,1	29,9	11,8	38,8	21,6	0,50		0,2	
		33,5	17,3	18,5	90,5	30,8	0,75		0,7	17
		37,3	19	19,3	83,3	37,3	0,63		0,6	
		38,8	20,3	20,5	103	34,5	0,75		0,8	
		34,8	21,3	14,5	55,8	20,5	0,50		0,2	
		61,3	35,3	145	625	229,3	10,7		10,2	18
		52,7	22	123	620	224,7	16,3		8,2	
		85,7	29,7	260	990	330,0	33,3		25,1	
		34,3	20	30,7	88	37,7	1,3		1,7	

All concentrations are expressed in ppm, unless otherwise indicated; 1, 2, 3 - Median and threshold values of heavy metal concentrations for 30 samples of surface sediment from the lagoon of Venice; (2) Core data between 100 and 200 cm (after Consorzio Venezia Nuova, 1999); (3) Investigated data from the Pili area (deep core: - 20 m); 4, 5, 6 - Class

Consorzio Venezia Nuova, 1999) and, moreover, because from a mineralogical point of view these sediments are mostly coming from the Piave river output and only limitedly to those of the Adriatic Sea. Furthermore, Piave sediments are more significant than those linked to the loads from river affluents in the south lagoon, since they are mainly composed of carbonates (Jobstraibizer & Malesani, 1973; Ministero dei Lavori Pubblici, Magistrato alle Acque di Venezia through its concessionary Consorzio Venezia Nuova, 1999 - Jobstraibizer) naturally and poorly enriched with trace elements (Jobstraibizer et al., 1995). Moreover, Donazzolo et al. (1984) are among the few authors who give tables that avoid graphic extrapolations and other elaborations for each single sample; finally, data relative to the end of the seventies can be considered particularly significant identifying the end of the industrial boom of the Porto Marghera, considered the source area (Basu & Molinaroli, 1994) for a large part of contaminated substances present in the Venice lagoon sediments, and the introduction of a more specific law for environmental protection.

Therefore, the comparison between Donazzolo's data (Donazzolo et al. 1984) and Basu-Bonardi's unpublished data appears to be the simplest and the most significant considering the amount of available information on the northern basin of the Venice Lagoon.

Of the 30 sampling stations sampled by Basu and Bonardi in 1996, the 19 stations closest to the 20 sites sampled by Donazzolo et al. (1984) were considered (Fig. 1). As can be deduced from Table 3, the average distance between sampling points is about 1.1 ± 1.8 km, varying from a minimum of 0 km in correspondence of stations 23BB and 163DON to a maximum of 9.0 km (stations 36BB and 145DD).

Table 3 shows the concentrations of Fe, Cr, Co, Ni, Cu, Zn, and Pb measured by the different authors for the stations taken into consideration.

Concerning the samples taken in 1996, the average Fe concentration is equal to 2.29 ± 0.87 %. Among the trace elements considered, Zn and Cr are the most abundant (76 ± 43 ppm and 61 ± 11 ppm); followed by Pb (27 ± 17 ppm), Cu (25 ± 12 ppm), Ni (22 ± 7 ppm) and lastly Co (9 ± 3 ppm).

If the data of Donazzolo et al. (1984) are considered, we find that

---

A of Protocol 8/4/93; (9) Class B; (10) Class C; 7, 8, 9, 10, 11 - Mean concentration values of pollutants (contaminants?) in surface sediments in the following lagoon areas: (7) north lagoon; (8)central lagoon; (9) south lagoon; (10) industrial canals; (11) lagoon channels; 12, 13, 14, 15, 16, 17, 18 - Mean metal concentrations provided for by Protocol 8/4/93 subdivided according to depth: (12) 0-15 cm; (13) 15-50 cm; (14) 50-100 cm; 15 (100-200 cm) and geographic areas (12, 13, 14, 15) north lagoon; (16) central lagoon; (17) south lagoon; (18) industrial canals.

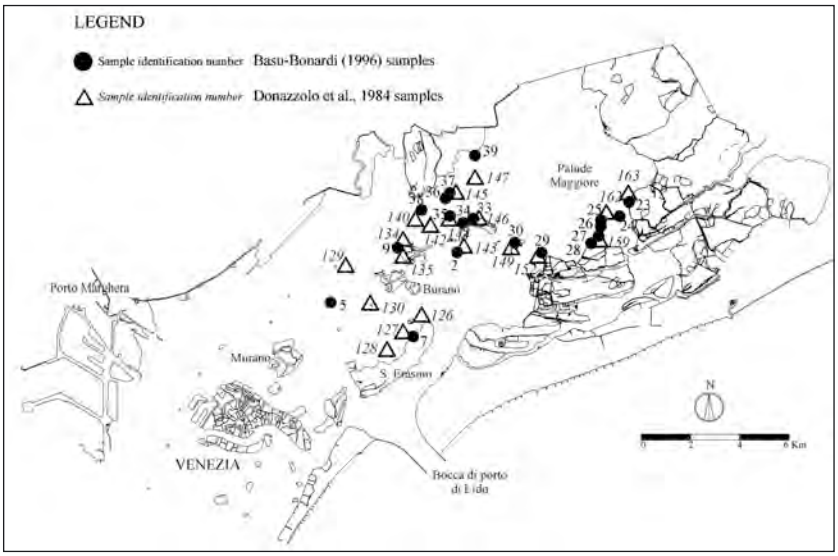

Fig. 1 - Sediment samples location of Basu-Bonardi and Donazzolo et al. (1984).

mean Fe concentrations are equal to 1.60 ± 0.37 ppm. Among the trace elements, the most abundant is always Zn (71.2 ± 21.8 ppm), while Cr, on the contrary, appears to be the element, among those considered, with the lowest concentration measured (13.6 ± 5.7 ppm). Pb, Cu, Ni and Co show, instead, mean content equal to 46.7 ± 8.5 ppm, 24.8 ± 7.2 ppm, 20.9 ± 3.31 ppm, and 13.9 ± 2.12 ppm, respectively.

Thus, considering mean concentrations of the single elements for all sampling stations studied, we see how the contents of the single analytes are difficult to compare (Fig. 2). Only Cu, Ni and Zn have similar mean concentrations; in fact, Basu and Bonardi's mean Cu concentrations are only 1% lower than those measured by Donazzolo et al. (1984), while those of Ni and Zn differ, respectively, by 4 and 6%. Contrarily, Fe concentrations with a percent difference on average equal to 30 %, and especially Co (-51 %), Pb (-73 %) and Cr (78 %) are correlatable between them with difficulty. In fact, the mean contents of Co and Pb measured by Donazzolo et al. (1984) are decidedly more considerable than those measured by Basu and Bonardi, while those of Cr are considerably less.

A preliminary interpretation of the differences found can be attributed to the type of acid digestion used to extract the elements studied. In fact, leaching with nitric acid 8N, like that adopted by Donazzolo et al. (1984), does not allow the total extraction of trace metals retained in the

Tab. 3 - Considered element concentrations in Basu-Bonardi (BB) and Donazzolo et al. (1984) (DON) samples and average percent difference on the two measures.

BB	DON	Distance (km)	Fe (BB) %	Fe (DON) %	% Diff.	Cr (BB) ppm	Cr (DON) ppm	% Diff.	Co (BB) ppm	Co (DON) ppm	% Diff.	Cu (BB) ppm	Cu (DON) ppm	% Diff.	Ni (BB) ppm	Ni (DON) ppm	% Diff.	Zn (BB) ppm	Zn (DON) ppm	% Diff.	Pb (BB) ppm	Pb (DON) ppm	% Diff.
2T	143	0,3	1,63	1,80	-10%	48	13,8	71%	5	14,0	-180%	22	30,4	-38%	22	22,6	-3%	74	90,0	-22%	19	52,0	-174%
5T	129	1,5	1,30	1,30	0%	68	12,0	82%	4	13,8	-245%	13	19,0	-46%	14	19,4	-39%	63	52,0	17%	11	41,4	-276%
	130	1,8		1,63	-25%		12,6	81%		14,0	-250%		24,4	-88%		18,4	-31%		92,6	-47%		45,8	-316%
7T	126	1,2	1,08	1,14	-6%	33	10,4	68%	4	17,0	-325%	12	18,8	-57%	18	19,6	-9%	43	62,0	-44%	10	43,0	-330%
	127	0,6		1,16	-7%		10,8	67%		18,2	-355%		20,2	-68%		18,0	0%		58,0	-35%		42,0	-320%
	128	1,3		1,16	-7%		9,6	71%		18,2	-355%		19,6	-63%		17,2	4%		54,0	-26%		47,6	-376%
9T	134	0,4	1,50	1,50	-39%	42	10,8	67%	4	11,2	-180%	19	33,8	-182%	24	17,2	4%	64	86,4	-101%	23	38,6	-286%
	135	0,4		1,50	0%		12,0	71%		14,2	-255%		23,8	-25%		20,0	17%		74,0	-16%		43,8	-90%
23	163	0,0	2,08	1,50	28%	76	10,4	86%	9	14,8	-64%	19	17,8	6%	18	21,4	-19%	68	46,0	32%	20	45,6	-128%
24		0,6	1,94		23%	58		82%	7		-111%	15		-19%	15		-43%	63		27%	20		-128%
25	162	0,6	1,93	1,45	25%	58	11,0	81%	7	13,0	-86%	15	18,8	-25%	15	20,6	-37%	52	52,4	-1%	20	42,4	-112%
26		0,4	1,45		0%	11		0%	13		0%	15		-25%	15		-37%	59		11%	15		-183%
27	159	0,5	2,02	1,72	15%	63	12,8	80%	10	14,4	-44%	19	19,6	-3%	19	24,6	-29%	78	50,0	36%	23	41,8	-82%
28		0,4	1,68		-2%	56		77%	11		-31%	15		-31%	15		-64%	59		15%	17		-146%
29	152	0,6	1,79	1,50	16%	55	11,8	79%	10	12,6	-26%	15	19,0	-27%	14	21,6	-54%	60	56,0	7%	13	42,8	-229%
30	149	0,4	1,91	0,90	53%	62	7,6	88%	11	11,2	-2%	19	11,6	39%	16	13,6	15%	63	34,0	46%	21	31,2	-49%
33	146	0,5	3,94	2,40	39%	37	34,0	8%	11	12,6	-15%	37	34,0	8%	34	24,2	29%	89	68,0	24%	32	43,0	-34%
34			2,92		18%	76		55%	11		-15%	33		-3%	26		7%	81		16%	83		48%
35	142	0,6	3,14	1,97	37%	83	18,0	78%	10	13,6	-36%	34	34,2	-1%	26	25,4	2%	87	106,0	-22%	30	58,8	-96%
	144	0,3		2,13	32%		17,4	79%		14,8	-48%		33,4	2%		24,4	6%		100,0	-15%		70,2	-134%
36	145	9,0	3,77	1,96	48%	83	14,6	82%	13	10,8	17%	37	31,2	16%	32	24,0	25%	98	90,0	8%	41	50,6	-23%
37		0,5	3,11		37%	81		82%	13		17%	42		26%	35		31%	110		18%	49		-3%
38	140	1,2	3,18	1,72	46%	89	15,4	83%	11	14,4	-31%	43	32,0	26%	28	23,2	17%	112	86,7	23%	34	50,2	-48%
	142	0,9		1,97	38%		18,0	80%		13,6	-24%		34,2	20%		25,4	9%		106,0	5%		58,8	-73%
39	147	1,5	3,19	1,50	53%	71	8,2	88%	10	11,0	-10%	45	21,0	53%	29	17,4	40%	113	60,0	47%	32	44,8	-40%
Average		1,1	2,29	1,60	30%	61	13,6	78%	9	13,9	-51%	25	24,8	-1%	22	20,9	4%	76	71,2	6%	27	46,7	-73%
Minimum		0,00	1,08	0,90		11	7,60		4	10,80		12	11,60		14	13,60		43	34,00		10	31,20	
Maximum		9,03	3,94	2,40		89	34,00		13	18,20		45	34,20		35	25,40		113	106,00		83	70,20	
St. Dev.		1,76	0,87	0,37		20	5,66		3	2,12		12	7,23		7	3,31		21	21,77		17	8,45	

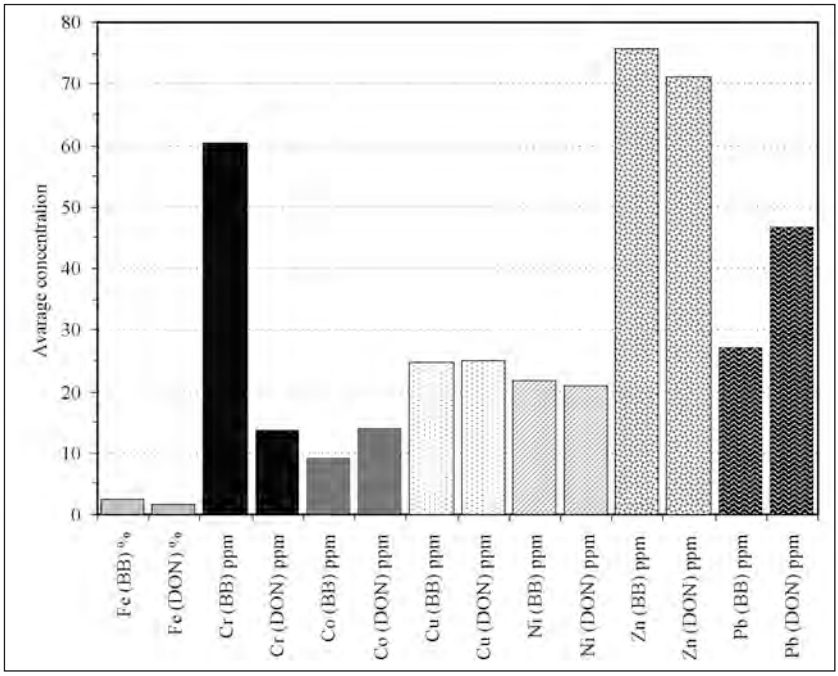

Fig. 2 - Average concentrations for the considered elements in Basu-Bonardi (BB) and Donazzolo et al. (1984) (DON) samples.

lattice position in silicate minerals. Only leaching made with a strong acid mixture containing hydrofluoric acid allows the extraction of the residual lithogenic component, or, alternately, using X-ray fluorescence technique. In any case, comparing the data of Donazzolo et al. (1984) with those obtained, we note that a similar explanation can be considered valid for Ni, Zn, Fe, and Cr. By a non total extraction, one could extract only a percentage, however difficult to estimate (Nirel & Morel, 1990), as one can easily note from the various percentage differences found between the two considered measurements of these elements that can be closely associated with fragmented particles (Table 3),. Higher concentrations of Co and Pb measured by Donazzolo et al. (1984), on the contrary, cannot be estimated in these terms. Nevertheless, one cannot even consider that there might have been a considerable decrease in Co and Pb loads of anthropogenic origin, since studies like that of Frignani et al. (1997) show that now sediments in the Porto Marghera area are 10% less contaminated with respect to sediments from 1930 to 1970.

Consequently, also other factors must be present to contradict the dif-

ferent measurements obtained. However, these in the case considered are not assessable, because accurate texture, composition and total organic carbon content data of sediments are lacking.

4. *Concluding Remarks.*

As one can deduce from the simple comparison of the two datasets of information for a limited number of elements concerned, it is impossible to make a comparison between the two. This is because of the different methods used and a possible textural and compositional difference of the samples themselves. Lacking exact boundary indications, as shown in Table 1, for the various studies, which aimed to define the possible contamination of surface and subsurface sediments of the lagoon of Venice, it seems clear that a comparison between these data is most of the times especially difficult, for which the authors can not make reference to published data. In fact, it would be necessary to define both grain-size and mineralogic characteristics of the sediments to be analyzed from a geochemical point of view in order not to over - or under-estimate possible contamination by heavy metals themselves.

Acknowledgements.

This work was carried out within the framework and with the financial support of the CORILA Project - Targeted subproject 3.2 (Work packages Hydrodynamics and Morphology). The authors thank Jane Frankenfield Zanin, CNR-ISDGM, Venice for her effective editing of the paper.

References.

Barillari A., 1978. Prime notizie sulla distribuzione dei sedimenti superficiali nel bacino centrale della Laguna di Venezia. Atti Ist. Ven. di Scienze, 136, 125-134.

Barillari A., 1981. Distribuzione dei sedimenti superficiali nel bacino meridionale della Laguna di Venezia. Atti Ist. Veneto di Scienze, 139, 87-109.

Barillari A., 1982. Relazioni tra alcuni elementi in traccia e proprietà dei sedimenti in due aree campione della Laguna di Venezia. Atti Ist. Veneto di Scienze, Lettere ed Arti, Rapporti e Studi, vol. VIII, 87-103.

Basu A. & Molinaroli, E., 1994. Toxic metals in Venice lagoon sediments: Model, observation, and possible removal. Environmental Geology, 24, 203-216.

Battiston G.A., Degetto S., Gerbasi R., Sbrignadello G., 1989. Determination of Sediment Composition and Chronology as a Tool for Environmental Impact Investigations. Marine Chemistry, 26, 91-100.

Bernarsi S., Costa F., Vazzoler S., Zonta R., Cecchi R., Ghermandi G., 1988. A Preliminary Investigation on the Distribution of Heavy Metals in Surface sediments of the Cona Tidal Marsh (Venice Lagoon). Il Nuovo Cimento, vol. 11C, N.5-6, 667-678.

Brambati A., 1968. Mixing and settling of fine terrigenous material (< 16 mm) in the northern Adriatic Sea between Venice and Trieste. Studi Trentini di Scienze Naturali, vol. XLV(2), 103-117.

Byscaye P.E., 1965. Mineralogy and sedimentation of recent deep-sea clay in the Atlantic Ocean and adjacent areas and oceans. Geol. Soc. Am. Bull., 76, 803-832.

Campesan G., Fossato V.U., Barillari A., Dolci F., Stocco G., 1987. Metalli pesanti e idrocarburi clorurati nei sedimenti della Valle di Brenta (Laguna di Venezia). Ist. Veneto di Scienze, Lettere ed Arti, Rapporti e Studi, vol. XI, 21-28.

Cochran J.K., Frignani M., Salamanca M., Bellucci L.G., Guerzoni S., 1998. Lead-210 as a tracer of atmospheric input of heavy metals in the northern Venice Lagoon. Marine Chemistry, 62, 15-29.

Donazzolo R., Orio A.A., Pavoni B., 1982. Radiometric Dating and pollutants profiles in a sediment core from the Lagoon of Venice. Oceanologica Acta, Volume Spécial, Décembre 1982, Les Lagunes Côtières, Actes du Symposium international sur les lagunes côtières, Bordeaux, France, 8-14 septembre 1981, 101-106.

Donazzolo R., Orio A.A., Pavoni B., Perin G., 1984. Heavy metals in sediments of the Venice Lagoon. Oceanologica Acta, vol. 7 - N°1, 25-32.

Frignani M., Bellucci L. C., Langone L., Muntau H., 1997. Metal fluxes to the sediments of the northern Venice Lagoon. Marine Chemistry, 58, 275-292.

Jobstraibizer, P. & Malesani, P., 1973. I sedimenti dei fiumi veneti. Memorie Società Geologica Italiana, 12, 411-452.

Jobstraibizer P., Are D., Carlin A., 1995. Metalli pesanti nei sedimenti della Laguna di Venezia. Plinius, 14, 181-182.

Loring D.H. & Rantala R.T.T., 1992. Manual for the geochemical analyses of marine sediments and suspended particulate matter. Earth Science Reviews, 32(1992), 235-283.

Menegazzo Vitturi L., Molinaroli E., Pistolato M., Rampazzo G., 1987. Geochemistry of recent sediments in the Lagoon of Venice. Rendiconti Soc. Italiana di Mineralogia e Petrografia, vol. 42, 59-72.

Ministero dei lavori pubblici, Magistrato alle Acque di Venezia tramite il suo concessionario Consorzio Venezia Nuova, 1999. Interventi per il recupero morfologico della Laguna di Venezia. Mappatura dell'inquinamento dei fondali lagunari, Studi ed indagini - Relazione di sintesi, pp. 1 - 107.

Ministero dei lavori pubblici, Magistrato alle Acque di Venezia tramite il suo concessionario Consorzio Venezia Nuova - Jobstraibizer, P., 1999 . Interventi per il recupero morfologico della Laguna di Venezia. Mappatura dell'inquinamento dei fondali lagunari, Studi ed indagini - Relazione finale, Appendice 1: Mineralogia e chimismo di trenta campioni: Interpretazione dei dati analitici e considerazioni a cura del prof. Jobstraibizer del Dipartimento di Mineralogia dell'Università di Padova, 21 pp.

Nirel P.V.M. & Morel F.M.M., 1990. Pitfalls of sequential extractions. Water Research, 24, 1055-1056.

Pavoni B., Donazzolo R., Marcomini A., Degobbis D., Orio A.A., 1987. Historical Development of the Venice Lagoon Contamination as Recorded in Radiodated Sediment Cores. Marine Pollution Bull., vol. 18, No. 1, 18-24.

Pavoni B., Marcomini A., Sfriso A., Orio A.A., 1988. Multivariate analysis of heavy metal concentrations in sediments of the Lagoon of Venice. The Science of the Total Environment, 77, 189-202.

Perin G., Bonardi M., Fabris R., Simoncini B., Manenete S., Tosi L., Scotto S., 1997. Heavy metal pollution in Central Venice Lagoon bottom sediments: evaluation of metal bioavailability by geochemical speciation procedure. Environmental Technology, vol. 18, 593-604.

Sfriso A., Marcomini A., Zanette M., 1995. Heavy Metals in Sediments, SPM and Phytozoobenthos of the Lagoon of Venice. Marine Pollution Bull., vol. 30, No. 2, 116-124.

Wilson M.J., 1987. A handbook of determinative methods in clay mineralogy. Blackie & Son, London, 308 pp.

Zonta R., Zaggia L., Argese E., 1994. Heavy metals and grain-size distributions in estuarine shallow water sediments of the Cona Marsh (Venice Lagoon, Italy). The Science of the Total Environment, 151, 19-28

THEMATIC AND LAND SUBSIDENCE MAPS OF THE LAGOON OF VENICE FROM ERS SAR INTERFEROMETRY

T. Strozzi[1], L. Tosi[2], U. Wegmüller[1], P. Teatini[3],
L. Carbognin[2], R. Rosselli[4]
[1]*Gamma Remote Sensing, Muri BE, Switzerland*
[2]*Istituto per lo Studio della Dinamica delle Grandi Masse, CNR, Venezia,*
[3]*Dipartimento di Metodi e Modelli Matematici per le Scienze Applicate, Università di Padova*
[4]*Consorzio Venezia Nuova - Servizio Informativo, Venezia*

Abstract.

Within the Co.Ri.La. project 3.2 on Hydrodynamics and Morphology, interferometric radar images from the ERS-1/2 satellites from 1993 to 2000 have been used to generate a subsidence map of the Lagoon of Venice. The SAR interferometric land subsidence map pictures very well the different displacement rates of the various compartments of the Lagoon. The SAR interferometric displacement map is discussed in comparison to the levelling results available through the ISES project. A geocoded thematic map of the Lagoon of Venice at 30 m resolution is also presented.

1. *Introduction.*

The European Remote Sensing Satellites ERS-1 and ERS-2 are the first of a series of spacecrafts intended to provide a pre-operational service of ocean, ice and land observations for the benefit of a large user community. One of the main instruments of both ERS satellites is a Synthetic Aperture Radar (SAR) operating at 5.3 GHz (C-band) with one polarization for imaging the Earth's surface. Recently, the development of SAR interferometry has proved that not only the amplitude of the radar signal

but also the phase carries important information for remote sensing applications (Bamler and Hartl, 1998, Rosen et al., 2000, Strozzi et al., 2001). In particular, differential SAR interferometry can be used to measure coherent displacements at cm to mm resolution. Spectacular new results resulted for geophysical sciences with earthquake displacement, volcano deformation, glacier dynamics and land subsidence being mapped. With regard to land subsidence, SAR interferometry exhibits complementary characteristics to the levelling surveys, because it has the capability to map large urban areas at low cost and high spatial resolution. The high precision levelling surveys, on the other hand, are used outside of the cities and to set up a reference point for the SAR subsidence analyses. In the case of the Venetian area, where high precision levelling surveys are currently available only around the Lagoon margin and along two lines from Venezia to Treviso and from Mestre to Padova, SAR interferometry has the capability to monitor the vertical displacements of all the built-up areas not fully covered with levelling results.

Within the Co.Ri.La. project on Hydrodynamics and Morphology, interferometric radar images from the ERS-1/2 satellites from 1993 to 2000 have been used to generate a single subsidence map. The SAR interferometric displacement data contributes to the control of the ground vertical movements as one of the possible components of the erosion and deposition processes. The SAR interferometric land subsidence map of the Lagoon of Venice very well pictures the different displacement rates of the various compartments of the Lagoon. The SAR interferometric displacement map is discussed in comparison to the levelling results available through the ISES (Intrusione Salina e Subsidenza) project (Tosi et al., 2000, Carbognin et al., 2001). Finally, a geocoded thematic map of the Lagoon of Venice at 30 m resolution computed with a Tandem interferometric coherence, the backscattering intensity and the backscattering intensity change is also presented.

2. *Differential SAR interferometry.*

With SAR interferometry the phase difference of two satellite radar images acquired from slightly different positions and at different times is computed (Bamler and Hartl, 1998, Rosen et al., 2000, Strozzi et al., 2001). The phase signal derived from an image pair relates both to topography and line-of-sight surface movement between the acquisitions, with atmospheric phase distortions, signal noise and inaccuracy in the orbit determination as main error sources. The basic idea of differential SAR interferometry is to subtract the topography related phase (for instance

Table 1 - Interferometric SAR images used in the computation of the land subsidence map of the Lagoon of Venice.

Orbits	Dates	Perpendicular Baseline	Time interval
07782_00477	10.01.93_24.05.95	3 m	864 days
00477_10497	24.05.95_23.04.97	7 m	700 days
10497_20517	23.04.97_24.03.99	-21 m	700 days
11289_05487	12.09.93_08.05.96	-17 m	969 days
25160_18012	07.05.96_30.09.98	-11 m	876 days
18012_26529	30.09.98_17.05.00	-49 m	595 days

simulated from a Digital Elevation Model) from the interferogram to derive a displacement map. The main characteristics of this technique are a spatial resolution on the order of 30 m and a sub-cm vertical accuracy. The main limitation is the possibility to derive subsidence information only over built-up or sparsely vegetated areas (i.e. where stable structures permit the formation of a coherent phase signal over time).

Nine SAR images from the European Remote Sensing Satellites ERS-1 and ERS-2 from 1993 to 2000 have been used in this study (Tab. 1). In order to generate a single subsidence map with reduced errors, 6 differential interferograms have been combined. Land subsidence was computed by assuming displacement in the vertical direction only. The map was geocoded to the Italian cartographic system Gauss-Boaga, zone 2, datum Roma 1940 with a pixel spacing of 30 m.

In addition to the interferometric phase itself, the interferometric coherence, which is a measure for the variance of the interferometric phase, is a very useful source of information on scene properties often complementary to the backscattered intensity. A geocoded thematic map of the Lagoon of Venice at 30 m resolution was computed by combination of a Tandem interferometric coherence, the backscattering intensity and the backscattering intensity change and is presented in Fig. 1.

3. *Land subsidence map of the Lagoon of Venice and comparison with ISES levelling surveys.*

The SAR-derived subsidence map of the Lagoon of Venice for the time period 1993-2000 at a spatial resolution of 30 m is shown in Fig. 2. The pixel corresponding to the benchmark Nodale 63 (ex 24') in Treviso

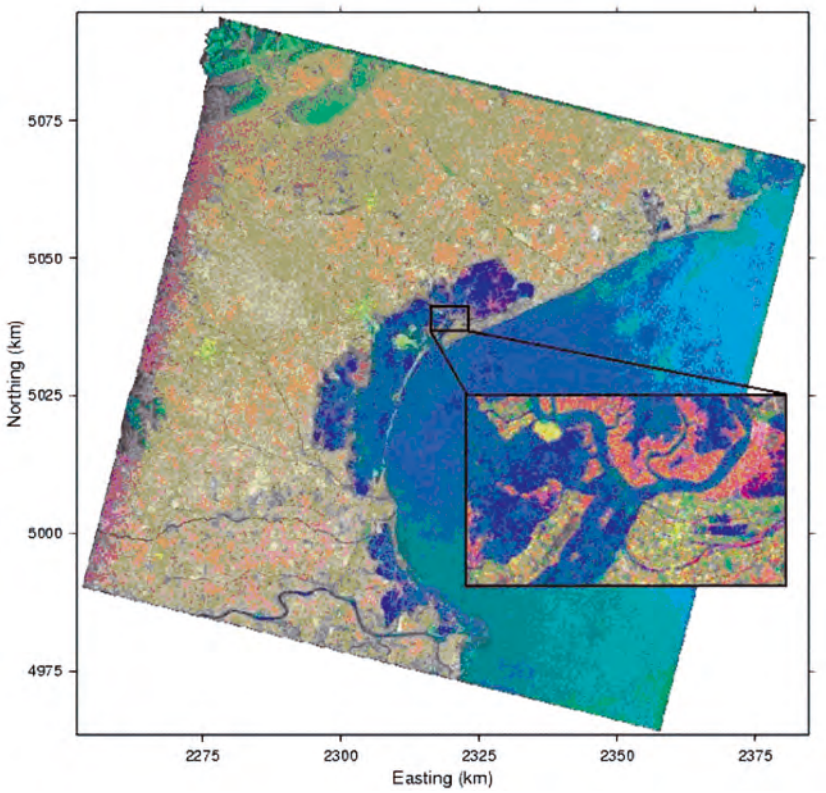

Fig. 1 - RGB color composite of interferometric coherence of the ERS-1/2 Tandem pair of the 7 and 8 May 1996, the averaged backscattering intensity for the time period 1993-2000 and the backscattering intensity change for the time period 1993-2000. The thematic map has a resolution of 30 m (see inset).

(that has been already considered stable in the ISES project) was considered the stable reference. The vertical displacement rates of the built-up areas are represented in a color scale between +1.0 and -5.0 mm/year. The incoherent areas (i.e. where it was not possible to measure subsidence) are shown without colors. The land subsidence rates from SAR interferometry are compared to those determined with levelling surveys in the frame of the ISES project along the lines Mestre - Venezia, Brondolo - Mestre - Jesolo, and Brondolo - Litorale di Lido - Jesolo (see Figs. 3 to 5).

For the 87 points where information is available from both surveying techniques (levelling benchmarks and corresponding SAR pixels) the standard deviation of the difference of the vertical displacement rates bet-

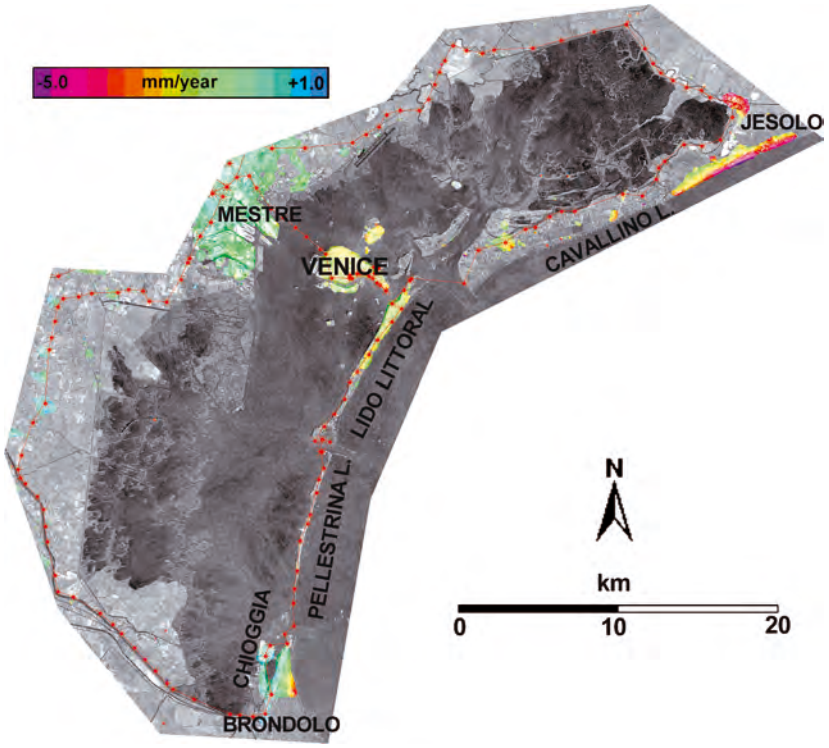

Fig. 2 - Land subsidence map (in mm/year) of the Lagoon of Venice for the time period 1993-2000 with superimposed the levelling lines used for comparison.

ween levelling surveys and SAR interferometry is 0.9 mm/year. From this number and previous works (Strozzi et al., 2001) we conclude that the accuracy of the SAR interferometric subsidence rates is on the order of ±1 mm/year, which is also the expected accuracy of the levelling surveys (Carbognin et al., 2001).

In the following, we will analyze the vertical displacement rates in the areas of Mestre-Venezia, Jesolo and the north of the Lagoon, Chioggia and the south of the Lagoon. In particular, we will give emphasis to the comparison between the 2-dimensional coverage from SAR interferometry and the linear results from levelling surveys.

The area of Mestre, Venezia and Lido Littoral (Fig. 2) is overall stable with altimetric variations included in 2 mm/year. From Figs. 3 and 4 there is a very good correspondence between the results from SAR inter-

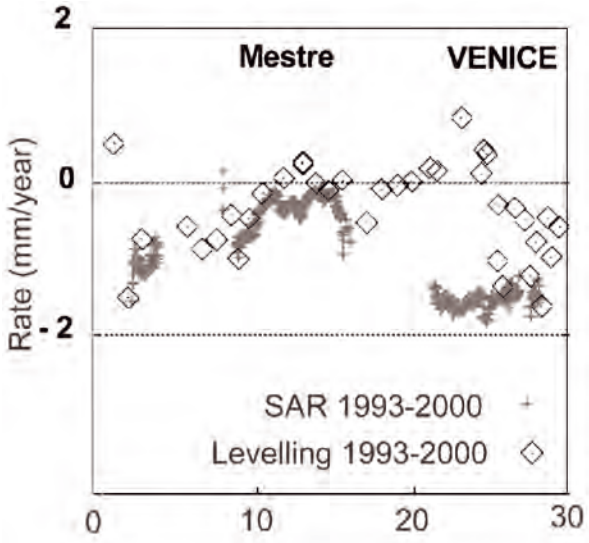

Fig. 3 - Subsidence rates (in mm/year) for the time period 1993-2000 from SAR interferometry (red crosses) and levelling surveys (black diamonds) along the levelling line Treviso - Mestre - Venezia.

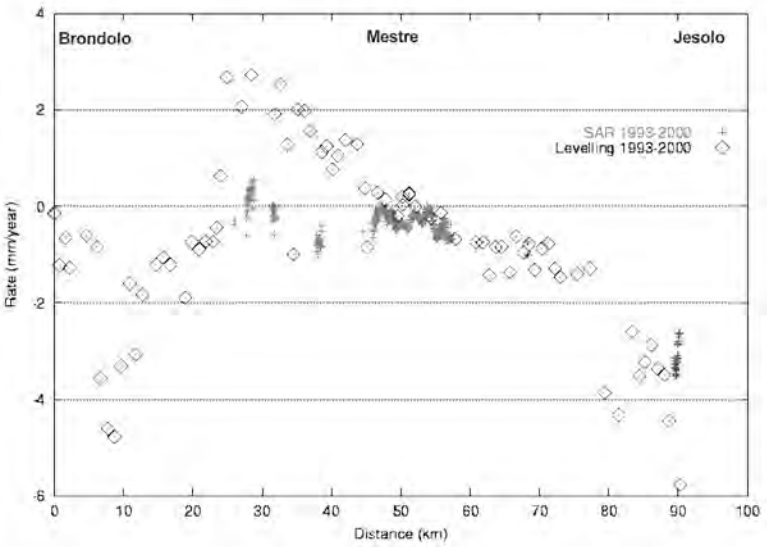

Fig. 4 - Subsidence rates (in mm/year) for the time period 1993-2000 from SAR interferometry (red crosses) and levelling surveys (black diamonds) along the levelling line Brondolo - Mestre - Jesolo.

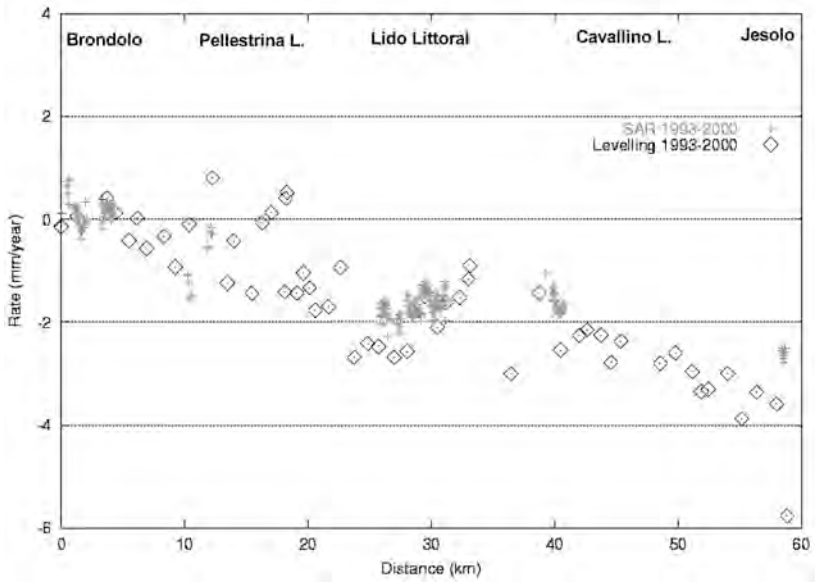

Fig. 5 - Subsidence rates (in mm/year) for the time period 1993-2000 from SAR interferometry (red crosses) and levelling surveys (black diamonds) along the levelling line Brondolo - Litorale di Lido - Jesolo.

ferometry and levelling surveys around Mestre. Along the western part of the profile in Venezia there is a certain difference between the values obtained from SAR interferometry and levelling surveys (with nevertheless a difference of less than 2 mm/year). On the other hand, for the eastern part of the profile in Venezia and for Lido Littoral (Fig. 5) the agreement between the two techniques is again very good. It is very interesting to observe an uplift of the ground in the southwest of Mestre, which is particularly evident from the levelling surveys (see Fig. 4).

For the northern part of the Lagoon, along the coast of Cavallino and Jesolo littoral (Fig. 6), we observe important subsidence rates that confirm the results of levelling surveys (see Figs. 4 and 5). In Jesolo Littoral there is a clear gradient of the subsidence rate from the coastline to the more stable areas inland. The pixels with valuable information from SAR interferometry inside of the Lagoon between Murano, Burano and S. Erasmo indicate a land subsidence rate of 1-2 mm/year with local values up to 3 mm/year (Fig. 7).

Also in the Chioggia area (Fig. 8) there is a strong gradient of the subsidence rate from the Sottomarina littoral to the stable area of the city of

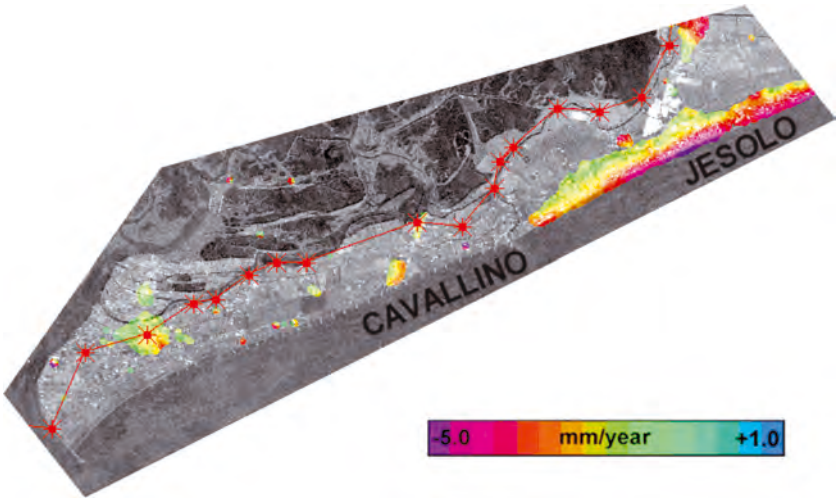

Fig. 6 - Land subsidence map (in mm/year) for the area of Cavallino - Jesolo during the time period 1993-2000 with superimposed the levelling lines used for comparison.

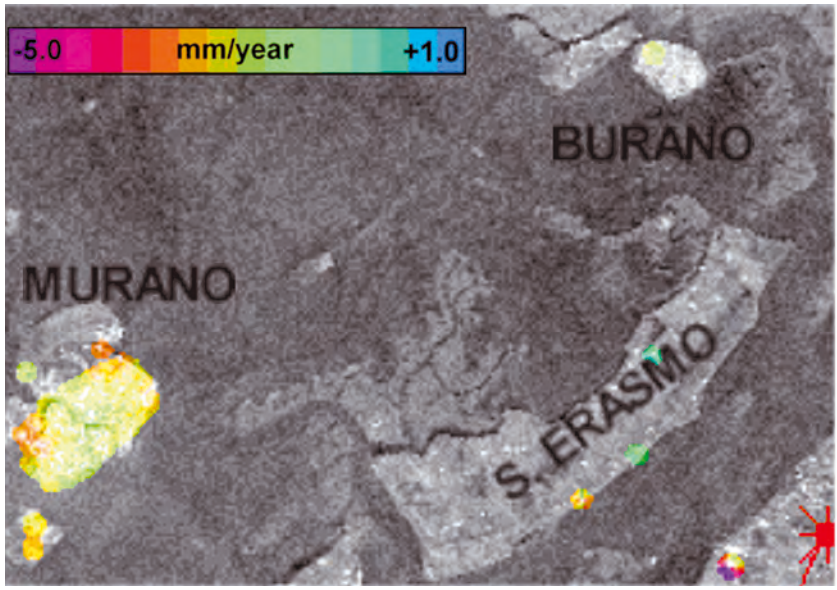

Fig. 7 - Land subsidence map (in mm/year) for the islands of Murano, Burano and S. Erasmo during the time period 1993-2000.

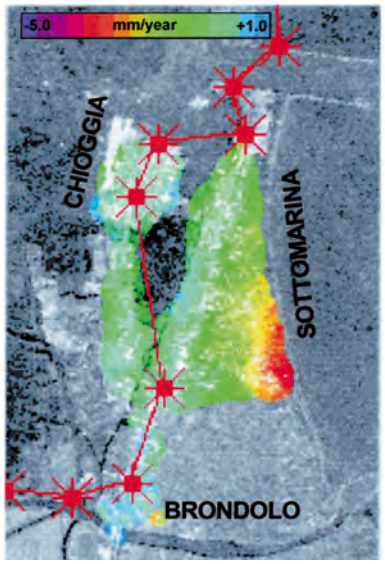

Fig. 8 - Land subsidence map (in mm/year) for the area of Chioggia during the time period 1993-2000 with superimposed the levelling lines used for comparison.

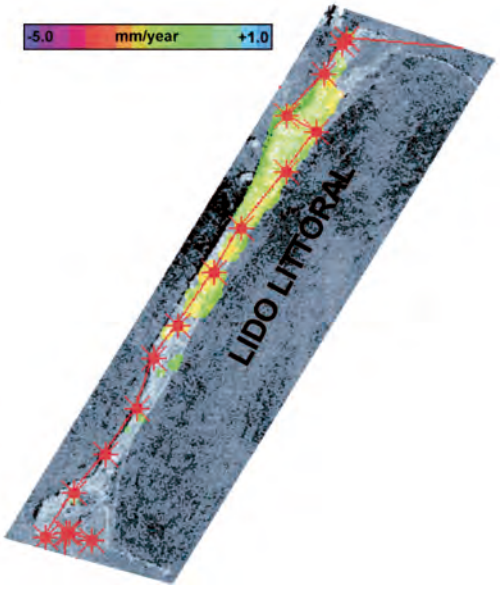

Fig. 9 - Land subsidence map (in mm/year) for Lido littoral during the time period 1993-2000 with superimposed the levelling lines used for comparison.

Chioggia. The very few pixels with valuable information from SAR interferometry for the area to the west of Chioggia indicate important subsidence values (larger than 3-4 mm/year), as observed with the levelling surveys. Between Brondolo and Lido Littoral the subsidence rates measured with SAR interferometry are very similar to those determined with levelling surveys (Fig. 5). Finally, along the Lido littoral (Fig. 9) a subsidence rate of about 2 mm/year is almost uniformly distributed over its central part.

4. *Conclusions.*

The SAR interferometric land subsidence map of the Lagoon of Venice gives confirmation to the first results available through the ISES project (Carbognin et al., 2001). Significant land subsidence rates were observed for the areas of Cavallino and Jesolo in the north of the Lagoon and for the area of Valli in the southern part. The SAR interferometric land subsidence map of the Lagoon of Venice, with an accuracy on the order of ±1 mm/year, also shows important gradients of the subsidence rate along the coastlines of Lido di Jesolo and Chioggia. Finally, we noticed a difference between the results of SAR interferometry and levelling surveys for the area in the southwest of Mestre, where the rebound determined with levelling surveys is not be completely confirmed with SAR data.

Land subsidence values could be measured with SAR interferometry only for urban and other not too small built-up areas, and therefore only for a few zones inside of the Lagoon. We expect more information for very small built-up areas by applying a different SAR interferometric technique specifically developed for point targets (Ferretti et al., 2001). The implementation of this technique for the Lagoon of Venice is part of a project that GAMMA is currently performing with ISDGM within the framework of a Data User Programme (DUP) of the European Space Agency (ESA). First results of this method should be available in about one year.

Acknowledgments.

This activity was performed in the frameworks of an ESA Data User Program and of the Co.Ri.La. project 3.2 "Hydrodynamics and Morphology of the Venice Lagoon".

We acknowledge the Venice Water Authority, Consorzio Venezia Nuova, Servizio Informativo for support. Levelling surveys courtesy ISES project (founded through the Consorzi di Bonifica Adige-Bacchiglione, Bacchiglione-Brenta and Delta Po-Adige; the Venice Water Authority; the Provincia di Padova and Provincia di Venezia; the Comune di Chioggia and the ISDGM-CNR).

ERS SAR data copyright ESA, processing GAMMA. The Italian National Geologic Survey is acknowledged for the DEM.

References.

Bamler R., & Hartl P., 1998. Synthetic aperture radar interferometry. Inverse Problems. 14:R1-R54.

Carbognin L., Teatini P., & Tosi L., 2001. Relative land subsidence in the lagoon of Venice, Italy, at the beginning of the new millennium. In Int. Conf. of UNESCO-BAS Project "Expert assessment of land subsidence related to hydrogeological and engineering geological conditions in the regions of Sofia, Skopje and Tirana", M. Matova ed., Geological Institute "Acad. Strashimir Dimitrov" of Bulgarian Academy of Sciences, 7-14.

Ferretti A., Prati C., & Rocca F., 2001. Permanent scatterers in SAR interferometry. IEEE TGRS, 39(1), 8-20.

Rosen P., Hensley S., Joughin I., Li F., Madsen S., Rodríguez E., & Goldstein R., 2000. Synthetic aperture radar interferometry. Proceedings of the IEEE, 88(3): 333-382.

Strozzi T., Wegmüller U., Tosi L., Bitelli G., & Spreckels V., 2001. Land subsidence monitoring with differential SAR interferometry. PE&RS, 67(11):1261-1270.

Tosi L., Carbognin L., Teatini P., Rosselli R., & Gasparetto Stori G., 2000. The ISES project subsidence monitoring of the catchment basin south of the Venice Lagoon, Italy. Land Subsidence (eds Carbognin, Gambolati & Johnson), La Garangola, Padova, Italy, II: 113-126.

Tosi L., Carbognin L., Teatini P., Strozzi T., & Wegmüller U., 2002. Evidences of the present relative stability of Venice, Italy, from land, sea and space observations. Geophysical Research Letters, 29 (13), 10.1029/2001G.L013211.

Werner C., Wegmüller U., Strozzi T., & Wiesmann A., 2000. GAMMA SAR and interferometric processing software. Proceedings of the ERS-ENVISAT Symposium, Gothenburg, Sweden, 16-20 October 2000.

RESEARCH LINE 3.3.
Efficiency of lagoon metabolism

TROPHIC STATE AND PRIMARY PRODUCER CHANGES IN THE CENTRAL PART OF THE VENICE LAGOON

A. Sfriso, C. Facca,
S. Ceoldo and P. F. Ghetti
Dipartimento di Scienze Ambientali,
Università Cà Foscari, Venezia

1. *Introduction.*

The main objectives of the WP1 (Primary production) activity (Research line: 3.3 - Efficiency of the lagoon metabolism) is to monitor the changes in the trophic level (nutrients and primary production) in the central part of the Venice lagoon. Sets of data collected on weekly/monthly basis in different years and in the same areas and stations by using the same sampling and analytical procedures will be compared and updated with data collected during the present research schedule. In addition the taxonomic composition, density and role of the main primary producers (seaweeds, seagrasses, phytoplankton, microphytobenthos) of the Venice lagoon will be also the object of spatial campaigns in the whole lagoon and temporal samplings in different seasons and areas.

The WP1 activity develops into several sub-activities which are distinct but strongly integrated research programmes:

1. Spatial and temporal changes in the seaweed distribution, biomass, net and gross primary production in the central part of the Venice Lagoon and study of the main producers of the whole lagoon;
2. Biomass, primary production and nutrient concentrations in *Zostera marina* and *Cymodocea nodosa*. Those rhizophytes account for ca. 2/3 of the seagrasses which populate the lagoon;
3. Spatial and temporal changes in the Venice macrophytes composition: Taxonomic changes. Updating activity. Introduction of non-native species. Utilisation of macroalgal communities, taxonomic ratios and sensitive species to assay the pollution and trophic level of the lagoon environment;

4. Spatial and temporal changes in the phytoplankton biomass (clorophyll *a* and phaeopigments), taxonomic composition and biovolumes. Study of microphytobenthos communities. Utilisation of microalgal communities as ecological integrity descriptors for the lagoon environment;
5. Spatial and temporal changes in relevant environmental variables related to the lagoon trophic state, the dominant primary producers and the clam fishing activities. In the water column: Dissolved oxygen, pH, Eh, transparency (Secchi disk). In the surface sediments: Density and fine grain-size percentage;
6. Spatial and temporal changes in sedimentation fluxes (SPM = settled particulate matter) and nutrient amounts vehicolated by SPM in the central part of the Venice lagoon;
7. Spatial and temporal changes of nutrient concentrations in the water column, surface sediments, SPM and tissues of the dominant macrophytes of the Venice lagoon.

The integration and comparison of historical data sets (macro and microphyte biomass, primary production, nutrient concentrations and relevant physico-chemical parameters) collected by the unit researchers during the last 15 years have been completed during the first year according to the programme work-plan (Sfriso *et al.*, 2002a,b; Rigollet *et al.*, 2002; Facca *et al.*, 2002a). The distribution of both the algal biomass and some physico-chemical parameters in the central part of the Venice lagoon, and the annual trends of the same variables in several sampling areas monitored during three periods environmentally significant (excessive *Ulva* growth (1970-1990), its decline (1990-94), intense catching of the bivalve *Tapes philippinarium* Adams & Reeve (1994-2001)) have been taken into consideration. At present, the annual trends of the parameters reported in the different sub-activities in three new lagoon areas (San Nicolò, Celestia, Tresse), selected in order to complete the available information on the trophic state of the lagoon, are in progress. In addition a new macrophyte and phytoplankton sampling campaign has been planned for June 2002 in order to update the distribution and relevance of the different lagoon producers in the presence of new environmental conditions due to the starting of a shell farming culture in ca. 3000 ha (Orel *et al.*, 2000). Algal biomass and distribution together with some physico-chemical parameters and nutrient concentrations in the water column will be sampled in the 55 stations monitored during the three previous environmental scenarios. Moreover additional stations (70, at least) will be selected in order to survey the whole lagoon.

The new sub-activities deal with the determination of the micro and macroalgal composition and the characterisation of the dominant algal communities in order to update the information on the primary producers of the lagoon and compare the results with those obtained in the '80s. In addition some taxonomic ratios and sensitive species will be preliminary used as environmental quality descriptors to assay the pollution and trophic level of the lagoon environment.

2. *Results and discussion.*

Data are presented by analysing the environmental conditions monitored during three significantly different scenarios:

- ➢ Excessive growth of macroalgae, especially *Ulva rigida* C. Ag. (1970-1990),
- ➢ Decrease and disappearance of huge macroalgal biomasses (1990-1994),
- ➢ Intensive catching of the bivalve *Tapes philippinarum* Adams & Reeve (1994-2002).

2.1. *Macroalgal and phytoplankton biomass distribution and macroalgal production.*

The integration and comparison of the available data (Sfriso *et al.*, 2002a,b) show the significant decrease of the macroalgal standing crop (SC) and the net (NPP) and gross (GPP) primary production. At present (3rd scenario), SC, NPP, GPP are ca. 1.6%, 2.9%, 2.4% of those monitored in 1987 (1th scenario), accounting for ca. $0.56*10^6$, $1.5*10^6$ and $9.7*10^6$ tonnes fwt, respectively. By the analysis of the annual trends in single stations it appears that the macroalgal biomass decreased from values up to ca. 20 kg m^{-2} to values ranging between ca. 350 g m^{-2} and <10 g m^{-2}.

Phytoplankton, despite the macroalgal decline, in the period between the first two scenarios did not show significant changes. The annual mean chlorophyll *a* concentrations were systematically lower than 5 μg dm^{-3}. During the 3rd scenario both the mean chlorophyll *a* concentrations and the cell biovolumes decreased to ca. 1/3 of the values monitored during the 1th scenario (Sfriso *et al.*, 2002a; Facca *et al.*, 2002b). In addition, phytoplankton blooms recorded systematically between '70s and '90s, missed in the '90s. Abnormal phytoplankton blooms were only monitored in 2001.

2.2. *Physico-chemical parameters and nutrient concentration in the water column.*

The algal biomass and macroalgal production decrease and the catching of the bivalve *Tapes philippinarum* by hydraulic and mechanical dredges caused strong changes of several environmental parameters related to them. During the '90s water turbidity increased significantly whereas the mean dissolved oxygen saturation, pH and redox potential decreased remarkably (Sfriso *et al.*, 2002b). In particular, the mean values of these variables recorded during the summer campaigns (55 sampling sites) of the three different scenarios decreased from 274% to 113%, from 8.82 to 8.01 and from 378 to 294 mV, respectively. At present water transparency is frequently lower than 30 cm, while oxygen saturation and pH peaks up to 394% and 9.54, as monitored during the 1th scenario, are missing.

On average the RP (reactive phosphorus) concentration in the water column is ca. 1/3 of the one monitored during the 1th scenario. In contrast, the mean concentration of DIN (inorganic dissolved nitrogen) is, in general, higher (about twice as much) than in the past because of the reduced algal assimilation and, probably, the decrease of denitrifying processes. At present, in fact, the lagoon environment is more oxidised than in the past when anoxia occurred frequently.

2.3. *Physico-chemical parameters and nutrient concentrations in the surface sediment.*

During the 3rd scenario, characterised by intense bivalve fishing activities, surface sediment grain-size and density changed significantly. In particular the fine (<63 μm) fraction percentage decreased in the inner lagoon areas, affected by high sediment resuspension caused by hydraulic and mechanical dredges, while it increased near the lagoon mouths because of the increase of the sediment fluxes.

Nitrogen, phosphorus and carbon concentrations in the 5 cm sediment top layer also changed (Sfriso *et al.*, 2002b). Nutrient were significantly different during the 1th and 3rd scenarios. The mean nitrogen and phosphorus concentrations in the whole central lagoon (55 sampling sites) during the 3rd scenario were remarkably lower and homogeneously spread than in the 1th one. In particular the mean organic phosphorus (OP) halved (from 104 to 59 μg cm^{-3}) and the total nitrogen decreased of ca. 25% (from 1.21 to 0.93 mg cm^{-3}). The concentration of organic carbon (OC), which is a structural element, shows changes which depend on the considered area. Peak values up to 900% of those monitored during the 1th sce-

nario in some areas North of Venice, which are affected by intense fishing activities but poor of water exchanges, contributed to increase the mean OC value of ca. 30%. Nevertheless, the OC concentration decreased significantly in several areas South of Venice affected by high hydrodynamic. In general, the impact of clam fishing played a more relevant role in nutrient changes than the decrease of the macroalgal biomass.

2.4. *Settled particulate matter (SPM) fluxes and erosion/sedimentation processes.*

SPM fluxes recorded on a yearly basis in some sampling sites during the last 15 years increased about five-twelvefold, mostly because of the clam fishing impact (Sfriso, 2000). At Sacca Sessola, an area particularly affected by the environmental changes which characterise the three scenarios, SPM fluxes (July-June 1989-90, 1992-92 and 1998-99) were ca. 65, 275 and 759 kg m^{-2} yr^{-1}, dwt, respectively. Therefore, at present, SPM fluxes at Sacca Sessola account for ca. 2-3 kg m^{-2} d^{-1}, dwt. Peaks of SPM fluxes up to 5 kg m^{-2} d^{-1}, dwt have been monitored. The effect of those marked SPM fluxes on the presence, distribution and growth on the primary producers is considerable and huge amounts of nutrients and pollutants are spread in the whole lagoon. However, despite the high amount of settled sediment, wide areas of the central lagoon are affected by erosive processes and loss of fine material. By measurements carried out in some areas of the central lagoon it was estimated that since the beginning of clam fishing activities, the central lagoon has suffered a mean bathymetric loss ranging from 1.5 to 3.5 cm per year.

2.5. *Algal taxonomy.*

The environmental changes monitored since the '90s are also coupled with strong changes in the composition and dominance of the lagoon primary producers. As far as phytoplankton is concerned, the abnormal sediment resuspension causes the resuspension of the microphytobenthic communities which populate surface sediments and also a change in the composition of the water column communities (Facca *et al.*, 2002b). In fact, a significant increase of benthic taxa, especially pennate diatoms is systematically recorded in the water column.

Macroalgae, in spite of the dramatic biomass decrease observed since the '90s show a significant increase of taxa (Sfriso *et al.*, 2002c). At present taxa recorded in the lagoon are more than twice as much those sampled during the '80s. That is due to the lack of anoxic crises due to bio-

mass collapse, the introduction of non-native species (by means of fish markets, cargo boats and liners) and the refinement of several taxonomic keys which allow a better identification of the species. Moreover, the utilisation of algal communities and sensitive species together with the determination of the species abundance and taxonomic ratios (Rhodophyceae/Chlorophyceae) allow to assay the environmental quality and ecological integrity of the lagoon and, in association with nutrient concentrations, to classify the trophic state of the examined ecosystem.

3. *Conclusions.*

The integration and comparison of data recorded from the WP1 research group in these last 15 years shows strong changes both in the composition and abundance of the lagoon primary producers and in most of the environmental variables strictly linked to their growth cycles. Bivalve spread and catching after the macroalgal biomass decrease, ulteriorly affected the producer presence and growth in the lagoon. In addition the amounts and distribution of nutrients and pollutants accumulated in the surface sediments changed significantly.

The ongoing project will allow to complete this information, in particular the trophic state of the lagoon will be updated. The compilation of the composition of the lagoon producers and their role in the lagoon primary production is in progress. The carrying out of the sub-activities planned in the WP1 project: a) Annual samplings in three steering stations and b) a summer mapping of the primary producers (macrophytes and phytoplankton) and nutrient concentrations in the water column of the whole lagoon, will allow further integration and comparisons with the data collected in these last 15 years and a better classification of the ecological quality and trophic state of the Venice environment.

References.

Facca C., Sfriso A., Ghetti P.F., 2002a. Phytoplankton composition and distribution in the central part of the Venice lagoon, Submitted to *Plant Biosystem.*

Facca C., Sfriso A., Socal, 2002b. Changes in abundance and composition of phytoplankton and microphytobenthos due to increased sediment fluxes in the Venice lagoon, Italy. *Estuarine, Coastal and Shelf Science*. 54: 773-792

Orel G., Boatto V., Sfriso A., Pellizzato M., 2000. *Piano per la gestione delle risorse alieutiche delle lagune della Provincia di Venezia*. In: Provincia di Venezia (Ed.), Sannioprint, Benevento, 102 pp.

Rigollet V., Sfriso A., Marcomini A., de Casabianca M.L., 2002. Heavy metals in sediments populated by *Zostera marina* at Thau Lagoon (France) and Venice Lagoon (Italy). Submitted to *Environmental Pollution.*

Sfriso A., 2000. Eutrofizzazione e inquinamento delle acque e dei sedimenti nella parte centrale della laguna di Venezia. MAV, CVN, Rapporto Finale. 3 vol.

Sfriso A., Facca C., Ghetti P.F., 2002a. Temporal and spatial changes of macroalgae and phytoplankton in shallow coastal areas: The Venice lagoon as a study case. Submitted to *Global Change Biology.*

Sfriso A., Facca C., Ceoldo S., Silvestri S., 2002b. Nutrient concentrations in the surface sediments of the central part of the Venice lagoon in the last fifteen years: updating and comparison between different scenarios. Submitted to *Oceanologica Acta*.

Sfriso A., la Rocca B., Godini E., 2002c. Inventario di taxa macroalgali in tre aree della laguna di Venezia a differente livello di trofia. *Società Veneziana di Scienze Naturali*. 27, 85-99.

PRELIMINARY RESULTS ON DEGRADATION OF ORGANIC COMPOUNDS BY MICROBIAL COMMUNITIES IN VENICE LAGOON

F. Baldi[1,2], R. Marcon[1], M. Pepi [2] and F. Zecchini[2]
[1]*Department of Environmental Science, Ca' Foscari University, Venice.*
[2]*Interuniversity Consortium for Environmental Chemistry, Marghera (Venice), Italy.*

1. *Introduction.*

Studies of microbial population in the Venice Lagoon are lacking. The importance of microbes in degradation of organic matter together with nutrient recycling is an important task in marine and brackish water environments. In Venice Lagoon inputs of organic compounds from urban wastes combine with organic compounds mainly hydrocarbons from the industrial activity in Marghera (VE). In the framework of CORILA project, our research unit have the task to investigate bacterial degradation of organic compounds in sediments of Venice Lagoon. In this preliminary survey, an innovative test BIOLOG™ was used. This test is very successful applied in determining microbial populations in soils and just recently is used for marine sediments (Ivanova et al. 1998; Ivanova et al. 2000, Kaye, et. al., 2000; Mayr et al., 1999). PAH (polycyclic aromatic hydrocarbons) degradation was considered an important task. PAHs are a wide class of organic molecules with two or more condensed aromatic rings, which polluted several areas in the Venice Lagoon. Many studies deals with PAH microbial degradation in soils and very few in marine ecosystems (Daane et al., 2001, Hedlund, et al., 1999; Hedlund, et al., 2001a; Hedlund, et al., 2001b; Maki et al, 2001).

2. *Materials and methods.*

2.1 *Sampling area.*

Four sampling stations were located and sediments from 3 sites were collected: Celestia, S. Erasmo e Foce Dese. Initially we studied microbial population from station 2 (Celestia site), as it is polluted by polycyclic aromatic hydrocarbons (PAH).

2.2 *Characterisation of microbial population in sediments.*

In order to characterise microbial populations in lagoon sediments we set up BIOLOG™test. This procedure has used with plate to characterise population by principal components analysis (PCA) (Di Giovanni et al., 1999). In this paper ECOPLATE™ system is used, an innovative method to determine the degradation profile of aerobic microbial population. This uses 96-well microplates to characterise communities on the basis of sole carbon source utilisation. This test was formerly performed with BIOLOG GN™ plates designed for gram negative bacteria. Recently ECOPLATES ™, specific for microbial community studies (31 carbon sources, 1 water control, 3 replicates), are available. The procedure was based on recovery of suspended bacteria from 20 g of air-dried sediment, incubated overnight at 28°C. This was done with diluted yeast extract medium (YE, 25 mg-l^{-1}) (Garland and Mills, 1991). The test was repeated six times to evaluate the oxidation reproducibility of microbial community. The pre-incubated inocula were transferred in 32 different wells containing 32 different organic compounds included water control. These compounds are intermediate of general metabolic pathways of prokaryotes and are the following: water, D-malic acid, methyl-pyruvate, methyl-succinate, propionic acid, pyruvic acid, succinamidic acid, N-acetyl-L-glutamic acid, alanin-amide, D-alanine, L-alanine, L-alanine-glycine, L-asparagine, L-glutamic acid. L- glutamic glicyl acid, L-pyro-glutamic acid, L-serine, putrescine, 2,3 butandiol, glycerol, adenosine, 2'-deossi-adenosine, inosine, tymidine, uridine, adenosine-5'-monophosphate, timina-5-monophosphate, uridine-5'-monophosphate, fruttose-6-phosphate, glucose-1-phosphate, glucose-6- phosphate, D, L-alpha-glycerol- phosphate. Plates were incubated for 24 h, 48 h, and 72 h. if organic compound oxidation occurred, a violet colour developed inside the well due the solubilization of formazan, the reduced form of tetrazolium salt (insoluble form). The intensity of colour was determined in each well as number of pixels by using the program NIH Image 1.62b7f.

2.3 *Isolation of PAH-degrading bacteria.*

To isolate PAH-degrading bacteria from sediment, a slurry (1:100, w: v) was made to prepare enrichment cultures. 1 g of sediment was diluted in 100 ml mineral medium containing per litre: 0.7 g KCl, 1 g $MgSO_4$, 2 g KH_2PO_4, 3,7 g $Na_2HPO_4.2H_2O$, 1 g NH_4NO_3, 24 g NaCl. An aliquot of this slurry was freshly distributed in new mineral medium containing plus different PAH: naphthalene, phenantrene, fluorene, fluoran-

thene, pyrene, and biphenyl amended separately in each culture as sole carbon and energy sources. After a suitable time of incubation in liquid culture, bacteria were cultivated in solid (1.6% agar) mineral medium containing different PAH. Crystals of these hydrocarbons were adhered on cover slip plates, and vapour from PAH crystal sublimation was assimilated by microbial cell growing on agar plates. One forming colony was transferred in complex medium containing per litre: 24 g NaCl, 5 g peptone, 2.5 g yeast extract, 1 g glucose, 1.6 g agar. After growth strains were stored in cryovials at -80°C.

2.4 *Oxygen consumption in naphthalene.*

The growth of VE-SN1 strain was indirectly followed by measuring O_2 consumption in mineral medium amended with naphthalene. Measurements were performed with an automated system (OxiTop model OC 110). OxyTop bioreactors (500 ml) were filled with 200 ml of mineral medium plus 2% of naphthalene crystals. Culture was continuously mixed with a magnetic stirrer and oxygen consumption was revealed by its lowering partial pressure (hPa) in the headspace of bottle reactor. Pressure was converted in biological oxygen demand (mg $O_2.l^{-1}$) by a formula defined by company protocol. Developed CO_2 from bacterial metabolism was entrapped by concentrated NaOH (pellets) placed in 3 internal chambers of OxiTop reactor. At the end of oxygen consumption phosphate and ammonium ($Na_2HPO_4.2H_2O$, 1 g NH_4NO_3) were supplied to investigate on inhibition of naphthalene degradation.

3. *Results and discussion.*

The microbial community isolated from sediment oxidised the major fraction of nutritional compounds in 22 wells out of 31. 4 out of 22 wells were considered borderline (+/-) growth. The substrate oxidation was feeble and determined on the basis of colour developed in each well and determined by imaging analysis to avoid bias due to subjective eye-detection.

Standards deviations of six duplicate tests were determined in each well (fig. 2). The reproducibility was good, and the oxidising pattern was the same in all wells, except for acceptable variations of colour (grey intensity). No oxidation was observed in the control with water. This starting value was 120 ± 20 pixel, above this threshold (140) the test was considered positive.

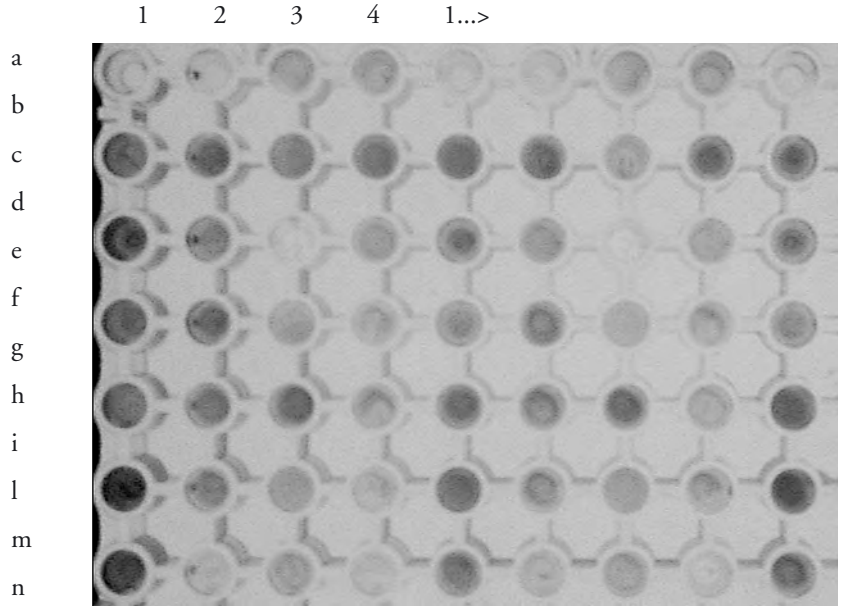

Fig. 1 - Photo of BIOLOG™ plate was taken by Kodak DC110 digital camera. Intensity of grey colour was determinated by NIH Image 1.62b7f. Grey intensity was determined in each well. Control wells containing water are placed at the three 1a positions.

The test was negative with beta-methyl-D glycoside, D-galactic acid gamma-lactone, L-treonine, glucose-1-phosphate, phenil-ethyl-amine, alfa-D-lactose. The degradation of 4-hydroxibenzoic acid occurred in these populations capable to degrade aromatic compounds by dioxygenases, but not for 2- hydroxibenzoic acid, which is easily degradable, due to the hydroxyl- substituting group close to the carboxylic group in the benzene ring. The microbial population is capable of growing on fatty acids and hence produces lipases because substrates such as Tween 80 and Tween 40 containing palmitic and oleic acid respectively are oxidised. Glucanases to degrade polysaccharides are secreted by the microbial community since: - D-xilose, D-galacturonic acid, D- mannitol, N-acetyl.glucosamine, glycogen, glucosaminic acid, itaconic acid, D-cellobiose, give positive test. The use by microbes of some aminoacids, such as putresceine, L-arginine, L-phenil-alanine, L-serine, pinpointed the production of active proteases. This test indicated that the microbial population in the station 2 of Venice Lagoon is highly eutrophic respect to other population isolated from unpolluted areas.

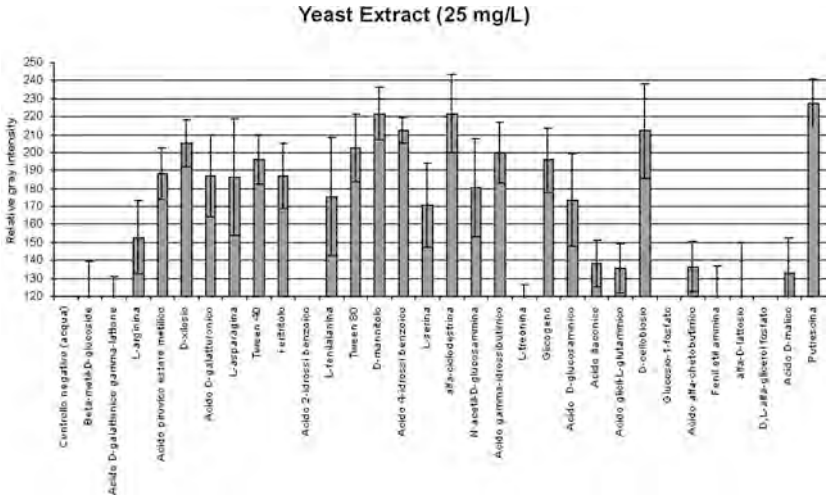

Fig. 2 - Relative grey intensity determined by image analysis was reported in relation to some nutritional compounds in six duplicate samples. Bacteria were detached by shaking 20 g of sediment and incubated overnight in yeast extract medium (25 mg.1^{-1}).

In order to isolate important PAH-degrading strains, enrichment cultures were prepared. Several strains

were isolated belonging to both Gram- and Gram+ bacteria. As species are not yet identified they are named as follows: VE-SN1, which uses naphthalene as carbon and energy source. VE-SB1 degrades biphenyl as carbon and energy source. VE-SF1 degrades fluorene as carbon and energy source. VE-SP1 uses phenanthene as carbon and energy source. We isolated also a strain VE-SC1 able to growth on cellulose as carbon and energy source.

Recently VE-SN1 was studied in detail for its ability to growth on naphthalene. Microbial degradation of PAH is scarcely investigated in marine and brackish ecosystems. New species and strains have been recently isolated. Our strain consumes oxygen at high rate (1100 μg O_2.d^{-1}) in Oxytop reactors. This rate was calculated by O_2 pressure (hPa) which lowered in the headspace and than converted in BOD ($mgO_2.l^{-1}$) (Fig. 3).

The O_2 consumption dramatically stops after 39 hours of incubation at 28°C. This stop was not due to nutrients deficiency. Oxygen, naphthalene and salts were amended in the spent medium. The strain did not start to degrade naphthalene again. Investigations are in progress to deter-

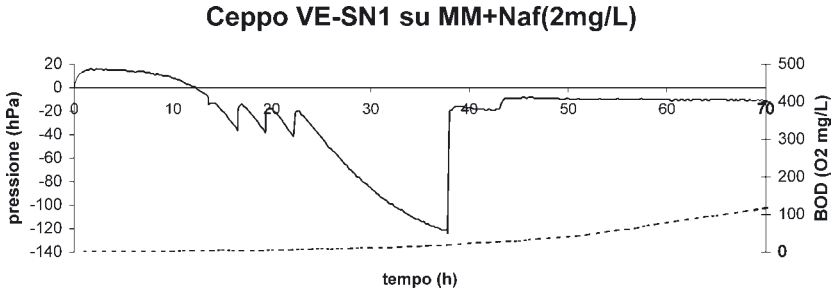

Fig. 3 - O2 consumption measured as pressure decrease (hPa) in the presence of mineral medium amended with 2 mg.1-1 of naphthalene (solid line) and BOD in relation to time (h) (dashed line).

mine if a toxic intermediate is produced during naphthalene degradation. Derivative oxidised water-soluble molecules are often more toxic than the starting molecules, because these species are more bio-available. In natural ecosystem these chemical species are consumed by other strains or species, which are complementary in the nutritional pathway. Under laboratory conditions this does not occur and the toxicity of intermediate molecules are often revealed.

4. *Conclusions.*

Further studies are needed to understand the characteristic of microbial community by BIOLOG™ test in the Venice Lagoon, collecting more samples from different ecosystems. The study of degradation of persistent and toxic molecules is started. At the moment few important strains have been isolated. Their phenotypic and genetic characterisation will be studied to understand the key microbes, which are able to transform and degrade these refractory molecules in lagoon sediments.

References.

Daane L.L., Harjono I., Zylstra G.J. and Haggblom M.M., 2001. Isolation and characterization of polycyclic aromatic hydrocarbon- degrading bacteria associated with the rhizosphere of salt marsh plants Appl Environ Microbiol. 67:2683-91.

Di Giovanni G.D., Watrud L.S., Seidler R. J. and Widmer F., 1999. Comparison of Parental and Transgenic Alfalfa Rhizosphere Bacterial Communities Using Biolog GN Metabolic Fingerprinting and Enterobacterial Repetitive Intergenic Consensus Sequence-PCR (ERIC-PCR) Microb Ecol. 37:129-139.

Garland J.L. and Mills A.L., 1991. Classification and characterization of heterotrophic microbial communities on the basis of pattern of community-level sole-carbon-source utilization. Appl. Environ. Microbiol. 57:2351-2359

Hedlund B.P., Geiselbrecht A. D., Bair T.J. and Staley J.T., 1999. Polycyclic aromatic hydrocarbon degradation by a new marine bacterium, *Neptunomonas naphthovorans* gen. nov., sp. nov Appl Environ Microbiol. 65:251-9.

Hedlund B.P., Geiselbrecht A.D. and Staley J.T., 2001. Marinobacter strain NCE312 has a Pseudomonas-like naphthalene dioxygenase FEMS Microbiol Lett. 201:47-51.

Hedlund B. P., and Staley J.T., 2001. *Vibrio cyclotrophicus* sp. nov., a polycyclic aromatic hydrocarbon (PAH)- degrading marine bacterium Int J Syst Evol Microbiol. 51:61-66.

Ivanova E.P., Kiprianova E.A., Mikhailov V.V., Levanova G..F, Garagulya A.D., Gorshkova N.M., Vysotskii M.V., Nicolau D.V., Yumoto N., Taguchi T. and Yoshikawa S., 1998. Phenotypic diversity of *Pseudoalteromonas citrea* from different marine habitats and emendation of the description Int J Syst Bacteriol. 48 Pt 1:247-256.

Ivanova E.P., Romanenko L.A., Chun J., Matte M.H., Matte G.R., Mikhailov V.V., Svetashev V.I., Huq A., Maugel T. and Colwell R.R., 2000. *Idiomarina* gen. nov., comprising novel indigenous deep-sea bacteria from the Pacific Ocean, including descriptions of two species, *Idiomarina abyssalis* sp. nov. and *Idiomarina zobellii* sp. nov Int J Syst Evol Microbiol. 50 Pt 2:901-907.

Kaye J.Z. and Baross J.A., 2000. High incidence of halotolerant bacteria in Pacific hydrothermal-vent and pelagic environments. FEMS Microbiol Ecol. 32:249-260.

Maki H., Sasaki T. and Harayama S. 2001. Photo-oxidation of biodegraded crude oil and toxicity of the photo- oxidized products. Chemosphere. 44:1145-51.

Mayr C., Winding A. and Hendriksen N.B., 1999. Community level physiological profile of soil bacteria unaffected by extraction method. J Microbiol Methods. 36:29-33.

COMPARATIVE SENSITIVITY OF BIOLUMINESCENT BACTERIA (MICROTOX TEST), GAMETES AND EMBRYOS OF THE SEA URCHIN *PARACENTROTUS LIVIDUS* TOWARD HEAVY METALS

A. Volpi Ghirardini, C. Losso, D. Marchetto,
G. Pessa, M. Picone and A. Arizzi Novelli
Dipartimento di Scienze Ambientali, Università Cà Foscari, Venezia

1. *Introduction.*

The integrated use of laboratory and field methods is nowadays recognized as the most suitable approach for assessing the occurrence or absence of ecological impairments in coastal marine and transitional environments. In this context, a battery of laboratory single-species toxicity bioassays is becoming of fundamental importance to assess water and sediment quality as a result of chemical pollution. Point and non-point sources of chemical pollutants affect the environmental quality of the Lagoon of Venice. In this ecosystem, a battery of reliable and sensitive toxicity bioassays can be used to monitor sediment quality, partly contributing to the proper management and recovery of polluted areas.

Carrying out methodological for some years our research group has been researches in order to develop reliable toxicity bioassays for environmental quality assessment of the Lagoon of Venice, mainly focusing on sediments. Methods already set up include a modified solid-phase bioassay protocol revealing *Vibrio fisheri* bioluminescent bacteria directly to suspended sediment (test Microtox®) (Volpi Ghirardini *et al.*, 1998; Volpi Ghirardini *et al.*, 1999; Bona *et al.*, 2000) and two short-chronic bioassays using the authoctonous Mediterranean echinoid *Paracentrotus lividus* (sperm cell and embryo toxicity bioassays) exposed to elutriates (Volpi Ghirardini *et al.*, 2001a) and pore water (unpublished data). Each method has been subjected to an iterative procedure of evaluation (repeatability, intralaboratory reproducibility, sensitivity, discriminatory ability

and correspondence with pollution levels) allowing progressive definition of their fiel of applicability to the Venetian lagoon environment. For each method the variability scale of responses along sediment pollution gradients was found. These methods are recognized worldwide (Volpi Ghirardini and Pellegrini, 2001) and also in Italy they have recently been proposed for monitoring estuarine and coastal marine environments (AA.VV., 2001 a, b).

In the Corila Project "Processi metabolici: produttività, cicli di nutrienti ed effetti dei contaminanti sul biota. Integrazione fra approccio sperimentale e modellistica ambientale e di rischio" application of these "biological models" has been proposed with two objectives: a) to contribute to the evaluation of toxic effects of priority contaminants which affect the Lagoon (using autochthonous species), to develop Ecological Risk Assessment models; b) to highlight pathological situations, causing possible dysfunction in lagoon metabolism, due to the accumulation of toxicity factors in sediments.

In order to investigate if the proposed toxicity bioassays can really contribute as "weight of evidence" in estimating of the quality of sediments in the Lagoon, it is necessary both to know their comparative sensitivity toward pure substances and to evaluate if range concentrations found in the environmental samples (i.e. marine waters, pore waters, sediments, etc.) can be directed by toxicity bioassays. Based on these objectives during the first year of the project a study was carried out to provide more exhaustive information on the comparative sensitivity of sea urchin to eight heavy metals (As, Cd, Cr, Ni, Pb, Cu, Zn and Hg) and to investigate if exposure to environmental concentrations (i.e. marine water, pore waters, sediments, etc.) recordered in researches carried out in the Lagoon can be detected by tests (Arizzi Novelli *et al.*, 2002a). Toxicity data (EC50 and NOEC may be useful in contributing to "objective a" (i.e. to assess toxic effects of priority contaminants for the Lagoon using autochthonous species) of the Corila project.

The present paper summarized the results of this study granted by Corila (detailed results are reported in Arizzi Novelli *et al.*, 2002a) and founded on the comparative sensitivity towards heavy metals of sea urchin fertilization test, sea urchin embryo test and Microtox test.

2. *Material and methods.*

Sperm cell and embryo toxicity test procedures were applied as reported in detail in previous papers (Volpi Ghirardini and Arizzi Novelli, 2001; Arizzi Novelli *et al.*, 2002b). These methods were developed in harmony with U.S.A standard methods and were tested for precision, intralaboratory reproducibility, comparability with Atlantic sea urchins using the same reference toxicant (Volpi Ghirardini and Arizzi Novelli, 2001) and reliability using organic (Volpi Ghirardini *et al.*, 2001b) and organometallic (Arizzi Novelli *et al.*, 2002b) substances. Preparation of solutions, quality control procedure and statistic analyses used to study heavy metal toxicity are detailed in the extended paper (Arizzi Novelli *et al.*, 2002a). EC50 data for Cd, Cr, Ni, Pb, Cu, Zn previously produced by our laboratory and already published (Passarini *et al.*, 2000) were used for test Microtox. Data for As and Hg were available in the literature (Kaiser and Devillers, 1994).

3. *Results and discussion.*

The toxicity data obtained for the two sea urchin bioassays are briefly summarized. The EC50 (mg/L) ranged from 0.017 mg/L (Hg^{2+}) to 16.21 mg/L (Pb^{2+}) for the sperm cell test, and from 0.046 mg/L (Hg^{2+}) to 3.06 mg/L (Cr^{3+}) for the embryo toxicity test. Both tests were able to discriminate heavy metal toxicity, showing differences in EC50 values of three and two orders of magnitude for sperm and embryo toxicity tests, respectively. Considering the data in mM/L, to better rank the toxicity of the heavy metals, the order of toxicity was $Hg^{2+} > Cu^{2+} > Zn^{2+} > As^{3+} \geq Cr^{3+} \geq Cd^{2+} \geq Pb^{2+} \geq Ni^{2+}$ (sperm cell test) and $Hg^{2+} \geq Pb^{2+} > Cu^{2+} > Zn^{2+} >$ Cd2+ $> Ni^{2+} > As^{3+} \geq Cr^{3+}$ (embryo test). Comparing sperm cell and embryo toxicity data, some considerations have been reported on the different effects of metals on the basis of known or presumed biological targets (Arizzi Novelli et al., 2002a). The NOEC values for sperm cell and embryo toxicity tests ranged from 0.01 mg/L (Hg^{2+}) to 1.9 mg/L (As^{3+}) (sperm cell test) and from 0.0025 mg/L (Pb^{2+}) to 0.2 mg/L (Cr^{3+}) (embryo toxicity test). Values showed differences of two orders of magnitude in both tests. The higher sensitivity of the embryo toxicity test with respect to the sperm cell test is also clear from the NOECs.

In order to investigate the applicability of sea urchin bioassays in assessing toxic concentrations of heavy metals in the Lagoon of Venice, results

for both tests were compared with environmental concentrations recorded in previous studies in different matrices, such as water column before and some hours after dredging (Collavini *et al.*, 2000) and pore water (Bertolin *et al.*, 1997). This comparison gave information on the most probable contaminants that the bioassays are able to detect on the basis of their "sensitivity limits". Result highlighted the fact that embryo toxicity test rather than the sperm cell test better reveals toxicity due to heavy metals in these matrices and that the sperm cell test can detect only sever contamination (Arizzi Novelli *et al.*, 2002a).

The comparative sensitivity toward heavy metals of both sea urchin tests and Microtox test (logarithmic scale) was investigated (Fig. 1). Comparing sea urchin bioassays it is evident that sensitivity of the embryo toxicity test is higher than that of the sperm cell test for Ni, Pb, Cd and Zn. The sensitivity of both test is comparable for As, Cr and Cu, while embryo test is less sensitive toward Hg. Both sea urchin tests are more sensitive than Microtox test with two exceptions: Hg (comparable EC50 shown by all tests) and Pb (only the embryotoxicity test is more sensitive than Microtox, while the sperm cell test, surprisingly, turned out to be less sensitive by almost two orders of magnitude). In all tests, as expected Hg^{2+}, is the most toxic of the heavy metals investigated.

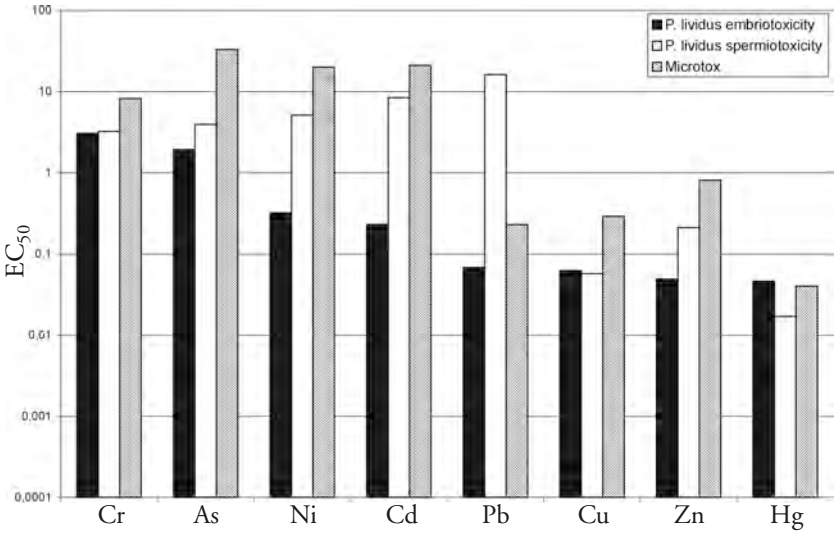

Fig. 1 - Comparative sensitivity of bioluminescent bacteria (Microtox test), gametes and embryos of the sea urchin *Paracentrotus lividus* toward heavy metals.

4. *Conclusion.*

The study demonstrated that both sea urchin tests were able to discriminate heavy metals toxicity showing differences in EC50 values of three and two orders of magnitude for sperm and embryo toxicity tests, respectively. The embryo test seemed particulary sensitive to Cd^{2+}, Ni^{2+}, Pb^{2+} and Zn^{2+}, whereas both tests showed similar sensitivity for Cu^{2+}, Cr^{3+} and As^{3+}. Comparison of the sensitivity limits of tests (NOEC) with heavy metals concentrations recordered in the Lagoon of Venice in previous studies in different matrices, demonstrated the potential ability of both bioassays to detect priority contaminants in this ecosystem.

Evaluation of the comparative sensitivity toward heavy metals of the two sea urchin tests and Microtox test demonstrated that the "sea urchin biological model", combining endpoints, is more effective in detective heavy metals toxicity in aqueous matrices than the Microtox test.

References.

AA.VV., 2001a. Giornata di studio "Indagini ecotossicologiche negli ambienti marini costieri in riferimento al D.L.152/99", Roma 6 marzo 2001, Biologia Marina Mediterranea 8 (2): 1-163.

AA.VV., 2001b. Ecotossicologia: acque dolci e marine. Atti Corso Unichim, Milano 28-29 novembre 2001.

Arizzi Novelli A., Losso C., Ghetti P.F. and Volpi Ghirardini A., 2002a. Toxicity of heavy metals using sperm cell and embryo toxicity bioassays with *Paracentrotus lividus* (Echinodermata: Echinoidea): comparisons with exposure concentrations in the lagoon of Venice (Italy). Env. Toxicol. Chem., accepted.

Arizzi Novelli A., Argese E., Tagliapietra D., Bettiol C. and Volpi Ghirardini A., 2002b. Toxicity of tributyltin and triphenyltin toward the early life stages of *Paracentrotus lividus* (Echinodermata: Echinoidea) Env Toxicol Chem 21 (4): 859-864.

Bertolin A., Mazzocchin G.A, Budello D. and Ugo P., 1997. Seasonal and depth variability of reduced sulphur species and metal ions in mud-flat pore-waters of the Venice lagoon. Mar Chem 59 (1-2):127-140.

Bona F., Cecconi G. and Maffiotti A., 2000. An integrated approach to assess the benthic quality after sediment capping in Venice lagoon. Aquatic Ecosystem Health and Management 3: 379-386.

Collavini F., Zonta R., Arizzi Novelli A. and Zaggia L., 2000. Heavy metals behaviour during resuspension of the contaminated anoxic sludge of the Venice canals. Toxicol Environ Chem 77:71-187.

Kaiser K.L.E. and Devillers J., 1994. Ecotoxicology of chemicals to *Photobacterium phosphoreum*. Gordon and Breach Science Publishers, Amsterdam.

Passarini F., Rampazzo G., Volpi Ghirardini A., Sperni L., Salizzato M. and Pavoni B., 2000. Extraction, identification and quantification of heavy metals in Venice lagoon sediments using toxicity tests with microorganisms, Annali di Chimica, 90: 91-101.

Volpi Ghirardini A. e Pellegrini D., 2001. I saggi di tossicità nella valutazione della qualità di acque e sedimenti di ambienti marini e di transizione: indicazioni per la scelta, la messa a punto, la valutazione e l'utilizzo dei metodi Biol. Mar Mediterranea 8 (2): 1-16.

Volpi Ghirardini A. and Arizzi Novelli A., 2001. A sperm cell toxicity test procedure for the Mediterranean species *Paracentrotus lividus*, Environ Technol 22: 439-445.

Volpi Ghirardini A., Arizzi Novelli A., Borsetto B., Delaney E. e Tagliapietra D., 2001a. Valutazione della tossicità dei sedimenti della laguna di Venezia mediante l'impiego di *Paracentrotus lividus* (Echinodermata: Echinoidea) Biol Mar Mediterranea 8 (1): 489-496.

Volpi Ghirardini A., Arizzi Novelli A., Likar B., Pojana G., Ghetti P.F., Marcomini A., 2001b. Sperm cell toxicity test using sea urchin *Paracentrotus lividus* Lamarck (Echinodermata: Echinoidea): sensitivity and discriminatory ability towards anionic and nonionic surfactants. Env Toxicol Chem 20 (3):644-651.

Volpi Ghirardini A., Ghetti P.F., Di Leo V. and Pantani C., 1998. Microtox® solid-phase bioassay in sediment toxicity assessment. Verh Internat Verein Limnol 26: 2393-2397.

Volpi Ghirardini A., Birkemeyer T., Arizzi Novelli A., Delaney E., Pavoni B. and P.F. Ghetti, 1999. An integrated approach to sediment quality assessment: the Venetian lagoon as a case study. Aquatic Ecosystem Health and Management 2 (4): 435-447.

USE OF BIOCHEMICAL, CELLULAR AND PHYSIOLOGICAL BIOMARKERS IN THE ASSESSMENT OF ENVIRONMENTAL QUALITY IN THE LAGOON OF VENICE: PRELIMINARY RESULTS

C. Nasci, L. Da Ros, N. Nesto, F. Meneghetti, A. Cella
Istituto di Biologia del Mare, CNR, Venezia

1. *Introduction.*

Over the last century, the coastal marine environments, including lagoon and estuaries, have been subjected to increasing anthropogenic inputs of xenobiotic substances which have greatly affected the health of these ecosystems. Therefore, the need of sensitive tools to be used in defining possible threats or damages to marine organisms and ecosystems has become more and more evident. Since the early eighties, many scientific efforts have been focused on the development of indices of biological effect as "early warning system" of adverse environmental changes, to be used in association with analytical chemical methods in monitoring programs on a world-wide scale (Goldberg *et al.*, 1975; Bayne *et al.*, 1988). Several studies based on chemical analysis have been carried out in the Venice lagoon to investigate the anthropogenic contamination (Fossato & Siviero, 1974, 1975; Fossato & Canzonier, 1976; Fossato & Craboledda, 1979; Campesan *et al.*, 1981, Nasci et al., 1985, 1991, 1998, 2000; Fossato *et al.*, 1989), but only in the last few decades the so-called "biomarker approach" has been applied in the lagoon environment quality assessment (Livingstone *et al.*, 1995; Livingstone & Nasci, 2000; Focardi *et al.*, 1998; Lowe & Da Ros, 2000). Field studies pose great difficulties, due on one hand to the complex and fluctuating nature of the environment itself, and, on the other, to the animal differences in their susceptibility to stress, resulting in an increased variability of biomarker responses. This is particularly evident in the Venice lagoon, which has been subjected to an heavy input of contaminants but also, in the last ten years, to intense fishing activity, mainly on *T. philippinarum*, with deleterious

effects on sediment resuspension and on benthic communities (Pranovi & Giovanardi, 1994; Pranovi *et al.*, 1998).

In this project a multiparametric approach has been applied. It consisted in measuring a suite of biomarkers determined at different degrees of biological organization from biochemical to physiological levels in sentinel organisms from differently impacted lagoon areas. Toxicity tests and pollutant concentrations in sentinel organisms, sediments and water will be carried on in the same sites by other research groups for a better understanding of the environmental data.

This approach could ultimately contribute to obtain:

- reliable biomarkers to be used as sensitive screening tools for environmental/ecological impact assessment
- development/validation of rapid, simple and cost-effective tests for measuring biological responses to lagoon stress factors .

To this end, on seasonal basis in the mussel, *Mytilus galloprovincialis*, a well-known and extensively used "sentinel" organism in environmental monitoring programs, the following biomarkers will be measured:

- *biochemical*, as catalase (Livingstone *et al.*, 1993) and aldheyde dehydrogenase activities (Forlin *et al.*, 1995). The catalase is an antioxidant enzyme detoxifying oxyradicals which can be increased by stress conditions. The aldheyde dehydrogenase is involved in the oxydative biotransformation of endogenous and xenobiotic compounds in more soluble and excretable products and it is inducible by exposure to pollutants;
- *cellular*, as neutral red retention time (Lowe *et al.*, 1995). This test is used to evaluate the condition of the lysosomal membranes by considering the retention time of neutral red dye into the lysosomal compartment before it leachs into the cytoplasm, being the elapsing time a measure of the membrane stability;
- *physiological*, as condition index (Lucas & Benninger, 1985) and survival in air (Eertman *et al.*, 1993). The condition index gives an indication of the animal physiological activity (growth, reproduction and secretion, etc.), and it is used to describe the fitness of the organisms; while the survival in air is employed to determine pre-existing stress undergone in the bivalve population normally adapted to periodical aerial exposure.

2. *Materials and method.*

Specimens of *M. galloprovincialis* were collected in October 2001 from three sites in the lagoon showing different type and degree of pollution (fig. 1):

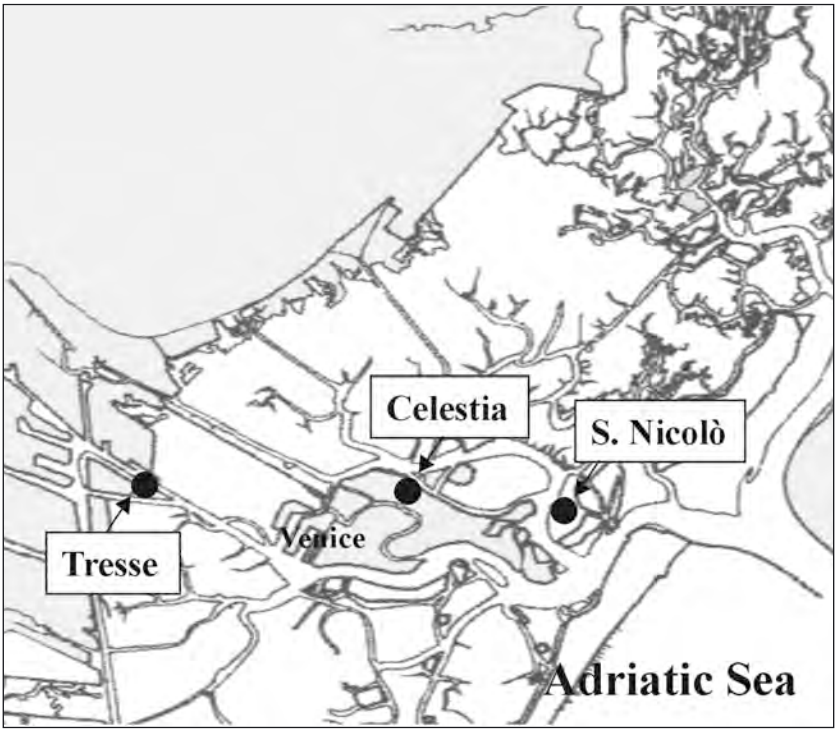

Fig. 1 - Sampling sites in the Venice Lagoon.

• Tresse (industrial contamination);
• Celestia (urban contamination);
• S. Nicolò (control site).

Collected mussels were kept in refrigerated box until the arrival in the laboratory where the organisms were processed for the different analyses.

The enzymes activity was determined in S9 cytosolic fraction of pool of digestive glands and all assays were carried out in five replicates. Catalase activity was measured following the decrease in absorbance at 240 nm, due to the H_2O_2 consumption $2H_2O_2 \varnothing 2H_2O_2 + O_2$ (Aebi, 1974). Aldehyde dehydrogenase was detected monitoring the increase in the absorbance at 340 nm, due to the reduction of NAD^+ propionaldehyde + NAD^+ + H^+ ∅ propionic acid + NADH (Förlin *et al.*, 1995).

The neutral red retention test was performed on the haemocytes of 10 individuals according to well established protocols (Lowe *et al.* 1995; Ringwood *et al.*, 1998).

After the incubation with the neutral red staining, the hemocytes were inspected under a microscope at time 15 minutes and then every 30 minutes to determine when loss from the lysosomes to the cytosol was evident. The test was terminated when dye loss was observed in 50 % of the small granular haemocytes (Lowe & Pipe, 1994; Ringwood et al., 1998).

The condition index was determined on 30 individuals after dehydratation in the oven (90° C for 48 hours) using the following ratio IC = dry weight of the wet meat / dry weight of the shell (Lucas & Benninger, 1985).

The survival in air was applied to a sample of 30 individuals placed in a constant room temperature of 18°C and 100 % humidity, with daily recording of the dead specimen was done. The LT50 (lethal time for the 50% of the sample) was calculated according to Kaplan & Meier (1958).

Data were compared using one-way analysis of variance (ANOVA) for biochemical analyses, the non-parametric Kruskal-Wallis test for neutral red assay and condition index, the Wilcoxon & Gehan test for the surviving curves (STATISTICA software package).

3. *Results and discussion.*

The results are reported in tab.1. Aldehyde dehydrogenase shows a significative higher value in the sample from Celestia (urban site) than in the S. Nicolò (control site) and Tresse (industrial site) ones, which exhibit similar levels. The catalase activity was similar in all the three samples, with values ranging from 0.79 to 0.96 mmol/min/g wwt.

Tab.1 - Biochemical, cellular and physiological parameters (mean ±SE) measured in *M. galloprovincialis* from different sites of the Venice Lagoon (October 2001).

	ADH (nmol/min/g w.wt.)	**CAT mmol/min/g w.wt.)**	**NR (min.)**	**IC**
S. Nicolò	29.62 ± 3.08	0.94 ± 0.10	58.5 ± 5.7	0.106 ± 0.005
Celestia	52.36 ± 8.14	0.96 ± 0.10	42 ± 5.8	0.071 ± 0.002
Tresse	27.13 ± 4.13	0.79 ± 0.13	33 ± 8.5	0.160 ± 0.007

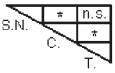

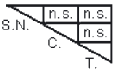

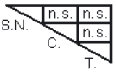

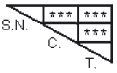

Statistical comparison: Anova for ADH and CAT, Kruskal-Wallis for NR and IC.
* = $p < 0.05$; *** = $p < 0.001$, n.s. = not significant.

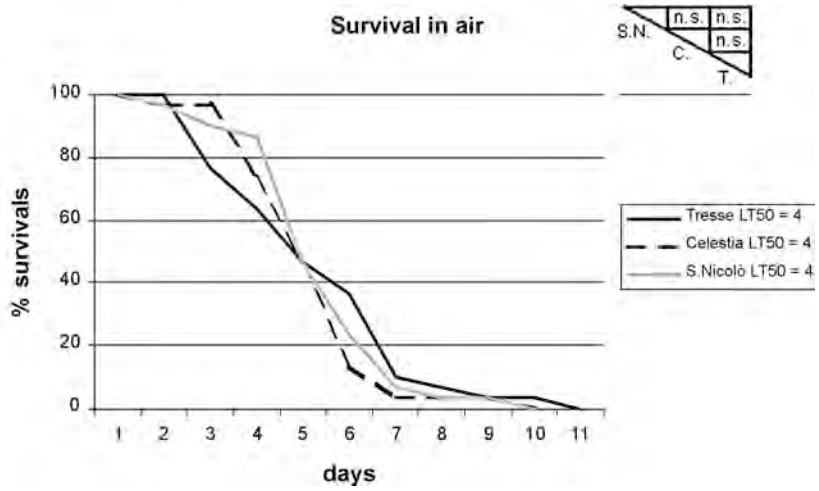

Fig. 2 - Surviving curves in *M. galloprovincialis* from different sites of the Venice Lagoon (October 2001). Statistical comparison (Wilcoxon & Gehan): n.s. = not significant.

As for the neutral red assay, the control sample S. Nicolò presents higher values of retention time to both the Celestia and Tresse ones, even though the differences are never significant.

As regards the physiological parameters, the condition index indicates the highest value at the industrial site showing a decreasing trend from Tresse> S Nicolò> Celestia. The survival curves show no statistical differences among the three sample and the related LT50 is the same for all three (LT50 =4 days) (fig. 2).

These preliminary results didn't reveal any significant difference among the areas as regards to the biological response at cellular and physiological level as survival in air in contrast with the condition index data. As for the biochemical parameters, only the aldehyde dehydrogenase showed an induction in the sample from Celestia, while catalase activity seems depressed in the industrial sites.

In the lagoon the mussels are generally exposed on a chronic basis to a complex mixture of contaminants. This often results in an acclimatation of the organisms to the severe environmental condition, through the activation of compensatory mechanisms (Nasci *et al.*, 1998). Moreover the biological responses to the presence of xenobiotics could be affected both by genetic and physiological variability of the organisms (size, age, growing rate, nutritional state, reproductive cycle) and by environmental parameters (temperature, salinity, dissolved oxygen, redox potential) (de Kock & Kramer, 1994; Lowe *et al.*, 1995). Consequently these prelimi-

nary results could be better understood and explained after the seasonal samplings will be completed and after the correlation with the contaminant level in the environment and in the biota will be made.

References.

Aebi H., 1974. Catalase. In: Methods of Enzymatic Analysis. Bergmeyer, H.U. (ed.). Academic Press, London, 671-684.

Bayne B.L., Clarke K.R. and Gray J.S., 1988. Background and rationale to a practical workshop on biological effects of pollutants. Mar. Ecol. Prog. Ser., 45, 1-5.

Campesan G., Fossato V.U., Stocco G., 1981. Metalli pesanti in mitili (*Mytilus sp.*) della Laguna veneta. Rapporti e Studi dell'Istituto veneto di scienze, lettere ed arti 8, 141-152.

De Kock W.C., Kramer J.M., 1994. Active biomonitoring (ABM) by translocation of bivalve molluscs. In: Kramer, K.J.M. (Ed.), Biomonitoring of Coastal Waters and Estuaries, CRC. Press Boca Raton, FL, 51-84.

Eertman R.H.M., Wagenvoort A.J., Hummel H., Smaal A.C., 1993. "Survival in air" of the blue mussel *Mytilus edulis* L. as a sensitive response to pollution-induced environmental stress. J. Exp. Mar. Biol. Ecol. 170, 179-195.

Focardi S., Fossi M.C., Leonzio C., Aurigi S., Casini S., Corsi I., Corsolini S., Monaci F., Sanchez-Hernandez J.C., 1998. Bioaccumulation and biomarkers responses to organochlorines, polycyclic aromatic hydrocarbons and trace metals in Adriatic Sea fish fauna. Rapp. Comm. Int. Mer Mèdit. 35, 1998.

Förlin L., Lemaire P., Livingstone D.R., 1995. Comparative studies of hepatic xenobiotic metabolizing and antioxidant enzyme in different fish species. Mar. Env. Res. 39, 201-204.

Fossato V.U., Campesan G., Craboledda L., Stocco G., 1989. Trends in chlorinated hydrocarbons and heavy metals in organisms from the Gulf of Venice. Archo Oceanogr. Limnol. 21, 179-190.

Fossato V.U., Canzonier W.J., 1976. Hydrocarbon uptake and loss by the mussel *Mytilus edulis*. Mar. Biol. 36, 243-250.

Fossato V.U., Craboledda L., 1979. Chlorinated hydrocarbons in mussels, Mytilus sp., from the Laguna Veneta. Archo Oceanogr. Limnol. 19, 169-178.

Fossato V.U., Siviero E., 1974. Oil pollution monitoring in the Lagoon of Venice using the mussel *Mytilus galloprovincialis*. Mar. Biol. 25, 1-6.

Fossato V.U., Siviero E., 1975. Idrocarburi alifatici in mitili prelevati da una stazione del Golfo di Venezia, scelta quale riferimento nella valutazione del grado di inquinamento della Laguna. Atti dell'Accademia Nazionale dei Lincei 8 (4), 641-646.

Goldberg E.D., 1975. The mussel-watch a first step in global marine monitoring. Mar. Pol. Bull. 6, 111.

Kaplan E.L., Meier P., 1958. Nonparametric estimation from incomplete observations. J. Amer. Statist. Assoc. 53, 457-481.

Livingstone D.R., Lemaire P., Matthews A., Peters L., Bucke D., Law R.J., 1993. Pro-oxidant, Antioxidant and 7-Ethoxyresorufin o-Deethylase (EROD) activity responses in liver of dab (*Limanda limanda*) exposed to sediment contaminated with hydrocarbons and other chemicals. Mar. Poll. Bull. 26 (11), 602-606.

Livingstone D.R., Lemaire P., Matthews A., Peters L.D., Porte C., Fitzpatrick P.J., Förlin L., Nasci C., Fossato V., Wootton N., Goldfarb P., 1995. Assessment of the impact of organic pollutants on goby (*Zosterisessor ophiocephalus*) and mussel (*Mytilus galloprovincialis*) from the Venice lagoon, Italy: biochemical studies. Mar. Env. Res. 39, 235-240.

Livingstone D.R., Nasci C., 2000. Biotransformation and antioxidant enzymes as potential biomarkers of contaminant exposure in goby (*Zosterissor ophiocephalus*) and mussel (*Mytilus galloprovincialis*) from the Venice Lagoon. In: Lasserre, P., Marzollo, A. (Eds), The Venice Lagoon Ecosystem. Inputs and Interactions between Land and Sea, UNESCO, Paris and The Parthenon Publishing Group, Lancs and N.Y. Press, 357-373.

Lowe D.M., Da Ros L., 2000. Cellular biomarkers of contaminant exposure and effect in mussel (*Mytilus galloprovincialis*) and goby (*Zosterissor ophiocephalus*) from the Venice Lagoon. In: Lasserre, P., Marzollo, A. (Eds), The Venice Lagoon Ecosystem. Inputs and Interactions between Land and Sea, UNESCO, Paris and The Parthenon Publishing Group, Lancs and N.Y. Press, 375-385.

Lowe D.M., Fossato V.U., Depledge M.H., 1995. Contaminant - induced lysosomal membrane damage in blood cells of mussel *Mytilus galloprovincialis* from the Venice Lagoon: an in vitro study. Mar. Ecol. Prog. Ser. 129, 189-196.

Lowe D.M., Pipe R.K., 1994. Contaminant induced Lysosomal membrane damage in marine mussel digestive cells: an in vitro study. Aquat. Toxicol. 30, 357-365.

Lucas A., Beninger P.G., 1985. The use of the physiological condition indices in marine bivalve aquaculture. Aquaculture 44, 187-200.

Nasci C., Campesan G., Fossato V.U., 1985. Indici fisiologici e biochimici di stress in *Zosterisessor ophiocephalus* della Laguna di Venezia. Oebalia 11 (3), N.S., 883-885

Nasci C., Campesan G., Fossato V.U., Tallandini L., Turchetto M., 1991. Induction of cytocrome P-450 and mixed function oxygenase activity by low concentrations of polychlorinated biphenyls in marine fish *Zosterisessor ophiocephalus* (Pall.). Aquat. Toxicol 19, 281-290.

Nasci C., Da Ros L., Campesan G., Fossato V.U., 1998. Assessment of the impact of chemical pollutants on mussel, *Mytilus galloprovincialis*, from the Venice Lagoon, Italy. Mar. Env. Res. 46(1-5), 279-282.

Nasci C., Da Ros L., Nesto N., Sperni L., Passarini F., Pavoni B., 2000. Biochemical and histochemical responses to environmental contaminants in clam, *Tapes philippinarum*, transplanted to different polluted areas of Venice Lagoon, Italy. Mar. Env. Res. 50, 425-430.

Pranovi F., Giovanardi O., 1994. The impact of hydraulic dredging for short-necked clams, *Tapes spp*. on an infaunal community in the lagoon of Venice. Sci. Mar. 58 (4), 345-353.

Pranovi F., Giovanardi O., Franceschini G., 1998. Recolonization dynamics in areas disturbed by bottom fishing gears. Hydrobiologia 375/76, 125-135.

Pulsford A.L., Thomas M.E., Lemaire-Gony S., Coles J., Fossato V.U., Pipe, R.K., 1995. Studies on the immune system of the goby, *Zosterisessor ophiocephalus,* from the Venice Lagoon. Mar. Pollut. Bull. 30(9), 586-591.

Ringwood A.H., Conners D.E., Hoguet J., 1998. Effects of natural and anthropogenic stressors on lysosomal destabilization in oysters *Crassostrea virginica*. Mar. Ecol. Prog. Ser. 166, 163-171.

OPTIMIZATION OF METAL SPECIATION TECHNIQUES IN VARIOUS ENVIRONMENTAL MATRICES AND APPLICATION TO THE STUDY OF POLLUTION IN THE LAGOON OF VENICE

E. Argese, C. Bettiol, S. Bertini,
L. Gobbo, C. Rigo
Dipartimento di Scienze Ambientali, Università Ca' Foscari, Venezia,

Metals play an important role in the deterioration of the Venice lagoon ecosystem. Since these pollutants are persistent in the environment, they can be hardly removed from the most contaminated sites, where they can reach very high levels and, as a consequence, cause serious problems to the community of organisms living therein. The presence of metals can influence negatively the efficiency of the lagoon metabolism, through the inhibition of the anabolic and catabolic processes that control the autoregulation and autodepuration capacity of the system.

This research is aimed at acquiring knowledge on the relationships between the chemical forms of metals and their bioavailability, on metal mobility in the various environmental compartments, on the pathways of introduction in the food chain and on bioaccumulation mechanisms. A particular attention is posed to metals such as mercury and arsenic, which are of great importance both for environmental and human health.

In the first part of the project, a procedure of geochemical speciation of metals in sediments has been optimized. This procedure partitions metals, by means of sequential selective extractions, in five fractions, corresponding to different forms of association in which metals are present in sediments. Each form is characterized by a different possibility of release to the overlying water column, as a function of the environmental conditions to which the sediment is subjected.

The speciation procedure has been applied to sediment samples collected in three sites of the lagoon of Venice with different water exchange, pollution tipology, organic matter content and granulometric distribution.

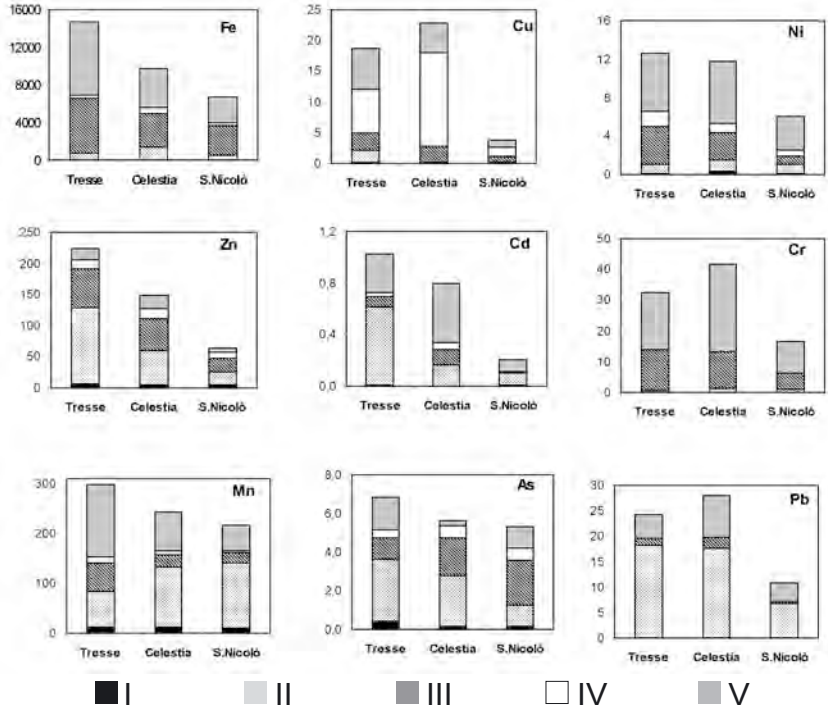

Fig. 1 - Total concentrations of metals and concentrations determined in the five fractions by the geochemical speciation procedure in sediment samples from the three sites. I) exchangeable, II) bound to carbonates, III) bound to Fe-Mn oxides/hydroxides, IV) bound to organic matter and sulphides, V) residual.
Concentrations are in mg/kg dry weight.

The results obtained are reported in figure 1. Concentrations are lower in the S. Nicolò site, which is located near one of the lagoon inlets and was intentionally chosen as a reference "blank".

In general, the Tresse and Celestia sites present a comparable metal contamination; however, in the first one the levels of Cd and Zn are higher, while the second site presents a higher concentration of lead. The Celestia site, though located far from the industrial area of Porto Marghera, shows a certain degree of contamination, that can be ascribed to sources of urban origin; in fact, it is known that the sludge of the inner canals of Venice contain high levels of metals [Argese et al., 1997]. Moreover, this site could be affected by pollutant inputs from the Murano island, where the glass industry is concentrated.

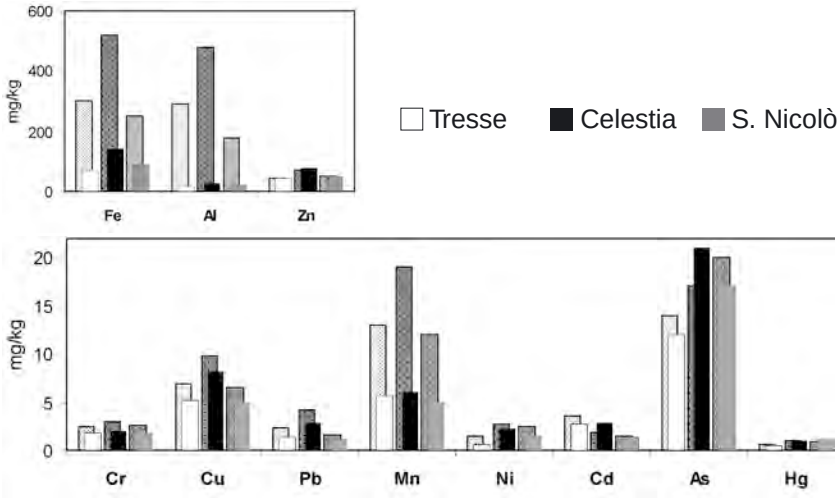

Fig. 2 - Concentrations of metals determined in the samples of *Mytilus galloprovincialis* collected in the three sites. The shaded values represent the concentrations determined in non-depurated organisms.
Concentrations are in mg/kg dry weight.

A further necessary step in the evaluation of the efficiency of lagoon metabolic processes in relation to the presence of pollutants involves the study of metal contamination in organisms. To this purpose, analytical methods for total metal content determination in biological samples have been set-up and validated by using certified reference materials. These methods have then been applied to the analysis of mussel (*Mytilus galloprovincialis*) samples collected in the same areas and at the same time of sediment sampling.

The differences between metal concentrations in mussels from the three sites are not very marked (fig. 2). Some metals, such as Cu, Pb, Ni, Zn and Hg, seem to present higher levels in the Celestia site. Though sediments collected at S. Nicolò were significantly less contaminated, mussels in general do not show lower levels in this site, with respect to the other ones. Therefore, the evidence of a relationship between metal concentrations in sediments and mussels appears rather complex.

The results illustrated in fig. 2 show also the importance of sample treatment before analysis; for various metals, in fact, a depuration step is necessary in order to acquire correct values of bioaccumulated concentrations.

Apart from the determination of total concentrations, the identification and quantification of various chemical forms of an element in envi-

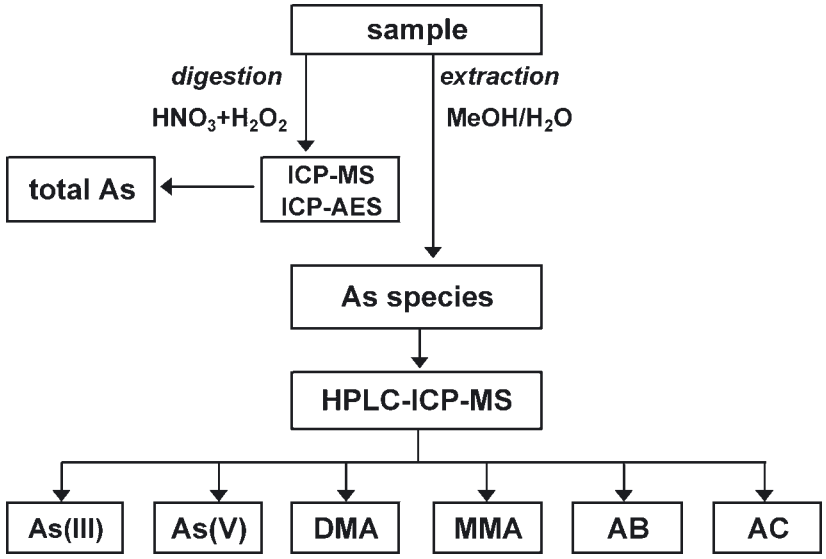

Fig. 3 – Scheme of the analytical procedure for the speciation of arsenic in biologial samples.

ronmental samples is of fundamental importance from an ecotoxicological point of view. These compounds differ not only in their physicochemical behaviour, but also can be subject to different accumulation and biotransformation processes in organisms, besides showing very different toxic effects [Stoeppler, 1992].

In this context, a procedure for the speciation of arsenic in biological samples is at an advanced stage of development (fig. 3). The phases of collection and treatment of samples, and the methods of extraction and separation of the various arsenic species, have been optimized. The analytical approach used for the determination of the arsenic species is the coupling of a separation technique, HPLC, with a very sensitive detector, such as ICP-MS [Larsen et al, 1997]. The compounds investigated are the inorganic species arsenite e arsenate, and the organic species monometilarsonic acid (MMA), dimetilarsinic acid (DMA), arsenobetaine (AB) and arsenocoline (AC). An example of a chromatogram obtained by anion-exchange HPLC-ICP-MS of a standard solution of the six arsenic species mentioned above is reported in figure 4.

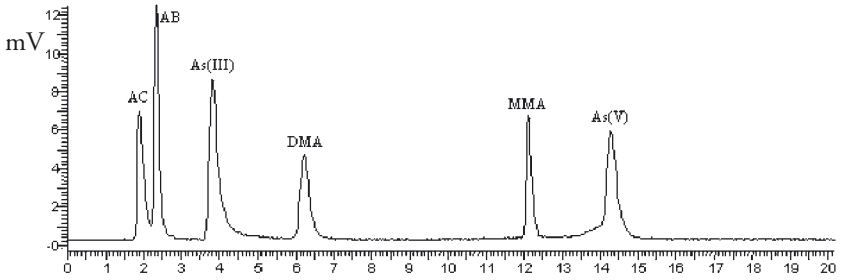

Fig. 4 – Chromatogram from anion-exchange HPLC-ICP-MS of a mixture of six arsenic standards (AC, AB, DMA, MMA 10 μg/l, As(III) and As(V) 20 μg/l).

References.

Argese E., Ramieri E., Bettiol C., Pavoni B., Chiozzotto E. and Sfriso A., 1997. Pollutant exchange at the water/sediment interface in the Venice canals. Water, Air & Soil Pollution, 99: 255-263

Larsen E.H., Quètel C.R., Munoz R., Fiala-Medioni A., Donard O.F.X., 1997. Arsenic speciation in shrimp and mussel from the Mid-Atlantic hydrothermal vents. Marine Chemistry, 57: 341-356

Stoeppler M., 1992. Hazardous Metals in the Environment. Elsevier Science, The Netherlands.

ESTROGENIC COMPOUNDS IN THE VENICE LAGOON: ANALYSIS AND SPATIAL DISTRIBUTION

G. Pojana, F. Busetti, A. Collarin, E. Badetti and A. Marcomini
Dipartimento di Scienze Ambientali, Università Cà Foscari, Venezia

The Venice lagoon can be considered an exemplar case of study for estrogenic compounds, because the high variety of inputs, such as untreated municipal wastewaters, treated industrial wastewaters, treated municipal wastewaters. Such substances are triggering an increasing interest because of their ubiquitous presence and their possible effects on aquatic organisms. A wide range of chemicals, resulting from human and animal metabolism, as well as from the use of synthesis compounds, is being discovered to induct estrogenic effects, because the relatively low specific specificity of receptors, even at concentrations in the ng/L range. A correct evaluation of lagoon metabolism should consider an estimation of removal from lagoon water of such compounds associated with production and degradation processes of organic matter. Moreover, area distribution of such compounds has to be established in order to identify sources and concentration gradients, and evaluate exposure concentration referred to effect concentrations.

Very accurate analytical procedures for the determination of such compounds in target environmental matrices are necessary to achieve such information. A new analytical method for the simultaneous determination of estrogenic compounds of metabolic (estradiol, estrone, estriol) and synthetic (mestranol, ethinylestradiol, diethilstylbestrol, bisphenol-A, benzophenone, nonphenol, carboxylated ethoxylated nonilphenols) origin by means of liquid chromatography coupled with mass spectrometry-ion trap via electrospray interface (HPLC-ESI-MS-IT), was developed. Such method was applied to the analysis of surface waters, collected in selected sampling stations (Fig. 1). Analyzed water samples indicate (Tab. 1) that concentrations of estradiol ed ethinylestradiol resulted

generally higher than LOEC (Low Observed Effect Concentration), while for other compounds, such as bisphenol A and nonphenol, determined concentrations were lower than NOEC (No Observed Effect Concentration) or in between NOEC and LOEC.

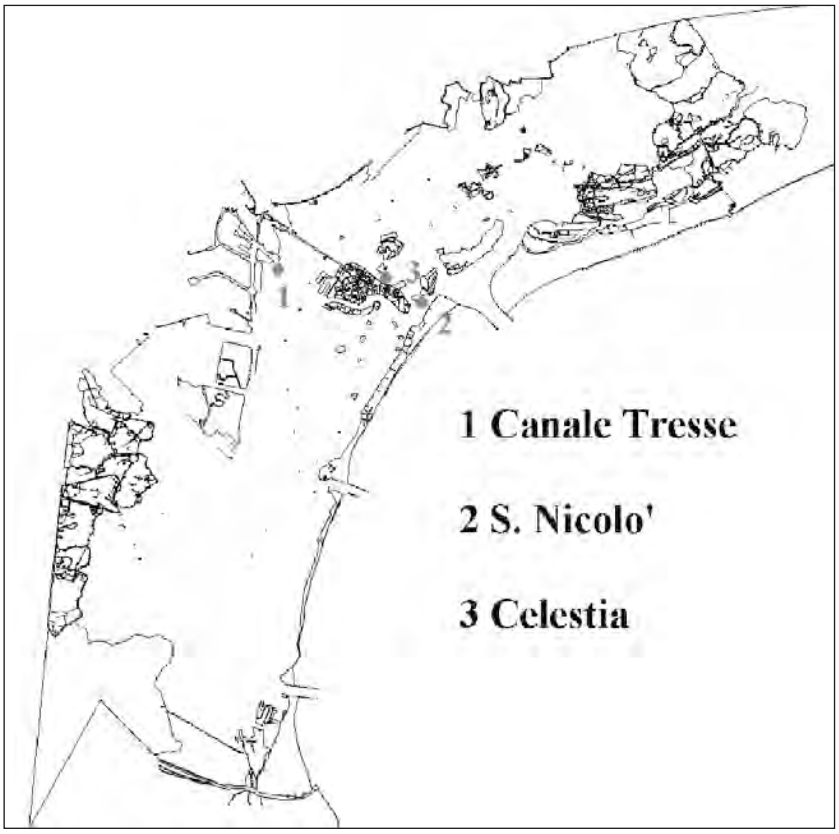

Fig. 1 – Location of sampling stations.

Tab. 1 - Concentration range of some determined estrogenic compounds in grab lagoon water samples collected in stations of Fig. 1.

Compound	Station 1	Station 2	Station 3
	Concentration in aqueous samples (ng/L)		
estradiol	3 - 36	3 - 13	8 - 175
ethinylestradiol	8 - 35	0.5 - 7	8 - 46
bisphenol-A	3 - 30	2 - 5	2 - 6
nonilfenol	4 - 40	4 - 25	6 - 23
benzophenone	1 - 35	20 - 35	15 -25

ANALYSES OF ORGANOTIN COMPOUNDS (TRI-, DI-, MONO- BUTYL- AND PHENYL-TIN) IN SEDIMENTS AND GASTROPODS OF THE LAGOON OF VENICE

B. Pavoni, F. Pellizzato, L. Sperni, E. Centanni
Dipartimento di Scienze Ambientali,
Università Cà Foscari, Venezia

Organotin compounds are a wide class of metallorganic compounds, mainly of anthropogenic origin, characterized by a $R_nS_nX_m$ general structure, with R as an alkyl or aryl substitute, and X an anionic species (i.e. halide, oxide or hydroxide), introduced since 1940s in different industrial applications, for example as stabilizers and catalyzers in PVC industries, which still represents their main employment. In the late 1950s organotin biocide properties were discovered which later gave rise to their applications as timber preservatives, fungicides, pesticide and coformulant in antifouling biocides (mid 1960s) applied on the hulls of the ships, on the aquaculture cages and released by shipyard activities [Hoch, 2001]. The most frequently found organotin compounds are: tributyltin (TBT) and triphenyltin (TPhT) and their degradation products mono- (MBT and MPhT) and di-substituted (DBT and DPhT). These were also selected for this investigation in the lagoon of Venice.

Once released in the aquatic environment, organotins are partitioned into different matrixes and degraded, with a progressive loss of organic groups from the Sn cation by photolysis, microbial activity, metabolism in some species of microalgae, or electrophilic and nucleophilic substitutions. Life time of organotin compounds in water is relatively low and is estimated to be in the range from four days to two weeks, in relation to the compound analyzed, but reaches a persistence of four years in the sediments. Their high lipophylicity enhances bioaccumulation in the biota as a consequence of ingestion and absorption through epithelia and membranes from water. Their toxicity towards organisms, which depends on nature and numbers of alkyl and aryl groups present in the molecule, is significant also at very low concentrations (1 ng/L) and at different tro-

phic levels: shell calcification anomalies in oysters [Alzieau *et al.*, 1986], ormonal disfunction in gastropods [Brian *et al.*, 1986] and immunologic disfunction in fishes [Suzuki *et al.*, 1992] are reported.

Since organotin final fate, bioavailability and toxicity in the environment depend on the chemical form of each congeners, the analytical procedure adopted in this investigation enables the determination of the named organotin congeners even at very low concentrations and in presence of many interferences. Such a procedure was validated by optimizing the following steps: extraction, derivatization with pentylmagnesiumbromide, preconcentration, clean-up and determination by GC-MS. Procedure accuracy and precision were determined by using certified materials and participating in inter-laboratory exercises.

The chemical analysis of samples collected from three stations in the lagoon of Venice showed that the organotins in the sediments are at relatively low levels (fig.1): the most contaminated sites were Tresse (TBT: 101±10, DBT: 61±8, MBT: 92±14 ng/g d.w.) and Celestia (TBT: 101±4, DBT: 65±28, MBT: 70±5 ng/g d.w.), and to a lesser extent Lido (TBT: 30±5, DBT: 9±1, MBT: 9±1 ng/g d.w.), in agreement with the different sources of pollution of this class of contaminants in each area. Phenyltin derivatives in the stations considered were at concentrations lower than the detection limit of the analytical procedure (LOD < 2 ng/g).

Levels of organotin significantly higher were found in biota tissues. Concentrations in the entire tissue of *H. trunculus* sampled in the central zone of Lido were: TBT, 286±20; DBT, 332±58; MBT, 325±145; TPhT, 42±28 ng/g d.w., and those found in S. Nicolò del Lido: TBT, 316±121; DBT, 405±176; MBT, 217±95; TPhT, 76±30 ng/g d.w.. A comparative analysis of the organotin content in muscle and visceral tissue reveals that there is no preferential bioaccumulation of the original congeners (TBT and TPhT) in the former. The degradations products (DBT and MBT), instead, are more concentrated in the visceral tissue rather than in the muscle, suggesting different metabolism and pathways of the pollutants in the body.

Levels of concentrations confirm the possibility of using these organisms as indicators of organotin contamination.

Organotin compounds are responsible for the appearance of *Imposex* (i.e. the imposition of male sexual characters on females) [Gibbs *et al.*, 1987] in many species of gastropod, including *H. trunculus*. Individuals of this gastropod were also biologically inspected to determine the imposex level, in terms of the Vas Deference Sequence Index (VDSI) as introduced by Gibbs *et al.* (1987) and modified for *H. trunculus* by Axiak *et al.* (1995).

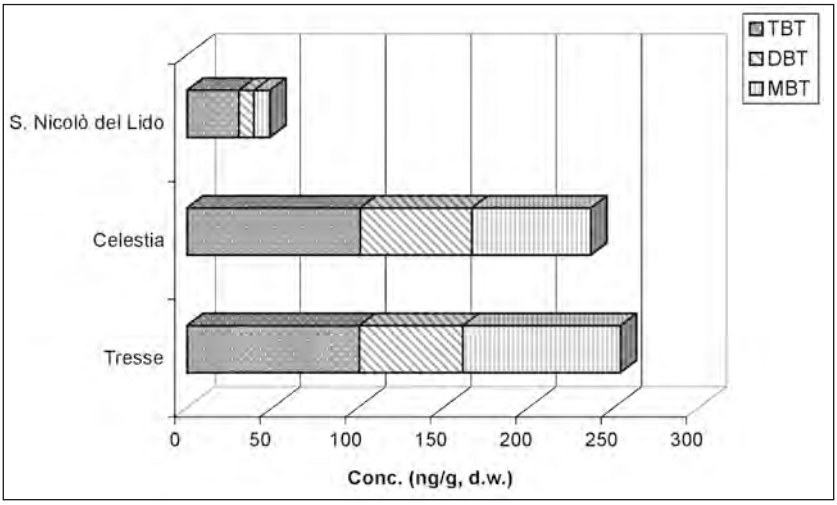

Fig. 1: Concentration of butyltin compounds (ng/g d.w.) in sediments of the sampling sites in the Lagoon of Venice.

This index determines 8 stages (from 0 to 5) of the biological effects, according to the absence/presence of a penis and a vas deference in female individuals. In the monitored stations imposex frequency was 100%.

References.

Alzieu C., Sanjuan J., Michel P. & Borel M., 1986. Tin contamination in Archacon Bay effect on oyster shell anomalies. *Mar. Poll. Bull*. 17, 494-498

Axiak V., Vella A.J., Micallef D., Chircop P. & Mintoff B., 1995. Imposex in *Hexaplex trunculus* (Gastropoda: Muricidae): first results from biomonitoring of tributyltin contamination in the Mediterranean. *Mar. Biol.* 121, 685-691

Brian G.W., Gibbs P. E., Burt G.R. & Hummerstone L.G., 1986. The decline of the gastropod *Nucella lapillus* around South-West England: evidence for the effects of tributyltin from anti-fouling paints. J. *Mar. Biol. Assoc.* UK. 66, 611-640

Gibbs P.E., Bryan G.W., Pascoe P.L. & Burt G.R., 1987. The use of the dog-whelk, *Nocella lapillus*, as an indicator of tributyltin (TBT) contamination. *J. Mar. Biol. Ass.* UK, 67, 507-523

Hoch M., 2001. Organotin compounds in the environment-an overview. *Appl. Geochem.*, 16, 719-743

Suzuki S., Matsuda R., Saito Y., 1992. Molecular species of tri-*n*-butyltin compounds in marine products. *J. Agric. Food Chem.* 40, 1437-1443

IDENTIFICATION OF A REMINERALIZATION MODEL AND ANALYSIS OF THE PRELIMINARY RESULTS

R. Pastres, S. Ciavatta, A. Petrizzo, D. Zanchettin
Dipartimento di Chimica Fisica, Università Cà Foscari, Venezia

Abstract.

In this paper we give a first account of our attempt of identifying a mathematical model for the simulation of the remineralization processes in a coastal lagoon and we present and discuss the preliminary results. The 1D dynamic model simulates the seasonal evolution of dissolved oxygen, nitrate, ammonia, sulphates and sulphides in the pore water of a sediment core. Precipitation and dissolution are described as non-equilibrium processes, while the concentrations of DIC species and pH are computed on the basis of the assumption that the carbonate system is at equilibrium.

1. *Introduction.*

The analysis of the dynamics of the processes which lead to the degradation of the organic matter in the sediment and to the release of inorganic Carbon, Nitrogen and Phosphorous back to the water column is of paramount importance for estimating the efficiency of the metabolism in an ecosystem. In spite of that, these processes have not been investigated in a systematic way in the lagoon of Venice and, up to now, no attempt of describing them by means of a deterministic mathematical model can be found in the literature. Furthermore, the majority of remineralization and early diagenesis models have been applied so far to deep sea sediments, which receive an approximately constant flux of organic carbon from the overlying water and whose temperature show limited seasonal variation. In these conditions, a steady-state solution of the governing equations is usually appropriate and leads to the estimation of the fluxes of nitrogen, carbon and phosphorous which are released back to the water

column [Rabouille and Gaillard, 1991]. However, a steady-state solution would not be adequate for describing realistically the degradation processes in the sediment of shallow coastal lagoons, such as the lagoon of Venice. In these systems, the seasonal fluctuations in the flux of organic matter and in the temperature are relevant moreover the bioturbation represents an important mixing mechanisms in the first layers of the sediment. As a result, the degradation of the organic matter and the subsequent release of phosphorous, ammonia and sulphide follow a seasonal pattern which can be described only by means of a dynamic model. In this paper we give a first account of our attempt of identifying such a model and we present and discuss the preliminary results.

2. *Methods.*

The degradation of the organic matter in a sediment core is the result of a sequence of complex redox processes. These processes are mediated by bacteria, which use for their own metabolism the Gibbs free energy released by the oxidation of the organic carbon to carbon dioxide. The free energy yield depends on the electron-acceptor species, as can be seen from Table 1, which shows the standard free energy of the most common reaction [Morel and Hering, 1993]. The different free energy yields give rise to an "ecological succession" among microbes, which, in turn, originates the so-called "biochemical zonation" within a sediment core.

As can be seen from (Tab.1), the degradation of the organic matter in the absence of molecular oxygen produces inorganic compounds, such as

Tab 1 - Standard free energy of the most common reaction of degradation of the organic matter, OM. The chemical composition of the organic matter is assumed to be: OM=(CH2O)106(NH3)16(H3PO4) [Morel, 1993].

	Processs	-ΔrG0 (kJ mol^{-1})
A	Aerobic respiration OM + 106 O_2 →106 CO_2 + 16 NH_3 + H_3PO_4 +106 H_2O	119
B	Denitrification OM + 84.8 NO_3^- + 84.8 H^+ → 106 CO_2 + 42.4 N_2 + 16 NH_3 + H_3PO_4 + 148.4 H_2O	113
C	Reduction of Mn ^{IV} OM + 212 MnO_2 + 424 H^+ → 106 CO_2 + 212 Mn^{+2} + 16 NH_3 + H_3PO_4 + 318 H_2O	96.9
D	Reduction of Fe ^{III} OM + 424 FeOOH + 848 H^+ → 106 CO_2 + 424 Fe^{+2} + 16 NH_3 + H_3PO_4 + 742 H_2O	46.7
E	Reduction of S^{VI} OM + 53 SO_4^{-2} + 53 H^+ → 106 CO_2 + 53 HS^- + 16 NH_3 + H_3PO_4 + 106 H_2O	20.5
F	Methanogenesis OM → 53 CO_2 + 53 CH_4 + 16 NH_3 + H3PO_4	17.7

NH_4^+ and HS^-, which are reoxidized when they reach the oxic layer. These secondary reactions represent important "sinks" for the oxygen and, hence, must be considered in the model, together with transport processes, which cause the redistribution of the chemicals along the vertical.

In order to simulate the degradation of the organic matter in a sediment core and the processes of early diagenesis, it is therefore necessary to take into account both the chemical/biochemical processes and the transport ones, which, in general, include the diffusion and the advection (i.e. burial and advection of pore water). This leads to the definition of a system of partial differential equation, which can be written as:

$$\frac{\partial c}{\partial t} = -v\frac{\partial c}{\partial z} + D(z)\frac{\partial^2 c_w}{\partial z^2} - f(c\ ,\beta, t)$$

where **c** is the state vector, v is the infiltration velocity, D is the diffusivity, which includes the bioturbation and therefore depend on the depth z, and **f** is the reaction term and β is the vector of parameter. The components of the state vector are the concentration in the interstitial water of the nine state variables listed in (Tab 2). Eq. (1) was solved by using an explicit finite-difference scheme, with a time step of 300 seconds and a vertical step of 10^{-2} m. A yearly simulation took about 600 seconds on a Digital 533Mhz Workstation. The structure of the model and the main interactions among the state variables are represented in (Fig. 1).

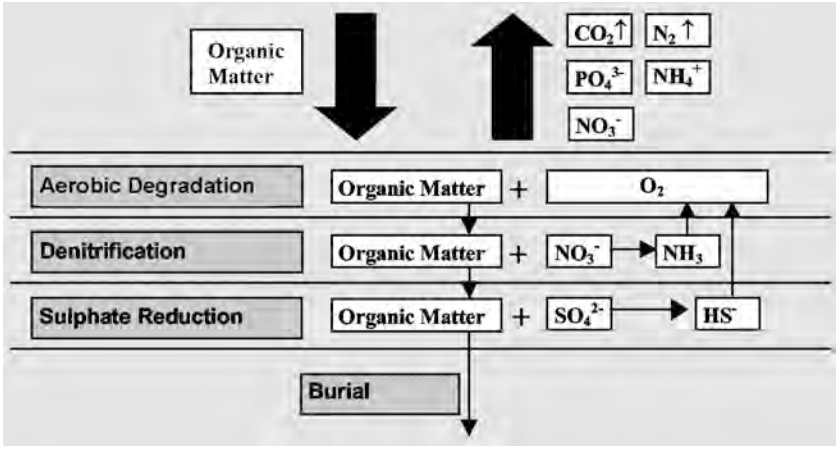

Fig. 1 - The main processes of the remineralization model.

The state variables were chosen on the basis of the current general literature [Wang and Van Cappellen, 1996, Chapelle, 1995, Rabouille and Gaillard, 1991], with the aim of keeping the complexity of the system as low as possible. The reduction of Mn^{II} and the methanogenesis were not included in the model as, in marine sediments, sulphate is, by far, the most abundant electron acceptor. Instead, the reduction of Fe^{III} was taken into account because a number of papers, [Giordani et al., 1996, Azzoni et al., 2001] suggest that the presence of Fe^{II} may reduce the damages caused by the occurrence of anoxic crisis in eutrophicated mediterranean coastal areas. The remineralization model was then coupled with a physical-chemistry model, in order to compute the carbonate equilibria and to take into account the pH-dependent precipitation-dissolution heterogeneous equilibria. The reaction terms, which include the heterogeneous equilibria, are shown in (Tab. 2). In accordance with [Wang and Van Cappellen, 1996] the "biochemical zonation" was simulated by using a set of control parameters, fci, i=1, …4 in (Tab. 2). At each time step, in each layer the control parameter is set to 1 if the concentration of the electron acceptor exceeds a given threshold, indicated with c_{lim} in (Tab. 3), [Chapelle, 1995], or to 0 if it falls below the threshold. Then, the most energetically favoured process is activated, while the other ones are inhibited.

3. *Results and discussion.*

As it was mentioned in the introduction, as far as we know, there are very few specific studies about the remineralization processes in the lagoon of Venice. This makes it very difficult to choose the initial values of the parameters and to fix the initial and boundary condition of the model in a realistic way. The initial and boundary values for dissolved oxygen, sulphate, sulphide and pH were taken from [Bertolin et al., 1997]. Boundary concentrations of ammonia and nitrate in the overlying water column were taken from a set of monthly data which were collected in the frame of a monitoring program carried out by the Venice Water Authority [Pastres, 1997, 1999]. A time-varying flux of organic carbon was imposed at the upper boundary, on the basis of the statistical analysis of chlorophyll a data which were collected in the same monitoring activity. The seasonal evolution of the other forcing functions, i.e. water temperature, was modelled by using a simple trigonometric function, whose coefficients were best-fitted against time series of high frequency temperature observations which were taken in shallow area of the lagoon

[Cossarini, 1999]. The values of the parameters were chosen in accordance with the general literature [Blackburn and Blackburn, 1993, Wang and Van Cappellen, 1996, Chapelle, 1995, Rabouille and Gaillard, 1991, Hunter et al., 1998].

Tab. 2. - The state vector and the state equations.

Organic Carbon (w)	C_{org}	Carbon dioxide (w)	CO_2
Dissolved Oxygen (w)	O_2	Ammonium (w)	NH_4^+
Nitrate (w)	NO_3^-	Sulphyde (w)	HS^-
Sulphate (w)	SO_4^{2-}	Ferric iron(w)	Fe^{III}
Ferrous iron(w)	Fe^{II}		

$$\mathbf{Adv + Diff} = -Pv\frac{\partial C_i}{\partial z} + P(D_B + D_m/\tau^2)\frac{\partial^2 C_i}{\partial z^2}$$

$$\frac{\mathbf{dC_{org}}}{\mathbf{dt}} = Adv + Diff - (1-P)\left(fc1\frac{\mu_{corg-O}(T)O_2}{K_{SO}+O_2} + fc2\frac{\mu_{corg-N}(T)NO_3^-}{K_{SN}+NO_3^-} + fc3\frac{\mu_{corg-F}(T)Fe^{III}}{K_{SF}+Fe^{III}} + fc4\frac{\mu_{corg-S}(T)SO_4^{-2}}{K_{SS}+SO_4^{-2}}\right)C_{org}$$

$$\frac{\mathbf{dO_2}}{\mathbf{dt}} = Adv + Diff - (1-P)fc1\,cs_{Corg-O}\left(\frac{\mu_{corg-O}(T)O_2}{K_{SO}+O_2}\right)C_{org} - P\,cs_{O2-N}\,\mu_{oxamm}(T)\left(\frac{O_2}{K_{SON}+O_2}\right)NH_4^+ - P^2\,\mu_{ox}(T)(cs_{O2-HS}\,HS^- + cs_{O2-Fe}\,Fe^{II})O_2$$

$$\frac{\mathbf{dNO_3^-}}{\mathbf{dt}} = Adv + Diff - (1-P)\,fc2\,cs_{Corg-N}\left(\frac{\mu_{corg-N}(T)NO_3^-}{K_{SN}+NO_3^-}\right)C_{org} + P\,\mu_{oxamm}(T)\left(\frac{O_2}{K_{SON}+O_2}\right)NH_4^+$$

$$\frac{\mathbf{dFe^{III}}}{\mathbf{dt}} = Adv + Diff - (1-P)\,fc3\,cs_{Corg-F}\left(\frac{\mu_{corg-F}(T)Fe^{III}}{K_{SF}+Fe^{III}}\right)C_{org} + P^2\,\mu_{ox}(T)cs_{O2-Fe}\,Fe^{II}\,O_2$$

$$\frac{\mathbf{dSO_4^{-2}}}{\mathbf{dt}} = Adv + Diff - (1-P)\,fc4\,cs_{Corg-S}\left(\frac{\mu_{corg-S}(T)SO_4^{-2}}{K_S+SO_4^{-2}}\right)C_{org} + P^2\,\mu_{ox}(T)cs_{O2-HS}\,HS^-\,O_2$$

$$\frac{\mathbf{dNH_4^+}}{\mathbf{dt}} = Adv + Diff + (1-P)cs_{Corg-N}\left(fc1\frac{\mu_{corg-O}(T)O_2}{K_{SO}+O_2} + fc2\frac{\mu_{corg-N}(T)NO_3^-}{K_{SN}+NO_3^-} + fc3\frac{\mu_{corg-F}(T)Fe^{III}}{K_{SF}+Fe^{III}} + fc4\frac{\mu_{corg-S}(T)SO_4^{-2}}{K_{SS}+SO_4^{-2}}\right)C_{org} - P\,cs_{O2-N}\mu_{oxamm}(T)\left(\frac{O_2}{K_{SON}+O_2}\right)NH_4^+$$

$$\frac{\mathbf{dFe^{II}}}{\mathbf{dt}} = Adv + Diff + (1-P)\,fc3\,cs_{Corg-F}\left(\frac{\mu_{corg-F}(T)Fe^{III}}{K_{SF}+Fe^{III}}\right)C_{org} - P^2\,\mu_{ox}(T)cs_{O2-Fe}\,Fe^{II}\,O_2 + [-k_{pFeS}fc_{pFeS}(\Omega_{FeS}-1) + k_{dFeS}fc_{dFeS}(\Omega_{FeS}-1)]$$

$$\frac{\mathbf{dHS^-}}{\mathbf{dt}} = Adv + Diff + (1-P)\,fc4\,cs_{Corg-S}\left(\frac{\mu_{corg-S}(T)SO_4^{-2}}{K_S+SO_4^{-2}}\right)C_{org} - P^2\,\mu_{ox}(T)O_2HS^- + [-k_{pFeS}fc_{pFeS}(\Omega_{FeS}-1) + k_{dFeS}fc_{dFeS}(\Omega_{FeS}-1)]$$

$$\frac{\mathbf{dCO_2}}{\mathbf{dt}} = Adv + Diff + (1-P)cs_{Corg-CO2}\left(fc1\frac{\mu_{corg-O}(T)O_2}{K_{SO}+O_2} + fc2\frac{\mu_{corg-N}(T)NO_3^-}{K_{SN}+NO_3^-} + fc3\frac{\mu_{corg-F}(T)Fe^{III}}{K_{SF}+Fe^{III}} + fc4\frac{\mu_{corg-S}(T)SO_4^{-2}}{K_{SS}+SO_4^{-2}}\right)C_{org}$$

$$\mu_i(\mathbf{T}) = \mu_i(25°)\bullet 1.07^{T-25°}$$

Tab. 3 - Parameters of the remineralization model.

SYMBOL	DESCRIPTION	SYMBOL	DESCRIPTION
P	porosity	CS	Stoichiometric coefficients
ô	tortuosity	K_{SO}	Half-saturation constatn for oxygen
v	Burial velocity (solid)	K_{SN}	Half-saturation constant for nitrate
	Advection velocity of pore water (dissolved)		
D_{Bo}	Bioturbation diffusivity at the water-sediment interface	K_{SS}	Half-saturation for sulphate
D_M	Molecular diffusivity	K_{SON}	Half-saturation constant for ammonium
T	Temperature	fc(1-4)	Control parameters
$\mu_{Corg\text{-}O}(T)$	Maximum specific aerobic respiration rate	C_{Limi}	Threshold concentrations
$\mu_{Corg\text{-}N}(T)$	Maximun specific denitrification rate	k_{pFeS}	FeS precipitation rate
$\mu_{Corg\text{-}S}(T)$	Maximum sulphate reduction rate	k_{dFes}	FeS dissolution rate
$\mu_{oxamm}(T)$	Maximum ammonium oxidation rate	S_{fFeS}	FeS solubiilty product
$\mu_{ox}(T)$	Maximum sulphyde oxidation rate	Ω	Saturation quotient

The preliminary results are summarized in (Fig. 2), which compares the seasonal evolution of the vertical profiles of sulphides with a set of experimental porewater data which were collected in a sediment core of the central part of the lagoon of Venice [Ugo, 2002]. The data set was partially presented in [Bertolin et al., 1993]. As it was stated in the introduction, the results should be regarded as preliminary ones because they were obtained by using initial estimates of the parameters which were not site-specific. However, as it can be seen in (Fig. 2), the model responds correctly to the seasonal evolution of the two forcings, i.e. the flux of organic carbon and the temperature. The increase in water temperature in the spring causes an increase in the bacterial activity: as a result the hydrogen sulphides, produced by the degradation via sulphate reduction, accumulates below the oxic layers during the summer and the autumn. The concentration of sulphides decrease in the following winter, when the production rate slow down and, therefore, the transport processes become effective in avoiding its accumulation. The experimental profiles show the same qualitative behaviour: the maximum concentrations are reached in the summer and in the yearly autumn, at depths ranging between 20 and 40 cm.

The simulation is in good quantitative agreement with the autumn and winter observed profiles and reproduces correctly the position of the sulphide maxima, but there is a systematic discrepancy between the model results and the spring and early summer data. The reasons of such a disagreement will be systematically investigated, in order to improve the performances of the model.

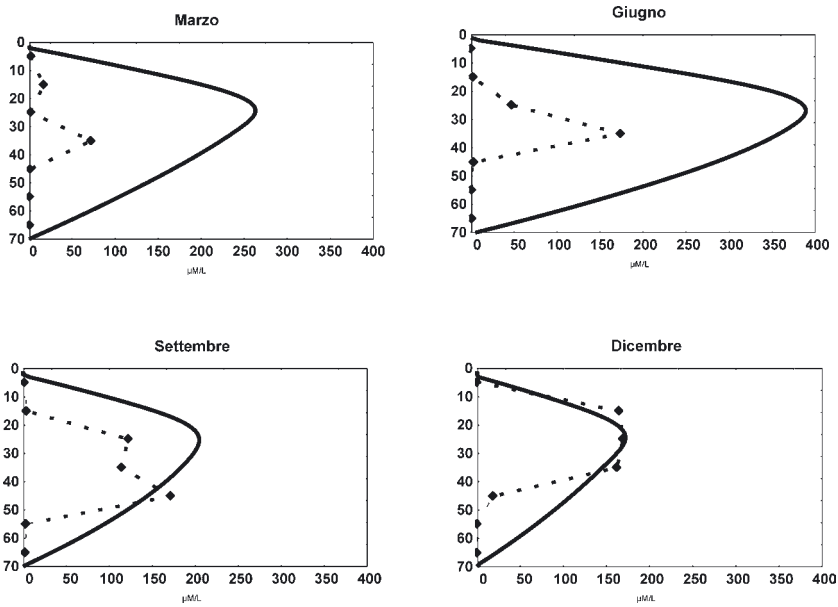

Fig. 2 - Seasonal evolution of the simulated and observed profiles of sulphides in a sediment core of the central part of the lagoon of Venice.

4. *Concluding remarks.*

Remineralization processes, which occur mainly in the sediment, play a central role in the metabolism of a shallow lagoon, as the degradation of organic matter releases phosphorous and nitrogen in inorganic forms. These internal fluxes of nutrients may be important for sustaining the primary production during the summer, when the external loads of these nutrients are lower than in the other seasons. To this regard, a dynamic model on one side offers the opportunity of obtaining information about the dynamic of these processes by analysing the data which are already available and, on the other, can provide an estimation of the releases of N and P, as a function of the flux of organic carbon from the water column to the sediment. The results presented in the previous section indicate that the model here presented could be a valuable tool for carrying out such an estimation. However, in order to achieve this aim, it will be necessary to calibrate the model. This key step, which will be preceded by a thorough sensitivity analysis, may highlight the fact that some experi-

mental information is still lacking and, therefore, may prompt further field studies. Such a "feedback" is, in our opinion, an extremely important aspect of the modelling activity, especially within the frame of large interdisciplinary projects such as the ones which are coordinated by CoRiLa.

References.

Azzoni R., Giordani G., Bartoli M., Welsh D.T., Viaroli P., 2001. Iron, sulphur and phosphorous cycling in the rhizosphere sediments of a eutrophic Ruppia cirrhosa meadow (Valle Smarlacca, Italy). Journal of Sea Research 45, 15-26

Bertolin A., Mazzocchin G.A., Rudello D., Ugo P., 1997. Seasonal and depth variability of reduced sulphur species and metal ions in mud-flat pore-waters of the Venice lagoon. Marine Chemistry 59, 127-140.

Blackburn T.H., Blackburn N.D., 1993. Rates of microbial processes in sediments. Phil. Trans. R. Soc. Lond. A 344, 49-58.

Chapelle A., 1995. A preliminary model of nutrient cycling in sediments of a Mediterranean lagoon. Ecological Modelling 80, 131-147.

Cossarini, 1999. Fattibilità di un confronto quantitativo tra i risultati di un modello tridimensionale di qualità dell'acqua e serie storiche spazio-temporali: applicazione al bacino lagunare veneziano. Master Thesis in Environmental sciences, Univ. of Venice.

Giordani G., Bartoli M., Cattadori M., Viaroli P., 1996. Sulphide release from anoxic sediments in relation to iron availability and organic matter recalcitrance and its effects no inorganic phosphorous recycling. Hydrobiologia 329, 211-222.

Hunter K.S., Wang Y., Van Cappellen P., 1998. Kinetic modeling of microbially-driven redox chemistry of subsurface environments: coupling transport, microbial metabolism and geochemistry. Journal of Hydrology 209, 53-80.

Morel F.M.M. and Hering J.G., 1993. Principles and applications of aquatic chemistry. John Wiley & Sons, US.

Pastres R., Solidoro C., 1997. Trattamento ed analisi dei dati anche mediante un modello di qualità dell'acqua (ex art. 55 del Capitolato Speciale) - Rapporto finale - Interventi per l'arresto del degrado connesso alla proliferazione delle macroalghe in laguna di Venezia 1995-1996. Consorzio Interuniversitario "La chimica per l'ambiente" - Consorzio "Venezia Nuova", Venezia.

Pastres R., Solidoro C., 1999. Trattamento ed analisi dei dati anche mediante un modello di qualità dell'acqua (ex art. 55 del Capitolato Speciale) - Rapporto finale - Interventi per l'arresto del degrado connesso alla proliferazione delle macroalghe in laguna di Venezia 1997-1998. Consorzio Interuniversitario "I.N.C.A." - Consorzio "Venezia Nuova" - Istituto Nazionale di Oceanografia e Geofisica Sperimentale, Venezia.

Rabouille C., Gaillard J.F., 1991. A coupled model representing the deep-sea organic carbon mineralization and oxygen consumption in surficial sediments. Journal of Geophysical Research, Vol. 96, No. C2, 2761-2776.

Ugo P., 2002. Personal Comunication.

Wang Y., Van Cappellen P., 1996. A multicomponent reactive transport model of early diagenesis: Application to redox cycling in coastal marine sediments. Geochimica et Cosmochimica Acta Vol.60 N16, 2993-3014.

ESTIMATION OF FLUXES AND RECONSTRUCTION OF HISTORICAL TRENDS OF PCDD/Fs AND PCBS IN THE VENICE LAGOON

M. Dalla Valle[1], A. J. Sweetman[1], K. C. Jones[1] and A. Marcomini[2]
[1]*Department of Environmental Science, Institute of Environmental and Natural Sciences, Lancaster University, Lancaster, UK.*
[2]*Dipartimento di Scienze Ambientali, Università Cà Foscari, Venezia*

1. *Introduction.*

The Venice lagoon has a long history of industrial activity and from the 1950s the inner lagoon area of Porto Marghera expanded as chemical and oil refining plants were developed. Although emissions from the industrial area have been consistently reduced because of the decline of the chemical industry and the adoption of new abatement technologies, high concentrations of PCDD/Fs, polychlorinated biphenyls (PCBs), polycyclic aromatic hydrocarbons (PAHs) and heavy metals still affect sediments, especially in the central lagoon, thus providing a potential source for the lagoon ecosystem and for human exposure, through the ingestion of seafood. Other sources are represented by atmospheric deposition, the discharge of untreated municipal effluents from the historical centre and the emissions associated with heavy aquatic traffic, due to local transportation, fishing activities, cruisers and oil tankers [Fattore et al., 1997]. Extensive sampling campaigns have been conducted in recent years, especially in the central part of the lagoon. Surface sediment, water, settleable particulate matter (SPM) and biota (clams, mussels, crabs and fishes) have all been analysed and physico-chemical data and environmental parameters have been recorded [Dalla Valle et al., 2002] (i.e. temperature, pH, organic carbon fraction in sediment and particulate matter, particulate matter concentration and fluxes). Four sites in the central lagoon were the focus of investigation, selected to represent contamination gradients. These are (Fig 1): Alberoni, close to the Malamocco Channel (site A); Sacca Sessola (site B), in an area of intense fishing activity; San Giuliano (site C), close to the mainland and to the Osellino Canal and Fusina (site D), in front of the industrial area

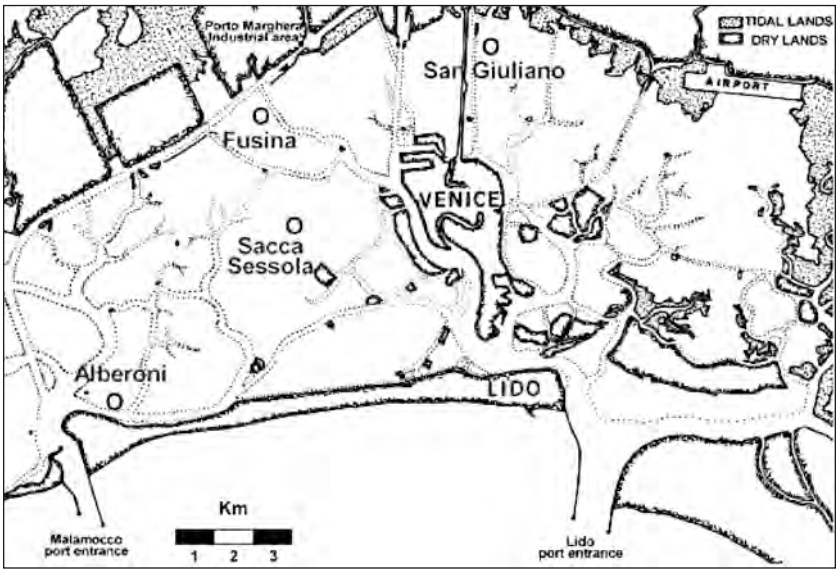

Fig. 1 - Map of the central lagoon.

and the industrial canals. The contaminant contribution of rivers from the catchment area and of atmospheric deposition were also investigated. The central part of the lagoon, between the Malamocco and Lido channels linking the lagoon to the Adriatic Sea, covers a water surface of ca. 132 km^2 and is quite well mixed hydrologically. PCDD/F emissions are now much lower than in the past [Frignani et al., 2001], but contaminated sediment in some areas of the industrial canals and surrounding areas can act as a significant long-term secondary source of PCDD/F to elsewhere in the lagoon as it becomes transported and re-distributed. High re-suspension of bottom sediments is caused by intensive fishing for clams (*Tapes Philippinarum*), shipping activity and tidal currents. These processes favour high sediment-water exchange, whilst the shallow warm waters of the lagoon encourage high biological productivity and air-water exchange.

2. *Estimation of PCDD/F fluxes.*

2.1 *Methods.*

The central part of the lagoon was chosen to evaluate the equilibrium status and to develop a mass-balance model to predict the steady state

concentrations and fluxes of individual PCDD/F congeners for key environmental compartments. Firstly the distance from the equilibrium of the congeners distribution was assessed by comparing fugacity values in each compartment. In fact, the comparison of fugacity values of a congener in the different environmental compartments allows to estimate the proximity to the equilibrium and fluxes direction. Actual fugacity values can be easily calculated from experimental concentrations in the compartments from the relationship: C = Z·f. Since air concentration values were not available, they had to be estimated from experimental findings resulting from an atmospheric deposition survey.

Then the QWASI (Quantitative Water Air Sediment Interaction) model was applied [Mackay, 2001], as it allows - once environmental parameters (e.g. total water surface, mean depth, organic carbon content in sediment), physical-chemical characteristics (such as PLs, log(Kow) and Henry's law constant), inputs and advective flows are known - to predict concentration values in all environmental media. The model, based on the fugacity concept, enables also to estimate the intermedia fluxes at the steady state condition.

2.2. *Results and discussion.*

The air/sediment fugacity ratios show a different behaviour in the different zones of the central lagoon (Fig.2). In the industrial district the

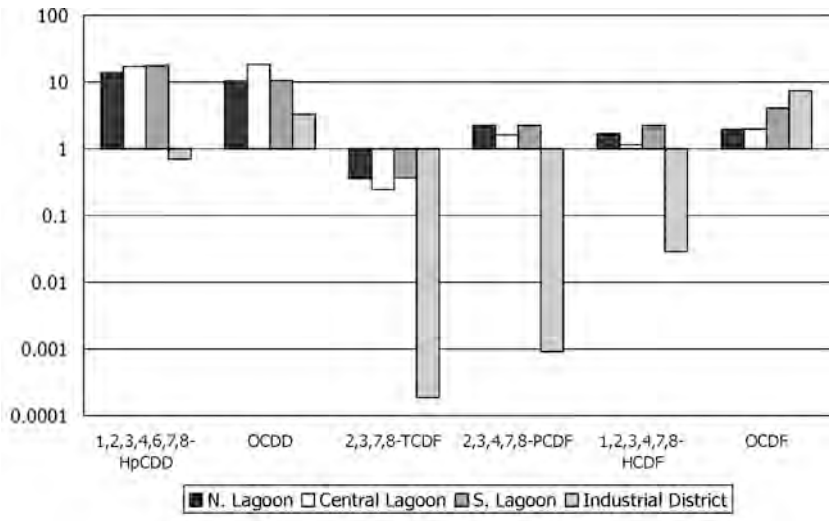

Fig. 2 - Air/sediment fugacity ratios in different lagoon areas.

ratio is close to 1 for the heavier congeners (HpCDD, OCDD and OCDF) while it is well below 1 for the lighter ones (TCDF, PeCDF and HCDF). For these congeners a net transfer from the sediment to the water column and then to the atmosphere is likely to occur. For the rest of the lagoon, a net deposition is likely to occur for HpCDD and OCDD, while the other congeners are close to equilibrium, except for TCDF, for which the fugacity ratio is between 0.24 and 0.36 (possible volatilisation).

The air/water fugacity ratio is calculated using non-filtered water samples, thus fugacity values, when above the detection limit, refer to bulk water. Fugacity ratios in this case exhibit the same result, suggesting deposition for the heavier congeners and volatilisation for the lighter ones (Fig. 3).

The sediment-SPM ratio was calculated from fugacity values obtained from matched samples of sediment and suspended particulate matter in four sampling sites located in the central part of the lagoon (Fig. 4). The ratio is always very close to 1, with minor differences among the stations, suggesting conditions very close to equilibrium.

The PCDD/F pattern predicted by the QWASI model for the sediment reflects exactly the input profile, with a dominance of OCDD, HpCDF and OCDF over the other congeners (Fig. 5). In water (non filtered) the profile is almost identical, due to the influence of SPM, while

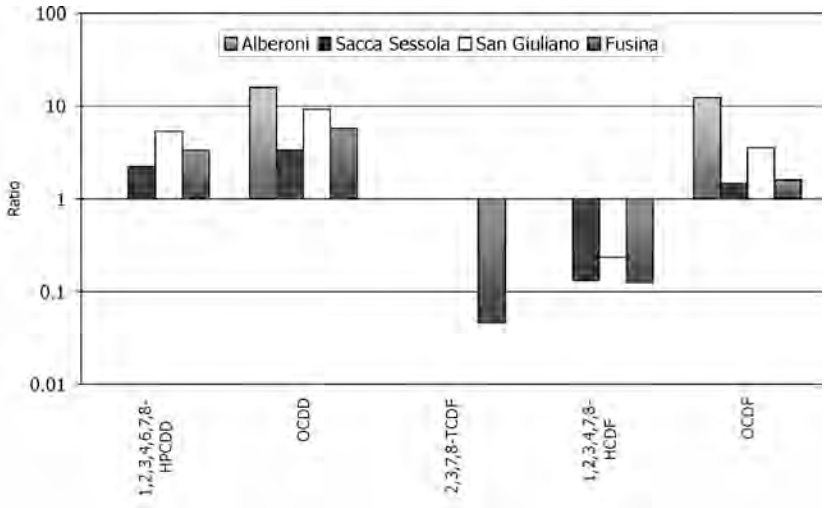

Fig. 3 - Air/water fugacity ratios in four station of the central lagoon.

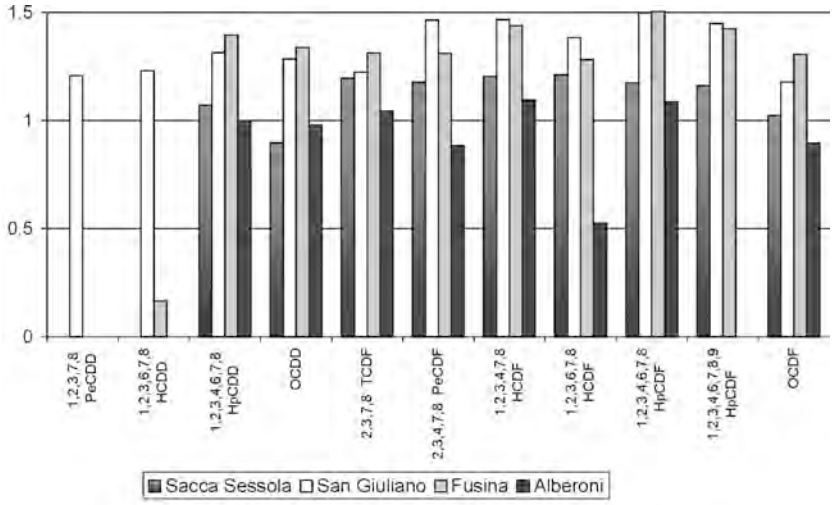

Fig. 4 - Sediment/SPM fugacity ratio in four stations of the central lagoon.

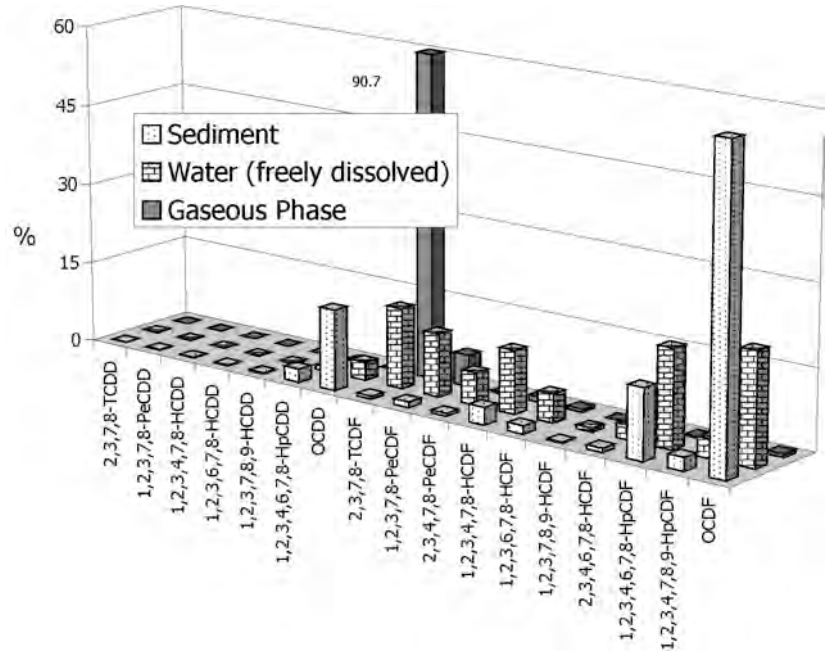

Fig. 5 - Congeners profile as predicted by the QWASI model.

the profile of the freely dissolved congeners is enriched in TCDD, TCDF, PeCDF and HCDF, while the importance of the heavier furans is similar. The atmospheric profile is completely different, with a clear dominance of TCDF, due mainly to its higher values in vapour pressure and in the Henry's law constant. In the gaseous phase TCDF represents about 90 % of the total dioxins and furans concentration.

3. *Comparison between dated cores and industrial deposition patterns.*

Extensive surveys on the sediment of the canals in the industrial district were carried out in recent years, providing a clear picture of the distribution pattern of PCDD/Fs. The samples of surficial sediment show, except for some localised spots affected by local and limited sources, a very similar pattern, dominated by OCDF and to a minor extent by HpCDF and OCDD (Fig. 6).

The pattern profile in the sediment of the industrial canals does not show a significant variation over time meaning that the fingerprint of the industrial district has maintained fairly constant during at least the last 50 years. Only the concentration levels vary, with a peak during the 1950s - 1960s and a significant decrease during the past two decades. Results from several surveys have shown that the total concentration of PCDD/Fs peaked between the 1960s and 1970s, with a dominance of PCDFs over PCDDs, and concentrations of OCDD and OCDF higher than lower chlorinated homologues [Dalla Valle et al., 2002]. OCDF is a marker compound for industrial activities in the lagoon, with its concentration and relative importance in the total PCDD/Fs pattern decreasing with increasing the distance from the industrial district. Over the last few years a comprehensive field investigation was undertaken which included the annual monitoring of PCDD/Fs in river and atmospheric deposition as well as the examination of salt marsh and industrial canal cores. The PCDD/Fs congeners profile of the surficial sediment taken from two salt marsh sites has been compared to the one relating to the atmospheric deposition on the same zones (southern and northern lagoon). The resulting statistical correlation found was for both the samples higher than 97%, while the correlation between the same samples and the atmospheric deposition pattern in the industrial district was lower than 40%. In the deeper layers the correlation with the corresponding atmospheric deposition decreases gradually to ca. 40-50% in the 15-18cm layer (where the PCDD/Fs concentration is maximum) then it rises again (Fig. 7, 8). This

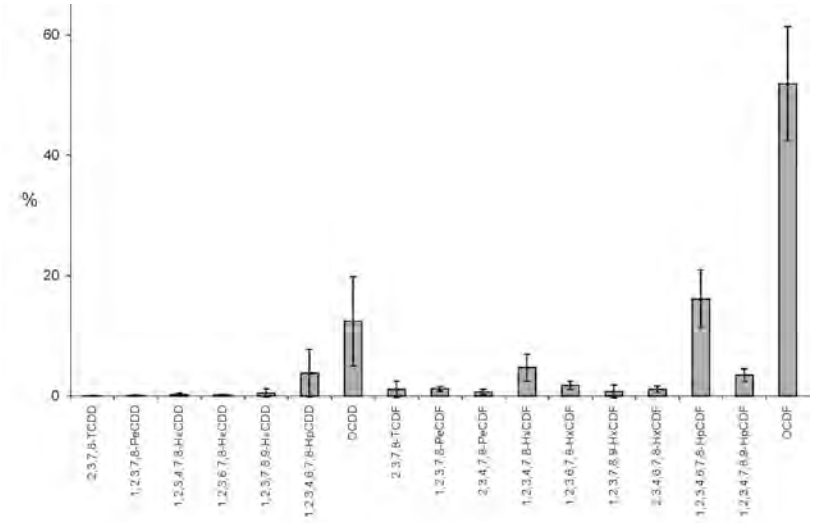

Fig. 6 - Congeners profile in the industrial lagoon surficial sediment (n = 37).

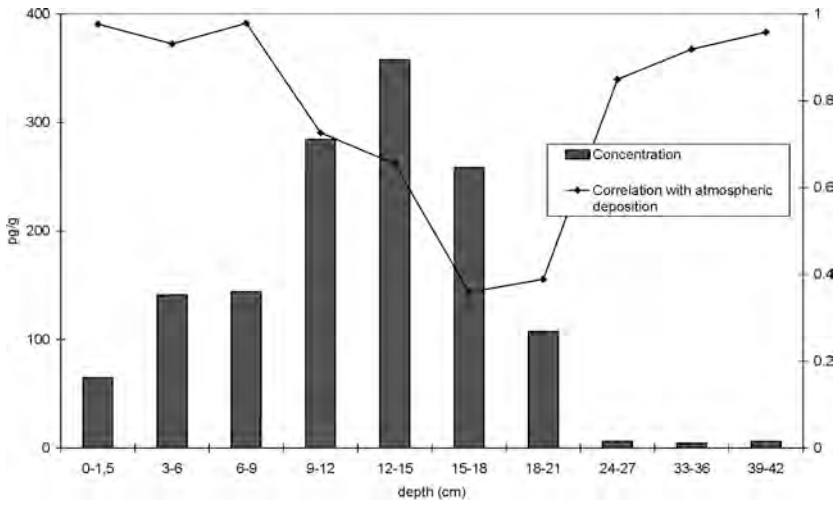

Fig. 7 - PCDD/Fs concentrations in salt marsh sediment (Northern Lagoon) and statistical correlation with the atmospheric deposition pattern.

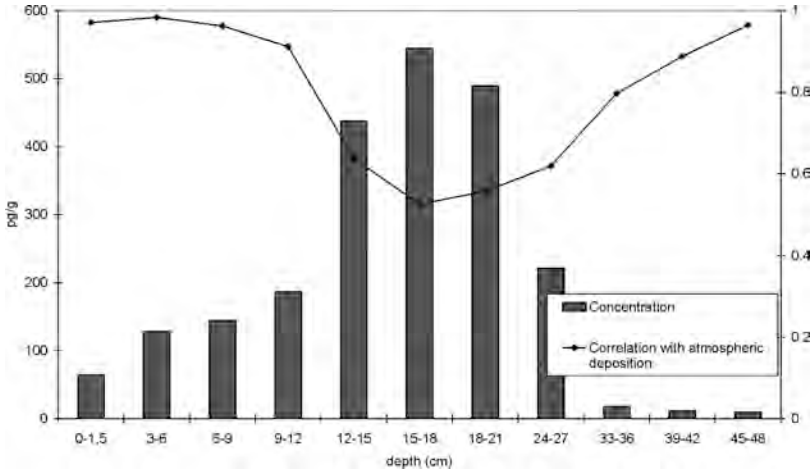

Fig. 8 - Total PCDD/Fs concentration in salt marsh sediment (Southern Lagoon) and statistical correlation with the atmospheric deposition pattern.

means that the profile on the surface and in the deep layers is dominated by the PCDD fraction, OCDD in particular, typical of an urban or general anthropic impact, while the medium levels (dated around the 1960s) are very similar to the pattern found in the sediment of the industrial canals. The correlation in fact between the deposition in the industrial district and the 12-15cm layer in the core taken in the northern lagoon and 15-18cm layer in the southern lagoon core is respectively 91% and 99%. The two layers can be dated around the 1960s. The correlation between the pattern of the atmospheric deposition in the industrial area, or of the sediment of the industrial canals, is higher in the Southern lagoon core for all the layers, as a consequence of the prevailing wind direction.

In conclusion:

1) the salt marsh sediment has been proved as a suitable and powerful tool to estimate the past trend of atmospheric deposition;
2) the deposition patter over the lagoon is a result of the sum of two different inputs, one influenced by the industrial district while the other can be regarded as background;
3) the influence of the industrial district was much higher in the past, peaking around the 1960s. Its influence in the atmospheric deposition is nowadays extremely reduced in its extent and range.

4. *Reconstruction of temporal trends of PCDD/Fs and PCBs.*

4.1. *Methods and materials.*

As follows from the considerations above and according to recent investigations carried elsewhere [Fox et al., 1999, 2001], the salt marsh cores have proved to be a suitable record of atmospheric total deposition. The objectives of this study were to:

a) reconstruct the historical trends of PCDD/Fs and PCBs in the Venice lagoon, in each environmental compartment;
b) develop a dynamic multimedia environmental model for the Venice lagoon which can be applied to other classes of pollutants.

A dynamic multimedia environmental model was developed in order to reconstruct the temporal trend of selected congeners of PCDD/Fs and PCBs in the Venice lagoon. The fugacity-based model, an evolution of Mackay's QWASI model, considers 5 compartments (air, water, suspended particulate matter in water, soil and sediment), their inputs, outputs and intermedia fluxes. Given an input scenario, the model also predicts the future concentrations in each compartment for some selected chemicals, namely: PCB 105, PCB 118, PCB 156, PCB 167, PCB 180, PCB 170, 1,2,3,4,6,7,8-HpCDD, OCDD, TCDF, 1,2,3,7,8-PeCDF, 1,2,3,4,7,8-HCDF, 1,2,3,4,6,7,8-HpCDF, OCDF. The central part of the lagoon, with a total surface of ca. 132 km^2, was considered. Inputs to the model environment were estimated from the study of dated sediment cores.

4.2. *Results and discussion.*

The trend observed for all congeners of PCDD/Fs reflects the history of production and usage of the examined compounds, with a peak in the atmosphere and in water around the 1960s and a delayed peak for soil and sediment. The peak concentrations in sediments were reached between the 1960s and 1990s, depending on the congener, reflecting the input profile, which has been estimated by studying two dated sediment cores sampled in two salt marshes. Salt marshes have been recently proved to be useful and reliable in reconstructing temporal trends of POPs (persistent organic pollutants).

A good agreement is observed between experimental results and concentrations predicted by the model for the year 2000, the difference is significant only for a few congeners (Table. 1). For all PCDD/F congeners the ratio predicted/measured concentration, averaged for the central lagoon, was always lower than a factor 6 for the sediment and within a

Tab. 1 - Comparison between experimental and predicted concentrations of selected PCDD/F and PCB congeners.

Congener	Sediment			Water		Air
	Predicted concentration (ng/kg)	Measured concentration (avg ± st.dev.) (ng/kg)	Predicted/ Measured	Predicted concentration (pg/L)	Measured concentration (min - max) (pg/L)	Predicted concentration fg/m3
1,2,3,4,6,7,8-HpCDD	77	12 ± 17	6.4	2.5	0.4 - 0.7	360
OCDD	260	44 ± 52	5.9	18	1.5 - 2.8	608
2,3,7,8-TCDF	3	2.7 ± 3.0	1.1	0.1	< 0.5	184
1,2,3,7,8-PeCDF	2	4.0 ± 4.5	0.6	0.1	< 0.5	226
1,2,3,4,7,8-HCDF	15	11 ± 12	1.4	0.4	0 - 0.9	25
1,2,3,4,6,7-8-HpCDF	101	63 ± 62	1.6	3.5	1.1 - 4.3	358
OCDF	27	138 ± 173	0.2	0.9	1.9 - 10.5	398
						ng/m^3
PCB 118	284	153 ± 175	1.9	11	50 - 90	1.8
PCB 105	837	44 ± 52	35	30	0 - 10	0.7
PCB 167	3938	60 ± 47	66	144	30	0.2
PCB 156	832	101 ± 90	8	27	20 - 30	0.1
PCB 180	4217	413 ± 448	10	148	160 - 210	0.4
PCB 170	130	193 ± 207	0.7	7	110 - 120	0.5

Tab. 2 - Sensitivity analysis for 1,2,3,4,7,8-HCDF.

Parameter	Air		Water		Water particles		Sediment	
	-10%	+ 10%	-10%	+ 10%	-10%	+ 10%	-10%	+ 10%
Air residence time	-	-	-	-	-	-	-	-
Air-side air-water MTC	-	-	-	-	-	-	-	-
Atmospheric heigth	-	-	-	-	-	-	-	-
Deposition velocity	9.8%	-9.8%	0.05%	-0.04%	-	-	-	-
Diffusion in soil	-	-	-	-	-	-	-	-
Degradation in air	-	-	-	-	-	-	-	-
Degradation in sediment	0.4%	-0.5%	2.5%	-2.6%	2.5%	-2.6%	2.5%	-2.6%
Degradation in water	0.05%	-0.05%	0.5%	-0.5%	0.01%	-0.01%	-	-
Aerosol concentration	10.0%	-10.0%	0.4%	-0.3%	-	-	-	-
SPM concentration	-	-	-	-	-	-	-	-
Henry's law constant	-0.2%	0.2%	-2.4%	2.1%	-11.3%	9.2%	-11.3%	9.2%
Kow	1.1%	-0.9%	9.4%	-9.3%	9.8%	-9.8%	9.9%	-9.9%
Molecular diffusivity in air	-	-	-	-	-	-	-	-
Molecular diffusivity in water	-	-	-	-	-	-	-	-
Rain velocity	1.7%	-1.7%	-0.03%	0.03%	-	-	-	-
Sediment depth	1.1%	-0.9%	9.5%	-9.5%	9.1	-9.0	9.8%	-9.8%
SPM deposition	0.02%	-0.01%	0.2%	-0.1%	10.0%	-10.0%	-0.02%	0.01%
Diffusion length path in sed.	0.9%	-0.8%	8.1%	-8.0%	-0.1%	0.1%	-0.1%	0.1%
Sediment-water effective diff.	-0.9%	0.8%	-8.9%	8.3%	0.1%	-0.1%	0.1%	-0.1%
Scavenging ratio	1.7%	-1.7%	0.1%	-0.1%	-	-	-	-
Soil-water effective diffusivity	-	-	-	-	-	-	-	-
Temperature	-10.8%	9.8%	-8.5%	7.0%	0.1%	-0.1%	0.1%	-0.1%
Vapour pressure	-11.1%	9.1%	-0.03%	0.03%	-	-	-	-
Water residence time	-0.03%	0.03%	-0.2%	0.2%	-0.2%	0.2%	-0.2%	0.2%
Water-SPM exchange rate	-	-	-	-	-	-	-	-
Water side air-w MTC	-0.06%	0.05%	0.07%	-0.06%	-	-	-	-
Water side w-sed MTC	-0.02%	0.01%	-0.2%	0.2%	0.01%	-0.01%	0.04%	-0.03%

factor 5 difference for the water concentration. The predicted concentration for PCBs in sediment are comparable with the experimental results for PCB 118, PCB 170 and PCB 156, while for the other congeners the concentrations are overestimated by at least an order of magnitude. Water concentrations are comparable with experimental findings, with the exception of PCB 180 for which concentrations were about an order of magnitude lower. Concentrations in the atmosphere were estimated, with values ranging between 100 and 1800 pg/m^3. Corresponding measured values are not available, and for this reason a sampling campaign has been recently undertaken.

Future trends for the same congeners were predicted, assuming a constant decrease of the inputs tending to a zero emission in the year 2050. The reduction in environmental levels depends primarily on the assumed degradation rates, with derived congener-specific half-lives range between 10 and 50 years.

A sensitivity analysis was performed to identify the parameters that most influence the model output and possibly the environmental behaviour of the studied compounds (Table 2). They were: degradation constants, Kow, Henry's law constant, vapour pressure, active sediment depth, sediment resuspension and deposition rates and water residence time in the lagoon. Other parameters seem to influence the model output (i.e. the concentration) for only one compartment. Air concentration is very sensitive to deposition velocity, aerosol concentration, scavenging ratio and precipitation rate. Diffusion constants in water and air have little influence.

References.

Dalla Valle M., Marcomini A., Sfriso A., Sweetman A.J. and Jones K.C., 2002. Estimation of PCDD/F distribution and fluxes in the Venice lagoon, Italy. Submitted to Chemosphere.

Fattore E., Benfenati E., Mariani G., Fanelli R. and Evers E.H.C., 1997. Pattern and sources of polychlorinated dibenzo-p-dioxins and dibenzofurans in sediment from the Venice Lagoon, Italy. Env. Sci. Technol. 31, 1777-1784..

Fox W.M., Connor L., Copplestone D., Johnson M.S. and Lee R.T., 2001. The organochlorine contamination history of the Mersey estuary (UK) revealed by analysis of sediment cores from salt marshes. Marine Environmental Research 51, 213-227.

Fox W.M., Johnson M.S., Jones S.R., Leah R.T. and Copplestone D., 1999. The use of sediment cores from stable and developing salt marshes to reconstruct historical contamination profiles in Mersey estuary, UK. Marine Environmental Research 47, 311-329.

Frignani M., Bellucci L.G., Carraro C. and Favotto M., 2001a. Accumulation of polychlorinated dibenzo-p-dioxins and dibenzofurans in sediments of the Venice Lagoon and the industrial area of Porto Marghera. Marine Pollution Bulletin, Vol. 42, No. 7, 544-553.

Mackay D., Joy M. and Paterson S., 1983. A quantitative water, air, sediment interaction (QWASI) fugacity model for describing the fate of chemicals in lakes. Chemosphere 12, 981-997.

Mackay D., 2001. Multimedia Environmental Models. The Fugacity Approach, 2nd edition. Lewis publishers. Boca Raton, Florida, USA.

REVIEW OF PRELIMINARY CONCEPTUAL MODEL OF THE LAGOON ECOSYSTEM, AND APPLICATION OF ECOLOGICAL RISK ASSESSMENT MODEL TO THE FOOD WEB

C. Micheletti, E. Semenzin, A. Critto, A. Marcomini
Dipartimento Scienze Ambientali, Università Ca' Foscari, Venezia

The Ecological Risk Assessment (ERA) has been applied within a decision support system developed according to a risk management framework, since it possesses features such as process reiterativety, capability of comparing and prioritizing different risks, and finally capability of merging scientific issues and management needs in the choice of the assessment endpoints.

According to the US EPA procedure (1998) and to ECOFRAME (ECOFRAME AQUATIC WORKGROUPS, 1999) tiered approach, a first tiered ERA was undertaken to estimate risk for the food web of the Venice lagoon. The risk was estimated by comparing the bioaccumulation in the tissue of selected organisms and the effect levels reported in the literature.

Persistent and toxic contaminants accumulated in sediments and in suspended particulate matter, as well as those dissolved in water, tend to concentrate in the tissue of organisms at the bottom of the food chain, possibly reaching harmful concentrations; moreover, the contaminants may adversely affect the top levels of the food web (particularly fish communities) by bio-magnification.

As far as the monitoring activity is concerned, it is essential to identify organisms or trophic groups exposed to the highest risk.

According to the proposed research program, the first tier of analysis was carried out, i. e. the Problem Formulation phase of ERA was accomplished which included the definition of preliminary conceptual model of the lagoon's ecosystem and the selection of the bioaccumulation model used for assessing the aquatic organism exposure.

The conceptual model focused on the detailed description of the food web, allowing the subsequent ecological risk assessment models to be applied. The selected food web model (Libralato et al., 2002) consisted of

27 elements (a single specie or trophic groups, detritus and the suspended and labile organic matter) distributed on 4 levels. At the bottom level there are the primary producers, followed by the benthic organisms, grouped according to size (micro-meiobenthos and macro-benthos) and feeding strategies (detritivore, herbivorous filter feeder, carnivorous, omnivorous). Finally, at the top level there are fishes, both autochthonous species and marine species that spend in the lagoon only a part of their life cycle.

Based on this frame, the food web organisms exposure was estimated, by applying bioaccumulation models. After a literature review, the Food Chain model (Gobas, 1993) was selected which is steady-state model for estimating concentrations of hydrophobic organic substances in various organisms of aquatic food-webs, including fish, benthos, macrophytes, aquatic plants etc., from chemical concentrations in the water and sediments. The model combines the toxicokinetics of chemical uptake, elimination and bioaccumulation in individual organisms and the trophodynamics of food-webs to estimate chemical concentrations in different organisms of food-webs. This food-web model differs from simple four-level generic food-chain models (e.g. Thomann 1989, Clark et al. 1990) since it includes multiple feeding interactions, and despite its genericity, it can be applied to food-webs on a site specific basis. The model is relatively simple and requires only few input data, which makes it easy to apply for practical use.

The model is generic in the sense that it can make model predictions for any aquatic food-chain. However, it requires site-specific input information to make realistic estimates of concentrations in actual food-webs. By means of a friendly interface, it is possible to introduce data concerning chemical properties, the environmental conditions and characterization of the organisms of the food-web included the fish diet matrix composition.

The Food Chain model (Gobas, 1993) required the adaptation of the previous food web model (Libralato et al., 2002) in order to include six trophic groups (Fig. 1): phytoplankton, zooplankton, detritivorous benthos, filter feeders benthos, carnivorous-omnivorous benthos, fishes. For the first five trophic groups, only the bio-concentration was considered (i.e. partitioning of hydrophobic substances between lipid fraction of the organisms and total organic carbon fraction of sediments) while for fishes the bio-magnification (i.e. the uptake through the diet) was also included.

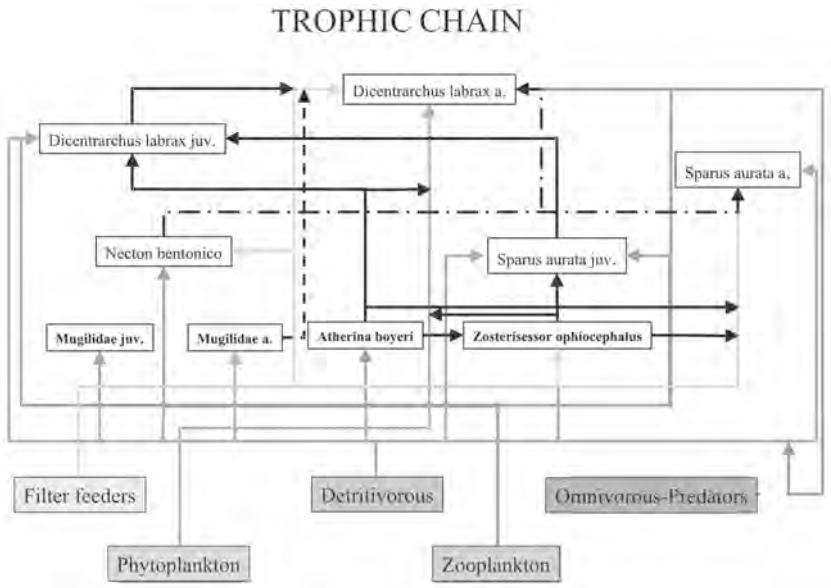

Fig. 1 - Food web model adapted from Libralato et al. (2002) and used by the Food Chain model to estimate the bioaccumulation of the hydrophobic organic pollutants in the organisms.

References.

Clark K.E., Gobas F.A.P.C. and Mackay D., 1990. Model of Organic Chemical Uptake and Clearance by Fish from Food and Water, Environ. Sci. Technol. 24, 1203-1213.

Gobas A.P.C.F., 1993. A model for predicting the bioaccumulation of hydrophobic organic chemicals in aquatic food webs:application to Lake Ontario. Ecological Modelling, 69: 1-17.

Libralato S., Pastres R., Pranovi F., Raichevich S., Granzotto A., Giovanardi O.E., Torricelli P., 2002. Comparison between the energy flow nwtworks of two habitats in the Venice Lagoon, Mar. Ecol., In Press.

Thomann R.V., 1989. Bioaccumulation model of organic chemical distribution in aquatic food chains. Environ. Sci. Technol. 23:699-707.

US-EPA, 1998. Guidelines for Ecological Risk Assessment. Washington DC: Risk Assessment Forum. EPA/630/R-95/002F.

RESEARCH LINE 3.4.
Chemical contamination

METALS REMOBILIZATION FROM SEDIMENTS OF THE VENICE LAGOON

G. Capodaglio[1], C. Chapman[2], CMG van den Berg[2], F. Corami[1], C. Turetta[3], E. Magi[4] and F. Soggia[4].
[1]*Dipartimento di Scienze Ambientali, Università Ca' Foscari, Venezia.*
[2]*Oceanography Laboratories, Liverpool University, UK.*
[3]*Istituto per Studio della Dinamica Ambientale, CNR, Venezia*
[4]*Dipartimento di Chimica, Università degli Studi di Genova.*

1. *Introduction.*

Studies carried out to evaluate sediment contamination in the Lagoon of Venice emphasized important problems of pollution in the central Lagoon[1-3] However very few is known about the contaminants mobility, the exchanges between water and sediments can be responsible for secondary pollution deriving from re-mobilization of pollutants introduced in the past time.

Processes responsible for these fluxes are the upward flow of pore water caused by diffusion and bioturbation. In coastal areas, characterized by low depth and organic rich waters, changes of oxygen concentration in the waters can produce variations in trace components cycling, that can generate both upward and downward fluxes[4,5]. These events are common in transition environments such as that in the Lagoon of Venice.

The aim of this research program is to investigate the mobility of trace elements using benthic chambers at two sites characterized by high metal concentration. Here we report preliminary results obtained to evaluate the mobility of Pb, Cd and Cu and Fe; samples were analysed for nutrients, metals in dissolved and particulate phases; thiol compounds as candidates for specific complexing ligands were also determined in the dissolved phase.

2. *Experimental.*

Experiments were carried out in July 2001 in two polluted areas of Lagoon of Venice; the first was carried out in the Tresse channel area bet-

Fig. 1 - Sites used for the benthic chamber experiments, (1) a Tresse channel area, R) (b) Campalto Isle area.

ween July 9th and 11th and the second in the Campalto area between July 23rd and 25th (see figure 1). Water samples were taken over a period of more than 45 hours every 3-4 hours from six 125L benthic chambers covering one area of about 3 m^2; to avoid changes in the ratio volume/surface due to collecting samples, the chambers were used in sequence: 2 samples of 2 L each and one third of 15 L were collected from the first chamber, then the next samples were gathered from the subsequent chamber and so on until the end of the experiment. Water was pumped up by a peristaltic pump and filtered by a membrane filter (0.45 µm) or by a cartridge filter (0.2 µm); aliquots were collected for determination of nutrients, thiols and metals. Particulate matter obtained by filtration was used to determine metal content in particulate form.

Measurements of nutrients were performed by an Autoanalyzer Techicon II, according to the Hansen and Grasshoff methods[6]. Metal concentrations in the dissolved phase were determined by three different

Tab. 1 - Accuracy tests by CASS-4 Nearshore Sewater Reference material. Concentration in μg/l.

	Cr		Mn		Fe		Co	
Certified±Toll. Interv.	0.144	±0.029	2.78	±0.19	0.713	±0.058	0.026	±0.003
Found value (SD)	0.167	0.006	2.86	0.11	0.727	0.043	0.032	0.005

	Cd		U		V		Zn	
Certified±Toll. Interv.	0.026	±0.003	3.0		1.18	±0.16	0.381	±0.057
Found value (SD)	0.030	0.004	2.67	0.16	1.22	0.045	0.360	0.023

	Cu		Sb		Ag	
Certified±Toll. Interv.	0.592	±0.055	--		--	
Found value (SD)	0.663	0.068	0.274	0.004	0.0078	0.0003

technique: by Inductively Coupled Plasma-Sector Field Mass Spectrometry (ICP-SFMS) after acidification by nitric acid (UPA Romil) and diluted ten time by ultrapure water (Milli Q, Millipore); by Anodic Stripping Voltammetry (ASV) after acidification by HCl and UV irradiation, details about the analytical procedure are previously reported[7]. Aliquots of larger samples was also analysed for the Cu and Fe concentration by Adsorptive Cathodic Stripping Voltammetry (AdCSV)[8,9]. Thiols were determined by Cathodic Stripping Voltammetry (CSV) following the methodology previously reported[10]. Particulate metals were determined by ICP-AES after digestion by a HNO_3 8M by a CEM DS 2000 microwave digestor[11]. Accuracy tests were carried out by analysis of one certified coastal seawater sample (CASS-4, National Research Council of Canada) (see table 1) and by comparison obtained by different analytical methodologies (see table 2).

Tab. 2 - Metal concentration in some samples obtained by different analytical methodology.

	sample 0	sample 3	sample 6	sample 9	sample 12	sample 15
I experiment						
Cd-ASV	0.67	0.21	0.36	0.21	0.26	
Cd-ICPMS				0.35	0.23	
Cu-ASV	21	15	17	16	20	
Cu-ICPMS				10	15	
II experiment						
Cu-CSV	27	21	22	24	23	26
Cu-ICPMS	26	23	26	25	28	27

3. *Results and Discussion.*

Measurements of salinity, Eh, particulate content are reported in figure 2 and 3. The potential measurements (mv Vs. Ag/AgCl, KCl 3П) show different trends for the two experiments, the first, in the Tresse area (close to the industrial area), showed that sub-oxic conditions were reached after about 18 hours. The second experiment carried out in the Campalto area, did not show any systematic changes in the potential (the mean value was 49±12mV); that was a consequence of partial emersion of the chambers during two low tide events, the first after 21 h and the second after 45 h. It is likely that this emersion would have caused oxygenation of the water. Fluctuations of salinity and nutrients that seemed related to the tide levels were evident for both experiments indicating that external water was exchanging with the benthic chambers. The nutrient concentrations for the two experiments were significantly different, the mean concentration of nitrate and ammonia in the Tresse area were 12.1 and 9.2 μmol/l respectively, while the mean concentrations were 2.6 and 0.8 μmol/l in the Campalto area. The evaluation of fluxes of nitrogen species during the experiments is made difficult by the fluctuation; therefore, fluxes were calculated making use of averaged concentrations obtained using a moving-average (3 data points wide); the results obtained are reported in figure 2c and 3c for the two experiments respectively. Although definitive conclusions require some more experiments, in the Tresse area an initially positive flux of both ammonia and nitrate became approximately zero, and then again positive (about 30 nmol/cm^2/h) after 40 hours, at the end of the experiment; at the same time an increase in particulate matter was observed (figure 2). In the Campalto experiment, where the potential was always positive, no significant fluxes of nitrogen species were observed. The iron concentration determined in the two benthic chambers agree with the potential measurements, a remarkable increase in the iron concentration was apparent for the first experiment after 21 hours, both in the dissolved phase, determined by AdCSV, and in the particulate phases; the experiment carried out in the Campalto area did not showed any significant variation of concentration (see figure 4b).

Cadmium, copper, lead and thiols concentrations did not follow an expected trend. Steady trends for thiols were expected due to releases from the sediments and either metals going into or coming out of the sediments as a function of redox conditions or as a consequence of sediment bioturbation. The dissolved cadmium concentration during the first experiment decreased from an initial value of 0.67 nmol/L to a value of

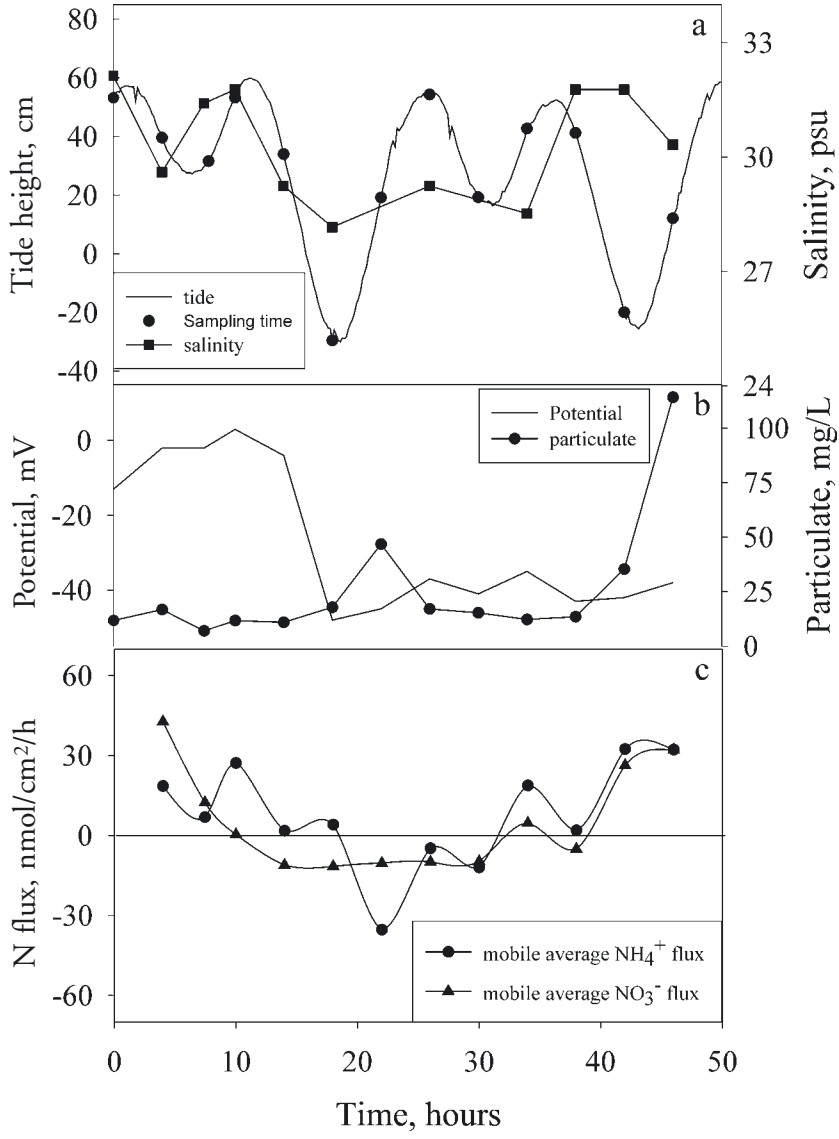

Fig. 2 - Measurement carried out during the first benthic chambers experiment.

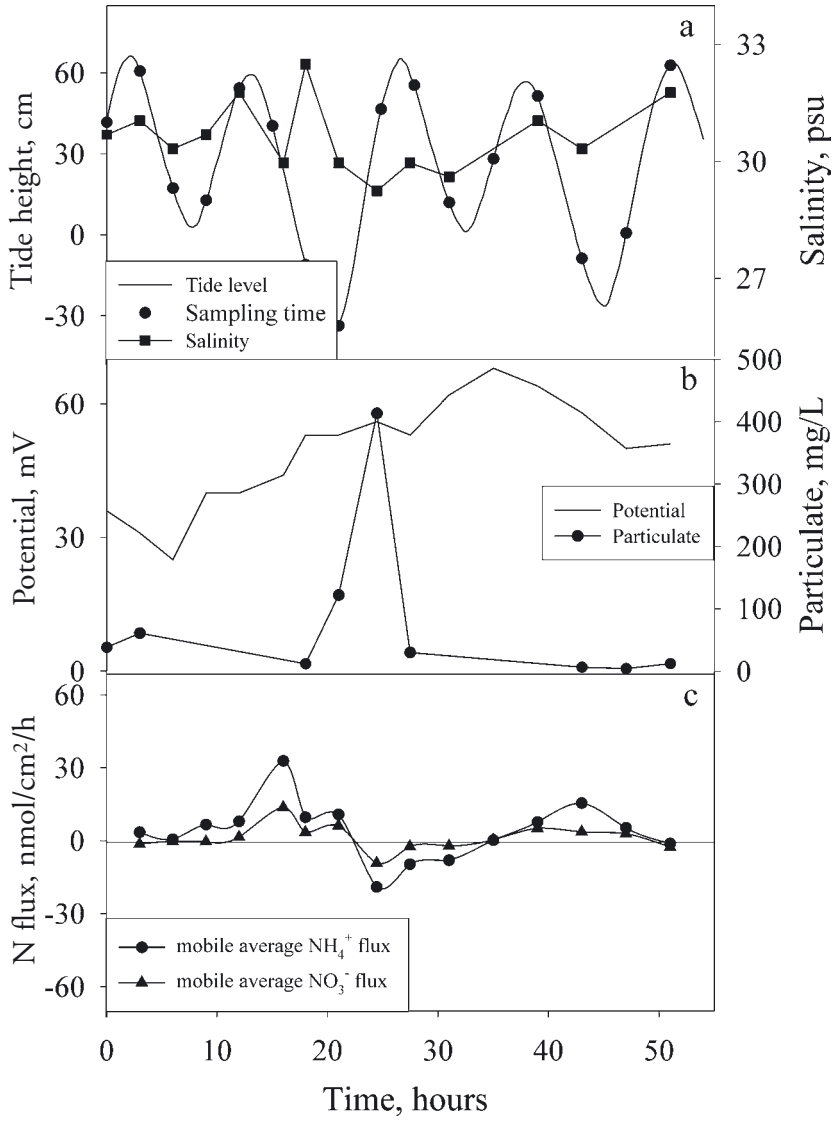

Fig. 3 - Measurement carried out during the second benthic chambers experiment.

about 0.22 nmol/l after 10 hours; in correspondence with the decrease in the potential value (18 hours) an increase were observed until 0.5 nmol/L and a subsequent reduction to the previous concentration. Its concentration trend was very different during the second experiment, it remained practically constant for 28 hours (0.55±0.11 nmol/L), later the concentration increase exponentially until a final value of 9.5 nmol/L. Considering that sub-oxic conditions were not observed in this experiment the positive flux should derive from diffusion or bioturbation phenomena; therefore, the results should be evaluated in consideration of bioturbation studies carried out in the same area contemporary to our experiment[12].

The concentrations of copper, lead and thiols on the other hand were found to change systematically, to some extent corresponding to the fluctuations in the tidal height though not always as the co-variation appears to break down during the last 10 h of the experiment. The mean concentration of Pb and Cu for the first experiment were 1.73±0.31 nM and 19.9±6.9 nM respectively, for the second the mean concentration were respectively 0.51±0.31 nmol/L and 27.5±9.3 nmol/L. Possible explanations for these fluctuations are 1) tidal pumping causing flux of compounds out of the sediments, and 2) tidal flow causing leakage of the benthic chambers producing the observed variation of concentrations to reflect changing in the Lagoon waters composition; in this case a contribution of water intrusion combined with tidal pumping effects can be hypothesized. The amount of particulate matter was also found to vary during the experiment which could be in agreement with a partial remobilization of sediments. Considering that metal concentration are only partially in phase with tide height and, at the beginning of the experiment, there was a correspondence of the maximum of concentration with the maximum of tide height, the leakage due to water intrusion did not seem to have a sensible effect on the concentration. Also the thiol concentrations were found to go up and down (see figure 5), and the mean concentration was 108 ±23 nmol/L.

The results obtained for the second experiment show that the thiol concentrations changes with the tide but the variation did not appear to be closely in phase with the tidal height, the mean concentration was 117±31 nmol/L. The preliminary data of copper and lead did not show a systematic trend in their concentrations, the mean concentration for Cu and Pb were 27.5±9.3 nmol/L and 0.51±0.39 nmol/L.

Data analysis is proceeding, and data interpretation is in progress considering also the day light cycle. Further experiments will be carried out

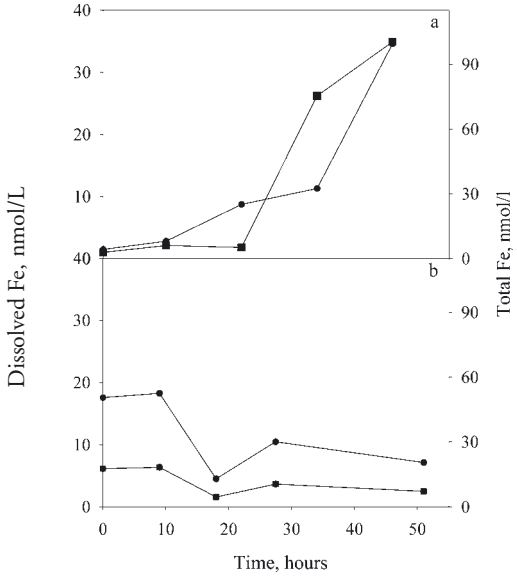

Fig. 4 - Iron concentration in the benthic chambers during the first experiment (a) and the second experiment (b).

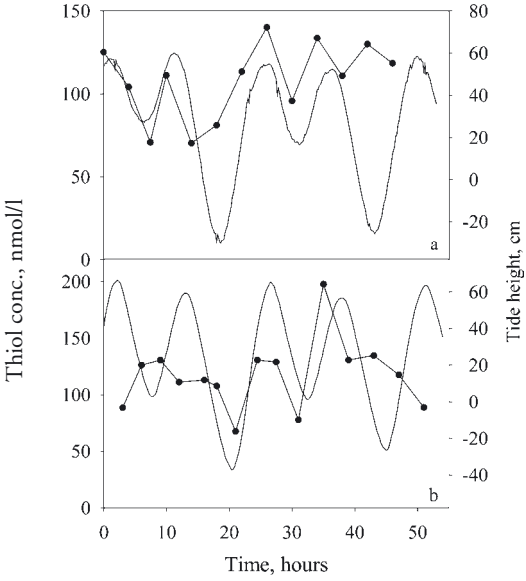

Fig. 5 - Thiol concentration during the first experiment (a) and the second (b). Tide height (——), thiol concentration (—●—).

to verify whether metals and thiols are indeed pumped out of the sediments using an in-situ probe. Subsequent experiments will be carried out with improved anchorage of the chambers, and with controlled lighting of the chambers.

Acknoledgement.

This work was supported by the CORILA under the Project "Role of aerosol and secondary pollution to the contamination of the Lagoon of Venice". The authors thank V. Zampieri for the technical support.

References.

1) Alberotanza L., Donazzolo R., Orio A.A., Pavoni B., and Zandonella A., 1987. La Dinamica dell'Inquinamento nella Laguna e nel Golfo di Venezia. Una applicazione del Confronto tra dati chimici e dati telerilevati. Inquinamento 29, 82-90.
2) Battiston G.A., Degetto S., Gerbasi R., and Sbrignadello G., 1989. Determination of sediment Composition an Chronology as a Tool for Environmental Impact Investigations. Marine Chemistry 26, 91-100.
3) Frignani M., Bellucci L.G., Langone L., and Muntau H., 1997. Metal fluxes to the sediments of the northern Venice Lagoon. Mar. Chem. 58, 275-292.
4) Simpson S.L., Apte S.C., Batley G.E., 1998. *Environ.Sci.Technol.*, 32, 620-25.
5) Zago C., Capodaglio G., Ceradini S., Abelmoschi M.L., Soggia F., Cescon P., Scarponi G., 2000. *Sci.Total Environ.*, 246, 121-37.
6) Hansen H.P. and Grasshoff K., 1983. In: *Methods of seawater analysis (II ed.)* (K. Grasshoff, Ehrhardt and Kremling, eds Verlag Chemie, Weinheim, pp. 347.
7) Capodaglio G., Barbante C. and Cescon P., 2001. In: "Environmental Contamination in Antarctica: A Challenge to Analytical Chemistry", S. Caroli, P. Cescon and D.W.H. Walton Eds., Elsevier Pergamon, Oxford, Chapt. 5, pp107-154.
8) Rue E.L., Bruland K.W., 1995. Complexation of iron(II) by natural ligands in the Central North Pacific as determined by a new competitive ligand equilibration/adsorption cathodic stripping voltammetric method. *Mar. Chem.*, 50, 117-138.
9) Campos M.L.A.M., van den Berg C.M.G., 1994. Determination of copper complexation in sea water by cathodic stripping voltammetry and ligand competition with salicylaldoxime, *Anal. Chim. Acta*, 284, 481-496.

10) Le Gall A.-C., van den Berg C.M.G., 1993. Cathodic stripping voltammetry of glutathione in natural waters. *Analyst*, 118, 1411-1415.
11) Frache R, Abelmoschi M.L., Grotti M., Ianni C., Magi E., Soggia F., Capodaglio G., Turetta C., Barbante C., 2001. Effects of ice melting on particulate Cu, Cd and Pb profiles in Ross Sea waters (Antarctica). Int. J. Environ. Anal. Chem., 79, 301-313.
12) Mugnai C., Frignani M., Gerino M., Bellucci L.G. Bioturbation in Sediments of the Venice Lagoon and its Possible Role on Water-Sediment Interactions. In this volume.

BIOTURBATION IN SEDIMENTS OF THE VENICE LAGOON AND ITS POSSIBLE ROLE ON WATER-SEDIMENT INTERACTIONS

C. Mugnai[1], M. Frignani[1], M. Gerino[2],
S. Sauvage[2], L. G. Bellucci[1]
[1]*Istituto di Geologia Marina, CNR, Bologna*
[2]*Centre d'Ecologie des Systèmes Aquatiques Continentaux, CNRS, Toulouse, France*

1. *Introduction.*

Bioturbation, the process of mixing that results from benthic macrofauna burrowing, feeding and reworking, has profound effects on both physical and geochemical proprieties of the surficial sediments (Aller, 1982). In fact, the rates of organic matter decomposition, as well as the biogeochemical cycles such as those of carbon and nutrients are mediated by bioturbation (Berner, 1980). In addition, fluxes of chemicals at the sediment-water interface are deeply influenced by the movement of interstitial fluids induced by mixing.

Bioturbation occurs in several different ways, as shown in Fig. 1. Some organisms, such as crabs and snails, mix surface sediment simply by crawling or plowing through it. The simple physiological activities of macrobenthos, such as feeding and moving, generate omni-directional particle transport. Other species cause rapid vertical particle transfer by two independent processes: bioadvection (Fisher et al., 1980) and "non-local mixing" (Boudreau, 1986). The former is produced by organisms, mainly polychaeta, which are called "conveyor-belt feeders" (Rhoads, 1974) that feed at depth in the sediment and defecate at the surface. Since they have the capacity to accumulate sediment at the surface, their effects on a tracer profile are similar to those due to a rapid sediment accumulation. The latter, called non-local transport, is generated by head-up vertical oriented organisms, which cause an active transport of sediment trough their gut from the sediment-water interface, where they mix sediment seeking food, to their egestion depth (Smith *et al.*, 1986/87, François *et al.*, 1997). A second type of non-local transport, called regeneration, is attri-

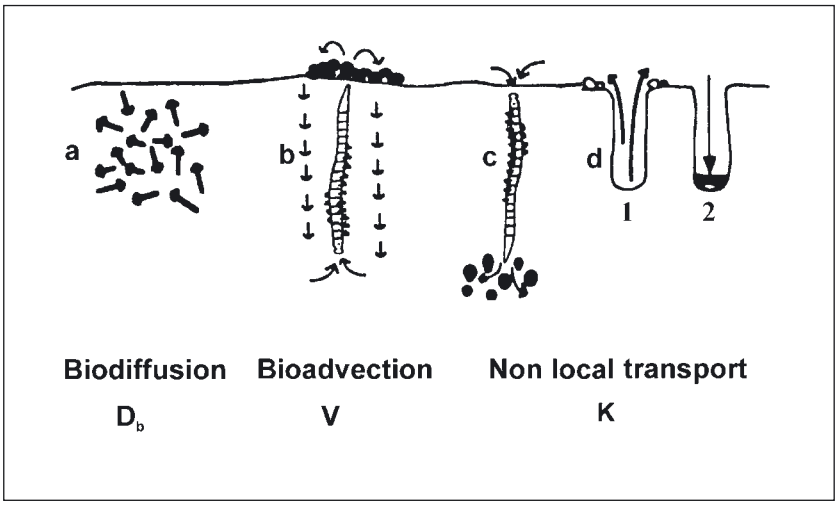

Fig. 1. - Mechanisms of bioturbation: a) biodiffusion; b) bioadvection by upward conveyor belt; c) mixing by downward conveyor belt; d) regeneration: 1- active phase (digging), 2- passive phase (burrow filling).

butable to large burrow digging organisms, such as crustaceans. It causes a net downward movement of surficial sediment, which drops into the burrow after it has been deserted (Gardner *et al.*, 1987).

The movement of organisms during bioturbation causes the displacement of pore waters, whereas the irrigation is the flushing of burrows with overlying seawater. These mechanisms bring about enhanced solute exchange between sediment and waters. The aim of this work was to assess rates and mechanisms of bioturbation at two selected sites of the Venice Lagoon, in the perspective to contribute to the understanding of its role in sediment-water interaction and pollutant transfer from sediments to overlying waters.

2. *Materials and methods.*

Experiments were carried out during July 2001 at two sites (Fig. 2) close to the locations chosen for flux measurements using benthic chambers (Chapman *et al.*, same volume). At each site four tubes were inserted into the bottom, one of them full of sediment without macrofauna (as a control). The luminophores, fluorescent sediment particles (63-350 μm),

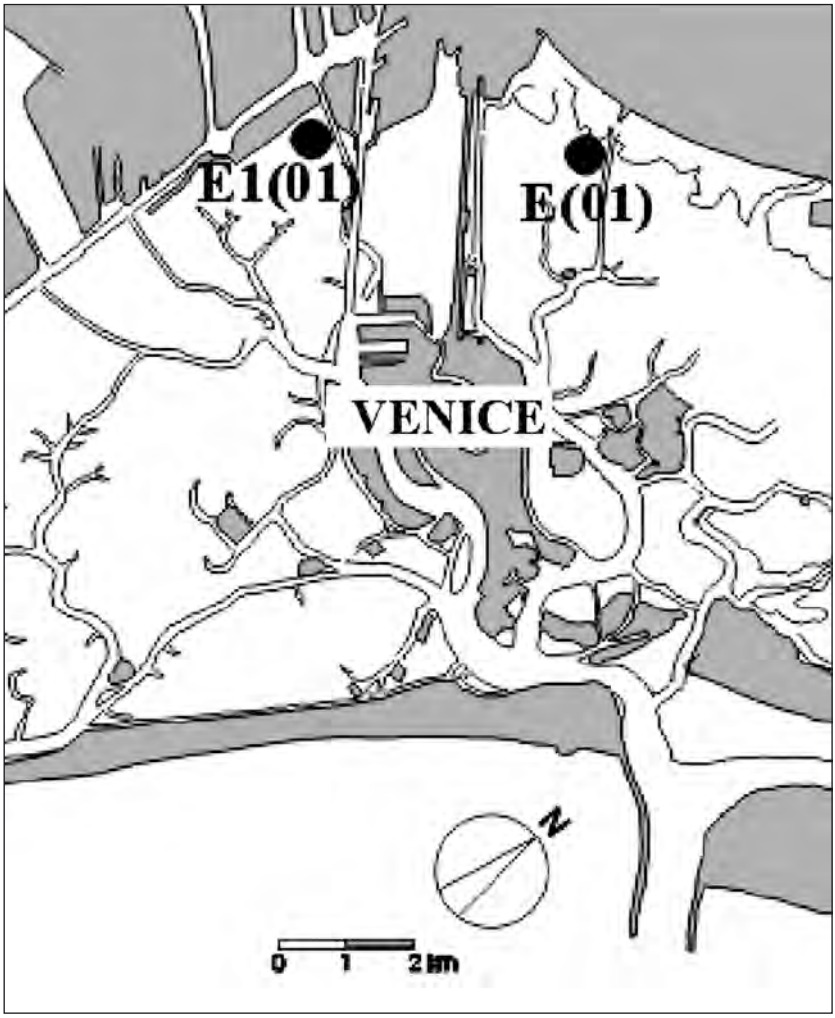

Fig. 2. - Study area and experimental sites.

were supplied at the sediment surface as a frozen cake thus obtaining a tracer pulse input. After two weeks the tubes were recovered and the sediment sliced in sections 0.5 to 5 cm thick. Sediments were then lyophilized, subsampled and counted for fluorescent dyed particles with a UV microscope. The results are expressed as concentration-depth profiles of luminophores (normalized against the total tracer inventory) as in Fig. 3.

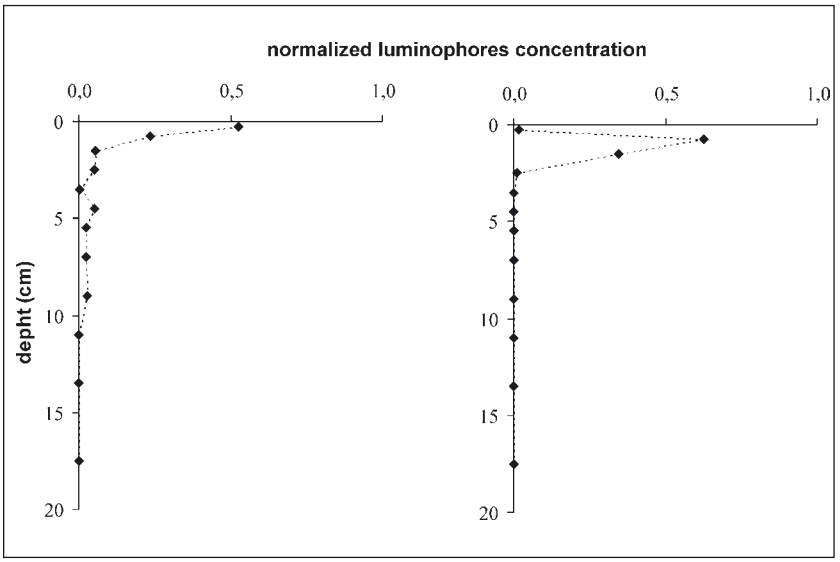

Fig. 3. - Selected luminophores profiles.

3. *Results and discussion.*

After two weeks we were able to recover all the six test tubes and only one control (E1). The control at site E1 shows a subsurficial peak that could be ascribed either to rapid sediment accumulation or to bioadvection. Since the first process was unlikely at the time, and we know from two previous experiments that the site is characterized by advective mixing (Gerino *et al.*, submitted), we believe that the control was rapidly colonized by organisms and underwent bioturbation just like the test tubes.

Each profile of Fig. 3 is typical of one of the two experimental sites. In particular, when the tracer distribution shows a maximum at the surface and concentration decreases almost exponentially with depth, the pattern is typical of biodiffusive mixing (Goldberg & Koide, 1962; Guinasso & Schink, 1975; Cochran, 1985; Wheatcroft *et al.*, 1990). This is produced by organisms that move sediment particles in a random manner over short distances. On the contrary, tracer peak values in the subsurface sediment, associated with absence of tracers at the sediment surface, can be explained by bioadvection (Robbins *et al.*, 1979; Fisher et al., 1980; Rice,

1986; Gerino *et al.*, 1994). Site E1(01) appears to be subject mainly to bioadvection, because all profiles show a well defined subsurficial peak with a variable enlargement due to a small biodiffusive component. In turn, non-local transport is characterized by deeper tracer peaks originated by the subsequent filling of burrows with surface sediment or egestion of fecal pellet at depth by surface deposit feeders denominated "inverse conveyors". Results show that at site E(01) biodiffusion prevails, with the presence of some peaks downcore, due to the effect of non-local transport.

Exact mathematical modelling of bioturbation is extremely difficult because of the variety, irregularity and complexity of the various processes. The usual approach has been to lump all processes together and describe bioturbation simply in terms of a biological mixing or "biodiffusion" coefficient (Berner, 1980). However, experimental tracer profiles account for the presence of different types of biological mixing. Furthermore, short time scale experiments have proven to be able to distinguish these different mechanisms that are probably active in sediment-water interactions. In order to quantify all bioturbation processes, a biodiffusive-bioadvective transport-reaction model under non steady state boundary conditions was used (Gerino *et al.*, 1994, 1998), with the addition of a non-local component. As experiments were conducted over a very short period of time, sedimentation rate is not taken into account in the model. The basic equation is:

$$\frac{\partial C(z,t)}{\partial t} = D_b \frac{\partial^2 C(z,t)}{\partial z^2} - V \frac{\partial C(z,t)}{\partial z} + K(z,t) - R(z,t)$$

in our case: $$R(z,t) = K(z,t)\frac{z_2 - z_1}{0.5}$$

and $$K(z,t) = \begin{cases} Ke & for \quad z \in [z_1, z_2] \\ 0 & for \quad z \notin [z_1, z_2] \end{cases}$$

where C is the normalized tracer concentration, t is the time (y), Db is the biodiffusive mixing rate ($cm^2\ y^{-1}$), V is the bioadvective transport rate ($cm\ y^{-1}$) and z (cm) is depth. K (y^{-1}) represents the "injection function", that simulates the non-local deposition of tracer elsewhere in the

sediment column, and Ke (y^{-1}) is a constant parameter estimated from the model. R(y^{-1}) is the removal function that determines the fraction of tracer displaced from the surface (Smith *et al.*, 1986/87; Boudreau, 1997). The depths z_1 and z_2 represent the upper and lower limits of the non-local injection. The non-local transport is thus quantified by a flux of sediment "injected", called Total Removed Sediment (TRS, g cm^{-3} y^{-1}) calculated from Ke, z_1 and z_2, the bulk dry density (g cm^{-3}) and the volume of the supplied frozen cake. The model allows the calculation of the theoretical tracer concentration, given suitable values of the parameters D_b, V, z_1, z_2, and K. These parameters are obtained through the best fit to the experimental profiles using the least square method.

The application of the model to our data allowed the estimate of D_b (1.5-6.2 cm^2 y^{-1}), V (15.2-26.1 cm y^{-1}) and K (0-65.7 y^{-1}) that account for the rates of biodiffusion, bioadvection and non-local injection of tracer, respectively. The set of parameters for each single core, including TRS, is reported in Table 1. These values appear clearly higher than those obtained for the same sites by Gerino *et al.* (submitted) from experiments carried out in 1998-1999. The differences are very relevant for site E, where the more recent experiments account for an increased importance of the non-local and bioadvective processes. This might be ascribed to the effect of the enhanced temperature, since the previous experiment at site E was conducted in autumn. Temperature, in fact, is an important key-factor in controlling bioturbation rates (Gerino *et al.*, 1998) and should be taken into account in further studies. Like in the previous experiment, a great heterogeneity characterizes the experimental profiles of this site.

Tab. 1. - Bioturbation coefficients from model simulations and TRS values.

Core	Db cm^2 y^{-1}	V cm y^{-1}	Ke y^{-1}	z_1 cm	z_2 cm	TRS gcm^{-3} y^{-1}
E(01)A	1.7	19.0	65.7	2	8	454
E(01)B	6.0	-	29.2	2	10	151
E(01)D	4.0	-	7.3	4	5	303
E1(01)A	1.5	26.1	-	-	-	
E1(01)B	6.2	16.2	-	-	-	
E1(01)C	5.1	21.5	-	-	-	
E1(01)D	2.0	15.2	-	-	-	

Db: biodiffusive mixing rate; V: bioadvective mixing rate; Ke: downward transport of tracer displaced by "non-local mixing"; z_1, z_2: upper and lower limits of the "non-local mixing" zone; TRS: total removed sediment from the surface and injected between z_1 and z_2 by non-local transport.

In the present study only a strong bioadvective component was detected at site E1, whereas the previous experiment (May 1999) showed the presence of non-local transport in all the experimental cores. This can be attributed to differences in benthic community composition between the two experiments. In particular we expect that at site E1(01) conveyor-belt organisms, like the polychaete *Capitella capitata*, are more represented than in the previous experiment (when they resulted scarce). The results of biological analyses on sediment samples, collected at the same sites during our experiments, will probably confirm this hypothesis.

These results provide evidence of rapid and intense sediment reworking that can significantly enhance the exchanges of dissolved species between sediments and overlying waters. For instance Hammond *et al.* (1999) found a discrepancy between fluxes of nutrients measured by benthic chambers and those estimated from the gradients of concentration in pore waters. They explained the difference invoking an extra flux due, in the field experiments, to the contribution of irrigation and macrofaunal activity. Therefore, for a clear understanding of role and mechanisms of the secondary contamination (Chapman *et al.*, this volume) it is important to estimate the relative influence of the different processes. In the future it will be necessary to carefully distinguish particle bioturbation from fluid bioturbation, in that the two often take place at distinctly different rates because of irrigation (Aller, 1977). Hence, it is important to separate the effects of particle mixing, which includes the displacement of pore waters, and irrigation. As others, these two processes are quantified through the coefficients D_B and D_I, respectively, whereas the biodiffusional flux of a dissolved solute is expressed by J_{BI}. Future experiments will be carried out to link bioturbation to sediment-water fluxes and approach the solution of a diagenetic equation that assess the role of all different mechanisms on pollutant transfer from sediment to the overlying waters. On the other hand, the insertion of a sedimentation term in the equation that models bioturbation will let us to simulate the formation of the sediment record and will enable the prevision of the effects of changes of the contaminant inputs, very important in deciding any monitoring program.

Acknowledgements.

This research was funded by the Consortium for Coordination of Research Activities Concerning the Venice Lagoon System (CORILA).

The authors are indebted with G. Capodaglio for his support in field operations. This is contribution No. 1283 of the Istituto di Geologia Marina, CNR, Bologna.

References.

Aller R.C., 1977. The influence of macrobenthos on chemical diagenesis of marine sediments. Ph.D. dissertation, Yale University, New Haven, Connecticut.

Aller R.C., 1982. The effects of macrobenthos on chemical properties of marine sediment and overlying water. In: McCall and M.J.S Tevesz (Eds.), Animal-Sediment Relations. Plenum Press, 53-102.

Berner R.A., 1980. Early diagenesis. A theoretical approach. Princeton University Press, New Jersey.

Boudreau B.P., 1986. Mathematics of tracer mixing in sediments: II - Nonlocal mixing and biological conveyor-belt phenomena. Am. J. Sci., 286, 199-238.

Boudreau B.P., 1997. Diagenetic models and their implementation. Springer-Verlag, Berlin.

Chapman C., Capodaglio G., van den Berg C.M.G., Corami F., Turetta C., Magi E., Soggia F., 2002. Metals remobilization from sediments of the Venice Lagoon. This volume.

Cochran J.K., 1985. Particle mixing rates in sediments of the eastern equatorial Pacific: evidence from ^{210}Pb, ^{239}, ^{240}Pu and 137Cs distributions at MANOP sites. Geochim. Cosmochim. Ac., 49, 1195-1210.

Fisher J.B., Lick W.J., McCall P.L., Robbins J.A., 1980. Vertical mixing of lake sediments by tubificid oligochaetes. J. Geophys. Res, 85, C7, 3997-4006.

François F., Poggiale J.C., Durbec J.P., Stora G., 1997. A new approach for the modelling of sediment reworking induced by a macrobenthic community. Acta Biotheor., 45, 295-319

Gardner L.R., Sharma P., Moore W.S., 1987. A regeneration model for the effect of bioturbation by fiddler crabs on ^{210}Pb profiles in salt marsh sediments. J. Environ. Radioactiv., 5, 25-36.

Gerino M., Stora G., Durbec J.P., 1994. Quantitative estimation of biodiffusive and bioadvective sediment mixing: in situ experimental approach. Oceanol. Acta, 17, 5: 547-554.

Gerino M., Aller R.C., Lee C., Cochran J.K., Aller J.Y., Green M.A., Hirschberg D., 1998. Comparison of different tracers and methods used to quantify bioturbation during a spring bloom: 234-Thorium, luminophores and chlorophyll a. Estuar. Coast. Shelf Sci. 46, 531-547.

Guinasso Jr. N.L., Schink D.R., 1975. Quantitative estimates of biological mixing rates in abyssal sediments. J. Geophys. Res. 80, 21, 3032-3043.

Hammond D.E., Giordani P., Berelson W.M., Poletti R., 1999. Diagenesis of carbon and nutrients and benthic exchange in sediments of the Northern Adriatic Sea. Mar. Chem., 66, 53-79.

Rhoads D.C., 1974. Organism-sediment relations on the muddy sea floor. Oceanogr. Mar. Biol. Ann. Rev., 12, 263-300.

Rice D.L., 1986. Early diagenesis in bioadvective sediments: relationships between the diagenesis of beryllium-7, sediment reworking rates, and the abundance of conveyor-belt deposit-feeders. J. Mar. Res., 44, 149-184.

Robbins J.A., McCall P.L., Fischer J.B., Krezoski J.R., 1979. Effect of deposit feeders on migration of ^{137}Cs in lake sediments. Earth Planet. Sc. Lett., 42, 277-287.

Smith J.N., Boudreau B.P. and Noshkin V., 1986/87. Plutonium and ^{210}Pb distributions in northeast Atlantic sediments: subsurface anomalies caused by non-local mixing. Earth Planet. Sc. Lett., 81, 15-28.

Wheatcroft R.A., Jumars P.A., Smith C.R., Nowell A.R.M., 1990. A mechanistic view of the particulate biodiffusion coefficient: step lenghts, rest period and transport directions. J. Mar. Res., 48, 177-207.

EXCHANGES OF ORGANIC POLLUTANTS AT THE SEDIMENT-WATER INTERFACE IN THE VENICE LAGOON

I. Moret[1,2], R. Piazza[1], A. Gambaro[1,2], S. Ferrari[1] e L. Manodori[2]
[1]*Dipartimento di Scienze Ambientali, Università Ca' Foscari, Venezia*
[2]*Istituto per la Dinamica dei Processi Ambientali, CNR, Venezia*

1. *Introduction.*

The sediment-water interface is place of continuous exchange of organic compounds, of nutrients and of metals[1,2,3]. In particular the particulate organic material (POM) present in the water column over the sediment surface can settle on the sediment causing a flux of organic pollutants towards it. For many of these compounds the sediment constitutes the final reservoir. However several factors, chemical, physical and biological can cause them to remobilize by reversing the previous flux. For example partial decomposition of organic matter causes the formation of dissolved organic matter, which concentrates in the pore water; concentration differences between the pore water and the water over it can promote fluxes of these substances at the sediment-water interface[2]. The practice of benthic chambers[1,2,4] has proved to be a valid approach for gauging the fluxes of some metals and some nutrients at the sediment-water interface.

This work studies the exchange of organic pollutants at the sediment-water interface in the Venice lagoon. The results of two experiments, using benthic chambers, are presented; the behaviour of polychlorobiphenyls (PCB), polycyclic aromatic hydrocarbons (PAH) and aliphatic hydrocarbons (AH) are studied.

2. *Experimental.*

The two experiments were carried out, using two sets of benthic chambers, in two polluted areas of the central lagoon, the first near the

Trezze canal (45°26.44'N, 12°16.556E), named site 1, and the second in the Campalto area (48°28.219'N, 12°18,83'E), named site 2.

Owing to the reversal of a benthic chamber the first experiment was carried out utilizing four chambers; the first sampling was carried out 3 hours before the positioning of the benthic chambers, the second 9 hours after the positioning, the third after 21 hours, the fourth after 33 hours and the fifth after 45 hours.

The second experiment was carried out utilising five benthic chambers; the first sampling was carried out before the positioning of the chambers, the second 9 hours after positioning, the third after 18 hours, the fourth after 27 hours, the fifth after 39 hours and the sixth after 51 hours.

11 l of water samples were collected using a electric rotary pump and pumping the water into a stainless steel container. In the laboratory water samples were filtered though GF/F Whatman glass filters (0.7 mm). So organic pollutants in the aqueous phase ("dissolved" PCBs, "dissolved" PAHs and "dissolved" AHs) were determined in the filtrate and "particulate" organic pollutants ("particulate" PCBs, "particulate" PAHs and "particulate" AHs) in the particulate matter collected on the glass filters. Continuous liquid-liquid extraction[5] for 24 h, using 10 l of the filtered water and 200 ml of a mixture of pentane-methylene chloride, 2+1 v/v, were used for the "dissolved" pollutant determination. The extraction mixture, dried by anhydrous Na_2SO_4 and joined to 3 x 5 ml of pentane used for washing off the residual Na_2SO_4, was reduced to 5 ml under a gentle stream of nitrogen and subjected to clean-up.

Before extraction five carbon-13-labelled PCBs (^{13}PCBxxx), carbon-13-labelled phenanthrene and perdeuterated hexadecane were added to the water samples for use as internal standards in the quantification of PCBs, PAHs and AHs, respectively; the added PCBs were: ^{13}PCB28 used for the trichlorobiphenyl homolog; ^{13}PCB52 used for the tetrachlorobiphenyl homolog; ^{13}PCB118 used for the pentachlorobiphenyl homolog; ^{13}PCB153 used for the hexachlorobiphenyl homolog; ^{13}PCB180 used for the heptachlorobiphenyl homolog.

The clean-up[6] was performed by adsorption chromatography using a glass column (i.d. = 6 mm) slurry packed with 2 cm (top) of pesticide grade Florisil,RS 60-100 mesh (Carlo Erba, Milano, Italy) and with 1 cm (bottom) of Alumina Oxide 60 70-230 mesh (Merck, Darmstadt, Germany). These adsorbents, previously washed with hexane, were activated prior to use in a muffle furnace at 600 °C for 4 h. Organic pollutants were eluted with n-hexane collecting 30 ml. The eluate, reduced under a gentle stream of nitrogen to 100 μl, was analysed by gas chromatography-mass spectrometry (GC-MS).

For the determination of "particulate" organic pollutants the filters with the filtered matter corresponding to 10 l of lagoon water were extracted in a sonication bath for 2 h using an aliquot of 60 ml of the pentane-methylene chloride mixture. The extract solution was treated in the same way as the extract solution obtained from the water and analysed by GCMS.

Samples were analysed with a Hewlett Packard Model 6890 Gaschromatograph coupled with a Hewlett Packard Model 5973 Mass Selective Detector (mass analyzer: quadrupole) using a fused silica capillary column (HP 5 - Trace Analysis, 60 m x 0.25 mm x 0.25 mm; Hewlett Packard, Avondale, PA, USA). The operating conditions for the PCB and AH analysis were: injector temperature, 280°C; transfer line temperature, 280°C; oven temperature program, 70 °C (1 min), 10 °C/min to 150 °C, 10 min at 150 °C, 3 °C/min to 280 °C, 30 min at 280 °C; carrier gas (helium) flow, 0.8 ml/min (constant flow mode); injection mode, pulsed splitless (carrier gas flow, 2.2 ml/min for 3 min; split valve open after 1 min). The operating conditions for the PAH analysis were: injector temperature, 300 °C; transfer line temperature, 280°C; oven temperature program, 70 °C (1,5 min), 10 °C/min to 150 °C, 1 min at 150 °C, 5°C/min to 280 °C, 30 min at 280 °C; carrier gas (helium) flow, 1.0 ml/min (constant flow mode); injection mode, splitless. Data were acquired in the electron impact (EI) mode (70 eV) using the selected ion monitoring (SIM) technique.

All organic pollutants were quantified by direct comparison of their peak area in the chromatogram with that of the internal standard. The values of concentration, calculated this way, were corrected for an instrumental response factor, which accounts for the diversity in the GCMS response[7].

Accuracy and repeatability of the analytical determinations were tested previously[8].

Tab. 1 shows a list of all the pollutants quantified in this work.

3. *Results and discussion.*

Tab. 2 reports the average and the relative standard deviation of the concentrations of the PCBs, PAHs and AHs found at the two sites in the two experiments. Figs. 1 and 2 show the trends of the concentration of the three groups of pollutants; the trends are shown separately for the "dissolved" fraction, the particulate fraction and the sum of the two fractions. The trends obtained in the two experiments are quite different.

Tab. 1 - List of the compounds (PCB, PAH, AH) quantified in this work.

PCB	PAH	AH
IUPAC No.	acenaphtene	n-hexadecane
18, 17, 31+28, 20+33, 52, 49, 44, 41+64, 74,	acenaphthylene	n-
70, 66, 95, 91, 60+56, 92, 90+101, 99, 97,	fluorene	heptadecane
87+115, 85, 136, 110, 151, 135, 149, 118, 146,	dibenzothiophene	n-octadecane
153, 132, 105, 141, 179, 137, 176, 138, 158,	phenantrene	n-nonadecane
187, 183, 128+167, 156, 180	antracene	n-eicosane
	2-methylphenanthrene	n-heneicosane
	4H-cyclopenta[*def*]phenanthrene	n-docosane
	1-methylphenantrene	n-tricosane
	fluoranthene	n-tetracosane
	pyrene	n-pentacosane
	benzo[*ghi*]fluoranthene+ benzo[*c*]phenanthrene	
	benzo[*a*]anthracene	
	chrysene+triphenylene	

Tab. 2 - Average and relative standard deviation (D.S.R. %) of the PCB, PAH and AH concentrations found in the two experiments.

	PCB concentration pg/l			**PAH concentration ng/l**			**AH concentration ng/l**		
	Dis.	Part.	Sum D+P	Dis.	Part.	Sum D+P	Dis.	Part.	Sum D+P
SITE 1									
average	**1309**	**885**	**2193**	**14**	**15**	**29**	**52**	**27**	**78**
D.S.R.%	38	41	24	32	29	11	34	33	33
SITE 2									
average	1113	1642	2755	16	18	34	80	121	201
D.S.R.	39	31	31	64	54	56	52	42	50

Dis.= "dissolved" fraction
Part.= particulate fraction
Sum D+P= sum "dissolved" fraction plus particulate fraction concentrations.

Looking closely at Fig. 1 it can be observed that the concentrations of the pollutants bound to the particulate matter remain quite constant; the value of the particulate PCB concentration at the starting moment is an exception. "Dissolved" pollutant concentrations show variations that are not correlated with each other nor with the tide trend and this cannot be connected with benthic fluxes.

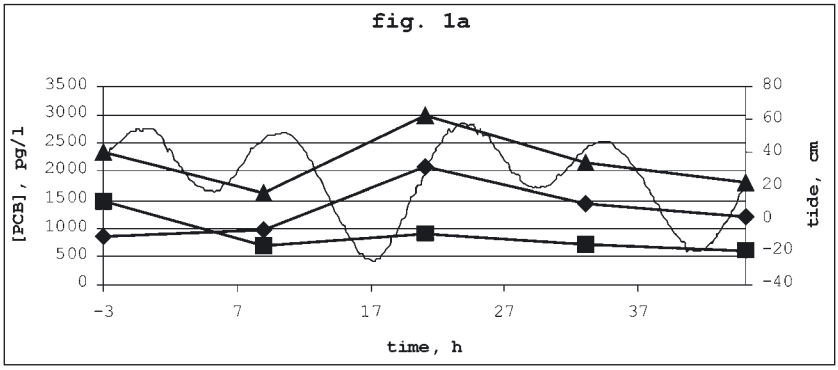

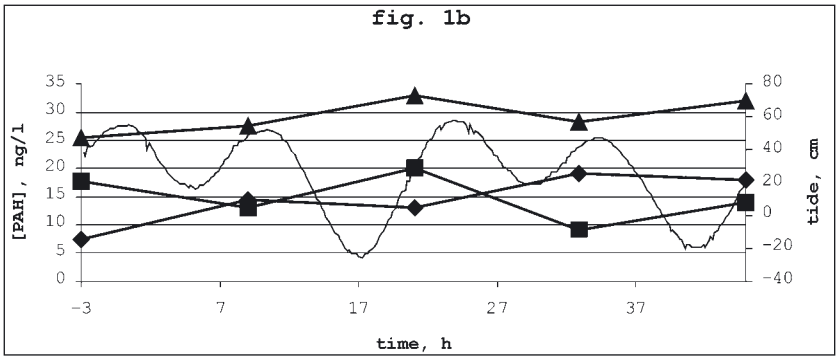

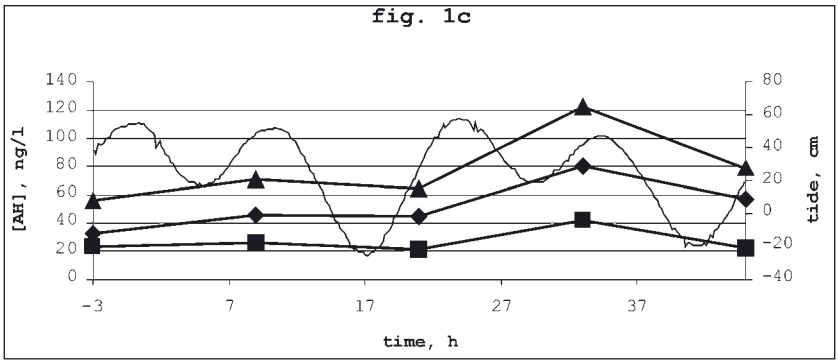

Fig. 1 - Site 1: trend of the tide (——) and of the concentration of the PCBs (fig. 1a), PAHs (fig. 1b) and of the AHs (fig. 1c) for matrix (◆, water; ■, particulate; ▲, sum water+particulate).

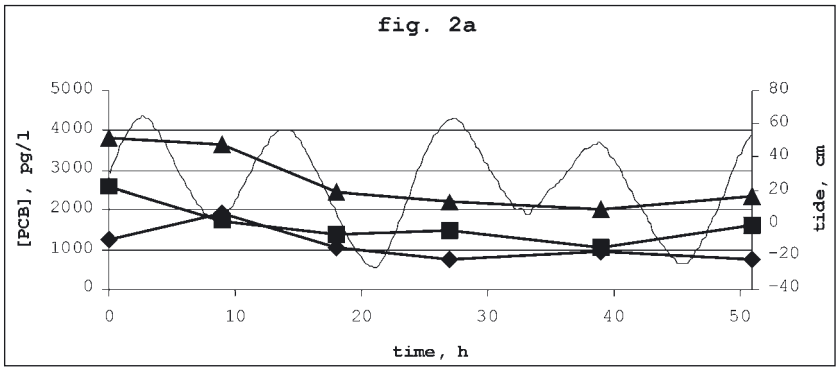

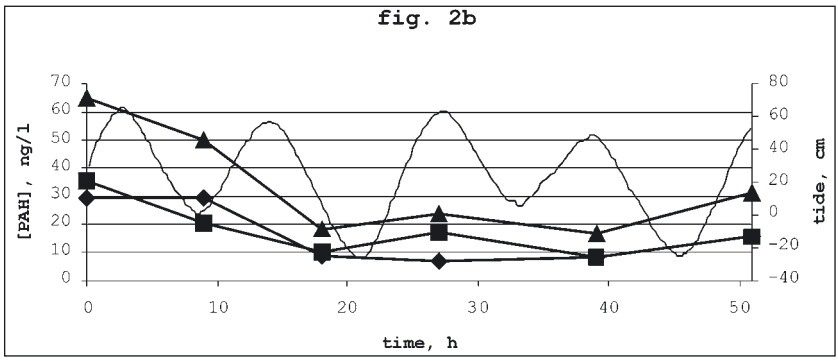

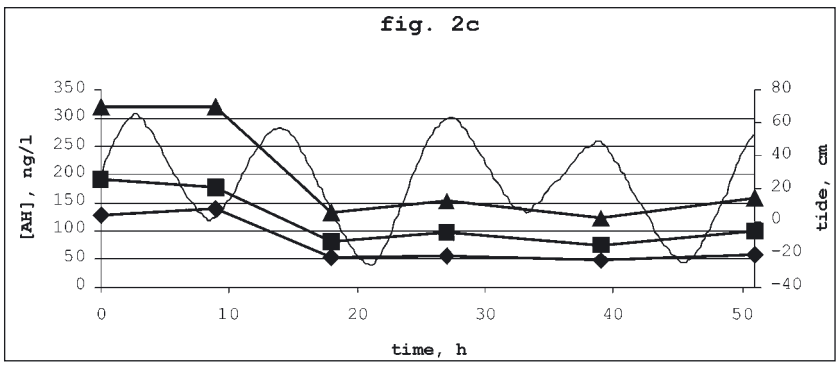

Fig. 2 - Site 1: trend of the tide (——) and of the concentration of the PCBs (fig. 2a), PAHs (fig. 2b) and of the AHs (fig. 2c) for matrix (◆, water; ■, particulate; ▲, sum water+particulate).

Looking closely at Fig. 2 it can be observed that the concentrations of the pollutants show similar trends with an initial phase characterized by declining concentrations, followed by reasonably constant concentrations; it is therefore possible to conjecture a deposition process from the water to the sediment. In this case too, there are no evident correlations with the tide trend.

Fig. 3 shows the trend for the distribution of PCBs for homolog in the "dissolved" and in the "particulate" fractions as found in the second experiment. It can be observed that: the concentrations of the "dissolved" trichloro and the tetrachloro homologs are proportionately greater in the second sampling; the concentrations of the "particulate" hexachloro homolog is proportionately greater in the fifth and sixth samplings.

Fig. 4 shows the trend for the concentration of PAHs for compounds in the "dissolved" and in the "particulate" fractions as found in the second experiment. It can be observed that in the "dissolved" fraction trend the PAHs with greater molecular weight are predominant in the first and second samplings while in the "particulate" fraction are always predominant.

Fig. 5 shows the trend for the concentration of AHs for compounds in the "dissolved" and in the "particulate" fractions as found in the second experiment. It can be observed that in the "dissolved " fraction the concentration of the n-docosane is always predominant and that in the "particulate" fraction the concentration of the n-hexadecane and of the n-heptadecane is always greater than that of the other hydrocarbons.

These results emphasize the complexity of studies of organic pollutant fluxes at the sediment-water interface. Other experiments, already programmed, are necessary for us to be able to draw initial conclusions on the trends of these fluxes.

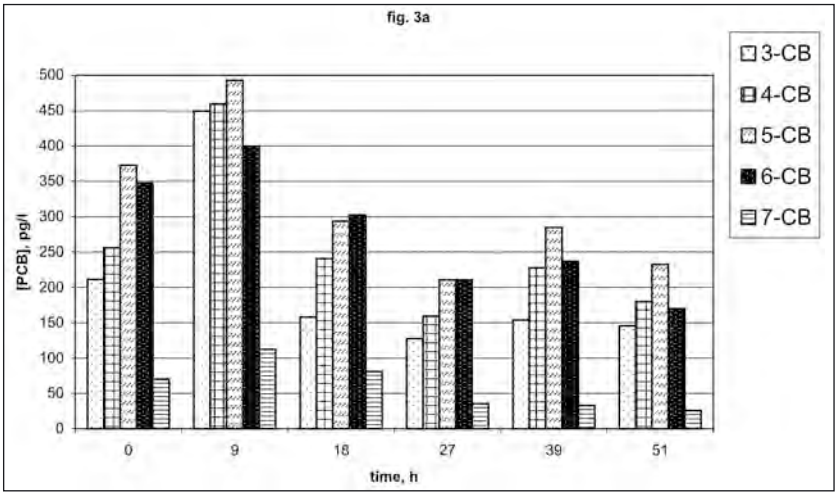

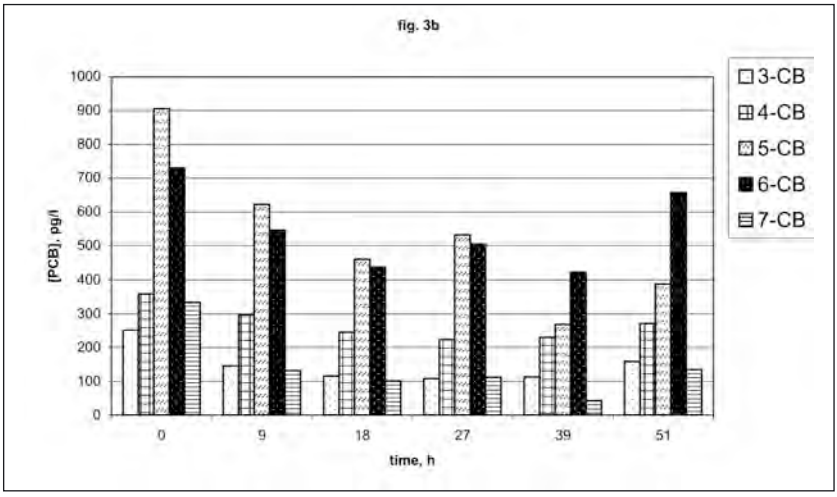

Fig. 3 - Trend of the PCB distribution for homolog in the "dissolved" (fig. 3a) and in the particulate (fig. 3b) fractions as found in the second experiment.

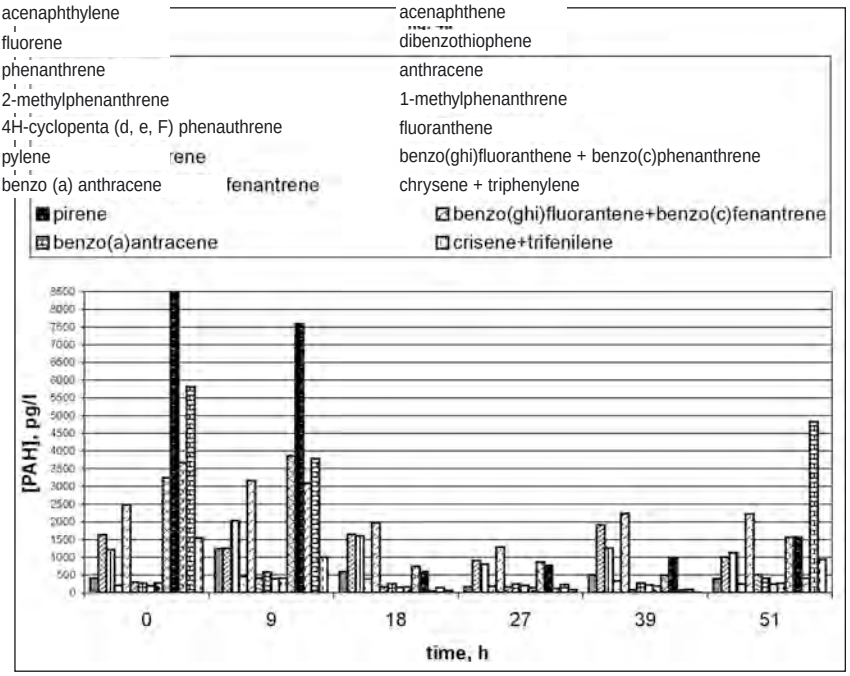

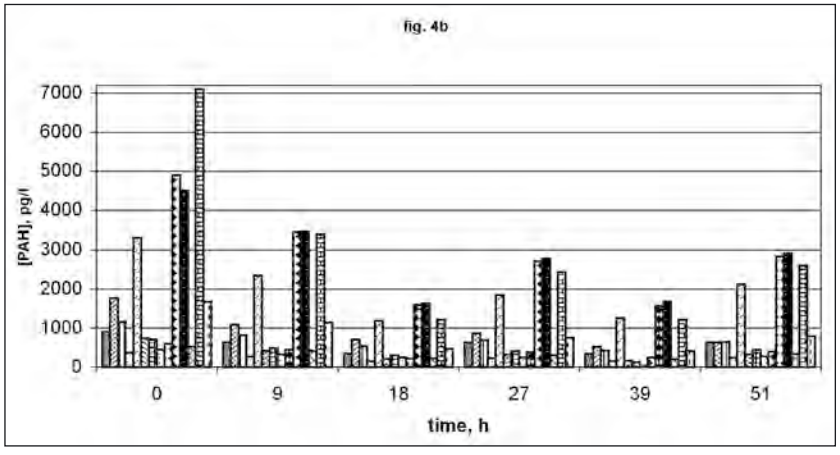

Fig. 4 - Trend of the PAH concentration in the "dissolved" (fig. 4a) and in the particulate (fig. 4b) fractions as found in the second experiment.

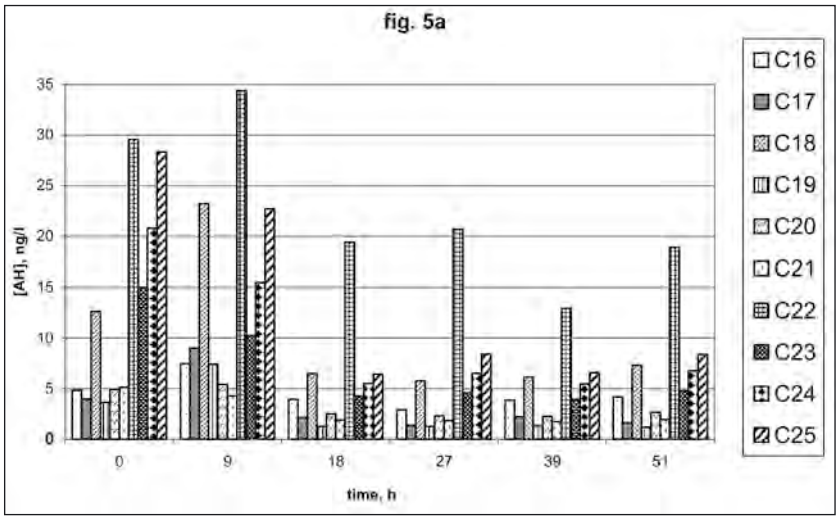

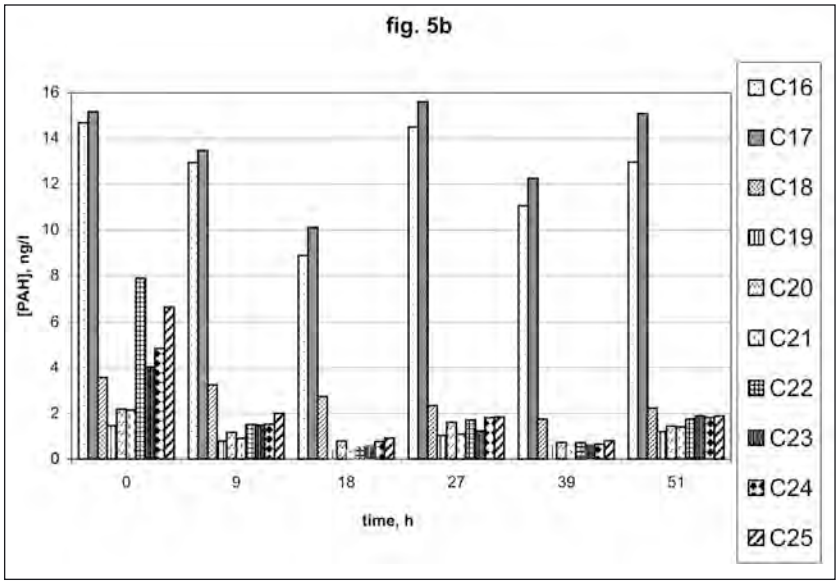

Fig. 5 - Trend of the AH concentration in the "dissolved" (fig. 5a) and in the particulate (fig. 5b) fractions as found in the second experiment.

References.

1) Zago C., Capodaglio G., Ceradini S., Ciceri G., Abelmoschi L., Soggia F., Cescon P., Scarponi G., 2000. Benthic fluxes of cadmium, lead, copper and nitrogen species in the northern Adriatic Sea in front of the River Pò outflow, Italy. The Science of the Total Environment. 246, 121-137.
2) Landén A., Hall P. O.J., 2000. Benthic fluxes and pore water distributions of dissolved free amino acids in the open Skagerrak. Marine Chemistry. 71, 53-68.
3) Giblin A.E., Hopkinson C.S., Tucker J., 1997. Benthic metabolism and nutrient cycling in Boston Harbor, Massachusetts. Estuaries. 20, 346-364.
4) Ciceri G., Maran S., Martinetti W., Quierazza G.,1992. Geochemical cycling of heavy metals in a marine coastal area: benthic flux determination from porewater profiles and in situ measurements using benthic chamber. Hydrobiologia. 235/236, 501-517.
5) Moret I., Piazza R., , Gambaro A., Benedetti M., Paneghetti C., Cescon P., 1999. Polychlorobiphenyls (PCBs) in the sediment and surface water of the Venice lagoon. Organohalogen compounds. 40, 223-226.
6) Erickson M.D., 1997. Analytical Chemistry of PCBs. CRC Press - Lewis Publishers, New York.
7) Moret I., Piazza R., Benedetti M., Gambaro A., Barbante C. and Cescon P., 2001. Determination of polychlorobiphenyls in Venice Lagoon sediments. Chemosphere 43, 559-565.
8) Natale A., 2001. Determinazione di policlorobifenili (PCB) ed idrocarburi policiclici aromatici (IPA) in acqua superficiale della laguna di Venezia. Thesis. Venice University.
9) Moret I., Piazza R., Benedetti M., Gambaro A., Paneghetti C., di Domenico A., Miniero R., Cescon P., 2000. Organohalogen Compounds, 46, 443-445.

THE MICROLAYER'S ROLE IN THE TRANSPORT OF MICROPOLLUTANTS IN THE VENICE LAGOON

A.M. Stortini[1], C. Turetta[2], F. Corami[3],
L. Manodori[3], S. Ferrari[3], G. Capodaglio[3]
[1]*Department of Chemistry, University of Florence, Italy.*
[2]*Institute for the Dynamics of Environmental Processes,*
National Research Council (IDPA-CNR), Venice, Italy.
[3]*Department of Environmental Science, Ca' Foscari University, Venice, Italy.*

1. *Introduction.*

Interactions between ocean and atmosphere play an important role in climate control, heat flux, CO_2 up-take, as well as the exchange of trace gases and the particulate matter. The surface film present at the air-sea interface has emerged as the primary cross-over point between the bulk water (liquid phase) and the atmosphere (gas phase)[1].

Nowadays the microlayer is considered not only as a layer present on oceanic and coastal waters, it also represents a gradient-region with own physical, biological and chemical properties[1]. Notwithstanding current information that has emerged over the last few decades, the microlayer's role as a modulator of the exchange of matter and energy, is still not well understood. In 1995, a group of experts (IMO/FAO/UNESCO-IOC/WMO/WHO/IAEA/UN/UNEP: Joint Group of Experts on the Scientific Aspects of Marine Environmental Protection – GESAMP, report N. 59), illustrated the state of art of aspects about surface film and microlayer arguments[1]. Characterisation of surface film (or microlayer when assumed to be a portion of the sampled surface film) emerged as an important tool for the evaluation of transport processes between the different phases. According to this group of experts, the surface film has an important role in economic affairs (e.g. fisheries), as well as global scale climatic changes.

The thickness of the microlayer is considered to be around 1 mm, and many processes contribute to its enrichment in some classes of compounds. Photochemical, microbiological and ecological aspects are invol-

ved in defining the microlayers composition[2,3]. Another aspect is the attenuation of radiative energy by means of the conductive or thermal sublayer (a portion of microlayer)[4]. Photodegradation of natural and anthropogenic compounds can influence the distribution of organic and inorganic microcomponents. Photolysis of compounds by UV radiation can induce changes in the ecological characteristics of the aquatic environment, e.g., the photolysis of Fe(III)-siderophore complexes can increase the bioavailablity of Fe[3].

The principal aspect that differentiate the water surface layer with respect to the bulk portion derives from its potential role as a pollutant reservoir, which is related to its capacity to accumulate surface active substances, both natural and man-made. Besides, dry and wet atmospheric depositions can also contribute to the accumulation of pollutants in the microlayer, and this is frequently observed in heavily industrialised areas along the U.S. coasts[5]. Studies on some embryos in offshore aquatic populations near Los Angeles gave evidence of increases in mortality, malformation and chromosomic anomalies[6]. These incidents, according some authors, are higher for eggs and larvas living in the microlayer, because of they are a neustonic population (a population typically resident in the first few millimeters of massive waters). The anthropogenic compounds principally associated with microlayer are: pesticides, polycyclic aromatic hydrocarbons, organotin compounds, organochloride compounds, debris, oil combustion deposition, etc[7,8]. For some of these products, an increase in concentration from 2 to 1000 times, with respect to the bulk water are hypothesised.

Here we will present some preliminary results, highlighting differences in composition between the microlayer and subsurface water, in two different areas of the central basin of the Venice Lagoon (Sacca Sessola and Murano sites). The aim of this study is to evaluate the role of the aquatic surface microlayer on micropollutant accumulation processes, transported by aerosol into the Venice Lagoon.

2. *Sampling method.*

To choose the best methodology for microlayer sampling, in relation to the aims of this study was an essential step. Many methods for sampling of the aquatic microlayer are reported in the literature[9]. The rotating drum, proposed many years ago by Harvey[10], nowadays represents one of the best methods, due to the thickness of the collected film, the

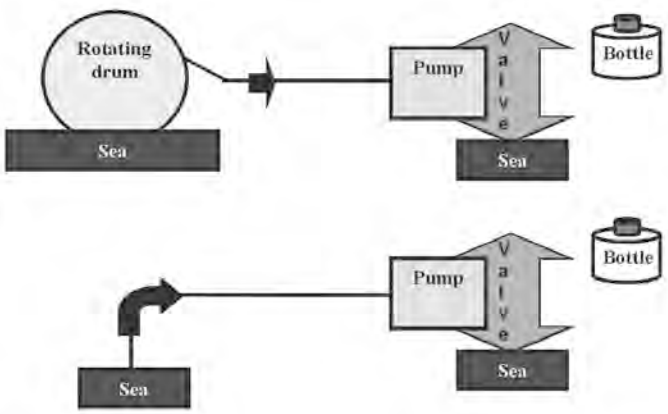

Fig. 1 - Functional sketch of the sample collecting system for microlayer and subsurface water (MUMS).

selectivity of the collected material, and the microlayer sampling rate.

The principle of the Harvey methodology is based on the collection of an aquatic surface film by capillarity. The sampler here used is the Multi-Use Microlayer Sampler (MUMS)[11; 12]. The collector consists of a rotating drum (the material is chosen according the application), located in a floating structure. The adsorbed film is removed from the drum by a Mylar scrapper. The liquid is recovered by a Teflon system, composed of: a pipeline, a three-way valve and a membrane pump. This apparatus guarantees complete control over sample collection, as well as the washing of the pipeline. A second channel is set up for the simultaneous collection of subsurface water, here considered between 0.30-0.50 m deep (see figure 1). Movement of the floating structure is gave by an electrical motor; all the system are powered by batteries, and all the principal functions of the apparatus are radio controlled.

3. *Analytical methodologies.*

3.1 *Inorganic component.*

To avoid sample contamination, any sample manipulations were carried out in an atmospheric controlled area (laminar flux – class 100). Trace metals analysis was performed by an inductive coupled plasma magnetic sector field mass spectrometer (Element, Finnigan MAT)

Tab. 1 - Concentrations of some trace elements in subsurface water and microlayer samples sampled from Sacca Sessola and Murano.

Sample	*Description*	Sampling date (mm/dd/yy)	*Site*	*Concentration µg/L*									
dissolved				*Mo*	*U*	*Cr*	*Mn*	*Ag*	*Co*	*Cu*	*V*	*Fe*	*Sb*
LV/2001/2/MM	*Microlayer*	*07/18/01*	*Sacca Sessola*	*10.2*	*3.15*	*0.141*	*2.04*	*0.003*	*0.305*	*1.44*	*6.67*	*4.40*	*0.35*
LV/2001/2/AM	*Subsurfacewater*	*07/18/01*	*Sacca Sessola*	*10.3*	*3.25*	*0.122*	*1.18*	*0.000*	*0.296*	*1.08*	*2.13*	*0.10*	*0.32*
LV/2001/4/MM	*Microlayer*	*07/27/01*	*Murano*	*11.1*	*3.16*	*0.310*	*6.47*	*0.006*	*0.406*	*2.16*	*7.07*	*69.3*	*0.36*
LV/2001/4/AM	*Subsurface water*	*07/27/01*	*Murano*	*10.0*	*3.10*	*0.460*	*9.33*	*0.010*	*0.525*	*2.90*	*3.06*	*151.*	*0.38*
particulate				*Pb*	*U*	*Cr*	*Mn*	*Ag*	*Co*	*Cu*	*V*	*Fe*	*Al*
LV/2001/2/PM	*Microlayer*	*07/18/01*	*Sacca Sessola*	*82.2*	*2.0*		*511*		*11.3*	*73.3*	*71.1*	*13.8**	*21.3**
LV/2001/2/PA	*Subsurfacewater*	*07/18/01*	*Sacca Sessola*	*32.0*	*0.9*		*280*		*6.0*	*44.0*	*30.0*	*6.4**	*9.8**
LV/2001/4/PM	*Microlayer*	*07/27/01*	*Murano*	*106.3*	*3.4*		*687*		*17.5*	*81.3*	*118.8*	*26.3**	*40.0**
LV/2001/4/PA	*Subsurface water*	*07/27/01*	*Murano*	*42.1*	*1.3*		*210*		*7.1*	*36.8*	*42.1*	*9.7**	*15.3**

**Concentration in mg/L*

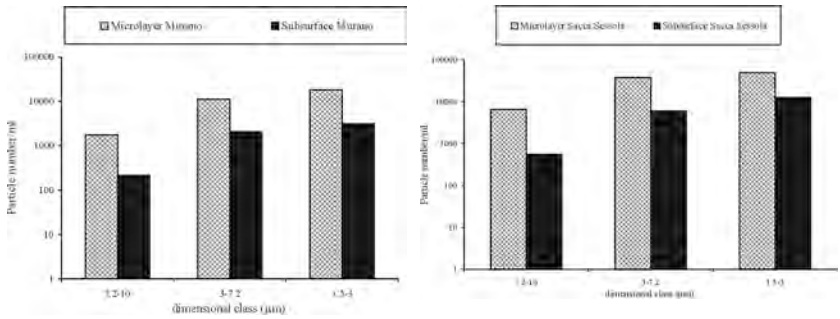

Fig. 2 - Granulometric distribution of particulate matter in the microlayer and in the subsurface water.

equipped with a Teflon spray chamber and a microconcentric nebulizer. Measurements were carried out in low (M/ΔM = 300) and medium (M/ΔM = 4000) resolution mode. To reduce the matrix effects due to salinity and to limit sample handling contamination, samples were diluted 10 time and the diluted samples were used for the direct determination of the trace metals. The quantification was carried out using the standard addition method.

3.2 *Organic pollutants.*

The sample treatment consists of a liquid-liquid continuous extraction, for 24 hours. The method was optimised. To obtain the best sample extraction, a mixture of solvents was used (pentane + dichloromethane, 200 ml, 2:1). Before the extraction, internal standards were added to the samples to quantify and to validate both the extraction and the measurement procedures. The analytical procedure follows a series of steps beginning with the solvent extraction procedure, followed by cycles of evaporation-condensation-diffusion pre-concentration, purification and the determination by a High Resolution Gas Chromatographic/Low Resolution Mass Spectrometry (HRGC-LRMS).

4. *Results.*

4.1 *Particulate matter.*

The samples were characterised by the granulometric distribution of particulate matter, for comparison with the distribution between the dimensional classes of aerosol samples (sampled in the same period).

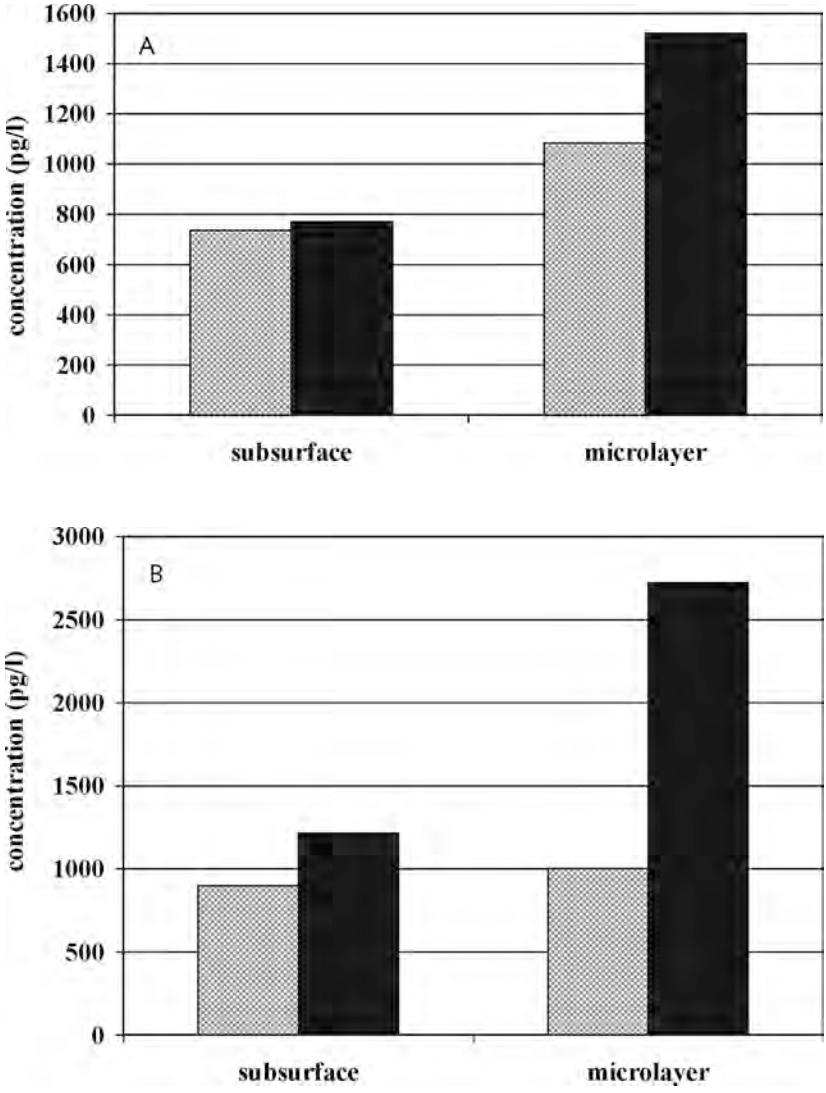

Fig. 3 - PCB concentrations in subsurface water and microlayer samples collected in Sacca Sessola (A) and Murano (B). Concentration in dissolved phase ( ) and in particulate phase ( ).

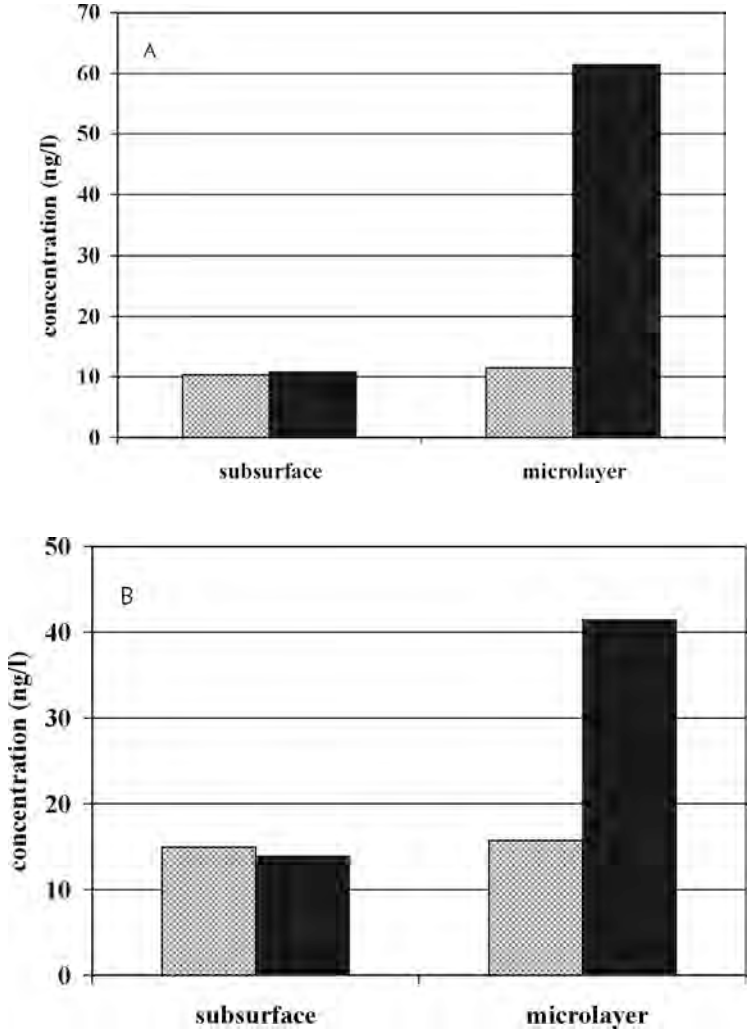

Fig. 4 - PAH concentrations in subsurface water and microlayer samples collected in Sacca Sessola (A) and Murano (B). Concentration in dissolved phase ( ) and in particulate phase ( ).

Preliminary results show an increase in particulate matter concentrations in the microlayer with respect to subsurface water. Besides which, both for the microlayer and for the subsurface samples, particles < 7.2 μm are the predominant granulometric fractions.

Trace element concentrations in microlayer and subsurface water samples are reported in Table 1. For the most part, the elements in the dissolved phase were not enriched in the microlayer with respect the subsurface water, within the examined elements only vanadium, which is linked with the use of fossil fuel, had an enrichment factor of 3-4 times, while in the particulate fraction all the examined elements showed an enrichment factor of 2 or higher; therefore the aerosols seem to contribute to the trace elements concentration essentially in the particulate form.

The PCB and PAH concentrations are reported in Figures 3 and 4, for samples collected in the Sacca Sessola and Murano sites respectively. The preliminary results show an enrichment of these pollutants in the microlayer in particulate form; which is not evident in the dissolved fraction. This was observed for both the pollutants, but was particularly evident for PAH's in the Sacca Sessola site. Further elaboration and interpretation of the data obtained from these sites is in progress.

References.

1) WHO 1995. The sea-surface microlayer and its role in global change. IMO/FAO/UNESCO-IOC/WMO/WHO/IAEA/UN/UNEP: Joint Group of Experts on the Scientific Aspects of Marine Environmental Protection (GESAMP). Reports and studies N°. 59. WMO Geneva 1995.
2) Zhou X. & Mopper K., 1997. Photochemical production of low-molecular-weight carbonile compounds in seawater and surface microlayer and their air-sea exchange. Marine Chemistry, 56, 201-203.
3) CEE AIRWIN Project (Structure and role of biological communities involved in the transport and transformation of persistent pollutants at the marine Air-Water Interface - AIRWIN - Project Reference: EVK3-2000-00030).
4) Soloviev A.V., Schlüssel P., 1994. Parameterization of the temperature difference across the cool skin of the ocean and of the air-ocean gas transfer on the basis of modelling surface renewal, Journal of Physical Oceanography, 24, 1339-1346.
5) Longwell A.C., Chang S., Hebert A., Hughes J.B. & Perry D., 1992. Pollution and developmental abnormalities of Atlantic fishes. Environmental Biology of Fishes 35, 1-21.

6) Cross J.N., Hardy J.T., Hose J.E., Hershelman G.P., Antrim L.D., Gossett R.W. & Crecelius E.A., 1987. Contaminant concentrations and toxicity of sea-surface microlayer near Los Angeles, California. Marine Environmental Research 23, 307-323.
7) Södergren A., Larson P., Knulst J., 1990. Bergqvist Transport of incinerated organochlorine compounds to air, water, microlayer and organisms. Marine Pollution Bulletin, 21, 18-24.
8) Knulst J. & Södergren A. 1994. Occurence and toxicity of persistent pollutants in surface microlayers near an incineration plant. Chemosphere, 29 (6), 1339-1347.
9) Garrett W.D. & Duce R.A., 1978. Advanced study institute on air-sea interaction instrumentation.
10) Harvey G.W., 1966. Microlayer collection from the sea-surface. A new method and initial results. Limnol. Oceanogr., 11, 608-613.
11) G. Loglio, Stortini A.M., Tesei U., Buso P., Schiavuta E. e Cini R., 1999. Problemi sulla caratterizzazione del microstrato oceano-atmosfera in zona costiera antartica. Incontri di Chimica Analitica dell'Ambiente, XIII – Il ruolo della chimica analitica nello studio della contaminazione ambientale a livello planetario. Acquario di Genova – Dipartimento di Chimica e Chimica Industriale. Genova 17-18 dicembre 1998 (riassunti).
12) Stortini A.M., Piccardi G. e Cini R., 2000. Studio del film di superficie: Valutazione ed ottimizzazione del metodo di raccolta. Incontri di Chimica Analitica dell'Ambiente, XIV – Qualità dei dati analitici – Qualità dell'ambiente. Dip. Chimica e di Chimica Industriale, Univ. Pisa, Pisa 5-6 Aprile 2000 (riassunti).

DETERMINATION OF TRACE ELEMENTS AND ORGANIC POLLUTANTS (PCB, PAH) IN THE ATMOSPHERIC AEROSOL OF THE VENICE LAGOON

A. Gambaro[1,2], L. Manodori[2], S. Ferrari[1], G. Toscano[1], A. Varga[1], I. Moret[1,2], G. Capodaglio[1,2]
[1]*Dipartimento di Scienze Ambientali, Università Ca' Foscari di Venezia, Italy*
[2]*Istituto per la Dinamica dei Processi Ambientali, CNR, Venezia*

1. *Introduction.*

It has recently become apparent that transport via the atmosphere is an important route by which both natural and pollutant compounds are transported from continents to both coastal and open sea.

Previous scientific research on the Lagoon of Venice showed that several processes contribute substantially to the input of pollutants into this delicate environment such as atmospheric transport, remobilization of sedimented pollutants and fresh waters draining from the catchment basins of the Lagoon (Bellucci et al., 1999; Jimenez et al., 1998). We know very little about the atmospheric contribution of trace elements and of organic pollutants to the contamination of the Venice Lagoon.

The aim of this study is to investigate the role of aerosols in the contamination of the Venice Lagoon ecosystem. This study was carried out to determine the trace elements, PCB and PAH concentrations in samples of atmospheric aerosols.

2. *Materials and Methods.*

Figure 1 shows the selected sites for the aerosol sampling. The sampling was carried out at four stations selected due to the speed and the direction of the wind, with the aim of characterising the aerosol derived from the possible sources of the Venice Lagoon.

Fig. 1 - Aerosol sampling sites: St. 1, urban and industrial sources; St. 2, inland sources; St. 3, marine sources; St. 4, "long range" sources.

Station 1 is located in the Moranzani locality, down-stream of the urban and industrial zone of Mestre (Marghera) where there are steel-works, chemical factories, oil refineries and power stations. The sampling of aerosol was carried out when the wind was blowing from the north-east collecting the aerosol derived from the urban and industrial sources.

Station 2 is located in the locality of Osellino-Tessera upstream of the urban zone of Mestre and down-stream of the Venice international air-port (Marco Polo). The sampling of aerosol was carried out when the wind was from the north-east collecting the aerosol derived from inland sources without the urban and industrial sources of Mestre.

Station 3 is located in the locality of Punta Sabbioni on a platform of the lighthouse at the Lido inlet. The sampling of aerosol was carried out when the wind was from south-east collecting the aerosol derived from marine sources (Adriatic Sea).

Station 4 is located in the locality of Teolo in the Euganei hills. The sampling of aerosol was carried out when the wind was from north-east square collecting the aerosol from "long range"sources.

Aerosol sampling was carried out in two periods: between 16th - 20th July at Stations 1, 3, 4 simultaneously, and between 26th - 30th July at Stations 2, 3, 4 simultaneously.

Aerosol samples were collected for trace element analysis onto cellulo-se filters (Whatman 41) using Tish High-Volume air samplers fitted with

PM_{10} size selective inlets. During sampling with a rate of about 1 m^3/min particles with aerodynamic diameters < 10 μm were classified into six size intervals with cutoff aerodynamic diameters of 7.2, 3, 1.5, 0.95, 0.49, <0.49 μm. The sampled filters were weighed and successively mineralized in acid mixture using a microwave digestion system. Elemental analysis of the aerosol samples was carried out by ICP-SFMS for the following elements: Li, Pb, U, Cd, Al, V, Mn, Fe, Cu, Zn, Co.

The origin of atmospheric aerosol reaching the Lagoon was investigated by means of tracers such as:

- Al and Li, which show the crustal contribution.
- Pb, V show principally the anthropogenic contribution to the atmospheric aerosol.

Aerosol sampling for PCB and PAH analysis was performed using a High-Volume air sampler equipped with a quartz filter before the sorbent material, which consisted of polyurethane foam (PUF). This sampler allowed the separate analysis of the "particulate" and "vapour" phases of atmospheric aerosol. For the determination of "particulate" PCBs and PAHs the quartz filter was extracted for 24 hours by Soxhlet apparatus using an aliquot of 240 ml of a mixture of pesticide grade n-pentane and dichloromethane (2:1, v/v).

For the determination of "vapour" PCBs and PAHs the PUF was extracted for 24 hours by Soxhlet apparatus using an aliquot of 480 ml of the same mixture.

The extract cleanup was done by column chromatography, using a column packed with Florisil and Alumina. The microcontaminants were eluted with n-hexane (30 ml). The eluate was reduced under a gentle stream of nitrogen to 100 μl and the PCBs and PAHs were determined by gaschromatography-mass spectrometry (Moret et al., 1999).

Five carbon-13-labeled PCBs and carbon-13-labeled phenantrene were added to the samples before extraction for use as internal standards for the microcontaminants quantification.

3. *Results and Discussion.*

The preliminary results of the granulometric distribution of the atmospheric aerosol collected at the different stations show a bimodal distribution with greater percentage of fine particles at stations 1, 2, 4 although the pattern is different between them. Greater percentage for coarse particles is observed at station 3.

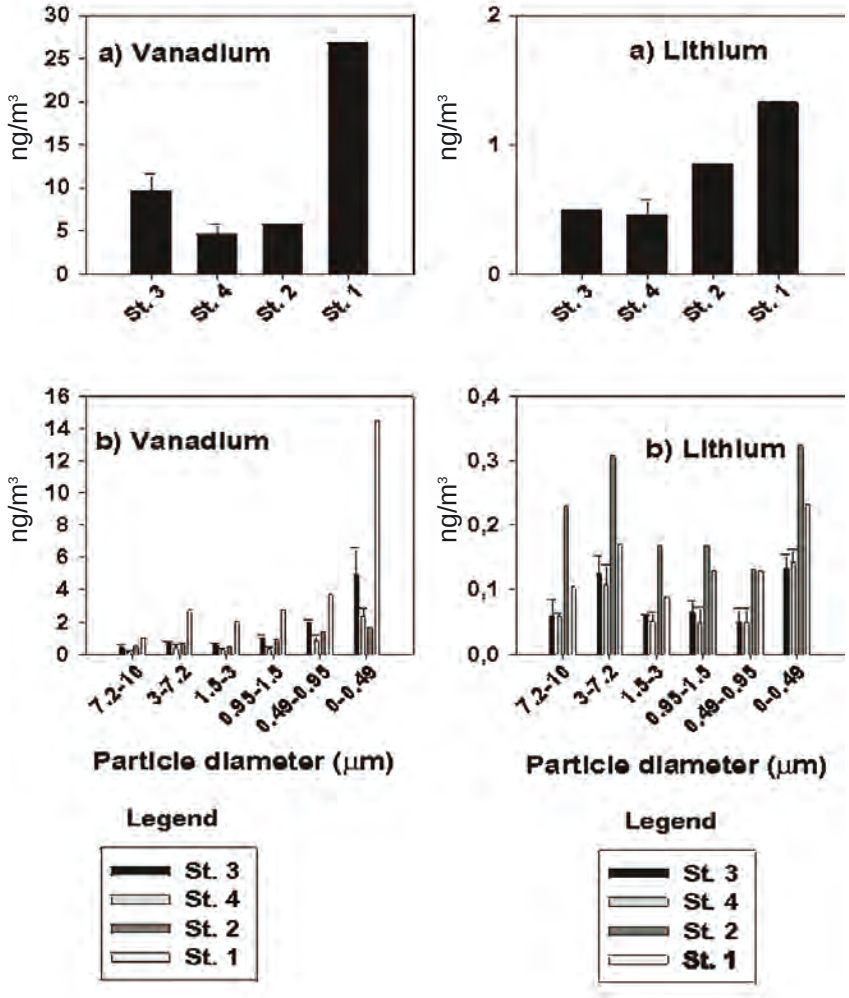

Fig. 2 - Total (a) and size distribution (b) concentrations of vanadium and lithium in the atmospheric aerosol collected at the investigated sites.

Figure 2 shows the preliminary results of the total and size distribution concentrations of vanadium (as element of industrial origin) and lithium (as element of natural origin) in the atmospheric aerosol collected at the various stations. The preliminary results obtained show that the elements such as V, with a clear anthropogenic origin, had a higher concentration at station 1 and in the fine fraction of aerosol, while other elements such

as Li showed similar concentrations at all sites with a bimodal distribution probably due to the crustal origin of this element.

The preliminary total PAH (expressed as sum of 17 compounds) and PCB (expressed as a sum of 54 congeners) concentrations in the aerosol samples collected at the investigated sites are reported in Figure 3. It can be observed that, the PCB concentrations were quite similar at all stations even if the highest levels were present at station 1. The PAH concentrations are highest at station 2 even though the concentrations present in the other stations are not negligible. In our previous work (Gambaro et al., 2002) it had been reported than the PCB and PAH concentrations were higher in the dissolved phase than in the particulate phase.

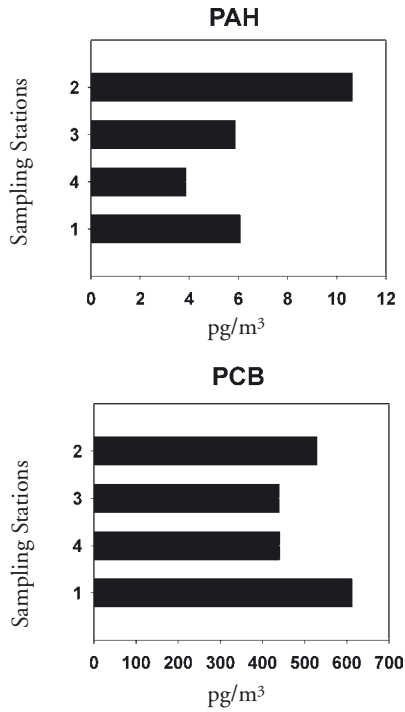

Fig. 3 - Total PAHs and PCBs concentration in the aerosol samples collected at the investigated sites.

To investigate the role of aerosols in the contamination of the Venice Lagoon ecosystem it is very important to estimate the flux of the contaminants from the atmosphere to the Venice Lagoon. Figure 4 reports the average daily flux values of V, Pb, PAHs and PCBs at the investigated

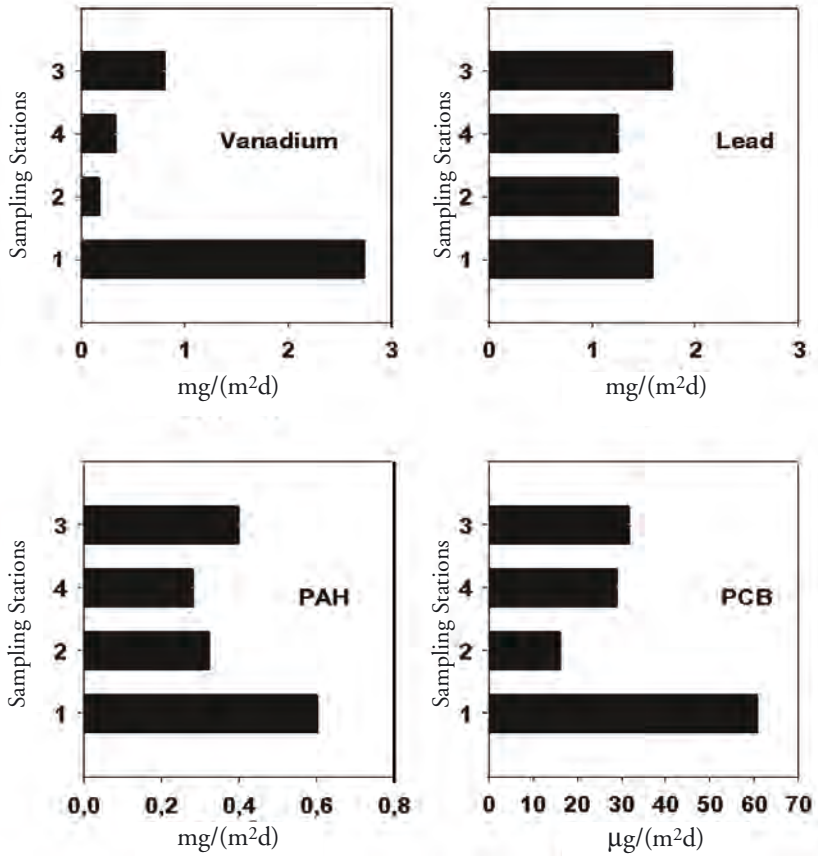

Fig. 4 - Average daily fluxes of vanadium (mg/(m^{2}d)), lead (mg/(m^{2}d)), PAHs (mg/(m^{2}d)), PCBs (µg/(m^{2}d)) at the investigated sites.

sites. It can be observed that the average daily flux of V, PCBs and PAHs were higher at station 1 whereas the flux of Pb is quite similar at all stations.

4. *Conclusion.*

To our knowledge this is the first study on the atmospheric aerosol flux of trace elements, PCBs and PAHs towards the Venice Lagoon system. Although the period of this study was short and the data are sparse, the preliminary results obtained show that:

- the concentrations of the inorganic and organic pollutants in the atmospheric aerosol are not negligible,
- for the study of the chemical contamination of the Venice Lagoon the marine aerosols contribution have to be considered.

Further experimental data are expected from the ongoing work and will allow a more thorough evaluation of the issue.

Acknowledgement.

This work was supported by the CORILA under the Projects "Role of aerosol and secondary pollution to the chemical contamination of the lagoon of Venice" and by the National Research Council of Italy (CNR). The authors thank A.M. Stortini and W. Zampieri for their sampling support.

Bibliography.

Bellucci L.G., Raccanelli S., Frignani M., and Carraio C., 1999. Polychlorinated biphenyls in sediments of the Venice Lagoon and their toxicity with respect to other organic microcontaminants. Organohalogen Comp. 43, 295-298.

Gambaro A., Moret I., Piazza R., Capodaglio G., Cescon P., 2002. Determinazione di microinquinanti organici (PCB, IPA, IA) nell'aerosol della laguna di Venezia. In: Attualità ed interdisciplinarità della Chimica Analitica, Convegno in memoria del Prof. Arnaldo Liberti, Roma, R21.

Jimenez B., Hernandez L.M., Eljarrat E., Rivera J. and Fossi M.C., 1998. Congener specific analysis analysis of polychlorinated dibenzo-p-dioxins and dibenzofurans in crabs and sediments from the Venice and Orbetello Lagoons, Italy. Environ. Sci. Technol. 32, 3853.

Moret I., Piazza R., Gambaro A., Benedetti M. and Cescon P., 1999. Polychlorobiphenils (PCBs) in the sediment and surface water of the Venice Lagoon.Organohalogen Comp. 40, 223-226.

RESEARCH LINE 3.5.
Quantity and quality of exchanges between lagoon and sea

CURRENT STRUCTURE IN FRONT OF THE LAGOON OF VENICE AS DERIVED FROM THE COASTAL HF RADAR DATA

V. Kovačević[1], M. Gačić[1], I. Mancero Mosquera[2], A. Mazzoldi[3], and S. Marinetti[4]

[1]*Istituto Nazionale di Oceanografia e di Geofisica Sperimentale, Trieste*
[2]*Escuela Superior Politécnica del Litoral, Guayaquil, Ecuador, presently at Istituto Nazionale di Oceanografia e di Geofisica Sperimentale, Trieste*
[3]*Istituto per lo Studio della Dinamica delle Grandi Masse, CNR, Venezia*
[4]*ITEF-CNR, Padova*

1. *Introduction.*

The dynamics of the Venetian Lagoon system is characterized by locally determined factors, such as a geometry and a topography, which to a certain extent interact with the principal forcing mechanisms (tides, fresh water runoff, and those meteorologically driven). The Lagoon communicates with the open sea through three relatively narrow inlets, in which the currents are almost totally driven by the tides. The possible interaction with the adjacent open sea area, relatively deep (20 m) with respect to the lagoon itself, is one of the aims imposed by a complex multidisciplinary research project conducted by CORILA. Thus it has become one of the research topics within the framework of the sub-task 3.5 "Quantity and Quality of the exchange between the Lagoon and the open-sea". Its realization is provided by installing a high-frequency (HF) Coastal Radar in conjunction with the current measurements within the inlets (Fig. 1).

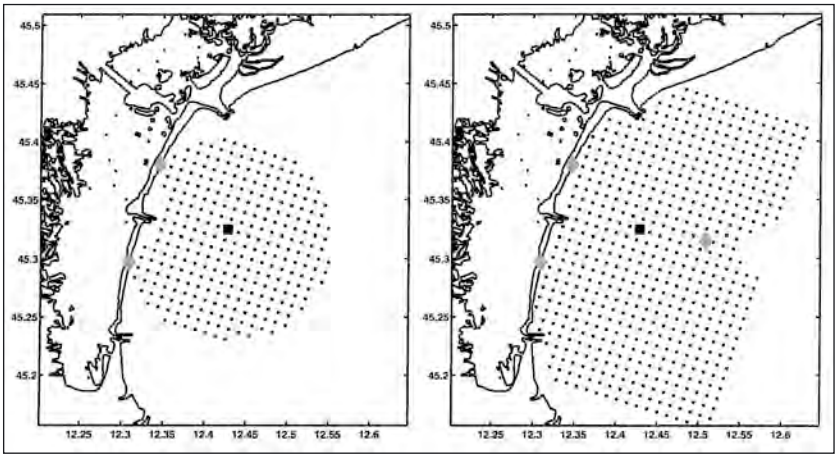

Fig. 1 - The regular spatial grid covered by two (left) and three antennas (right) operating simultaneously. The antennas are denoted by gray solid diamonds. The location for which the power spectrum has been calculated is denoted by a black square. Positions of the ADCP current meters inside the inlets are denoted by black solid circles.

2. *Data and methods.*

The Coastal Ocean Dynamics Applications Radar (CODAR) SeaSonde (by COS, LTD) is a system of antennas which emit electromagnetic radiation at about 25 MHz, and receive the backward signal, dispersed from the surface sea waves of exactly the half of the wave-length of the emitted radiation (Crombie, 1955). Algorithms were developed (Lipa and Barrick, 1983), which, on the basis of a Doppler shift, determine the radial currents obtained by a single receiving antenna, and subsequently combine the radials from at least two antennas in order to calculate the total currents. Individual current measurements have typical speed and direction uncertainties of about 4 cm/s and 12°, respectively. In our case, the two antennas, about 10 km distant from each other, situated on the islands of Lido and Pellestrina, have been continuously operating since November 2001. The third antenna, mounted on the Oceanographic platform "Acqua Alta", was operating intermittently. However, after resolving the power supply problems, its mode of operation is going to be changed, and it will operate continuously within a short period of time. The advantage of a three-antenna system lies in the fact that a much wider area of the sea surface (of about 280 km^2) will be covered in front of the Lagoon, almost double with respect to the one covered by two

antennas only (Fig. 1). The average currents within 1 m from the sea surface are available every hour at a regular spatial grid with a resolution of about 750 m. Maximum range reached is about 15 km off the coastline.

We have analysed the current data collected between November 2001 and March 2002. In particular, a spectral analysis has been applied to the November 2001 time series at one location about 5 km distant from the Malamocco inlet (Fig. 1), which was one of the three locations without gaps. The harmonic analysis has been performed on a 90-days long time series (November 2001 – January 2002) on a grid covered by the two antennas. Thus, a spatial distribution of the harmonic parameters, amplitudes and phases, is determined for the most significant constituents, M2 and K1. Averaging the hourly data at the same grid over a monthly period, mean monthly current structure and a corresponding eddy kinetic energy (a measure of the total variance) is obtained for the months November 2001, December 2001, January 2002, February 2002, and March 2002. The evolution of the current field during an episode of the strong north-easterly bora wind is followed using a sequence of hourly current maps between December 6 and December 9, 2001. Also in this case the area covered is determined from two antennas.

3. *Preliminary results.*

Inspection of the power spectrum at a grid point indicated in Fig. 1, reveals the most significant characteristics of the current variability in front of the Lagoon (Fig. 2). The tidal motion is evident, but not so energetic as a low frequency signal, at time scales of the order of several days. On the contrary, in the lagoon inlets semi-diurnal and diurnal tidal con-

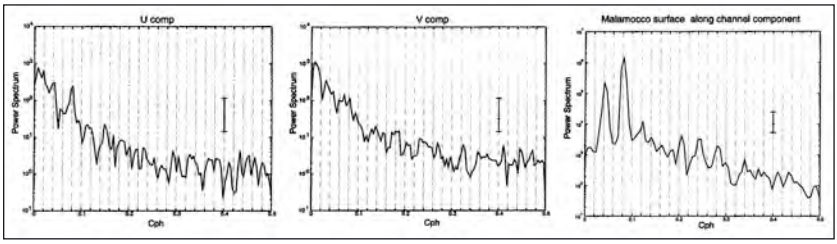

Fig. 2 - Power spectrum and the confidence limits for the east-west (left) and north-south current components (center) at the location indicated in Fig. 1, compared to that of the along-channel component in the Malamocco inlet right.

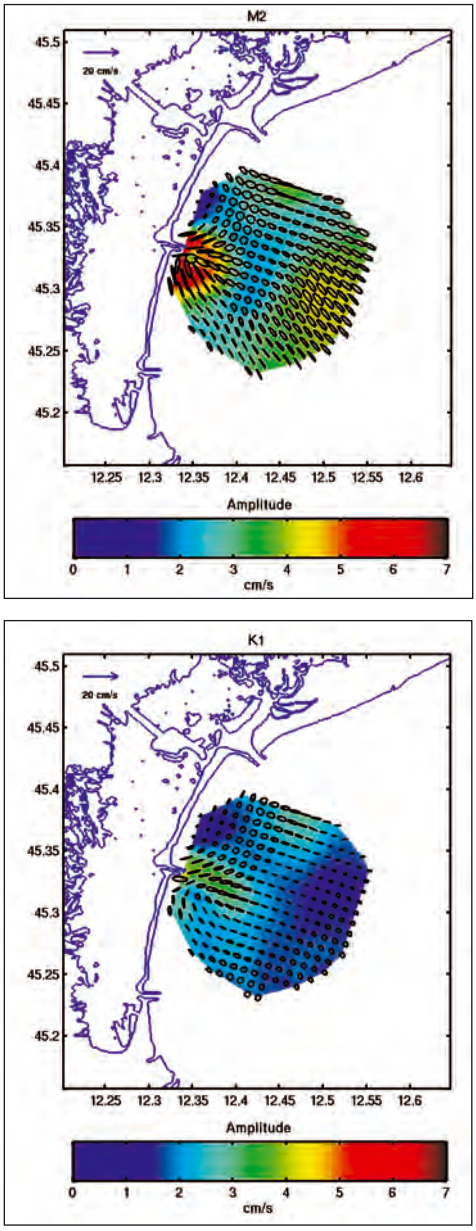

Fig. 3 - Spatial distribution of the tidal ellipses and amplitudes for the major semi-diurnal (M2) and diurnal (K1) constituents.

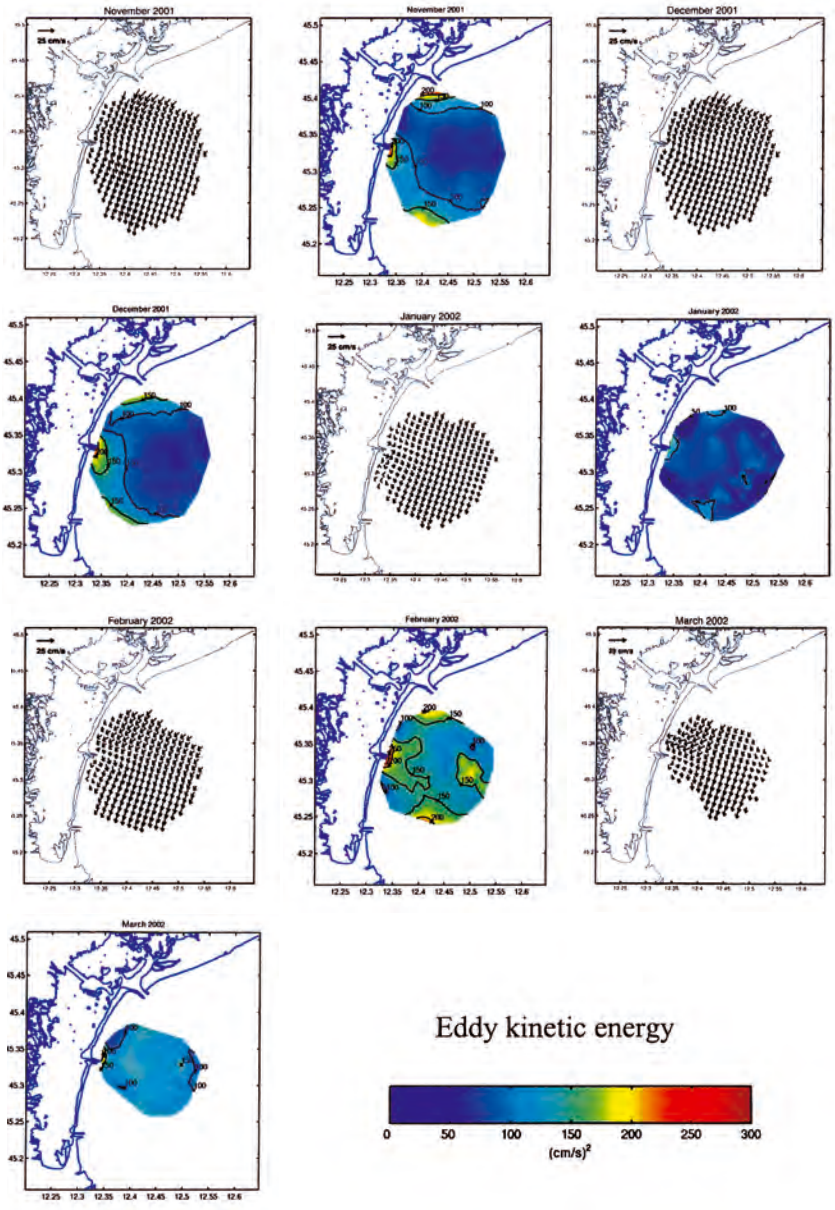

Fig. 4 - Maps of the mean monthly surface currents in the period November 2001 – March 2002, and a corresponding eddy kinetic energy per unit mass.

stituents play much more important role, and exceed significantly the residual, low-frequency currents, as reported for the Malamocco inlet in Fig. 2.

The maps of the amplitude distribution for M2 and K1 (Fig. 3) confirm that a tidal signal is much lower than in the inlets, where it reaches amplitudes of about 70 cm/s and 30 cm/s for M2 and K1, respectively. Tidal signal from the inlets dissipates quite quickly, within 3-4 km offshore. Thus M2 amplitudes away from the inlets are within 2-4 cm/s, while those of K1 drop below 2 cm/s. Current ellipses associated with the tidal flow are radially polarized in the vicinity of the inlets, whereas they become almost circular at a distance of 3-4 km from them.

The monthly mean current structure is represented in Fig. 4 for a 5-month period, from November 2001 to March 2002. Inspection of these maps reveals that a long term current flow is prevalently southward, parallel to the coast, with velocities of about 10-15 cm/s. This type of flow is coherent with the branch of the general cyclonic circulation cell which embraces the whole Adriatic Sea, and in particular, its northernmost basin, adjacent to the Venetian Lagoon (see Cushman-Roisin et al., 2001, for an overview). Eddy kinetic energy per unit mass is obtained as follows:

$$EKE = \Sigma[(u_i - u_a)^2 + (v_i - v_a)^2]/2$$

where u_i and v_i are eastward and northward hourly components, T is the total number of hours in a monthly time interval, subscript "i" counts the hourly data, while u_a and v_a are the corresponding monthly means.

This quantity is proportional to the flow variance, which contains variations around the monthly mean at both tidal and sub-tidal frequency scales. Once again a variability close to the inlets is put into evidence, while further from the coast it diminishes. In November and December 2001 monthly mean maps reveal a mean current field intensity of about 12-13 cm/s, while in January 2002 it is lower than 10 cm/s. In addition, the current field in January is much less energetic. Both facts may indicate that during this month the current field was not affected much by forcing such as a meteorological one. Indeed, the time series of wind data available from the platform 'Acqua Alta' (not shown here) were an indicator of a low meteorological activity during January 2002. On the contrary, it was much more energetic during the rest of the studied period.

An episode, characterised by a strong north-easterly bora wind blowing for a couple of days in December 2001, has been taken as an example of response to extreme wind conditions. Evolution of the currents is

depicted through a sequence of six hourly maps, unequally distributed in time (Fig. 5). The corresponding flow in the Malamocco inlet is going to be reported as well. The first snapshot on 6th of December at 13 GMT (1), has been taken as a representative of the current flow during the weak wind conditions. Mean hourly wind effectively is lower than 5 m/s. In the inlet, the tidal current is almost zero (slack water). In the open sea distant from the coast and islands, southward flow of about 10 cm/s is evident, while close to the islands the presence of small scale clock-wise eddies is hinted. The second snapshot (2), taken four hours later still corresponds to low wind conditions. Generally, the flow is weak, except near the inlets, where it is about 10 cm/s. Inside the inlet maximum ebb current of about 50 cm/s is observed. The day later at 23 GMT (3) the wind conditions indicate ENE bora wind of about 13 m/s mean hourly speed. The CODAR map shows onshore surface flow of about 10-15 cm/s, coinciding with the almost maximum flood current in the inlet of about 50 cm/s. On 8th December at 16 GMT (4) the ENE bora reaches speeds of about 17 m/s. The south-westward velocity in the north-eastern portion of the area is about 20 cm/s, while it diminishes in the southern part. Along the lagoon islands, the flow is parallel to the coast, and there are no longer small scale eddies evident near the shore. Relatively strong currents near the Lido and Chioggia inlets are just at the margins of the covered area, and there is no possible justification for it. The flow inside the inlet is characterized by a maximum ebb tide of about 30 cm/s. The next two snapshots (5 and 6), taken on the 9th December at 10 GMT and 20 GMT, respectively, correspond to the ENE and NE bora with the mean hourly speed of about 18 m/s. The next surface map (5) shows the flow parallel to the shore of about 20 cm/s, while in the central zone the flow is weak, and slightly divergent. In the inlet there is an ebb current of about 30 cm/s. The surface map (6), on the contrary, represents southward and south-westward flow, more intense near the shore (about 30 cm/s), decreasing offshore (20 cm/s). Simultaneously, in the inlet the flow intensity of about 70 cm/s denotes the maximum ebb tide.

This example of the evolution of the current field in front of the lagoon during an episode of bora wind illustrates that the effect of the wind acts most probably through the on-shore piling up the water, caused by the Ekman transport in the surface layer. Consequently, the pressure gradient is established, which in turn leads to the geostrophic balance and causes a southward flow parallel to the coast. Weak small-scale eddies, near the islands, observed during calm weather conditions, disappear and the current field becomes more homogeneous.

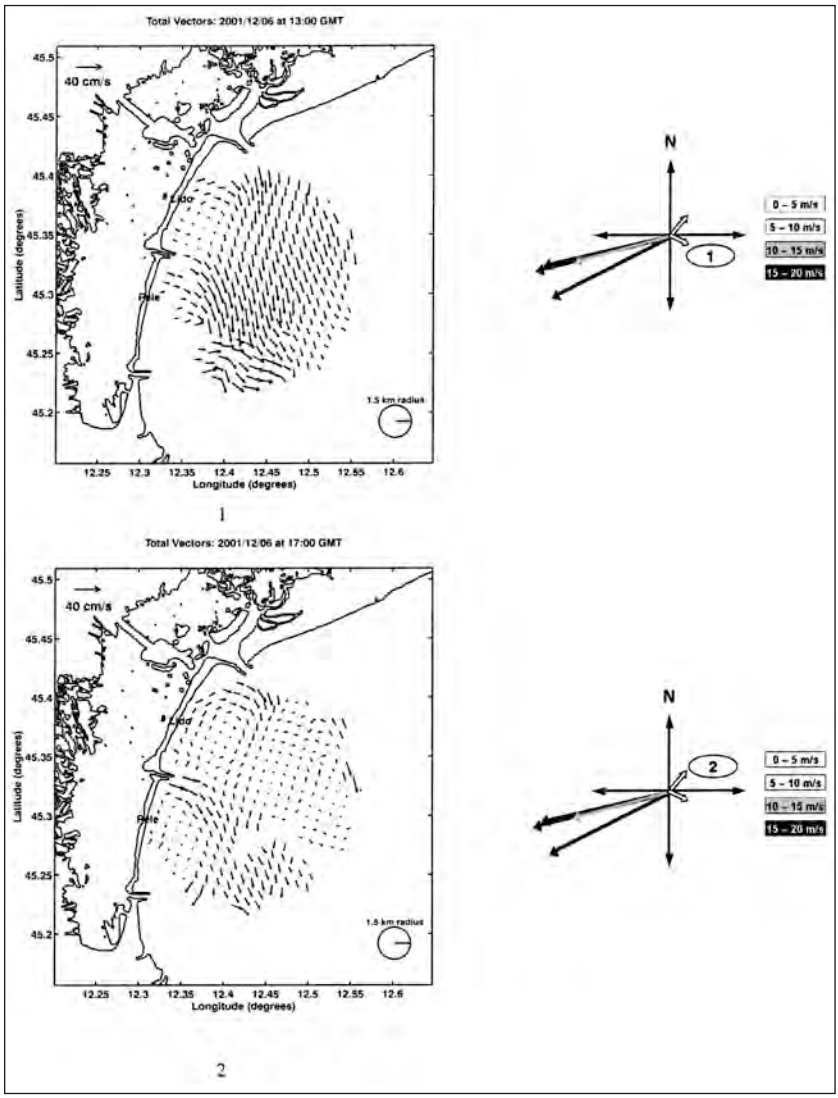

Fig. 5 - A sequence of six hourly maps, and corresponding mean hourly winds in the period 6-9 December 2001.

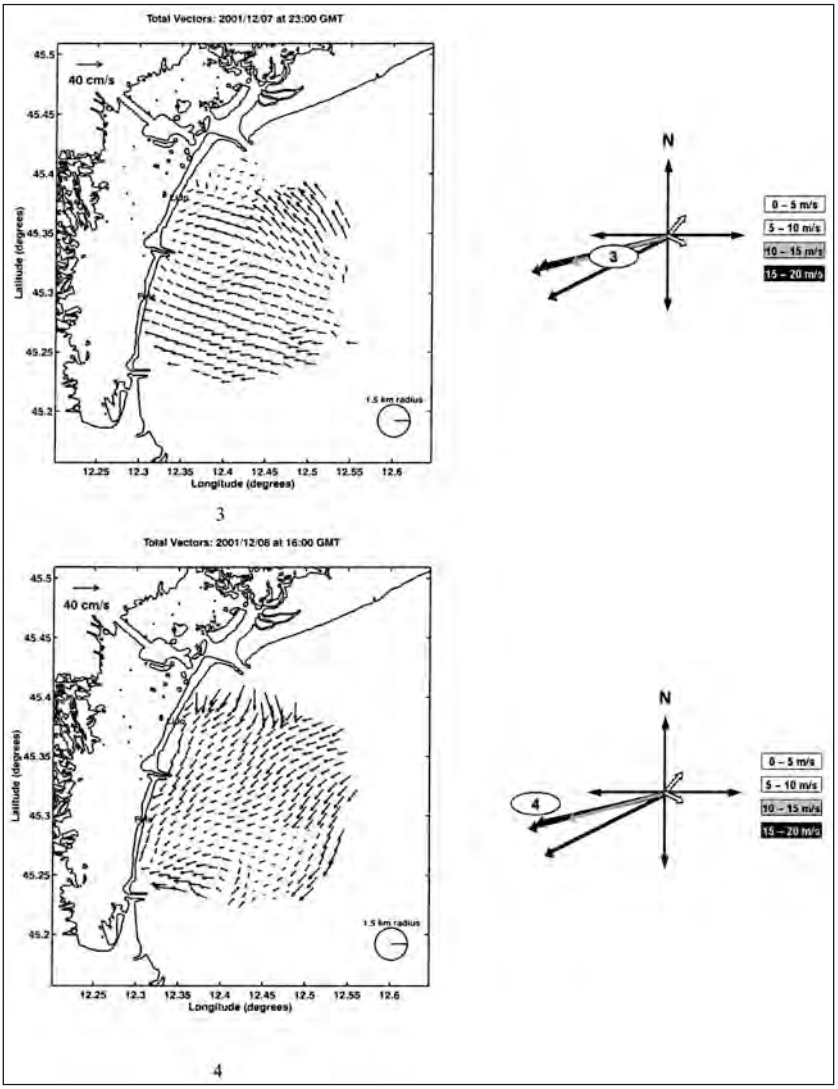

Fig. 5 - Continued.

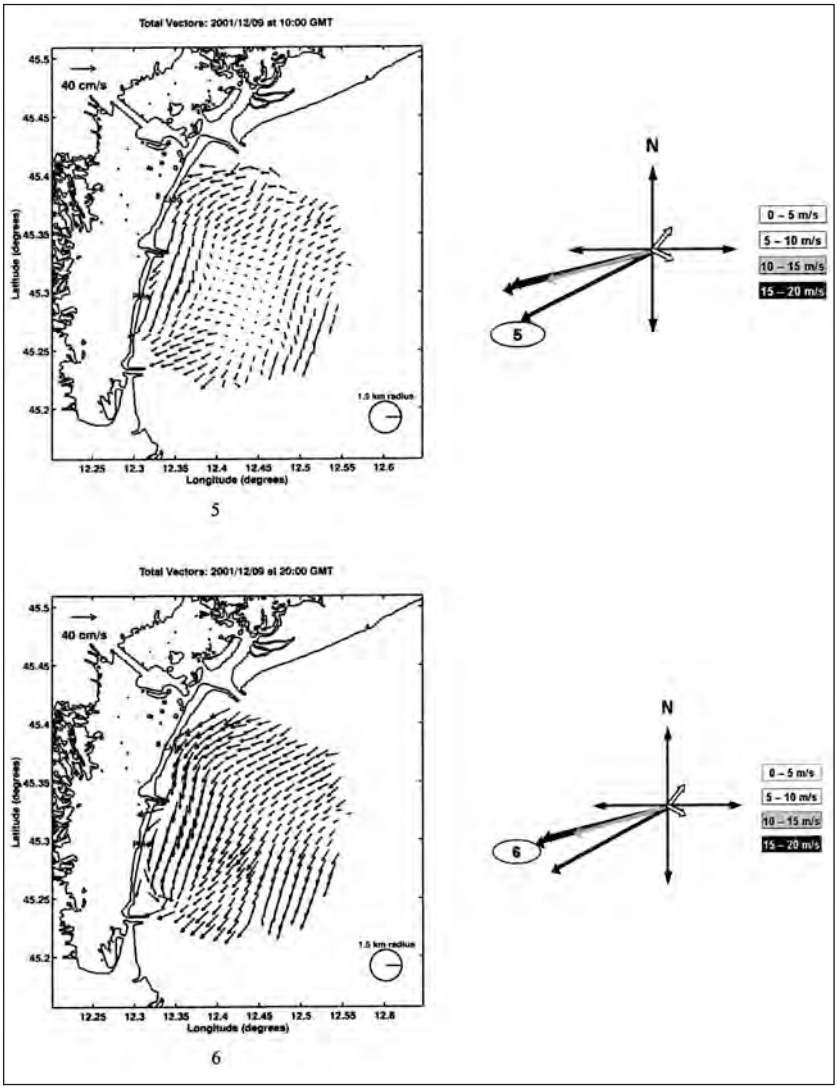

Fig. 5 - Continued.

4. *Concluding remarks.*

It is noteworthy to mention that these are preliminary results, which require a more detailed analysis, especially in the sub-tidal frequency range. Thus, the future efforts will be focused more in detail on the dynamical aspects of the connection between the residual flow (obtained by subtracting a tidal signal from the raw hourly data) and the strong wind conditions, connected to the both NE bora and SE sirocco winds (onshore piling up of water which results in the geostrophic flow parallel to the coast). Once the third antenna at the Oceanographic platform will be operating in the continuous mode, the investigated area will be extended, and this will enable studying the flow structure in the vicinity of all three inlets. Moreover, surface current data on such an area will make possible comparing the circulation results derived from ecological-hydrodynamical numerical modelling and those measured by HF radar. Ongoing measurements will contribute to long-term time series construction (of about a year), which is crucial for determining with a sufficient resolution all important tidal constituents in the current field.

Acknowledgement.

Isaac Mancero Mosquera undertook this work with the support of the "Programme for Training and Research in Italian Laboratories of the Abdus Salam International Centre for Theoretical Physics, Trieste, Italy".

References.

Crombie D.D., 1955. Doppler spectrum of sea echo. Nature 175, 681-682.

Cushman-Roisin B., Gačić M., Poulain P.-M. and Artegiani A., (Eds.) 2001. Physical Oceanography of the Adriatic Sea. Kluwer Academic Publishers, Dordrecht, Boston, London, 304 pp.

Lipa B.J. and Barrick D.E., 1983. Least-Squares method for the extraction of surface currents from CODAR crossed-loop data: application at ARSLOE. IEEE Journal of Oceanic Engineering, OE-8, 226-253.

ANALYSIS OF CURRENT MEASUREMENTS IN INLETS OF THE VENETIAN LAGOON*

M. Gačić[1], A. Mazzoldi[2], V. Kovacevic[1], F. Arena[1],
I. Mancero Mosquera[3], G. Gelsi[1] and G. Arcari[2]
[1] *Istituto Nazionale di Oceanografia e di Geofisica Sperimentale, Trieste*
[2] *Istituto per lo Studio della Dinamica delle Grandi Masse, CNR, Venezia*
[3] *Escuela Superior Politécnica del Litoral, Guayaquil, Ecuador, presently at Istituto Nazionale di Oceanografia e di Geofisica Sperimentale, Trieste*

1. *Introduction.*

One of the most important oceanographic problems related to the temporary lagoon closures is the water flow pattern in the inlets and the exchange rate variability at different time scales. From the flow rates, estimates of residence and water renewal times can be obtained, which are key parameters for determining the impact of temporary closures on the lagoon water characteristics and ecosystem. The Venice Lagoon has three inlets (Fig. 1) which are at most 900 m wide (Lido) and at most 20 m deep (Malamocco). The flow is presumably tidally driven, but no experimental evidences whatsoever exist on a possible contribution of the wind forcing and freshwater discharge. So far, there has not been any systematic experimental study aimed at estimating the water flow rate through the lagoon inlets and its temporal variability. Only some numerical modeling studies have been carried out and have shown some features of the water exchange patterns giving also some rate estimates (Umgiesser, 2000) without however detailed validations with experimental data.

* These preliminary results were published in a paper: Gačić, M., V. Kovačević, A. Mazzoldi, J. Paduan, F. Arena, I. Mancero Mosquera, G. Gelsi and G. Arcari, 2002: Measuring Water Exchange between the Venetian Lagoon and the Open Sea. EOS, Transaction, American Geophysical Union, 83, 20, 217-222.

Fig. 1. - The LANDSAT-Thematic Mapper image showing the Venice lagoon on 9 August 1986. Red dots indicate the locations of the bottom-mounted ADCP in the lagoon inlets, while yellow dots denote positions of the CODAR antennas. Coastal HF radar coverage is delimited by a yellow line.

2. *The experimental set-up and preliminary measurement results.*

During the year 2000, a research plan was developed to address the most relevant oceanographic issues concerning lagoon - open-sea interaction. The study program, among other activities, consisted in two-year simultaneous current measurements in all three lagoon inlets. This was complemented with the high-frequency coastal radar (CODAR) surface

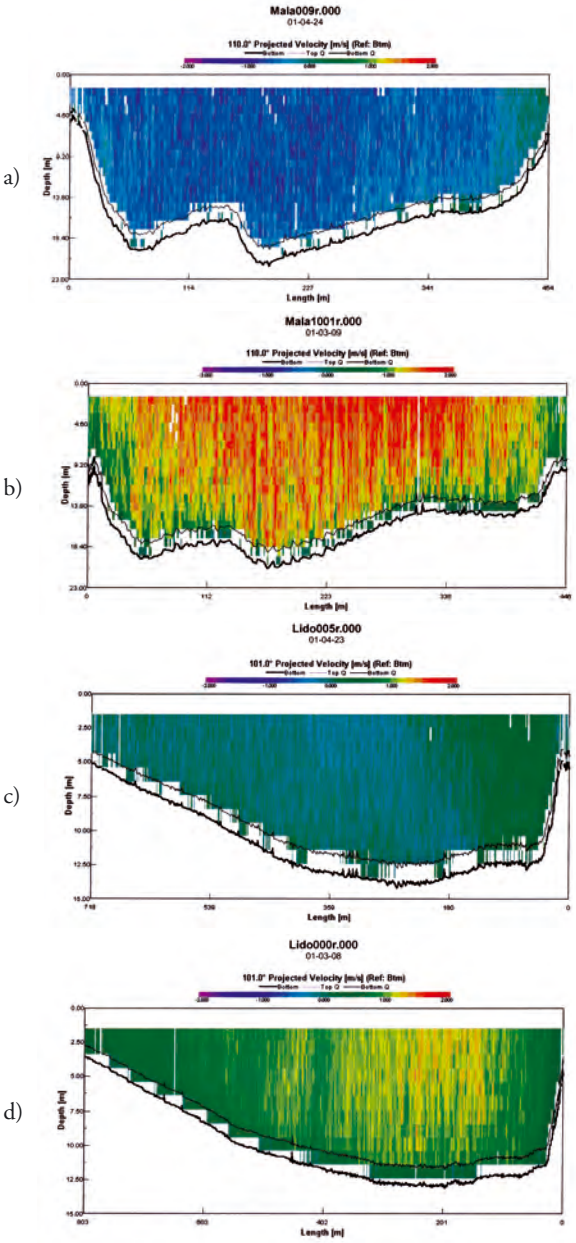

Fig. 2a, b, c and d. - Transects showing the distribution of the inflowing current components in the Lido inlet for various tidal phases.

current measurements in the area in front of the lagoon inlets. The locations of CODAR antennas and the spatial coverage of the surface current measurements are shown in Fig. 1. Here we will limit our presentation to results of some preliminary analyses of inlets' current measurements.

The project realization started in January, 2001. The measurements have been carried out with both bottom-mounted and ship-borne Acoustic Doppler Current Profilers (ADCP) so that in each inlet one ADCP was installed. Since the aim of these measurements is to study time-dependent variability of inlet currents as well as of water exchange rates, it was necessary to determine the relationship between the vertically averaged currents measured with the ADCP at a single location, and the flow rate. In the preparatory phase, it was also necessary to determine the most representative location of a mooring in each inlet; the criteria for choosing the ADCP locations was that the linear correlation between the inlet flow rate and the vertically averaged current over a unit column area is maximum. This preparatory phase consisted of a series of current profiling and the water flow rate calculations on a transect where the bottom-mounted ADCP was supposed to be moored. The measurements were carried out with a ship-borne ADCP in various phases of tides. The profiling exercises have shown that the water flow is rather homogeneous across entire inlets' cross-sections with weak horizontal and vertical shears (Figs. 2 a, b, c and d). Subsequently, for different locations on transects the linear regression between the total water flow rate and the vertically averaged current was calculated. The linear relationship between the two variables very well approximates their interdependence, as illustrated from the scatter plot of the vertically averaged current speed and the total water flow rate for the transect in the Lido inlet and in Malamocco for locations where the ADCP's were subsequently installed (Fig. 3a and b). From the figure one can also see that the currents can reach up to 1.5 m/s with the corresponding flow rate of about 10.000 m^3/s (for a comparison Po, the biggest Adriatic river has an average discharge rate of 1500 m^3/s reaching only exceptionally a value of 11.000 m^3/s).

The fixed current records initiated 17 June, 2001 at selected locations (Fig. 1). The vertical resolution has been set to 1 meter and the current speed and direction have been recorded every 10 minutes as an average of 60 pings. The first successful instrument and data recovery took place 30 July 2001 and here we present some preliminary results on current pattern and variability in two inlets (Lido and Malamocco) from these first data sets. The prevalent variability in current field is, as expected,

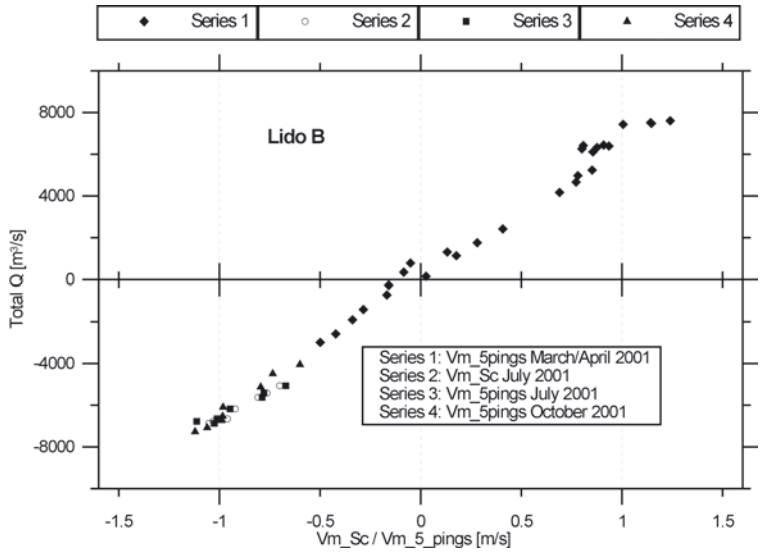

Fig. 3a. - Scatter plot of the vertically averaged current-speed along a water column of the unit width versus the inlet flow rate as obtained with a ship-borne ADCP measurements in Lido. Positive values of the current component along the inlet axis stay for the water outflow.

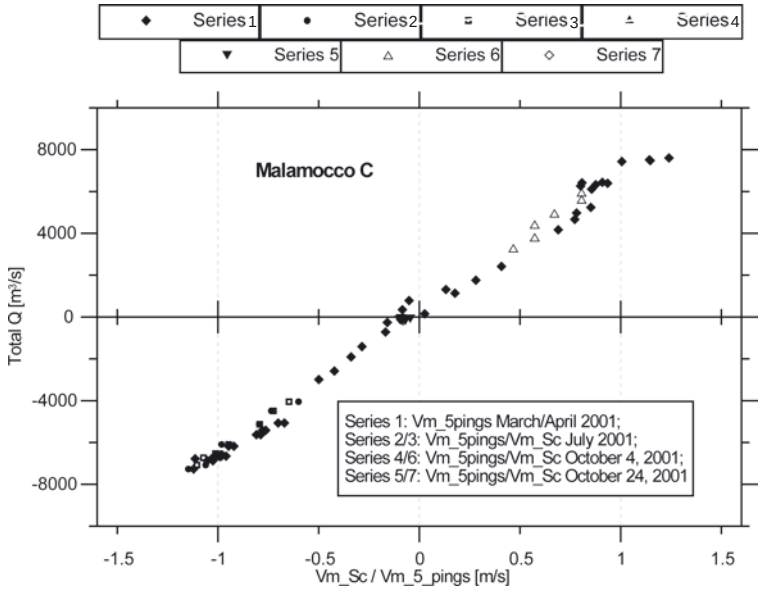

Fig. 3b. - The same as in Fig. 3a, but for the inlet of Malamocco.

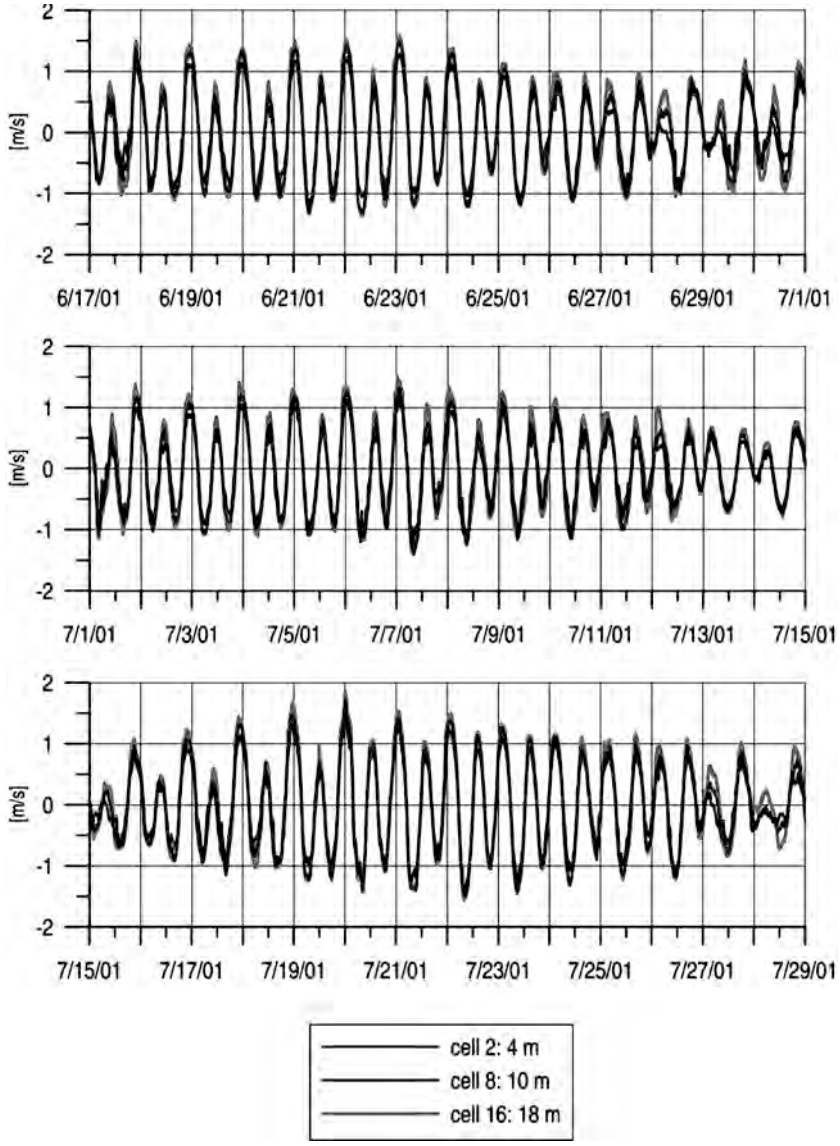

Fig. 4 - Time-series of the current component along the Malamocco inlet axis for several ADCP cells. Cell number together with its nominal distance from the sea floor (in meters) is denoted in the legend.

Tab. 1.- Ellipse parameters from the harmonic analysis of current data (at six meters from the bottom) in two inlets of the Lagoon of Venice. The letter "M" indicates the magnitude of the major axis, while "m" indicates the minor one, "inc" is the orientation of the major axis, "ph" indicates phase with respect to the inflowing current component. The letter "e" before each variable name refers to the error.

Site	const	period (h)	M (mm/s)	eM (mm/s)	m (mm/s)	em (mm/s)	inc (°)	einc (°)	ph (°)	eph (°)
Lido	K1	23.93	312	32	-7	8	-5	1	0	5
	M2	12.42	707	36	0	13	-8	1	- 141	2
Malomocco	K1	23.93	295	23	-19	16	-15	3	-8	5
	M2	12.42	702	25	-5	16 I	-18	1	- 155	2

Tab. 2. - Amplitude ("amp") and phase ("ph") from the harmonic analysis of sea surface elevations (SSE) at the two inlets of the Lagoon of Venice. The letter "e" before each variable name refers to the error.

Site	const	amp (m)	eamp (m)	ph (°)	eph (°)
Lido	K1	0.189	0.022	62	7
	M2	0.249	0.009	263	2
Malamocco	K1	0.189	0.021	62	6
	M2	0.248	0.008	262	2

associated with a tidal signal (Fig. 4), and the polarization of current oscillations is mainly along inlet axes. The oscillations are barotropic and no net residual flow can be evidenced from the visual inspection of the data.

Harmonic analysis was applied to the ADCP data and information on tidal parameters of the seven most important tidal components was obtained. The largest amplitude shows a semidiurnal M2 component (the major ellipse axis at Lido and Malamocco is about 70 cm/s). The second strongest tidal component is the diurnal K1 which represents less than one half of the M2 amplitude. Minor axes of all the components are of the order of errors and thus tidal currents appear perfectly polarized. The phase-difference between the two inlets for M2 component shows that the semi-diurnal tidal oscillations at Malamocco lead those at Lido by 29 minutes (Tab. 3). This is opposite to the phase-lag obtained

Tab. 3. - Phase differences ("phd") between Malamocco and Lido, for SSE and currents. The letter "e" before each variable name refers to the error. Negative sign means that Malamocco leads Lido.

	const	**phd** (°)	**ephd** (°)	**phd** (**hh:mm**)
Current	K1	-8	7	-00:32
	M2	-14	3	-00:29
SSE	K1	0	9	00:00
	M2	-1	3	-00:02

from the sea level measurements as well as from numerical modeling results since the overall features of the semi-diurnal tidal wave in the Adriatic Sea were explained in terms of progressive Kelvin waves (Mosetti, 1986). Our results in fact show that the tidal currents in the lagoon inlets are controlled by local along-inlet sea-level differences which on their turn are determined by the geometry of the inlet itself. In fact, the geometry of the lagoon in the area of Lido inlet is complicated and blocks the tidal exchange causing the tidal oscillations in Lido lagging those in Malamocco. Moreover, lagoon geometry near the Malamocco inlet is characterized by a channel which extends as a continuation of the inlet axis and facilitates the current response to the sea-level slope. The most energetic diurnal component (K1) shows the absolute value of the phase-lag between Lido and Malamocco of 32 minutes, and also in this case the phase-lag has the opposite sign of what one would expect from the explanation of dynamics of the diurnal component in the Adriatic Sea in terms of topographic waves progressing crosswise from the eastern to the western coast (Malacic et al., 2000).

Since we have had sea level data available for both inlets and for the entire current measurement period, the phase-lag between various tidal components in sea-level and in current-field was also calculated (Tab. 4). In the most energetic diurnal component K1 currents lead the sea-level by about 60° in both inlets, i.e. the maximum inflowing currents occurs about 4 hours before the sea-level maximum. At the frequency of the most energetic semi-diurnal component (M2), currents lead the sea-level for the phase-lag of about 50° or in absolute terms for about two hours. This differs appreciably from the expected phase-lag of 90° but this is probably due to the complicated bathymetry of the lagoon interior.

Table 4. Phase differences ("phd") between the SSE and inflowing current at two locations. The letter "e" before each variable name refers to the error. Positive sign means that inflow leads SSE.

Site	**const**	**phd** (°)	**ephd** (°)	**phd** (hh:mm)
Lido	K1	62	9	04:06
	M2	44	3	01:30
Malamocco	K1	70	8	04:42
	M2	57	3	02:00

From the current meter data it is also shown that the variability at tidal frequencies explains almost entirely the flow variance through inlets (about 97% of the total variance was shown to be related to the tidal oscillations). It is, however, important to mention that during the measurement period which was a summer season, the wind variations are characterized by a sea-breeze diurnal cycle. Therefore, diurnal flow variability in addition to tides, can be contaminated by the wind, but it is quite impossible to separate a wind-induced daily signal from the diurnal tide. An estimate of a possible wind contribution can be obtained only by comparing summer and winter current variance at the diurnal frequency, since the sea-breeze wind-regime occurs only during the summer-season.

3. *Conclusions.*

The presented preliminary data analysis reveals that the tidally-induced flow generates a total average water exchange rate per cycle through all three lagoon inlets on the order of 10.000 m^3/s. Comparing this value with the total volume of the lagoon of about $5{,}5\times10^8$ m^3, one obtains the residence time on the order of a day. This means that the lagoon is rather well ventilated and quickly flushed by the tidally induced flow. Although we analyzed a relatively short data record, this preliminary results revealed that the lagoon water flow variability is mainly controlled by tides. Surprisingly, the wind and run-off contributions seem negligible. However, the complete two-year measurement program will provide a more complete insight into the functioning of the system Venice Lagoon – Northern Adriatic. Furthermore, the wind and freshwater run-

off contributions to the lagoon - open sea exchange will be better assessed by having available data from different seasons, especially from autumn and winter when these two forcing functions are at their maximum. Additionally, a detailed analysis of the water flow through inlets in situations characterized by "acqua alta" events will give the flushing pattern of the lagoon in these extreme conditions.

Acknowledgement.

I. Mancero Mosquera has participated in the research with the support of the "Programme for Training and Research in Italian Laboratories" of the Abdus Salam International Centre for Theoretical Physics, Trieste. C. Fragiacomo helped with the satellite image preparation.

References.

Malacic V., Viezzoli D. and Cushman-Roisin B., 2000: Tidal dynamics in the northern Adriatic Sea. Journal of Geophysical Research, 105, 26265-26280.

Mosetti R., 1986: Determination of the current structure of the M2 tidal component in the northern Adriatic by applying the rotary analysis to the Taylor problem. Bollettino di Oceanologia Teorica ed Applicata, 4, 165-172.

Tosi L., Carbognin L., Teatini P., Strozzi T. and Wegmueler U., 2002: Evidence of the present relative land stability of Venice, Italy, from land, sea, and space observations, Geophys. Res. Lett., Vol. 29, No. 12, June, 2002.

Umgiesser G., 2000: Modeling residual currents in the Venice Lagoon. In: *Interactions between Estuaries, Coastal Seas and Shelf Seas,* Ed. T. Yanagi, Terrapub, Tokyo, 107-124.

MODELING THE WATER EXCHANGES BETWEEN THE VENICE LAGOON AND THE ADRIATIC SEA

A. Cucco, G. Umgiesser
Istituto per lo Studio della Dinamica delle Grandi Masse, CNR, Venezia

1. *Introduction.*

The Lagoon of Venice is a complex and unique environment both for the ecological aspects and for its hydrodynamics. In the last decades owing to the improvement in the frequency of the flooding events more research has been focused to protect the historical city from the invasion of the high water.

To understand the dynamic of spreading of water in the lagoon area, it is necessary to analyse the hydrodynamic behaviour of the three inlets of Lido, Malamocco and Chioggia that connect the lagoon with the open sea. With this aim an interdisciplinary project based on empirical measurements and on modeling studies has been carried out. This paper is concerned with the modeling aspect of the project and has the aim of analysing the exchanges of water between the sea and the lagoon through the three inlets.

Up to now only few numerical modeling studies have been carried out to estimate the water exchange rates through the three inlets and its time dependent variability (Umgiesser, 2000). The results obtained from these analysis have never been validated with detailed experimental data.

In this work a 2D hydrodynamic model has been calibrated and validated with experimental elevation tide and flow rates data measured by tide gauges and bottom-mounted Acoustic Doppler Current Profilers (ADCP) installed inside the three Venice Lagoon inlets. This allows for the analysis of different circulation patterns inside the three inlets caused by various forcing scenarios.

This work is therefore able to contribute to the open question of how the exchange rates through the lagoon inlets vary under different meteorological conditions. This is insofar important because the answer to this question will help to better understand the equilibrium in the lagoon both in terms of hydrodynamics and ecology.

2. *The hydrodynamic model.*

In this application, an unified hydrodynamic model of the Venice Lagoon and of the Adriatic Sea, based on the finite element method, has been used (Umgiesser & Bergamasco, 1993; Umgiesser & Bergamasco 1995). This approach is totally justified by the necessity to investigate the dynamic of the water exchanges between the Adriatic Sea and the Venice Lagoon.

The hydrodynamic model used is a two-dimensional finite element model. The finite element method gives the possibility to follow the morphology and the bathymetry of the area and to represent with higher resolution the zones where hydrodynamic activity is more important. The numerical computation has been carried out on a spatial domain that represents the entire Venice lagoon and the Adriatic Sea through a finite element grid.

The grid contains 10948 nodes and 20013 triangular elements (figure 1, 2). The bathymetric data necessary for the hydrodynamic model have been provided by CORILA.

The model considers as open boundaries the channel of Otranto, elsewhere as closed boundary the whole perimeter of the Adriatic Sea and the Venice lagoon.

The model uses finite elements for spatial integration and a semi-implicit algorithm for integration in time. The terms treated implicitly are the water levels and the friction term in the momentum equation and the divergence term in the continuity equation, all other terms are treated explicitly. The model resolves the vertically integrated shallow water equations in their formulations with levels and transports:

$$\frac{\partial U}{\partial t} - fV + gH\frac{\partial \zeta}{\partial x} + RV + X = 0$$

$$\frac{\partial V}{\partial t} + fU + gH\frac{\partial \zeta}{\partial y} + RU + Y = 0$$

$$\frac{\partial \zeta}{\partial t} + \frac{\partial U}{\partial x} + \frac{\partial V}{\partial y} = 0$$

where ς is the water level, U and V the vertically-integrated velocities (total or barotropic transports), g is the gravitational acceleration, $H=h+\varsigma$ the total water depth, h the undisturbed water depth, t the time and R the friction coefficient. The terms X and Y contain all other terms like the

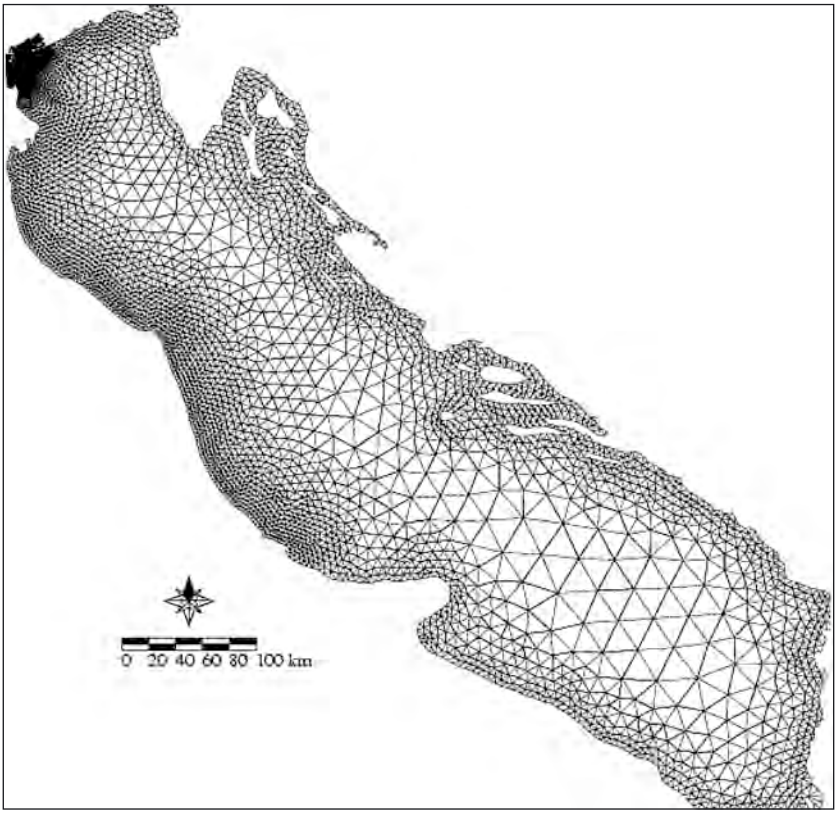

Fig. 1 - Grid of the Adriatic Sea and the Venice Lagoon. The model consists of 10948 nodes and 20013 elements.

wind stress, the nonlinear terms and those that need not to be treated implicitly in the time discretization.

At the open boundaries the water levels are prescribed while at the closed boundaries only the normal velocity is set to zero and the tangential velocity is a free parameter. This correspond to a full slip condition.

3. *Results.*

3.1 *Water level calibration.*

All simulations presented in this work have been carried out using a time step of 300 seconds. This time step could be achieved due to the

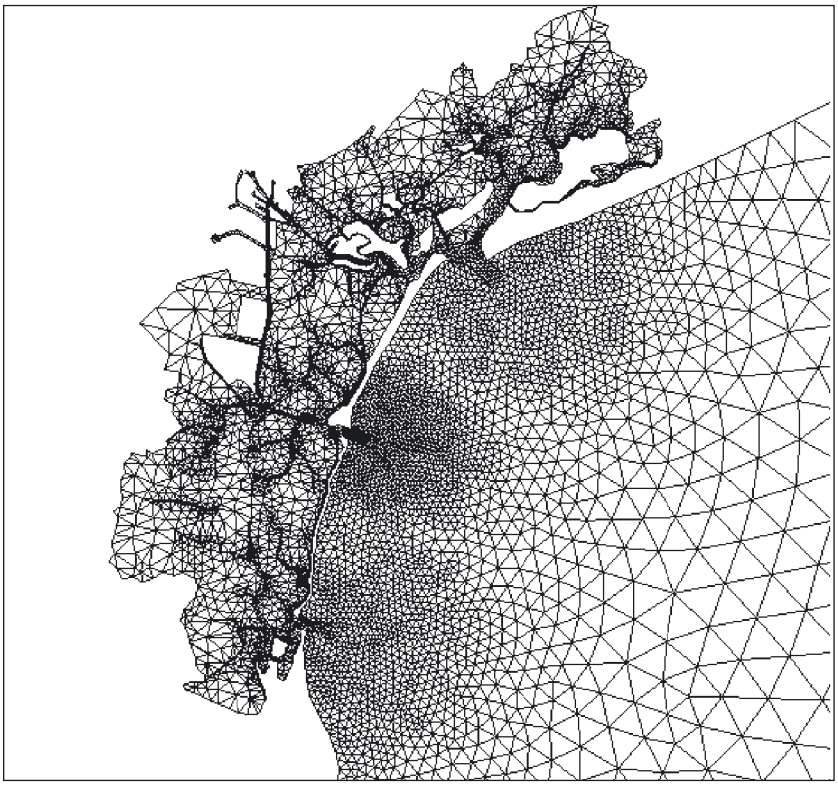

Fig. 2 - Zoom for the Venice Lagoon area.

unconditionally stable scheme of the finite element model. At the open boundary of Otranto the water level has been imposed.

A spin up time of 15 days has been always used for the simulations. This time was enough to damp out all the noise that has been introduced through the initial conditions.

As forcing the tide and the wind have been prescribed. The most important tidal constituents are M2, S2, K1, N2, K2, O1 and P1. In this work a tide with all of the principal constituents has been considered.

For the wind forcing, two typical wind regimes have been taken into account. The first is the bora, a strong wind from the north-east, the other is the scirocco, a south-easterly wind. These winds have been chosen to be spatially constant over the Adriatic sea and the lagoon, with a wind speed of 10 m/s for the bora and 5 m/s for the scirocco. A simple drag laws has

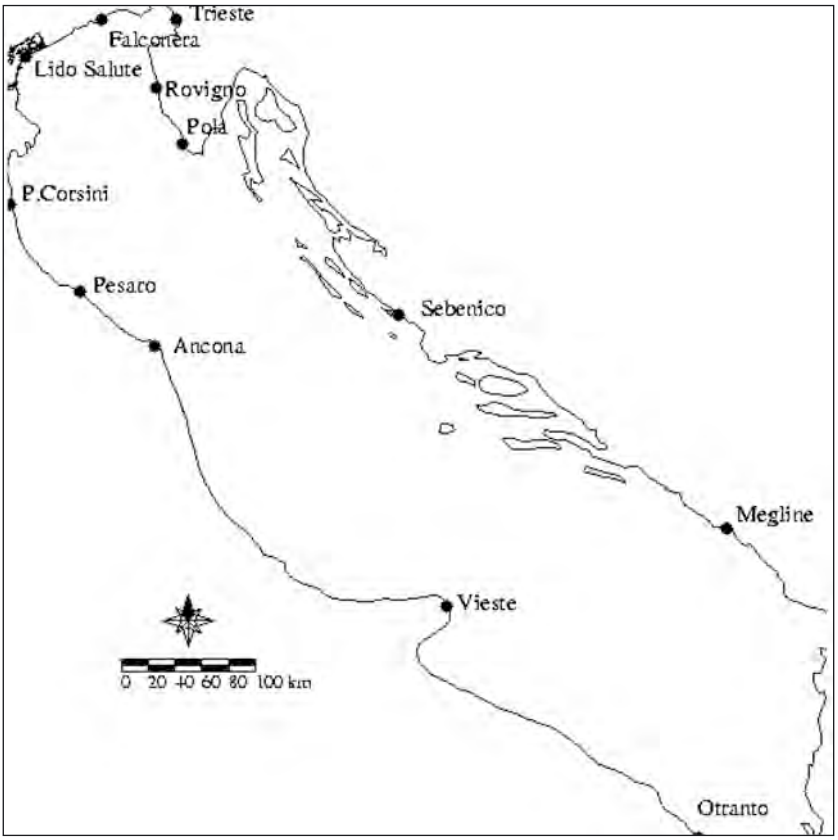

Fig. 3 - Location of the tide gauges used to calibrate the model.

been used for the wind stress with a drag coefficient of C_D=2.5×10^{-3}. Other types of forcing have been neglected. Especially the river runoff is not taken into account.

The model has been calibrated using the sea level data measured by 13 tide gauges located along the coast of the Adriatic sea and inside the lagoon (figure 3). All the simulation presented in this section have been extended to one full year (2001). The tidal forcing prescribed at the open boundary has been modified during this phase. A series of calibrations have been carried out. During the calibration the harmonic constants at Otranto are varied until a satisfactory result for the Lido inlet close to the Venice Lagoon has been found.

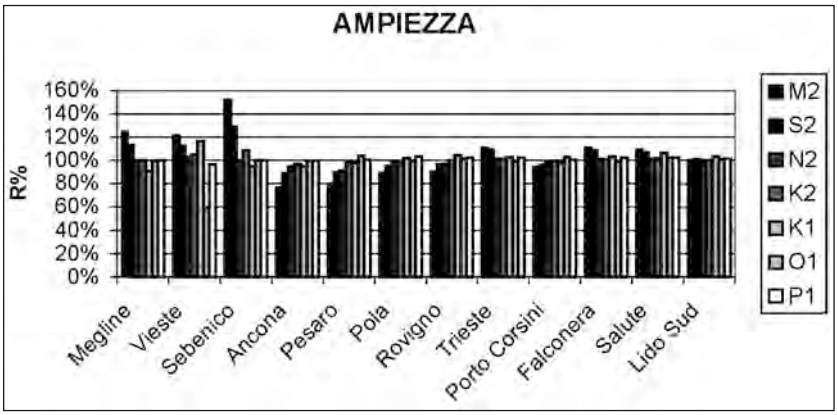

Fig. 4 - Relative ratio between modeled and measured amplitude of the harmonic components along the Adriatic Sea.

The calibrated model reproduces faithfully the tidal oscillation in most part of the northern and central Adriatic sea and inside the Venice Lagoon (figure 4). The southern areas, being close to the Otranto channel, are influenced by the imposed parametrization. In any case in the zones far from the open boundary the circulation is more easily reproducible. In fact, close to the inlets of Venice Lagoon, the harmonic costants are reproduced with an accuracy of 98.7%.

3.2 *Flux data validation.*

Once the model has been calibrated with the water levels, it has been applied to estimate the exchanges through the three inlets. Results obtained have been compared with empirical data measured by ADCP probes installed inside Lido and Malamocco inlet. In the following the first preliminary results of the comparison between numerical and experimental data are reported.

A bottom-mounted ADCP mooring has been installed in each inlet of the Venice Lagoon. The aim of these measurements is to study time-dependent variability of inlet currents as well as of water exchange rates. Once chosen the most representative ADCP locations in each inlets, the data collection get started. From 17th June 2001 current speed and direction have been recorded every 10 minutes inside Lido and Malamocco inlet. At Chioggia the measurements started from 8th May 2002. The flow rates have been calculated through linear regression from the vertically integrated measured currents. (For more information see Ga_i_ et

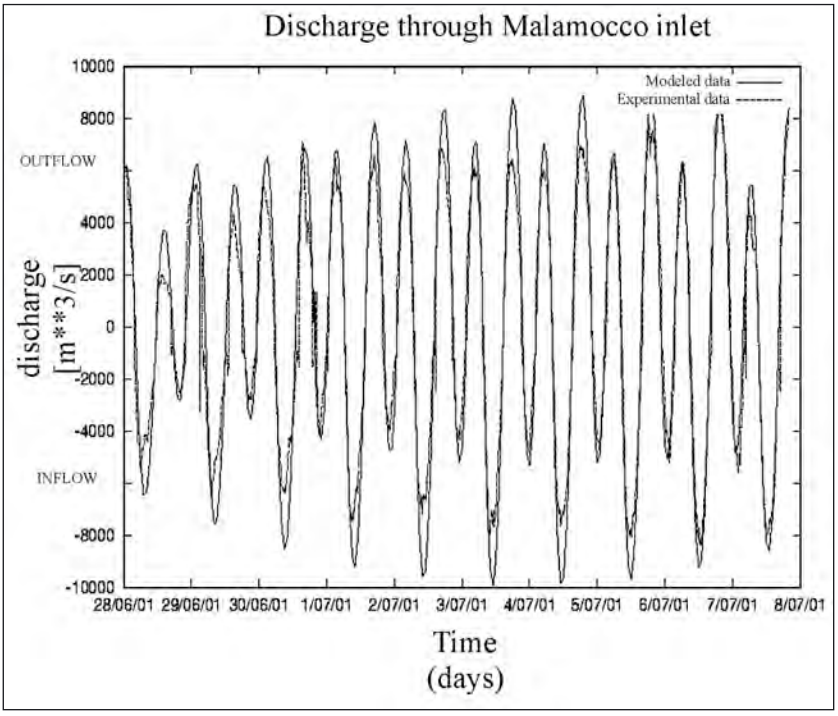

Fig. 5 - Discharge through Malamocco inlet computed by the model and measured with bottom mounted ADCP probe. The time series is extend to 10 days summer period.

al., 2002). These experimental data have been used to validate the discharge rates obtained from numerical simulations.

A preliminary analysis has been carried out considering ADCP data collected at Lido and Malamocco during June - July 2001. This data set, being collected during the summer period, is to be considered without strong signals caused by wind or pressure forcing. From the harmonic analysis of the discharge time series was found that the signal is entirely due to the principal tide components less than a residual of about 2% of total amplitude. Tidal currents inside Lido and Malamocco inlets have been investigated with a simulation that comprises the 8 first months of 2001. No meteorological forcing has been imposed on the model, only the tide forces the basin. The computed discharge through Malamocco and Lido inlets has been considered.

In figure 5 the measured and modeled discharge rates trough Malamocco inlet are plotted. The time series start from 28 June 2001 and

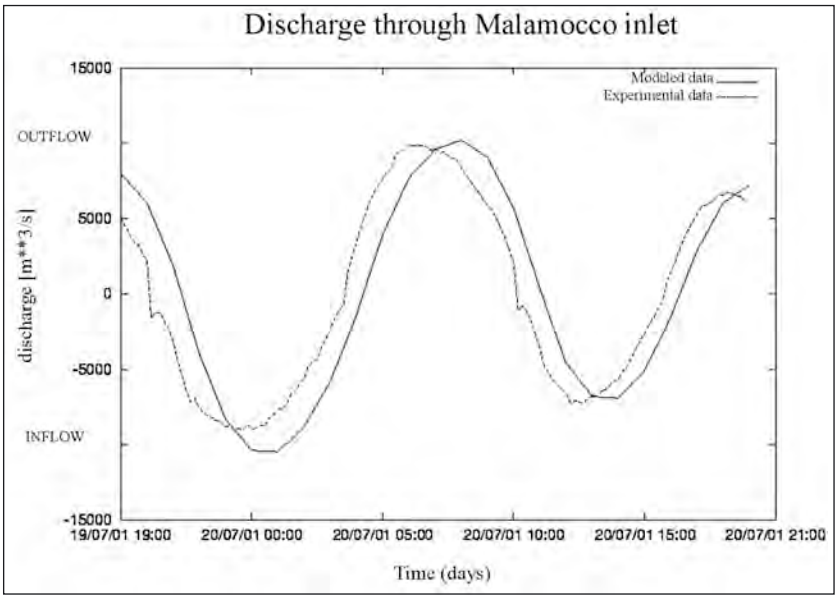

Fig. 6 - Discharge through Malamocco inlet computed by the model and measured with bottom mounted ADCP probe from 7 P.M.. 19th to 8 P.M. 20th July 2001.

extend to 8 July 2001. As we can see the modeled results overestimates the intensity of the measured discharge in all the cases. What concerns the Lido the average computed discharge is about 18% greater than the real data. At Malamocco analogous difference have been detected: about 17% of the measured value.

Also the phase of the two signals presents some difference. In figure 6 one day discharge time series has been plotted for Malamocco inlet. Both for Malamocco that Lido, there is a delay of about one hour of the computed fluxes with respect to the measured one.

To better understand the main difference between the modeled and the experimental data set, a spectral analysis and a frequency phase determination of the signals have been carried out. In figure 7 the amplitude spectrum of the modeled and experimental data is reported for Malamocco. It is to be noticed immediately the presence of two peaks corresponding to the main diurnal and semidiurnal frequencies which are related to the principal tide components (K1, M2 and S2). The main difference between the modeled and the real data is related to the overestimation of the semidiurnal frequencies amplitude, with a difference of 26% for Malamocco and of 24% for Lido with respect to the measured amplitude.

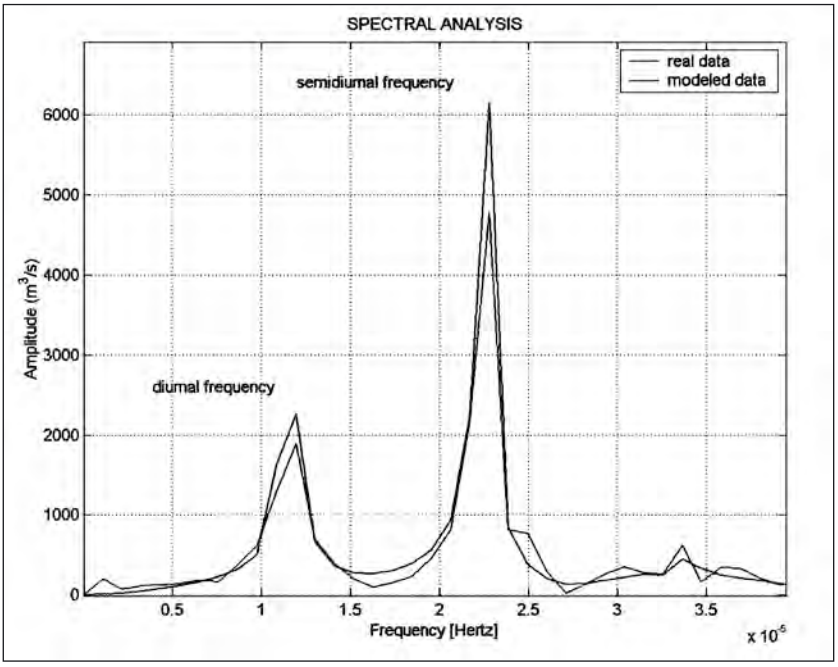

Fig. 7 - Amplitude spectrum of the modeled and measured discharge time series for Malamocco inlet.

As well as the amplitude the phase signal differs in the two cases both for Malamocco that for Lido. To estimate the delay between the modeled and the real data, the phase shift of the frequency spectrum has been calculated. For Lido the average phase shift of the peaks frequency band is 29° for semidiurnal and 12° for diurnal components. This corresponds to a delay of the modeled data respect to the real one of 57 minutes for semidiurnal and of 55 minutes for diurnal components. Analogous results have been detected for Malamocco with average phase shift of 27° for semidiurnal and of 18° for diurnal frequency band, corresponding to delay of 53 minutes and 1hour and 03 minutes.

The one hour delay of the modeled data signal with respect to the real one is to be related to the tidal wave propagation simulated by the model. In fact the model being calibrated using harmonic analysis methods, presents some uncertainty given by an average approximation valued at the 8%. This difference causes an erroneous estimation of the tidal wave signal both for what concerns the amplitudes and the phase of the single components. In figure 8 a one day water level time series computed by the model

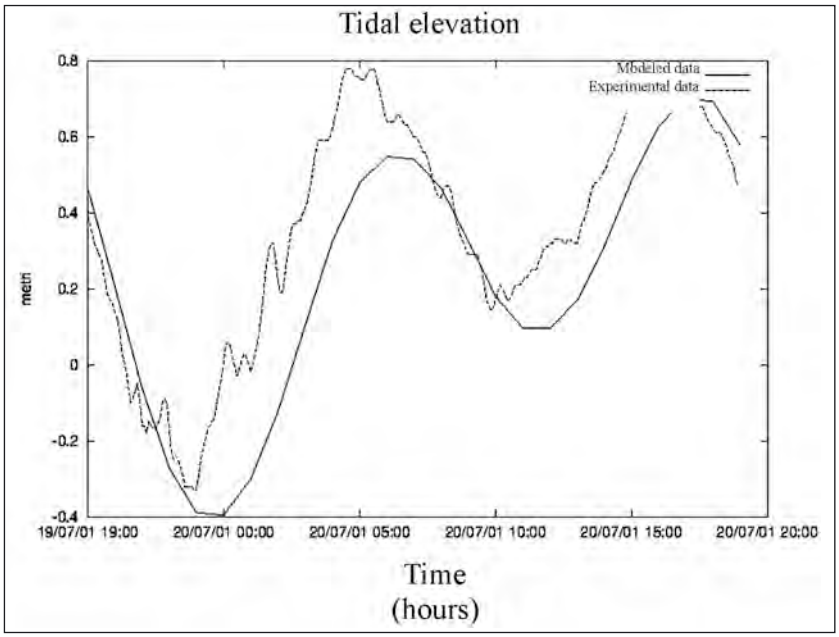

Fig. 8 - Water level elevation at Malamocco inlet computed by the model and measured with tide gauge for 24 hours period.

and one measured with tide gauge outside Malamocco inlet is plotted to show the phase shift and amplitude error that has been encountered.

3.3 Instantaneous and residual circulation.

The circulation of water inside the Venice lagoon and through the three inlets of Lido, Malamocco and Chioggia has been analysed. The instantaneous and residual circulation are described. Three idealised cases have been studied. First we consider one year simulation with only tidal forcing prescribed at the open boundary, second we consider as forcing the wind acting on the sea surface too. The residual circulation has always been described by Umgiesser (2000), but in this case the numerical domain comprised only the lagoon without the Adriatic Sea. It was not particularly adequate to describe the fluxes through the inlets.

No wind case.

In the first case only the tide forces the model. No wind has been prescribed. The results are presented after the system has reached a dynamic steady state.

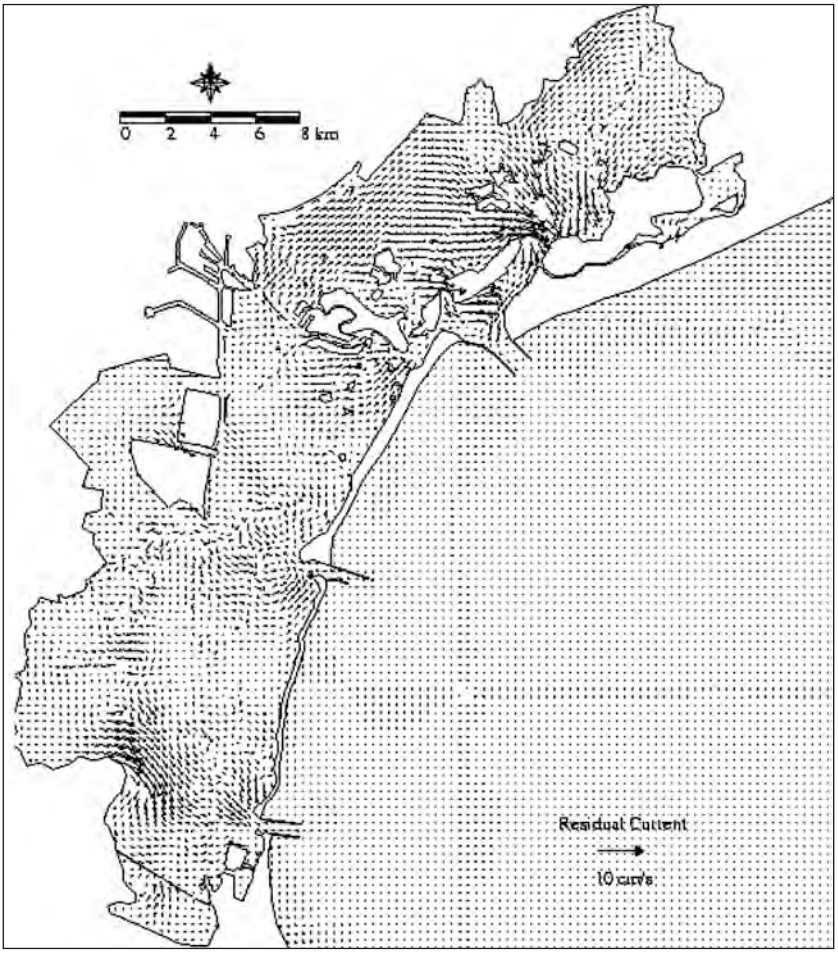

Fig. 9 - Residual currents for a complete tide and no wind forcing.

The tidal level at the three inlets is the same, no different tidal elevation or phase shift results from the simulation. During a typical spring tide the tide oscillates between $\pm$ 0.52 m.

The tidal forcing the lagoon is subjected to generate instantaneous currents that are almost periodic during a tidal cycle. In the case of the three inlets these fluctuating currents reach different values inside the channels. Higher currents have been observed at Malamocco with maximum value of 100 cm/s while lower values have been measured inside the other two inlets with peak velocities of 90 cm/s and 73 cm/s respectively at Lido and Chioggia.

Water flows through Malamocco and Lido inlet with higher velocity during the ebb than during the flood cycle. No asymmetric behaviour of current velocity between flood and ebb tidal cycle has been observed at Chioggia.

Filtering out the fluctuating part of the tidal currents the residual currents can be obtained (figure 9). In the case of no wind, residual currents of 10 cm/s have been computed close to the Lido inlet. Inside the inlet the intensity of these currents is weak, generally less then 5 cm/s.

In figure 10 the computed discharge through horizontal sections displaced inside the three inlets has been plotted. As it can be seen, the two most important inlets are Malamocco and Lido, with maximum discharge values of 10718 m^3/s and 10051 m^3/s. Chioggia only carries maximum values of 5638 m^3/s. Moreover, the Malamocco inlet is connected to the central part of the lagoon through the Petroli channel. The average depth of this straight channel is about 14 m and the reduced friction in this channel makes it possible that there is actually entering more water through Malamocco than through Lido even if the Lido basin is the largest one.

The averaged discharge values computed during a one month simulation has been analysed. The entity of discharge rates obtained are gene-

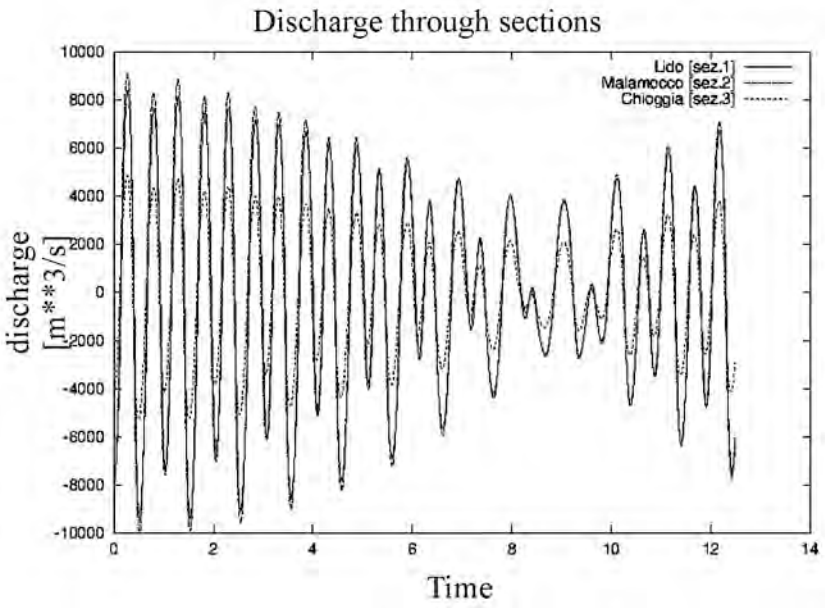

Fig. 10 - Discharge through the three inlets for 12 days simulation. The figure shows high values of computed discharge during spring tide (initial period).

rally smaller than the instantaneous discharges. The values are about 60 m^3/s for Lido and Chioggia, 0.2% of the maximum instantaneous discharge observed at Malamocco, and about 30 m^3/s for Malamocco.

Scirocco wind case.

In a second simulation the entire basin has been forced both with the tide and scirocco wind.

The presence of wind as forcing changes considerably the circulation pattern of the lagoon and the dynamics of the water exchanges with the Adriatic Sea.

During a scirocco wind of 5 m/s, the average sea level computed at the three inlets shows a set up of 0.10 m on the medium sea level. The tide arrives simultaneously at the three inlets and no different elevation values have been observed.

The wind acting on the surface increases the intensity of instantaneous currents inside the three inlets and in the lagoon. Maximum values of about 120 cm/s have been observed at Malamocco. At Chioggia the peak velocity registered has reached 108 cm/s while inside Lido inlet the maximum value of the current is about 100 cm/s. Scirocco wind drives water toward North-Northwest direction enhancing the current entering from Chioggia inlet and reducing that entering from Lido and Malamocco. Otherwise during ebb tide water flows with higher values through Malamocco and Lido inlet than through Chioggia one.

No main difference with the previous case has been observed about maximum instantaneous discharge intensity. Peak values of 10280, 10797 and 5122 m^3/s have been registered at Malamocco, Lido and Chioggia.

The action of wind changes radically the residual circulation pattern (figure 11). Scirocco wind pushing water northward gives rise to residual velocity of 15 cm/s at Chioggia and in the southern areas of the lagoon. Lower values have been computed in the northern areas and inside Malamocco and Lido inlet. This vigorous circulation enhances the average discharge intensity at the three inlets. Water inflows mainly through Chioggia with a residual flow of 740 m^3/s and outflows through Lido and Malamocco with values of 500 and 240 m^3/s.

Bora wind case.

Finally the effects of bora wind on tidal circulation has been taken into account.

At the three inlets water levels ranges from + 0.55 m to – 0.49 m on

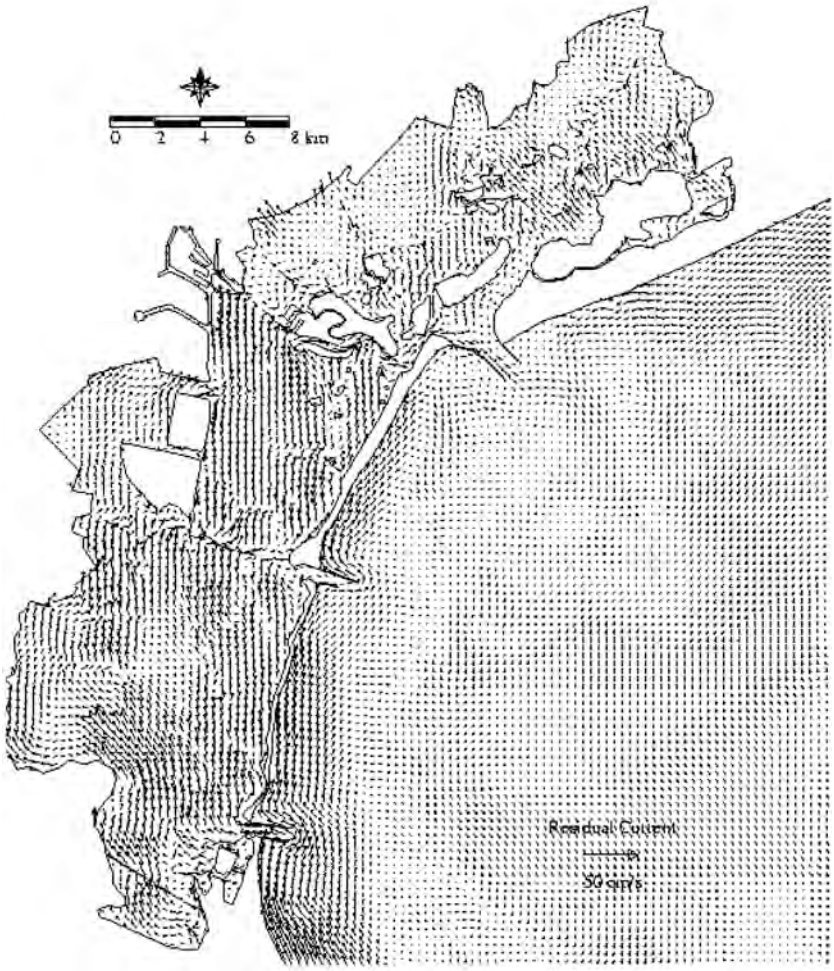

Fig. 11 - Residual currents for a complete tide and scirocco wind (5).

the medium sea level. Because of the wind effect the average sea level is higher in the southern part than in the northern part of the lagoon.

During this numerical experiment the wind direction coincides closely with the major axis of the Venice Lagoon, further enhancing the total flow. Currents velocity of up 125 cm/s have been observed at Chioggia. At Lido and Malamocco lower values of peak velocity have been registered, respectively 93 cm/s and 112 cm/s. These top velocities gives rise to

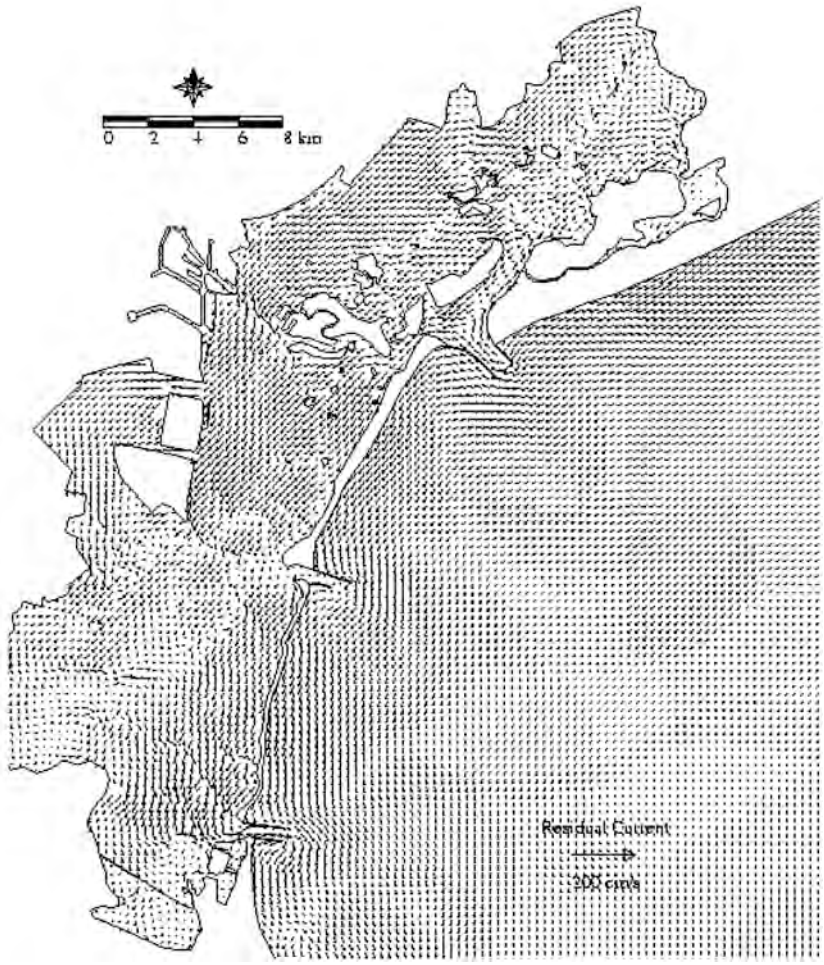

Fig. 12 - Residual currents for a complete tide and bora wind (10).

maximum discharge values of 6782 m^3/s at Chioggia, 9903 m^3/s at Lido and 10223 m^3/s at Malamocco inlets.

The residual circulation driven by bora wind is quite different with respect to the previous two conditions (figure 12). Water flows through Lido inlet (2140 m^3/s of average discharge) with maximum residual current values observed of 30 cm/s and flows out mainly through Chioggia inlet (1900 m^3/s) and to a minor extent through Malamocco inlet (240 m^3/s).

4. *Conclusions.*

In this works the water flow rates through the three inlets of the Venice Lagoon have been investigated using an hydrodynamic model. The model has been calibrated and validated comparing the water levels and the discharge rates, computed with the numerical analysis, with empirical data measured by tide gauges and ADCP probes.

From the results obtained it is clear that a better calibration of the model is need. The phase shift can be compensated by imposed different phase angles for the harmonic constant at Otranto. The amplitude can be better calibrated by changing the friction parameter at the inlets.

Once the model has been made operative, the current system inside the three inlets has been studied under varying external forcing: periodic tide and the wind acting on the surface.

Some typical situations have been simulated. One year real astronomical tide with different wind forcing has been run. The wind regimes were the situation of no wind, scirocco wind and bora wind. The results show the importance of meteorological forcing on enhancing the intensity of the peaks current velocity and on creating different sea level set up inside the three inlets.

Acknowledgements.

This work was carried out with the financial support of CORILA in the framework of the CORILA Project 3.1 and 3.2.

References.

Bergamasco A., Carniel S., Pastres R. and Pecenik, 1998. A unified Approach to the Modeling of the Venice Lagoon-Adriatic Sea Ecosystem. Estuarine Coastal and Shelf Science, 46,438-492.

Gacic M, Kovacevic A., Mazzoldi A., 2002. Measuring Water Exchange between the Venetian Lagoon and the Open Sea. EOS, number 20, volume 83.

Orlic M., Gacic M. e Le Violette P., 1992. The current and circulation of the Adriatic Sea, Oceanologica Acta, vol.15, n.2, pg.109-124.

Umgiesser G. & Bergamasco A., 1993. A staggered finite element model of the Venice Lagoon. In: K. Morgan, E. Ofiate, J. Periaux & Zienkiewicz, O. C. (eds), Finite Elements in Fluids. Pineridge Press.

Umgiesser G. & Bergamasco A., 1995. outline of a Primitive Equation Finite Element Model. Rapporto e Studi, vol. XII. Venice, Italy: Istituto Veneto di Scienze, Lettere ed Arti. Pages 291-320.

Umgiesser G., 2000. Modeling residual currents in the Venice Lagoon, in Interactions between Estuaries, Coastal Seas and Shelf Seas, pp. 107-124.

ANALYSIS OF THE CIRCULATION OF THE LAGOON OF VENICE UNDER SCIROCCO WIND CONDITIONS

D. Melaku Canu[1], G. Umgiesser[1], N. Bonato[2], M. Ferla[2]
[1]*Istituto per lo Studio della Dinamica delle Grandi Masse, CNR, Venezia*
[2]*Servizio Idrografico e Mareografico Nazionale, Venezia*

Abstract.

Data collected by 20 tide gauges located in the lagoon of Venice, were used to test the response of the finite element hydrodynamic model, SHYFEM, during no-wind periods. The calibrated model has then been applied to a high tide event, under Scirocco wind conditions. The results demonstrate the capability of SHYFEM to reproduce the tide levels at the sampled stations, during the no-wind periods. Also during Scirocco winds the reproduced tidal elevations are in good agreement with the measured ones, even if there are some differences during the peak values. These are probably due to the high uncertainty and variability of the experimental forcing conditions (such as wind gusts) at the inlets that are only partially caught by the measurements system.

Introduction.

The Lagoon of Venice is the largest Italian lagoon; it exchanges with the sea 385 million of cubic meter per day on average and receives, on average, 33 m^3/s of water from the drainage basin, through the main 9 rivers. The average depth is of 1 meter and the average residence time is of 10 days, increasing from the inlets to the main land border.

The lagoon is a transitional environment between land and water, it is an ecosystem where continually changing environments succeed one another from the mainland to the sea.

The lagoon in fact can also be divided up as follows: the open lagoon with 418.22 square km; the closed lagoon, with its 84.74 square km, the

banks which cover a surface area of 7.46 square km and the inner islands and reclaimed areas for 29.12 square km. The boundaries between each of the sub-environment are continually changing, due to the physical and human actions.

The analysis of those interacting actions is necessary to understand the actual trends and dynamics. And experimental investigations and analysis, besides models, such as the SHYFEM hydrodynamic model (Umgiesser & Bergamasco, 1993, Umgiesser, 1997), can be valuable tools in supporting both ecological and physical-morphological studies of the Lagoon of Venice.

The objective of this work is the analysis of the responses given by a hydrodynamic finite element model, SHYFEM, in the application to the Lagoon of Venice.

The analysis has been made in order to test the capability of the model to simulate both, no wind conditions and Scirocco wind conditions.

The comparison of the model results with experimental values, collected by the National Hydrographic and Mareographic Service – Venice Office, allows us to test the goodness of the model responses. After the calibration, the analysis of the circulation has been made comparing the no wind scenario with the Scirocco scenario. The comparison shows how the circulation pattern in the lagoon of Venice is sensitive to wind conditions.

1. *The Data.*

1.1 *The Tide gauge system managed by the SMI, the National Hydrographic and Mareographic Service – Venice Compartment Office.*

Tide level observations in the Lagoon of Venice have been systematically made since the 2nd half of the XIX century, mostly by the IGM (Geographic Military Institute).

Regularly measures were made after 1871, when the Genio Civile of Venice established the first reference tide gauge in the city, at Campo Santo Stefano. These observations were then used in 1910 to determine the 0 point sea level of Venice, by averaging the high and the low tide values measured from 1884 to 1909.

A second reference gauge was set up in Venice in 1906 at Punta della Salute, this gauge was then moored in 1923 at the location where it is still now. The Punta della Salute tide gauge is now the reference for the lagoon of Venice and for all the other Northern Adriatic lagoons and estuaries.

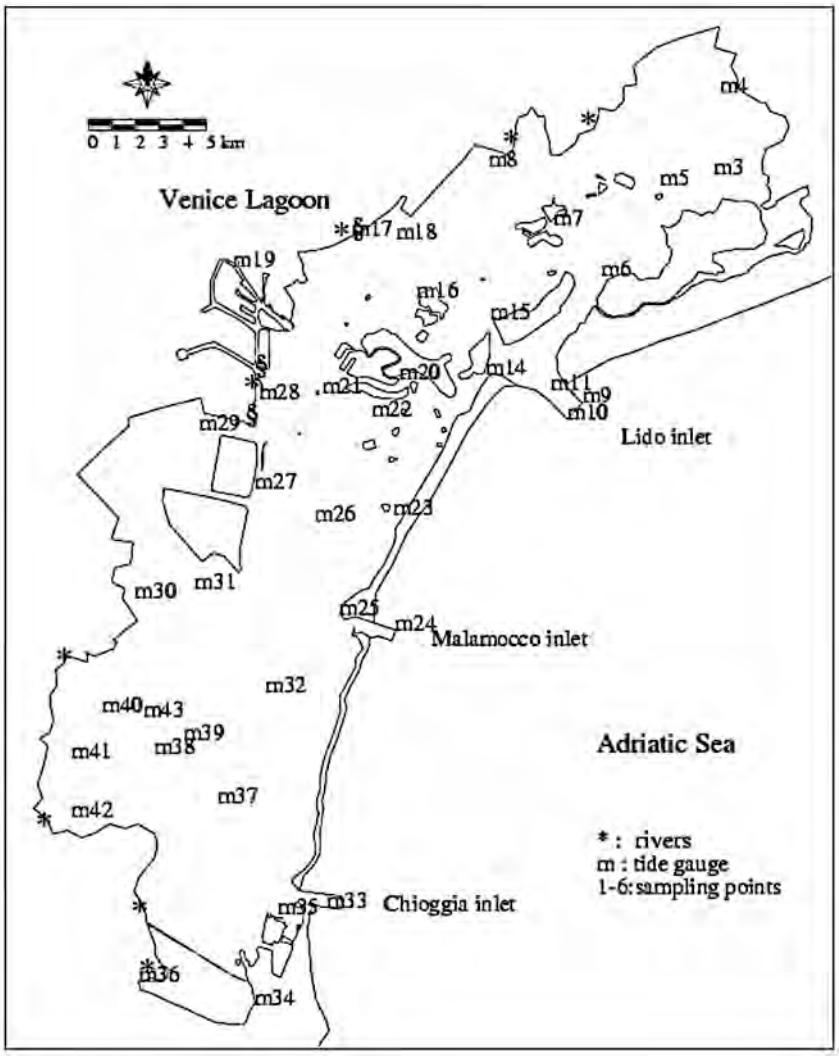

Fig. 1 - SMI tide gauge system in the Lagoon of Venice.

Actually the tide gauge system located in the city of Venice is one of the widest ever set up and it is a source of valuables scientific information on relevant issues such as mean tide level variations and for the safeguard of Venice from the high tides.

During the past decades several tide gauges have been set up in the lagoon of Venice and along the coast (Fig. 1). They are generally formed

by a concrete made rectangular plant cabin covered by two pitches. The concrete structure is sustained by a pole system sticked on the sea floor.

Actually the IMS office of Venice manages 54 stations, 7 of them are located outside the lagoon, and 6 of them also take meteorological parameters.

1.2. *Methodology of measurement.*

Close to some reference gauges, such as Punta Salute, Diga Sud Lido and Trieste, a datum point, determined by a high precision topographic survey done by SIMN, has been set up. Inside each cabin a small horizontal plate has been positioned. The height of the plate is either determined by the available datum point or, if a datum point is not available, by comparing the medium water level during neap tide with a tide gauge where a datum point is present. During these neap periods the water level can be considered to be nearly horizontal. For every station a complete history is archived that allows for the quality control of the data collected. Through this tide gauge records it is possible to evidence events that have influenced the re-calibration of the instrument and also other long term processes such as the variation of the bottom level (subsidence). Through this long history of records it was possible to validate long lasting time series with a very high level of precision and accuracy.

At this point it must be pointed out the difficulty that may involve the interpretation of the tidal time series close to the inlets during events of high water. Even if a certain amount of data exists both for the dikes at the inlets and along the Italian coast it is difficult to establish the exact water level variation during these events. In these cases the water level shows strong oscillations due to the presence of strong waves in the vicinity of the tide gauge, and the post processing not always can get rid of the strong random signal present in the recordings.

1.3. *Acquisition, elaboration and usage of the tidal data.*

The data observed at the tide and meteorological cabins that are run by SIMN (Venice) are needed for various other activities of this office. They are

- Diurnal forecasting of the tidal level
- Forecasting of high tides
- Statistical analysis of the tide data (maximum and minimum, harmonic constants…)
- Study of exceptional high water events
- Correlation studies between tide and meteorological parameters

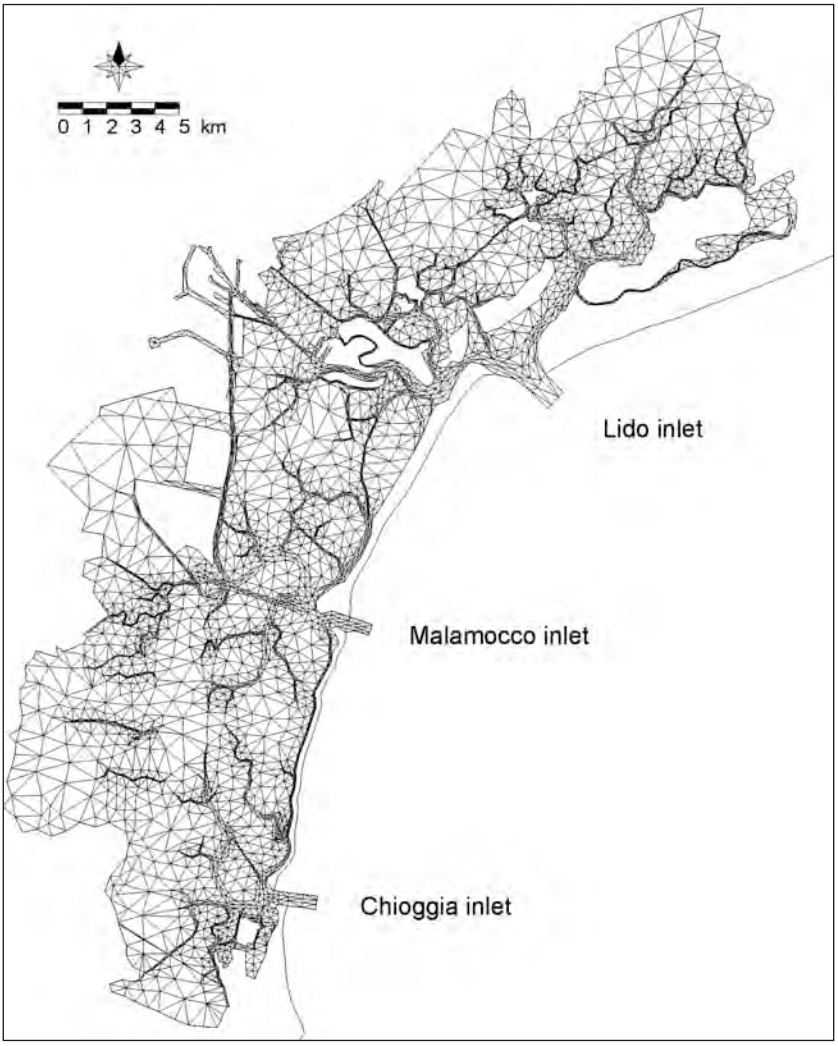

Fig. 2 - The model grid of the Venice Lagoon.

The tide gauges used for the observations are of the classical type, using a floating body placed inside a tube that is placed vertically in the water and is closed at the bottom. The tube has little holes on its side (diameter 2-3 cm) to allow the exchange of water between the tube and the surrounding environment, effectively damping the fast water level oscillation in the tube (wind waves). The old instruments were of mechanical

type, using a small pen for registering the water level on endless paper. These instruments are still used in some of the tide gauges, but have been slowly substituted by the electronic tide gauges with a floating sensor. These new instruments are often equipped with real time transmission of the data to the central office. The frequency of the data logging is set to one datum every 10 minutes.

The data collected is processed by a procedure, called MAREA, which has been developed by this office. The software can process data by digitalization of the paper records, data inserted directly through the keyboard and data read in from a file coming either from registered data on mass storage in the cabins or directly transmitted to the office through wireless communication. This procedure allows for an easy consultation, correction, validation and elaboration. Some of the more important applications are the selection of minimum and maximum values during the day, month and year, the selection of hourly values in a given period and the statistical presentation of data used by SIMN for the yearly determination of the high and low tidal values.

2. *The Hydrodynamic model SHYFEM.*

The hydrodynamic module solves the two dimensional barotropic shallow water equations using a semi-implicit algorithm. The spatial discretization of the equations is done on a triangular finite element grid (Fig. 2). These linear finite elements give enough flexibility to describe the complex geometry and bathymetry of the Venice Lagoon.

The model equations are:
where η is the water level, u,v the horizontal velocities in x and y direction, while U and V are the vertically-integrated velocities, g is the gravi-

$$\frac{\partial U}{\partial t} + u\frac{\partial U}{\partial x} + v\frac{\partial U}{\partial y} - fV + gH\frac{\partial \eta}{\partial x} + RU + X = 0 \qquad (1)$$

$$\frac{\partial V}{\partial t} + u\frac{\partial V}{\partial x} + v\frac{\partial V}{\partial y} + fU + gH\frac{\partial \eta}{\partial x} + RV + Y = 0 \qquad (2)$$

$$\frac{\partial \eta}{\partial t} + u\frac{\partial U}{\partial x} + v\frac{\partial V}{\partial y} = 0 \tag{3}$$

$$U = \int_{-h}^{\zeta} u dz \qquad V = \int_{-h}^{\zeta} v dz \tag{4}$$

tational acceleration, H=h+η the total water depth, h the undisturbed water depth, t is time and R is the friction coefficient. The terms X and Y include all other terms like the wind stress and the non-linear terms. Evaporation is assumed to equal the precipitation, and therefore they are not explicitly computed.

The wind stress uses a constant drag coefficient, and the friction coefficient is determined through the Strickler formula.

Water levels are described by linear form functions defined on the nodes (intersections) of the grid while the velocities are described by constant form functions over one element, which corresponds to the definition of the velocities on the centre of the elements.

The model also treats shallow water flats, subjected to dry and flooding periods. It takes the shallow water flats out of the algebraic system during the dry period and adds them again, once the surrounding water level is higher than the water inside the dry element. This specific implementation conserves the mass in each element.

3. *Results.*

3.1. *Comparison between simulated and measured levels.*

The hydrodynamic model has been used to simulate the hydrodynamic under no wind conditions (C1, November 1999 and C2, June 1992) and Scirocco wind condition (S1, November 2000). The model was forced using experimental tide levels at the inlets as shown in figures 3 and 4, and wind stress at the surface as shown in figure 5.

The simulated levels at the selected tide gauges are then compared with the experimental levels measured at the same stations. The comparisons of measured levels at stations 5 and 16 during the no-wind period of November 99 with the simulated levels -at the same stations- given by the simulation C1 is shown in figure 6. The simulated curves are in good agree-

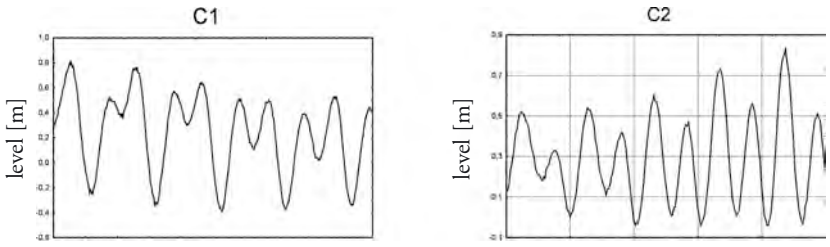

Fig. 3 - Physical forcings at inlets: levels at station m 10 for the no wind simulations C1 and C2.

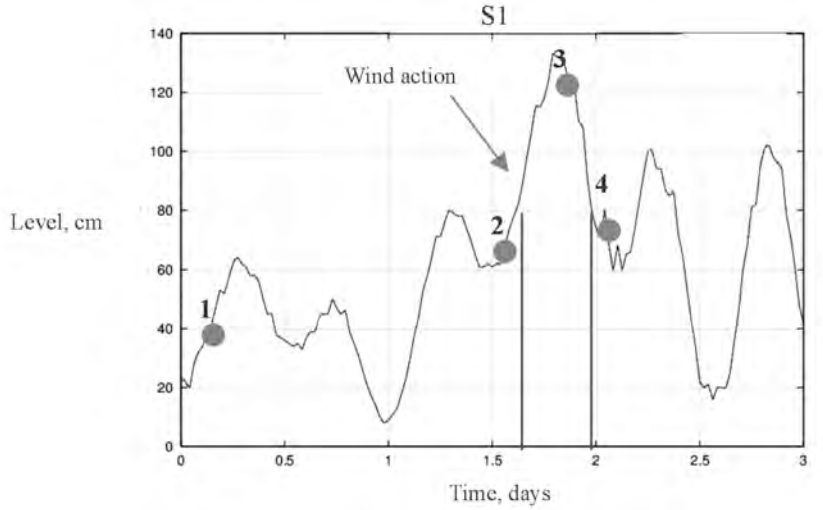

Fig. 4 - Physical forcings at inlets: levels at station m 10 for the Scirocco wind simulations S1.

ment with the experimental data, both in phase and in intensity. The same good results are obtained for the simulation C2 as shown in figure 7 by the comparison of simulated and measured values of June at stations 20 and 27.

For the Scirocco wind simulation of November 2000 we can see from Figure 8 that there are small differences between the simulated and observed values, in correspondence of the strong wind action. These differences at the peak level are probably due to the uncertainty in the registration and the high variability of the wind regime that is only partially measurable.

The comparison against measured data can be seen as a validation of the hydrodynamic model results. Therefore we can use the model to analyse the circulation of the lagoon with a rather good degree of confidence on the results obtained.

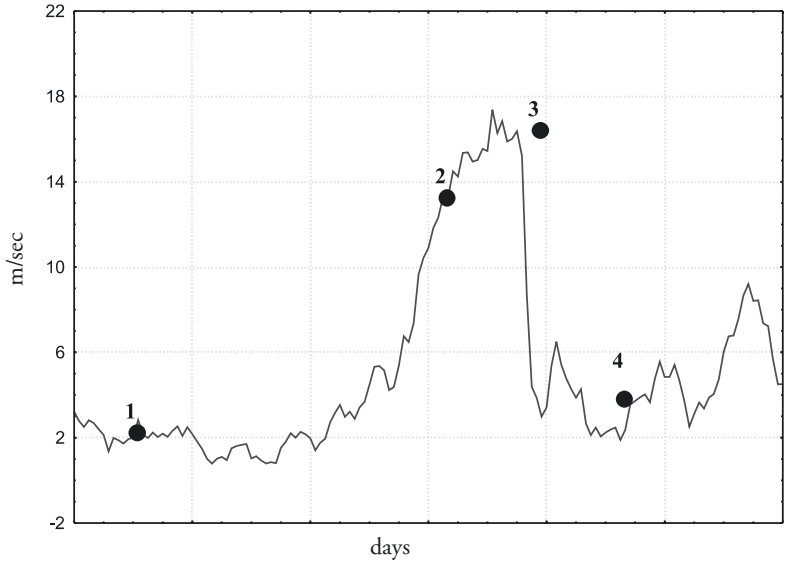

Fig. 5 - Recorded Scirocco wind speed used in the S1 simulation.

3.2. *Analysis of the circulation.*

Through the analysis of the spatial distribution of the water levels in the lagoon of Venice (fig. 9) we can observe the differences between the circulation patterns induced under the S1 and C1 conditions. For the C1 (no-wind) simulation we observe that the tide effect spreads from the inlets to the internal areas parallel to the Lido strips, with low differences along the North-South direction and slightly higher differences along the East-West direction.

The circulation pattern induced by the Scirocco wind action is more complex: the water is here pushed to the North, where it reaches values that are 40-50 cm higher than the values assumed at the southern sites. The evolution can be seen from Figure 10, where the spatial distribution of water levels are shown (see Figures 4 and 5). In the first plot that shows the levels at the beginning of the simulation, the values are almost uniform all over the basin, while in the second one, after 1 day of moderate wind action, the North–South gradient can be seen. It will increase in the third plot that shows the levels after one-day-and-a-half of wind action, when the wind reaches the higher speed. In the last plot, which shows the levels at the end of the event, the North-South gradient becomes weaker.

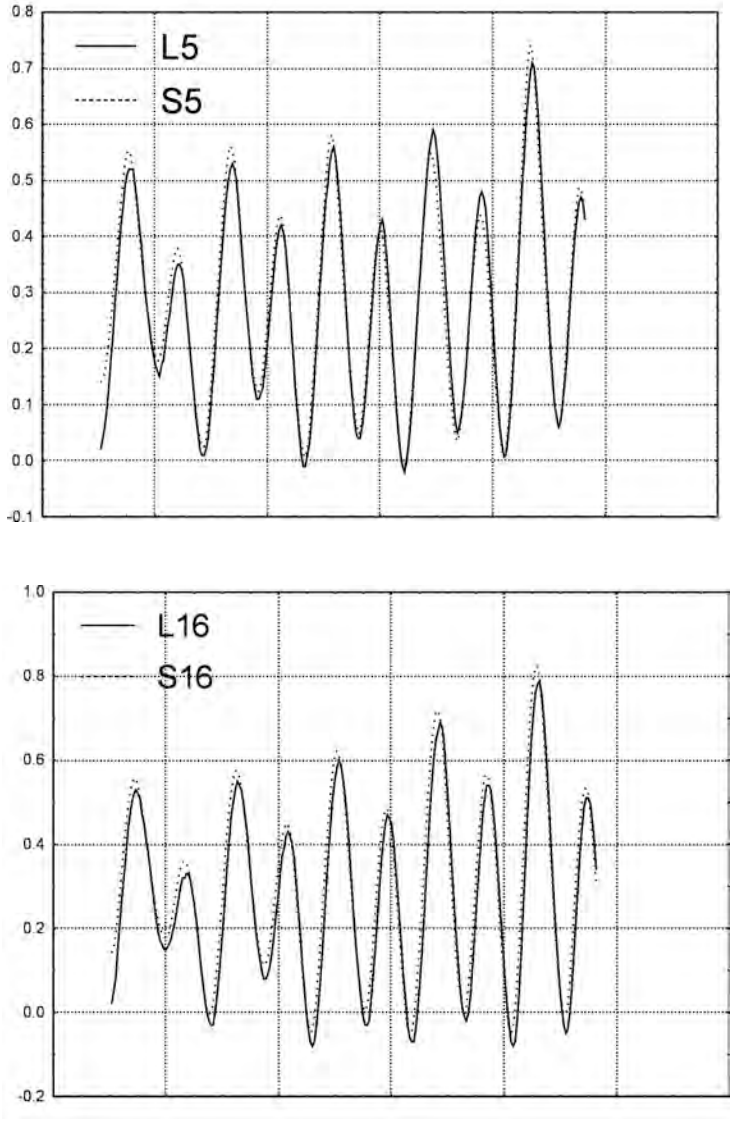

Fig. 6 - Comparison between measured (L) and simulated (S) levels at the stations M5 and M16 in November 1999.

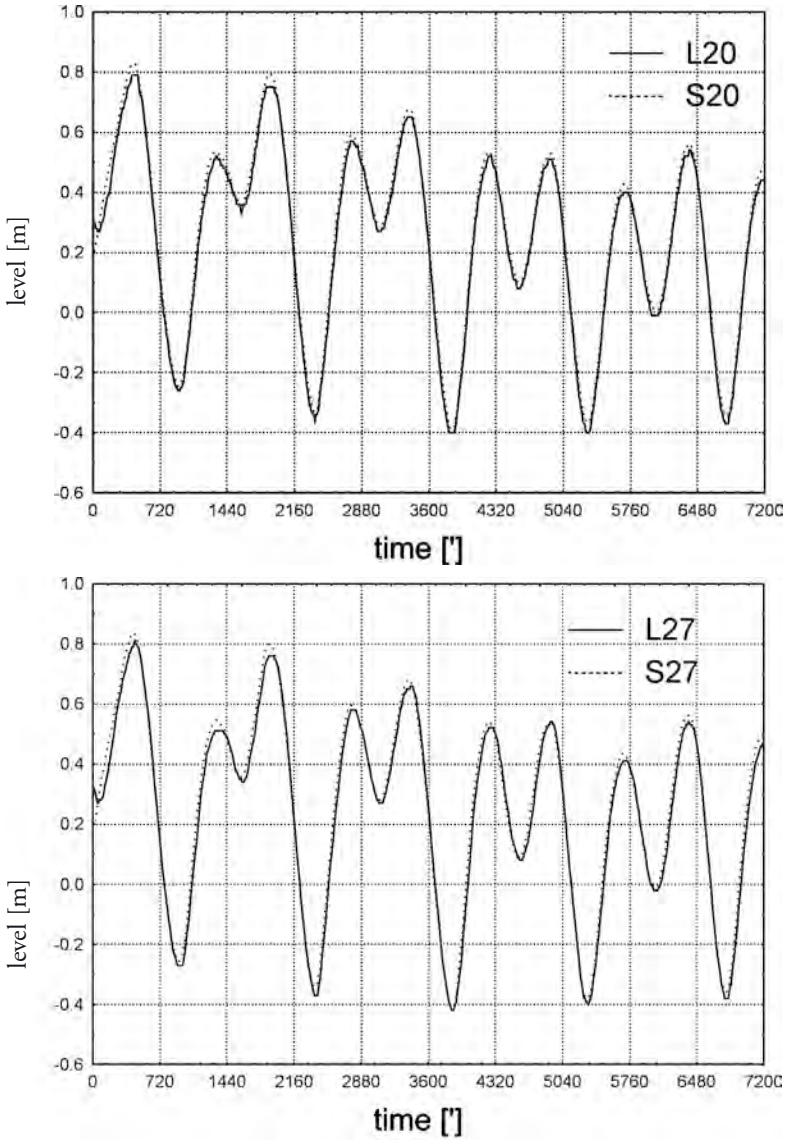

Fig. 7 - Comparison between measured (L) and simulated (S) levels at the stations M20 (a) and M27 (b) in June 1992(C2).

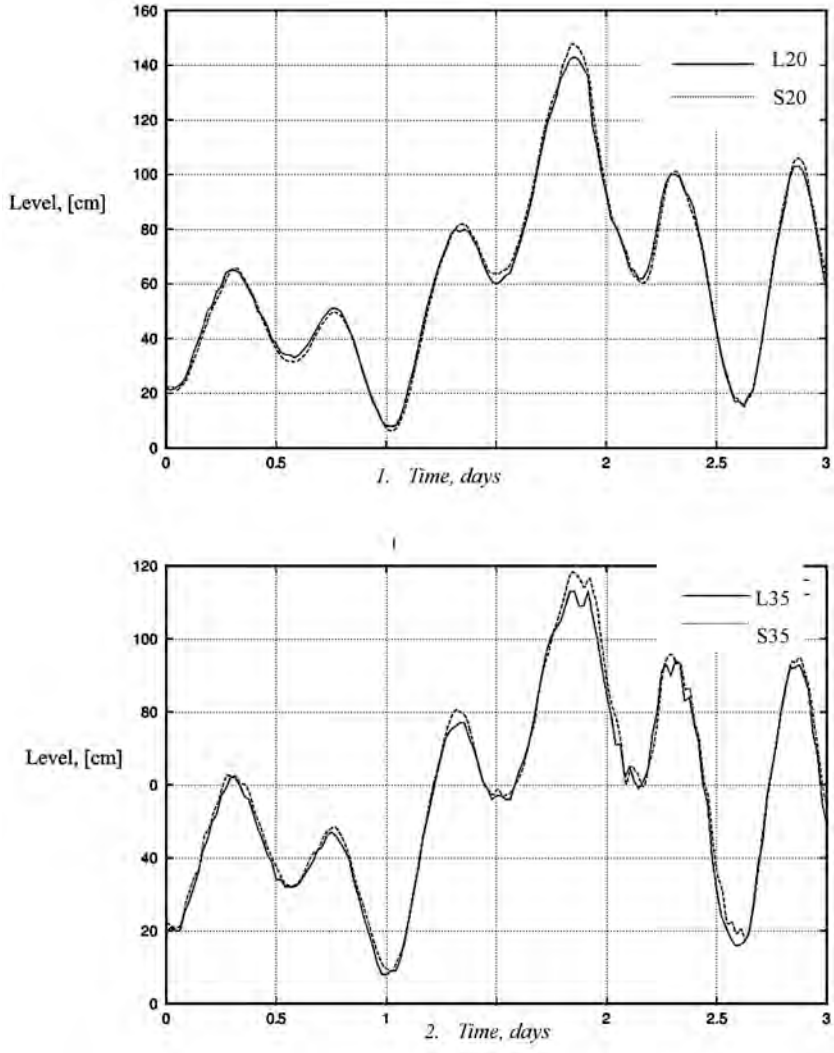

Fig. 8 - Comparison between measured (L) and simulated (S) levels at the stations M20 and M35 in November 2000 (S1).

The quantitative confirmation of these observed differences is given by the analysis of the fluxes along opportunely positioned transects, at the inlets and along the internal borders between the lagoon sub-basins (North, Central and Southern, see Lagoon picture in Figure 12). From

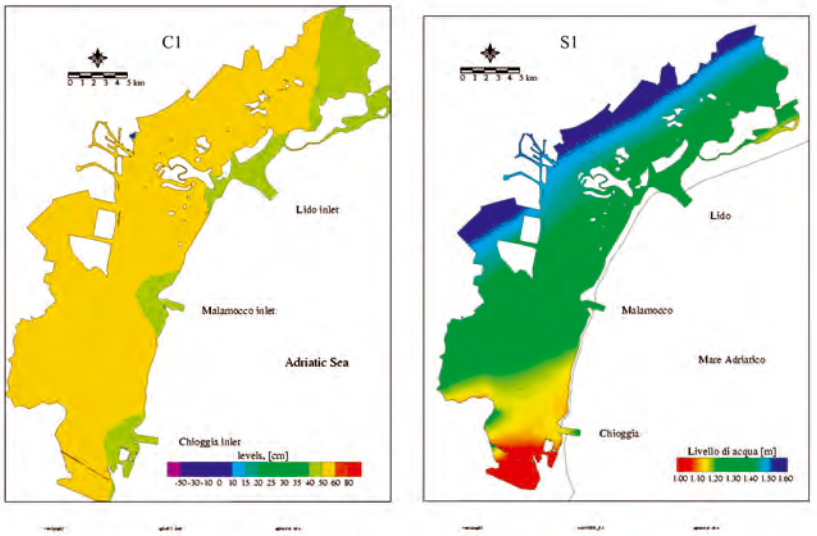

Fig. 9 - Spatial distribution of water levels in the Lagoon of Venice, during the high tide, for the simulations C1 and S1 (no-wind and Scirocco wind respectively).

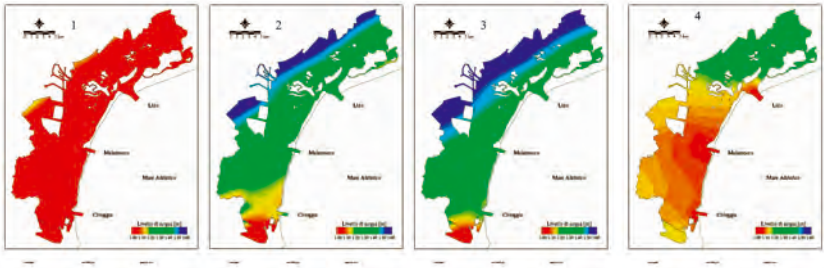

Fig. 10 - Evolution of water levels in S1 simulations. Numbers 1-4 refer to the time steps shown in Fig. 4 and 5.

figure 11 we can see that during the Scirocco wind event the water enters the Chioggia inlet reaching flux values that are as twice higher (up to 4000 m^3/s) than the fluxes that normally enter this inlet during the high tide (normally around 2000 m^3/s). At the end of the Scirocco wind event the water flows from the north to the south-east in order to restore the water level equilibrium. At this time the outflowing fluxes measured at the Northern inlets -Lido and Malamocco- reach high values, around 10000 m^3/s, higher than the usual outflowing values, that are around 6000 m^3/s.

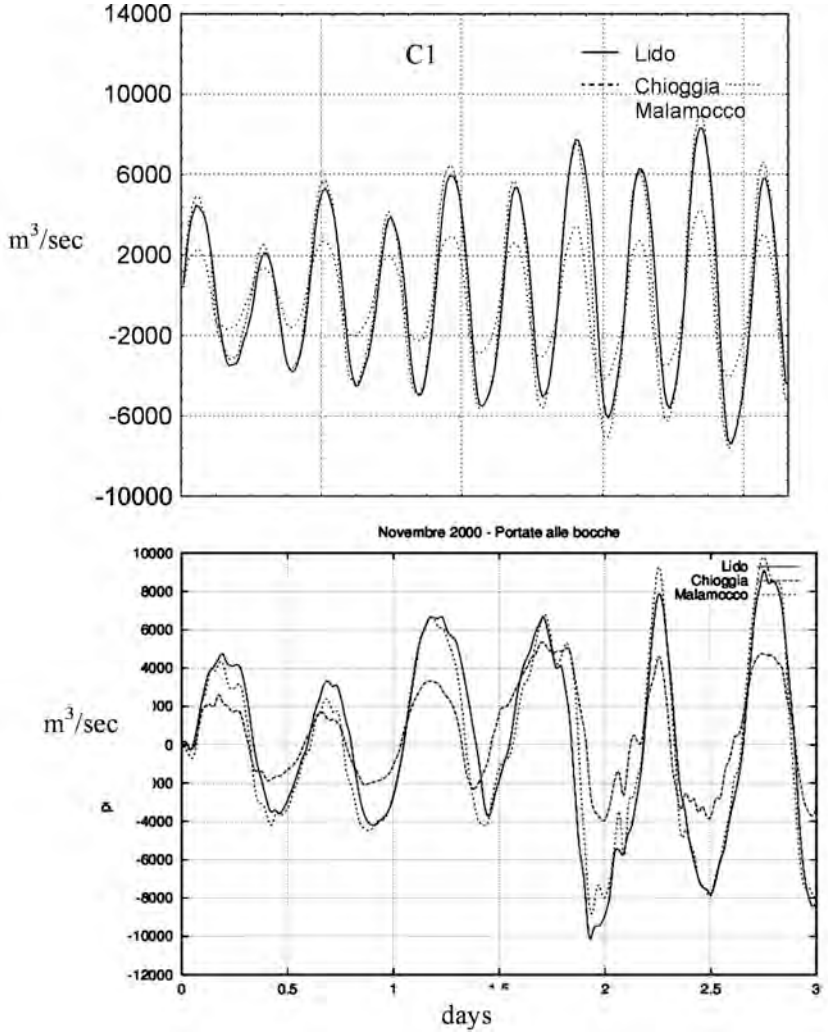

Fig. 11 - Fluxes at the three inlets for simulations C1 (no-wind) and S1 (Scirocco wind). Positive values indicative inflows, negative values outflows.

Also the fluxes on transects 'Laguna Centrale' and 'Laguna Sud' are higher than the references when the Scirocco wind is blowing, as shown in figure 12. Here they reach values around 4000 m^3/s higher than the reference values that are around 500 m^3/s.

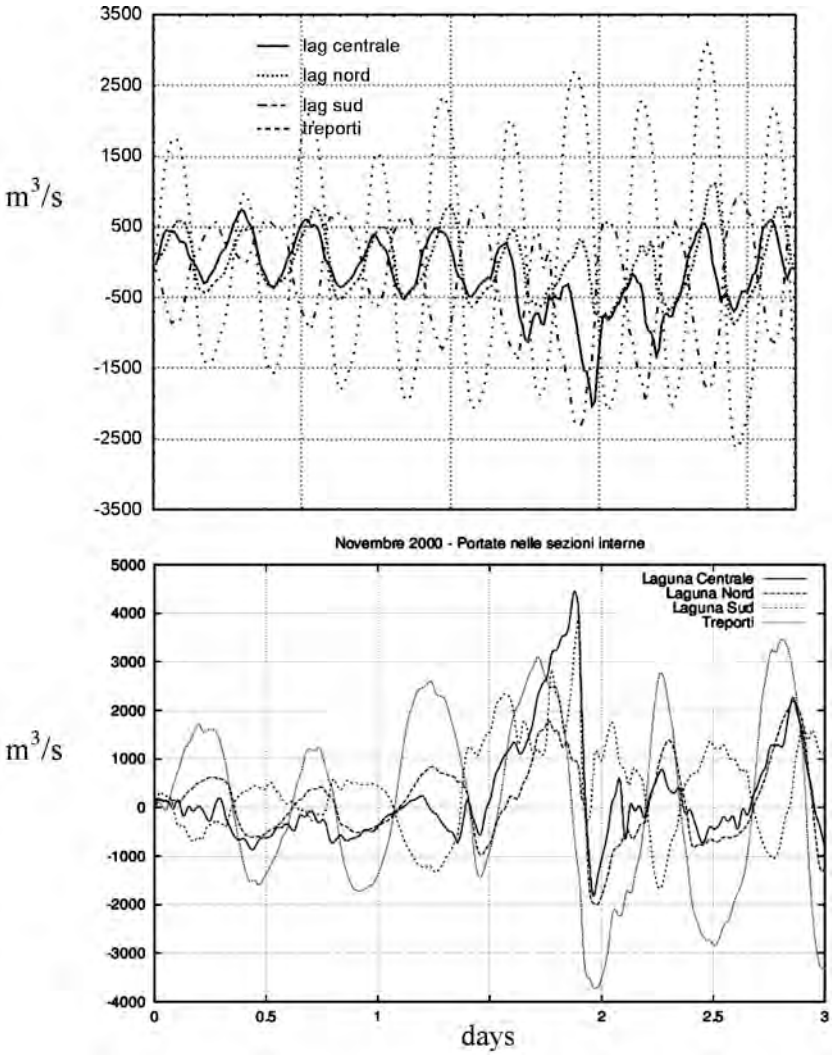

Fig. 12 - Fluxes through the internal transect for simulations C1 (no wind) and S1 (Scirocco wind). Northward fluxes are assumed as positive.

The same differences in the absolute values can be seen at the end of the Scirocco wind event, when, again, the values of water fluxes at the two southern transects assume high negative values, induced by the restoring equilibrium.

Fig. 12 - Continued.

4. *Conclusions.*

The comparison of the simulation results with the data measured by the SMI, confirmed the capability of the SHYFEM model to simulate the hydrodynamic of the Lagoon of Venice, under no-wind and Scirocco-wind conditions.

The model has then been used to analyse the effects of changing wind forcings on the hydrodynamic of the Lagoon of Venice. And it shows that the hydrodynamics is strongly influenced by the wind action, both in direction of water mass circulation and in the absolute values of the water fluxes.

References.

Umgiesser G. & Bergamasco A., 1993. A staggered grid finite element model of the Venice Lagoon. In: *K.Morgan, E. Ofiate, J .Periaux, & Zienkiewicz, O.C. eds Finite Elements in Fluids*.Pineridge Press.

Umgiesser G., 1997. Modelling the Venice Lagoon. *International Journal of Salt Lake Research 6*: 175-199, Kluwer academic Publishers. (The Netherlands).

VARIABILITY OF HYDROCHEMISTRY, INORGANIC AND ORGANIC MATTER AND PLANKTON BETWEEN THE VENICE LAGOON AND THE ADRIATIC SEA. PRELIMINARY RESULTS (YEAR 2001)

F. Bianchi[1], E. Ravagnan[1], F. Acri[1],
F. Bernardi-Aubry[1], A. Boldrin[1], E. Camatti[1],
G. Campesan[1], D. Cassin[1], A. Comaschi[1],
M. Turchetto[1], E. Van Vleet[2], M. Bressan[3]
[1]*Istituto di Biologia del Mare, CNR, Venezia*
[2]*College of Marine Science, University of South Florida, St. Petersburg Florida USA*
[3]*Dipartimento di Biologia, Università di Padova*

Abstract.

Exchanges and fluxes of organic and inorganic substances, both dissolved and particulate, and plankton organisms between the Venice lagoon and the Adriatic sea have been taken into account in a multidisciplinary study started since the beginning of year 2000 (CORILA, line 3.5, WBS2). Preliminary results about the variability of these parameters, obtained from intensive field experiments carried out at the Lido inlet, as well as synoptic surveys performed at Lido, Malamocco and Chioggia, related to February-December 2001, are reported and discussed.

1. *Introduction.*

Several attempts have been done in order to quantify exchanges and fluxes between the lagoon of Venice and the Adriatic Sea. Many of them were mainly focused on physics by ISDGM/CNR (1978a, 1978b, 1979) and OGS (1992-93, unpublished data), while fluxes and budgets of biogeochemical parameters on the water column are still lacking.

This approach was taken into account by the Istituto di Biologia del Mare of Venice since 1982, when fluxes were investigated during one or more tidal cycles in some minor areas of the Northern lagoon: i) a first

detailed study of some biogeochemical parameters was carried on in 1982 in the channel Borgognoni during one tidal cycle (Barillari *et al.*, 1985); ii) fluxes from/into Palude di Cona were assessed during seasonal surveys from 1983 to 1985, by means of contemporary samplings at its exchanging points (Bianchi *et al.*, 1987a, 1987b; Boldrin *et al.*, 1987); iii) the biological variability of Palude della Rosa was assessed during intensive seasonal campaigns in 1991-92, characterising in this way fluxes of inorganic and organic matter, both dissolved and particulate, phyto- and zooplankton communities and primary productivity, and calculating nutrients and suspended matter budgets in this small ecosystem (Acri e*t al.*, 1995; Bianchi *et al.*, 1999).

The CORILA project, started in the year 2000, through the research line 3.5 "Quantity and quality of the exchanges between the Venice lagoon and the Sea", gave us the opportunity to extend this approach to the three inlets of the Venice lagoon, in order to assess, through a series of intensive seasonal experiments, the exchange rates of the main biogeochemical parameters, as oxygen, nutrients, inorganic and organic seston, plankton, organic biological compounds and micropollutants. The aim is to estimate their annual and seasonal mean values, and, in particular, their exchange rates in extreme meteorological conditions. In this paper, some preliminary results related to the period February-December, 2001, are reported and discussed.

2. *Materials and methods.*

Accordingly, the planned strategy for the above mentioned parameters involves sampling over few tidal cycles, during extreme meteorological conditions and in various seasons and/or different freshwater discharge conditions.

To give an exhaustive picture of the quantities involved in such processes at different time-scale, the following sampling strategy was adopted:

1) to assess the annual variability and exchange rate, intensive seasonal campaigns were carried out at each inlet, following 8 tidal cycles (48h) during a spring tide phase, with 3 hours interval (high tide, ebb, low tide, etc.);
2) to follow the gradual modifications between seasons, monthly surveys were performed simultaneously at the three inlets, during one spring tidal cycle (6h) in high tide, ebb and low tide.

The stations taken into account are located in the middle of each inlet,

in the same position of the ADCP currentmeters mooved by ISGDM/CNR and OGS (see Gacic *et al.*, this volume).

Measurements of the hydrological properties of the water column were performed by multiparametric probe casts from surface to bottom, while discrete samplings were made by Niskin bottles deployed at a fixed depth (5 m), an intermediate level estimated as representative of the whole water column.

The following parameters were examined:

- transparency, with a Secchi disk;
- temperature and salinity, with multiparametric probes (IDRONAUT 801 and HYDROLAB Datasonde4), calibrated against a Guildline Autosal 8400B laboratory salinometer;
- transmittance as percent of the incident beam, by a transmissometer connected to a multiparametric probe;
- dissolved oxygen, according to Winkler's method (Strickland and Parsons, 1972);
- dissolved nutrients (ammonia, nitrites and nitrates, orthophosphates and orthosilicates), filtered through Whatman GF/F fiberglass filters (porosity = 0.7 μm) and analysed with a Systea-Alliance auto-analyser, according to the methods generally indicated by Strickland and Parsons (1972) and Hansen and Koroleff (1999);
- chlorophyll *a*, assessed according to Holm-Hansen *et al.* (1965), after filtration through Whatman GF/F filters and measurement of the acetone extract before and after acidification by means of a Perkin Elmer LS5B spectrofluorometer;
- particulate organic carbon (POC) and nitrogen (PN), determined on Whatman GF/F filters after elimination of inorganic carbon by HCl, with a Perking Elmer 2400 CHN elemental analyser, according to Hedges and Stern (1984);
- total suspended matter (TSM), filtered through pre-weighted Whatman GF/F fiberglass filters and weighted by a gravimetric method; organic and inorganic percentage was assessed after incineration at 400°C (Strickland and Parsons, 1972);
- phytoplankton numerical abundances and taxonomy on samples fixed in neutralized formalin with hexamethylentetramine and counted under an invertoscope according to the method of Uthermöl (1958);
- zooplankton numerical abundances and taxonomy on samples collected from bottom to surface by a Clarke-Bumpus sampler equipped with a 200-μm net, then fixed in neutralized formalin and counted quantitatively under a stereomicroscope.

Naturally produced organic compounds (fatty acids, sterols, triacylglycerols, wax esters and phospholipids produced by marine plants, animals and bacteria), as well as anthropogenic compounds (petroleum hydrocarbons, faecal sterols, chlorinated hydrocarbons and pesticides) have also been taken into account. Samples collected for organic biomarker analysis were immediately extracted at the Istituto di Biologia del Mare and then returned to the University of South Florida for continued analysis, performed by Iatroscan TLC-FID chromatography (i.e., thin layer chromatography - flame ionization detection). Use of this instruments allows quantitative analysis of specific lipid classes found in each sample (dissolved organic matter and suspended particulate matter).

In this paper, data concerning two cruises carried out in March (preliminary phase) and November (first experimental period), as well as monthly results from the three inlets, are reported and discussed; as naturally produced organic and anthropogenic compounds, data related to the May 2001 preliminary cruise are reported here.

3. *Results and discussion.*

3.1. *March 2001.*

3.1.1. *Hydrology.*

The spring campaign was characterised by high water level ("acqua alta"): a maximum height of 104 cm was reached in the second half of the 8th of March, when strong and persistent winds from East-North-East blew. So, a coastal transport of diluted water from the Northern rivers (mainly Sile and Piave) took place. This signal is evident in the second half of the vertical salinity distribution (fig. 1), when values < 33 PSU were measured on the whole column. As transparency regards, this diluted water showed higher seston concentration, as detected by Secchi disk readings $\leqslant$ 0.5 m and transmittance values < 10% of the incident beam (fig. 2).

3.1.2. *Dissolved nutrients, particulate matter and chlorophyll.*

As nutrients regard, DIN (as sum of ammonia, nitrite and nitrate) assumed averages of 23.3 μM, with a maximum of 34.2 μM related to the minimum in salinity of 31.5 PSU. During the "acqua alta", DIN concentrations were slightly higher. Nitrogen fractions were mainly due to nitrate (80%), while ammonia and nitrite accounted respectively for 17 and 3% of the total. Ammonia contribution to total nitrogen increased during

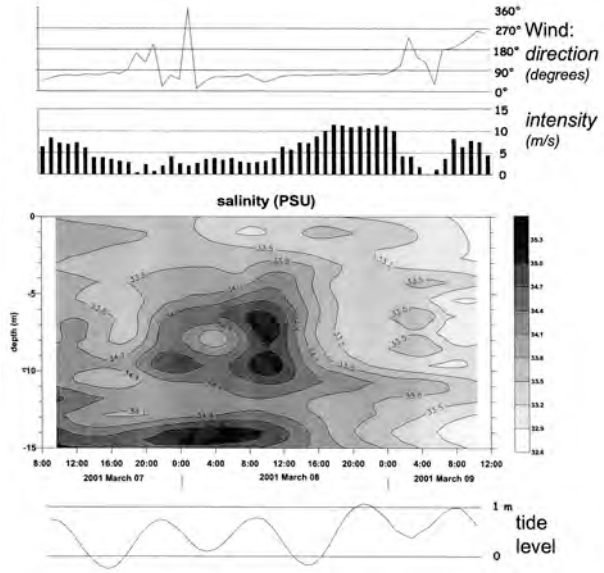

Fig. 1 - March, 2001. Vertical distribution of salinity at Lido during the sampling period. Wind direction and intensity, as well as tidal level, are reported.

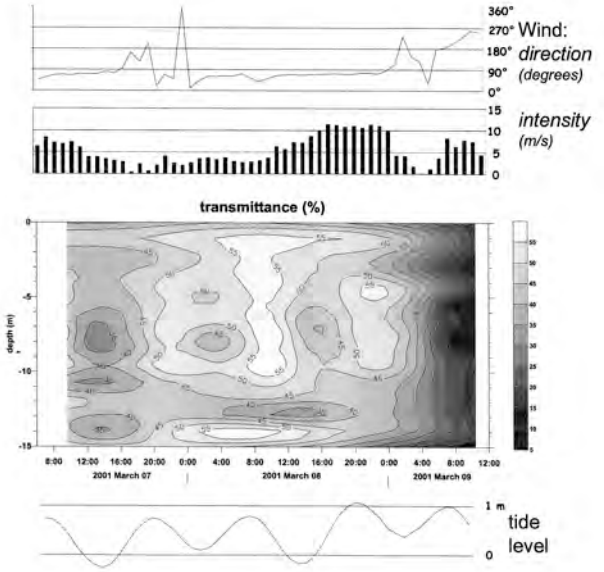

Fig. 2 - March, 2001. Vertical distribution of trasmittance by incident beam at Lido.

high water (from 2-3 μM to values > 5 μM). Significant inverse correlations between salinity versus DIN and salinity versus ammonia were found (respectively: r=- 0.894 and r=- 0.595, both n=32 and $p \leqslant 0.01$).

Orthosilicate showed the same behaviour, increasing from 5-8 μM to values > 11 μM during the "acqua alta".

Particulate matter distribution was in strong correspondence with the optical properties of the waters: TSM minima (3-6 mg/dm^3) matched with high transmittance readings (50-60%), while the highest TSM concentrations (between 21 and 28 mg/dm^3) were found at the end of the "acqua alta", when transmittance was < 10%. The inorganic fraction, always dominant in this campaign (average = 76%), increased slightly its percentages to values > 80% of the total during the "acqua alta".

Chlorophyll *a* average concentration was 1.4 μg/dm^3, with ratios between active and non-active products around 1.4. No differencies were observed when "acqua alta" occurred.

3.1.3. *Phyto- and zooplankton abundances and taxonomy.*

Phytoplankton abundances ranged between $1220 \cdot 10^3$ (low tide, 7th March) and $2134 \cdot 10^3$ cells/dm^3 (high tide, 8th March). Community structure was discriminated by the tidal height: in high tide diatoms dominated (more than 50% of the total), while in low tide nanoflagellates were prevalent (> 50%).

As taxonomy, coccolithophorids were well represented in high tide (around 10-15%), decreasing their percentages to 5-10% in low tide.

All samples were characterised by some common species, like *Skeletonema costatum*, *Emiliana huxley*, *Pseudonitzschia seriata* complex and some cryptophyceans.

Zooplankton species composition appeared to be differentiated between the tidal phases: in low tide, the copepod *Acartia tonsa* (38% of the total) and some larval stages, mainly belonging to decapods (21%), dominated the community, while in high tide the calanoid *Paracalanus parvus* (40%), some cladocerans (15%) and other copepods (14%) prevailed.

3.2. *November 2001.*

3.2.1. *Hydrology.*

In November, the "acqua alta" occurred again, this time since the beginning of the sampling period (14th November). It was caused by strong winds from East-North-East, blowing with an intensity up to 20 m/s. So, in the middle, the picture of salinity showed the same distribu-

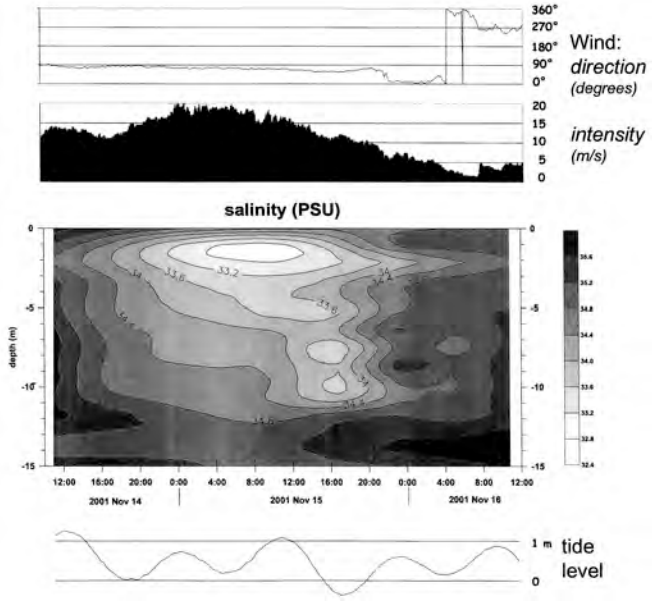

Fig. 3 - November, 2001. Vertical distribution of salinity at Lido.

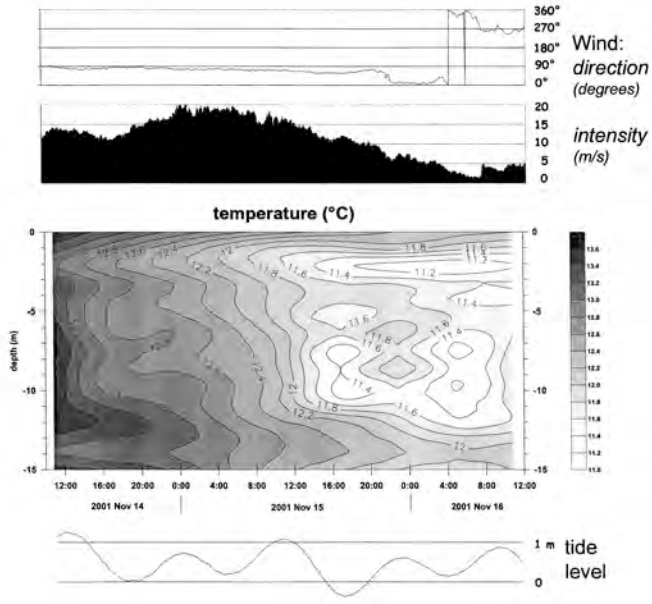

Fig. 4 - November, 2001. Vertical distribution of temperature at Lido.

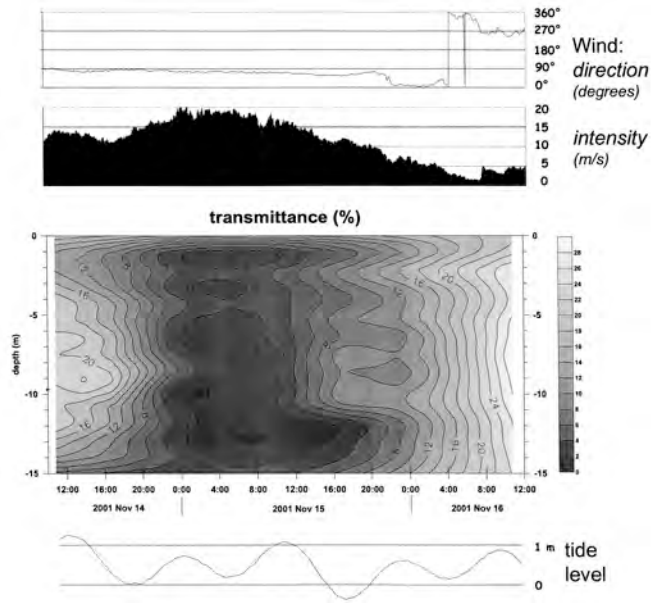

Fig. 5 - November, 2001. Vertical distribution of trasmittance at Lido.

tion as in March, with a minimum of about 33 PSU (fig. 3). Cold winds caused, as secondary effects, a decrease in water temperatures, clearly evident in the temperature pattern of figure 4, and resuspension of sediments on the whole water column, as showed by the transmittance vertical distribution (fig. 5).

3.2.2. *Dissolved nutrients, particulate matter and chlorophyll.*

The diluted waters sampled during the "acqua alta" were more rich in nutrients, DIN increasing from 16 to 30 μM, orthosilicate from 10 to 20 μM, orthophosphate from 0.1 to 0.4 μM, with respective maxima related to the salinity minimum. DIN was mainly represented by nitrate (average = 70%), decreasing to 62% during "acqua alta", while ammonia increased up to 34%.

Particulate matter showed two peaks of 44 mg/dm^3 and 37 mg/dm^3, both related to high tide, mainly due to the inorganic fraction (> 80%).

Phytoplankton biomass as chlorophyll *a* was on average 1.2 μg/dm^3, with slight higher values in high than in low tide. The variation of chlorophyll *a*/pheopigment ratio, lower than 0.8 in high water, indicated the prevalence of degradation products on alive chlorophyll.

3.2.3. *Phyto- and zooplankton adundances and taxonomy.*

Phytoplankton abundances varied between $160 \cdot 10^3$ and $1184 \cdot 10^3$ cells/dm^3. No quali- and quantitative differences between high and low tide were observed during the "acqua alta". Nanoflagellates and diatoms dominated (respective averages = 60 and 40%). As taxonomic composition, tychopelagic species prevailed (*Navicula* spp, *Amphora* spp, *Pleurosigma* spp, *Cocconeis* spp, *Diploneis* spp).

Zooplankton abundances ranged between 503 and 2131 ind/m^3, both in low tide. As species composition, some differencies between tides occurred: the copepod *Paracalanus parvus* and the cladoceran *Penilia avirostris* dominated in high tide, while *Acartia clausi* prevailed in low tide, typical species of the seasonal period.

3.3. *Seasonal surveys at the three inlets.*

3.3.1. *Hydrology.*

The montly pictures may contribute to describe the interannual variability at each inlet. As temperature regards, the annual cycle was evident in the trend of figure 6. No differencies were detected among the inlets. A wider range can be recognized for measurements related to low tide, showing the strong influence of the atmosphere on the lagoon.

Salinity values at Lido inlet were lower than Malamocco and Chioggia (fig. 6). Lido and Malamocco showed significant differencies between high and low tide (Lido: ANOVA F-test = 9.0, $p < 0.05$; Malamocco: F-test = 4.7, $p \leqslant 0.05$).

3.3.2. *Dissolved nutrients, particulate matter and chlorophyll.*

Among nutrients, DIN showed a typical seasonal pattern, with maxima in winter (around 20-25 μM) and a summer minimum common to all inlets, due to the biological uptake (August, about 2 μM; fig. 6). The "acqua alta" signature of November can be recognized in the highest concentration measured at Lido (up to 30 μM), due to the nitrogen-rich riverine outflow. Our data pointed out that nitrate mean concentration increased in high tide while ammonia rose in low tide conditions, for the three inlets. The percent mean variations were:

- Lido: nitrate from 74 to 70%, ammonia from 22 to 27%, respectively in high and low tide;
- Chioggia: nitrate from 67 to 50%, ammonia from 28 to 46%, in high and low tide;

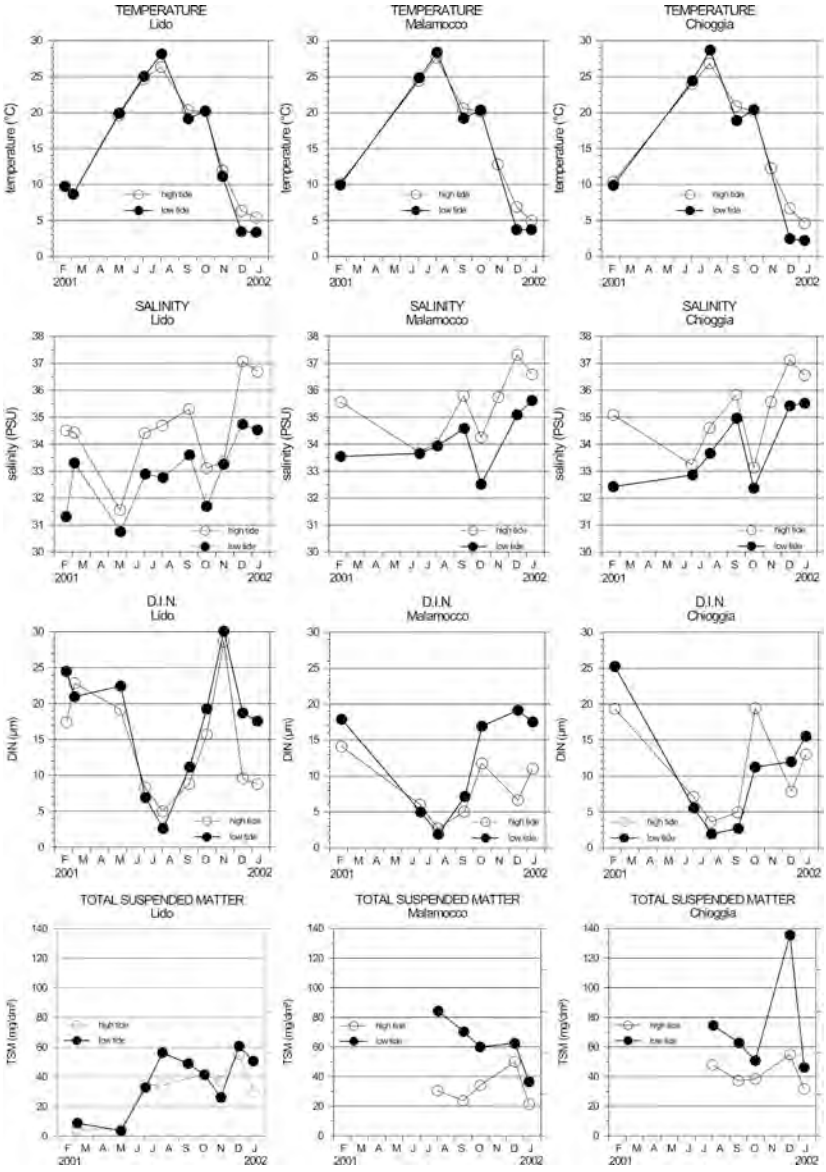

Fig. 6 - Time trends of temperature, salinity, dissolved inorganic nitrogen (DIN), total suspended matter (TSM) at Lido, Malamocco and Chioggia in high and low tide.

• Malamocco: nitrate from 57 to 51%, ammonia from 39 to 44%, in high and low tide.

In August, in low tide, nitrate concentrations fell down to values close to the detection limit (< 0.1 μM, percentage = 1% of DIN), while ammonia increased up to 90% of total: this phenomenon was in concomitance with a peak in chlorophyll concentration.

Orthosilicate annual averages were about 13 μM, with no differencies between tidal phases. The annual trend was opposite to the nitrate one, with low values in winter and a peak in August, in concomitance with the chlorophyll maximum, a signal that the microalgae responsible were not diatoms.

Orthophosphate showed very low values (average = 0.1 μM), with no particular trend.

Total suspended matter distribution peaked commonly during summer, but each inlet had a slight different behaviour (fig. 6): Lido showed low values in correspondence with "acqua alta", probably due to the dilution effect, and peaked in summer and winter; seston content peaked only in summer at Malamocco, while Chioggia, after the summer maximum, had another one in December (up to 140 mg/dm^3), probably due to local events. Only TSM content at Malamocco was different between tides (ANOVA F-test = 8.3, $p \leqslant 0.05$).

TSM composition was mainly due to the inorganic fraction (average = 70%). The organic percentage rose up to 35-40% at the three inlets in August, when peaks of chlorophyll were detected in low tide at Lido (28.4 μg/dm^3), Malamocco (28.9 μg/dm^3) and Chioggia (36.7 μg/dm^3; fig. 7).

3.3.3. *Phyto- and zooplankton abundance and taxonomy.*

As phytoplankton, the sources of variability could be the following:

1. species seasonal succession;
2. quali- and quantitative differencies among the three inlets;
3. quali- and quantitative differencies between high and low tide.

1) In the considered period, abundances ranged from $0.108 \cdot 10^3$ (December, high tide, Malamocco) to $12145 \cdot 10^3$ cells/dm^3 (September, low tide, Chioggia). The September maximum did not match the chlorophyll peak, as observed in August: in this sample, the phytoplankton abundances reached 5107 10^3 cells/dm^3, with a prevalence of very small forms, mainly represented by nanoflagellates (75% of total) and *Nitzschia frustulum*, all < 10 μm. In addition, the probably presence of some filamentous colonies of cyanobacteria, that

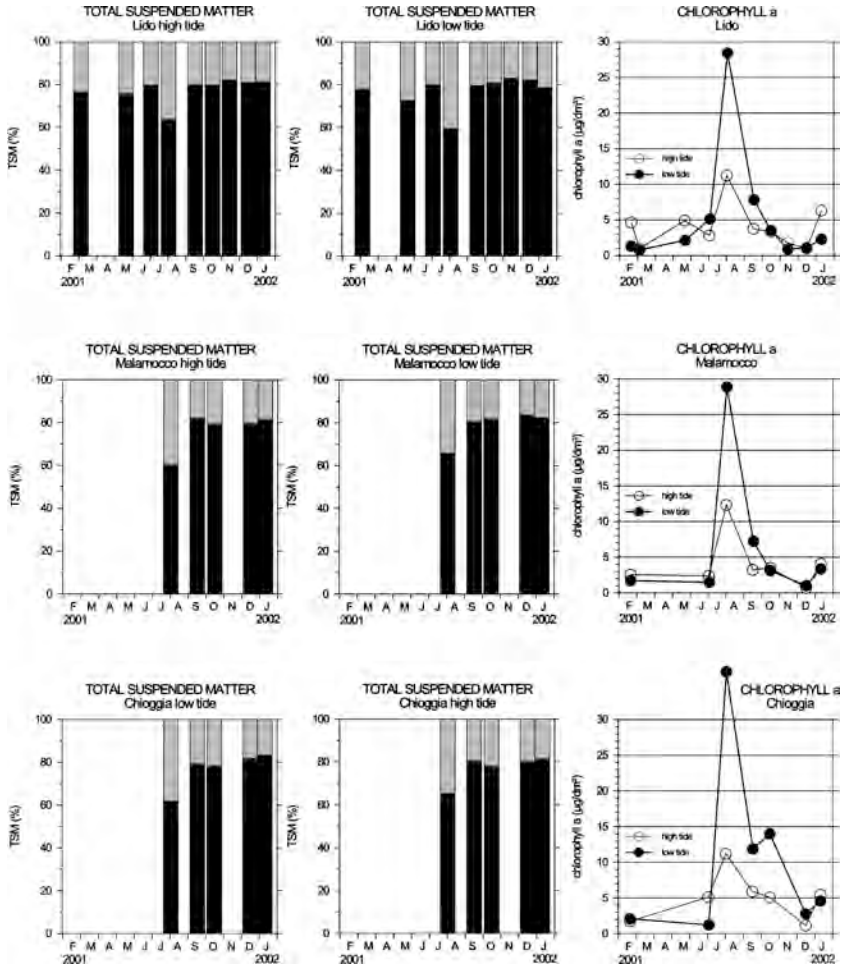

Fig. 7 - Stacked bars related to inorganic (black) and organic (gray) TSM fractions in high (left) and low tide (center) and temporal variations of chlorophyll a (right) at Lido (above), Malamocco (middle) and Chioggia (bottom). The highest percentages of organic material in August match the chlorophyll peak at each inlet.

could have been retained onto filters, but not observed under the microscope, may contribute to clarify this discrepancy (Socal, com. pers.). During the considered annual cycle, the taxonomic composition was dominated by nanoflagellates and diatoms (90% of the total), while dinoflagellates and coccolithophorids accounted for the remai-

ning 10%. According to what already known at the inlets of the Venice lagoon, a typical seasonal succession in species composition may be confirmed: i) in late winter small colonies with a high growth rate can be found (*Skeletonema costatum*, *Pseudonitzschia delicatissima* complex and *Chaetoceros* spp.); ii) in summer high abundances, mainly by nerithic (*Cerataulina pelagica*) and brackish species (*Nitzschia frustulum*), were observed; iii) minima of tychopelagic diatoms were typical in deep-winter.

2) As spatial variability, small quantitative differencies were detected among the three inlets. Chioggia showed relative higher numerical abundances, with *Skeletonema costatum* percentages of 6-7% of total.
3) As tidal variability, in high tide some nerithic diatoms were more abundant in February (*Skeletonema costatum* and *Pseudonitzschia delicatissima* complex) and July (*Cerataulina pelagica* and *Chaetoceros* spp.), while in low tide higher phytoplankton concentration occurred in August, September and October, because of *Nitzschia frustulum* percentages up to 25%.

In summer, zooplankton showed higher numerical values in ebb tide, due almost exclusively to the copepod *Acartia tonsa*, dominant in this period in the inner lagoon (Comaschi *et al.*, 1994), and to some larval stages of decapods and molluscs. In the cold season, zooplankton biomass remained low, both in high and in low tide. The September peak in high tide was due to the copepod *Paracalanus parvus*.

The preliminary data showed that zooplankton composition at Lido was similar to that of the coastal area of the Northern Adriatic, while Malamocco was more influenced by inner lagoon populations, with *Acartia tonsa* as dominant species.

3.4. *Naturally produced organic compounds.*

Results from the May 2001 preliminary cruise at Lido indicated that most of the lipids found in the dissolved organic matter (DOM) were present as the free fatty acids (70-80%), witj lower levels of sterol esters, wax esters, triacylglycerols and phospholipids). Total lipid concentrantions in the DOM were generally present in much lower concentrations than those found in the suspended particulate material (SPM). Lipids present in the SPM were primarily free fatty acids and phospholipids with approximately 30-70% of the total lipids divided between these two lipid classes. Smaller amounts of sterol esters, wax esters and triacylglycerols were also found in the SPM. Concentrations of total lipids were generally 1-10$\mu g/dm^3$ in the SPM fraction and <2 $\mu g/dm^3$ in the DOM.

References.

Acri F., Alberighi L., Bastianini M., Bianchi F., Boldrin A., Cavalloni B., Cioce F., Comaschi A., Rabitti S., Socal G., Turchetto M., 1995. Variazioni ad alta frequenza dei parametri idrobiologici nella laguna di Venezia. In: Proceedings of the Sixth SITE Symposium, Venice (Italy), 16, 31-34.

Barillari A., Bianchi F., Boldrin A., Cioce F., Comaschi Scaramuzza A., Rabitti S., Socal G., 1985. Variazioni dei parametri idrologici, del particellato e della biomassa planctonica durante un ciclo tidale nella laguna di Venezia. In: Proceedings of the Sixth AIOL Symposium, Livorno (Italy), 227-234.

Bianchi F., Boldrin A., Cioce F., Rabitti S., Socal G., 1987a. Variazioni stagionali dei nutrienti e del materiale particellato nella laguna di Venezia. Bacino settentrionale. Ist. veneto Sci. Rappti Studi 11, 49-67.

Bianchi F., Boldrin A., Cioce F., Socal G., 1987b. Concentrazione di nutrienti nella laguna di Venezia. Bacino settentrionale. In: Proceedings of the Seventh AIOL Symposium, Trieste (Italy), 155-164.

Bianchi F., Acri F., Alberighi L., Bastianini M., Boldrin A., Cavalloni B., Cioce F., Comaschi A., Rabitti S., Socal G., Turchetto M., 1999. Biological variability in the Venice Lagoon. In: Lasserre, P., and Marzollo, A., (Eds.), The Venice Lagoon Ecosystem. Inputs and Interactions Between Land and Sea., Parthenon Publishing Press, 97-125.

Boldrin A., Rabitti S., Bianchi F., Cioce F., 1987. Dinamica della sostanza sospesa nella laguna di Venezia. Bacino settentrionale. In: Proceedings of the Seventh AIOL Symposium, Trieste (Italy), 165-174.

Comaschi A., Acri F., Alberighi L., Bastianini M., Bianchi F., Cavalloni B., Socal G., 1994. Presenza di *Acartia tonsa* (Copepoda:Calanoida) nella laguna di Venezia, Biol. Mar. Medit., 1, 273-274.

Hansen H.P. and Koroleff F., 1999. Determination of nutrients. In: Grasshoff, K., Cremling, K., Erhardt, M. (Eds.), Methods of Seawater Analysis, Wiley-VCH Verlag, 159-228.

Hedges J.I. and Stern J.H., 1984. Carbon and nitrogen determination of carbonate-containing solids. Limnol. Oceanogr., 19, 984-989.

Holm-Hansen O., Lorenzen C.J., Holmes R.W., Strickland J.D.H., 1965. Fluorometric determination of chlorophyll. J. Cons. perm. Int. Explor. Mer., 30, 3-15.

ISDGM/CNR 1978a. Campagna di misure 15-18 giugno 1977. Bocca di porto di Malamocco. Technical Report TR98, 156 pp.

ISDGM/CNR 1978b. Relazione preliminare sui risultati delle campagne di misura in laguna, nell'ambito del "Modello scambio laguna-mare in termini di parametro salinità". Technical Report TR99, 144 pp.

ISDGM/CNR 1979. Campagna di misure 16 e 27 ottobre 1978. Bocca di Porto di Malamocco. Technical Report TN77, 44 pp.

Strickland J.D.H. and Parsons T.R., 1972. A practical handbook of seawater analysis. Bull. Fish. Res. Bd. Canada, 167, 311 pp.

Uthermöl H., 1958. Zur Vervollkomnung der quantitativen Phytoplankton-Methodik. Mitt. Int. Ver. Limnol., 9, 1-38.

NUMERICAL ANALYSIS OF THE NUTRIENT FLUXES THROUGH THE VENICE LAGOON INLETS

C. Solidoro[1], G. Cossarini[1], R. Pastres[2]
[1]*Istituto Nazionale di Oceanografia e di Geofisica Sperimentale, Trieste*
[2]*Dip. Chimica Fisica Università Cà Foscari, Venezia*

Abstract.

Nutrient fluxes through open boundaries greatly influence the evolution of biological compartments and trophic status of the lagoon of Venice. They are nutrient input from the hydrographic network of rivers and channels, from the urban centres and from the industrial area and sewage plants, the exchanges with the atmosphere and the sediment, and the fluxes through the lagoon inlets towards and from the Adriatic Sea.

Among these fluxes, the exchanges at the lagoon inlets probably are the less investigated, even if they clearly are of major importance in controlling the evolution of the nutrient content available for the autotrophic communities. This can easily be seen while recognizing that-in term of water fluxes-up to 60% of the lagoon volume is exchanged during a single tide cycle. Nonetheless, so far only a small number of estimations of such fluxes is presently available. Furthermore, these estimations gives contrasting indication, so that doubts persist even on the sign of the fluxes.

In this paper we use a pre-existing 3D coupled transport water quality model of the lagoon for assessing time evolution of the exchange fluxes at the three lagoon inlets. Model results show that the lagoon exports nutrient, during almost all the year. A more detailed analysis indicates that there are differences among the three sub-basins. The Northern Sub-basin, which receives the greatest amount of nutrient input from the river basin, export nutrients through the whole year, both through the Lido inlet and towards the Central Subbasin. The Central Sub-basin exports nutrient through the Malamocco inlet during most of the year, while it receives nutrients from the sea in August and September. Exchanges between the

Southern and the Central Basins are very small, as to indicate that this sub-basin is independent from the other ones. Fluxes through the southern inlets are alternately positive and negative, but always pretty small, indicating a substantially balanced situation for the Southern Basin.

1. *Introduction.*

The lagoon of Venice is the largest Italian Lagoon, it is located in the northern part of the Adriatic Sea, it covers an area of around 500 km^2 and exchanges with the sea through three inlets. Average depth is around 1 meter, as a result of the combination of large shallow area connected by a network of channels, whose depth is however shallower than 2 meters in the majority of the cases. Deeper channels are the ones connected to the inlets. The lagoon is usually subdivided into three sub-basins, which are separated by areas (the watersheds) along with the flow of matter is low.

A network of river and artificial channels input into the lagoon an important amount of contaminants from the drainage basin, in which around 1500000 inhabitants live, but which produces a nutrients load comparable to the one produced by 4000000 equivalent inhabitants.

Part of this load is uptaken by autotrophic communities and enters into the biological cycles. The remaining part is transported to the nearby areas, and – under specific condition – eventually exported to sea. The sea, however, might act as a source of nutrients, too, since exchanges through the inlets can be positive or negative, depending on time and specific conditions.

Exchanges at the lagoon inlets are probably the less known and analysed among the exchanges which occur at the open boundaries.

The present paper offers an estimate of the time evolution of nitrogen fluxes at the three inlets, to be compared to the ones already published. Our estimate is obtained by using a previously released 3D water quality-transport model, whose results have been corroborated by comparison against a large data-set of experimental observations (Cossarini et al. 2002, Solidoro et al. 2002).

2. *Previous estimations of fluxes at the inlets.*

In spite of their importance in controlling trophic evolution and water quality within the lagoon, exchanges of nutrients through the three lagoon inlets has been only marginally investigated, and even poorly quantified.

Sfriso et al. (1994), using data from a monitoring program for the period Jan '91- Dec '91, calculated a net import flux through the two inlets of Malamocco and Lido of 10.440 t N for the period between February and August. The estimation is obtained using the mean difference of TIN between sea and lagoon, which is positive for the period February-August, and an estimate of the water exchanged between lagoon and sea (~$58x10^9$ m^3/y). This positive flux represents an input which is four time greater than the nitrogen input from the discharge points located in the central part of the lagoon (i.e. an area covering a part of the northern subbasin and a part of the central subbasin centred to the Venice island), and which is of the same entity of the denitrification flux, 11.000 t N/y, estimated for the same area (Sfriso & Marcomini, 1994). However, it should be considered that the authors used a rather small number of measurement (7 sampling points for the central lagoon, plus 4 points in the channel of the two inlets, plus one point in the sea; sampled 9 times during the year), and a very simple exchange model. In addition, the monitoring program refers to the early '90, when the lagoon was suffering from a massive proliferation of macraolgae, which no longer occurs.

A former estimation (CVN, 1990) drafts a quite different situation respect to the one proposed by Sfriso et al. (1994). In agreement with these findings – based on data of dissolved nitrogen which were collected in a monitoring program of the lagoon inlets status (A.3.3. CVN, 1988) and on data of particulate nitrogen from Rossi (1979) – the lagoon would import 1300 t/y of nitrate and nitrite and export 970 t/y of ammonium, 2890 t/y of DON and 2890 t/y of PON. Therefore, the lagoon would globally export 5450 t/y of nitrogen toward the Adriatic Sea.

An even larger export was estimated by the same authors (CVN, 1990), based on an elaboration of data of N concentration within the lagoon (A 3.3. CVN, 1988), which have been regrouped and averaged for different subbasins, and information on N concentration in the Adriatic Sea derived from measurements performed at the CNR oceanographic station. Results indicated an export toward the Adriatic Sea of 18.450 t/y of nitrate and nitrite and 4.950 t/y of ammonium.

The situation is even more complex if the fluxes of nitrogen are considered which are related to the suspended and floating organic matter. These fluxes have indeed been recognised to constitute an important term of the global balance, which should not be neglected in comparison with the fluxes associated to the dissolved phase (Flindt et al., 1997; Salomonsen et al., 1997).

3. *Water quality model estimation of fluxes.*

The estimations of exchanges at the inlets discussed in the previous paragraph are obtained by elaborating experimental data and basing on simplified assumption on transport dynamic. Basically, the differences in concentration between the lagoon and the sea are computed, and used to derive fluxes, or fluxes are derived from simplified mass balances. In one case purposely measured data were used. We have assessed time evolution of fluxes at the three inlets by using a 3D coupled water quality model, previously presented and whose results have been corroborated by comparison against a large data set. (Cossarini et al. 2000; Solidoro et al. 2002).

Mathematical models describe the space and time of evolution of a set of variables, thought to be representative of the main feature of a system (state variables), by mimicking the main interactions between major ecosystem compartments and transport processes. In practice, the spatial domain is subdivided in a number of areas (grid points of the model) thought to be homogeneous in respect to the variables considered, and a mass balance is defined for each state variables in each of the grid points. Then, the (instant) variation in time of each state variable Ci is computed as the sum of the variation induced by transport processes and the variation due to biological/chemical transformations.

The model equations read as:

$$\frac{\partial C_i(x,y,z,t)}{\partial t} = \nabla(K(x,y,z)\cdot\nabla C_i(x,y,z,t)) + f(C_i(x,y,z,t),\beta,t) + u(x,y,z,t) \quad (1)$$

where C_i represent the state of the vector of the 13 compartments chosen for the description of the state of system, *f* is the local term of bio/chemical reaction that takes into account the relations between the state variables and *b* is the vector of the parameters that regulate these relations. *K(x,y,z)* is the eddy diffusivity tensor, that describes the diffusion transport due to the effects of the tidal dispersion. Finally, *u* represents exchanges of energy at the air-water interface, calculated from daily meteoclimatic data for the 1998, input of nutrient form the drainage basin, civil and industrial sources (Regione Veneto, 2000).

Model results give us the possibility to analyse the evolution of spatial distribution of the state variables continuously in time. Among the other things, this enables us to investigate the mechanisms which drive plankton and nutrients evolution and to estimate the fluxes among sub-basins and major biological compartments, which are poorly quantified. In fact,

the comparison among model predictions and experimental information, both on fluxes (i.e. flow rates of denitrification, primary production, nutrient released from sediment) and on time evolution of temperature, nutrients, plankton, corroborates, or at the very least does not falsify, the model. Furthermore the data set used in the corroboration is a pretty large one, which covers the whole seasonal evolution of several water quality parameters in different area of the lagoon (Cossarini et al., 2000; Solidoro et al. 2002). Therefore we can have some confidence also on the estimates the model offers about also processes, like nutrient exchanges at the inlets, even if we recognise that we are dealing with a number of simplifying assumptions.

4. *Results and discussion.*

The model does not consider the nitrogen fluxes bound to floating macroalgae, because these processes are poorly quantified and because in the last ten years there has been a drastic reduction in macroalgae standing stocks. (CVN 2023 linea F, 2000).

The model indicates an annual export of 2175 t/y nitrogen. In particular, the lagoon exports 1445 t/y of nitrate and 401 t/y of ammonium. The loss of nitrogen due to export of organic matter is estimated as 329 t/y.

Fluxes are characterised by high seasonal variability, Fig. 1. Maximal negative values of nitrate flux are found during fall and winter months, in correspondence with maxima in river input. An inversion of the sign of the flux is observed in September for nitrate and in August for ammonium, when the nitrogen input from the drainage basin is at its minimum value, and nutrient content in lagoon water is very low, also because of biological activity. The flux bound to organic matter shows the maximal values during spring and summer months and minimum ones during winter month, clearly following the evolution of phototrophic compartments.

The model allows one to compare exchanges at the open boundaries and fluxes among biological compartments. Fig. 2 depicts the yearly averaged fluxes of the entire nitrogen cycle. The solid arrows represent fluxes within the food web, the obliqueus arrows on the left indicates imports of NO3- and NH4+ from rivers and other sources, while the double head arrows stands for the net exchanges with the Adriatic Sea. Dashed arrows are the fluxes related to denitrification and sediment burial. All fluxes are

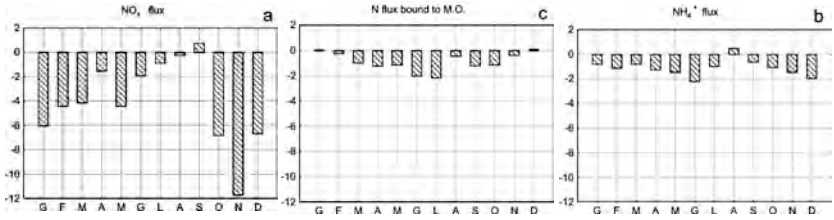

Fig. 1a, b and c - Mean month fluxes of nitrate (a), ammonium (b) and nitrogen bound to organic matter (c) through the lagoon inlet estimated by the model for the 1998.

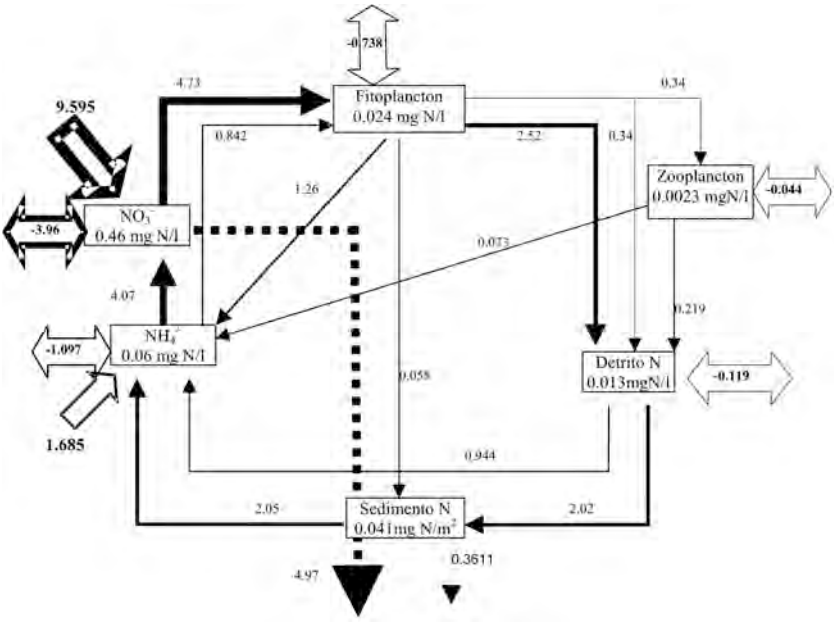

Fig. 2 - Scheme of nitrogen cycle in the lagoon. Fluxes are expressed in t N/y.

given in t/day, but the values in the boxes, which are the yearly averaged concentration of the state variables and are expressed in mg/l (mg/m2 for the sediment compartment).

The model indicates that phytoplankton primary production amounts to 5.5 t N/day and is supported mainly by nitrate. More than 75% of this flux is recycled to ammonia, either directly or through passage in the detritus and sediment compartments, and subsequent mineralization.

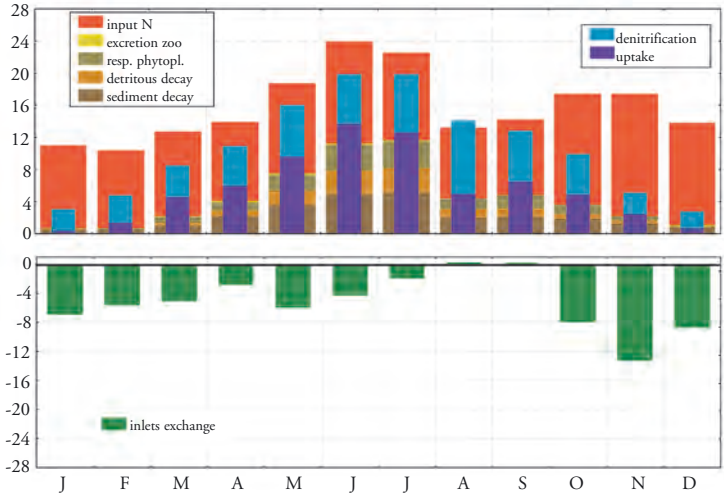

Fig. 3 - Seasonal evolution of DIN balance terms for the whole lagoon. Production terms are piled in the larger, red, column, while narrow, blue, bar refer to loss terms. Bottom panel reports seasonal evolution of fluxes through the inlets.

Around 14% of primary production is exported to the Adriatic Sea and only a small fraction, around 6%, is transferred to higher level. It is worth to note that recycling process generates an (averaged) daily flux of nitrogen of 4 t/d, which is to be compared, and added, to the 11 t/d coming from external sources. Sediments contributed to this flux for more than half, and detritus for around a quarter. All the recycled nitrogen is originated as ammonia, but a significant part of it (70%) is oxidised to nitrate. New and regenerated nitrogen is utilised for phytoplankton growth (36%), consumed in denitrification processes (31%), and exported to the sea, which therefore is an important sink.

Fig. 3 summarises the time evolution of fluxes and offers a comparison among sources and loss terms of dissolved inorganic nitrogen mass balance. In fact for each month 2 bars are reported. The narrower one is a pile bar which indicates the sum of nitrogen uptaken from phytoplankton and denitrification, while the larger bar represents the sum of the sources terms, namely the input from external sources, zooplankton excretion, phytoplankton respiration, mineralization of sediment and detritus. As indicated in the legend, different contributions are reported with different colours. Exchanges at the three inlets are reported in the second plot, in the bottom part of the figure. Inspection of the figure reveals that, when considering the lagoon as whole, the 'biological' nitro-

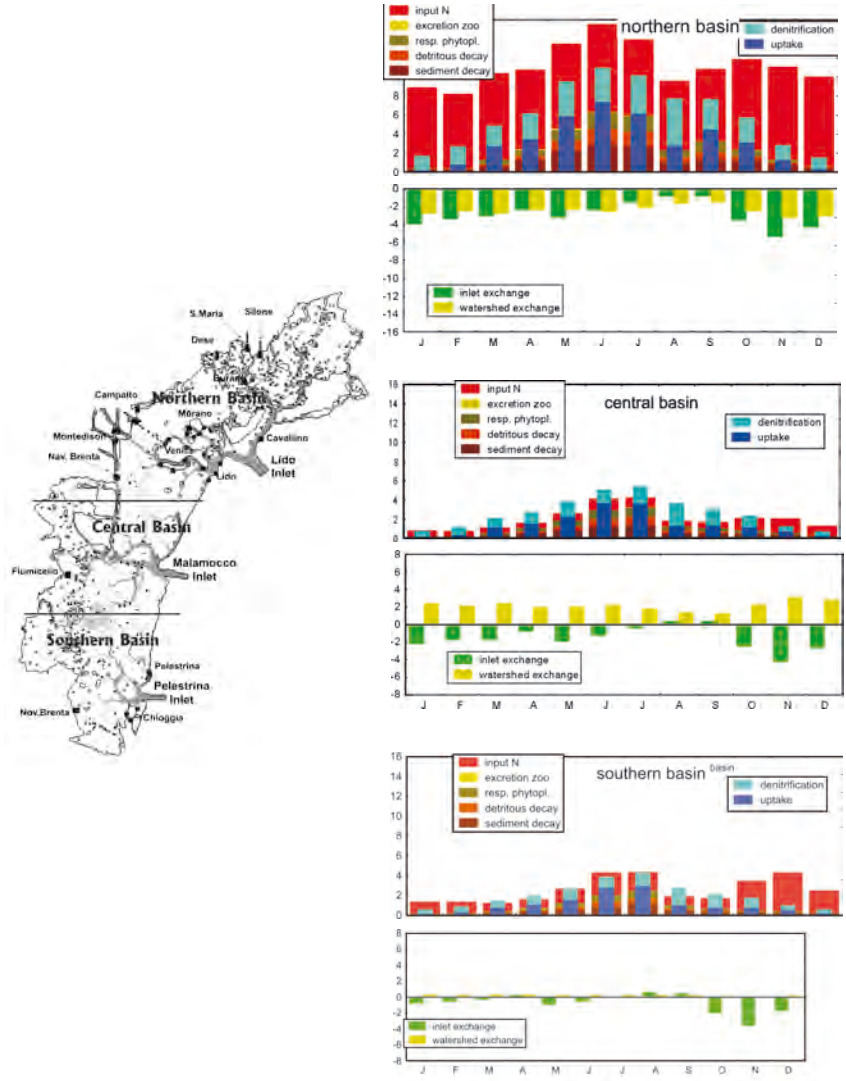

Fig. 4 - Seasonal evolution of DIN balance terms for the 3 subbasin. On the right, map of the lagoon; location (square) and name of the input sources are superimposed.

gen demand (large bar) is always significantly smaller than the sum of external inputs and recycling (narrow bar), with the exception of August. As a consequence a surplus of nitrogen exists, and there is a negative flux to the sea. Conversely, a positive flux (import) of nitrogen occurs in

August, when there is a deficiency of nitrogen lagoon. An import of nitrogen occurs also in September, in spite of a positive balance among production and loss terms within the lagoon. This might be due to the fact the exchanges are determined also by local features of the area in the vicinity of the inlets, which might be masked when averaging all over the lagoon. It must be stressed, however, that in August and September the difference in production and loss terms is small, the balance almost even, and the fluxes through the inlets almost negligible.

In general, it is therefore possible to summarise the situation by saying the lagoon abates part of the nutrient loads it receives, and exports the residual part to the sea. Export is larger in wintertime, when plankton productivity is lower.

A more detailed analysis can be performed by inspecting the time evolution of fluxes in the separate subbasins. Fig. 4 reports time evolution of fluxes which compose the nitrogen balance, arranged as in the previous Fig. 3, but averaged for the three different subbasin. It is immediately clear that the northern part of the lagoon receives the most part of nutrient load, which is consistent with the fact the major rivers and the industrial plant insist in this area (see map of Fig. 4). When added to recycling, input reach values which average around 12 t/day. Phytoplankton uptakes only a fraction of the nitrogen input in the system, and exports all over the year, both towards the Adriatic sea (dark green bar in lower panel of Fig. 3a) and towards the central sub-basins (light green bar in the lower panel of Fig. 3a). In this subbasin the situation is different. Recycling is more important than river inputs, and therefore the availability of nitrogen presents a seasonal evolution which follow the biological activity, with a maximum in summertime, while in the previous case river input were the dominant contribution. Moreover, a deficit of nitrogen would be present within the central subbasin all over the year, since nitrogen demand for phytoplankton growth and denitrification is larger than recycling and river input, which adds up to around 2.5 t/day. However, fluxes from the northern subbasin, about 2 t/day, are always more than sufficient to compensate such a deficit, and actually when those are taken into account too, a surplus of nitrogen originates for this subbasin too. As a consequence also the central subbasin exports matter through its inlet, and to a smaller extent to the southern basin too.

Exchanges with the southern basins are very small (around 0.2) as to indicate that this subbasin is independent from the other ones. Input and recycling are pretty low in the southern subbasin, but they are, most of the time, of the same order of nitrogen demand. Fluxes through the sou-

thern inlets are alternately positive and negative, but always pretty small, so confirming a substantially balanced situation. Fluxes became markedly negative only in October, November and December, when – as in other sub-basins – biological consumption is reduced and the amount of exported nutrient depends mainly on river input. In the specific case, it is the input from the Novissimo Brenta (Nov.Brenta in the map of Fig. 4) which transits through the sub-basin and gives rise to a flux toward the sea of around 2-4 t N/d.

5. *Conclusion.*

In the present paper a 3D trophic-diffusive model of water quality, corroborated by comparison of model output against experimental observations and information on rate of fluxes and processes, is used to assess time evolution of nitrogen exchange between the lagoon of Venice and the Adriatic Sea. Even if we recognise that we are dealing with a number of simplifying assumption, the use of such a model offers advantages in respect to more simplified methodologies adopted in previously published estimations.

The analysis of model results puts in evidence that the northern subbasin receives the most part of nutrient load from rivers. There is a surplus, and Northern Subbasin exports nutrients all over the year both towards the Adriatic Sea and the central subbasin. In the Central Subbasin, river input and matter recycling are not high enough as to cope with plankton requirements, but when inflows from the Northern Subbasin are taken into account too, a surplus exists also in this subbasin, and – as in the previous case – we have a net outflow towards the Adriatic Sea all over the year, except August and September. Southern Sub-basin exchanges very little with Central Subbasin, so it might be seen as isolated from the rest of the lagoon. It exchanges little with the sea too, and fluxes are both positive and negative. This implies that Southern Subbasin is the one more influenced by the sea, and who is more likely to present marine features, in comparison with the other subbasins. As a whole, however, the lagoon exports nutrient to the sea, almost 2175 t N/y. The maximal export fluxes are during wintertime, when the lagoon dilutes and disperse in the sea the input discharged by the rivers of the drainage basin. During summertime the lagoon suffers a small deficit of nitrogen that is supplied by the exchanges with the Adriatic Sea, which might therefore become, for a short interval of time and for a small amount, a source of nutrient for the lagoon.

Reference.

Cossarini G., Solidoro C., Pastres R., 2001. Modello tridimensionale di qualità dell'acqua della laguna di venezia: analisi numerica del funzionamento dell'ecosistema e del ciclo dell'azoto. Atti XXV, Congresso Nazionale SiTE, 2001.

CVN, 1990. Rapporto sullo stato attuale dell'ecosistema lagunare. Rapporto finale Studio 1.3.9

CVN, 1988. Distribuzione delle concentrazioni di inquinanti e delle velocità di corrente in diverse sezioni delle bocche di porto Studio 1.3.2.

CVN 2023. linea F, 2000. Rapporto sullo stato attuale dell'ecosistema lagunare. Consorzio Venezia Nuova.

Flindt M.R., Kamp-Nielsen L., Marques J.C., Pardal M.A., Bocci M., Bendoricchio G., Salomonsen J., Nielsen S.N., Jorgensen S.E., 1997. Description of the three shallow estuaries: Mondego River (Portugal), Roskilde Fjord (Denmark) and the Lagoon of Venice (Italy). Ecological Modelling, Vol. 102, pp 17-31.

Rossi A., 1979. Distribuzioni di clorofilla e di carbonio, azoto e fosforo totale nel particellato sospeso in acque superficiali del bacino settentrionale della laguna veneta. Tesi di laurea, Università degli studi di Padova, Facoltà di Scienze, Istituto di Biologia Animale.

Regione Veneto, 1998. Piano per la prevenzione dell'inquinamento e il risanamento delle acque del bacino idrografico immediatamente sversante nella laguna di Venezia. Regione Veneto Segreteria Regionale all'Ambiente, Direzione Tutela dell'Ambiente.

Salomonsen J., Flindt M.R., Geertz-Hansen O., 1997. Significance of advective transport of Ulva lactuca for a biomass budget on a shallow location. Ecological Modelling, Vol. 102, pp 129-132.

Sfriso A., Marcomini A., Pavoni B., 1994. Annual nutrient exchanges between the central lagoon of Venice and the northen Adriatic Sea. The science of the Total Environment, Vol. 156, pp 77-92.

Solidoro C., Cossarini G., Pastres R., 2002. Modelling nitrogen and phytoplankton in the lagoon of Venice. Marine Ecology Progress Series (Submitted).

VELFEEM (VENICE LAGOON FINITE ELEMENT ECOLOGICAL MODEL) DEVELOPMENT OF THE MODEL AND FIRST ANALYSIS ON THE INFLUENCES OF PHYSICAL FORCING ON THE ECOLOGICAL PROCESSES

C. Solidoro[1], D. Melaku Canu[1,2], G. Umgiesser[2].
[1]*Istituto Nazionale di Oceanografia e di Geofisica Sperimentale, Trieste*
[2]*Istituto per lo Studio della Dinamica delle Grandi Masse, CNR, Venezia*

Abstract.

The paper illustrates the development of a hydrodynamic water quality model for the lagoon of Venice, VELFEEM, which is a site specific implementation of a generic water quality transport model, FEEM, obtained by coupling a finite element hydrodynamic model and a standard water quality model.

The water quality module is based on EUTRO, the generic code released by US-EPA, but has been improved by adding zooplankton dynamic and properly selecting the values of the kinetic constants. In its present form the model simulates the evolution of phyotplankton, zooplankton, nutrients (phosporus, nitrogen, amonnia) detritus, BOD and dissolved oxygen.

The transport model is based on a advective-diffusion two-dimensional hydrodynamic model, which uses a finite element discretization of the basin, so allowing variable resolution and a good trade off between computational demand and need for high resolution.

The model has been used to analyze ecosystem response in climatological condition, to begin with, and then to compare the effects induced by different scenarios of external forcing, such as modification in the total nutrient load input from the river basin, modification in the wind regime, modification in the exchange with the Adriatic Sea through the inlets.

1. Introduction.

The objective of our research project is to set up a hydrodynamic water quality model for the lagoon of Venice.

Beside to constitute a research instrument, to be used in analysing water quality fluxes evolution under different scenario of meteorological and physical forcing, the model might be used as a management tool, capable to offer a contribution in the evaluation of ecological consequences of implementation of possible policy options.

In particular, and in consideration of the intervention that are under discussion for the lagoon of Venice, the model might be used for the evaluation of the most suitable zones of a water basins for different activities and the identification of optimal strategies for aquaculture, for the revision of Water Quality Target and the estimation of Maximum Permissible Load, for the assessment of the impact of settlement/restoration of wetlands. It might also be used in the assessment of the environmental effects related to interventions proposed to prevent the periodical flooding of large parts of the historical city occurring in winter and known as *acqua-alta* (high tide), such as the proposed mobile gates at the inlets or other permanent morphological modifications. Furthermore the model might constitute a base for the implementation of a model suite to address the assessment of cycles of toxics and heavy metals.

The model is obtained by coupling a transport model and a water quality model, namely the primitive equation finite element hydrodynamic model, SHYFEM, developed for the lagoon of Venice some years ago (Umgiesser and Bergamasco 1993), and an improved version of the ecological model EUTRO, a sub-model of the water quality modelling System WASP, released by the U.S. Environmental Protection Agency (EPA) (Ambrose et al., 1993).

A finite element parameterisation has been chosen for the transport model because it allows for variable and optimal spatial resolution, while keeping the computational effort at a reasonable level. In fact, the basin is described by a horizontal model grid made out of triangles that vary in size and form to best adapt to the geometrical and topographic constraints. EUTRO has been chosen as a starting point for the ecological module because WASP is a model for a generic aquatic ecosystem widely known and tested under a variety of different conditions (Desmedt et al., 1998, Vuksanovic et al., 1996, Warwick et al., 1999, Kellershohn & Tsanis et al., 1999, Tufford & McKellar, 1999).

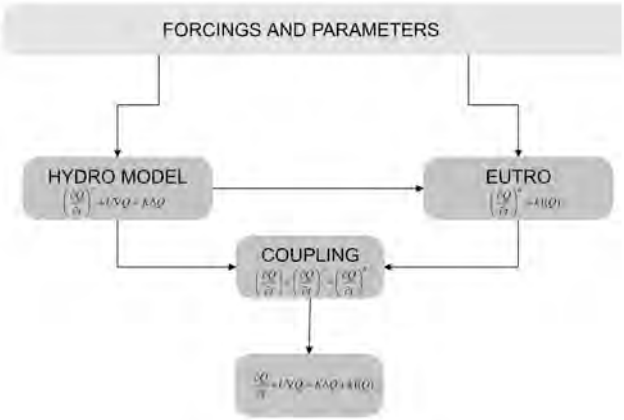

Fig. 1 - Schematic description of the structure of the integrated model FEEM.

The coupling between EUTRO and SHYFEM constitutes a structure (there after labelled Finite Element Eutrophication Model, FEEM), which is meant to be a generic water quality program that presents some advantages with respect to the WASP SYSTEM, without loosing the capability provided by EUTRO for full eutrophication dynamics. Indeed, while in the WASP SYSTEM the hydrodynamic module which computes box volumes and fluxes between boxes is a very simple 1D link-node model, and 2D or 3D set-ups are possible only for simple cases, transport phenomena are fully solved (at the cost of a still acceptable, even if larger, computational effort) in FEEM. In addition, the original EUTRO formulation has been here updated to a more general formulation, by including the possibility of modelling explicitly the zooplankton density, kept constant in time at a prescribed level in the WASP SYSTEM, by introducing an additional state variable.

The paper illustrates development of FEEM, and first steps of the application of FEEM to the lagoon of Venice. Presently this is only meant to illustrate the feasibility of site specific applications, but obviously – in a future step, and once validated against experimental data – the resulting model, thereafter named VELFEEM (Venice Lagoon Finite Element Ecological Model), might constitute a useful tool to test hypotheses about specific ecosystem mechanisms and an important part of a Decision Support System.

We like to stress here, however, that site-specific applications of FEEM might be easily implemented for other areas too. In fact, several case stu-

dies are presently going on (the application to the Adriatic Sea FEEM-AS, to the Lake Peipsi PE-FEEM, Gulf of Taranto FEEM-TA; lagoon of Cabras CA-FEEM).

The paper discusses also sensitivity of model output to changes in nutrients loading and in the intensity of physical forcing such as wind and tide actions.

The model will be briefly presented in sections 2 and 3, while in the section 4 first simulation results will be described and commented.

2. *The FEEM Model.*

The integrated model is an advective-diffusion two-dimensional ecological model made by coupling a finite element hydrodynamic model SHYFEM (Umgiesser & Bergamasco, 1993) that resolves the water balances, with the ecological model EUTRO-WASP (Water Quality Simulation Analysis), and a heat flux module. (Melaku Canu, 2001 (c)).

This system simulates the evolution and interaction of 9 ecological state variables, namely, zooplankton, phytoplankton, ammonia, nitrate, phosphate, organic nitrogen, organic phosphorous, carbonaceous biochemical oxygen demand, and dissolved oxygen. The evolution of the state variables describes the main steps of the four biogeochemical cycles of nitrogen, phosphorous, oxygen and carbon.

At each time step, the values of the variables in the spatial domain, and also the values of aggregate indexes - such a the water quality aggregated index TRIX, (Vollenveider et al. 1997) - are given.

The integration of the submodels in FEEM is described in detail in Umgiesser et al., (2001). Basically, the global temporal variation of any state variable is split into the sum of two contributions - a physical term, and a biological-reactive term - solved within two independent modules (Fig. 1).

2.1 *The transport model.*

The hydrodynamic finite element model solves the two dimensional barotropic shallow water equations on a grid of finite elements. The equations consist of the continuity equation and the momentum equation in their formulation with transports.

$$\frac{\partial \eta}{\partial t} + \frac{\partial u}{\partial x} + \frac{\partial v}{\partial y} = 0 \qquad (1)$$

$$\frac{\partial U}{\partial t} + u\frac{\partial U}{\partial x} + v\frac{\partial U}{\partial y} - fV + gH \cdot \frac{d\eta}{dx} + R \cdot U + X = 0 \qquad (2)$$

$$\frac{\partial V}{\partial t} + u\frac{\partial V}{\partial x} + v\frac{\partial V}{\partial y} + fU + gH \cdot \frac{d\eta}{dy} + R \cdot V + Y = 0 \qquad (3)$$

where η is the water level, u,v the horizontal velocities in x and y direction, f the Coriolis parameter, U,V the vertically-integrated velocities (total or barotropic transports) with

$$U = \int_{-h}^{\varsigma} u dz \qquad V = \int_{-h}^{\varsigma} v dz$$

g is the gravitational acceleration, $H=h+\eta$ the total water depth, h the undisturbed water depth, t the time and R the bottom friction coefficient.

The terms X,Y contain all other terms like the wind stress and the non-linear advective terms. The friction coefficient is determined through the Strickler formula, and the wind stress uses a constant drag coefficient.

These equations are solved in time by a semi-implicit algorithm. In this procedure the unknown transports from the momentum equation are substituted into the continuity equation resulting only in a linear system to be solved for the water levels. With the knowledge of the new water levels the unknown transports may be solved for explicitly.

The spatial discretization of the equations is done on a triangular finite element grid. These linear finite elements give enough flexibility to describe the complex geometry and bathymetry of sites like the Venice Lagoon. On this grid the water levels are described by linear form functions, with the water levels defined on the nodes (intersections) of the grid. On the other hand, the velocities are described by constant form functions over one element, which corresponds to the definition of the velocities on the center of the elements.

This "staggered" approach of defining the various variables and unknowns is well known from the finite difference technique and allows for propagation properties that conserve energy and mass. The same is also valid in this case for the finite elements.

The model is forced through the open boundaries where the water levels are prescribed and through the wind stress on the water surface.

The transport and diffusion of a dissolved substance is done through an explicit up-wind algorithm that is mass conserving. The dissolved sub-

stance is represented by linear form functions with the variables defined on each node. The variables used in the model are the temperature, salinity and all state variables of the ecological module EUTRO.

The model treats also shallow water flats. These shallow water flats during a tidal cycle are sometimes covered with water, and sometimes are dry. During the dry period these elements are taken out of the algebraic system and are later added again, once the surrounding water level is higher than the water inside the dry element. The specific implementation done here conserves the mass in each element.

2.2 *The water quality model.*

The ecological model has been developed by starting from the EUTRO code of WASP, the water Analysis Simulation program released by the US Environmental Protection Agency EPA (Ambrose et al. 1993). The module has been extracted from the original code, adapted to our case study and improved (Melaku Canu, 2001 (c)). Now it simulates the evolution of the 9 state variables ammonia NH3, nitrate NOX, phosphate OPO4, phytoplankton Phy, zooplankton Zoo, organic nitrogen ON, organic phosphorous OP, carbonaceous biogeochemical oxygen demand CBOD, and dissolved oxygen DO. The variables are connected together in four interacting systems: the nitrogen cycle, the phosphorous cycle, the oxygen cycle and the carbon cycle as shown in fig. 2.

The main improvement in respect to the original EUTRO module is the inclusion of an additional state variable for describing the dynamic of zooplankton community, which is now simulated explicitly. In the original WASP the phytoplankton mass balance equation did contain a loss term that is ascribed to grazing pressure, but such a term was computed assuming a constant predefined value for the density of zooplankton, and transferred directly to the organic matter compartment. Therefore, the original EUTRO could be seen as a particular case of NPD model, that is as one of those models in which the matter is thought to be cycling through the major compartments Nutrient, Plankton and Detritus. These models are commonly used in oceanography, where the ecosystem submodels are coupled to general circulation models of very large area, and where, as a consequence, the discretization, both spatial and temporal, and the level of details one can take into consideration, cannot be very fine. Such a hyper-aggregated representation of the ecosystem functioning is however less suitable for smaller systems, such as lagoon or coastal area, where one is usually interested in processes covering temporal scales of the

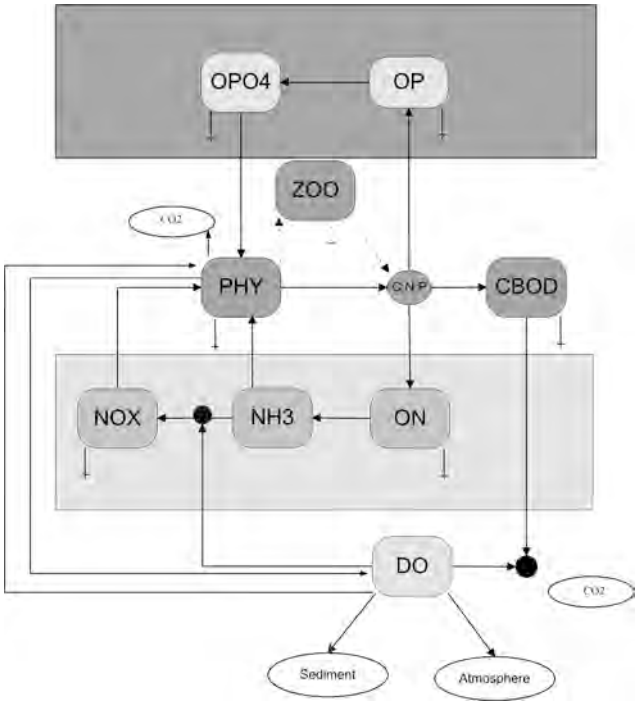

Fig. 2 - Schematic description of the structure of the Water Quality submodel EUTRO0D.

order of months or seasons, and high spatial resolution is frequently a plus. Clearly, the parameterisation used in the original EUTRO is a particularly “rich” case of the NPD models, since the compartment 'N' is expanded up to 3 distinct state variables, and other 3 state variables are used to described the compartment 'D'. It therefore appears very much appropriate to release the constrain of a unique pool for plankton community, and to distinguish, at the very least, between an autotrophyc phytoplankton community and an heterotrophic zooplankton community, upscaling in this way the model to a member of the class of the NPZD models, where the zooplankton becomes a state variable. The importance of such an extension can hardly been underestimated, since NPD systems can exhibit only the so-called ‘bottom-up’ dynamics, in which the availability of nutrient is the only driving factor controlling plankton evolution, whereas the inclusion of a predator-prey relationship enables also the arising of ‘top-down’ controlled dynamics, in which the

driving factor is the dynamic of the grazer. This is important even if one is focused mainly on phytoplankton dynamics (for example because one feels that there is not enough zooplankton data for a full calibration), and zooplankton is considered only as a 'closure' term for phytoplankton. Indeed, there is a big difference in phytoplankton evolution between the case in which grazing is parameterized by fixing the zooplankton at a constant value and the case in which zooplankton is left to evolve. In fact, only in the latter case predator-prey oscillation can arise. This might imply substantial differences on the phytoplankton evolution at monthly and seasonal scale.

In the updated version of EUTRO (thereafter labeled Eutro0D) a new state variable describes the dynamics of a generic herbivorous zooplankton compartment (ZOO), meant to be representative of the pool of all the herbivorous zooplankton species. Consequently, the evolution of phytoplankton, considered as a pool of primary producers, is driven by light intensity, temperature and concentration of nutrients in water, and by the dynamic of the grazers.

Phytoplankton growth is described by combining a maximum growth rate under optimal conditions, and a number of dimensionless factors, each ranging from 0 to 1, and each one referring to a specific environmental factor (concentration of nutrients, temperature, light availability), which reduces the phytoplanktonic growth insofar as environmental conditions are at sub-optimal levels. Phytoplankton stochiometry is fixed at the user-specified ratio, so that no luxury uptake mechanisms are considered, and the uptake of nutrients is directly linked to the phytoplankton growth, and described by the same one-step kinetic law. More specifically, the influence of inorganic phosphorous and nitrogen availability on phytoplankton growth/nutrients uptake is simulated by means of Michealis-Menten-Monod kinetics. Phytoplankton uptakes nitrogen both in the forms of ammonia and nitrate, but ammonia is assimilated preferentially, as indicated in the ammonia preference relation. The influence of temperature is given by an exponential relation, while the functional forms for the limitation due to sub-optimal light condition can be chosen between two alternative options, namely the formulation proposed by Di Toro et al. (1971) and the one proposed by Smith (1980). In Eutro0D we introduced a new option for the light limitation on growth using a Steele formulation (Steele, 1962) that can use hourly light input values. Again, the choice between different available functional forms (Ditoro, Smith, and Steele) is made by setting the index LGHTSW equal to 1, 2 or 3. The new version is therefore able to simulate diurnal variations depending on light intensity. Finally, the two more frequently used

models for combining maximum growth and limiting factors, the multiplicative and the minimum (or Liebig's) model, are both implemented, and the user can choose which one to adopt.

The evolution of the zooplankton is described by the grazing term, and by the mortality term. The grazing term is described by the Holling type II relationship between phytoplankton and zooplankton concentration and by the grazing parameter while the mortality term is described by a first order cinetic. The zooplankton assimilates the ingested phytoplankton with an efficiency EFF, and the fraction not assimilated, ecologically representative of faecal pellets and sloppy feeding, is transferred to the organic matter compartments (dotted lines Fig. 2). Finally, zooplankton mortality is described by a first order kinetics. The code has been written by adopting the standard WASP nomenclature system, and the choice between the different available functional forms is performed by setting the index IGRAZ. A choice of 0 (the default value) corresponds to the original EUTRO version, giving the user the ability to choose easily between the extended version or revert to the original one.

Nitrogen and phosphorous are returned to the organic compartment (ON, OP) via phytoplankton and zooplankton respiration and death. After mineralization, the organic form is again converted in the dissolved inorganic form available for phytoplankton growth.

The DO mass balance is influenced by almost all of the processes going on in the system. The reaeration process acts to restore the thermodynamic equilibrium level, the saturation value, while respirations activities and mineralization of particulated and dissolved organic matter consume DO and, of course, photosynthetic activity produces it. Other terms included in the DO mass balance are the ones referring to redox reactions such as nitrification and denitrification. The reaeration rate is computed from the model in agreement with either the flow-induced rate or the wind-induced rate, whichever is larger. The wind-induced reaeration rate is determined as a function of wind speed, water and air temperature, in agreement with O'Connor (1983), while the flow-induced reaeration is based on the Covar method (Covar, 1976), i.e., it is calculated as a function of current velocity, depth and temperature.

3. *VEELFEM, The Application of FEEM to the Venice Lagoon.*

The lagoon of Venice is the largest Italian lagoon. It is located in the Northern Adriatic sea and covers a surface area of around 550 Km2. It is crossed by a network of deeper channels, but the average depth is around 1

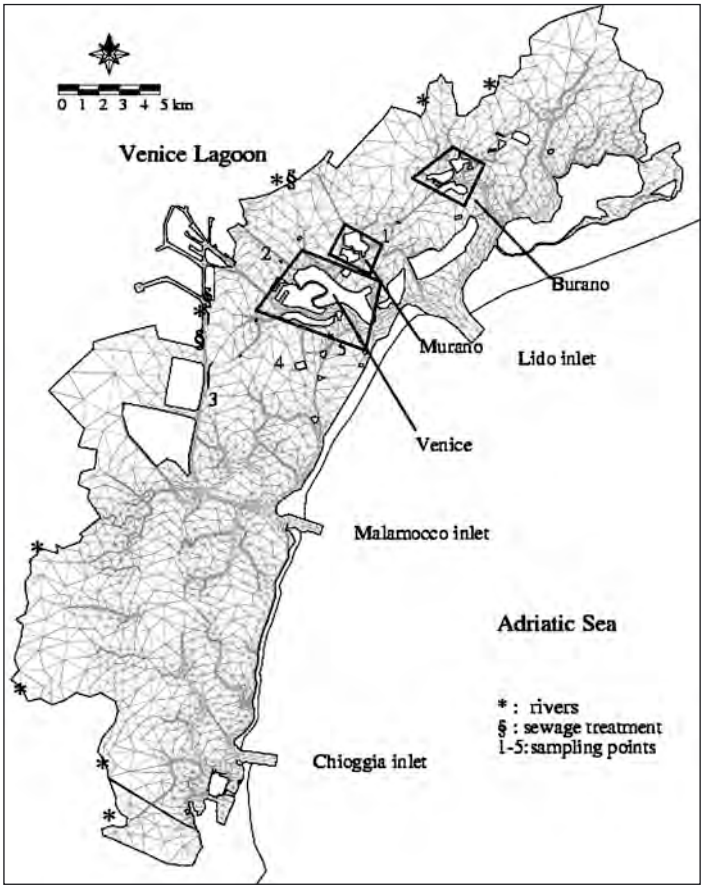

Fig. 3 - Finite Element Grid of VELFEEM.

meter. The average residence time around 10 days, varying from 1 day for the area close to the inlets to 30 days for the internal areas. The lagoon is a transitional environment between land and sea and both the influences of sea and of the main land have driven its ecological and morphological evolution, together with human actions. The lagoon exchanges with the sea 385 million of cubic meter per day on average, through three inlets (Bocca di Lido, Bocca di Malamocco and Bocca di Chioggia), and it receives, in average, 2.8 million cubic meters of freshwater per day from the drainage basin, through the main 9 rivers. It is subject to the import of nutrients and salty water from the sea, and to the riverine input of sediment, fresh water, pollutants and nutrients from the main land. Those processes interact together in

the morphological balance between erosion and silting; they also induce strong gradients in salinity and nutrient concentration, affecting the water quality and, in turn, the natural habitats distribution and composition.

The lagoon has to cope with the considerable amount of nutrients loads, that often caused eutrophication problems. In fact the Lagoon is located in one of the more densely populated Italian Regions, where intensive agriculture and important industrial activities are settled. Furthermore the city of Venice and the islands of Murano and Burano are not provided by the proper sewage treatment system: the old systems are still used, and the sludge is directly dumped into the lagoon after encountering a very rough first step of the biological degradation.

A huge effort has been made to preserve and investigate this ecosystem, mainly from an experimental point of view, but, in the last ten years, also a good number of modelling studies have been performed. In spite of this there still is a lot of modelling work to be done, including research in coupled ecological-transport models. In fact, several 0D ecological models have been proposed for nutrient cycles and macro algae proliferation (Coffaro & Sfriso, 1997, Coffaro & Bocci, 1997, Coffaro et al., 1997, Solidoro et al., 1997a, 1997b, 1997c, Pastres et al., 1995, 1997) and a box model has been set up, in order to include exchanges with the Adriatic Sea in a mass balance of nutrients (Bergamasco and Zago, 1999), but, as far as we know, only two 3D fully coupled ecological-transport models have been presented in the literature. Furthermore, one of these (Bergamasco et al., 1998) includes a primitive equations physical submodel (POM) and covers all the lagoon, but with a very coarse spatial discretization and an extremely simplified ecological sub model, while the other one - which was originally focussed only on the central part of the Lagoon of Venice (Solidoro et al., 1997a, 1997b, 1997c; Pastres et al. 1995, 1997) and has been recently updated to all the lagoon (Solidoro et al. 2001) - includes standard water quality submodel, but adopts several simplifying assumptions in its transport module, so that this model cannot resolve accurately processes which occur on time scales shorter than the tidal cycle. Also, recently, several companies have started working on the development of coupled hydrodynamic-ecological modelling, sponsored by the municipality or governmental agencies. This models, however, have not been present to the scientific community, as yet.

VEELFEM couples a primitive equation physical submodel and a standard water quality module (Melaku Canu et al. 2001 (c), Melaku Canu et al. 2002, Umgiesser et al. 2002). The finite elements numerical scheme gives enough flexibility to describe the complex geometry of the Venice Lagoon. The bathymetry is discretized by around 5000 elemets,

with a spatial resolution which varies from 30 meters to 1 km. The lagoon, the inlets and the river point sources are indicated in fig. 3, in which the model grid is plotted. The figure gives a striking example of the level of detail which can be reached by a finite element discretization and therefore of the potentiality of this approach in comparison with the more traditional finite difference approach.

Initial conditions for the ecological module are set in agreement with the values given in Regione Veneto (2000), while boundaries and loadings are entered in agreement with experimental data, as described in detail in Melaku Canu et al. (2001). The fig. 3 reports also the spatial indication of the non-point sources, i.e., the area around the populated islands of the lagoon, which receives urban loads. Light intensity and temperature are assumed to be spatially constant over the grid domain, and their values have been derived from an experimental data set of daily values, properly averaged. (Pastres and Solidoro. 1999). Daily values of light intensity are then split by the model into hourly values, taking into consideration the information, available, about how the length of the photoperiod changes during the year. The hydrodynamic model is forced also by tide at the three inlets and by a wind stress field.

As for biological submodel, we have used parameter values from literature on previous modelling works about the Venice Lagoon (Pastres and Solidoro, 1999; Solidoro et al. 2000, Pastres et al. 2001, Solidoro et al. 2002). As for physical submodel calibration has been performed versus tidal gauges. (Melaku Canu et al., 2001 (b))

Likely, there still is space for improving the capability of the model to reproduce quantitatively real evolution. However a formal calibration of a model of this complexity and of this computational demand is very difficult, and as not been performed as yet. Instead, after some empirical calibration, we have focused on the comparison between model predictions under different scenarios of forcings. The assumption is that the emerging indication are robust, at least qualitatively, in respect of minor modifications in some parameter values.

3.1 *Description of scenario.*

In order to compare the variability in water quality induced by changes in external conditions and physical forcing, we have defined 4 scenarios, by considering a reference scenario and by varying - one at a time – wind, tide, and nutrient load. The model is run for one year under each of the four scenarios, and results are compared. Each simulation took around 4 days of computer time, by using a medium power workstation

Our reference scenario is described by simulation *ref*. Here the total amount of nutrient loading is given by the DRAIN project results, and is 3996 tons/year for the total nitrogen and 228 tons/year for the total phosphorous. This is the most update estimate available. (Zonta et al., 2001). Total loading from the drainage basin are input assuming that the whole river network present a constant concentration of nutrients, while the amount of water discharged from each river (and therefore the amount of loading discharged from it) varies in agreement with the water flow average values given by Bernardi et al. (1993). In order to simulate seasonality, these average values have been multiplied by a sinusoidal function. The tide used in the reference scenario is an idealized sinusoidal M2 tide, typical for the Northern Adriatic. Wind action is not included.

The *tide* scenario differs from the reference scenario for the tide, that is now given by the experimental value of sea levels measured in 1987. This simulation is made in order to see how the tide forcing affects the water quality and its variability in time and space.

The *wind* scenario is done to investigate the variability due to the wind action: the model is here forced by an experimental wind stress data file measured in the lagoon of Venice in 1987.

A fourth scenario *nut* is made to evaluate the variation in water quality induced by changes in nutrient load from the drainage basin. This is the intervention more frequently planned when thinking of preservation of water body subjected to eutrophication. On this purpose a run has been performed in which total loads of N and P are , respectively, 26% and 58% higher than in *ref* . These values are the estimate given in 2000 by Regione Veneto (Regione Veneto 2000), and therefore the difference between *ref* and *nut* gives also an idea of the uncertainty in Water Quality due by uncertainty in nutrient loading.

4. *Result and discussion.*

The water quality of a basin is defined in terms of actual and potential primary productivity[1]. Usually it is assessed by taking into account chlorophyll and DO concentration, which are proxies for actual primary

[1] Clearly, from a broader point of view other parameters should to be considered as well, such as level of toxicant and pollutants, and presence of pathogenic bacterial. In literature, however, these aspects are kept distinct and dealt with in a different context, while water quality model traditionally address only the parameters related to eutrophication.

production, as well as concentrations of nutrients, which can be seen as proxies for potential fertility. Indeed, in agreement with the new Italian legislation, in the lagoon of Venice water quality targets regard concentration of Nitrogen and Phosphorus, which should be below a given threshold, and the trophic index TRIX, which is defined as linear combination of chlorophyll density and the logarithms of nutrients and DO (Vollenweider et al. 1997).

$$TRIX=\frac{1}{2}[Log_{10}(Chla*(DO*100/02sat)*DIN*PIN)+1.5]$$

where *Chla* is the phytoplankton concentration, expressed in Chlorophyll a, *DO* is the dissolved oxygen concentration, *O2sat* is the oxygen saturation value, *DIN* is the total dissolved inorganic nitrogen and *PIN* is the particulate inorganic nitrogen. It might be worth to note here that the index can be seen as the first component of a principal component analysis on water quality data collected in a monitoring program which is currently going on in the lagoon, that is as a (diagnostic) variable which summarises an important fraction of total variability of the system (Solidoro and Cossarini, 2001).

The model simulations give the temporal evolutions of the spatial distributions of the state variables. From these, it is possible to compute the value of trophic indexes, too, including TRIX.

Effects of physical forcing, and namely of riverine input and tidal exchanges are clearly recognisable in spatial distribution of the state variables. As an example, while analysing the ref scenario it is possible to note that nutrient concentration is higher in the northern basin, and lower in the southern, and that a gradient from the main land toward the sea inlet is also present. Fig. 4 presents the yearly averaged spatial distribution of total dissolved nitrogen, but this pattern is maintained throughout the whole year, and it suggests that, in general, phytoplankton blooms are not nutrient limited. This is confirmed by the time evolutions of dissolved inorganic nitrogen, (not shown) which emphases as during the blooming season there is only a low depletion of nutrient. More specifically, depletion is higher close to river estuaries, where nutrient concentration is higher and phytoplankton blooms more intense, and lower in the vicinity of the inlets. However, even when nutrients are at their minimum values, their concentration is higher than the respective half saturation constants so that nutrient availability controls the phytoplankton dynamics only for short interval of time, and only in the less eutrophic area, which are those

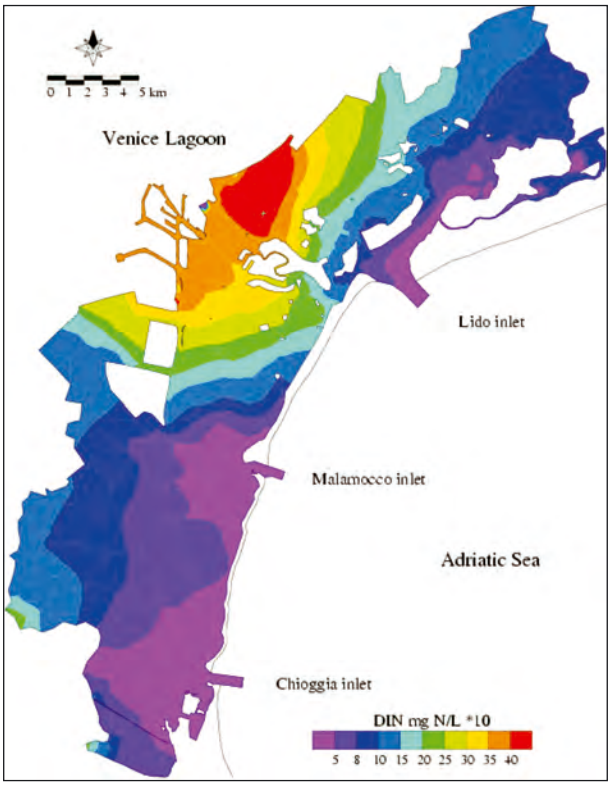

Fig. 4 - Yearly averaged spatial distribution of total dissolved nitrogen in the reference scenario (ref).

far from the point sources of nutrients.Phytoplankton dynamic is clearly light and temperature driven. In winter time the concentration values are low in the whole basin, at levels around 0.015 mg/L of Carbon, then in April, when temperature rises, first blooms appear. Blooming season lasts until September, when temperature is again too low for supporting photosynthesis. Within the blooming season nutrients are uptaken, and their concentration became, in some situation and for short intervals, so low as to limit phytoplankton growth. However it is possible to note that blooms start where water is shallow, and therefore irradiance and temperature reach values favorable to growth faster, and wherever nutrient concentration is higher, that is close to the river mouths, around the city of Venice, where urban loads are input and, more generally, in the northern part of the lagoon. The highest blooms are reached in June and July with

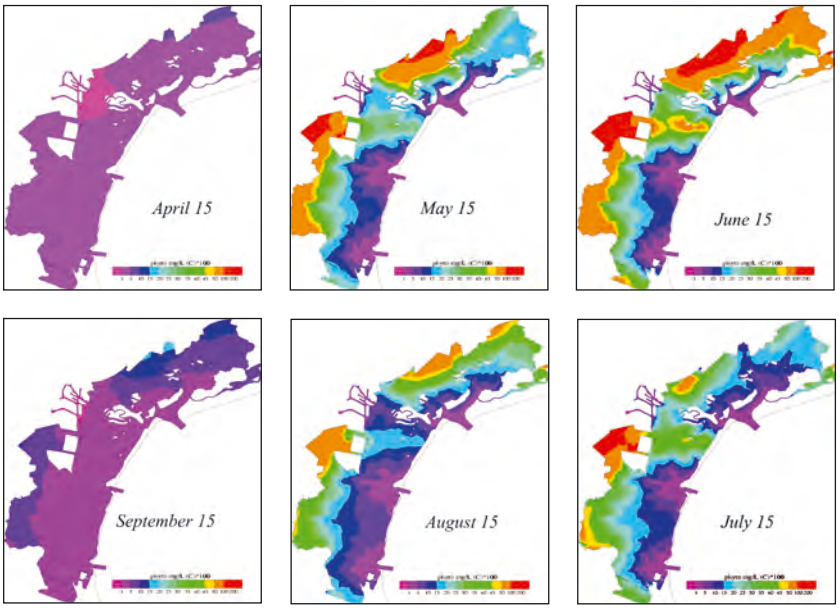

Fig. 5 - Spatial distributions of phytoplankon in six different moments of the year.

values of 4-4.5 mg C/L. Tidal exchanges with the sea, which present a lower concentration of phytoplankton, are clearly noticeable too. Fig. 5 illustrates, as an example, spatial distributions of phytoplankton in six different moments of the year. The spatial distribution of CBOD concentration levels exhibits a similar pattern, but in this case – besides rivers and urban loads - it possible to notice also the direct influence of the phytoplankton blooms, CBOD concentration rises in correspondence to them. The oxygen concentration gradient is negative from the main land toward the sea inlet, during the coolest season, specifically during the months of January and December, and it goes in the opposite direction during the other months. Clearly, for this variable as well for the other one, smaller scale features can be identified which are superimposed to this general pattern, because of the peculiarity of the different location, and of the combination of differing interacting processes. These features are common to all the scenarios here considered, even if the figures above described refer to the reference scenario *ref.*

The implementations of the *wind* and *tide* scenarios produce little changes in phytoplankton distribution. Conversely, easily recognisable modifications are induced in the dynamic and spatial distribution of

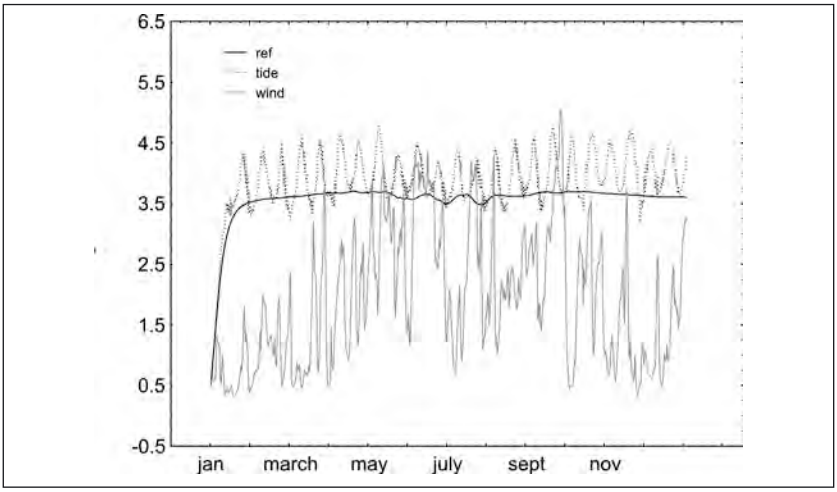

Fig. 6 - Comparison of average nitrogen evolution under the sceanrio ref, tied, and wind.

nutrients and, as a consequence of TRIX. In addition, nutrients and TRIX are the parameters which should be monitored in agreement with the indication given in the Italian legislation, and therefore we focus on them in our analysis.

The incorporation of realistic values of tide does not affect significantly the spatial distribution, but introduces an oscillation in the response, since beside the M2 tide there is now the neap/spring cycle, which was not included in the ref scenario. The comparison of the continuos and dotted lines in fig. 6 clearly illustrates this for the sampling point number 1. By contrast, the introduction of realistic wind stress alters also the averaged value of the response, as it is illustrated, always in fig. 6, by grey line.

The comparison among evolution of concentration of total Dissolved Inorganic Nitrogen in other locations (sampling points 2-4 of figure 2) puts in evidence as the introduction of realistic values of physical forcing alters in different way different locations, depending on the exposure to tidal expansion and sensitivity to winds. Points which are close to the inlets, such as station 5, present higher tidal induced oscillation, and results given by different scenarios are similar. On the contrary differences among scenarios are emphasized in points which are far from the inlets, like station 3 (results not shown here).

The comparison of spatial distribution confirms that little differences are found among the ref and the tide scenario, while a different pattern is

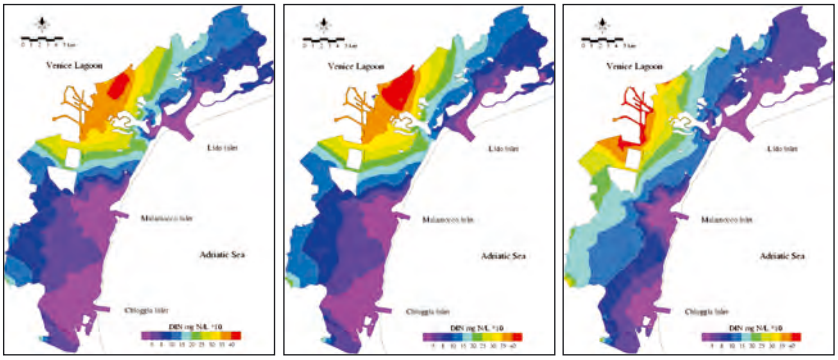

Fig. 7 - Illustrate this by comparing the yearly averaged spatial distribution of DIN for the 3 scenarios ref, wind and tide.

found under the *wind* scenario. In the latter case wind induced currents alter the spatial distribution of nutrient which results higher in the area close to the main land in the southern part of the lagoon, and lower in the vicinity of the sea and in the northern part, as if a sort of squeezing and anticlockwise rotation would have exerted on the variable field. Fig. 7 illustrate this by comparing the yearly averaged spatial distribution of DIN for the 3 scenarios ref wind and tide. Similar consideration can be made if a passive traces is considered (not shown here).

Differences in the water quality under the different scenarios can be visualized also by comparing the spatial distribution of the trophic index, which indeed is meant to summarize the information contained in the other parameters too. First raw of Fig. 8 illustrates the comparison of the yearly averaged value of TRIX, while the second and thirds raws gives a suggestion on the temporal variability of such an average, by reporting, for each location, respectively the minimum and maximal value reached during the year.

When analysing the mean annual distribution of TRIX, *ref* and *tide* scenarios are similar, with water quality just slightly higher, as a consequence of the introduction of real tide. Instead, model reproduction of the mean annual distribution of TRIX turn out to be more sensitive to the parameterisation of the wind stress. Specifically, it can be seen as the inclusion of a realistic scenario of wind gives better condition for the most part of the lagoon. A statistical test (t-test) confirms that differences in the maps are statistically significant in all the cases . It should be noted here that the palette (colorbar) has been chosen in agreement with the discretization in classes given by the Italian water quality act (dlgs. 192, 1999)

values lower than 4 indicates good water quality conditions, values higher than 6 indicates bad conditions.

The assessment of water quality level, however, cannot be made by considering only the yearly averaged values, since the averaging procedure masks the variability of the signal while in reality, beside the mean value, one is interested also in the probability that critical conditions arise. Since bad water quality moments are traced by very high level of the trophic index, the inspection of the third raw in figure 8, in which it is reported the worst situation reached in each point of the lagoon during the year, seems appropriate. The analysis of these maps indicates that the wind scenario gives the worst situation, while the safest condition is the result of the tide scenario. This is consistent with what we have already observed, that is that the introduction of realistic value of physical forcings enhances the variability of the signal, so that even if the average value is lower, the possibility that critical conditions (high values of TRIX) arise in some moment is higher . The comparison of maps in fig. 8 confirms that the highest variability is induced by the wind scenario.

Finally, in order to assess to which extent mean annual distribution of TRIX, and therefore our evaluation of water quality level in the lagoon, is sensitive to realistic parameterization of wind and tide, we have run a simulation under the nut scenario, and used the sensitivity to a change in the nutrient load as a reference term. The comparison among different sensitivities has been made by analysing 4 whisker-box plots (figure 9), which illustrate – for each scenario – mean values and spatial variability of the yearly average values of every point of the lagoon. Clearly, an increment of nutrient load significantly affects ecosystem dynamics, but it is interesting to note that variation in TRIX, though significantly higher than those produced by other scenarios here considered, is not so high as to make them negligible in comparison. Actually, it is possible to appreciate that the variations induces by the introduction of realistic winds is as high as about 20% of the variation induces by reduction of nutrient loads. However, a statistical test (t-test) proves that all the distribution are statistically different.

5. *Conclusions.*

The coupled hydrodynamic-ecological model VELFEEM set up for the Lagoon of Venice has been used to run four different one-year simulations varying the forcings conditions and the boundary conditions.

The model provides full space and time evolution of the state variables, and reproduces their time and space variability.

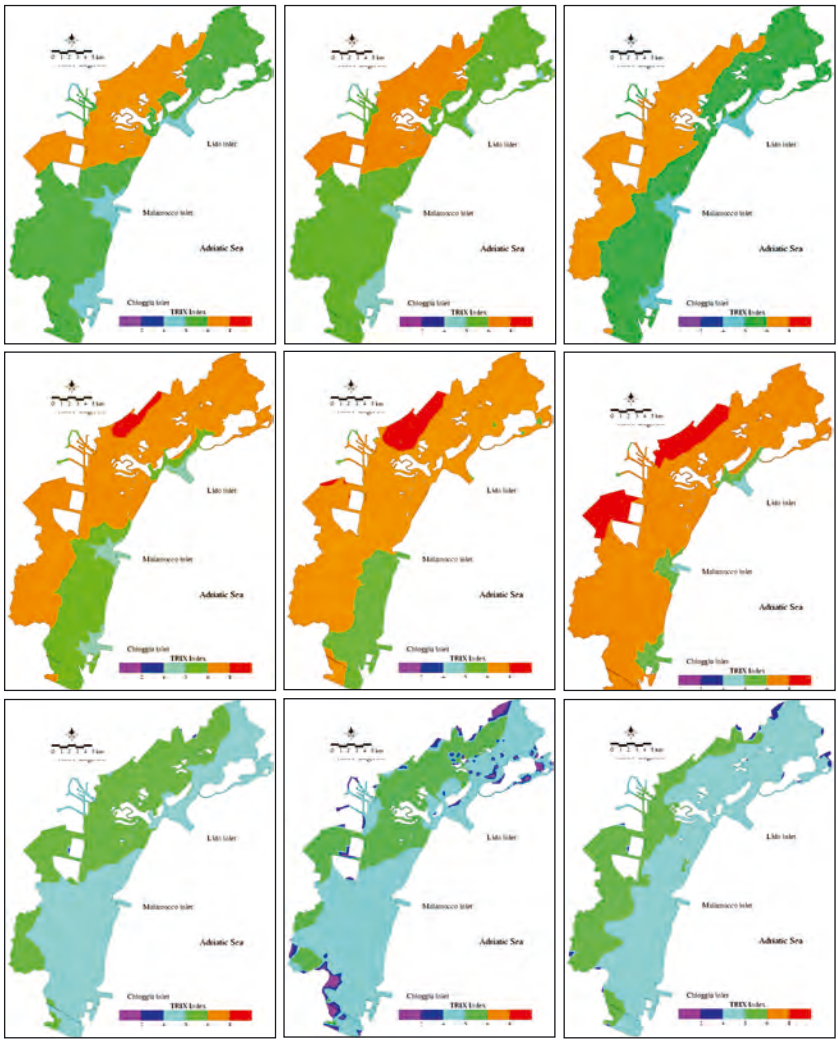

Fig. 8 - Comparison of the yearly averaged value of TRIX (first raw), the maximum value of TRIX reached during the year in each loactions (second raw), the minimum value of TRIX reached during the year in each loactions (third raw). Scenario ref (1st column), tide (2st column), wind (third column).

Model output is sensitive to variation in the physical forcings, and in particular to the parameterization of the wind stress. Indeed the variation induced by modification in the wind stress are smaller, but not negligible,

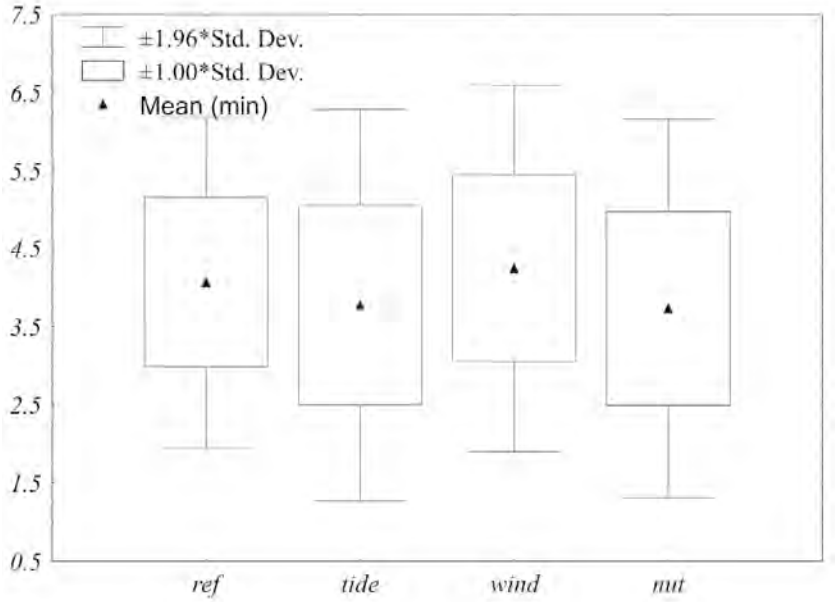

Fig. 9 - Comparison among mean values and spatial variability of the yearly average of TRIX for every point of the lagoon, under different scenarios.

in comparison with the ones produced by significant variation in the nutrient load.

Results exemplify how a numerical model can be used as Decision Support System in water quality management. They confirm that water quality is strongly affected by nutrient load, and therefore a reduction of nutrient load can be an important step towards improvement of water quality, but put in evidence that a proper parameterisation of physical forcing, and in particular of wind stress, is important, because the uncertainty induced by oversimplifications in the descriptions of this factors is relevant.

Accordingly, the effort recently made in order to estimate the nutrient load coming from the watershed are to be considered valuable, but resources should be devoted to the investigation of other important processes, too. This includes the role played by physical forcing in the definition of the water quality level, and the modality of exchanges between lagoon and sea. Certainly, a proper parameterization of these processes would increase the accuracy of our model prediction.

Ecological submodel: Mass balance equations and functional form.

Mass balances			
			General Reactor Equation
$Q(PHY) = (GP1 - DP1 - GRZ) * PHY$	*1*		*phytoplankcton Phy [mg C/L]*
$Q(ZOO) = (GZ - DZ) * ZOO$	*2*		*zooplankton Z: mg C/L]*
$Q(NH3) = (N_{alg1} + ON1 - N_{alg2} - N1)$	*3*		*ammonia NH3 [mg N/L]*
$Q(NOX) = (N1 - NO_{alg} - NIT1)$	*4*		*nitrate Nox [mg N/L]*
$Q(ON) = (ON_{alg} - ON1)$	*5*		*Organic nitrogen ON [mg N/L]*
$Q(OPO4) = (OP_{alg1} + OP1 - OP_{alg2})$	*6*		*Inorganic phosphorous OPO4 [mg P/L]*
$Q(OP) = (OP_{alg3} - OP1)$	*7*		*Organic phosphorous OP [mg P/L]*
$Q(CBOD) = (C1 - OX - (\frac{5}{4} * \frac{32}{14} * NIT1))$	*8*		*Carbonaceous biogeochemical oxygen demand CBOD mg O_2/L*
$Q(O) = DO1 + DO2 + DO3 - (OC * RES) - \left(\frac{64}{14} * N1\right) - OX - SOD$	*9*		*Dissolve oxygen DO [mg O_2/L]*

Where

Functional expressions		*Description*
$GP1 = L_{mut} * L_{light} * K1C * K1T^{(T-T_n)}$	*10*	*phytoplankton growth rate with nutrient and light limitation*
$DP1 = RES + K1D$	*11*	*phytoplankton respiration and death rate*
$GPP = GP1 * PHY$	*12*	*phytoplankton growth*
$DPP = DP1 * PHY$	*13*	*phytoplankton death*
$GRZ = KGRZ * \frac{PHY}{PHY + KPZ} * ZOO$	*14*	*grazing rate coefficient*
$GZ = EFF * GRZ$	*15*	*zooplankton growth rate*
$DZ = KDZ * ZOO$	*16*	*zooplankton death rate*
$PHSNK = (1 - EFF) * GRZ * PHY$	*17*	*grazing inefficiency on phytoplankton*
$N_{alg1} = NC * DPP * (1 - FON)$	*18*	*source of ammonia from algal death*
$N_{alg2} = PN * NC * GPP$	*19*	*sink of ammonia for algal growth*
$NO_{alg} = (1. - PN) * NC * GPP$	*20*	*sink of nitrate for algal growth*
$ON_{alg} = NC * (DPP * FON + PHSNK + DZ)$	*21*	*source of organic nitrogen from phytoplankton and zooplankton death*
$N1 = KC_{nit} * KT_{nit}^{(T-T_n)} * NH3 * \frac{DO}{K_{nit} + DO}$	*22*	*Nitrification*
$NIT1 = KC_{denit} KT_{denit}^{(T-T_n)} * NOX * \frac{K_{denit}}{K_{denit} + DO}$	*23*	*denitrification*
$ON1 = KNC_{min} * KNT_{min}^{(T-T_n)} * ON$	*24*	*mineralization of ON*
$OP1 = KPC_{min} * KPT_{min}^{(T-T_n)} * OP$	*25*	*mineralization of OP*
$OP_{alg1} = PC * DPP * (1. - FOP)$	*26*	*source of inorganic phosphorous from algal death,*
$OP_{alg2} = PC * GPP$	*27*	*sink of inorganic phosphorous for algal growth*
$OP_{alg3} = PC * (DPP * FOP + PHSNK + DZ)$	*28*	*source of organic phosphorous from phytoplankton and zooplankton death*
$OX = KDC * KDT^{(T-T_n)} * CBOD * \frac{DO}{KBOD + DO}$	*29*	*oxidation of CBOD*
$C1 = OC * (DPP + PHSNK + DZ)$	*30*	*source of CBOD from phytoplankton and zooplankton death*
$DO1 = KA * (O_{sat} - DO)$	*31*	*reareation term*
$DO2 = PN * GP1 * PHY * OC$	*32*	*dissolved oxygen produced by phytoplankton using NH3*
$DO3 = (1 - PN) * GP1 * PHY * 32 * \left(\frac{1}{12} + 1.5 * \frac{NC}{14}\right)$	*33*	*growth of phytoplankton using NOX*
$PN = \frac{NH3 * NOX}{(KN + NH3) * (KN + NOX)} + \frac{NH3 * KN}{(NH3 + NOX) * (KN + NOX)}$	*34*	*ammonia preference*
$RES = K1RC * K1RT^{(T-T_n)}$	*35*	*algal respiration*
$SOD = (\frac{SOD1}{H} * SODT^{(T-T_n)})$	*36*	*sediment oxygen demand*
$L_{mut} = min(X1, X2)$ or $mult(X1, X2)$	*37*	*minimum or multiplicative nutrient limitation for phytoplankton growth*
$X1 = \frac{(NH3 + NOX)}{KN + NH3 + NOX}$	*38*	*nitrogen limitation for phytoplankton growth*
$X2 = \frac{OPO4}{KP + OPO4}$	*39*	*phosphorous limitation for phytoplankton growth*
$L_{light} = \frac{I_0}{I_s} * e^{-(KE * H1)} * e^{(1 - \frac{I_0}{I_s} * e^{-(KE * H1)})}$	*40*	*light limitation for phytoplankton growth*
$KA = F(WIND, VEL, T, T_{air}, H)$	*41*	*re-areation coefficient (Covar...., O'Connor....)*

With

Variables		
T	*[°C]*	*water temperature*
T_{air}	*[°C]*	*air temperature*
O_{sat}	*[mg/L]*	*DO concentration value at saturation*
I_0	*[lux/day]*	*incident light intensity at the surface*
H	*[m]*	*depth*
VOL	*[m^3]*	*volume*
VEL	*[m/sec]*	*current speed*
$WIND$	*[m/sec]*	*wind speed*

Reference.

Ambrose R. B., Wool T. A., Martin J.L., 1993. The water quality analysis simulation program, Wasp5: Model documentation. Environmental Research Laboratory, Athens, Georgia Vol. a, pp. 1-281, Vol. b. pp. 1-81.

Bergamasco A. and Zago C., 1999. Exploring the Nitrogen Cycle and Macroalgae Dynamics in the Lagoon of Venice Using a Multibox Model. Estuarine, Coastal and Shelf Science 48: 155-175.

Bergamasco A., Carniel S., Pastres R., Pecenik G., 1998. A Unified Approach to the Modelling of the Venice Lagoon-Adriatic Sea Ecosystem. Estuarine, Coastal and Shelf Science 46: 483-492.

Bernardi S., Cecchi R., Costa F., Ghermandi G., Vazzoler S., 1986. Trasferimento di acqua dolce e di inquinanti nella Laguna di Venezia. Inquinamento anno XXVIII n°1/2:2-20.

Coffaro G. and Bocci M.,1997. Resources competition between *Ulva Rigida* and *Zostera marina*: a quantitative approach applied to the Lagoon of Venice. Ecological Modelling. 102: 85-94.

Coffaro G. and Sfriso A., 1997. Simulation model of *Ulva rigida* growth in shallow water of the Lagoon of Venice. Ecological Modelling. 102: 55-66.

Coffaro G., Bocci M., and Bendoricchio G., 1997. Application of structural dynamic approach to estimate space variability of primary producers in shallow marine water. Ecological Modelling. 102: 97-114.

Covar A.P., 1976. Selecting the proper reaeration coefficient for Use in Water Quality Models. Presented at the U.S. EPA Conference on Environmental Simulation Modeling, April 19-22, 1976, Cincinnati Ohio.

Desmedt F., Vuksanovic V., Vanmeerbeeck S. and Reyns D., 1998. A time dependent flow model for heavy metals in the Scheldt Estuary. Hydrobiologia. 366:143-155.

Di Toro D.M., O'Connor D.J. and Thomann R.V., 1971. A Dynamic Model of the Phytoplankton Population in the Sacramento San Joaquin Delta. Adv. Chem. Ser. 106, Am. Chem. Soc., Washington DC, pp. 131-180.

Kellershohn D.A. and Tsanis I.K., 1999. 3D Eutrophication modeling of Hamilton Harbour: Analysis of remedial options. Journal of Great Lakes Research. 25(1):3-25.

Melaku Canu D., Umgiesser G., Solidoro C., 2001. (a) Short term simulations under winter conditions in the lagoon of Venice: a contribution to the environmental impact assessment of a temporary closure of the inlets. Ecological Modelling, Vol 138/1-3, pp 215-230

Melaku Canu D., Umgiesser G., Bonato N., Ferla M., 2001. (b) Analisi della circolazione nella Laguna di Venezia durante gli eventi di acqua alta. comunicazione LXXXVII Congresso Nazionale Società Italiana di Fisica. Milano. (submitted, this issue)

Melaku Canu D., 2001, (c). Developing an ecological model for the lagoon of Venice. Technical report n° 244 ISDGM-CNR. Marzo 2001

Melaku Canu D., Solidoro C., Umgiesser G., 2002. Modelling the response of the lagoon of Venice Ecosystem to variation in the physical forcings (under revision in Ecologial Modelling)

O'Connor D.J., 1983. Wind effects on Gas-Liquid Transfer Coefficients. Journal of Environmental Engineering, Volume 109, N° 9, pp. 731-752.

Pastres R., Solidoro C., Cossarini G., Melaku Canu D., Dejak C., 2001. Managing the rearing of Tapes philippinarum in the lagoon of Venice: a decision support system Ecol. Modelling , 138: 213-245

Pastres R., Franco D., Pecenik G., Solidoro C. and Dejak C., 1997. Local sensitivity analysis of a distributed parameter water quality model. *Reliability Engineering and System Safety Journal*. 57: 21-30 Elsevier (Northern Ireland).

Pastres R., Franco D., Pecenik G., Solidoro C. and Dejak C., 1995. Using parallel computers in environmental modelling: a working example. *Ecol. Modelling*. 80, 1: 69-86. Elsevier (Amsterdam).

Regione Veneto Segreteria Regionale all'Ambiente, 1998, aggiornamento 2000. Piano per la Prevenzione dell'inquinamento e il risanamento delle acque del bacino idrografico immediatamente sversante nella Laguna di Venezia

Smith R. A., 1980. The theoretical Basis for Estimating Phytoplankton Production and Specific Growth Rate from Chlorophyll, Light and Temperature Data. Ecological Modelling 10, pp. 243-264.

Solidoro C., Pastres R. Melaku Canu D., Pellizzato M., Rossi R., 2001. Modelling the growth of Tapes philippinarum in Northern Adriatic lagoons. Marine Ecology Progress Series, Vol. 199, pp 137-148.

Solidoro and Cossarini, 2001. Analisi ed interpretazione dei dati anche mediante un modello di qualità dell'acqua. Mela1. Techinical report Consorzio Venezia Nuova.

Solidoro C., Cossarini G., Pastres R., 2002. Nutrient dynamics in coastal ecosystems: modelling nitrogen fluxes in the lagoon of Venice. (submitted to Marine Ecology Progress Series)

Solidoro C., Brando E.V., Dejak C., Franco D., Pastres R. and Pecenik G., 1997(c). Simulation of the seasonal evolution of macroalge in the Lagoon of Venice. *Envinromental Modelling and Assesment* 2:65-71, Baltzer Science Pubblication (The Netherlands).

Solidoro C., Brando V.E., Dejak C., Franco D., Pastres R. and Pecenik G., 1997(b). Long term simulation of population dynamic of Ulva rigida in the Lagoon of Venice. Ecological Modelling 102: 259-272 Elsevier (Amsterdam).

Solidoro C., Pecenik G., Pastres R., Franco D. and Dejak C., 1997 (a). Modelling *Uva rigida* in the Venice Lagoon: Model structure identification and first parameters estimation. *Ecol Modelling* 94: 191-206 Elsevier (Amsterdam).

Steele J.H., 1962. Environmental Control of Photosynthesis in the Sea. Limnol. Oceanogr. 7:137-150.

Tufford D.L. and McKellar H.N., 1999. Spatial and temporal hydrodynamic and water quality modeling analysis of a large reservoir on the South Carolina (USA) coastal plain. Ecological Modelling. 114(2-3):137-173

Umgiesser G., Melaku Canu D., Solidoro C., Ambrose B., 2000. VELFEEM, a Finite Element Ecological Model for the Lagoon of Venice. Internally coupling FEM with a water quality module of WASP (in Environmental Modelling and Software, in press)

Umgiesser G. and Bergamasco A., 1993. A staggered grid finite element model of the Venice Lagoon. In: K.Morgan, E. Ofiate, J .Periaux, & Zienkiewicz, O.C. eds, Finite Elements in Fluids. Pineridge Press.

Vollenweider R.A., Giovanardi F., Montanari G., Rinaldi A., 1998. Characterization of the trophic conditions of marine coastal waters, with special reference to the nNW Adriatic Sea: proposal for a trophic scale, turbidity and generalized Water Quality Index. ", Environmetrics-Chichester, 9: 329-357

Vuksanovic V., Desmedt F. and Vanmeerbeeck S., 1996. Transport of Polychlorinated biphenyls (PCB) in the Scheldt Estuary simulated with the water quality model WASP. Journal of Hydrology. 174(1-2): 1-18.

Warwick J.J., Cockrum D. and McKay A., 1999. Modeling the impact of subsurface nutrient flux on water quality in the Lower Truckee River, Nevada. Journal of the American Water Resources Association. 35(4): 837-851.

Zonta R., Bettiol C., Collavini F., Fagarazzi O.E., Zaggia L., Zuliani A., 2001. DRAIN project- Fresh water and pollutant transfer from the drainage basin to the Venice Lagoon Project Report N. 15B June.

RESEARCH LINE 3.6.
Biodiversity in the Venice Lagoon

FISH DIVERSITY IN THE VENICE LAGOON: PRELIMINARY REPORT

D. Mainardi[1], R. Fiorin[1], A. Franco[1], P. Franzoi[1],
O. Giovanardi[2], A. Granzotto[1]
A. Libertini[3], S. Malavasi[1], F. Pranovi[1], F. Riccato[1], P. Torricelli[1]
[1]*Dipartimento di Scienze Ambientali, Università Cà Foscari, Venezia*
[2]*Istituto centrale per la ricerca scientifica e tecnologica applicata al mare, Chioggia (VE)*
[3] *Istituto di Biologia del Mare, CNR, Venezia*

1. *Introduction.*

The biodiversity is not an entity in itself, but it refers to the intrinsic property and universal attribute of all living forms that each individual is unique [Solbrig, 2000]. The concept encompasses the variety of the world's organisms together with the interrelatedness of genes, species and ecosystems that create the great, interdependent system of the life on earth. Genes, species and ecosystems reflect the different levels of complexity in biological organisation at which it is possible to measure biodiversity.

The coastal lagoons are environments subjected to remarkable fluctuations in many characteristics such as salinity, temperature, nutrient concentration, hydrodynamic conditions. The lagoonal species have evolved a very wide tolerance to the environmental variation while the habitat availability and resource partitioning mainly affect their distribution patterns. These ecosystems are important sites for fish, as nursery areas, overwintering sites and migration areas, which naturally support large numbers of fish [Elliot & Hemingway, 2002].

The lagoon of Venice supports high fish production. The environmental variability and unpredictability select for a low diversity of resident fish, highly specialized to cope with the environmental changes, and for an high abundance of transient species [Mann, 2000; Elliot & Hemingway, 2002]. The knowledge of fish diversity can be used to assess both the conservation options and resource exploitation.

This study presents a preliminary report on the fish fauna diversity in the lagoon of Venice at the species and community levels. Community attribu-

tes such as species composition, in terms of abundance, diversity and functional groups, have been investigated, while cytogenetic technics have been used to determine differences at the species level in the two most representative families (Syngnathidae and Gobiidae) of the lagoonal fish fauna.

2. *Materials and Methods.*

2.1. *Study site.*

The Venice Lagoon is the largest lagoon of the Mediterranean basin. It is characterized by the presence of macroalgae and seagrass meadows which show a high patchy distribution. Also morphological and physico-chemical parameters show a high heterogeneity in space and time, and this generates strong gradients [Sistema Veneziano; Sacchi, 1985] which give rise to a high habitat variability. To partially cover this high variability three sampling areas, located in two different basins were chosen: Ca' Zane (CZ) located in the Northern part of the Lagoon and Lido (LD) and Lago dei Teneri (LT), located southern of Venice (fig. 1).

2.2. *Field sampling.*

Fish were monthly collected by means of fyke nets with the aid of local fishermen from March to December 2001 in each sampling area. The fyke net is a traditional static gear used to exploit shallows and consists of a barrier about 40 m long that guides the fish towards four or more cone shaped unbaited traps. The nets are located to intercept the fish moving according to the tidal flows which in this area are the strongest of all Mediterranean basin (to 1m in height). These nets are often placed combined in a system which could cover more than one square kilometer; fish trapped are periodically (once every two days) collected by fishermen. The use of such a fishing gear could allow to obtain samples with a wide spatio-temporal distribution and probably better representative of fish community of the sampling area. All fish caught were transferred in laboratory where they were identified to the species level and counted.

2.3. *Community analysis.*

Due to the different number of nets used by fishermen during the fishing season, catch data were standardized as catch per unit effort (CPUE) by using the single trap as unit effort.

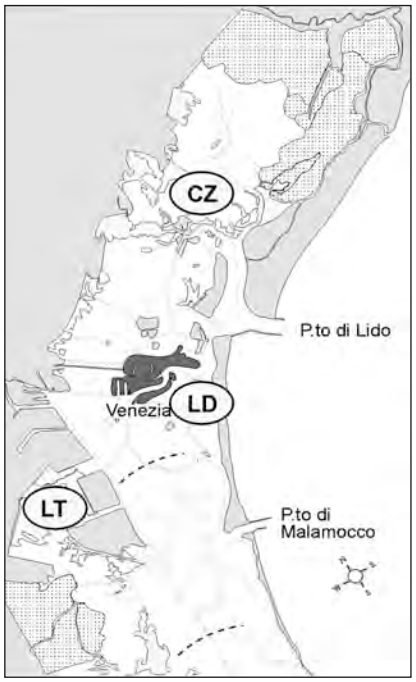

Fig. 1 - Lagoon of Venice and sampling areas. CZ=Ca' Zane, LD=Lido, LT=Lago dei Teneri.

To analyse the different spatio-temporal pattern of habitat/resources exploiting species data were grouped by season: Spring (March to May), Summer (June to September), and Autumn (October to December). On the basis of habitat utilization 6 functional groups (ecological guilds) were identified, instead on the basis of diet knowledge 10 trophic groups (dietary guilds) were identified. To describe species diversity of fish assemblages, Shannon index was calculated. A Bray-Curtis similarity matrix, performed on $\sqrt{\sqrt{x}}$ transformed data, was calculated and a Multidimensional Scaling (MDS) ordination [Kruskal & Wish, 1978] was performed in order to analyse the presence of spatio-temporal patterns. The analyses of community structure were carried out using PRIMER software package version 4.0 [Clarke & Warwick, 1994].

2.4. *Cytogenetics.*

The nuclear DNA contents were evaluated by flow cytometric essay of fish blood and kidney sample from five species of Syngnathidae (*Syngnathus abaster, S. taenionotus, S. typhle, Hippocampus guttulatus* and

Nerophis ophidion) and three species of Gobiidae (*Gobius niger, Zosterisessor ophiocephalus* and *Knipowitschia panizzae*). All the analysed specimens came from the Venice Lagoon. The preparation of the samples was according to the methods of Gold *et al.* [1991] and Ronchetti *et al.* [1995]. Three parameters were considered: the genome size (GS), the nuclear Adenine-Tymine base pair DNA content (AT-DNA) and the AT-DNA percentage of the whole GS (AT%). GS and AT-DNA values (picograms) were determined by comparison with the GS and AT-DNA values of chicken erythrocytes, used as internal standard.

3. *Results and Discussion.*

3.1. *Community Analysis.*

Forty-three fish species belonging to 21 families were detected in the three stations (tab. 1). The fish community was dominated, in terms of frequency of occurrence, by the following four species: the grass goby *Zosterisessor ophiocephalus*, the black goby *Gobius niger*, the sand smelt *Atherina boyeri*, and the flatfish *Solea vulgaris*, which occurred by each month of sampling in all the three stations. The seasonal trend in the number of species differed markedly across stations (fig. 2a): LT shows lower number of species than LD and CZ during spring months, whereas LD shows a relatively higher number of species through the year than CZ and LT being the only station showing an increase in the number of species in autumn months. Conversely, number of individuals tended to be higher in LT, especially during spring, when about 100 individuals/trap were recorded (fig. 2b).

These spatial differences were also reflected by the monthly trends of the Shannon diversity index (fig. 3): the index is higher in CZ during spring, and tends to increase in both LD and CZ during the autumn months; whereas in LT diversity values are lower during most of the year although with a fluctuating pattern.

Percentage composition in terms of the functional groups showed differences among the sampling areas, especially as regards the contribution of migrant juvenile species (mj), which were less abundant in LT during each season (tab. 2). This latter area was mostly dominated by sedentary species, which constituted more than 90% of the catches. Although sedentary species showed relatively high abundances in all the stations, "migrant juveniles" were represented with relatively high percentages both in CZ (more than 40% during spring and about 25% during summer)

Tab. 1 - Presence/absence of species in seasons; in brackets average ± S.D. number of traps are reported. Species are divided by family, trophic groups (TG: b+ = macrobenthivorous (preys > 5mm); b- benthivorous (preys < 5mm); pl = planktivorous; er = herbivorous; pi = piscivorous; il = iliofagous) and functional groups (FG: d = diadromous; er = estuarine resident; ma = marine adventitious; mj = migrant juvenile; msm = marine seasonal migrants; u = ubiquitous). Below average fish abundances and S.D. per trap are reported.

				CZ			*LD*			*LT*		
TG	FG	Family	*Species*	*Spring (35.5 ±6.36)*	*Summer (30.5 ±4.95)*	*Autumn (20.5 ±14.85)*	*Spring (58 ±17)*	*Summer (33.5 ±5.40)*	*Autumn (20.33 ±5.86*	*Spring (23.5 ±21.08)*	*Summer (45.5 ±21.92)*	*Autumn (36.33 ±5.68)*
b$^+$/pi	d	Anguillidae	*Anguilla anguilla*	x	x	x	x		x	x	x	x
pl/b$^+$	er	Atherinidae	*Atherina boyeri*	x	x	x	x	x	x	x	x	x
pi	ma	Belonidae	*Belone belone*				x	x	x		x	x
b$^-$/b$^+$	u	Blenniidae	*Blennius pavo*	x			x	x		x	x	
b$^-$/b$^+$	u		*Blennius gattorugine*						x			
b$^+$	ma	Callionymidae	*Callionymus rissoi*						x			
pi	ma	Carangidae	*Trachurus trachurus*						x			
pl	msm	Clupeidae	*Sardina pilchardus*				x					
pl	mj		*Sprattus sprattus*	x	x		x	x		x	x	
pi	d		*Alosa fallax*						x		x	
b$^-$/b$^+$	er	Cyprinodontidae	*Aphanius fasciatus*	x	x	x	x			x	x	x
pl	mj	Engraulidae	*Engraulis encrasicholus*	x	x	x	x	x	x	x	x	
b$^+$/pi	er	Gobiidae	*Zosterisessor ophiocephalus*	x	x	x	x	x	x	x	x	x
b$^+$/pi	er		*Gobius niger*	x	x	x	x	x	x	x	x	x
b$^+$/pi	u		*Gobius cobitis*			x	x		x			x
b$^-$	er		*Knipowitschia panizzae*	x	x		x	x		x		
b$^-$/b$^+$	mj		*Pomatoschistus minutus*	x		x	x		x	x		
b$^-$	er		*Pomatoschistus marmoratus*	x	x					x	x	x
b$^-$	er		*Pomatoschistus canestrini*	x								
b$^+$	u	Labridae	*Symphodus roissali*				x	x	x			
pi/b$^+$	msm	Moronidae	*Dicentrarchus labrax*	x	x				x	x	x	x
		Mugilidae	spp	x	x	x	x	x	x	x	x	x
il	mj		*Liza aurata*		x	x	x		x	x	x	x
il	er		*Liza saliens*	x	x	x	x		x	x	x	x
il	d		*Liza ramada*	x	x	x	x		x		x	x
il	msm		*Chelon labrosus*						x			
b$^-$/b$^+$	ma	Mullidae	*Mullus barbatus*		x			x				
b$^+$	d	Pleuronectidae	*Platichthys flesus*	x	x	x	x		x	x	x	x
pi/b$^+$		Salmonidae	*Salmo trutta*				x					
pi	ma	Scombridae	*Scomber scomber*	x								
b$^+$	mj	Soleidae	*Solea vulgaris*	x	x	x	x	x	x	x	x	x
b$^+$	ma	Sparidae	*Diplodus vulgaris*							x		
b$^+$	ma		*Diplodus sargus*	x								
b$^+$/er	ma		*Boops boops*					x				x
b$^+$	mj		*Sparus aurata*	x	x		x	x		x	x	x
b$^+$	msm		*Diplodus annularis*				x	x	x	x		
b$^+$	msm		*Lithognathus mormyrus*				x		x			
b$^-$/b$^+$	msm	Syngnathidae	*Syngnathus acus*			x	x		x			
b$^-$	er		*Syngnathus abaster*		x		x	x				
b$^-$/pi	er		*Syngnathus typhle*		x		x	x	x		x	
b$^-$/b$^+$	msm		*Syngnathus tenuirostris*			x			x			
b$^-$	u		*Hippocampus guttulatus*	x			x	x	x	x	x	
b$^-$	u		*Hippocampus hippocampus*						x			
b$^+$	ma	Triglidae	*Trigla hirundo*				x					
			Average	24.17	45.72	29.08	41.37	37.82	66.02	90.61	46.42	19.04
			Dev.st	2.86	34.38	8.51	42.71	18.15	18.94	56.44	24.47	2

and in LD (from 11% in autumn to 68% in spring). A peak in the frequency of marine coastal ubiquitous species occurred in LD during summer (18%), and diadromous species were more represented in CZ than in the other stations during each season (tab. 2). Two species, belonging to the "estuarine resident group" were dominant in the fish community in

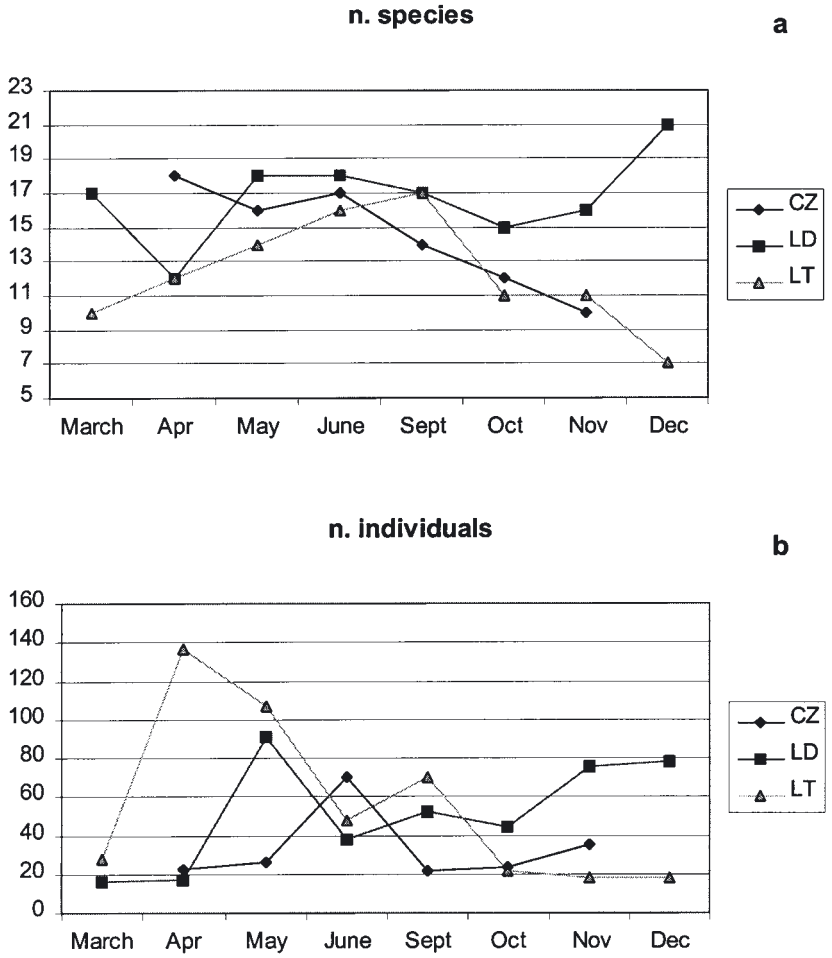

Fig. 2 - Monthly trends of number of species (a) and number of individuals (b) for the three sampled areas standardized as CPUE.

terms of relative abundance: the grass goby *Zosterisessor ophiocephalus* and the sand smelt *Atherina boyeri*, which showed average seasonal CPUEs well above 1 individual/trap in all the three stations. In tab. 2, the trophic groups data were also reported. The planktivorous/benthivorous (pl/b^-) group results to be the best represented group, being often the dominant one. Only LD in spring and summer shows a higher relative abundance of planktivorous (pl) and benthivorous/piscivorous (b^+/pi) respectively.

Tab. 2 - Percentage composition of fish community grouped by trophic and functional groups (TG and FG, respectively).

	CZ			LD			LT		
TG	spring	summer	autumn	spring	summer	autumn	spring	summer	autumn
b^+	22.61	14.59	8.61	0.49	2.48	1.71	4.50	3.34	1.05
b^-	0.69	0.39	0.00	0.44	0.88	0.29	5.13	0.04	0.05
pl	27.03	23.16	1.11	66.82	18.83	3.61	0.10	4.66	0.00
pi	0.05	0.00	0.00	0.02	1.12	0.39	0.00	0.21	0.12
il	1.11	2.36	25.49	0.52	0.40	16.64	0.56	2.03	33.64
b^+/pi	14.31	8.95	1.82	24.82	35.58	10.37	4.51	8.26	8.81
pl/b^-	33.34	49.14	60.07	6.30	19.07	64.23	80.00	80.66	53.99
b^-/b^+	0.86	1.37	2.90	0.58	17.47	2.55	5.21	0.78	2.31
b^+/er	0.00	0.00	0.00	0.00	1.28	0.00	0.00	0.00	0.04
b^-/pi	0.00	0.04	0.00	0.02	2.88	0.21	0.00	0.01	0.00
FG									
d	6.19	14.56	11.55	0.19	0.00	9.49	1.35	1.42	1.34
er	44.68	55.94	84.88	31.49	58.41	76.99	94.72	90.27	95.93
ma	1.41	0.29	0.00	0.03	2.57	0.41	0.05	0.18	0.24
mj	43.41	24.78	2.88	67.68	20.43	11.07	3.43	7.62	2.09
msm	4.11	4.43	0.46	0.25	0.88	0.58	0.43	0.15	0.09
u	0.21	0.00	0.23	0.36	17.70	1.46	0.03	0.36	0.32

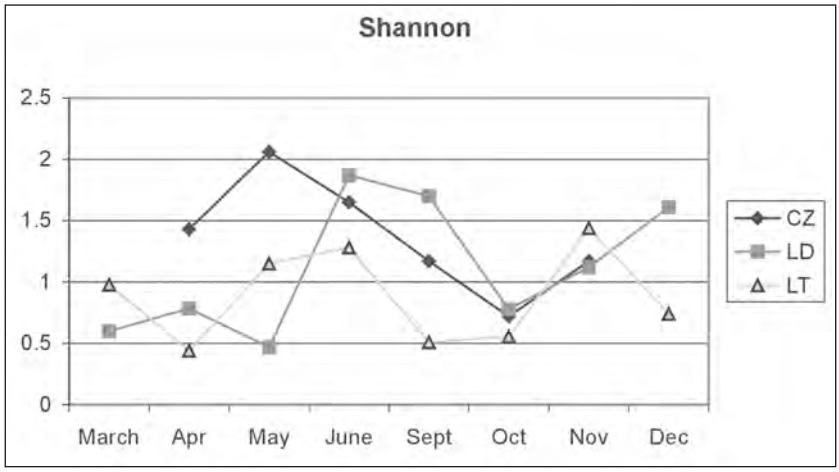

Fig. 3 - Monthly trends of Shannon diversity index for the three sampled areas standardized as CPUE.

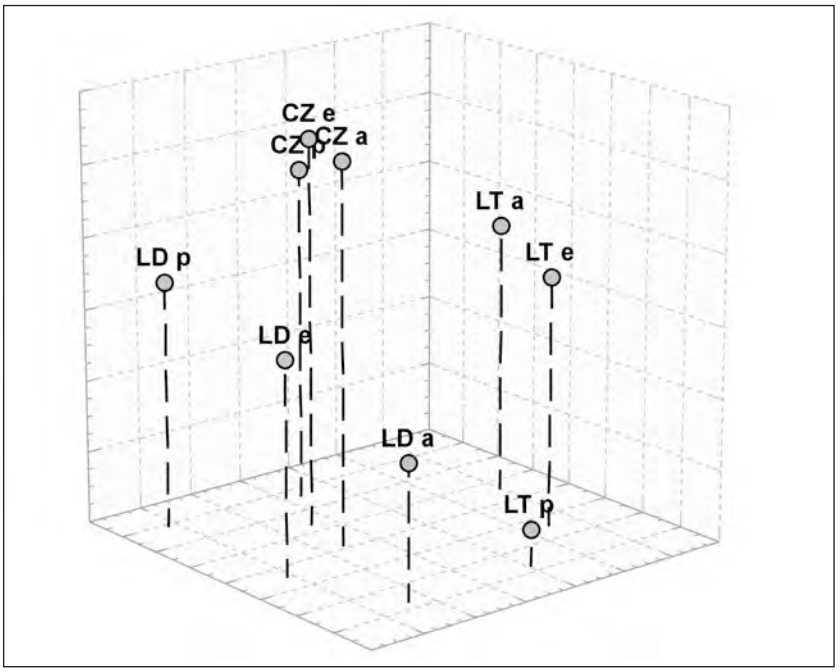

Fig. 4 - MDS plot for family data.

Finally, the MDS plot for family data (fig. 4) shows a good discrimination among the three stations. CZ shows a lower dispersion in comparison with LT and LD which appear more spread, as confirmed by the relative dispersion index (CZ =0.6, LD=1.13 and LT=1.27). The ordination for functional and trophic groups seems to be less informative, due to a strong seasonal effect which partially masks the spatial differences.

The list of species obtained by the present work shows that the composition of the fish assemblage in the Venice Lagoon consists, in terms of ecological guilds, of a 24% of estuarine residents, 21% of marine adventitious, 14 % of migrant juveniles, 16% of marine seasonal migrants, 14% of ubiquitous coastal species, and 11% of diadromous species. This seems to be rather similar to what reported by Elliot & Dewailly [1995] for the typical European estuarine fish assemblage (Atlantic seaboard).

The composition based on dietary preference guilds indicates the dominance of species feeding on invertebrates and fish: macro- and micro-benthivorous and piscivorous species represent the 80% of the fish assemblage, according with what has been found for both salt marsh and

European estuaries [Elliot & Dewailly, 1995; Mathieson, *et al.* 2000]. The rest of the fish community is dominated by detritivorous species (mullets) which have a stronger incidence during autumn and the beginning of the winter: this suggests that the fish community in the Venetian Lagoon has a more complex trophic structure during spring and summer when a higher incidence of predators is observed.

The venetian fish assemblage is dominated by three families which explain the higher percentage of similarity among the three sampling sites: Atherinidae, Gobiidae and Mugilidae. This result has been found also by Gordo & Cabral [2001] for a portuguese lagoon and this further suggests the similarity between the Venetian Lagoon and the estuaries on the Atlantic Seaboard in the fish assemblage composition.

The family Cyprinodontidae (represented in the Venice Lagoon by the only species *Aphanius fasciatus*) was important to discriminate LT from the other two stations, confirming the dominance of this family in the salt marsh areas as reported by Mathieson *et al.* [2000]. Furthermore, this site is characterised by low number of small estuarine resident species, high number of individuals and a strong seasonal pattern with spring peaks, suggesting that the geographic position and the salt marsh characteristics determine a peculiar, strongly specialised fish assemblage in this type of area.

By contrast, both in CZ and LD there is a higher contribution of marine species belonging mostly to the guilds of migrant juveniles and ubiquitous coastal species, which is consistent with the geographic position of these areas, that is near the sea mouths as concerns LD, and along the S. Felice canal (an important marine inlet) in the case of CZ. Further, the presence of higher number of species in these sites compared to LT, suggests the importance of the sea mouths in increasing the biodiversity of the fish estuarine assemblage, according with Arruda *et al.* [1988].

Further investigations will allow to analyse the main morphological and chemico-physical features which characterise the three areas in order to obtain a better understanding of the fish community patterns. The extension of this analysis to other areas of the Lagoon may then provide useful tool for the conservation and the management of the ichthyological resources.

3.2. *Cytogenetics.*

The table 3 reports the three parameters on nuclear DNA contents determined by flow cytometry (GS, AT-DNA, AT%) and already available data on karyotype morphology [Vitturi *et al.*, 1998; Libertini, unpublished] in five syngnathid species.

Tab. 3 - Genome size (GS), AT-DNA content (AT-DNA), AT-DNA percentage (AT%), diploid chromosome number (2n) and fundamental number of chromosome arms (NF) in five species of Syngnathidae. GS and AT-DNA are the diploid (2C) values and are given into picograms. DNA values are reported as the mean ± the standard deviation.

	S. taenionotus	*S. abaster*	*S. typhle*	*H.guttulatus*	*N.ophidion*
(2C) GS	0,98±0,014	1,03±0,013	1,02±0,036	1,12±0,016	3,94±0,037
(2C) AT-DNA	0,56±0,007	0,59±0,006	0,57±0,008	0,63±0,040	2,53±0,051
AT%	56,82±0,628	57,16±0,599	55,61±1,712	55,61±0,571	64,43±0,990
2n	44	44	44	44	58
NF	44	44	44	44	114

If compared with analogous cytogenetical data available from literature for other teleost fishes, the species belonging to the genera *Syngnathus* and *Hippocampus* here investigated are characterised by lower GS and chromosome number [Klinkhardt *et al.*, 1995], and AT% values similar to the most of the teleosts [Hudson *et al.*, 1980; Karel & Gold, 1987]. Therefore, a trend toward reduction in both DNA content (generally realised through hetero-chromatin loss) and chromosome number seems to have characterised the karyotypical evolution of these species. On the other side, *N. ophidion* has four-folds the DNA amount and more than twice of the NF of other syngnathids; these differences testifying a different karyological evolution between *Nerophis* and the other syngnathids during which polyploidisation might have occurred. Such opposite trends may be involved in a different management of genetic biodiversity at the individual level, realised through the effects of genome organisation on the recombination mechanisms [White, 1984; Olmo *et al.*, 1989]. In *Syngnathus* and *Hippocampus* intra-chromosomal crossing-over recombination would be promoted by terminal centromere chromosomes and low amount of hetero-chromatin. Conversely, in *Nerophis*, there is a higher tendency to maintain unchanged some DNA regions (i.e. the characters herein codified) and the preferential recombination units are the whole chromosomes which are randomly sorted during the first meiotic division, therefore the crossing-over would be hampered by the presence of a median centromere and large heterochromatin blocks [Libertini, unpublished] in the chromosomes. Moreover, *Nerophis* had a further source for increasing the genetic variability due by the doubling of the whole gene set through the polyploidisation event occurred in the past.

Although preliminary, the data on the GS in three goby species belonging to three different genera gave comparable 2C values of about two picograms. These values are intermediate between those ones found in syngnathids and resemble the values generally found in teleosts, with spe-

cial reference to the Percomorpha [Klinkhardt *et al.*, 1995]. Preliminary data on GS and AT% values characterising the three species of Gobiidae seem to be less differentiated than those found in syngnathids indicating a low level of cytogenetical differentiation among the genera in this family.

Further analyses on DNA nuclear content are presently on work in order to extend the cytogenetical study to other syngnathids and goby fish, to better understand the pathways of genome diversification among the taxa and to enhance the implications of this process on the management of genetic biodiversitity and on life-history.

References.

Arruda L.M., Andrade J.P. & Cunha M.M., 1988. Abundance, diversity, and community structure of the fish population in the Ria de Aveiro (Portugal). Oceanologica Acta 11, 235-240.

Clarke K.R. & Warwick R.M., 1994. Similarity-based testing for community pattern: the two-way layout with no replication. Marine Biology 118, 167-176.

Elliott M. & Dewailly F., 1995. The structure and components of European estuarine fish assemblages. Neth. J. Aquat. Ecol. 29, 397-417.

Elliot M. & Hemingway K.L., 2002. Fishes in Estuaries. Blackwell Science, Oxford.

Gold J.R., Ragland C.J., Birkner M.C. & Garrett G.P., 1991. A simple procedure for long-term storage and preparation of fish cells for DNA content analysis using flow cytometry. The Progressive Fish-Culturist 53, 108-110.

Gordo L.S. & Cabral H.N., 2001. The fish assemblage structure of a hydrologically altered coastal lagoon: the Obidos lagoon (Portugal). Hydrobiologia 459, 125-133.

Hudson P., Cuny G., Cortadas J., Haschemeyer A.E.V. & Bernardi G., 1980. An analysis of fish genomes by density gradient centrifugation. Eur. J. Biochem. 112, 203-210.

Karel W.J. & Gold J.R., 1987. A thermal denaturation study of genomic DNAs from North American minnows (Cyprinidae: Teleostei). Genetica 74, 181-187.

Klinkhardt M., Tesche M. & Greven H., 1995. Database of Fish Chromosomes. Westharp Wissenschaften. Magdeburg, Germany.

Kruskal J.B. & Wish M., 1978. Multidimensional scaling. Sage Publications, Beverley Hills, California.

Mann K.H., 2000. Ecology of coastal waters. Blackwell Science, Oxford.

Mathieson S., Cattrijsse A., Costa M.J., Drake P., Elliott M., Gardner J. & Marchand J., 2000. Fish assemblages of European tidal marshes: a comparison based on species, families and functional guilds. Mar. Ecol. Prog. Ser. 204, 225-242.

Olmo E., Capriglione T. & Odierna G., 1989. Genome size evolution in vertebrates: trends and constraints. Comp. Biochem. Physiol. 92B, 447-453.
Ronchetti E., Salvadori S. & Deiana M.A., 1995. Genome size and AT content in Anguilliformes. Eur. J. Histochem. 39, 259-263.
Sacchi C.R., 1985. Le sel de La Palice: réflexions sur le paralin méditerranéen. Mem. Biol. Mar. Ocean. 15, 71-89.
Solbrig O.T., 2000. The theory and practice of the science of biodiversity: a personal assessment. In: Kato, M. (Ed.), The biology of biodiversity, Springer-Verlag.
Vitturi R., Libertini A., Campolmi M., Calderazzo F. & Mazzola A., 1998. Conventional karyotype, nucleolar organizer regions and genome size in five mediterranean species of Syngnathidae (Pisces, Syngnatiformes). J. Fish Biol. 52, 677-687.
White M.J.D., 1984. Chromosomal mechanisms in animal reproduction. Boll. Zool. 51, 1-23.

BIODIVERSITY IN THE LAGOON OF VENICE: EFFECTS OF BIOCIDAL COMPOUNDS ON THE SURVIVAL OF BENTHIC FILTER-FEEDING ORGANISMS, WITH PARTICULAR REFERENCE TO COMPOUND ASCIDIANS

F. Cima, L. Ballarin, P. Burighel
Dipartimento di Biologia, Università di Padova

1.1 *Biocides in the lagoon of Venice.*

Biocides in the aquatic environment can negatively influence the fitness of many organisms acting at various levels of their biological cycles, such as fertilisation, embryonic and larval development, larval settlement, asexual reproduction and adult survival.

Thus, biocidal compounds such as those extensively used in the lagoon of Venice as components of antifouling paints for the protection of submerged manufacts such as piles, quays and boats, can affect the composition and/or the distribution of animal communities.

The lagoon of Venice is a coastal system of particular ecological relevance, as it represents the sum of many environmental typologies. In general, it is a shallow water basin with an incomplete water renewal and is characterised by many harbour activities, river outlets and channels crossing agricultural and urban areas.

1.2. *Ascidians as models for immunotoxic investigations.*

Animal survival is fundamental for the maintenance of biodiversity and, in all metazoans, immune system enables the survival of the organism allowing the recognition and the rejection of non-self materials (neoplastic cells, microorganisms, foreign agent), potentially dangerous to the organism itself. As a consequence, reduction in the intensity of immune responses can severely undermine the survival of organisms, which result less able to cope with parasites and infections.

Ascidians are filter-feeding animals, frequently found in the coastal environments. They represent a simple model for the study of natural

immune responses and their immune system has been the subject of many recent and past investigations.

Botryllus schlosseri is a colonial ascidian widely distributed in the lagoon of Venice, which resulted highly sensitive to organotin exposure [Henderson, 1987]. We already used *B. schlosseri* as a model organism in a research project aiming to clarify the cellular and molecular basis of the immunosuppression by organotins.

1.3. *Antifouling compounds: state of the art.*

From the mid 1960s to the end of 1980s organotin compounds (mainly tributyltin, TBT) were widely used as biocides in antifouling paints. Their low hydrosolubility favoured their accumulation in sediments and the subsequent slow release in the water column, whereas their high lipophilicity enables their entry in animal tissues and cells. These compounds resulted highly immunotoxic, even at low concentrations, in both vertebrates and invertebrates. They cause lymphocyte depletion, atrophy of thymus and lymphatic tissues in teleosts and mammals [Verschuuren et al., 1970; Vos et al., 1984; Snoeji et al., 1985; Guta-Socaciu et al., 1986; Devries et al., 1991; Dacasto et al., 1994], inhibit phagocytosis and provoke cytolysis of polymorphonuclear leukocytes [Elferink et al., 1986], resulting in a strong immunosuppression of cell-mediated immune responses.

The high toxicity of organotin compounds, which are dangerous also for human health, led to coastal ecosystem depauperation with remarkable consequences in fishing activity and, since 1982, induced many countries to control or ban their use. The E.C. Instruction 89/677 banned the use of TBT-based antifouling paints on boats less than 25 m in length and law proposals for the complete ban of TBT within 2003 were prepared. As a consequence, there has been a shift towards new biocidal compounds to be used in antifouling paint formulations as an alternative to TBT.

A recent survey of our research team indicates that zinc pyrithione (ZnP) and kathon 5287 (4,5-dichloro-2-n-octyl-4-isothiazolin-3-one) are the most used alternative antifouling compounds in the lagoon of Venice in the last decade. Despite their high diffusion in coastal waters and sediments, the fate of these compounds in the environment, their biogeochemical cycles, their bioavailability and their mechanisms of bioaccumulation in trophic chains remain almost completely unknown. Moreover, although negative effects on aquatic ecosystems of these alternative biocides have not been extensively studied for they are believed

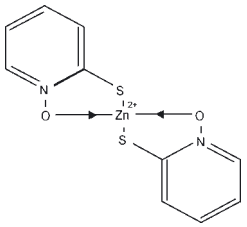

Fig. 1 - Zinc pyrithione (ZnP).

less toxic than organotins, these substances have the potential to cause environmental damage, as they must be toxic to a wide range of marine fouling species [Voulvoulis et al., 1999]. Therefore, environmental monitoring and acute toxicity tests on target organisms and cells represent a priority for safeguard of environment, biodiversity and human health.

1.4. *Zinc pyrithione.*

Zinc pyrithione is a zinc salt complex, resulting from the combination of 2-mercaptopyridine-1-oxide with zinc (II), mainly used in agriculture for its antifungal activity and in the formulation of antidandruff shampoos (fig. 1).

It was firstly synthesised in 1936 and registered in 1937. It has a medical use as bactericidal, antimycotic and antiseborroic compound [Pansy et al., 1953; Albert et al., 1956; Hyde and Nelson, 1984; Khattar et al., 1988]. As a bactericidal agent it is used to coat sponges and toothbrushes and is added in plastics, glues, mortars, stuccos, fabrics.

The solubility of ZnP in distilled water is very low (15-20 ppm) and increases when complexes with organic amines are formed (e.g. up to 300 ppm in concentrated detergents) [U.S. EPA, 2000].

Due to its excellent chelant properties, ZnP is an active metal complex, acting in particular on biological membranes. In addition, its low water solubility is responsible of its high stability and lipophilicity, which make it a good substitute of organotins in antifouling paint formulations.

1.5. *Comparison between immunotoxic effects of ZnP and TBT.*

ZnP has teratogenic effects on teleostean larvae [Goka, 1999], but so far no genotoxic activity has been reported [Skoulis et al., 1993]. It is cytotoxic towards cultured mammalian cells [Priestley and Brown, 1980],

probably due to the inhibition of DNA synthesis [Imokawa and Okamoto, 1982], and mutagenicity has also been reported [Snyder et al. 1965; Adam et al., 1995].

In the first year of the research project, we focussed our attention to ZnP in order to evaluate its effects on animal health and survival. Therefore, we investigated the capability of ZnP to affect immune responses through the evaluation of a series of immunotoxicity indexes.

We set up short-term cultures (60 min at 25 °C) of *B. schlosseri* haemocytes exposed to various concentrations (0.1 to 10 μM) of ZnP. The "amoebocytic index", i.e., the percentage of cells with amoeboid shape, and the "phagocytic index", i.e., the percentage of haemocytes containing phagocytised yeast cells, were significantly ($p < 0.05$) reduced after exposition to 0.1 and 0.5 μM ZnP, respectively. These effects were dose- and time-dependent, and irreversible, similarly to those reported for TBT [Cima et al., 1995; 1998], but, differently to TBT exposition, a significant ($p < 0.05$) detachment of cells from the substrate occurred after incubation at 0.5 μM. Detection of microfilaments and microtubules at light fluorescence microscope by means of FITC-phalloidin and anti-a-tubulin antibody, respectively, revealed thorn-shaped, cytoplasmic prolongations due to cytoskeletal alterations only in the actinic component. Isodynamic mixtures of ZnP and TBT showed an antagonistic interaction on their effects on the "amoebocytic index".

Like TBT [Cima and Ballarin, 1999], ZnP induced apoptosis, the extent of which was evaluated as "apoptotic index" considering the percentage of haemocytes showing both chromatin condensation with acridine orange and chromatin fragmentation with TUNEL reaction. Early and late apoptosis occurred after exposition to 0.1 and 0.5 μM, respectively. The latter concentration also significantly ($p < 0.001$) affected both oxidative phosphorylation and lysosomal activities through the inhibition of cytochrome-c-oxidase and acid phosphatase activity, respectively. Differently to TBT [Cima and Ballarin, 2000; Cima et al., 2002], no effect was observed on Ca^{2+} homeostasis, since no decrement in Ca^{2+}-ATPase activity occurred, although a little increase in cytosolic Ca^{2+} was detected after incubation at the highest concentration.

In conclusion, the pattern observed in the immunotoxicity indexes demonstrate that ZnP has a strong toxicity on cultured haemocytes at very low concentrations and interferes with fundamental cell activities. Therefore, this substitute biocide results as much toxic as TBT and, since many of its mechanisms of action are unknown, it does represent a potential risk for the environmental health, in particular for benthonic invertebrates.

References.

Adam W., Ballmaier D., Epe B., Grimm G.N., Saha-Höller C.R., 1995. N-hydroxypyridinethiones as photochemical hydroxyl radical sources for oxidative DNA damage. Angew. Chem. 34, 2156-2158.

Albert A., Gibson M.I., Rubbo D., 1956. The influence of chemical costitution on antibacterial activity. Part IV: the bactericidal actin of 8-hydroxyquinoline (oxine). Br. J. Exp. Pathol. 36, 119-130.

Cima F., Ballarin L., 1999. TBT-induced apoptosis in tunicate haemocytes. Appl. Organometal. Chem. 13, 697-703.

Cima F., Ballarin L., 2000. Tributyltin induces cytoskeletal alterations in the colonial ascidian *Botryllus schlosseri* phagocytes via interaction with calmodulin. Aquat. Toxicol. 48, 419-429.

Cima F., Ballarin L., Bressa G., Sabbadin A., 1995. Immunotoxicity of butyltins in tunicates. Appl. Organometal. Chem. 9, 567-572.

Cima F., Ballarin L., Bressa G., Burighel P., 1998. Cytoskeleton alteration by tributyltin (TBT) in tunicate phagocytes. Ecotoxicol. Environ. Safety 40, 160-165.

Cima F., Dominici D., Mammi S., Ballarin L., 2002. Butyltins and calmodulin: which interaction? Appl. Organometal. Chem.16, 182-186.

Dacasto M., Nebbia C., Bollo E., 1994. Triphenyltin acetate (TPTA)-induced cytotoxicity to mouse thymocytes. Pharmacol. Res. 29, 179-186.

Devries H., Penninks H., Snoeji A.H., Seinen W., 1991. Comparative toxicity of organotin compounds to rainbow-trout (*Oncorhynchus mykiss*) yolk-sac fry. Sci. Total Envir. 103, 229-243.

Elferink J.G.R., Deierkauf M., Van Steveninck J., 1986. Toxicity of organotin compounds for polymorphonuclear leukocytes: the effect on phagocytosis and exocytosis. Biochem. Pharmac. 35, 3727-3732.

Goka K., 1999. Embryotoxicity of zinc pyrithione, an antidandruff chemical, in fish. Environ. Res. 81, 81-83.

Guta-Socaciu C., Giurgea R., Rosioru C., 1986. Thymo-bursal and adrenal modification induced by triphenyltin compounds in chickens. Arch. Exper. Vet. Med. Leipzig 40, 307-311.

Henderson R.S., 1987. Effects of organotin antifouling paint leachates on Pearl Harbour organisms: a site-specific flowthrough bioassay. In: Proceedings of the Organotin Symposium of the Oceans '87 Conference, Halifax, Nova Scotia, Vol. 4, IEEE, New York, 1226-1233.

Hyde G.A., Nelson J.D., 1984. Sodium and zinc omadine. In: Kabara, (Ed.), Cosmetic and Drug Preservation: Principles and Practice, Marcel Dekker, New York, 115-128.

Imokawa G., Okamoto K., 1982. The inhibitory effetcs of zinc pyrithione on the epidermal proliferation of animal skins. Acta Derm. Vener. 62, 471-475.

Khattar M.M., Salt W.G., Stretton J.R., 1988. The influence of pyrithione on the growth of microorganisms. J. Appl. Bacteriol. 64, 265-272.

Pansy F.E., Stander H., Koenberger W.L., Donovick R., 1953. *In vitro* studies with 1-idroxy-2(1H)-pyridinethione. Proc. Soc. Exp. Biol. 82, 122-124.

Priestley G.C., Brown J.C., 1980. Acute toxicity of zinc pyrithione to human skin cells in vitro. Acta Derm. Vener. 60, 145-148.

Skoulis N.P., Barbee S.J., Jacobson-Kram D., Putman D.L., San R.H.C., 1993. Evaluation of the genotoxic potential of zinc pyrithione in the *Salmonella* mutagenicity (Ames) assay, CHO/HGPRT gene mutation assay and mouse micronucleus assay. J. Appl. Toxicol. 13, 283-289.

Snyder F.H., Buehler E.V., Winek V., 1965. Safety evaluation of zinc 2-pyridinethiol-1-oxide in shampoo formulation. Toxicol. Appl. Pharmacol. 7, 425-437.

Snoeji N.J., Van Jersel A.A.J., Pennincks A.H., Seinen W., 1985. Toxicity of triorganotin compounds: comparative *in vivo* studies with a series of trialkyltin compounds and triphenyltin chloride in male rats. Toxicol. Appl. Pharmacol. 81, 274-286.

U.S. EPA, 2000. Notice of filing a pesticide petition to establish an exemption from the requirement of a tolerance for a certain pesticide chemical in or on food federal register: September 20, 65, 56895-56901.

Verschuuren H.G., Ruitenberg E.J., Peetoom F., Helleman P.W., Van Esch G.J., 1970. Influence of triphenyltin acetate on lymphatic tissue and immune responses in guinea pigs. Toxicol. Appl. Pharmacol. 16, 400-410.

Vos J.G., Van Logten M.J., Kreeftenberg J.G., Kruizinga W., 1984. Effect of triphenyltin hydroxide on the immune system of the rat. Toxicology 29, 325-336.

Voulvoulis N., Scrimshaw M.D., Lester J.N., 1999. Alternative antifouling biocides. Appl. Organometal. Chem. 13, 135-143.

ECOGENETIC BIODIVERSITY IN *ZOSTERISESSOR OPHIOCEPHALUS* FROM THE LAGOON OF VENICE: I GENE-ENZYME POLYMORPHISMS

P. M. Bisol
Dipartimento di Biologia, Università di Padova

1. *Introduction.*

In the framework of investigations focused on biodiversity in the Lagoon of Venice, attention has been devoted to enzymatic variability in the gobiid *Zosterisessor ophiocephalus*. This fish is widespread in the lagoon and plays an important role on the brackish waters community.

The main point of the research is the evaluation of genetic polymorphisms and their ecological implications.

In fact, biological diversity includes the genetic variation within species, both among geographically separated populations and among individuals within single populations.

Natural selection and genetic drift can alter the distribution of variants in time and local differences in the physical and biological environment can cause differentiation in space.

Genetic variation in demographic parameters can have significant effects on population dynamics within species as well as affecting other species in the food web. These processes involve the recursive interaction of four different elements: a) variation in allele frequencies, b) variation in morphological or physiological design, c) variation in ecological performance, d) variation in demographic output (Feder and Watt, 1992).

Many agents affect the connections between such elements: environmental background and population structure, ontogeny and developmental processes, phenotypical responses and gene expression.

Hence the necessity for an interdisciplinary approach at the genomic, individual and population levels to investigate the relationships between genetic biodiversity and environmental factors.

This paper reports the first results obtained following the use of electrophoretic techniques and describes the enzyme polymorphisms in *Zosterisessor ophiocephalus.*

2. *Materials e Methods.*

Specimens of *Zosterisessor ophiocephalus* (40 per sample) were collected from four sampling locations in the Lagoon of Venice. The fish collection methods and sampling sites are described by Mainardi *et al.* in this volume.

The samples were kept alive in seawater until anatomical dissection, which was done in Mainardi's laboratory in Venice. Four fragments of skeletal muscle, liver, gills and the two eyes were prepared separately for each individual in Eppendorf tubes and transported to the Padua laboratory with dry-ice packs and stored at –80° until enzyme electrophoresis.

Tissue samples (about 10 mg) were mechanically homogenized in Eppendorf tubes in 200 μl of 0.02 M Tris/HCl pH 8 and centrifuged at 15,000 rpm for 15 min. The supernatants from each homogenate were preserved in small aliquots and stored for comparative analyses.

Two electrophoresis techniques were used: native and isolectrofocusing. In the first case, the enzyme molecules are separated according to their net charge, which at any particular pH depends on the ionisation of the free amino or carboxyl groups. In the second case, the enzymes are separated in a pH gradient, established by application of an electrical field to a mixture of amphoteric buffer substances known as carrier ampholytes.

Native electrophoreses were carried out by a SarthophorSystem (Sartorius), a convenient apparatus which employs cellulose acetate as supporting medium (Grunbaum, 1981). The analyses were performed on 3 ml of supernatant at constant voltage for 20-40 minutes. The running buffers were the following: Buffer A: Tris 8,30 g/l and Citric Acid 4,70 g/l pH 7.2; Buffer B: Tris 10,00 g/l and Boric Acid 3,00 g/l, pH 8.8.

PhastSystem, a programmable apparatus by Amersham-Pharmacia, performed Isoelectrofocusing electrophoresis utilising specific polyacrylamide gels with a mixture of carrier ampholytes Pharmalyte. 0.3 μl of supernatant were introduced on the upper surface of gels at broad pH range (*3-9*) and the electrophoreses were carried out at the following conditions:

Step	**Volt**	**Ampere (mA)**	**Watt**	**Temperature (°C)**	**Volt/h**	**Time (Min)**
Prerun	2000	2,5	3,5	15	75	10’
Sample loading	200	2,5	3,5	15	15	5’
Run	2000	2,5	3,5	15	410	20’

After electrophoresis, the enzyme stains were applied to the media in agar overlay according to Bisol et al. (1981) and incubated at 37 °C. Two staining buffers were used: 1) 0.1 M Tris/HCl 1, pH 7.4 and 2) 0.1 M Tris/HCl, pH 8.0.

Following is a summary of best experimental conditions for each enzyme:

Adenylate Kinase (AK: Enzyme Code 2.7.4.3): *Sartophorsystem*; Running buffer: A; Staining Recipe: 50 ml Buffer 2; 50 mg Glucose; 10 mg NADP; 10 mg ADP; 10 mg MTT; 20 mg $MgCl_2$; 5 mg PMS; 10 U Hexokinase + 10 U Glucose-6-Phosphate dehydrogenase.

Fumarate hydratase (FU: EC 4.2.1.2.): *Sartophorsystem*; Running buffer A; Staining Recipe: 50 ml Buffer 1; 50 mg Na Fumarate; 10 mg NAD; 10 mg MTT; 5 mg PMS; 10 U Malate dehydrogenase.

Glucose phosphate Isomerase (GPI: EC 5.3.1.9) *Phastsystem*; Staining Recipe: 50 ml Buffer 2; 10 mg Na Fructose 6-phosphate; 10 mg NADP; 10 mg MTT, 5 mg PMS; 10 U Glucose-6-Phosphate dehydrogenase.

Glyceraldehyde 3-P dehydrogenase (GAPDH: EC 1.2.1.12): *Sartophorsystem*; Running buffer A Staining Recipe: 50 ml Buffer 1; 100 mg Na Fructose-1,6-diphosphate; 10 U Aldolase; after incubation at 37°C for 30' add 150 mg Na Arsenate; 10 mg NAD; 10 mg MTT; 5 mg PMS 5.

Isocitrate dehydrogenase (ICD: EC 1.1.1.42): *Phastsystem*; Staining Recipe: 50 ml Buffer 2; Na Isocitrate 30 mg; NADP 5 mg, MTT 5 mg; $MgCl_2$ 10 mg; PMS 5 mg.

Lactate dehydrogenase (LDH: EC 1.1.1.27): *Sartophorsystem*; Running buffer: B; Staining Recipe: 50 ml Buffer 1; 30 mg L-Na Lactate; 15 mg NAD; 10 mg MTT; 5 mg PMS.

Malate dehydrogenase (MDH: EC 1.1.1.37): *Sartophorsystem*; Running buffer: A; Staining Recipe: 50 ml Buffer 2; ml; L-Na Malate 75 mg; NAD 20 mg; MTT 10 mg; PMS 5 mg.

Malic Enzyme (ME: EC 1.1.1.40): *Sartophorsystem*; Running buffer: A; Staining Recipe: 50 ml Buffer 2; 70 mg L-Na Malate; 20 mg NADP; 10 mg MTT; 5 mg PMS; 20 mg $MgCl_2$.

Phosphoglucomutase (PGM: EC 2.7.5.1) *Phastsystem*; Staining Recipe: 50 ml Buffer 2; 30 mg Glucose 1-phosphate (containing at least 1% glucose 1,6-diphosphate); 10 mg NADP; 10 mg MTT; 5 mg PMS; 20 mg $MgCl_2$ 10; U Glucose-6-Phosphate dehydrogenase.

Phosphogluconate dehydrogenase (PGD: EC 1.1.1.44): *Phastsystem*; Staining Recipe: 50 ml Buffer 2; 50 mg Na_3-6-Phosphogluconate; 10 mg NADP; 20 mg $MgCl_2$; 10 mg MTT; 5 mg PMS.

Superoxide dismutase (SOD: EC 1.15.1.1.) *Phastsystem*; Staining Recipe: 25 ml Buffer 2; 5 mg MTT; 5 mg PMS; light.

3. *Results.*

The electrophoretic and IEF profiles from 148 specimens of *Zosterisessor ophiocephalus* showed multiple forms and differential tissue expression for the enzymes analyzed. These features are common in teleost fish (Maranesi and Mantovani, 1997). Different proteins which have similar enzymatic properties can be justified by the occurrence of a) multiple gene loci coding for structurally distinct polypeptide chains, b) multiple allelism at a single locus, c) multimeric enzymes, made up of two or more polypeptide chains or subunits (Harris and Hopkinson, 1976). The application of the Mendelian law of monohybrid segregation and some statistical rules for combining the enzyme subunits allows genetic and molecular interpretations of the electrophoretic patterns. In other words, diploid organisms posses only two alleles at each locus, and if the number of identical subunits present in a homozygote is *n*, then in a heterozygote n+1 is the expected number.

In this way, 21 loci were postulated for the 11 enzyme systems assayed. The difference in tissue expression was estimated on the basis of the different staining intensities. In addition, all data were compared with the previous descriptions reported in the literature concerning *Zosterisessor ophiocephalus* (Callegarini and Ricci, 1973; McKay and Miller, 1991; Miller et al. 1994; Sorice and Caputo, 1999) and other Gobiidae (Wallis and Beardmore, 1980; 1984a; 1984b; Pezold and Grady, 1989; Aizawa et al., 1994). These comparisons are affected by a certain amount of approximation in reason of the different techniques and of limits in the descriptions. In fact, MacKey and Miller (1991) used protein solutions obtained homogenising together eye, gill and white muscle, while other Authors referred only to the tissues routinely used for the their high activity and clear resolution (Miller et al., 1994; Sorice e Caputo, 1999)

The following descriptions are given for each system in alphabetic order and the symbols for each locus are given in order of decreasing anodal mobility.

AK: A single locus active in muscle. No variant was observed.

FU: One locus, FU-1 expressed in liver and active also in muscle. No variability was observed.

GPI: Two loci, Gpi-1 and Gpi-2, both expressed in all studied tissues, forming one interlocus hybrid zone of heterodimers (fig. 1). Variability was observed only in one specimen at the GPI-2 locus: its three-banded pattern reflects the dimeric structure of enzyme and corresponds to heterozygote condition (Comparini et al. 1977).

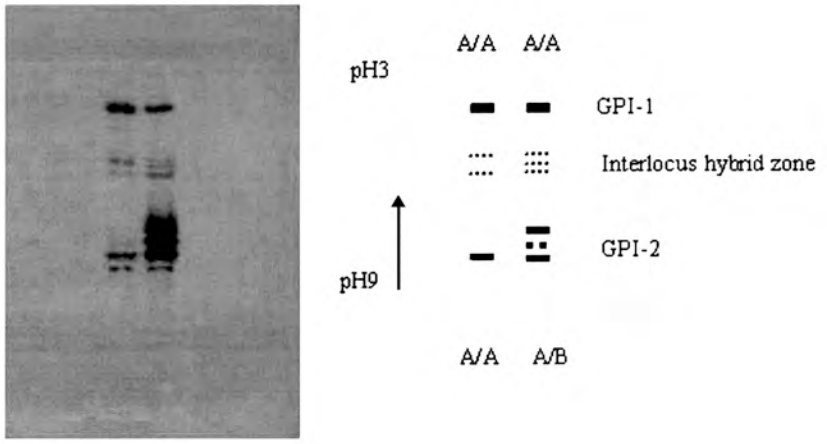

Fig. 1 - Isoelectrofocusing patterns (and their schematic interpretation) of GPI from two specimens Zosterisessor ophiocephalus. Dotted lines indicate the hybrid zone inter loci and intra locus.

GAPDH: Two loci, active in all tissues. No variant was seen.

ICD: Two loci, ICD-1 and ICD 2, both expressed in liver. ICD-2 resulted active also in the eye and muscle. No variant was seen.

LDH: The patterns from different tissues are illustrated in figure 2. The isozyme number and distribution of LDH in the analysed tissues indicate the presence of the three main isozymes usually described in fish (Basaglia, 1989). The fractions number 2 and 3, expressed in all tissue, represent the products of the loci LDH-A and LDH-B respectively. The fraction number 1, highly anodic, is expressed in the eye and corresponds to the LDH-C locus. The fractions with feeble staining (dotted lines in the schematic representation) have been putatively interpreted as interloci hybrid zones. According to Farias et al. (1997), the cathodic liver isozyme (fraction number 4) has been considered an artefact, probably arising from liver ADH reacting with traces of alcohol in the staining reagents.

MDH: Four non-variable fractions were seen in all specimens (fig.3). This pattern corresponds to two cytosolic and one mitochondrial isozymes encoded by three gene loci: MDH-A, MDH-B and MDH-M, respectively.
The fraction between the two more anodic fractions can be classified as a hybrid zone.

ME: Five bands characterised the patterns obtained for this isozyme (fig 3). The comparison of the mobility with those obtained from MDH

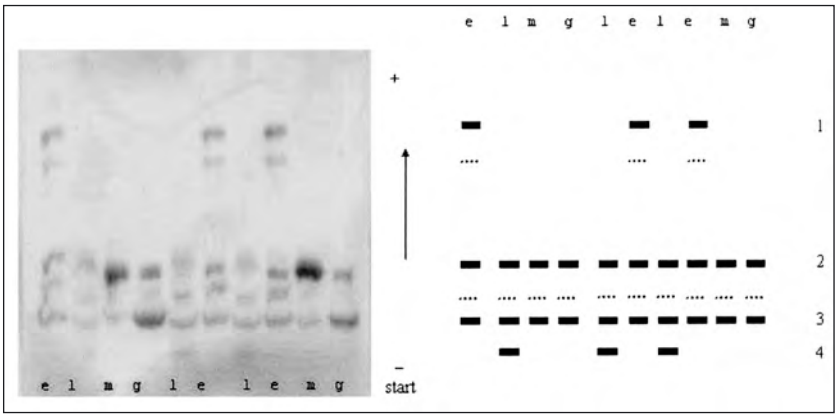

Fig. 2 - Electrophoresis patterns (and their schematic interpretation) of LDH isozymes of various tissue in Zosterisessor ophiocephalus. The small letters indicate the tissue of origin: e, eye; l, liver; m, muscle; g, gills. The dotted lines indicate putative interloci hybrid zone.

suggests that the most anodic fraction is ME, the others are MDH isozymes which can react also using NADP as co-enzyme.

PGM: Two loci, PGM-1 and PGM-2, both active in muscle and liver. In the eye only PGM-1 was active. The presence of two bands in one specimen at locus PGM-2 indicates the monomeric structure of enzyme.

PGD: One locus expressed in all tissues. No variants were seen.

SOD: One isozyme system, active in liver. No variant was seen.

4. *Conclusions.*

The survey of about 150 specimens of *Zosterisessor ophiocephalus* has permitted a more adequate description of the electrophoretic patterns in relation to the number of loci and the identification of the hybrid fractions.

The above description is largely in accordance with the most recent results for fish (Basaglia, 2002) and eliminates some disagreements in the data reported in literature for *Z. ophiocephalus* and other gobiids.

Judging from electrophoretic and IEF patterns in *Z. ophiocephalus*, some of the enzyme systems examined are tissue-specific. GPI, GAPDH, PGD and LDH (fraction 2 and 3) were found in all tissue, two enzymes (PGM-1, IDC-2) were present in three tissues, three other enzyme systems (FU, PGM-2 ICD-1) were detected in two tissues, SOD was active only in the liver.

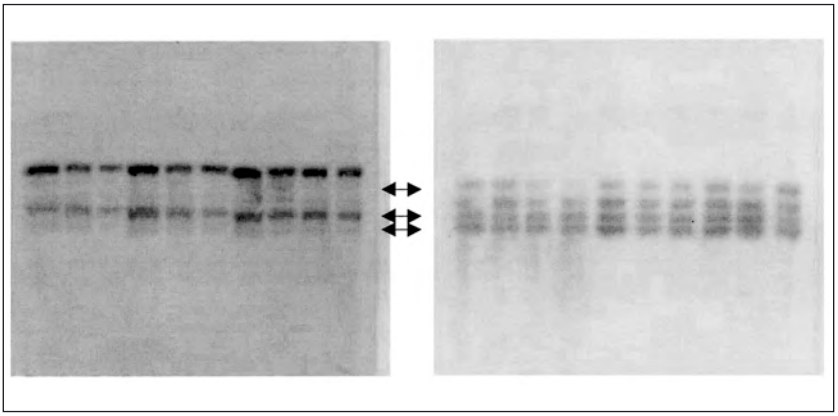

Fig. 3 - Cellulose acetate electrophoretic patterns of ME (left) and MDH (right) isozymes of muscle from 10 specimens of Zosterisessor ophiocephalus. ME is the most anodic fraction. The arrows indicate the MDH isozymes active also if stained at the ME condition.

Other important result concern the LDH patterns, in reason of the attribution to Alcohol dehydrogenase of the cathodic fraction active in the liver. Moreover, this study has detected that the ME isozymes are active also when the coenzyme utilised is NAD.

Despite the high number of specimens analysed, the level of genetic polymorphism is very low, and this is due to the detection of only two heterozygotes at the GPI and PGM loci. These results are in agreement with those of Miller et al (1994). However, other data are necessary in order to understand the significance of the low level of genetic variability and to evaluate the possible dynamics of enzyme polymorphisms in this species. For instance, the recruitment process could affect the genetic structure of gobiid populations.

References.

Aizawa T., Hatsumi M., Wakahama K., 1994. Systematic study on the *Chaenogobius* species (Family Gobiidae) by analysis of allozyme polymorphisms. Zoological Science 11, 455-465.

Basaglia F., 1989. Some aspects of isozymes of lactate dehydrogenase and glucosephosphate isomerase in fish. Comp. Biochem. Physiol., 92B, 213-226

Basaglia F., 2002. Multilocus isozyme systems in African lungfish, *Protopterus annectens*: distribution, differential expression and variation in dipnoans. Comp. Biochem. Physiol. 131 B, 89-102.

Bisol P.M., Pasquali P., Varotto V., 1981. Formal genetics of two loci,AP-1 and PGI-1, in the marine copepod Tisbe holothuriae. Vie et Mileu 31, 293-295.
Callegarini C., Ricci D., 1973. Lactate dehydrogenase (LDH) isozymes in some species of fresh water, euryhaline and salt water teleosts from the Po plain and its sea-coasts. Boll. Zool. 40, 25-30.
Comparini A., Rizzotti M., Rodinò E., 1977. Genetic control and variability of Phosphoglucose Isomerase (PGI) in eels from the Atlantic Ocean and the Mediterranean Sea. Marine Biology 43, 109-116.
Farias I.P., Paula-Silva M.N., Almeida-Val V.M., 1997. No co-expression of LDH-C in Amazon cichlids. Comp.Biochem. Physiol. 117B, 315-319.
Feder M.E., Watt W.A., 1992. Functional biology of adaptation. In Berry, R.J., Crawford, T.J., and Hewitt, G.M. (Eds) Genes in ecology. Blackwell Scientific Publications, 365-392.
Grunbaum B.W., 1981. Handbook for forensis of human bloodstain. Published by Sartorius GmbH.
Harris H. and Hopkinson D.A., 1976. Handbook of enzyme electrophoresis in human genetics. North Holland Publishing Company.
McKay S.I., Miller P.J., 1991. Isozyme criteria in testing of phyletic relationships between species of *Gobius* and related eastern Atlantic and the Mediterrenean genera (Teleostei: Gobioidei). J. Fish Biol 39(A), 291-299.
Miller P.J., Serventi M., Soregaroli D., Torricelli P., Gandolfi G., 1994. Isozyme genetics and the phylogeny of Italian freshwater gobies (Teleostei: Gobioidei). J. Fish Biol 44, 493-451.
Pezold F., Grady J.M., 1989. A morphological and allozymic analysis of species in the *Gobionellus oceanicus* complex (Pisces,Gobiidae). Bull. Mar. Sci. 45, 648-663.
Sorice M., Caputo V., 1999. Genetic variation in seven goby species (Perciformes:Gobiidae) assessed by electrophoresis and taxonomic inference. Marine Biology 134, 327-333.
Wallis G.P., Beardmore J.A., 1980. Genetic evidence for naturally occurring fertile hybrids between two goby species *Pomatoscschistus minutes* and *P. lozanoi* (Pisces,Gobiidae). Mar. Ecol. Prog. Series 3, 309-315.
Wallis G.P., Beardmore J.A., 1984 a. Genetic variation and environmental heterogeneity in some closely related goby species. Genetica 62, 223-237.
Wallis G.P., Beardmore J.A., 1984 b. An electrophoretic study of the systematic relationships in some closely related goby species (Pisces,Gobiidae). Biol.J. Linn. Soc. 22, 107-123.

IDENTIFICATION OF TRANSCRIBED GENES IN *MYTILUS GALLOPROVINCIALIS* AND *ZOSTERISESSOR OPHIOCEPHALUS*

P. Venier[1], A. Pallavicini[3], G. Lanfranchi[1,2]
[1]*Dipartimento di Biologia, Università di Padova*
[2]*CRIBI, Università di Padova*
[3]*Dipartimento di Biologia, Università di Trieste*

The Mediterranean mussel *Mytilus galloprovincialis* and the grass goby *Zosterisessor phiocephalus* represent model organisms in previous studies (Canova et al., 1998; Dolcetti at al, 2002) as well as in the Co.Ri.La Research Programme (2000-2004) on account of their ecological role and economic importance. However, the basic features of their genome and their gene functions are relatively unknown in comparison to other vertebrate and invertebrate species.

Actually, Fig. 1 shows the number of nucleotide and protein records present at the National Center for Biotechnology Information (Bethesda, MD, U.S.A.) in March 2002 for 11 reference organisms (fig. 1). The NCBI has been established in 1988 as a national resource for molecular biology information and for the better understanding of molecular processes affecting human health and disease. In addition to other bio informatics resources, the public databases of the NCBI can immediately feature the state of knowledge of any living organism for which nucleic acid or protein sequencing have been developed. In comparison to humans, fruit flies and other species reported in Fig. 1, the lack of data for *Z. ophiocephalus* and *M. galloprovincialis* is evident.

Advanced knowledge on genes and DNA-related functions is essential for understanding regular and abnormal development, life performance and reproductive success of the living organisms. In addition, genetic differences detected among individuals, populations and species are the basis of the biological richness of a given ecosystem.

On account of previous experience developed on human skeletal muscle (CRIBI; University of Padova, Prof. G. Lanfranchi and Prof. G. Valle) we could propose a molecular approach for the systematic identifi-

Nucleotide	Protein	
5600687	179571	Homo sapiens
337972	39281	Drosophila melanogaster
264871	83979	Arabidopsis thaliana
217099	62105	Caenorhabditis elegans
19340	32283	Saccharomyces cerevisiae
2253	447	Mus musculus domesticus
1473	1101	Oncorhynchus mykiss
407	8577	Escherichia coli K12
342	293	Mytilus edulis
170	129	Mytilus galloprovincialis
3	2	Zosterissessor ophiocephalus

Fig. 1 - Nucleotide and protein entries for 11 reference organisms at the National Center for Biotechnology Information (Bethesda, MD, U.S.A., March 2002).

cation of transcribed genes in the above-mentioned species (Aviv and Leder, 1972; Chomczynski and Sacchi, 1987; Diatchenko et al., 1999; Gubler and Hoffman, 1983; Ko, 1990; Lanfranchi et al., 1996; Soares and Bonaldo, 1998; Laveder et al., 2001).

As described in Fig. 2 (fig. 2) the expression of a finely selected subset of genes, i.e. transcription into intermediate RNA molecules and translation, provides the cells and the organism with the right amount of proteins necessary at any moment for basic functions as well as functions recruited during particular life stages or during unhealthy/stressful conditions.

Current bio-molecular techniques and specific software schematically described in Fig. 3 (fig. 3) allow the "back-copy" of transient RNA transcripts (mRNA) into double stranded DNA (cDNA, DNA complementary to the mRNA molecules), unidirectional cloning in a suitable *carrier* molecule, definition of a cDNA library (collection of bacterial clones containing specific *carrier*-cDNA inserts), amplification of the cDNA inserts with universal primers, selection and identification of the transcribed genes by systematic DNA sequencing. Finally, number and amount of the expressed genes resulting from software analysis of the sequence data allow the definition of the so-called "transcriptional profile", i.e. the molecular signature of the cellular response for a given tissue, life stage and environmental situation.

A number of potential results may develop from such molecular approach initially developed for *M. galloprovincialis* (Venier et al., 2001)

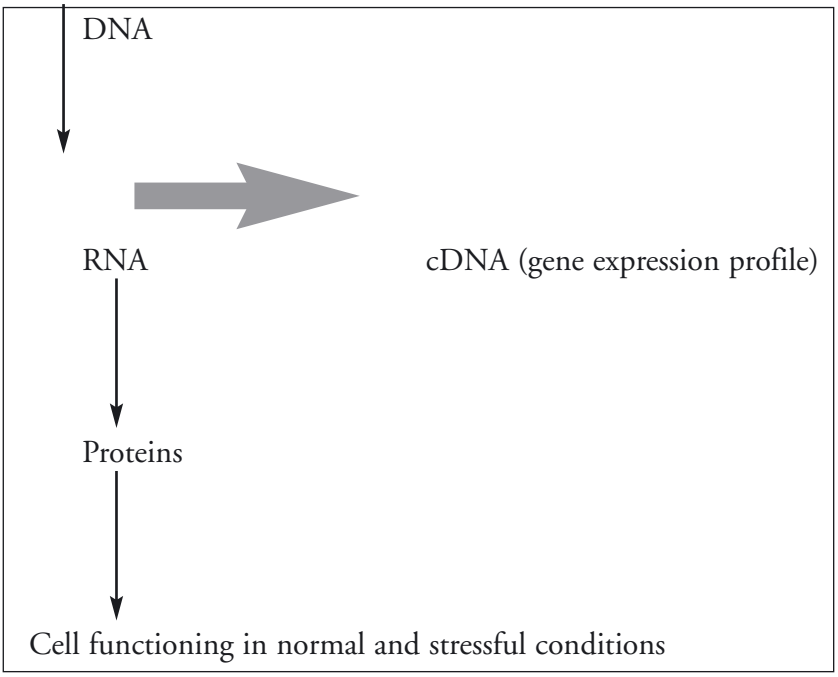

Fig. 2 - Finely regulated gene expression is essential for any living organism: the sub-set of the transcribed genes at any moment in a given cell type or tissue can be analysed through enzymatic synthesis of DNA, complementary copy of mRNA molecules (cDNA).

and now extended to the grass goby *Z. ophiocephalus* in the frame of the Co.Ri.La research project. 1) Identification of genes expressed in different tissues under physiological and stressing conditions with submission of new records to the public NCBI database. 2) Interspecies comparison based on selected genes, i.e. comparative genomics, in order to understand similarities and differences between phylogenetically close species, better described as 'ecotypes' (*M. edulis* and *M. galloprovincialis*). 3) Detection of sequence peculiarities to be used in the definition of new molecular diagnostic tools for surveying the ecological quality of national coastal waters (as stated by the DL 152/99). 4) Definition of a comprehensive catalogue of genes expressed by *M. galloprovincialis* and *Z. ophiocephalus* as starting point for the development of DNA-microarrays to be applied in environmental research and biomonitoring.

Methods have been set up for mussels and gobies during 2000-2001 and preliminary data, partially granted by Italian MURST, are now availa-

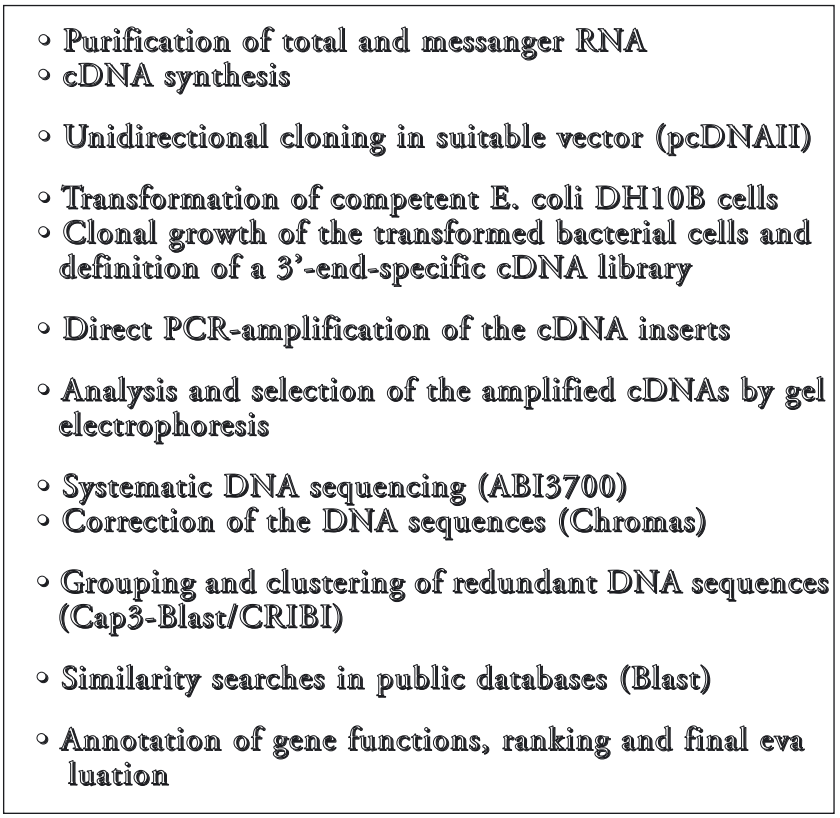

Fig. 3 - Procedural steps in the identification of actively transcribed genes of *M. galloprovincialis* and *Z. ophiocephalus*.

ble for *M. galloprovincialis*. The first round of DNA sequencing of the expressed sequence tags (3'-end-specific cDNA library from representative tissues of normal mussel) defined 285 DNA sequences corresponding to 159 non redundant transcripts (fig. 4). About half of them did not match any other record present in the NCBI database, thus suggesting differences between the active genes of the Mediterranean mussel and the nucleotide and protein sequences recorded from other organisms. *Such new sequences possibly indicate mussel-specific gene functions*. Other mussel transcripts showed different degree of similarity with sequences already present in the NCBI database. 10 mussel transcripts showed the highest similarity level ($>e^{-60}$) and recognised both mitochondrial and nuclear genes.

DNA sequences		285
Non redundant consensus sequences		159
Average length (base pairs)		330
Similarity search results (TBLASTX):		
◦ no similarity:		84 (52,8%)
◦ similarity:	$>e^{-60}$	10 (6,3%)
	$>e^{-30}$	39 (24,0%)
	$>e^{-20}$	47 (29,6%)
	$<e^{-20}$	28 (17,6%)

Fig. 4 - Transcribed genes of *M. galloprovincialis* (mRNAs from representative tissues of control mussels, pooled sample). Preliminary DNA sequencing defined 84 transcripts different from any other record present in the NCBI database and transcripts having different degree of similarity with gene functions already recorded as nucleotide or protein sequence (10 sequences showed the highest similarity level and included typical mitochondrial and nuclear genes).

Work is in progress for *Z. ophiocephalus* (purification of total and messanger RNA from various tissues, production of cDNA and creation of a 3'-end-specific cDNA library) in order to allow DNA sequencing and the first similarity searches.

References.

Aviv H. and Leder P., 1972. Purification of biologically active globin messanger RNA by chromatography on oligo-thymidylic acid-cellulose. Proc. Natl. Acad. Sci. 69, 1408-1412.

Canova S., Degan P., Peters L.D., Livingstone D.R., Voltan R. and Venier P., 1998. Tissue dose, DNA adducts, oxidative damage and CYP1A-immunopositive proteins in mussels exposed to waterborne benzo[a]pyrene. Mutat. Res. 399(1), 17-30.

Chomczynski P. and Sacchi N., 1987. Single-step method of RNA isolation by acid guanidinium thiocyanate-phenol-chloroform extraction. Anal. Biochem. 162, 156-159.

Diatchenko L., Lukyanov S., Lau Y.F., Siebert P.D., 1999. Suppression subtractive hybridization: a versatile method for identifying differentially expressed genes. Methods Enzymol. 303, 349-380.

Dolcetti L., Dalla Zuanna L., Venier P., 2002. DNA adduct levels in mussels and fish exposed to bulky genotoxic compounds. Mar. Environ. Res. (in press).

Gubler U. and Hoffman B.J., 1983. A simple and very efficient method for generating cDNA libraries. Gene 25, 263-269.

Ko M.S.H., 1990. An "equalized cDNA library" by the reassociation of short double-stranded cDNAs. Nucleic Acids Res 18, 5705-5711.

Lanfranchi G., Muraro T., Caldara F., Pacchioni B., Pallavicini A., Pandolfo D., Toppo S., Trevisan S., Scarso S. and Valle G., 1996. Identification of 4,370 expressed sequence tags from a 3'-end-specific cDNA library of human skeletal muscle by DNA sequencing and filter hybridization. Genome Res. 6, 35-42.

Laveder P., De Pittà C., Toppo S., Valle G. and Lanfranchi G., 2001. Specific subtraction of abundant mRNAs in skeletal muscle. Submitted.

Soares M.B and Bonaldo M.F, 1998. Constructing and screening normalized cDNA libraries. In: Birren B. et al. (Eds) Genome Analysis. A Laboratory Manual, Cold Spring Harbor Laboratory Press, Vol. 2, 49-157.

Venier P.A., Pallavicini A., Vezzi L., Dolcetti E., Crestanello G., Lanfranchi, 2001. Verso un catalogo dei geni di Mytilus galloprovincialis. In: 3rd Joined Meeting FISV (ABCD, AGI, SIBBM, SIMGBM, SIMA) (Riva del Garda, Italy), p. 269.

STUDIES OF THE BIODIVERSITY IN THE VENICE LAGOON: MOLECULAR PROBES OF ECOTOXICOLOGICAL SUSCEPTIBILITY

I. VALIDATION OF DNA DAMAGE DETECTION IN FISH (*Zosterisessor ophiocephalus, Pall*) AND MUSSEL (*Mytilus galloprovincialis, Lam*) BY MEANS OF COMET ASSAY

L. Tallandini
Dipartimento di Biologia, Università di Padova

1. *Introduction.*

The maintenance of population and species-level genetic integrity are necessary components of fitness and long-term survival of populations and species. Changes and/or disruption of genetic equilibriums at different biological complexity levels lead to direct effects on the decline of the biodiversity resource. Several factors can be acting in the loss of biodiversity; among these the effects of long-term, low-level chronic exposure of populations to chemical contaminants have lead to decline or disappearance of many populations.

Concern has therefore been developed to the risks arising from the potential chronic and transgenerational effects of environmental contamination. Among these, changes in genetic variability and allele frequencies have been observed, directly or indirectly caused by contaminant exposure.

Measures of genetic patterns indicate polymorphism gradients in polluted environments and significant deviations from Hardy Weinberg expectations were observed at contaminated locations (Battaglia et al 1980, Benton et al 1994, Bisol et al., 1994; Patarnello et al 1991, Roark and Brown 1996).

The concept that genetic patterns within populations may be altered by exposure to contaminants is therefore at the basis of a context-driven understanding of the effects of contamination on populations and ecosystems . However, in order to provide direct links to genotoxic syndromes, it is necessary to link explicitly evidences of genetic pattern alterations to contaminant exposure/effects (Belfiore and Anderson, 2001).

Different susceptibility to environmental stress of different populations and genotypes of the same species can be studied following the effects of pollution in the natural habitat by means of ecotoxicological biomarkers. This approach can be applied in Venice Lagoon on the solid basis of about twenty years of pollution monitoring through the whole basin and in specific areas of the lagoon, showing the presence of heavy metals, PAHs and PCBs.

Two biomarkers were chosen for our work:

- The biotransformation enzymes of the P450 family and particularly CYP1A, a isoenzyme induced by various polyciclic aromatic hydrocarbons (PAHs), Polychlorinated biphenyls (PCBs), chlorinated dibenzodioxine and chlorinated dibenzofurans, and recognized as a specific biomarker for these chemicals.
- The Comet assay (Single Cell Gel Electrophoresis): chosen for its capability of detecting and differentiating genotoxic and cytotoxic DNA damages induced by different genotoxic and cytotoxic agents; not a specific biomarker, but increasingly used for its ability in discriminate different degrees and types of DNA damages.

In our three-year work plan the general aims are:

a) an evaluation of the levels of detectable damages/alterations by the two biomarkers in fish *Zosterisessor ophiocephalus* (Pall.), collected in four sampling sites of Venice Lagoon during the four seasons, in order to assess the correlation of biomarkers with pollution levels;
b) a comparison between the results obtained from the two indicators and the genetic patterns of the collected populations through different seasonal studies.

The first step of planned work was the assessment and validation of biomarker protocols.

Cyt.P450 protocols were already defined, validated and currently employed in the laboratory, while Comet assay procedures were quite a novelty.

The first year of work focused therefore on the test and evaluation of the reliability of the comet assay as a biomarker in two distinct situations:

- experimental exposure of fish to PCB in monitored aquaria;
- detection of different environmental pollution effects on samples taken from their natural habitat.

1.1. *Comet Assay.*

Comet assay originally developed by Rydberg and Johanson (1978), improved by Ostling and Johanson (1984) and modified in alkaline conditions by Singh et al., (1988, 1994, 2000), is a method allowing the detection of DNA damage as double strand breaks (DSB), single strand

breaks (SSB), alkali labile sites (ALS) and even DNA cross-links (Tice, 1995; Singh, 2000; Tice, 2000).

Since the early 1990s, due to the advantages showed with respect to DNA bulk akaline unwinding and alkaline elution procedures, interest for this assay has been constantly increasing. Its main advantages are: high sensitivity, ability in detecting strand breaks and alkali labile sites at individual cell level, the opportunity to evaluate different responses to toxic and genotoxic agents inside a cell population, the chance to obtain significant results using of a low number of cells. (Singh, 2000) Furthermore, comet assay can also be used to study some aspects of DNA repair (Fairbairn et al 1995; Anderson and Plewa, 1998). Finally, the perspective of introducing selective molecular probes, which are able to discriminate among diverse kind of damages due to different classes of substances, is a possible added benefit.

Comet assay has been used in some works coupled with micronucleus test, with results indicating that the former is more sensitive with reference to the level of the toxicant agent and the time of response. One of the reasons may come from the fact that, with comet assay there is no need for cell division to evidence genotoxic agent effects (Belpaeme et al., 1996). In this perspective comet assay, showing a clear dose response even at low levels of at least one genotoxicant agent, could be much more sensitive in ecogenotoxicological studies (Padrangi et al., 1995; Belpaeme et al 1996; Singh, 2000).

Many known mutagens and genotoxic carcinogens have been tested with the comet assay. Evidences of the sensitivity of the test to detect directly and indirectly induced DNA damage have been observed for a number of agents, including oxidative, alkilating and intercalating agents. Furthermore, in the last 10 years reproducible protocols have been developed and comet assay was increasingly employed in order to correlate organism-exposure to environmental contaminants with observed effects on DNA (Mc Kelvey-Martin, 1993; Tice, 1995; Vrzoc and Petras, 1997; Henderson et al., 1998; Frenzilli et al., 2000; Singh, 2000; Livingstone et al., 2000; Tice et al., 2000).

2. *Experimental.*

2.1. *Exposure of fish Zosterisessor ophiocephalus (Pall.) to PCB (Aroclor 1254): DNA damage evaluation by means of comet assay.*

Eighty adult fish, weighing on average 38.78±20.22g with an average length of 15.16±2.58 cm, collected by a trawl net from a low polluted

area located in the Venice Lagoon near the town of Chioggia were divided in ten 90 litre tanks and kept at 20 ±1°C in continuously aerated sea water, 33‰ salinity.

After 7 days of acclimation the treatment started by adding a volume of Aroclor 1254 (1mg/ml ethanol) to the five exposure tanks in order to obtain a nominal PCB concentration of 10µg/l; in the control tanks an equal volume of the pure solvent was added. Three times a week half the water was replaced and the PCB concentration subsequently restored. During the whole experiment (28 days) fish were fed with mussels collected in the Adriatic Sea.

At 0 (controls), 7, 14, 21, 28 days (controls and treated) days fish were sacrified, five from the control pool and five from the exposed pool.

2.1.1. *Erythrocyte collection in fish (Zosterisessor ophiocephalus, Pall.).*

Blood samples were collected from dorsal aorta of fish using heparinized syringes and suspended (1:500) in a Ca++ Mg++ free Phosphate Buffered Saline (PBS).

2.1.2. *Alkaline SCGE assay in fish erytrocytes.*

For SCGE procedure the protocols of Singh et al. (1988) and Singh (2000) were followed with minor adjustments. A schematic representation of the procedure is reported in Fig.1.

After slide preparation, DNA unwinding, electrophoretic run, and staining with ethidium bromide, the slides were examined at 400X using a fluorescent microscope; computer software (Casti Imaging 2001), was used to score individual parameters for each examined nucleus. The software was developed on the basis of the public domain analysis program for SCGE (Helma and Uhl, 2000).

The observed images were described as (fig.2):

- Nuclei: in the case of a subspheric core
- Cometae: in the case of a tail exceeding the right edge of the subspheric core circle
- Apoptotic nuclei: in the case of DNA fluorescence completely migrated and almost detached from the subspheric core of the nucleus which appears drastically reduced due to the little DNA in the head.

The comet imaging included: total DNA, percent of DNA in the comet head and tail, Tail Length (TL) and Tail Moment TM (TM=TL x % fluorescence outside the nucleus) (Ashby et al., 1995; Helma and Uhl, 2000) (fig. 3).

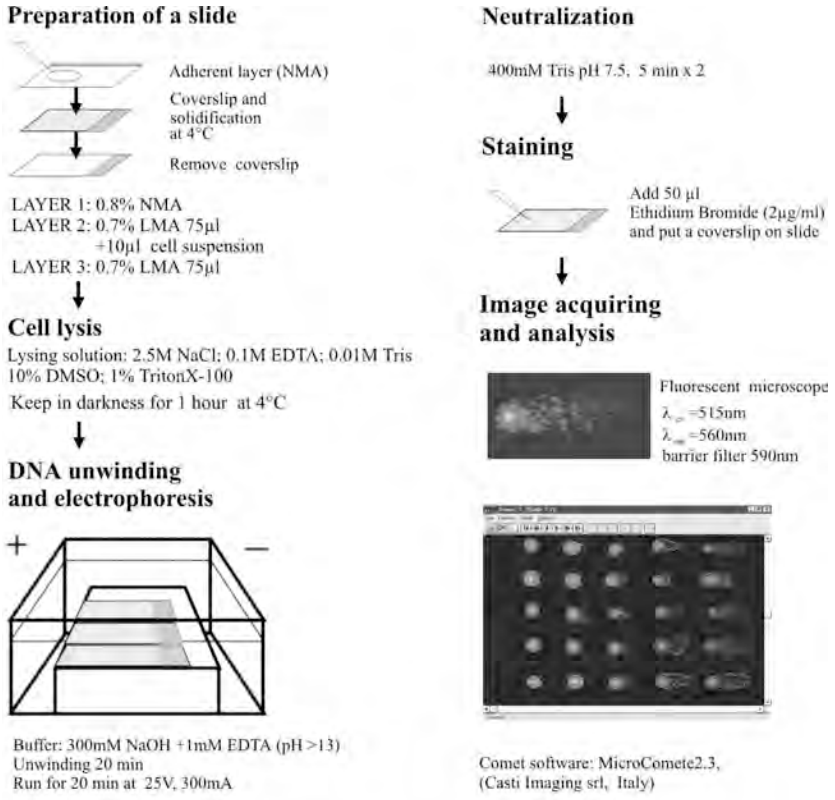

Fig. 1 - Comet assay protocol.

Routinely about 50 cells per animal were examined for each sample. Samples from five control and five exposed fish were used at each exposure time. Statistical analysis was performed by means of Student's t test and non parametric Wilcoxon test with the help of SPSS Systat software.

2.2. *Evaluation of DNA damage in mussels from the Venice Lagoon.*

2.2.1. *Mussel collection in field.*

Mussels (Mytilus galloprovincialis, Lam) were collected monthly, during a period of six month, August –January, in five sites of the Venice Lagoon: 1.Canale San Domenico, 2.Porto di Chioggia, 3.Canale Lombardo Esterno, 4.Porto di Malamocco, 5.Area Industriale di Marghera (Fig.4).

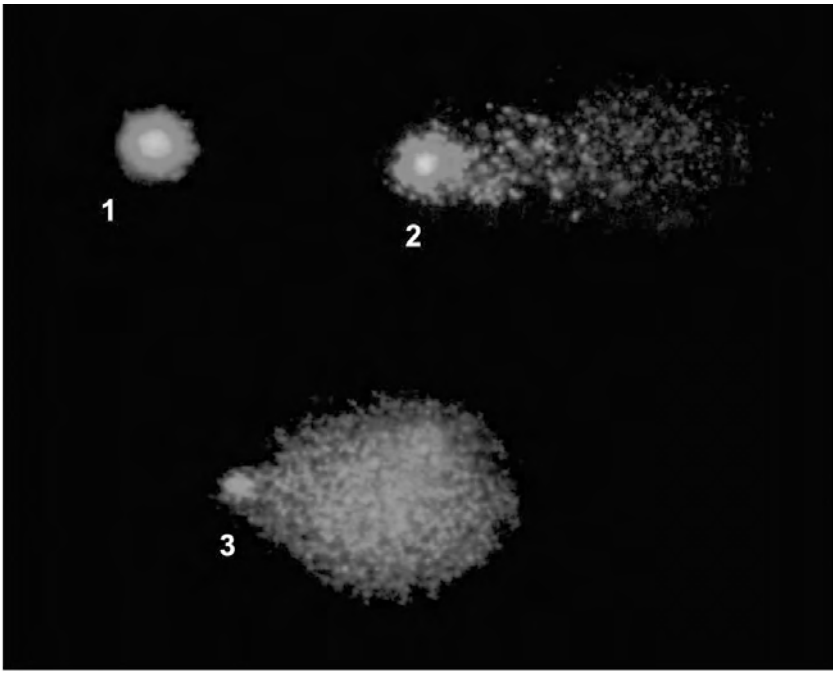

Fig. 2 - Erythrocytes nuclei after comet assay: 1) nucleus, 2)comet, 3) apoptosis.

At each collection time from each site 12 mussels, (length: 6±0.6 cm) were collected, quickly transferred in the laboratory, and stored one night in individual flasks in filtered aerated sea water to clear gut contents prior to the Comet assay.

2.2.2. *Procedure for Cell isolation from digestive gland.*

Comet assay was performed on mussel hepatocytes. For cell isolation the protocols of Lowe and Pipe (1994) and Mitchelmore and Chipman (1998) slightly modified were used. Digestive gland pieces were incubated with regular and slow agitation, for 60 minutes; at the end of incubation time cell suspension was filtered trough 100mm, 56 mm and 20 mm strainers in order to remove cell clumps and oocytes. The filtered suspension was then centrifuged at 200g for 5 minutes, resuspended in CMFS and then analysed using optical microscope for checking cell concentration and viability. The cell suspensions we used after centrifuging at 200g, were resuspended in CMFS to obtain approximately 10.000 cells in 10 μl.

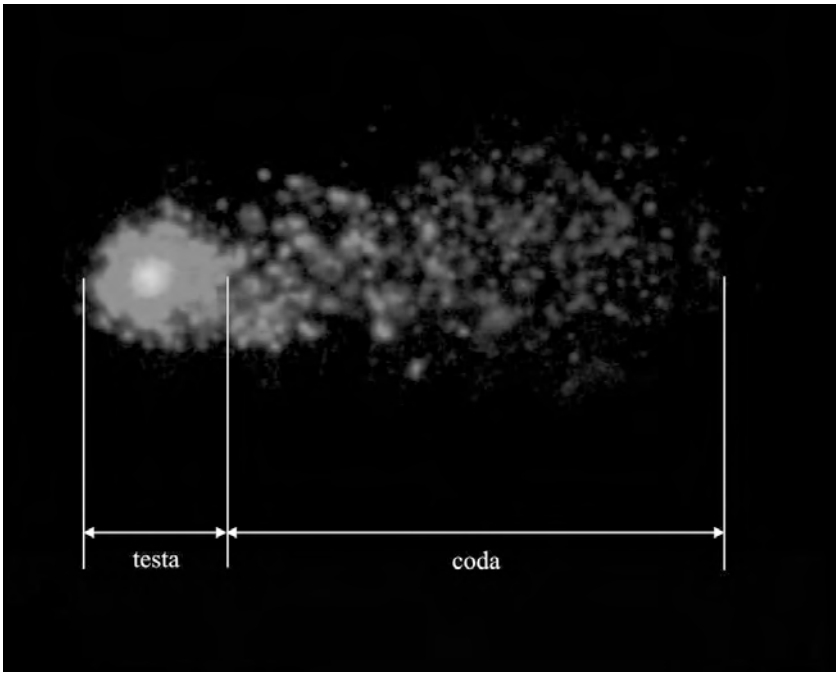

Fig. 3 - Schematic representation of cornet head and tail parameters (according to Helma and Uhl, 2000).

2.2.3. *Alkaline single cell gel electrophoresis of mussel hepatocytes.*

The comet assay procedure was performed following the same protocol used for fish erythrocytes, with minor modifications in buffer due to different osmotic and saline features between mussels and fish.

3. *Results.*

3.1. *Exposure of fish Zosterisessor ophiocephalus (Pall.) to PCB (Aroclor 1254): DNA damage evaluation by means of Comet assay.*

3.1.1. *Apoptotic events, cometae incidence and parameters.*

At each sample time (0,7,14,21,28 days) data for the Comet assay were analysed as percentage of cometae. In exposed fish after 7 days of treatment a very relevant incidence of apoptotic nuclei (up to 20% out of total) was observed. Apoptotic nuclei decreased at 14 and 21 days, being

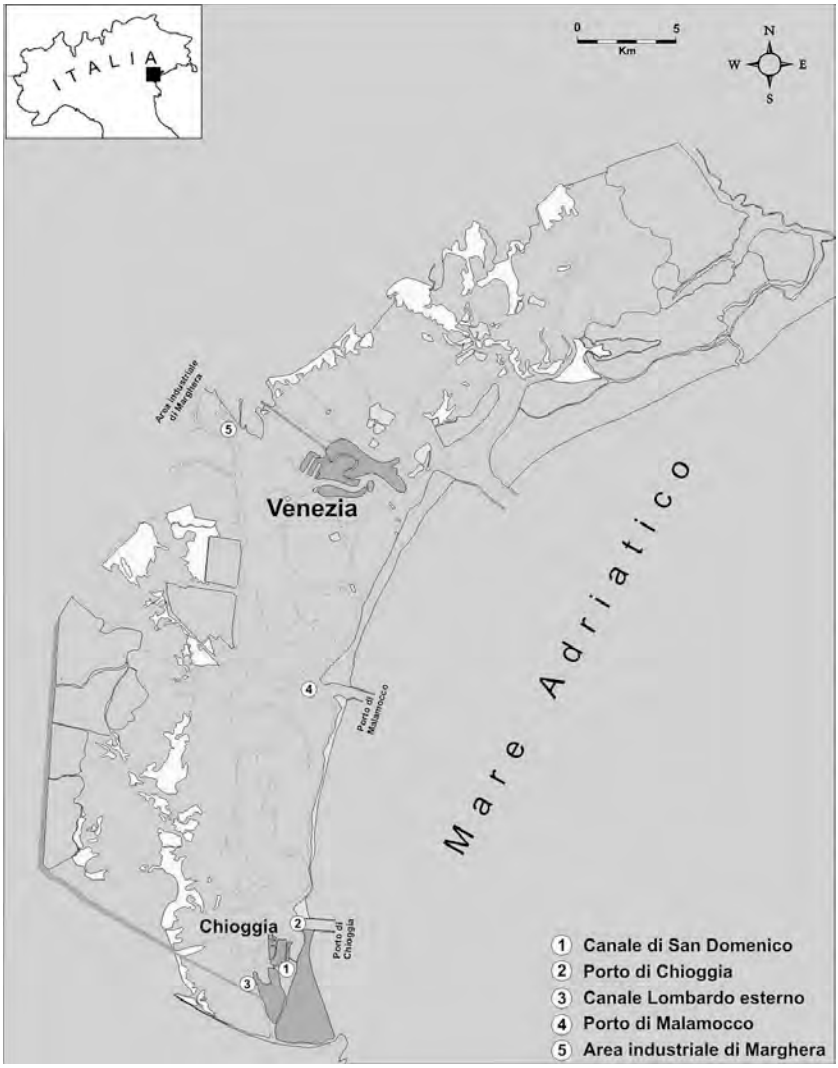

Fig. 4 - Venice Lagoon: location of the sampling sites.

completely absent at 28 days. The difference in apoptotic incidence between exposed and controls was highly significant ($P \leqslant 0.001$) at 7,14 and 21 days.

The mean percentage values of cometae during the experiment was equal to 16.2±7% in controls and 72.2±14% in exposed fish. The mean

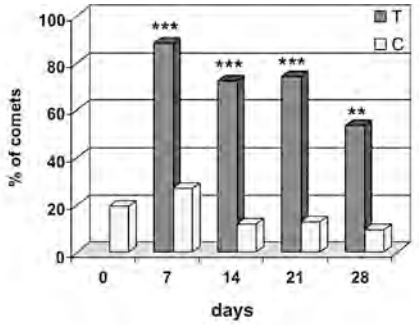

Fig. 5 - Percentage of cometae during the experiment in control (C) and treated (T) erythrocytes. (Asterisks indicate significant difference from control).****p<0.01 **p<0.05.

value differences between control and exposed fish were highly significant (P⩽ 0.001) at any time of the exposure (Fig 5).

Mean values for comet parameters (Tail Length and Tail Moment) were always higher in exposed fish than in control (P<0.001) for both parameters (fig.6). Furthermore, frequency distribution of Tail Length and Tail Moment values shows very marked and significant differences between control and exposed organisms. Finally the sums of Tail Lengths for all cells in control and exposed fish (normalized at each sample time at 250 cells) showed a significant difference (P<0,001) between control and exposed samples during the whole treatment. The higher values found in the exposed fish confirm the hypotesis of an Aroclor 1254–induced damage.

3.1.2. *Evaluation of DNA damage in mussels from the Venice Lagoon.*

The study concerned the evaluation of DNA damage from hepatocytes of mussels collected between August and January in five different sites of Venice Lagoon (see previous chapter).

The time span was chosen in order to discriminate between the effects on cell nuclei of environmental xenobiotics and seasonal exogenous (temperature, O2, salinity) and endogenous (biochemical and physiological parameters) variables. Recorded environmental variables were temperature, salinity and dissolved oxygen saturation in water.

3.1.3. *Apoptotic events, cometae incidence and parameters.*

Apoptotic events observed in our samples were comprised between 1.2% and 23.2% of cell population; Malamocco was the site with the lowest mean percentage (4.4%) of apoptotic events and also had the lowest measured percentage in a single sampling (1.2% in January).

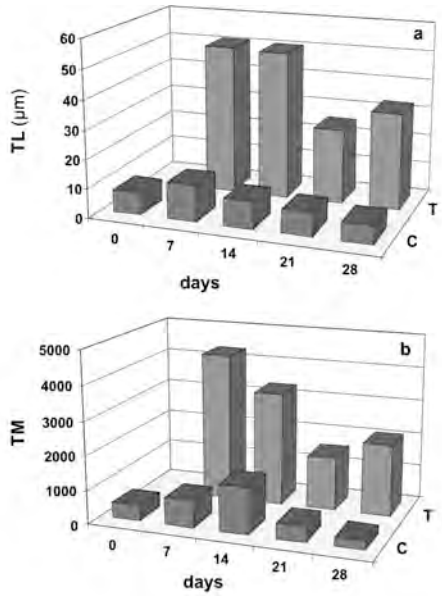

Fig. 6 - Mean values of Tail Lenght (a), and Tail Moment (b) in control (C) and treated (T) fish erythrocytes during the experiment.

Marghera was the site with the highest mean percentage (14.6%) with values spanning between 7.2% (January) and 23.2% (August). It has to be noted that in this site monthly apoptotic values have been at least twice than those of the other sites. Statistical analysis showed that the differences in mean and monthly values between Marghera and the other sites were highly significant ($0.01<P<0.05$), while the other sites showed no significant differences (fig. 7).

A linear regression of apoptotic cell percentage of all sites against water temperature showed significant positive correlation ($P\leqslant0.01$). Single site analysis evidenced that the site with highest correlation and significance between apoptotic cell percentage and water temperature was Marghera, ($P\leqslant0.01$) while Malamocco had the lowest ($P\leqslant0.03$).

Sample examination showed the presence of cometae in all sites during the whole sampling period with percentages between a minimum of 6% (Malamocco, December) and a maximum of 86% (Marghera, August). As it has been observed with percentage of apoptotic events there is a strong positive correlation between cometae percentage and temperature.

In the same way Marghera is the site with a significantly higher cometae count when compared with other sites: $P\leqslant0.01$ with Malamocco and

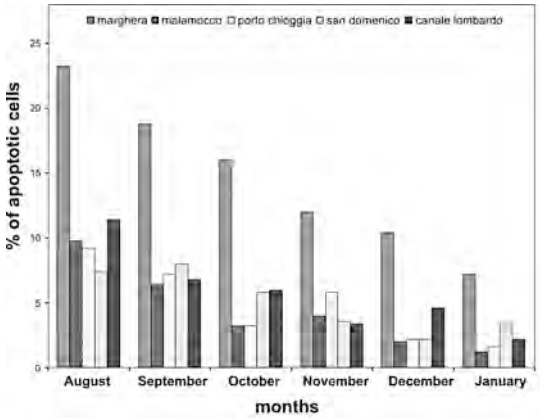

Fig. 7 - Mytilus sp. (digestive gland): apopotic cells percentage observed in the five site samples during a six month span monitoring.

Porto Chioggia, P≤0.03 with San Domenico and Canale Lombardo; these four sites show no significant differences among them.

Analysis of five monthly samples showed that mean TL and TM values were higher in Marghera then in the other sites except for TL value in November with respect to San Domenico and Canale Lombardo. Comparing the other sites, Canale Lombardo had higher TL and TM than Malamocco in October, November and December while in September only TL value was higher. Canale Lombardo had TL and TM higher than Porto Chioggia in October and November and San Domenico in October; in November San Domenico had higher TL and TM values than Malamocco and Porto Chioggia.

An overall ranking with respect to the alteration of nuclei can be evicted from the situation above:

Marghera > Canale Lombardo > San Domenico > Porto Chioggia > Malamocco.

The analysis of the distribution of damage classes for each site, during the six-month span of the experiment, confirms both temperature effect as co-factor on nuclei alteration and the evidence that this effect is maximum in the most polluted site: in Marghera, during August, 25% of sample nuclei had 90% of DNA outside central core thus showing strong suffering of the structural components of nucleus. In the same circumstances the percentage in Canale Lombardo was 12.8%, San Domenico 4,4%, Porto Chioggia 3.6% and Malamocco 2.8%.

These data are a further confirmation of the alteration ranking reported above.

4. *Conclusions.*

The two experimental works here reported clearly indicate that Comet assay can be a reliable and useful molecular biomarker.

In the first study fish were exposed in controlled conditions to PCB, and it was possible to detect an highly significant response to the treatment in terms of DNA alterations linked both to cytotoxic and genotoxic effects.

We can attribute the high incidence of apoptosis observed to an early cytotoxic effect, which has highest incidence at 7 days, and ends within 28 days of exposure. On the contrary, a comet-like alteration of DNA, linked to a genotoxic effect and detected during the whole experiment, showed the longest tail length and highest tail moment values, (i.e.: the highest damage), at the longest exposure time (28 days). These evidences agree with the MFO induction pattern by PCBs in Zosterisessor ophiocephalus (Pall.) (Nasci et al., 1991) and the model of MFO-linked genotoxic activation by PCBs. Experimental data strongly suggest in fact that MFO-produced intermediates are necessary in order to activate PCBs oxidative processes and/or adduct formation (Butterworth et al., 1995; Pereg et al., 2002).

In the second study by means of Comet assay data, we were able to discriminate different dystrophic levels in the five examined sites. A very significant dystrophy gradient: Marghera> Canale Lombardo> San Domenico> Porto Chioggia> Malamocco was observed. This gradient corresponds to the pollution levels detected in Venice Lagoon (Cescon et al., 2000; Fossato et al., 2000 a, b; Scarponi et al., 2000; Widdows & Nasci, 2000). It has to be underlined the very dramatic incidence of apoptotic events and comet-like alterations in hepatocytes of mussels collected in the sampling site of Marghera.

According to these data, Comet assay test would be a useful biomarker not only in controlled in vivo/in vitro experiments in the laboratory, but also in samples collected on the field. This fact gives us a suitable tool for the study of the relationships between genetic patterns and organism/population response to dystrophic environmental effects.

As reported above measures of genetic patterns can indicate polymorphism gradients in polluted environments, and significant deviations from Hardy-Weinberg expectations were observed at contaminated locations (Battaglia et al., 1980; Benton et al., 1994; Patarnello et al., 1991; Roark and Brown, 1996; Ghiotto, 2001). The two biomarkers we are employing, Cyt.P450 system, (specific and previously assessed), and

Comet assay, (assessed in this work), seem to fit well with pollution pattern of Venice Lagoon and give us the possibility to study functional (biochemical/ physiological) consequences of genetic changes. The study of phenotypic consequences of genetic changes are of increasing interest in order to relate ecotoxicity and genotoxicity data to consequences for populations and communities and, ultimately, biodiversity (Shugart and Theodorakis, 1998; Belfiore and Anderson, 2001).

References.

Anderson D. and Plewa M.J., 1998. "The International Comet Assay Workshop".

Ashby J., Tinwell H., Lefevre P.A., Browne M.A., 1995. The single cell gel electrophoresis assay for induced DNA damage (Comet assay): measurement of tail length and moment. *Mutagenesis*. vol. 10 n. 2: 85-90.

Battaglia B., Bisol P.M. and Rodinò E., 1980. Experimental studies on some genetic effects of marine pollution. *Helgoländer Meeresuntersuchungen*. 14th European Marine Biology Symposium. 33 (1-4): 587-595.

Belfiore N.M and Anderson S.L., 2001. Effects of contaminants on genetic patterns in aquatic organisms: a review *Mutation Research*. 489: 97-122.

Belpaeme K., Delbeke K., Zhu L., Kirsch-Volders M., 1996. Cytogenetic studies of PCB77 on brown trout (*Salmo trutta fario*) using the micronucleus test and the alkaline comet assay. *Mutagenesis* 11 (5): 485-492.

Benton M.J., Diamond S.A., Guttman S.I., 1994. A genetic and morphometric comparison of *Helisoma trivolvis* and *Gambusia holbrooki* from clean and contaminated habitats *Ecotoxicology-and-Environmental-Safety*. 1994; 29(1): 20-37.

Bisol P.M., Alay F., Gavilan J.F., Gonzalez F., Cabello Y.J., 1994. Influencia del ambiente sobre la estructura genetica de dos poblaciones de *Chilina dombeyana* (Bruguiere, 1789) (Mollusca, Gastropoda) del rio Biobio, *Boletin Soc. Biol.* Concepcion, Chile 65: 181-185.

Butterworth F.M., Pandey P., Mc Gowen R.M., Ali-Sadat S., Walia S., 1995. Genotoxicity of PCBs: recombionogenesis by biotransformation products. *Mutation Research*. 342, 61-69.

Cescon P., Barbante C., Capodaglio G., Cecchini M., Turetta C., Caroli S., Caimi S., Senofonte O., Delle Femmine P., Petrucci F. and Fuoco R., 2000. Microinquinanti inorganici nella laguna di Venezia. In: *La ricerca scientifica per Venezia*; Il progetto sistema Lagunare Veneziano. Ed. Istituto veneto di scienze, lettere ed arti II (I): 495-523.

Fairbairn W.D., Olive P.L. and O'Neill K., 1995. The comet assay: a comprehensive review. *Mutation research*. 339: 37-59.

Fossato V.U., Campesan G., Craboledda L., Dolci F. and Stocco G., 2000. Organic micropollutants and trace metals in water and suspended particulate matter. In: *La ricerca scientifica per Venezia; Il progetto sistema Lagunare Veneziano*. Ed. Istituto veneto di scienze, lettere ed arti, III: 39-46.

Fossato V.U., Campesan G., Craboledda L., Dolci F. and Stocco G., 2000. Persistent chemical pollutants in mussels and gobies from Venice Lagoon. La ricerca scientifica per Venezia; Il progetto sistema Lagunare Veneziano. Ed. Istituto veneto di scienze, lettere ed arti, III: 187-196.

Frenzilli G., Bosco E., Barale R., 2000. Validation of single cell gel assay in human leukocytes with 18 reference compounds. *Mutation Research*. 468 (2): 93-108.

Ghiotto R., 2000. Analisi di polimorfismi in molluschi bivalvi della laguna di Venezia. *Tesi di laurea* (a.a.1999/2000).

Helma C. and Uhl M., 2000. A public domain image analysis program for the S.C.G.E. (Comet Assay). *Mutation Research*. 466: 9-15.

Henderson L., Wolfreys A., Fedyk J., Bourner C. and Windebank S., 1998. The ability of the comet assay to discriminate between genotoxins and cytotoxins. *Mutagenesis*. vol. 13 n. 1: 89-94.

Livingstone D.R., Chipman J.K., Lowe D.M., Minier C., Mitchelmore C.L., Moore M.N., Peters L.D. and Pipe R.K., 2000. Development of biomarkers to detect the effects of organic pollution on aquatic invertebrates: recent molecular, genotoxic, cellular and immunological studies on the common mussel (*Mytilus edulis* L.) and other mytilids. *Int.J.Environmental and Pollution*, 13: 1-6.

Lowe D.M, Pipe R.K., 1994. Contaminant induced lysosomal membrane damage in marine mussel digestive cells: an in vitro study. *Aquatic-Toxicology*. 30(4): 357-365.

McKelvely-Martin V.J., Green M.H.L., Shmezer P., Pool-Zobel B.L., De Meo M.P., Collins A., 1993. The single cell gel electrophoresis assay (Comet assay):A European review. *Mutation research*. 288: 47-63.

Mitchelmore C.L. and Chipman J.K., 1998. DNA strand breakage in aquatic organisms and the potential value of the comet assay in environmental monitoring. *Mutation Research*. 399: 135-147.

Nasci C., Campesan G., Fossato V., Tallandini L., Turchetto M., 1991. Induction of cytochrome P–450 and mixed function oxygenase activity by low concentration of polychlorinated biphenyls in marine fish Zosterisessor ophiocephalus (Pall.) *Aquatic Toxicology* 19: 281-290.

Östling O. & Johanson K.J., 1984. Bleomicin, in contrast to gamma irradiation, induces extreme variation of DNA strand breakage from cell to cell, *Int. Journal of radiation biology* 52: 683-691.

Pandrangi R., Petras M., Ralph S., Vrzoc M., 1995. Alkaline single cell gel (comet) assay and genotoxicity monitoring using bullheads and carp. *Environmental and Molecular Mutagenesis*. 26: 345-356.

Patarnello T., Guinez R., Battaglia B., 1991. Effects of pollution on heterozygosity in the barnacle Balanus amphitrite (Cirripeda: Thoracica). Mar. Ecol. Prog. Ser. 70: 237-243.

Pereg D., Robertson LW., Gupta RC., 2002. DNA adduction by polychlorinated biphenyls: adducts derived from hepatic microsomal activation and from syntetic metabolites. Mutation Research. 139: 129-144.

Roark S., Brown K., 1996. Effects of metal contamination from mine tailings on allozyme distributions of population of great plains fishes. Environ, Toxicol. Chem.. 15: 921-927.

Rydberg B. & Johanson K.B., 1978. Estimation of DNA strand breaks in mammalian cells. In: *DNA repair mechanisms* Hanvalt PC, Friedberg E.C., Foxs CF Eds, Accademic Press, New York, 465-468.

Scarponi G, Turetta C., Capodaglio G., Barbante C., Cescon P., Ghetti P.F., Frache R., Papoff P., Fuoco R., Franco P., Lampugnani L., Caroli S., 2000. Valutazione chemiometrica della qualità di alcune componenti dell'ecosistema lagunare veneziano. Indice di tossicità di sedimenti. In: *La ricerca scientifica per Venezia; Il Progetto Sistema Lagunare Veneziano*. Ed. Istituto veneto di scienze, lettere ed arti II (I): 71-97.

Singh N.P., McCoy M.T., Tice R.R., Schneider E.L., 1988. A simple technique for quantification of low levels of DNA damage in individual cells. *Exp.Cell.Res*. 175: 184-191.

Singh N.P., Stephens R.E., Schneider E.L., 1994. Modification of alkaline microgel electrophoresis for sensitive detection of DNA damage. *Int. J. Radiat. Biol.* 66 23-28.

Singh N.P., 2000. Microgels estimation of DNA strand breaks, DNA protein crosslinks and apoptosis. *Mutation. Research.* 455: 111-127.

Tice RR, 1995. Application of the single cell gel assay to environmental biomonitoring for genotoxic pollutants. *In Biomonitors and biomarkers as indicators of environmental change*, edited by F.M. Butterworth. Plenum Press, New York, pp 69-79.

Tice RR., Agurell E., Anderson D., Burlinson B., Hartmann A., Kobayashi H., Miyamae Y., Rojas E., 2000. Single cell gel/comet assay: guidelines for in vitro and in vivo genetic toxicology testing. *Environmental And Molecular Mutagenesis*. 35 (3) :206-221.

Vrzoc M., Petras ML., 1997. Comparison of alkaline single cell gel (Comet) and peripheral blood micronucleus assays in detecting DNA damage caused by direct and indirect acting mutagens *Mutation-Research-Fundamental-And-Molecular-Mechanisms-Of-Mutagenesis*. 381 (1): 31-40.

Widdows J. & Nasci C., 2000. Effetti degli inquinanti nella laguna di Venezia: responsi fisiologici nei mitili (*Mytilus galloprovincialis*). Sintesi Generale del Progetto. In: La ricerca scientifica per Venezia; Il Progetto Sistema Lagunare Veneziano. ed. Istituto veneto di scienze, lettere ed arti, I: 103-104.

FIRST RESULTS OF A RESEARCH PROJECT ON THE DIFFUSION OF ALLOCHTHONOUS MARINE SPECIES (ZOOBENTHOS) IN THE LAGOON OF VENICE. MOLLUSKS: AFFINITIES AND DIFFERENCES WITH THE MEDITERRANEAN SITUATION

L. Mizzan and R. Trabucco
Museo di Storia Naturale di Venezia

The first results of an elaboration carried out by database especially developed from the available bibliographic data concerning the presence of allochtonous marine species in the Mediterranean, in particular for Mollusks, are given. After examining the published works a revision of the records, both taxonomic and of merits , has been made. This elaboration has revealed the effective presence in the Mediterranean of at least 138 out of the 185 species of exotic mollusks so far recorded. Once analysed the geographic areas of origin, the ecological characteristics and the methods of diffusion, the Mediterranean situation as well as the specific one of the Lagoon of Venice have been characterized, thus pointing out sensible differences in the spread of the exotic species in the compared environments and a remarkable Atlantic characterization for the Lagoon of Venice.

Finally some of the new data in course of publication in Bollettino del Museo di Storia Naturale di Venezia are presented, concerning the first results of the research campaign in the Lagoon of Venice, among which the first record for the Veneto Lagoon of two species of exotic mollusks: Anadara demiri (Piani, 1981) (Mollusca, Bivalvia, Arcidae) and *Musculista senhousia* (Benson in Cantor, 1842) (Mollusca, Bivalvia, Mytilidae).

1. *Introduction.*

1.1. *The Lagoon of Venice: climatic characterization.*

The Lagoon of Venice and in general the North Adriatic lagoons sensibly differ from other Mediterranean coastal lagoon environments

because of several contributory geographic, climatic, environmental and biological features which lend them remarkably North European affinities rather than typically Mediterranean, often defined as "sub-Atlantic" characteristics [Sacchi, 1979; Bianchi, 1988].

The narrow, elongated shape of the Adriatic magnifies the tidal phenomena, typically modest in the Mediterranean, and reduces the water exchange with the rest of the Mediterranean. This factor together with the high latitudes reached in the Gulf of Venice and the low depths of the basin increases the temperature range in the seasonal cycle. Moreover, many big rivers flow into the Gulf of Venice, some of which of Alpine origin, thus determining thermohaline values which are closer to North European environments than to Mediterranean ones. The thermic and pluviometric influence of the Eastern Alps as well as the periodic cold winds from northeast (Bora) are also to be considered. [Sacchi et al., 1989].

As a matter of fact, the populations themselves of the coasts of the North Adriatic basin show the significative absence of some typically Mediterranean species, a phenomenon called for this reason "north Adriatic hiatus" [Sacchi, 1977; Sacchi, 1983]. The sub-Atlantic characteristics of these environments are stressed by the presence of species typical of more northern areas with Atlantic affinity such as *Fucus* virsoides and *Littorina saxatilis*.

These environmental and biological peculiarities may in part explain the reason why the Lagoon of Venice represents the first Mediterranean arrival station for numerous new species as well as account for the fact that the acclimation in the Lagoon is not always followed by irradiation towards other Mediterranean environments, though similar for other aspects.

1.2. *Introduction of alien species in the Lagoon of Venice.*

The exotic species which have reached the Lagoon generally seem to have in common a wide ecological value. They easily adjust themselves to variations of salinity, temperature and often dissolved oxygen and usually tolerate high rates of water pollution. On the other hand, these characteristics are indeed those bestowing on these species the capacity to colonize new environments and compete with the indigenous species [Sacchi et al., 1989]. In some cases instead, the new species seem to develop such specializations as to allow them to penetrate into specific environments with still available niches. A point in case could be *Tricellaria inopinata* [d'Hondt and Occhipinti Ambrogi, 1985; Sacchi et al., 1992].

The development of intense maritime traffic with big vessels, shortest periods of navigation, methods of stocking and unloading of great quan-

tities of bilge-water, the growing imports and periods of stay in open or partially confined waters of still vital commercial species, together with several possible mechanisms in the different life stages (larvae or adults), have remarkably reduced the biogeographical isolation of these environments [Zibrowius, 1992; Occhipinti Ambrogi, 1995, Mizzan, 1999]. Besides the above mentioned mechanisms of "passive" penetration one should also take into consideration an ever growing responsibility for deliberate introduction of exotic species for water farming or inappropriate repopulation campaigns.

If these mechanisms of penetration can explain the increase of appearance of alien species in the Lagoon of Venice, like in other similar environments, the increase of cases of complete acclimation may be favoured in the Lagoon of Venice by the deeper and deeper phenomena of human interaction which interest it.

If the Lagoon of Venice has been for many centuries an environment strongly characterized by human presence, it is only in the last two hundred years that the intervention of man has been able to sensibly modify the characteristics of the system itself. As a matter of fact for over five hundred years the Magistrates of the Serenissima prevented the Lagoon from turning into a marsh by keeping, consciously or not, an ecological characterization for wide areas which was still substantially similar to the original one of these environments. For some decades we have been witnessing a decisive increase of human pressure with rapid changes on territory, environment and even populations. The hydrodynamic alterations of the basin, the increase of erosion of the sea bottom, water pollution and indiscriminate fishing as well as the general banalization of the systems have been reducing the competitiveness of indigenous species in comparison with alien ones.

The Lagoon of Venice is therefore on the one hand receiving, more and more often due to human intervention, voluntary or not, new alien species while on the other hand, owing to the alteration of the lagoon environment and its progressive degradation, its indigenous species are being negatively sorted out. Such a context ends by favouring the alien species which best resist or adjust to new conditions, thus fostering a spiral process whose serious effects on the maintenance of biodiversity and local populations is self-evident.

This research means to define the phenomenon of the Lagoon of Venice starting from the analysis of the Mediterranean situation and provide new data on the distribution of alien species in the Lagoon so as to explain their interactions with local elements.

2. *Instruments and methods.*

2.1. *Step 1. Bibliographic research and creation of a data bank on alien species.*

The first stage of research has consisted in gathering a substantial bibliography concerning the alien species of Mollusks so far recorded for the Mediterranean. The choice of this group has been made because of the wide diffusion of the Mollusk Phylum in every type of environment and climate, a circumstance which makes them good indicators of both populations and environmental conditions.

As for the Lagoon of Venice, the decision has been made to investigate also into exotic species belonging to other taxonomic categories and comparing the data with those provided by Mollusks.

The data have been successively critically analysed and put into a data bank (fig. 1).The data bank has been structured by records, each of them concerning a different species and tailor-made to insert the taxonomic data about present systematic position, examined bibliography, first finding and first record in the Mediterranean. The data inserted also refer to the type of record and the method of penetration of the species (tab. 1), the area in which it has been found so far and the recording stations ; the latter proves particularly useful to trace back the route followed by the species in the Mediterranean. Finally the data bank records are furnished with space for notes in order to record possible ecological peculiarities of the species or any other useful information. The processing of bibliographic data has concluded this first stage of work; in particular the periods of finding, the success and ways of penetration, the biogeographical areas of origin have been studied. The analysis has been carried out in parallel on the Mediterranean and on the Lagoon of Venice, so as to highlight affinities and differences between the two situations.

2.2. *Stage 2. Elaboration of the research program: sampling campaign 2002.*

The second stage of work will consist of a sampling campaign in the Lagoon of Venice to be carried out on a total of 17 stations which well represent the different conditions existing within the lagoon environment and are scattered on the entire area involved in the research. The acquired data will be successively analysed and processed in order to obtain up-dated information on the alien species and the interactions with indigenous species.

Some preliminary outings have already provided a first outstanding result, that is the spotting of two species never recorded before for the Lagoon: bivalves *Musculista senhousia* (Benson in Cantor, 1842) and *Anadara demiri* (Piani, 1981).

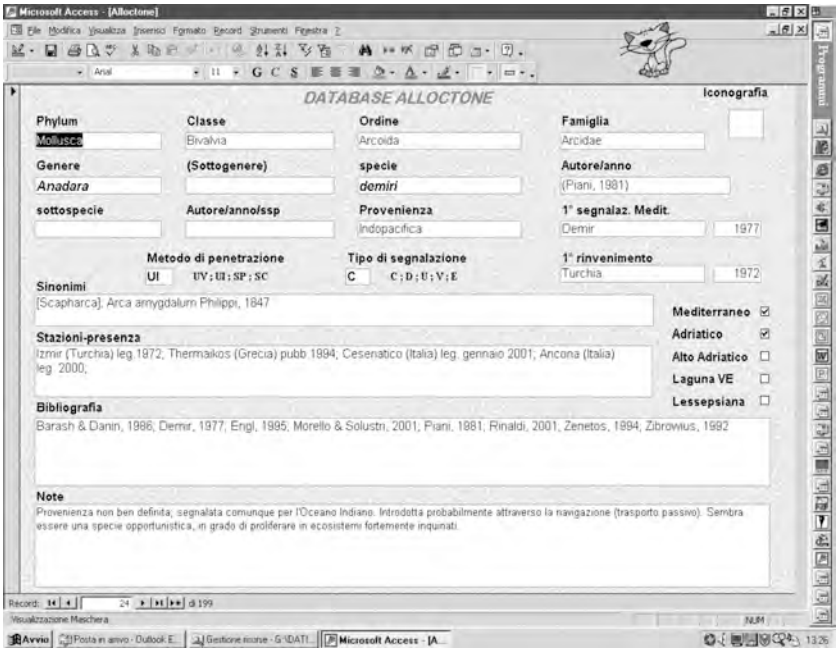

Fig. 1 - Slide of alien species database.

Tab. 1 - Account of database abbreviations.

Methods of penetration
UV: Human - Intentional UI: Human - Unintentional SP: Spontaneous SC: Unknown
Type of records
C: Certain D: Uncertain U: Single (including UR: Single finding and US: Single Records) V: Old records E: Wrong

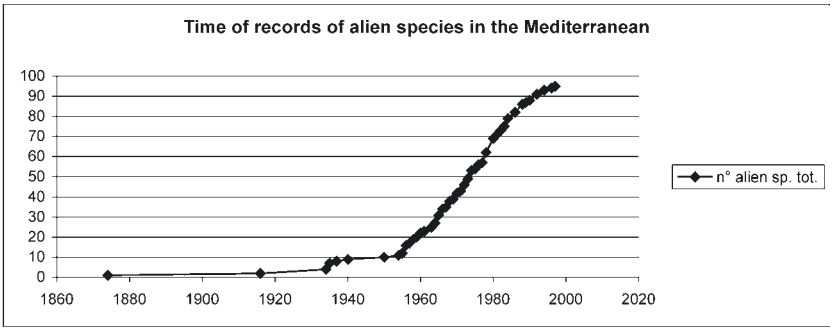

Fig. 2 - Findings of alien species in the Mediterranean.

3. *Results and discussion.*

During the filling in of the data bank records, an objective difficulty of identification of the species has been found because of the frequent confusion with local elements which has caused a high number of wrong identifications . It has not always been easy to either trace the period of penetration, since some records are not precise about the date of finding of the species, or define the area of origin: for instance, in several cases, some species considered allochthonous were actually authochtonous species whose presence or effective distribution were not sufficiently known. In addition, finding information has been difficult because of the dispersion of data, published on a number of scientific magazines, sometimes with limited circulation, or because of unclear titles and abstracts of the articles themselves.

After a critical revision of the data, the elimination of wrong records and the one-by-one assessment of uncertain records, the first information of the data bank have been processed.

198 species so far recorded for the Mediterranean have been examined, 14 of which concern taxonomic groups different from Mollusks and refer exclusively to the Lagoon of Venice. Among the other 184, concerning Mollusks, 137 have been assessed as “certain” (including “old” species, “single findings” and “single records”), 45 as “uncertain” and 2 as “wrong”. For the Lagoon of Venice 13 “certain” records of Mollusks have been assessed; among the 14 concerning other taxa, 12 have been considered as “certain” and 2 “uncertain”. All the following elaborations concern only “certain” records .

The graph (fig.2) shows that the first records of alien Mollusks for the Mediterranean go back to the last decades of 1800, which is likely to be due to the opening of the Suez Canal dated 1869, as confirmed also by

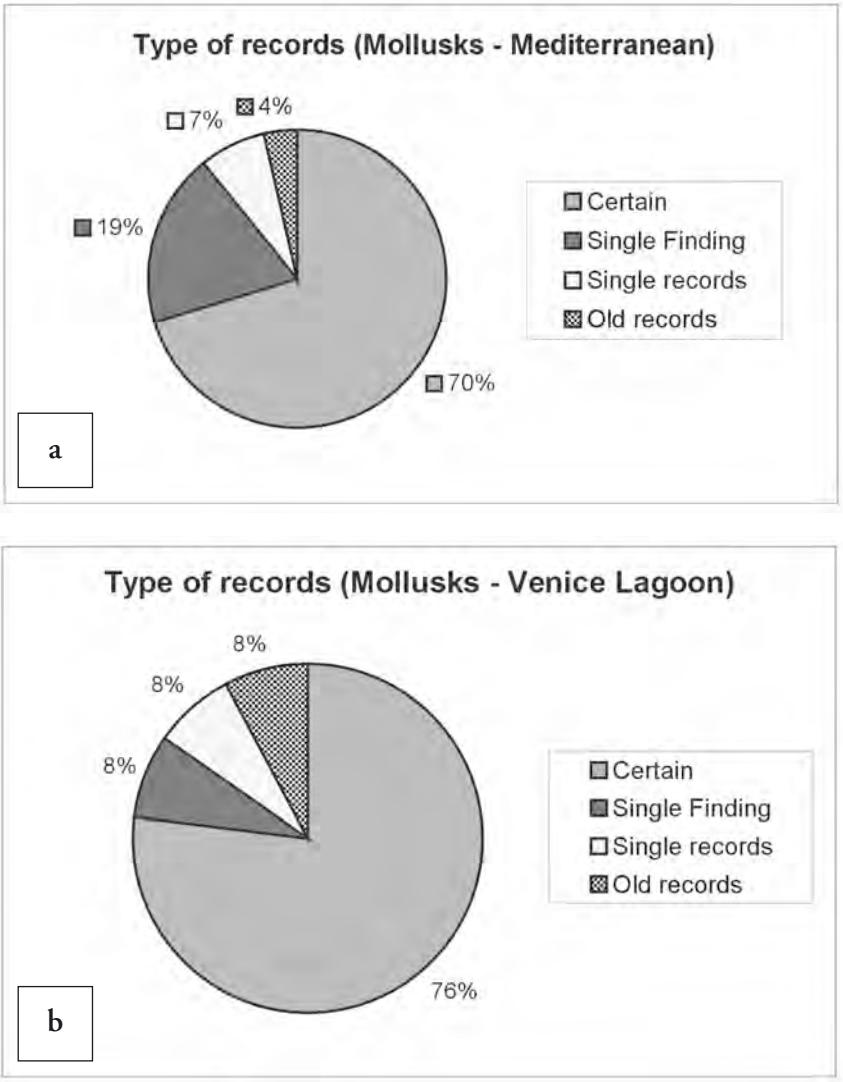

Fig. 3 - Successful penetrations of Mollusks in the Mediterranean (a) and in the Venice Lagoon (b).

the fact that most alien species are of Indo-Pacific origin. (Fig. 5a). The increase of records at the beginning of the last century, in particular during the thirties, was followed by a standstill during World War II and a successive renewal from the fifties onward.

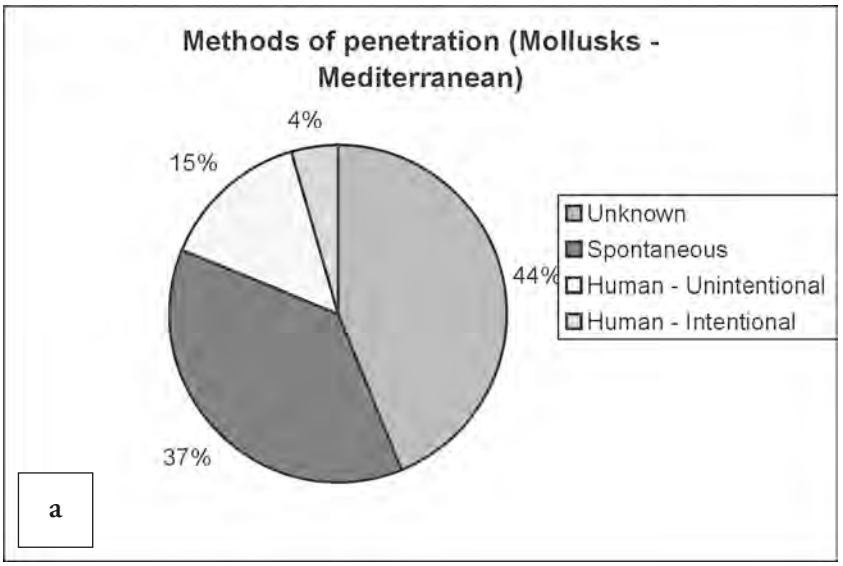

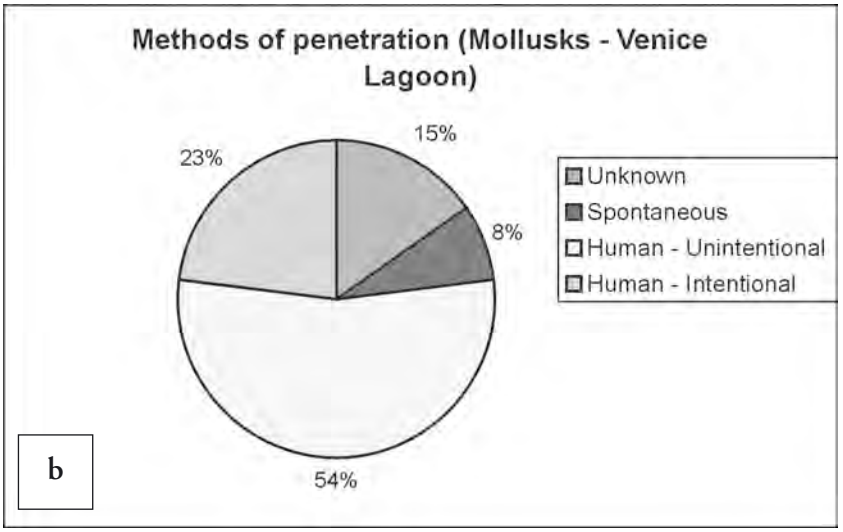

Fig. 4 - Methods of penetration of Mollusks in the Mediterranean (a) and in the Venice Lagoon (b).

The assessment of the "success of penetration" (fig.3a) shows that in the Mediterranean 70% of species (96) has definitely settled down (certain and repeated record); 19% (26 species) refers to single findings, 7%

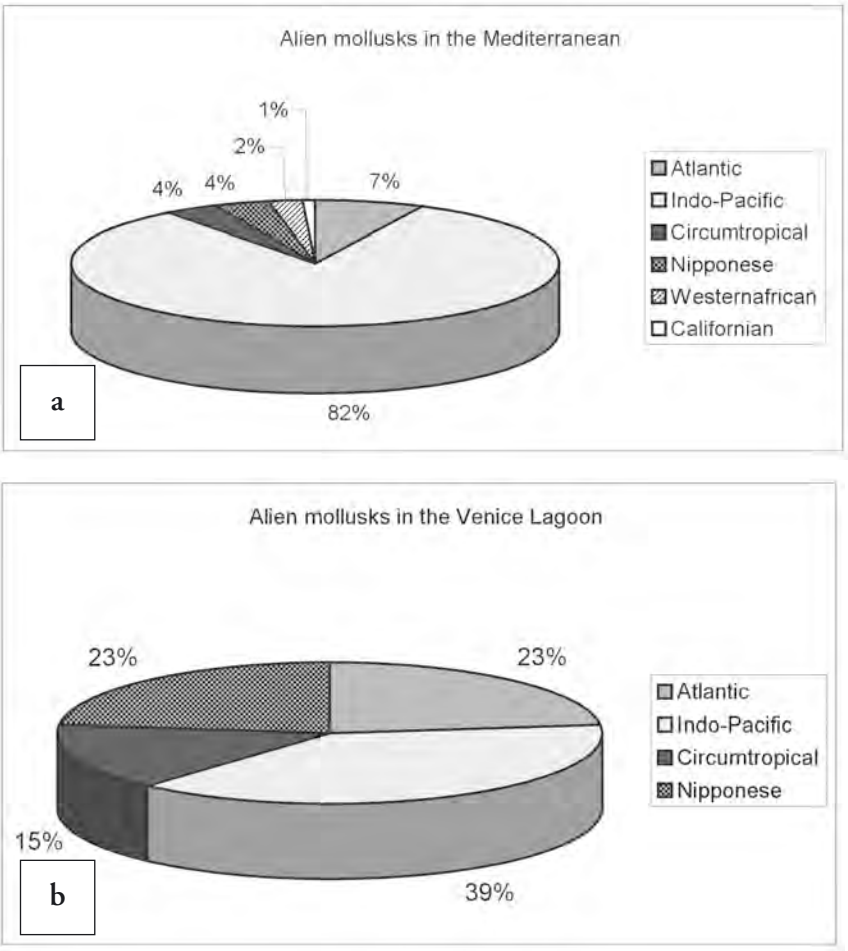

Fig. 5 - Biogeographical areas of origin of alien mollusks in the Mediterranean (a) and in the Venice Lagoon (b).

(10 species) to records which have never been repeated and 4% (5 species) to "old" records. In conclusion almost 3 out of 4 species come to acclimation, at least at local level (single area).

In the Lagoon of Venice (fig.3b) the success appears even greater since the species recorded as "certain" are 76% (10); one has been found only once (8%), one has been recorded only once (8%) and one considered as an "old" record.

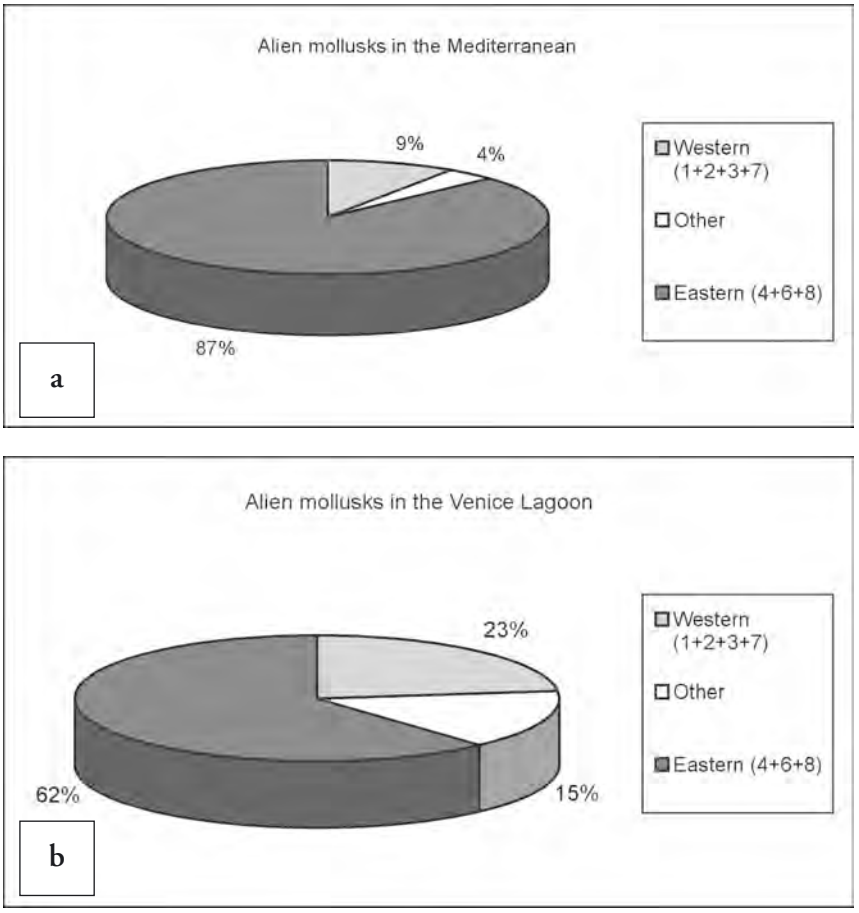

Fig. 6 - Division by longitude of biogeographical areas of origin: Mediterranean (a) Venice Lagoon (b).

The ways of penetration of alien Mollusks into the Mediterranean (fig. 4a) remain unknown for most of the species examined (60, that is 44%) although for 51 (37%) we can assume a spontaneous arrival, by which we essentially mean the crossing of the Suez Canal by species of wide ecological value, in particular euryhaline, given the presence of high salinity areas within the canal. The information on involuntary anthropic introductions (20 species, that is 15%) is of interest, while the voluntary ones represent only 4% of the total (6 species).

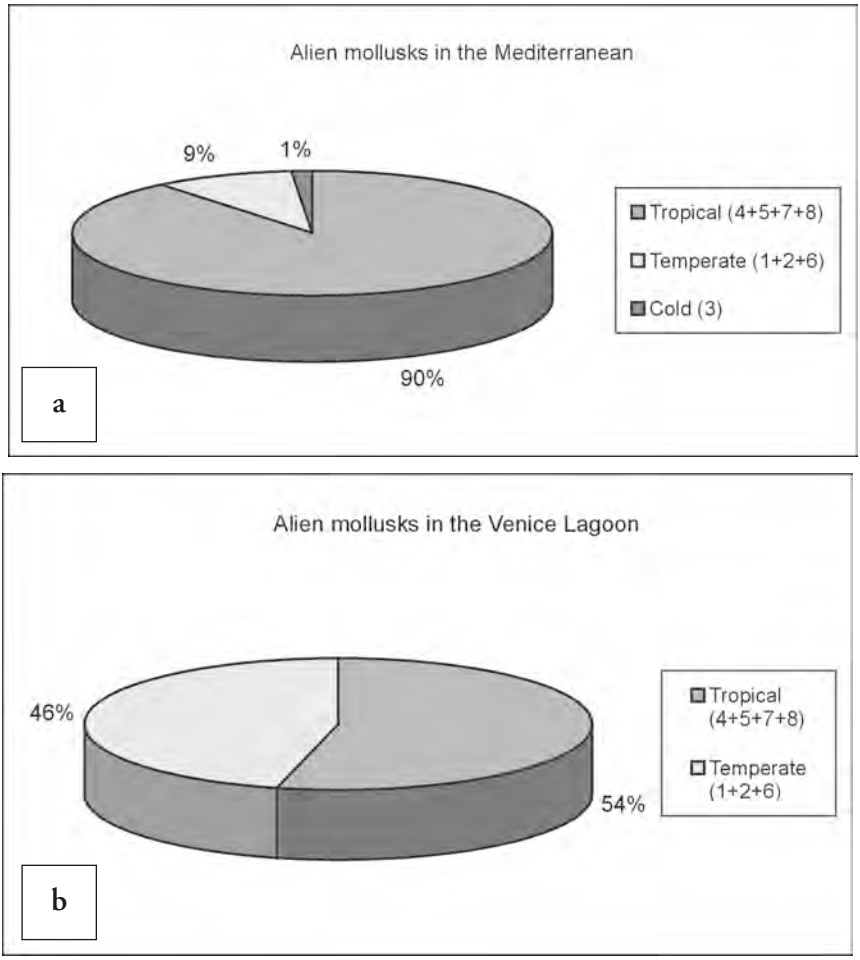

Fig. 7 - Division by climate zones of biogeographical areas of origin: Mediterranean (a) Venice Lagoon (b).

On the contrary, in the Lagoon the main vector is man, given the predominance of species introduced both intentionally (3, that is 23%) and involuntarily (7, that is 54%), justifiable with the presence of water farming activities and maritime traffic. Only 8% (1 species) may have come spontaneously, while the way of penetration for the remaining 15% (2 species), a percentage decidedly lower than that of the Mediterranean, is still unknown.

As for the biogeographical areas of origin (fig. 5a), the Indo-pacific elements prevail decidedly (82%, 113 species) and actually the distribu-

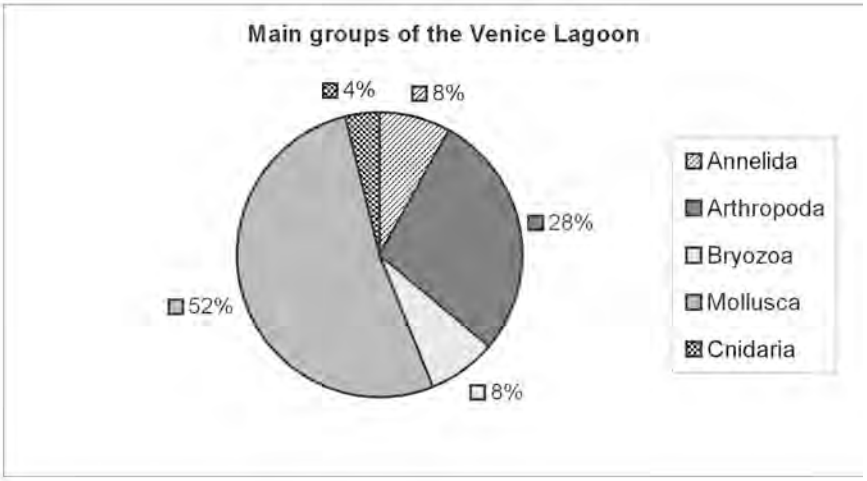

Fig. 8 - Distribution of alien species found in the Venice Lagoon by main taxonomic groups.

tion of most species recorded for the Mediterranean proves limited to the Eastern basin (Mar di Levante). As a whole the species of Atlantic origin are few (7%, 10 species); the remaining ones seem to be equally divided among circumtropical elements (4%, 5 species), Nipponese (4%, 5 species), Western African 82%, 3 species) and Californian (1%, 1 species).

In the Lagoon of Venice (fig. 5b) 5 species out of 13 (39%) are of Indo-Pacific origin, 3 Atlantic (23%), 3 Nipponese (23%) and 2 circumtropical (15%), which emphasizes a less important dominance of the Indo-Pacific component in comparison with the Mediterranean, a stronger diversification in the areas of origin and a greater Atlantic affinity.

According to a division of the areas of origin by longitude (fig. 6a), in the Mediterranean the eastern species prevail (119, that is 87%) over 13 western species (9%) and "others" (4%, 5 species).

In the Lagoon (fig. 6b) instead the eastern species go down to 62% (8 out of 13), while there are 3 western species (23%). The increase of the western component as well as the parallel decrease of the eastern fraction are clear.

Finally, according to a division of the areas of origin by climate zones, the Mediterranean situation is characterized as follows (fig. 7a): 122 tropical species (90%), 13 species from temperate areas (9%) and 2 species from cold areas (1%). In this case the advantage of thermophile species proves decidedly higher than expected, which could indicate for the Mediterranean a trend towards sub-tropical affinities.

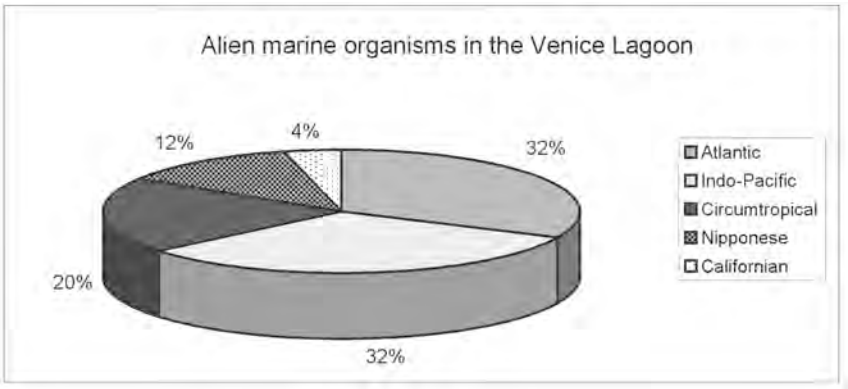

Fig. 9 - Biogeographical areas of origin of alien species found in the Venice Lagoon.

The data for the Lagoon of Venice (fig. 7b) confirm the Atlantic character compared to the Mediterranean basin, evident in the higher percentage of elements from temperate areas (46%, 6 species); the remaining 54% is anyhow represented by 7 tropical species.

For the Lagoon of Venice the decision has been made to investigate also into the other taxonomic categories, together with Mollusks (tab. 2, fig. 8), taking into consideration the area of origin. On a total of 25 elements, it has turned out that 8 are of Indo-Pacific origin (32%) and as many of Atlantic origin, while 5 species have circumtropical distribution

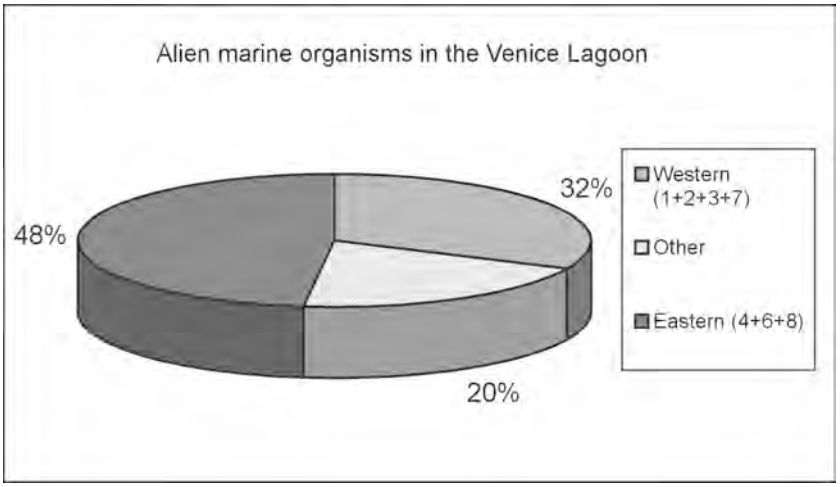

Fig. 10 - Division by longitude of biogeographical areas of origin of alien species found in the Venice Lagoon.

Tab. 2 - List of alien species in order of occurrence in the Venice Lagoon.

Species	Time of occurrence in the Lagoon	Reference record	Original spread area
Littorina saxatilis	XVIII sec.	Olivi, 1792	North European Atlantic coasts (very old record)
Ficopomatus enigmaticus	First World War	Fauvel, 1938	Subtropical and Temperate Eastern waters (Australia-New Zealand)
Hydroides dianthus	1934	Fauvel, 1938	North American Atlantic coasts
Callinectes sapidus	1950	Giordani Soika, 1951	North American Atlantic coasts
Crassostrea gigas	1966-67	Cesari and Pellizzato, 1985b	Nipponese
Scapharca inaequivalvis	1974-1976	Cesari and Pellizzato, 1985b	Indo-Pacific, through Suez and intermediate stages
Cuthona perca	1976	Perrone, 1995	North American Atlantic coasts
Ammothea hilgendorfi	1979-1981	Krapp and Sconfietti, 1983	Indo-Pacific
Elasmopus pectenicrus	1980-1981	Sconfietti, 1983	Lessepsian species known for Eastern Medit. (circumtropical)
Doris bertheloti	raccolto da Paolo Cesari	Perrone, 1989	North European Atlantic coasts
Callinectes danae	1981	Mizzan, 1993	North American Atlantic coasts
Paracerceis sculpta	1981	Forniz and Sconfietti, 1983	Circumtropical (North Amer ican Pacific and Atlantic coasts)
Rapana venosa	1981	Cesari and Pellizzato, 1985a	Nipponese
Garveia franciscana	1978	Morri, 1982	Circumtropical (San Francisco Bay -alien)
Tapes philippinarum	1983	Cesari and Pellizzato, 1985b	Nipponese
Saccostrea commercialis	1984	Cesari and Pellizzato, 1985b	Circumtropical
Tricellaria inopinata	1982-1983	D'Hondt and Occhipinti, 1985	New species; probably indopacific
Bursartella leachi	1985	Cesari et al., 1986	Circumtropical
Dyspanopeus sayi	1992	Froglia and Speranza, 1993	North American Atlantic coasts
Haminoea callidegenita	1992	Alvarez et al., 1993	Indopacific
Xenostrobus sp.	1992	Sabelli and Speranza, 1994	Indopacific
Caprella scaura	1994-1995	Sconfietti and Danesi, 1996	Indopacific
Celleporella carolinensis	1994-1995	Occhipinti and d'Hondt, 1996	American Atlantic coasts
Anadara demiri	2000	Present work	Indopacific
Musculista senhousia	2001	Present work	Indopacific

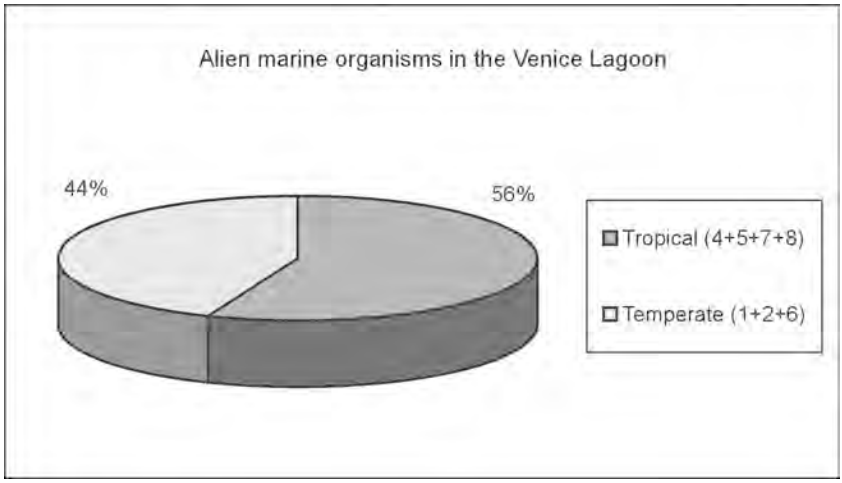

Fig. 11 - Division by longitude of biogeographical areas of origin of alien species found in the Venice Lagoon.

(20%), 3 Nipponese (12%) and 1 is from Australia-New Zealand area (4%) (fig. 9). In conclusion, the comparison clearly shows a greater diversification among classes but also highlights greater Atlantic and western affinities.

Finally, the investigation into the climate zones (fig.11) shows a division of the percentages which is very similar to that of Mollusks with 14 tropical species (56%) and 11 temperate species (44%), thus confirming both the significativeness of the data given above and the soundness of the choice of Mollusks as a representative group for the aims of the study.

4. *Conclusions.*

The gathering and successive processing and analysis of bibliographic data have allowed a characterization of the phenomenon of the introduction of alien species into the Lagoon of Venice compared with the Mediterranean.

The Lagoon area is characterized by a high rate of success of the penetrations, even higher than the one assessed for the Mediterranean, where 3 out of 4 exotic species come to acclimation, at least at local level.

The Lagoon of Venice differs decidedly also for what concerns the ways of entrance of alien species since man is the main responsible for that, while

the number of species penetrated in a spontaneous way is clearly lower. The low percentage of elements whose way of penetration is unknown testifies of the attention dedicated to the study of the phenomenon.

The "sub-Atlantic" character of the Lagoon of Venice is stressed by the high percentage of species of western origin, with Atlantic and temperate affinity, in comparison with the prevailing Indo-Pacific elements with clear tropical affinity noticed in the Mediterranean.

The data concerning all taxonomic groups found in the Lagoon of Venice prove to be very similar to those obtained by the examination of Mollusks.

References.

Alvarez L.A., Martìnez E., Cigarrìa J., Rolàn E., Villani G., 1993. *Haminaea callidegenita* Gibson and Chia, 1989 (Opisthobranchia: Cephalaspidea), a Pacific species introduced in European coasts. Iberus, 11 (2), 59-65.

Cesari P., Mizzan L., Motta E., 1986. Rinvenimento di *Bursatella leachi leachi* Blainville, 1817 in Laguna di Venezia. Lavori Soc. Ven. Sc. Nat., 11, 5-16.

Cesari P., Pellizzato M., 1985a. Insediamento nella Laguna di Venezia e distribuzione adriatica di *Rapana venosa* (Valenciennes) (Gastropoda, Thaididae). Lavori Soc. Ven. Sc. Nat., 10, 3-16.

Cesari P., Pellizzato M., 1985b. Molluschi pervenuti in Laguna di Venezia per apporti volontari o casuali. Acclimazione di *Saccostrea commercialis* (Iredale & Roughely, 1933) e di *Tapes philippinarum* (Adams & Reeve, 1850). Boll. Malacologico, 21, 237-274.

Fauvel P., 1938. Anellida Polychaeta della Laguna di Venezia. R. Com. Talass. It. Mem., 246, 1-26.

Forniz C., Sconfietti R., 1983. Ritrovamento di *Paracerceis sculpta* (Holmes, 1904) (Isopoda, Flabellifera, Sphaeromatidae) nella Laguna di Venezia. Boll. Mus. civ. St. Nat. Venezia, 34, 197-203.

Froglia C., Speranza S., 1993. First record of *Dyspanopeus sayi* (Smith, 1869) in the Mediterranean Sea (Crustacea: Decapoda: Xanthidae). Quad. Ist. Ric. Pesca Marittima, 5 (2), 163-166.

Giordani Soika A., 1951. Il *Neptunus pelagicus* (L.) nell'alto Adriatico. Natura, 42, 18-20.

d'Hondt J.L., Occhipinti Ambrogi A., 1985. *Tricellaria inopinata*, n. sp., un nuveau Bryozoaire Cheilostome de la faune méditerranéenne. P.S.Z.N.I.: Marine Ecology, 6 (1), 35-46.

Krapp F., Sconfietti R., 1983. *Ammothea hilgendorfi* (Böhm, 1879), an adventitious pycnogonid new for the Mediterranean Sea. P.S.Z.N.I.: Marine Ecology, 4 (2), 123-132.

Mizzan L., 1993. Presence of swimming crabs of the genus *Callinectes* (Stimpson) (Decapoda, Portunidae) in the Venice Lagoon (North Adriatic sea – Italy): first record of *Callinectes danae* Smith in European waters. Boll. Mus. civ. St. Nat. Venezia, 42, 31-43.

Mizzan L., 1999. Le specie alloctone del macrozoobenthos della Laguna di Venezia: il punto della situazione. Boll. Mus. civ. St. Nat. Venezia, 49, 145-177.

Morri C., 1982. Sur la présence en Méditerranée de *Garveia franciscana* (Torrey, 1902) (Cnidaria, Hydroida). Cah. Biol. Mar., 23, 381-391.

Occhipinti Ambrogi A., 1995. La Laguna di Venezia: ambiente di conservazione e di invasioni. S.It.E. Atti, 16, 115-117.

Occhipinti Ambrogi A., d'Hondt J.L., 1996. Introduzione di specie alloctone in Laguna di Venezia: *Celleporella carolinensis* Ryland, 1979 (Bryozoa: Ascophora). Boll. Mus. civ. St. Nat. Venezia, 46, 53-61.

Olivi A., 1792. Zoologia Adriatica ossia Catalogo ragionato degli animali del Golfo di Venezia e delle Lagune di Venezia. Bassano.

Perrone A.S., 1989. Una specie di nudibranchi doridiani nuova per il Mediterraneo: dati sulla morfologia di *Doris bertheloti* (d'Orbigny, 1839) (Opisthobranchia: Nudibranchia). Boll. Malacologico, 24 (9-12), 237-242.

Perrone A.S., 1995. Una specie di nudibranchi del genere *Cuthona* Alder & Hancock, 1855, nuova per il Mediterraneo: *Cuthona perca* (Marcus, 1958) (Opisthobranchia: Nudibranchia). Boll. Malacologico, 31 (1-4), 28-36.

Sabelli B., Speranza S., 1993. Rinvenimento di *Xenostrobus* sp. (Bivalvia: Mytilidae) nella Laguna di Venezia. Boll. Malacologico, 29, 311-318.

Sacchi C.F., 1977. Le symposium international sur les "Problèmes malacologiques de la Mer Adriatique et des lagunes" organisé par la Società Malacologica Italiana. Atti Soc. ital. Sci. nat. Museo civ. Stor. nat. Milano, 118 (2), 115-117.

Sacchi C.F., 1977. La "Lacune Nord-Adriatique" et son influence sur l'écologie des Gastéropodes dunicoles. Prémisses méthodologiques. Atti Soc. ital. Sci. nat. Museo civ. St. Nat. Milano, 118 (2), 213-225.

Sacchi C.F., 1983. Il Nordadriatico: crocevia di faune, intreccio di popoli. Atti Mus. civ. St. nat. Trieste, 35, 39-64.

Sacchi F., Occhipinti Ambrogi A., Sconfietti R., 1989. Les lagunes nord-adriatiques: un environnément conservateur ouvert aux nouveautés. Bull. Soc. Zool. de France, 114 (3), 47-60.

Sconfietti R., 1983. Segnalazione di *Elasmopus pectenicrus* (Bate) (Crustacea, Amphipoda) nella Laguna di Venezia. Boll. Mus. civ. St. Nat. Venezia, 33, 91-92.

Sconfietti R., Danesi P., 1996. Variazioni strutturali in comunità di Peracaridi agli estremi opposti del bacino di Malamocco (Laguna di Venezia). S.It.E., 17: 407-410.

Zibrowius H., 1992. Ongoing modification of the mediterranean marine fauna and flora by the establishment of exotic species. Mésogée, 51, 83-107.

BIODIVERSITY STUDIES AT MACROBENTHIC COMMUNITY LEVEL IN THE LIDO BASIN (LAGOON OF VENICE): A REVIEW

F. Maggiore, G. Taroni
Istituto per lo Studio della Dinamica delle Grandi Masse, CNR, Venezia

1. *Introduction.*

Population and community level processes are important measures of the relevance of global climatic changes and local disturbance (Pearson & Barnett, 1989). Human societies affect relationships between abiotic and biotic compartments of the ecosystem acting on bio-geochemical cycles on one hand and on population and community dynamics on the other hand. Therefore, biodiversity appears as the tangible currency, which is influenced by, and reflects, the state of the ecosystems (Barbault & Hochberg, 1992).

Biodiversity studies at community level consider how species assemblages form communities and interact with the environment to form ecosystems. Every species is identified by morphology and autoecology (physiological adaptations, feeding habit, life cycle, interspecific relationships), which define its functional role. The knowledge of functional diversity of the community provides information on main ecological processes, which maintain its structure and functioning (Piraino & Fanelli, 1997).

Based on these considerations, a research on the existing macrobenthic community studies was begun in the northern basin of the lagoon of Venice. The objective is to identify assemblages of species with the main distribution and ecological role and thus to reconstruct the scenario of macrobenthic community distribution at different times, pointing out, if possible, temporal changes in relation to environmental changes.

Data come from three studies carried out on the shallows: unpublished data of Giordani Soika consented by "Museo Civico di Storia Naturale" of Venice, the book "Le alghe della laguna di Venezia" (Comune di Venezia-Assessorato all'Ecologia, 1991), a report provided by Ministero dei Lavori Pubblici - Magistrato alle Acque (Biotecnica, 1994).

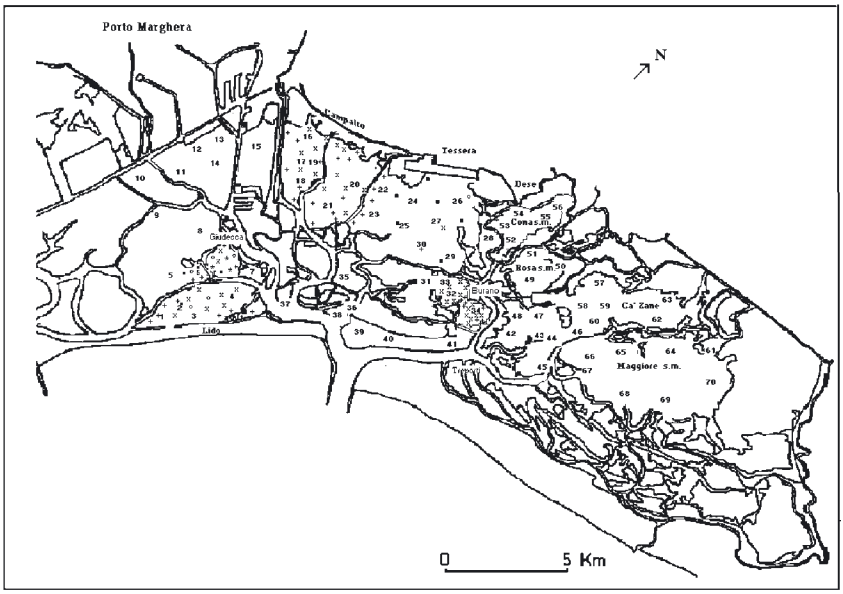

Fig. 1 - Station distributions in the Lido basin. Numbers mark Giordani Soika stations; symbols (*, °, x, +, n) the 1990s stations and symbol n in Tessera area marks stations without fauna in the 90's. s.m = salt marsh.

2. *Material and Methods.*

2.1. *Study area.*

Figure 1 shows sampling station distributions. Giordani Soika sampling area (summer and autumn 1948 and 1968) spreads from the watershed to the Maggiore salt marsh; the latest studies concern samples collected in winter and spring 1988 in three areas: between Venice and the Lido littoral, Tessera and Burano salt marsh (Comune di Venezia-Assessorato all'Ecologia, 1991) and samples collected in spring 1992 in the Campalto area (Biotecnica, 1994).

2.2. *Sample analysis.*

One of the problems in dealing with the comparison between the three data series lies in differences in sampling methods and seasons (tab. 1).

Furthermore, concerning Giordani Soika samples, although each sample was washed through a 1.0 mm mesh sieve, species quoted have a size, at the adult stage, equal or greater than one cm; the lack of the smaller size species might be due to the rough sorting method.

Tab. 1: Tools and season samplings in the studies quoted.

Authors	Tool	surface	mesh screen	season
Giordani Soika	Corer	0.01x4=0.04m²	1 mm	summer –autumn
Comune di Venezia	grab	0.03x4=0.09 m²	1 mm	winter-spring
Biotecnica	grab	0.03x4=0.09 m²	1 mm	winter-spring

With regard to the 1990s samples, the authors say that the fourth grab sample was washed through a 0,4 mm mesh to better quantify Chironomids; however they don't specify if they sort other invertebrates too.

2.3. *Data analysis.*

Data were worked out following two sequential approaches: 1) The correspondence analysis (Benzecri, 1973) and cluster analysis (k c-means method) (Hartigan, 1975) were applied to identify station groups characterized by the same assemblages of species. To determine the more important species in each station group, percentage mean abundance, a Constancy index, and a Fidelity index were calculated for each species (Bachelet & Dauvin, 1993). The Constancy index is the percentage ratio between the number of occurrences n_{ij} of the species *i* in a station group *j* and the number of stations n_j in the group *j* ($C_{ij}=n_{ij}/n_j$): the Fidelity index ($F_{ij}=C_{ij}/ C_{ij}$) is the percentage ratio between the Constancy of a species in a station group and the sum of its constancies in all station groups Important species were termed constant (C>50%), common (50%≥C>25%), exclusive (F=100%), and characteristic (100%>F≥67%). 2) The Grall & Glemarec (1997) ecological classification was utilized and adapted to define the ecological role of each species and to verify if homogeneous species assemblages in a functional point of view exist. The authors identified, along an organic enrichment gradient on soft bottom, five groups of species with similar abundance profiles. Borjia et al. (2000) verified the sequence of these ecological groups in Spanish estuarine environments. The following groups were identified:

GROUP 1: species very sensitive to organic enrichment and present in normal conditions. They include the specialist carnivores and some deposit-feeding tubiculous polychaetes;

GROUP 2: species indifferent to enrichment, always present in low densities with non-significant variations in time. These include suspension feeders, less selective carnivore and scavengers;

GROUP 3: species tolerant of excess organic matter enrichment. These species may occur in normal conditions but their popula-

tions are stimulated by organic enrichment. These are surface-deposit-feeding but also animals capable of switching their feeding behavior like tubicolous Spionids, Scrobicularidae, and Amphipods;

GROUP 4 : second-order opportunistic species. These are the small species with a short life cycle, adapted to a life in reduced sediment where they can proliferate. They are the subsurface deposit feeders essentially related to the cirratulids; and

GROUP 5: first-order opportunistic species. These are the deposit feeders that proliferate in sediments reduced up to the surface. Two species of polychaetes of universal distribution are typical of this group, *Capitella capitata* and *Malacoceros fuliginosus*. Some nematodes and oligochaetes are also present.

Species quoted in the analysed studies and their belonging to aforementioned ecological groups are listed in table 2.

3. *Results.*

The three data series were analysed one by one because of sampling method differences and to provide an outline of the zoobenthos distribution in the northern basin of the lagoon in the three periods.

Figures 2, 3 and 4 are the graphic output of the correspondence analysis performed, respectively, on the 1948, 1968 and the 1990s data; it seems, in all three cases, that station-points and species-points arrange themselves in a parabolic outline.

3.1. *The scenario in 1948.*

A succession of animal populations, whose distribution is established by the distance from the sea and channels, is shown along axis 1; a succession of four communities, defined by species with high percentage mean abundance, constancy and fidelity, is shown from the inside of the inlet towards the mainland and going off the channels (from the negative to the positive pole).

- The first one, characteristic of stations close to the inlet (polyhaline area), is made up of marine and mixed* species (*Loripes lacteus* and *Owenia fusiformis* community) living on sandy and sandy muddy bottom; 88% of these species belong to ecological group 1.
- The second one spreads towards the watershed, Campalto, Porto Marghera and salt marsh areas close to the channels (from the poly- to

Tab. 2: List of species recorded in the Lido basin by Giordani Soika (G), Comune di Venezia-Assessorato all'Ecologia (1990) (A) and Biotecnica, (1994) (B).

Ecological groups		Species		Authors
1	Mollusca	Bittium reticulatum (Da Costa, 1778)	Br	G, A,
		Chlamys varia (Linnaeus, 1758)		A
		Cyclope neritea (Linnaeus, 1758)	Cn	G, A, B
		Ensis minor (Chenu, 1843)	Em	G
		Dosinia lupinus (Linnaeus, 1758)		A
		Gibbula adriatica (Philippi, 1844)	Ga	A
		Hiatella arctica (Linnaeus, 1767)		A
		Loripes lacteus (Linnaeus, 1758)	Ll	G, A
		Nucula nucleus (Linnaeus, 1758)	Nn	G, A
		Mactra stultorum (Linnaeus, 1758)		A
		Mytilaster marioni (Locard, 1889)		A, B
		Paphia aurea (Gmelin, 1791)	Pa	G, A, B
		Solen marginatus Pulteney, 1799	Sm	G,
		Tapes decussatus (Linnaeus, 1758)	Td	G, A
		Tapes philippinarum (Adams & Reeve, 1850)	Tp	B
		Tellina distorta Poli, 1791		A
		Tellina nitida Poli, 1791		A
	Annelida	Clymenura clypeata (Saint-Joseph, 1894)	Ccl	A
		Euclymene oerstedi (Claparède, 1863	Eo	A
		Hydroides dianthus (Verrill, 1873)		A, B
		Owenia fusiformis Delle Chiaje,1841	Of	G, S
		Pectinaria koreni (Malmgren, 1866)	Pk	G, A, B
		Pherusa monolifera (Delle Chiaie, 1841)		S
		Terebella lapidaria Linnaeus, 1767		A,B
	Crustacea	Crangon crangon (Linnaeus, 1758)	Ccr	G
		Pilumnus hirtellus (Linnaeus, 1761)		B
2	Mollusca	Hamynoea navicula (da Costa, 1778)	Hn	A, B
		Nassarius corniculus (Olivi, 1792)		A
		Nassarius reticulatus (Linnaeus, 1758)	Nr	G, A,
		Philine aperta (Linnaeus, 1767)		A
	Annelida	Aponuphis bilineata (Baird, 1870)		S
		Eunice vittata (Delle Chiaje, 1828)		A, B
		Glycera rouxii Audouin & Milne-Edwards, 1833	Gr	G
		Glycera trydactila Schmarda, 1860	Gt	G, A, B
		Harmothoe extenuata (Grube, 1840)	Hh	G
		Nematonereis unicornis Schmarda, 1861		A
		Nephtys hombergi Savignyi, 1818	Nh	G
		Lumbrinereis gracilis (Ehlers, 1868)		A
		Mysta picta (Quatrefage, 1865)		A, B
		Syllis gracilis Grube, 1839	Sg	A, B
3	Mollusca	Abra alba (W. Wood, 1802)	Aa	G, A, B
		Abra nitida (O. F. Müller, 1776)	An	A
		Abra segmentum (Récluz, 1843)	As	A, B
		Abra tenuis (Montagu, 1803)	At	A
		Cerastoderma glaucum (Poiret, 1789)	Cg	G, A, B
		Corbula gibba (Olivi, 1792)		A
		Crassostrea gigas (Thunberg, 1793)		A
		Hydrobia acuta (Draparnaud, 1805)	Ha	A
		Mytilus galloprovincialis Lamarck, 1819		A
		Scrobicularia plana (Da Costa, 1778)	Sp	G, A, B
	Annelida	Hediste diversicolor (O. F. Müller, 1776)	Hd	G, A, B
		Heteromastus filiformis (Claparède, 1864)		A
		Paradoneis lyra (Southern, 1914)	Pl	A
		Perinereis cultrifera (Grube, 1840)	Pc	A, B
		Marphysa sanguinea (Montagu, 1815)	Ms	G, A, B
		Melinna palmata Grube, 1870	Mp	G
Ecological groups		Species		Authors
3	Annelida	Neanthes succinea (Frey & Leuchart, 1847)	Ns	G, A.B
		Notomastus latericeus M.Sars, 1851		A, B

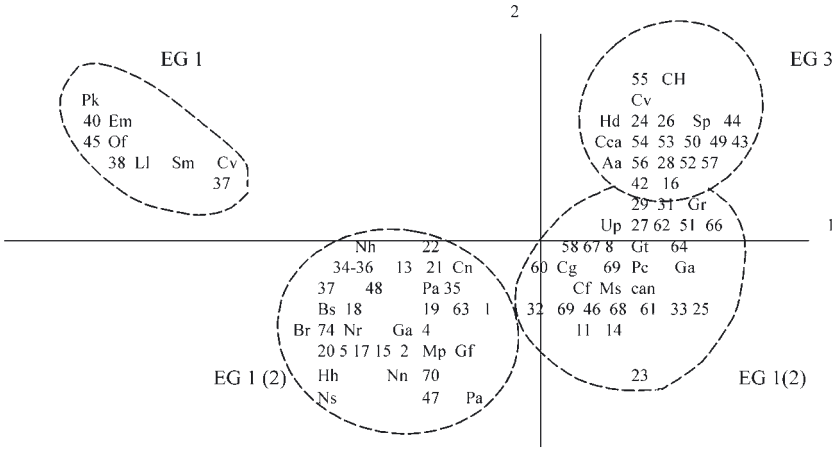

Fig. 2 - Correspondence analysis in 1948. Graphic shows station groups achieved with cluster analysis; abbreviated names are given in Table 2. EG= Ecological Group.

the mesohaline area); it is made up of mixed and marine species living on sandy muddy and muddy sandy sediments (*Nucula nucleus*, *Cyclope neritea* and *Nepthys hombergii community*) belonging to ecological group 1 (46%) and 2 (24%).

- The third one, characteristic of Porto Marghera, Tessera and salt marsh areas far away from the channels (from the poly- to the mesohaline area), is made up of mixed species (*Perinereis cultrifera* and Cirriformia filigera community) belonging to ecological group 1 (51%), 3 (23%)and 2 (20%).
- The fourth one, characteristic of basin marginal area and inner salt marsh areas (from the poly- to the oligohaline area) is made up of paralic* and mixed species (*Hediste* diversicolor and *Abra alba* community); 96% of these species belong to ecological group 3.

* The meaning of paralic and mixed species is that suggested by Guelorget and Perthuisot (1992).

3.2. *The scenario in 1968.*

Species-points and station-points arrange themselves along axis 1 (fig.3) showing a transition from the inlet (positive pole) towards basin marginal

*The meaning of paralic and mixed species is that suggested by Guelorget and Perthuisot (1992).

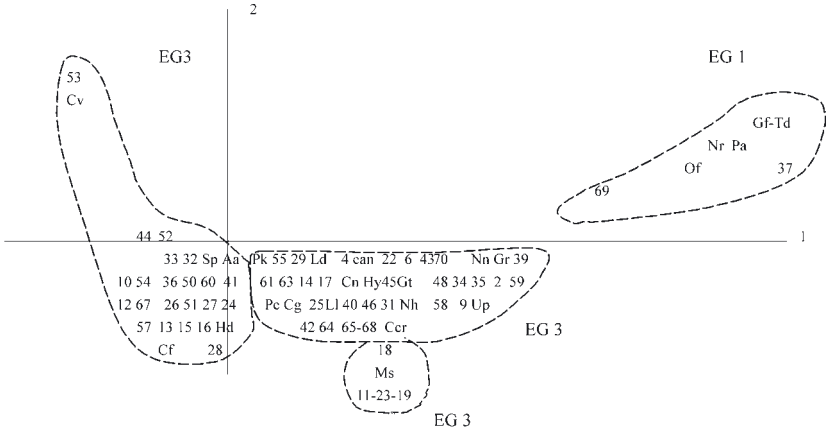

Fig. 3 - Correspondence analysis in 1968. See also legend of fig. 2.

areas (negative pole); stations are gathered in very close groups characterised by more abundant and constant or common species: *Nassarius reticulatus, Paphia aurea, Nepthys hombergii, Cyclope neritea, Hediste diversicolor, Cerastoderma glaucum, Marphisa sanguinea* and *Abra alba.*

Apart from *Nassarius* reticulatus and *Paphia aurea*, respectively, exclusive and characteristic in the group defined by them (st.37 e 69), no species has remarkable Fidelity index, thus the gradient appears more as a succession of populations, that differ in changes of dominance, rather than as well defined communities. Two great species assemblages, both made up of mixed and paralic species, are present:

- the first one, which spreads from the inlet towards the basin central area and some salt marsh zones (from the poly- to the mesohaline area), is dominated by *Nepthys hombergii*, *Cyclope neritea, Hediste diversicolor* and *Cerastoderma glaucum*;
- the second one, which lies in the basin marginal areas (oligo-, meso- and polyhaline), is dominated by Hediste diversicolor and Abra alba.

Gathering species in ecological groups, group 3 is widely present in the basin.

3.3. *The scenario in the 1990s.*

Species-points and station-points arrange themselves along axis 1 (fig.4) showing a transition from the *Zostera* (Burano salt marsh), Lido, Giudecca and Campalto stations close to the channels (positive pole)

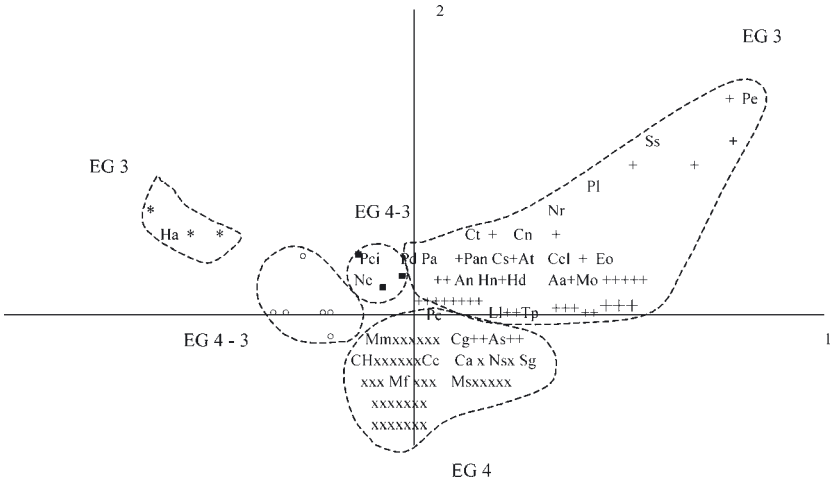

Fig. 4 - Correspondence analysis in the 1990s. Only significant species were taken into account. See also the legend of fig. 2.

towards the areas less revitalized by the sea action (negative pole). The five assemblages, identified by the cluster analysis, were defined by species with high percentage mean abundance and constancy, because no species has remarkable Fidelity index; as in 1968 the gradient appears more as a succession of populations differing in changes of dominance.

Two major species assemblages were pointed out:

- the first one, characteristic of stations close to the channels (+ in fig. 1), is mainly made up of paralic species belonging to the ecological group 3 (79%). The dominants for percentage mean abundance and constancy are *Abra segmentum and Hediste diversicolor;*
- the second one is characteristic of stations lying in inner position with regard to those of previous assemblages and, in any case, far-away from the channels (x in fig.1). The assemblage is made up of paralic species and opportunistic marine species (*Capitella capitata, Malacoceros fuliginosus*) indicators of strong organic enrichment; Chironomids distinctly dominate, followed by C. capitata and Abra segmentum. Most of species belong to ecological group 4 (68%), 3 (16%) and 5 (14%).

Other groups concern the few inner stations of Giudecca and Lido areas (*, °, _ in fig.1), they differ in dominance changes of Chironomids, *Hydrobia* acuta and *A. segmentum.*

4. *Conclusions.*

The differences in sampling methods (tools and sorting techniques) between the three considered periods don't allow assessing biodiversity changes in terms of species richness and community structure.

Macrofauna considered in Giordani Soika data consists of species whose size, at mature stage, is greater or equal to one cm; species of a lower dimensional nature were not quoted. On the contrary, they are recorded in the 1990s data (*Hydrobia acuta, Capitella capitata, Malacoceros fuliginosus, Chironomids*).

A characterization of the lagoon on the basis of a part of benthic macrofauna has been attempted, trying to investigate the autoecology of the same species.

The results can be analysed as follow:

1) Stations and species seem to arrange themselves in a parabolic outline (Guttman effect) implying that axis 2 was a quadratic function of axis 1 (Benzecri et al., 1973); this occurs when the system is controlled by a one dimensional phenomenon.
2) Zoobenthos distribution in 1948 corresponds with the zonation pattern proposed by Guelorget & Perthuisot (1992) for the paralic systems. Three zones were recognized:

- zone II-III (marine and mixed species) from the inlet towards Porto Marghera and some salt marsh stations;
- zone III-IV (mixed and paralic species) in the salt marshes and in the areas far away from the channels; and
- zone IV-V (paralic species) in the basin marginal areas and in the salt marsh inner areas.

This basic pattern was modified in the following periods.
In 1968 two zones were observed:

- the first one (zone III-IV) spreads from the inlet towards the basin central area and more revitalized salt marsh areas,
- the second one (zone IV) involves basin marginal areas.

The zonation pattern of the 1990s shifts to zones IV (+ in fig.1) and V (x, *, °, _ in fig.1) and it gets more complicated with the presence of opportunistic marine species (*Capitella capitata, Malacoceros fuliginosus*). Changes with regard to initial conditions (1948) were caused by spread of paralic species (*Hediste diversicolor, Abra segmentum* and *Cerastoderma glaucum*) in basin areas where mixed and marine species (*Loripes lacteus, Owenia fusiformis, Nucula nucleus*) lived in 1948.

3) High Fidelity index of dominant species in 1948 allowed defining station groups and, thus, community limits, while in the following

periods exclusive and characteristic species are absent in the species assemblages. Loripes lacteus, Owenia fusiformis and Nucula nucleus exclusive in their assemblages in 1948 strongly decrease in 1968 and in the 1990s as *Hediste diversicolor*, Abra segmentum and *Cerastoderma glaucum* become ubiquitous in the whole basin.

4) Gathering species in ecological groups allowed clarifying observed differences.

In 1948 group 1 is present from the inlet to Porto Marghera, in the shallows close to the Burano channel and in some salt marsh stations; it is enriched with species of group 2 going towards the basin inner areas and it is replaced by group 3 species in the marginal areas.

In 1968 group 3 is widespread in the basin and in the 1990s groups 3 and 4 dominate. It might be stressed that the occurrence of group 4 in the 1990s is due to the massive presence of Chironomids. Observed differences are due, in 1968, to the expansion of Cerastoderma glaucum and Hediste diversicolor distributions. Samplings were carried out from July to October, always in the same stations, but not always in the same month. Dominance variations observed might be due to the climatic variability that normally occurs from July to October. On the contrary, both species might be favoured by lagoon eutrophic conditions; their distribution, in fact, occurs in more contaminated areas (marginal, central and salt marsh areas); nutrient concentration data (Giordani Soika & Perin 1974) and some aspects of autoecology of species support this hypothesis. Both species are tolerant of excess organic matter enrichment; high mortality of C. glaucum, after anoxic protracted periods, has been observed, but it shows adaptive strategies to withstand stress conditions. In fact, the metabolism of *C. glaucum* is reduced under high summer temperatures decreasing the oxygen consumption and the adults migrate between different zones of sediments during dystrophic periods (Labourg & Lasserre, 1980; Wilson & Elkaim, 1997). *Hediste diversicolor* shows a broad fitness to enriched sediments due to the physiological tolerance to the exposure to sulfide (Vismann, 1990).

Data analysis of the 1990s supports this hypothesis; eutrophic conditions persist (Sfriso et al. 1992) and although samplings were carried out in winter and spring, the scenario follows the same pattern of 1968. Moreover, samplings of the 1990s provide more precise information on the relationships between community structure and environmental conditions because of a greater methodological refinement. In fact, in brackish waters, the animal assemblages identified (*Abra segmentum, Cerastoderma glaucum, Hediste diversicolor, Capitella capitata, Polydora*

ciliata, Chironomidi) are linked to nutrients and organic matter in the sediments (Amaral & Costa, 1999).

In conclusion, the one-dimensional factor stressed by the correspondence analysis is referable to the water dynamics which influences grain size distribution and trophic status establishing zonation patterns and ecological group distributions. Organic enrichment of sediments might have caused the decreasing of *Loripes lacteus, Owenia fusiformis* and *Nucula nucleus* and favoured more competitive species even if, according to Aleffi et al. (1995), the rarefying of *Nucula nucleus* seems to be due to a decreasing of the fine mud component in the sediments.

Finally some zoological remarks must be stressed concerning some species quoted by Giordani Soika.

Corophium volutator is frequently found in the Mediterranean. Ruffo (1982) examining *C. volutator* specimens coming from different Mediterranean sea areas ascribes this species to *C. orientale* specifying that the presence of *C. volutator* in the Mediterranean Sea must be confirmed. Giordani Soika's preserved specimens do not appear in that examined by him. *Cirriformia filigera* is found in marine environments; whereas *Cirriformia tentaculata* is a marine species living also in paralic systems (Guelorget & Perthuisot, 1992).

Concerning *Abra* alba and *A.segnmentum*, it should be stressed that Giordani Soika records *A. alba* where following authors (Comune di Venezia-Assessorato all'Ecologia, 1991; Biotecnica, 1994) record *A. segmentum*. A. alba is a marine species living close the estuary mouths and in brackish waters, while A. segmentum is strictly a paralic species.

Taking into account these observations, these species kept in the "Museo Civico di Storia Naturale" collections are being re-examined.

References.

Aleffi F., Chiozzotto E., Grim F., Orel G., Scattolin M., 1995. Ricerche sui popolamenti bentonici animali della laguna di Venezia. Atti S.IT.E. 16, 35-37.

Amaral M.J., Costa M.H., 1999. Macrobenthic communities of saltpans from the Sado estuary (Portugal). Acta Œcologica 20(4), 327-332.

Bachelet G., Dauvin J.C., 1993. Distribution quantitative de la macrofaune benthique des sable intertidaux du basin d'Arcachon. *Oceanologica Acta* - 16(1): 83-97.

Barbault R., Hochberg M.E., 1992. Population and community level approaches to studying biodiversity in international research programs. Acta Œcologica 13(1), 137-146

Benzecri J.P., 1973. L'analyse des données.V.2. Dunod Paris, 619 pp.

Biotecnica, 1994. Rilevamenti a supporto degli interventi urgenti per l'arresto e l'inversione del degrado ambientale nella zona di Campalto - Tessera. *Ministero dei Lavori Pubblici - Magistrato alle Acque - tramite il suo concessionario Consorzio Venezia Nuova.*

Borja A., Franco J., Pérez V., 2000. A marine biotic index to establish the ecological quality of soft-bottom benthos within European estuarine and coastal environments. Marine Pollution Bulletin 40 (12), 1100-1114.

Comune di Venezia - Assessorato all'Ecologia, 1991. Le alghe della laguna di Venezia. Arsenale editrice.

Giordani Soika A., Perin G., 1974. L'inquinamento della laguna di Venezia: studio delle modificazioni chimiche e del popolamento sottobasale dei sedimenti lagunari negli ultimi vent'anni. Bollettino Museo Civico Storia Naturale di Venezia 26, 25-68.

Grall J., Glémarec M., 1997. Using biotic indices to estimate macrobenthic community perturbations in the bay of Brest. Estuarine Coastal and Shelf Science 44 (suppl A), 43-53.

Guelorget O., Perthuisot J.P., 1992. Paralic ecosystems. Biological organization and functioning. *Vie Milieu* 42(2), 215-251.

Hartigan J., 1975. Clustering algorithms. Wiley & Sons, New York:351 pp.

Labourg P.J., Lasserre P., 1980. Dynamique des populations de *Cerastoderma glaucum* dans une lagune aménagée de la région d'Arcachon. Marine Biology 60, 147-167.

Pearson T.H., Barnett P.R.O., 1987. Long-term changes in benthic populations in some west European coastal areas. Estuaries 10 (3), 220-226.

Piraino S., Fanelli G., 1997. Biodiversità funzionale, ridondanza e specie cardine. *Biologia Marina Mediterranea* 4(1), 104-114.

Ruffo S., 1982. The Amphipoda of the Mediterranean. *Mem. Inst. Oceanogr, Monaco* 13

Sfriso A., Pavoni B., Marcomini A., Orio A.A., 1992. Macroalgae, nutrient cycles and pollutants in the lagoon of Venice. Estuaries 15(4), 517-528.

Vismann B., 1990. Sulfide detoxification and tolerance in *Nereis (Hediste) diversicolor* and *Nereis (Neanthes) virens* (Annelida:Polychaeta). Marine Ecology Progress Series 59, 229-238.

Wilson J.G., Elkaim B., 1997. Seasonal and geographical differences in oxygen consumption with temperature of *Cerastoderma glaucum* (Poiret) and a comparison with *C. edule*. Estuarine, Coastal and Shelf Science 45, 571-577.

RESEARCH LINE 3.7.
Forecasting and management models

ON THE GEOMORPHOLOGY OF TIDAL ENVIRONMENTS: THE LAGOON OF VENICE

M. Marani[1], E. Belluco[1], A. D'Alpaos[1], A. Defina[1], S. Lanzoni[1], G. Seminara[2], A. Rinaldo[1]
[1]*Dipartimento Ingegneria Idraulica, Marittima Ambientale e Geotecnica, Università di Padova*
[2]*Dipartimento Ingegneria Ambientale, Università di Genova*

Abstract.

Observational evidence is presented on the geometry of meandering tidal channels and on the drainage density of tidal networks evolved within coastal wetlands characterized by different tidal, hydrodynamic, topographic, vegetational and ecological features. We analyze at first the geometrical properties of tidal meanders, with possible dynamic implications on their evolution. In particular, it is shown that large spatial gradients of leading flow rates induce important spatial variabilities of meander wavelengths and widths, while their ratio remains remarkably constant in the range of scales of observation. This suggests a locally adapted evolution, involving the morphological adjustment to the chief landforming events driven by local hydrodynamics. In the second part of our study we perform theoretical and observational analyses of the drainage density of tidal networks. We show that, in spite of the apparent site-specific features of morphological variability, conventional measures of drainage density appear to be quite constant in space and time indicating a similarity of forms. We emphasize that such similarity is an artifact of the Hortonian measure. Since important morphological differences may only be captured by introducing measures of the extent of unchanneled flows, whose determination requires the definition of suitable drainage directions defined by hydrodynamic gradients, in this work we study for the first time the distribution of unchanneled lenghts in a tidal environment.

1. *Introduction.*

The development of drainage patterns across tidal basins controls the hydrodynamics and sediment exchanges between saltmarshes and tidal flats [e.g. *Myrick and Leopold, 1963; Pestrong, 1965; Boon, 1975; Pethick, 1980; Boon and Byrne, 1981; Leopold et al., 1993; Steel and Pye, 1997; Friedrichs and Perry, 2001*]. The importance of accurate observations and analyses of the planar patterns of tidal networks and of their drainage density is linked to the implications on the origin and long-term evolution of the complex of morphological structures which characterizes environments such as lagoons, deltas or estuaries. In order to perform morphometric analyses of tidal networks one needs an objective procedure for delineating the drainage area to any link or to any cross-section of a channel. A new method, based on flow hydrodynamics, for delineating drainage directions and contributing areas throughout the tidal network was proposed by *Rinaldo et al.* [*1999a*]. The method applied to three tidal environments and several of the embedded watersheds, quite different in their tidal, geologic, vegetational and hydrodynamic characteristics, revealed interesting geomorphic features, including a comparison of scaling relationships in measures of tidal landforms with analogous ones found in the fluvial system [e.g. *Rodrìguez-Iturbe and Rinaldo, 1997*]. It became apparent, however, that several features of the tidal channels, chiefly the width and the curvature of the axis, show strong variations in space unusual in fluvial morphology, even over length scales of hundreds to thousands of widths [*Marani et al., 2002a*]. Instead of finding scale invariant features of the type clearly prevailing in fluvial systems, a nearly complete lack of scaling features in all tidal systems analyzed was revealed. To investigate the generality of such results, we first examine the structure and the validity of the assumptions built in the Poissonian hydrodynamic model [*Rinaldo et al., 1999a*], and relax them selectively to probe its limits owing to a fair assessment of possible artifacts of the schemes adopted.

The observations of the geometry of tidal networks on which the present work is based are obtained from the digitalization of aerial photographs or published data and regard tidal environments with different morphological and tidal characteristics. The study areas are mainly the lagoon of Venice (Italy), Petaluma Bay (CA, USA) and Barnstable marsh (MA, USA). For in-depth descriptions of the environments considered and of the processing tools on aerial photographs and on digital terrain maps see [*Fagherazzi et al., 1999; Marani et al., 2002b*].

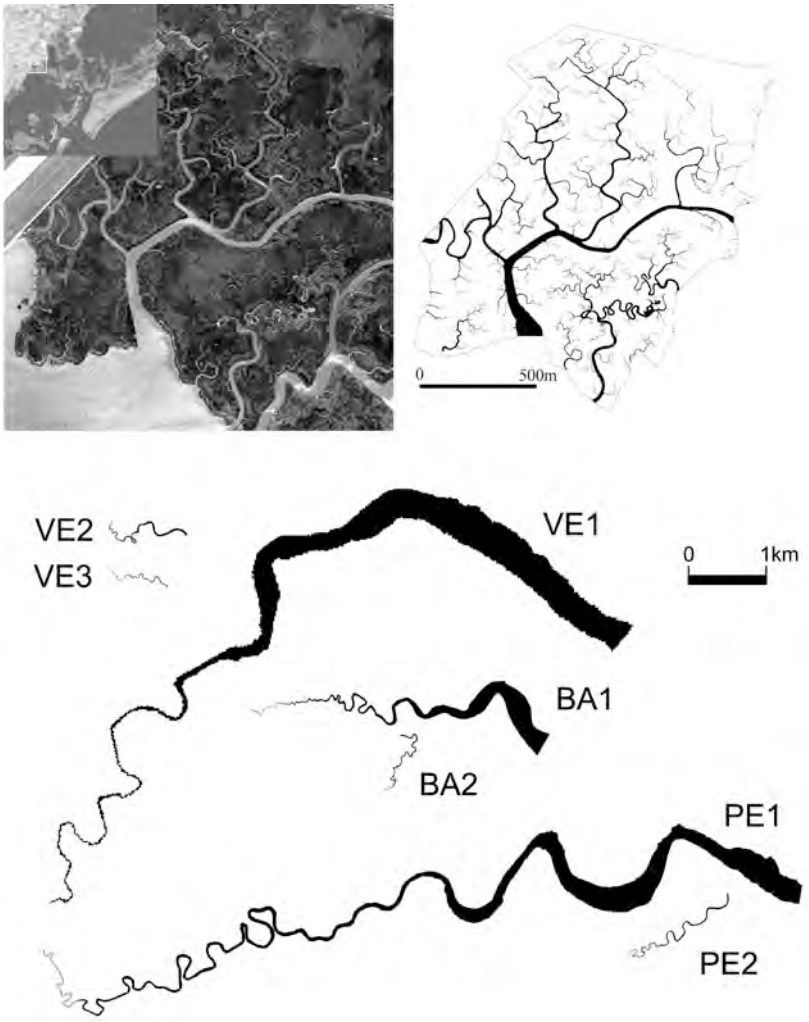

Fig. 1 - A sample of the database employed (after *Marani et al.*, [2002a]). Upper portion: digital image of a portion of the tidal flats in the Northern lagoon of Venice, localized within the lagoon (the *forma urbis* of the city of Venice appears in the bottom part of the uppermost left inset). Also shown is the automatic extraction of the channelized patterns, to scale, according to the techniques described in *Fagherazzi et al.* [1999]. Lower part: the planar geometry of seven meandering tidal channels (out of approximately 150 within our data base), extracted respectively from: the lagoon of Venice (Italy) (VE1, VE2, VE3); Barnstable (MA, USA) (BA1, BA2); and Petaluma (CA, USA) (PE1, PE2). It is seen the wide range of scales and of degrees of meandering sampled. Notice that the patterns are represented to scale, and that the pixel size varies from case to case, as described in *Fagherazzi et al.* [1999] and *Rinaldo et al.* [1999a].

2. *Tidal meanders.*

We introduce a set of mathematical tools for the objective, automatic analysis of tidal meanders [for details see *Marani et al., 2002a*]. The geometry of a tidal channel and the characteristics of its meanders (Fig. 1) may be described in terms of a number of geometrical properties like: i) its planar curvature $c(s)$, i.e. the inverse of the local radius of curvature, characterized as a function of the intrinsic coordinate s to track its planar development; ii) its intrinsic wavelength, L_s, computed along the s-coordinate; and iii) the cartesian wavelength, L_x, defined by the (cartesian) distance between the initial and the end sections of the meander. These sections are located through the inflection points of the axis, i.e. sites s_i where $c(s_i)=0$, and a meander may be defined as any portion of the channel along s containing three such inflection points. This definition is conceptually reasonable and leads to a relatively simple automatic procedure for delimiting meanders from observed data. The planar characterization of a meandering channel is completed by its half-width $B(s)$, whose planar development carries crucial geomorphological information also on the magnitude of landscape-forming flowrates shaping its cross-sections.

An interesting relationship between two of the parameters introduced above may be obtained by considering an empirical result known for fluvial environments, which relates the cartesian meander length to the channel width. Figure 2 shows observations [after *Leopold et al., 1964, Figure 7.41a and 7.46*] from: a) different fluvial environments; b) valleys left by ancient river courses, or relics of past wetter climates; c) glaciers' meanders; and d) gulf stream meanders, to which our data on tidal meanders have been added. The data indicate the validity of a linear relationship $L_x \alpha B$, as observed by *Leopold et al.* [*1964*]. It is relevant that the new data from our observations do not modify appreciably, within statistical significance, the linear relationship between L_x and $\overline{B}$ (average channel width within a meander). The dimensionless parameter $L_x / \overline{B}$ thus tends to be constant across very different environments. This suggests that when the physical mechanisms governing the spatial development of meanders act at a scale comparable with their width, the landforms generated exhibit strong similarities independently of the nature of the processes that shape them.

The above geomorphic characterization of tidal meanders cannot, of course, be considered complete because properties other than planar are to be considered. Topography is first considered. Topographic gradients are less significant in tidal environments than in hillslope and fluvial geomor-

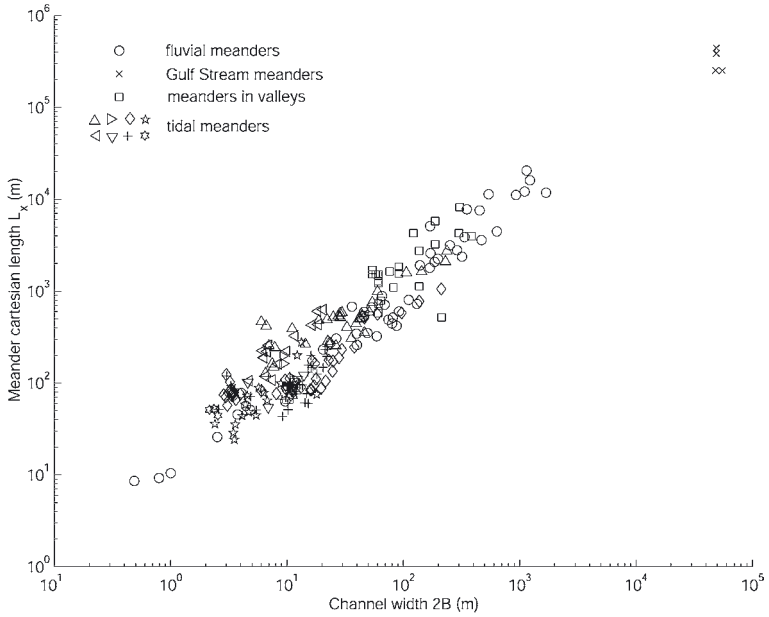

Fig. 2 - Cartesian meander length versus width for rivers (circles), fluvial valleys (squares), glacial meandering patterns (triangles) and the gulf stream (crosses) (after *Leopold et al., 1964*) compared to tidal meanders from this database (portrayed by the different symbols shown in the inset). Notice the different symbols pertaining to the development of the same tidal meander, corresponding to sites along the same observed pattern where width and amplitude have been measured. It is remarkable that a roughly constant ratio is maintained. The fact that the fluctuations induced by tidal patterns are no larger than those observed for such diverse morphologies as valleys, glaciers and the gulf stream is deemed suggestive (after *Marani et al.*, [2002a]).

phology [*Rinaldo et al., 1999a*], owing to the different dynamic implications. In fact, while slopes (and thus gravity) command basin-scale transport, tidal flows are driven mostly by free surface gradients that are weakly dependent on topography. Nevertheless, topographic curvatures can be suitably used to single out the channelized portion of the tidal environments [*Fagherazzi et al., 1999*]. Moreover, the bottom profile of tidal channels is usually characterized by an upward concavity which increases with channel convergence [*Lanzoni and Seminara, 2002*]. As a consequence, bottom slope, which may attain relatively high values in the landward reaches, tends to decrease progressively as one moves seaward, thus implying that the flow depth is likely to increase at a rate smaller than the width. Here we show the results of our survey of the width-to-depth ratio,

β=*2B/D*, in meandering tidal channels and creeks [*Marani et al., 2002a*]. Figure 3 shows, for a large sample of channels within the Lagoon of Venice, plots of channel depth D versus width *2B*. The data are derived from digitized maps for the large channels (say, *B>10 m*), and result from a direct survey in the test area. The plot in Figure 3 shows clear differences in β values. Although important fluctuations occur, saltmarsh creeks and tidal flat channels are seen to respond to different erosional processes resulting in different incisions. In saltmarshes, the ratio β lies consistently in the range 5-7, quite differently from the values typically observed in meandering rivers (usually 8<β<48; e.g. *Millar, 2000*). In tidal flats, less incised, river-like patterns are observed (8<β<50). Therefore saltmarsh creeks, where the role of vegetation and of cohesive properties of the sediment are likely to strongly affect the erosional processes, tend to be more deeply incised than their fluvial counterparts. On the contrary, the larger channels developing in tidal flats, where vegetation is less likely to play a major role and the role of sediment cohesion could be less crucial owing to generally increasing sand fractions, are more similar to fluvial landforms. Thus it is significant that certain regularities are observed in the planar properties though facing such different imprintings of the relevant erosional processes. This also awaits proper theoretical interpretation.

3. *The drainage density of tidal networks.*

The Poissonian model proposed by *Rinaldo et al.,* [*1999a*] identifies locally drainage directions, defined by the steepest descent of the water surface topography through free surface gradients in analogy to what happens in fluvial settings where topographic gradients drive the drainage. Watershed delineation in tidal basins is a difficult task, owing to the unsteady character of the flow field induced by tidal currents. Indeed, drainage directions vary both in space and in time, thus in principle preventing a unique definition of the divides characterizing a tidal network. This problem has been bypassed by the procedure for the delineation of time-independent watershed areas in tidal environments proposed by *Rinaldo et al.* [*1999a*]. Time-independent watersheds are delineated on the basis of the water surface topography obtained by suitably simplifying the classic two-dimensional shallow water equations. In particular, by assuming that tidal propagation across the intertidal areas (i.e., tidal flats and/or salt marshes) flanking the tidal channels is frictionally dominated and that, at any instant *t*, the local water surface elevation, say $\eta_1(x, t)$,

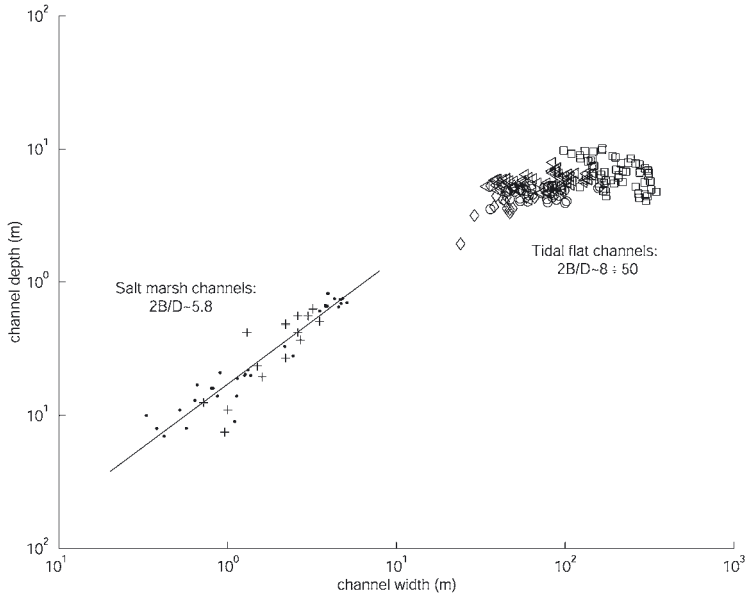

Fig. 3 - Width versus depth for a number of directly surveyed tidal channel sections in the lagoon of Venice. Crosses and dots indicate two different saltmarsh channels measured along their winding path. Diamonds, squares and triangles indicate tidal flat channels. As an excercise, we have fitted only saltmarsh data with a straight line (whose intercept is forced to zero), which is estimated to yield a slope $\beta \sim 6$ and $R^2 = 0.98$ (after *Marani et al.*, [2002a]).

above the instantaneous average tidal elevation $\eta_0(t)$ on the shallow flats is relatively small (i.e $\eta_1 << \eta_0$), *Rinaldo et al.* [*1999a*] showed that, for a nearly horizontal bottom topography, the free surface can be described by the following Poisson boundary value problem:

$$\nabla^2 \eta_1 = \frac{\lambda}{(\eta_0 - z_b)^2} \frac{\partial \eta_0}{\partial t} \qquad (1)$$

where z_b is the average bottom elevation of the intertidal regions, and λ is a friction coefficient (see *Rinaldo et al., 1999a* for details). In order to derive time-independent solutions, *Rinaldo et al.* [*1999a*] further simplified the problem by assuming the forcing at the right-hand side of (1) to be constant and tidal propagation within the creek network to be instantaneous compared to that on the shallow salt marsh or flats. As a conse-

quence , at each instant, the water level in the tidal channel network bordering the intertidal areas is spatially independent and equal to $\eta_0(t)$, that is $\eta_1=0$. The Poisson equation (1), subject to the no-flux condition $\partial\eta_1/\partial n=0$ on the boundary with the mainland and to the condition $\eta_1=0$ on the creek network, allows the determination of a spatial distribution of representative water levels. On the basis of the distribution of water depths flow directions can be obtained at any location on the salt marsh, by determining the steepest-descent direction, and the divides related to any channel cross-section may be identified.

It should be noted that, given the hypotheses underlying the procedure, the divides tend to be equidistant from the channel axes, independently from channel width and depth. This result appears rather surprising since the tidal wave propagates faster through larger (and deeper) channels and they thus influence larger portions of the surrounding shallow flats than smaller channels do. We thus propose herein a stringent test of limits and validity of the approximations embedded in the model of *Rinaldo et al.* [*1999a*]. In order to more closely describe the behaviour of the system we relax in the following the hypothesis that the tidal wave instantaneously propagates within the channel network and assume that tidal elevation, $\eta(x, t)$, varies in space and in time according to the solution of one-dimensional shallow water equations provided by *Dronkers* [*1964*] (see for details on the cited equations: *Dronkers, 1964*; *Lorentz, 1926*; *Zimmermann, 1982*; *Rinaldo et al. 1999b*). Mathematically the new problem reduces to the iterative solution, at a given instant t of the tidal cycle, of (1) by imposing $\partial\eta_1/\partial n=0$ on impermeable boundaries and $\eta_1=\eta-\eta_0$ along the channels. Here $\eta(x, t)$ is obtained by Dronkers equation, while $\eta_0=<\eta>$ denotes its average value over the tidal embayment considered. What emerges from the application of the modified version of the Poissonian model (see *Marani et al.* [*2002b*] for details) is that the divides do not coincide with the lines equidistant from channel axes, and that they migrate during the tidal cycle thus inducing a time variability of the watersheds. It is worthwhile to note that the values of watershed area tend invariably to the (constant) solution given by the model of *Rinaldo et al.* [*1999a,b*] both in the rising and in the falling phases of the tide, when the water level is slightly above the average elevation of the flats, and this tendency is enhanced as the flow resistance over the intertidal regions increases, a circumstance which is quite common in the actual system e.g. due to the presence of dense vegetation. This indicates that tidal propagation within the shallow storage zone adjacent to the channels is in these cases essentially governed by the planimetric configuration of the channel

network, which alone determines the configuration of the watersheds in the infinite-celerity scheme. This is very important from a morphological point of view since the maximum flood and ebb discharges occur when levels exceed or are just below the channel bank-full elevation, respectively [*Bayliss-Smith et al., 1978; Healey et al., 1981; French and Stoddart, 1992*]. Indeed Marani et al. [*2002b*] show that the infinite-celerity and finite-celerity Poisson models yield very similar results as far as maximum discharge is concerned. The above results therefore suggest that the time-invariant watershed delineation proposed by Rinaldo et al. [*1999a*] is suitable to predict peak discharges. In order to further test the robustness of our results we have also compared them to those obtained from a full-fledged semi-implicit, Galerkin finite element model [*Defina, 2000*] discretizing the complete shallow water equations over the whole lagoon of Venice and including a refined description of wetting/drying processes. It should be emphasised here that our interest towards a simplified model is justified by the fact that a finite-element model could not conceivably be used for the mathematical description of the evolution of a tidal environment over morphologically-meaningful periods of time as, due to the numerical burden involved, the duration of the simulation would basically be the same as the time interval being simulated. Figure 4 shows the comparison between the values of the maximum discharge computed through the time-dependent Poisson model described above and the finite-element model for some selected locations in the channel network of the northern lagoon of Venice. It is seen how the two sets of values compare quite favourably with discrepancies of the order of 15%. This leads to the conclusion that maximum discharges obtained through the Poisson models introduced are consistent with those determined through a complete hydrodynamic simulation. This has definite relevance for tidal morphodynamics because it has been shown that maximum discharge, tidal prism and channel area (and width) can be empirically related [*e.g. Rinaldo et al., 1999a,b*].

We then turn to the analysis of drainage density, whose basic definition, (according to *Horton's*, 1945), is the ratio of the network total length to its watershed area: $D=\Sigma L/A$, i.e. it is the inverse of a length (l_H). The Hortonian length l_H is a measure of how the catchment is dissected by the channel network, whereas the unchanneled mean path length l, indicates how efficiently the network 'serves' (i.e. drains or feeds water during ebb and flood) its catchment, determining the mean flow distance from a point on the marsh to the nearest channel. 'Overmarsh' paths for the salt marshes monitored within the lagoon of Venice are studied via flow direc-

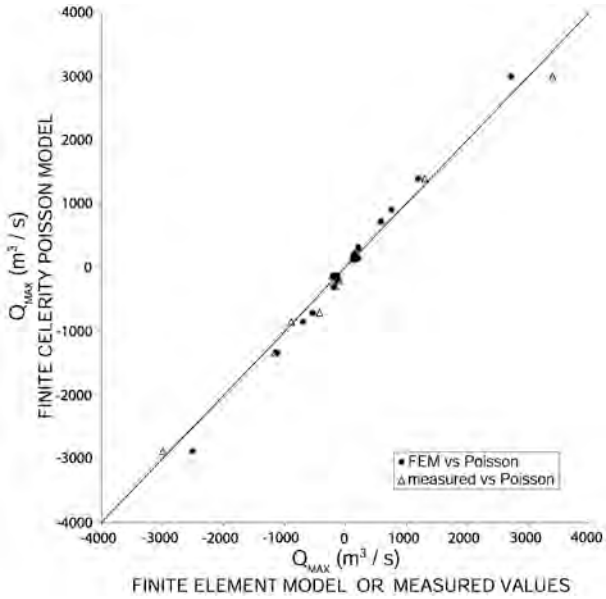

Fig. 4 - The values of maximum discharge obtained at different sections in the northern lagoon of Venice by use of the infinite-celerity Poissonian model are compared to direct observations and to the results from a full-fledged finite element model (after *Marani et al.*, [2002b]).

tions derived from relevant free-surface gradients, i.e. via the infinite-celerity Poissonian hydrodynamic model applied to the study areas [*Marani et al., 2002b*]. Thus for any unchanneled site defined within a tidal landscape we determine objectively the flow path to the nearest tidal channel and compute its length, thereby defining a random space function. Figures 5 and 6 show the semilog plot of the probability distributions of overmarsh pathways in different areas of the S. Felice and Pagliaga salt marshes, in the Venice lagoon. We observe that the approximately linear trends suggest exponential probability distributions of the type observed in fluvial environments by *Tucker et al.* [*2001*]. The slope of the semi-log plot is the mean of the exponential distribution, and thus the mean overmarsh path length, which appears to fluctuate considerably in space even in adjacent sites (Figs. 5 and 6). It is thus relevant to assess whether these are to be considered natural fluctuations around a mean behaviour or rather the symptoms of space-dependent processes influencing network development. In this view it is of practical and theoretical importance to

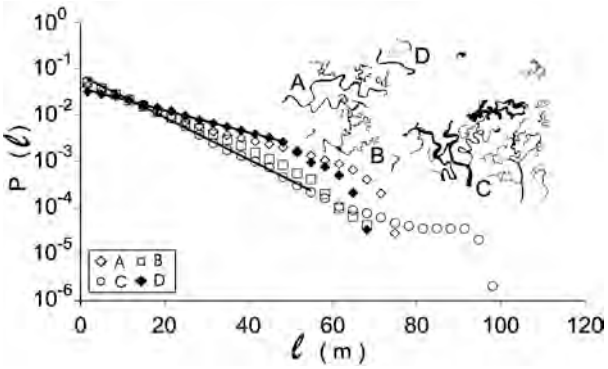

Fig. 5 - Probability density function of overmarsh path length *l* evaluated for several watersheds within the S.Felice salt marsh. Note that an approximately straight observational trend on the semi-log plot suggests an exponential distribution (after *Marani et al.*, [2002b]).

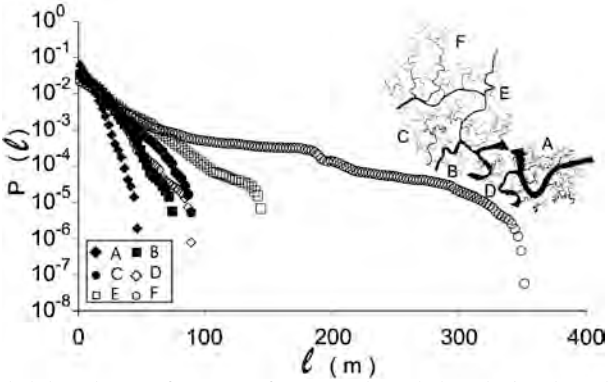

Fig. 6 - Probability density function of overmarsh path length *l* evaluated for several watersheds within the Pagliaga salt marsh. Note that an approximately straight observational trend on the semi-log plot suggests an exponential distribution (after *Marani et al.*, [2002b]).

study the dependence of total network length on other physical characteristics of the salt marshes and it would be desirable to relate total channel length to a feature of the salt marsh which would make the relationship independent from location. To this end, Figure 7 plots total channel length versus sub-basin area *A*. The experimental points from the different sites considered reasonably fall onto the same line, suggesting that total network length responds to the total area served regardless of tidal

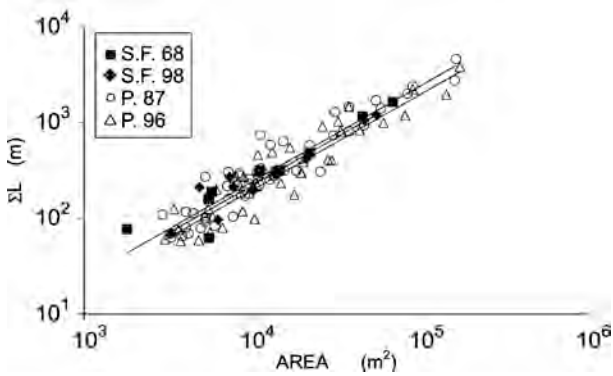

Fig. 7 - Relationship between total network length and basin area for several sub-basins in S. Felice and Pagliaga salt marshes showing a common linear trend. The data have been fitted to a power-law with unit exponent ($\Sigma L \cong \alpha A^{1\pm0.05}$). The best estimate are: a=0.024 m^{-1} for S. Felice 1968 (r^2=0.991); a=0.022 m^{-1} for S. Felice 1998 (r^2=0.978); a=0.024m^{-1} for Pagliaga 1987 (r^2=0.911); and a=0.020 m^{-1} for Pagliaga 1996 (r^2=0.885). Notice that $a=l_H^{-1}$ is the Hortonian drainage density (after *Marani et al.*, [2002b]).

amplitude. The data, fitted to a power law, yield roughly unit values of the exponents for both salt marshes and for all years of observation (details on the computations and statistics are reported in the caption). The linear relationship in Figure 7 agrees qualitatively with *Steel and Pye* [1997] who obtained a positive correlation (albeit apparently not a linear one) between total length and watershed area (defined through an arbitrary geometric construct) from a survey of 13 british salt marshes. The relation in Figure 7 suggests a rather spatially constant mechanism of network development and a constant Hortonian drainage density, the slope of the relationship $\Sigma L \alpha A$. With respect to differing mean overmarsh path lengths l, one wonders whether there is a common morphodynamics of tidal networks leading to structures nearly homogenous in space – or else the Hortonian measure may not be distinctive. To substantiate this observation, we plot mean overmarsh path lengths l versus sub-basin area A. The existence of a relationship between Hortonian characteristic length l_H and the mean overmarsh path length l, would confirm that the geometry of the network, including branching and meandering characteristics, is similar from place to place. The result is seen in Figure 8 which indicates that mean overmarsh path length exhibits a larger scatter than experienced by total length (Fig. 7), and no clear trend over the interval of areas spanned by the data is evident. This is due to rather different sub-basin shapes, branching and meandering characteristics of the tidal networks

cutting through the salt marshes. The results of Figures 7 and 8 indeed indicate that, since Hortonian drainage density remains relatively constant and mean overmarsh path length reflects instead different network features, there is not a similarity of forms from one location to another in the network structure and in the way the network dissects the salt marsh. Moreover, the Hortonian measure of drainage density is not particularly distinctive, as it happens [*Kirchner,* 1993*; Rodrìguez-Iturbe and Rinaldo,* 1997*; Rinaldo et al.* 1999*; Dodds and Rothman*, 2000] to topological measures for network comparison.

A conclusive test is illustrated in Figure 9, where the ratio l_H/l is plotted against link frequency [*Horton, 1945*], defined as the ratio of the number of channel links to the watershed area A. The ratio V'l_H/l' is a measure of the efficiency with which, for a certain Hortonian drainage density (i.e. a given total channel length per unit area), the salt marsh is dissected by the network: high values of l_H/l for a given l_H correspond to a spatial arrangement of channel links which efficiently reduces the mean overmarsh path length. Figure 9 shows the data from our field sites (Fig. 9a) jointly with the data from simple geometrical settings (Fig. 9b). Cases 1, 2, 3, 4 and 6 share the same values of total network length and basin area and thus the same Hortonian length l_H. These cases show how, for a fixed l_H, different branching structures and meandering characteristics yield different values of the efficiency l_H/l. Cases 5 and 7 have a larger

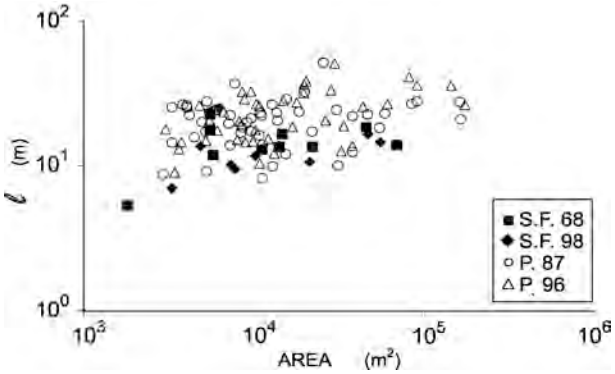

Fig. 8 - Relationship between mean overmarsh path length and basin area for several subbasins in S. Felice and Pagliaga salt marshes. The relationship does not indicate any clear trend. In particular, we have estimated the best relationship ($l \cong bA^c$) with the following results: S. Felice 1968: b=2.92, c=0.17 (r^2=0.22); S. Felice 1998: b=3.92, c=0.12 (r^2=0.11); Pagliaga 1987: b=10.69, c=0.06 (r^2=0.03); Pagliaga 1996: b=3.63, c=0.19 (r^2=0.22).

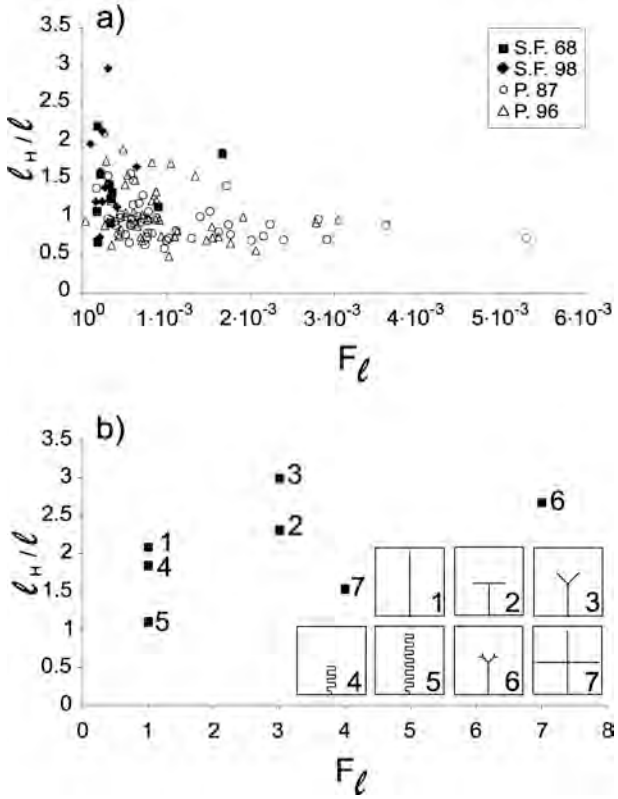

Fig. 9 - Ratio of Hortonian and mean unchanneled lengths vs link frequency for (a) various watersheds in the Pagliaga and S. Felice salt marshes and (b) for schematic test settings (after *Marani et al.*, [2002b]).

total network length and thus smaller values of l_H than the previous ones. The test cases illustrated explain the wide variability observed in Figure 9a, in spite of the constancy of l_H in Figure 7. We thus conclude that the traditional Hortonian morphological description does not provide a complete picture of the geometry of a tidal network and of its relationship with the salt marsh which it dissects. Our results seem also to support the known concept of inheritance of the major features of channelized patterns from sand- or mud-flat to a salt marsh [*e.g. Allen*, 2000; *Friedrichs and Perry*, 2001]. In fact, the constant value of the Hortonian drainage density l_H suggests that the total length of the channel network is uniquely defined by salt marsh area. Thus when the tidal landscape reaches an elevation that allows the colonization by alophytic vegetation, this

freezes the configuration of the network which can, from then on, only undergo minor changes immaterial to its basic structure. The impact of the above results on the general morphodynamic model of the lagoon of Venice, on which research is actively progressing, remains to be seen. In particular, forthcoming research will correlate link frequencies with ratios of tidal channel width to depth, as a general proxy for sediment and vegetational characteristics of a salt marsh.

4. *Conclusions.*

Our main conclusions concerning the features of tidal meanders and the morphological description of tidal networks and salt marshes observed in different coastal wetlands can be summarized as follows:

I) substantial differences with fluvial morphologies are observed. In particular, the observations emphasize the role of strong spatial gradients of characteristic geometric features, chiefly wavelength and width, that respond to gradients in landforming discharges. Remarkably, as the dominant discharge markedly increases seaward along a tidal channel, its width adjusts to an exponential growth, whose rate constant is site-specific;

II) as tidal meanders evolve, the (appropriate) meander wavelengths, radii of curvature and width vary by orders of magnitude (say, we recorded widths growing from a few meters to 200 m within a few km alongstream), thus rendering the meandering forms strongly non stationary. This and other results obtained, i.e. that in both fluvial and tidal environments the ratio of meander length to meander width remains roughly constant, seem to imply that the adjustment of meander morphology to varying dominant discharges is local and does not entail significant transition zones;

III) width-to-depth ratios, which bear strong implications on the erosional and migration mechanisms that originate and develop the meanders, substantially depend on location, thus supporting the significance of the observation of certain planar regularities independent of tidal, vegetational, hydrodynamic conditions and sediment types;

IV) the distributions of the flow lengths of unchanneled pathways in salt marshes within observational tidal networks show interesting features. Our introduction of suitable drainage directions, defined by hydrodynamic gradients, is based on a Poissonian model which proves robust and reliable upon comparison with complete models in a large spectrum of cases of practical interest. This bears important consequences for the prediction of the morphological evolution of lagoons and coastal wetlands;

V) drainage densities, i.e. the extent of tidal channelization, of various salt marshes have been observed and analyzed. We find a clear tendency to develop watersheds described by exponential decays of the probability distributions of unchanneled lengths;

VI) the total length of the channel network is found to be uniquely defined by salt marsh area. We suggest that this supports the concept of inheritance and thus salt marsh area might be a proxy of the dynamic forcing responsible for the formation of the network during its history. This implies that when the tidal landscape reaches an elevation that allows the colonization by alophytic vegetation, the configuration of the network freezes and can, from then on, only undergo minor changes not altering its basic structure;

VII) similarity of forms developing at different sites is not observed, although Hortonian measures indicate a robust relationship between total network length and marsh area. Such relationship is artificially independent from important factors such as marsh elevation and vegetation types, which indeed affect the relevant geomorphology. Mean unchanneled lengths, computed appropriately, resolve the lack of distinctiveness of Horton's drainage density.

References.

Allen J.R.L., 2000. Morphodynamics of Holocene salt marshes: a review sketch from the Atlantic and southern North Sea coasts of Europe. Quaternary Sci. Rev., 19 (17-18), 1155-1231.

Bayliss-Smith T.P., Healey R., Lailey R., Spencer T. and Stoddart D.R., 1978. Tidal flows in salt-marsh creeks. Estuarine Coastal Marine Sci., 9, 235-255.

Boon J.D., 1975. Tidal discharge asymmetry in a salt marsh drainage system. Limnology & Oceanography 20, 71-80.

Boon J.D., Byrne R.J., 1981. On basin hypsometry and the morphodynamic response of coastal inlet systems. Marine Geol., 40, 27-48.

Defina A., 2000. Two Dimensional Shallow Flow Equations for Partially Dry Areas. Water Resour. Res., vol. 36, 11, 3251-3264.

Dodds S. and Rothman D.H., 2000. Annu. Rev. Earth Planetary Sci., 77, 114-128.

Dronkers J.J., 1964. Tidal Computations. North-Holland, Amsterdam.

Fagherazzi S., Bortoluzzi A, Dietrich W.E., Adami A., Lanzoni S., Marani M., Rinaldo A., 1999. Tidal networks 1. Automatic network extraction and preliminary scaling features from digital terrain maps. Water Resour. Res., 35, 12, 3891-3904.

French J.R. and Stoddart D.R., 1992. Hydrodynamics of salt marsh creek systems: implications for marsh morphological development and material exchange. Earth Surf. Proc. Landforms, 17, 235-252.

Friedrichs C.T., Perry J.E., 2001. Tidal salt marsh morphodynamics, J. Coastal Res., 27.

Healey R.G., Pye K., Stoddart D.R. and Bayliss-Smith T.P., 1981. Velocity variation in salt marsh creeks, Norfolk, England. Estuarine Coastal Shelf Sci. 13: 535-545.

Horton R.E., 1945. Erosional development of streams and their drainage basins: Hydrophysical approach to quantitative geomorphology, Bull. Geol. Soc. Am., 56, 275-370.

Kirchner J.W., 1993. Statistical inevitability of Horton's laws and the apparent randomness of stream channel networks. Geology, 21, 591-594.

Lanzoni S., Seminara G., 2002. Long term evolution and morphodynamic equilibrium of tidal channels. J. Geophys. Res., vol. 107, pp. 1-13.

Leopold L.B., Wolman M.G. and Miller J.P., 1964. Fluvial Processes in Geomorphology. Freeman and Company, San Francisco.

Leopold L.B., Collins J.N. and Collins L.M., 1993. Hydrology of some tidal channels in estuarine marshlands near San Francisco. Catena, 20, 469-493.

Lorentz H.A., 1926. Verslag Staatcommissie Zuiderzee 1918-1926. Report, Government Zuiderzee Commission, Alg. Landsddrukkerij, Den Haag.

Millar R.G., 2000. Influence of bank vegetation on alluvial chennel patterns. Water Res. Resour., 36(4), 1109-1118.

Marani M., Lanzoni S., Zandolin D., Seminara G., Rinaldo A., Tidal meanders, 2002a. Water Resour. Res., in press.

Marani M., Belluco E., D'Alpaos A., Defina A., Lanzoni S., Rinaldo A., 2002b. On the drainage density of tidal networks. Water Resour. Res., in press.

Myrick R.M. and Leopold L.B, 1963. Hydraulics geometry of a small tidal estuary. U.S. Geol. Sur. prof. Paper, 422-B, 18.

Pestrong R., 1965. The development of drainage patterns on tidal marshes. Stanford Univ. Publ. Geol. Sci., Tech. Rep. 10, 87.

Pethick J.S., 1980. Velocity surges and asimmetry in tidal channels. Estuarine and Coastal Marine Science, 11, 331-345.

Redfield A.C., 1972. Development of a New England salt marsh, Ecol. Monogr., 24, 2, 201-237.

Rinaldo A., Fagherazzi S., Lanzoni S., Marani M., Dietrich W.E., 1999a. Tidal networks 2. Watershed delineation and comparative network morphology. Water Resour. Res., 35, 12, 3905-3917.

Rinaldo A., Fagherazzi S., Lanzoni S., Marani M., Dietrich W.E., 1999b. Tidal networks 3. Landscape-forming discharges and studies in empirical geomorphic relationships. Water Resour. Res., 35, 12, 3919-3929.

Rodrìguez-Iturbe I. and Rinaldo A., 1997. Fractal River Basins: Chance and Self-Organization, Cambridge Univ. Press, New York.

Steel T.J. and Pye K., 1997. The development of salt marsh tidal creek networks: evidence from the UK. Proc. of Canadian Coastal Conference 1997, Vol. 1, 267-280.
Tucker G.K., Catani F., Rinaldo A. and Bras R.L., 2001. Statistical analysis of drainage density from digital terrain data. Geomorphology, 36, 187-202.
Zimmermann J.T.F., 1982. On the Lorentz linearization of a quadratically damped forced oscillator. Physics Lett., 89A(3), 123-124.

MODELLING SUSPENDED SEDIMENT TRANSPORT IN TIDAL FLOWS: THEORY AND APPLICATION TO LONG TERM EQUILIBRIUM OF TIDAL CHANNELS

M. Bolla Pittaluga and G. Seminara
Dipartimento di Ingegneria Ambientale, Università di Genova

Abstract.

We derive a depth averaged model of suspended sediment transport. The development of the analysis leads us to revisit the asymptotic approach originally developed by Galappatti (1983), more recently generalised by Wang (1992) and widely employed in commercial codes. The formal asymptotic expansion of the exact solution is found to differ from Galappatti's approach. Moreover, rather than leading to a differential equation for the depth averaged concentration it actually provides higher order corrections for the leading order equilibrium approximation of the depth averaged concentration. Such corrections can be expressed in terms of spatial and temporal derivatives of the leading order solution. Based on the formal asymptotic expansion of the exact solution, we are then able to derive an analytical form for the flux of suspended sediment appropriate in slowly varying flows, which is suitable to applications to a variety of morphodynamic contexts including tidal and fluvial environments. Such approach is then applied to investigate the long term equilibrium of tidal channels.

1. *Introduction.*

River and Estuarine Morphodynamics is a discipline aimed at predicting the short - long term evolution of the interface between the flowing mixture of water and sediments and the underlying cohesionless (or cohesive) container. It is not uncommon for sediments to be dominantly transported in suspension in streams characterised by spatial and/or temporal variations of the hydrodynamics occurring on very large scales such

that, in some sense to be precisely defined below, the flow may be considered as 'slowly varying' in space and/or time. Typical examples are tidal flows and flood waves. Under the latter conditions, the problems of morphodynamics would benefit from the availability of an appropriate depth averaged model to evaluate the sediment flux transported in suspension.

In 1983 Galappatti (but see also Galappatti and Vreugdenhil, 1985) attempted to derive a depth averaged form of the convection diffusion equation for sediment concentration on the basis of an asymptotic approach relying on the existence of small parameters measuring the relative importance of advection and local variations of concentration versus turbulent diffusion and gravitational settling. The approach is then based on a classical regular perturbation expansion (see for instance, Nayfeh, 1973), except for the peculiar treatment proposed by the author for the boundary conditions. In fact, essentially the author does not expand the boundary conditions in terms of the small parameter, as is typical of classical perturbation approaches. Rather, he stipulates that the depth averaged value of the concentration is wholly determined by the lower order approximation of the solution, while higher order terms are forced to have vanishing depth average. The boundary condition at the bed interface is eventually reinforced by requiring that the sum of the lowest and higher order components of the solution must satisfy it. This leads to a relationship which the author treats as a differential equation for the depth averaged concentration.

We show that, with a classical perturbation expansion of the solution, rather than deriving a differential equation for the depth averaged concentration, one finds a sequence of higher order corrections for the depth averaged concentration expressed in terms of spatial and temporal derivatives of the leading order solution. Based on the classical perturbation expansion of the solution, we derive an analytical expression for the flux of suspended sediment suitable in slowly varying flows. Such result seems to be particularly useful in order to perform numerical investigations of long term morphodynamical processes as the use of 3D models would make computations of long term equilibrium extremely heavy.

The application of such model to the evaluation of the long term equilibrium profile of tidal channels proves effective: indeed the equilibrium configuration is determined, in a machine time some order of magnitude smaller than using a numerical model based on the solution of the convection diffusion equation coupled with the hydrodynamic equations. Results show that the effects of settling-lag and local variation of concentration are often not crucially important.

2. *Transport of Suspended Sediment by Slowly Varying Flows.*

2.1. *Formulation of the problem.*

Let us now consider the flow of a dilute mixture of water and fine sediment particles and refer the flow field to a cartesian coordinate system x^*, y^*, z^* with z^* vertical, x^* longitudinal and y^* transverse (hereafter a star apex will denote a dimensional quantity subsequently made dimensionless). The transport of suspended sediment under gravity is then governed by the convection-diffusion equation which, referring to the case of plane flows for the sake of simplicity, reads:

$$\frac{\partial C}{\partial t^*} + U^* \frac{\partial C}{\partial x^*} + \left(W^* - W_s\right)\frac{\partial C}{\partial z^*} = \frac{\partial}{\partial x^*}\left(\mathsf{D}_x^* \frac{\partial C}{\partial x^*}\right) + \frac{\partial}{\partial z^*}\left(\mathsf{D}_z^* \frac{\partial C}{\partial z^*}\right), \quad (1)$$

where

C: local volumetric sediment concentration;
(U^*, W^*): longitudinal and vertical components of the local velocity;
t^*: time;
W_s: particle fall velocity;
$(\mathsf{D}_x^*, \mathsf{D}_z^*)$: longitudinal and vertical components of the eddy diffusivity.

Let us make the relevant physical quantities dimensionless as follows:

$$t = \omega t^*, \quad (U, W) = \left(\frac{U^*}{U_0^*}, \frac{W^*}{W_0^*}\right), \quad x = \frac{x^*}{L_0^*}, \quad z = \frac{z^*}{D_0^*}, \quad (\mathsf{D}_x, \mathsf{D}_z) = \frac{\left(\mathsf{D}_x^*, \mathsf{D}_z^*\right)}{u_{*0} D_0^*}, \quad (2)$$

having employed the following scales:

ω: typical frequency of the flow field;
U_0^*: longitudinal velocity scale;
$W_0^* = \mathsf{D}_0^* U_0^* / L_0^*$: scale for vertical velocity;
L_0^*: longitudinal spatial scale;
D_0^*: reference flow depth;
u_{*0}: reference friction velocity.

Note that the scale for the vertical velocity arises from the equation of continuity.

Using the above dimensionless variables the equation (1) takes the form

$$\delta_1 \frac{\partial C}{\partial t} + \delta_2 U \frac{\partial C}{\partial x} + \left(\delta_2 W - 1\right)\frac{\partial C}{\partial z} = \frac{1}{kZ_0}\left[\frac{\partial}{\partial z}\left(\mathsf{D}_z \frac{\partial C}{\partial z}\right) + \delta_3 \frac{\partial}{\partial x}\left(\mathsf{D}_x \frac{\partial C}{\partial x}\right)\right], \quad (3)$$

where the following dimensionless parameters arise:

$$\delta_1 = \frac{\omega D_0^*}{W_s}, \qquad \delta_2 = \frac{U_0^* D_0^*}{W_s L_0^*}, \qquad \delta_3 = \left(\frac{D_0^*}{L_0^*}\right)^2, \qquad Z_0 = \frac{W_s}{k u_{*0}}, \quad (4)$$

Note that the parameters $\delta_j (j=1,3)$ are typically small for slowly varying flows like tidal flows and flood waves. In (3) k is the von Karman constant and Z_0 is the reference Rouse number.

Let us define a transformed vertical coordinate ζ as follows:

$$\zeta = \frac{z^* - \eta^*}{D^*} = \frac{1}{D}(z - \eta), \quad (5)$$

where D and η represent the local flow depth and the bottom elevation respectively, scaled by the reference flow depth D_0^*.

It is now convenient to set

$$\delta_2 = \delta, \qquad \delta_1 = \gamma\delta \ (\gamma \approx O(1)). \quad (6)$$

Employing the transformation (5) and neglecting the term proportional to δ_3, the convection-diffusion equation (3) becomes:

$$\frac{1}{kZ_0}\left[\frac{\partial}{\partial\zeta}\left(D_\zeta \frac{\partial C}{\partial\zeta}\right)\right] + D\frac{\partial C}{\partial\zeta} = \delta\left\{\gamma D^2 \frac{\partial C}{\partial t} - \gamma D\left(\frac{\partial\eta}{\partial t} + \zeta\frac{\partial D}{\partial t}\right)\frac{\partial C}{\partial\zeta} + D^2 U\frac{\partial C}{\partial x} - \left[UD\left(\frac{\partial\eta}{\partial x} + \zeta\frac{\partial D}{\partial x}\right) - DW\right]\frac{\partial C}{\partial\zeta}\right\}, \quad (7)$$

The boundary conditions to be associated with equation (7) impose vanishing sediment flux at the free surface. Furthermore, at the bed, we impose the so called 'gradient boundary condition' which essentially consists of an entrainment assumption whereby the net sediment flux is assumed to be proportional to the difference between the actual local instantaneous concentration and the value that concentration would attain at equilibrium with the local and instantaneous flow conditions, the proportionality constant, i.e. the entrainment coefficient, being equal to the particle velocity normal to the bed. The resulting form of the boundary conditions reads:

$$\frac{D_\zeta}{kZ_0}\frac{\partial C}{\partial\zeta} + DC = \delta\left\{DWC - DUC\frac{\partial h}{\partial x}\right\} \qquad (\zeta = 1), \quad (8)$$

$$\frac{D_\zeta}{kZ_0}\frac{\partial C}{\partial\zeta} + DC_e = \delta\left\{DWC - DUC\frac{\partial\eta}{\partial x}\right\} \quad (\zeta = \zeta_R), \quad (9)$$

where h is the free surface elevation scaled by the reference flow depth D_0*. Moreover, ζ_R is the conventional dimensionless value of the reference elevation where the boundary condition is imposed under uniform conditions. Several empirical expressions for C_e and ζ_R are available in the literature (see, for instance, Van Rijn, 1984). They correlate C_e with a dimensionless measure of the bottom stress, the so called Shields parameter θ, and with the particle Reynolds number R_p.

A closure relation for the eddy diffusivity D_ζ is also required and, assuming slow time variations of the flow field consisting of a quasi-steady sequence of equilibrium states, we can write

$$D_\zeta = D \frac{u_*}{u_{*0}} N(\zeta), \tag{10}$$

with u_* the instantaneous value of friction velocity and $N(\zeta)$ the vertical distribution of eddy diffusivity at equilibrium. Using the classical parabolic distribution for $N(\zeta)$ we write:

$$N(\zeta) = K\zeta(1-\zeta). \tag{11}$$

2.2. *Formal perturbation solution for the case* $\delta << 1$.

It is possible to obtain a formal perturbation solution of the differential equation (7), associated with the boundary conditions (8, 9), by expanding the concentration C in powers of the small parameter δ. By substituting from the latter expansion into the differential problem and equating likewise powers of δ we find a sequence of differential problems at the various orders of approximation. In the following, for the sake of brevity, we have just reported the solution of the differential problems.

At the leading order of approximation we find the classical Rouse solution

$$C_0(\zeta;x,t) = C_e(\vartheta, R_p)\left(\frac{1-\zeta}{1-\zeta_R}\cdot\frac{\zeta_R}{\zeta}\right)^Z, \tag{12}$$

where Z represents the local Rouse number.

At the following order of approximation the solution for the vertical distribution concentration C_1 takes the form

$$C_1(\zeta;x,t) = D\frac{\partial \overline{C_0}}{\partial t}\chi_{11} + \overline{U}D\frac{\partial \overline{C_0}}{\partial x}\chi_{14} + Z\overline{C_0}\left(\frac{\partial \eta}{\partial t}\chi_{12} + \frac{\partial D}{\partial t}\chi_{13}\right), \quad (13)$$

where $\overline{U}$ and $\overline{C_0}$ represent the velocity and the lower order concentration averaged on the flow depth respectively, while the functions χ_{1j} (j=1, 4) are reported in Appendix A.

It is worth to notice that a self similar vertical distribution of the velocity, appropriate for slowly varying flows, has been used, hence:

$$U = \overline{U}(x,t)\,F(\zeta), \qquad F(\zeta) = \frac{\sqrt{C_{f0}}}{k}\left(ln\frac{\zeta}{\zeta_0} + A\zeta^2 + B\zeta^3\right), \quad (14)$$

where C_{f0} represents the friction coefficient at the reference state (defined as $\overline{U}$ (x, t)=1) and ζ_0 is the conventional dimensionless value of the reference elevation for no slip in uniform flows.

2.3. *Derivation of an analytical relationship for the suspended sediment flux under slowly varying flows.*

Following the ideas outlined above, we can expand the suspended sediment flux in powers of the small parameter δ in the form $q_s = q_{s0} + \delta\, q_{s1} + O(\delta^2)$ where q_{s0} and q_{s1} have been scaled by with the reference flow discharge per unit width $U^*_0\, D^*_0$.

With the aid of (14) and the expansion of the concentration C we can write:

$$q_s = q(x,t)\,\psi(x,t), \quad (15)$$

where

$$q(x,t) = \overline{U}(x,t)\,D(x,t), \quad (16a, b)$$

$$\psi(x,t) = \int_{\zeta_R}^{1}\left[C_0 + \delta\, C_1 + O(\delta^2)\right]F(\zeta)d\zeta = \psi_0 + \delta\psi_1 + O(\delta^2).$$

By susbstituing (12) and (13) into (16b) we end up with the following relationships for Ψ_0 e Ψ_1

$$\psi_0 = \frac{\sqrt{C_{f0}}}{k} C_e \left[I_{02} + K_1 I_{01} \right],$$
$$\psi_1 = \frac{\sqrt{C_{f0}}}{k} \left[D \frac{\partial \overline{C_0}}{\partial t} q_{s10} + \overline{U} D \frac{\partial \overline{C_0}}{\partial x} q_{s11} + D_{,t} \overline{C_0} q_{s12} + \eta_{,t} \overline{C_0} q_{s13} \right], \tag{17}$$

where I_{0j} (j=1, 2) and q_{s1j} (j=0, 3) are integrals of functions of ζ_R and Z and their expressions are reported in Appendix B. All the above coefficients are then functions of some integrals which have been calculated numerically and then interpolated in order to obtain analytical expressions. Equations (15, 16, 17), together with the expressions of the coefficients I_{0j} (j=1, 2) and q_{s1j} (j=0, 3), provide a simple analytical procedure for the evaluation of the suspended sediment transport in slowly varying flows and can be easily incorporated into morphodynamic numerical models concerning fluvial or lagoon environments.

3. *Application: long term equilibrium of tidal channels.*

The latter formulation is then applied to study the morphodynamic equilibrium of tidal channels and, in particular, the effects of settling-lag and of the local variations of concentration on such equilibrium configuration. The theoretical analysis of *Lanzoni e Seminara* (2002), which neglected such effects, demonstrated the existence of a long term equilibrium configuration characterised by a vanishing net sediment flux in a tidal cycle and by a longitudinal bottom profile concave seaward and convex landward. The concavity increased as the channel convergence increased. Furthermore the depth at the inlet section of the channel was uniquely determined by channel geometry and tidal forcing and additionally the final equilibrium configuration gave rise to the emergence of the bed in the inner part of the channel, thus determining its length.

Figure (1) represents a comparison between the longitudinal bed profiles in the equilibrium configuration of a straight rectangular tidal channel in the case where the effects of sediment advection and local variation of concentration are accounted for or viceversa. The results show that the effects of settling-lag and local variation of concentration lead to a longitudinal bed equilibrium configuration which is practical identical to that obtained by the simpler model of *Lanzoni e Seminara* (2002). However note that the above effects are more pronounced during the initial phase of bed evolution when sediment transport is more intense.

The effect of the exchange of sediments between the channel and the sea on the long term equilibrium of tidal channels has also been investigated through a simplified model whereby the sediment flux during the ebb phase was assumed to be controlled by the transport capacity of the stream at the inlet section, while the sediment flux during the flood phase was taken to be driven by some fixed 'sea' sediment concentration. Space does not allow us to describe the analysis in detail. Briefly, it turns out that an excess of sediment supply from the sea induces sediment deposition but does not prevent the channel from reaching a new equilibrium configuration; on the other hand, a deficient exchange of sediments with the sea leads to an equilibrium profile quite close to that obtained on the basis of the equilibrium assumption employed in the present paper (figure 2). As mentioned above, such findings were not based on a detailed analysis of the hydrodynamics of the flow field in the region close to the inlet section. This is a subject for future developments. In fact, due to the asymmetry of the flow field during the ebb and flood phases, a net positive or negative sediment flux may arise at the inlet. The morphodynamic equilibrium of tidal inlets is strictly related to the above mechanism and will also require attention in the near future. A model, which neglects the above effect assuming that the sediment flux in the inlet section is always in equilibrium with the local sediment transport capacity of the flow field, suggests that equilibrium is reached when the bottom shear stress attains the threshold conditions for sediment motion in accordance with *Marchi*'s (1990) assumption. However, the effect of an excess of sediment supply as well as of the overtides discussed below, may alter the above picture.

Finally, we have examined the case when the tidal oscillation at the sea contains a contribution from an M_4 overtide out of phase relative to the M_2 component. The former component may alter the character of tide propagation in the channel, which may turn from flood- into ebb- dominant. As a result, the equilibrium configuration of the channel may be significantly affected: this is shown in figure (3) for different values of the phase lag between the M_2 and M_4 components.

4. *Conclusions.*

A depth averaged model of suspended sediment transport has been derived revisiting the asymptotic approach originally developed by Galappatti (1983) and more recently generalised by Wang (1992) and Katopodi (1992). Based on an asymptotic approach, the result of the theoretical analysis leads to an analytical form for the flux of suspended

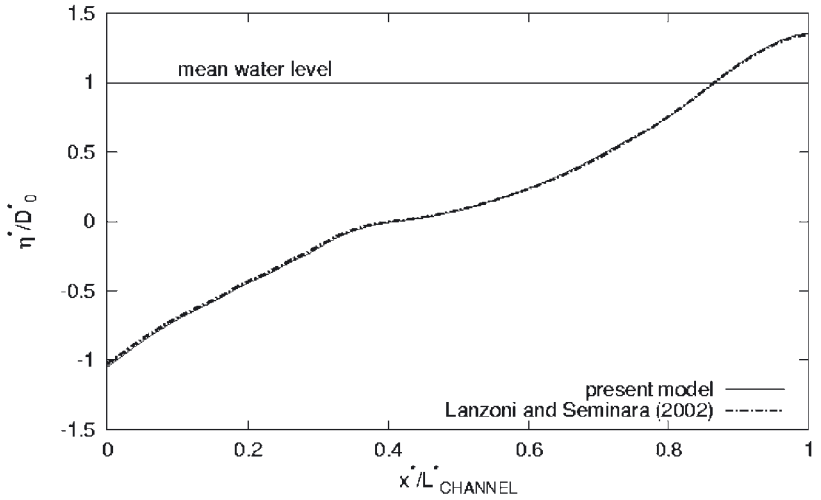

Fig. 1 - Comparison between the longitudinal bottom profiles of the channel at equilibrium in the case in which the effects of settling-lag and local variation of concentration are accounted for (solid line) or neglected (dotted line).

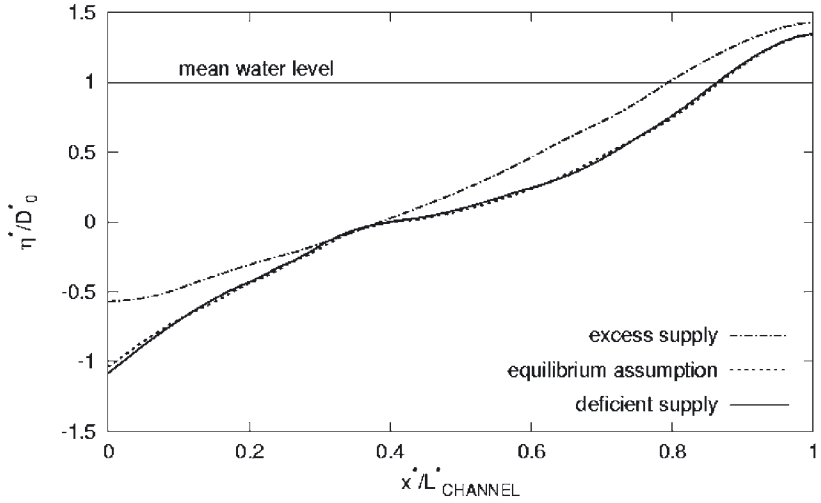

Fig. 2 - Effect of an excess or defect of sediment supply from the sea on the long term equilibrium of tidal channels.

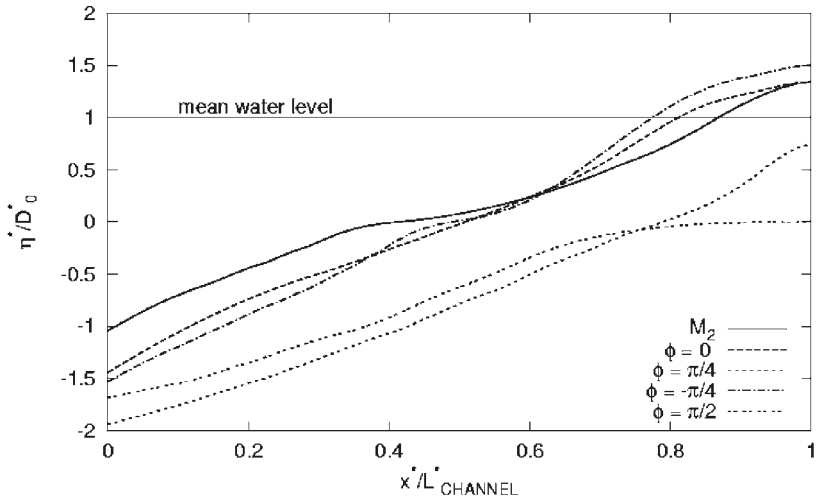

Fig. 3 - Equilibrium configurations of a tidal channel for different values of the phase lag f between the M_2 and M_4 components of the tidal oscillation at the sea. The ratio between the amplitudes of the M_4 and the M_2 components is 0.2.

sediment appropriate to slowly varying flows and suitable to applications to a variety of morphodynamical contexts, including tidal and fluvial environments. The model presented herein can be incorporated in a variety of depth integrated models with the great advantage of including unsteady and spatially varying effects in the evaluation of the flux of suspended sediment without the need to solve a 2D or 3D convection-diffusion equation for the concentration field. We have shown that such advantage proves remarkable when attempting to perform morphodynamic calculations of the long term equilibrium of tidal channels. Flows subjected to more rapid variations of geometry, like flows in tidal inlets or large scale bedforms are also suitable candidates for the application of the present approach.

APPENDIX A

The functions χ_{1j} (j=1, 4) appearing in equation (13) has the form:

$$\chi_{1j} = \gamma\left(C_{1j} - BC_{1j}\big|_1\right) \qquad (j = 1,2),$$
$$\chi_{13} = \gamma\left[\left(C_{13} - BC_{13}\big|_1\right) - \left(C_{15} - BC_{15}\big|_1\right)\right], \quad \chi_{14} = \left(C_{13} - BC_{13}\big|_1\right). \tag{A1}$$

In (A1) the functions C_{1j} (j=1, 5) are the solutions of the following initial value problems:

$$\begin{aligned} LC_{1j} &= a_j(\zeta) && (j = 1,5), \\ \frac{\partial C_{1j}}{\partial \zeta} &= 0 && (\zeta = \zeta_R) \quad (j = 1,5), \\ C_{1j} &= b_j && (\zeta = \zeta_R) \quad (j = 1,5), \end{aligned} \tag{A2}$$

with

$$L = \frac{1}{kZ}\left[\frac{\partial}{\partial \zeta}\left(N(\zeta)\frac{\partial}{\partial \zeta}\right)\right] + \frac{\partial}{\partial \zeta}, \qquad Bf = \frac{1}{kZ}N(\zeta)\frac{\partial f}{\partial \zeta} + f, \tag{A3}$$

and

$$a_1 = \phi_0(\zeta), \quad a_2 = a_3 = \frac{\phi_0(\zeta)}{(1-\zeta)\zeta}, \quad a_4 = \phi_0(\zeta)F(\zeta), \quad a_5 = G(\zeta)\frac{\phi_0(\zeta)}{(1-\zeta)\zeta}, \quad G(\zeta) = \int_{\zeta_0}^{\zeta} F(\xi)d\xi,$$
$$b_j = 1 \qquad (j = 1,5). \tag{A4}$$

APPENDIX B

The expressions of the coefficients appearing in the equation (17) are as follows:

$$I_{01}(\zeta_R, Z) = \int_{\zeta_R}^{1}\left(\frac{1-\zeta}{1-\zeta_R}\frac{\zeta_R}{\zeta}\right)^Z d\zeta,$$

$$I_{02}(\zeta_R, Z) = \int_{\zeta_R}^{1}\left(\ln\zeta + A\zeta^2 + B\zeta^3\right)\left(\frac{1-\zeta}{1-\zeta_R}\frac{\zeta_R}{\zeta}\right)^Z d\zeta, \tag{B1}$$

$$q_{s10} = \gamma\left(A_{11} + K_1 A_{11}^*\right),$$

$$q_{s11} = \frac{\sqrt{C_{f0}}}{k}\left[A_{14} + K_1 A_{14}^* + K_1\left(A_{11} + K_1 A_{11}^*\right)\right],$$

$$q_{s12} = Z\gamma\left(A_{13} + K_1 A_{13}^*\right) - Z\gamma\frac{\sqrt{C_{f0}}}{k}\left[A_{15} + K_1 A_{15}^* + K_2\left(A_{13} + K_1 A_{13}^*\right) + K_3\left(A_{12} + K_1 A_{12}^*\right)\right],$$

$$q_{s13} = Z\gamma\left(A_{12} + K_1 A_{12}^*\right),$$

$$K_1 = -\ln\zeta_0 - A\zeta_0^2 - B\zeta_0^3 \cong -\ln\zeta_0, \qquad K_2 = K_1 - 1, \qquad K_3 = \zeta_0 + \frac{3B}{4}\zeta_0^4 + \frac{2A}{3}\zeta_0^3 \cong \zeta_0.$$

and the coefficients A_{1j}, (j=1..5) read:

$$A_{1j}(\zeta_R, Z) = \int_{\zeta_R}^{1} C_{1j}(\xi;\vartheta,R_p)F_1(\xi)d\xi - BC_{1j}\Big|_1 \int_{\zeta_R}^{1} F_1(\xi)d\xi \qquad (j=1,5),$$
$$A^*_{1j}(\zeta_R, Z) = \int_{\zeta_R}^{1} C_{1j}(\xi;\vartheta,R_p)d\xi - BC_{1j}\Big|_1 (1-\zeta_R) \qquad (j=1,5), \tag{B2}$$

where

$$F_1(\zeta) = \ln\zeta + A\zeta^2 + B\zeta^3, \tag{B3}$$

The integrals I_{01}, I_{02}, A_{1j} and A^*_{1j} are functions of ζ_R and Z. We have calculated numerically each of the above quantities using Simpson's rule for a set of values for ζ_R and Z falling in the ranges:

$$\log\zeta_R \in [-3,-1], \qquad Z \in [0.01,6.30], \tag{B4}$$

with steps $\Delta\log\zeta_R$=0.05 and ΔZ=0.01.

We then used the calculated values to derive analytical expressions for each coefficient by performing interpolations of the general form

$$P(x,y) = \sum_{i=1}^{7}\sum_{j=1}^{7} p_{ij}\, x^{i-1} y^{j-1}, \tag{B5}$$

where x is equal to log ζ_R, y is the Rouse number and the coefficients p_{ij} have been obtained by a least square regression. The values of p_{ij} are not reported here for the sake of brevity but can be made available at request by the authors. Figures (4a,b) show a sample comparison between the interpolated values of the coefficient I_{01} and the values attained by numerical integration of the integral appearing in (B1). Note that the relative error of such comparison does never exceed 0.05 % (figure 5).

Acknowledgements.

This work has been funded by the Italian Ministry of University and of the Scientific and Technological Research under the National Project "Idrodinamica e morfodinamica di ambienti a marea" and cofunded by the University of Genova and by CORILA.

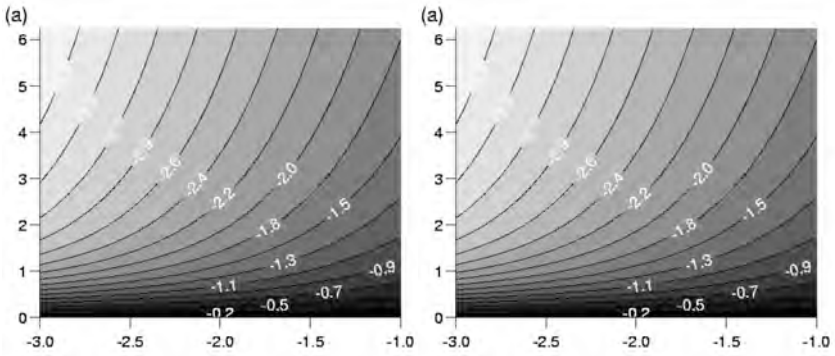

Fig. 4 - Comparison between the interpolated values of the coefficient I_{01} (b) and the values attained by numerical integration of the integral appearing in (B1) (a). The x axis represent the logZ_R, the y axis the Rouse number and the contour levels reports the log(I_{01}).

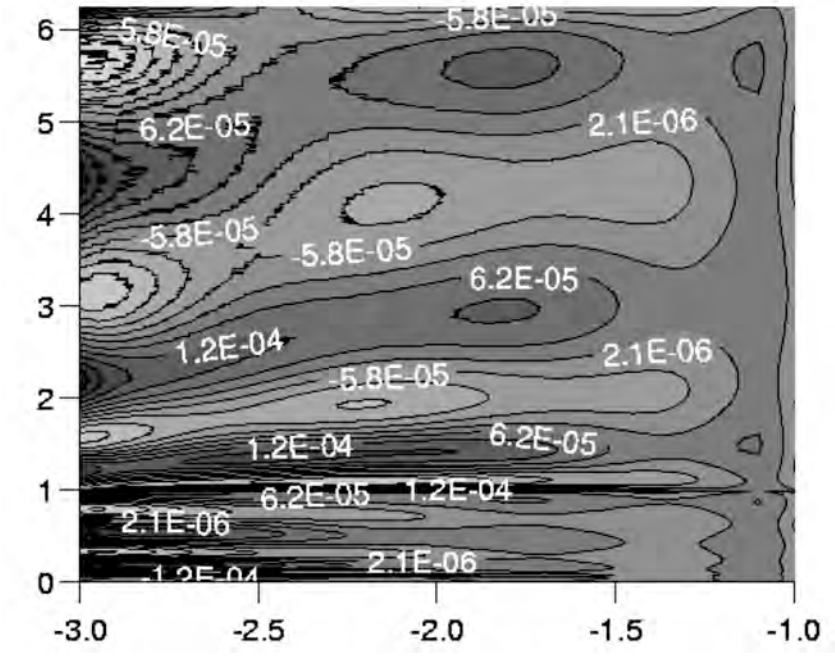

Fig. 5 - Relative error between the interpolated values of the coefficient I_{01} (b) and the values attained by numerical integration of the integral appearing in (B1).

This paper represents a shortened version of two papers: the former [Bolla Pittaluga and Seminara, 2002a] has been submitted for publication to *Water Resources Research*, the latter [Bolla Pittaluga and Seminara, 2002b] is in the process of being submitted for publication on *Journal of Geophysical Research*. The work is also part of the Ph.D. Thesis of Michele Bolla Pittaluga to be submitted to the University of Padova in partial fulfilment of his degree.

Bibliography.

Bolla Pittaluga M. and Seminara G., 2002a. Depth integrated modelling of suspended sediment transport, submitted to *Water Resources Research*.

Bolla Pittaluga M. and Seminara G., 2002b. Long term equilibrium of tidal channels: effects of settling-lag, sediment supply and overtides, to be submitted to *J. Geoph. Res*.

Galappatti R., 1983. A depth-integrated model for suspended transport, Delft University of Technology, Faculty of Civil Eng., Report No.83-7.

Galappatti R. and Vreugdenhil C.B., 1985. A depth-integrated model for suspended sediment transport, *J. Hydr. Res.*, 23 (4), 359-377.

Katopodi I. and Ribberink J.S., 1992. Quasi-3D modelling of suspended sediment transport by currents and waves, *Coastal Engineering*, 18, 83-110.

Marchi E., 1990. Sulla stabilità delle bocche lagunari a marea, Rend. Accademia Nazionale dei Lincei, Roma, Serie IX, 1, 137-150 (in italian).

Nayfeh A.H., 1973. Perturbation methods, *Wiley*, New York.

van Rijn L.C., 1984. Sediment transport, Part II: Suspended load transport, *J. Hydr. Eng.*, 110 (11), 1613-1641.

Wang Z.B., 1992. Theoretical analysis on depth-integrated modelling of suspended sediment transport, *J. Hydr. Res.*, 30 (3), 403-421.

MORPHODYNAMICS OF TIDAL CHANNELS: EXPERIMENTAL OBSERVATIONS

N. Tambroni, M. Bolla Pittaluga and G. Seminara
Dipartimento di Ingegneria Ambientale, Università di Genova

Abstract.

The paper reports on a laboratory investigation of the morphodynamic evolution of tidal erodible channels closed at one end and connected at the other end with a tidal sea.

The present experimental observations confirm the recent theoretical results of *Lanzoni* & *Seminara* (2002) and *Bolla Pittaluga* & *Seminara* (2002) suggesting that tidal channels can achieve a morphodynamic equilibrium characterized by an upward concave bed profile, vanishing net sediment flux in a tidal cycle and the formation of a 'beach' close to the landward end of the channel.

Observations concerning the morphodynamic evolution of the inlet and the formation of bedforms in the channel, are also reported.

1. *Introduction.*

The issue of whether morphodynamic patterns may achieve equilibrium conditions on long time scales is, needless to say, of major importance for all aspects related to the management of tidal environments. In spite of its relevance, the problem has only been partially investigated and still awaits to be fully explored.

Below we examine experimentally the issue of the possible existence of a long term longitudinal equilibrium profile of tidal channels, key features of estuarine and lagoon environments. A sound approach to the investigation of this complex problem can be constructed by isolating each of the above factors in the context of idealized models reproducing only part of the actual process. This research line has been recently pursued theoretically by *Schuttelaars* & *de Swart* (2000), *Lanzoni* & *Seminara* (2002) and

Bolla Pittaluga & *Seminara* (2002). In the latter contribution a straight, convergent channel, closed at one end and connected at the other end with a tidal sea was examined, at first neglecting the *sediment discharge* of rivers possibly debouching at the upstream end of the channel and the *lateral exchange of sediments* between the channel and the adjacent tidal flats. The main output of the latter work can be summarized as follows:

- The asymmetry of surface elevation leads to a net sediment flux within a tidal cycle which is directed landward.
- Starting from an initially flat bed, profile evolves towards an equilibrium configuration characterised by an upward concave profile (except in the beach region) and vanishing net flux of suspended sediments in a tidal cycle at any cross section.
- Equilibrium does not imply that the instantaneous sediment flux vanishes, though transport is generally very weak at equilibrium.

It is the aim of the present work to check the latter findings through a controlled laboratory experiment. The theoretical foundation of the experimental conditions reproduced in the experiments are discussed in the next section. Section 3 is devoted to a brief description of the experimental apparatus, section 4 reports on some preliminary observations and section 5 concludes the paper with some discussion.

2. *Formulation of the problem.*

2.1. *The hydrodynamic problem.*

Our attention is focused on a straight tidal channel of length L^*_e (hereafter the star apex will represent dimensional quantities) and mean flow depth at the mouth of the estuary D^*_0 (fig. 1). The cross section is rectangular and the local width B^* is assumed to vary along the landward oriented longitudinal axis x^* according to the following classical exponential law:

$$B^* = B^*_0 e^{-x^*/L^*_b} \tag{1}$$

where L^*_b is an efolding length (called convergent length) and B^*_0 is the channel width at the inlet. Neglecting the possible presence of tidal flats adjacent to the main channel, whose effect can be accounted for by properly modifying the continuity equation, the basic one-dimensional equa-

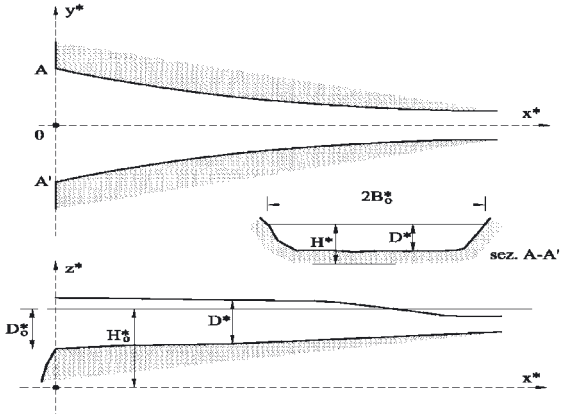

Fig. 1 - Sketch of the estuary and notations.

tions which govern mass and momentum conservation for a rectangular channel, read:

$$\begin{cases} B^* \dfrac{\partial D^*}{\partial t^*} + \dfrac{\partial \left(D^* U^* B^* \right)}{\partial x^*} = 0 \\ \dfrac{\partial U^*}{\partial t^*} + U^* \dfrac{\partial U^*}{\partial x^*} + g \dfrac{\partial H^*}{\partial x^*} + \dfrac{U^* \left| U^* \right|}{C^2 D^*} = 0 \end{cases} \tag{2-3}$$

where t^* denotes time, D^* is the local flow depth, H^* is the water surface elevation, U^* is the local cross sectional averaged velocity, g is gravity and C is the dimensionless Chezy coefficient, i.e the flow conductance.

The relevant variables of the problem can be made dimensionless as follows:

$$t^* = \omega^{*-1} t, \qquad \left(D^*, H^* \right) = D_0^* \left(D, H \right), \qquad U^* = U_0^* U, \qquad C = C_0 c, \tag{4}$$

where ω^*,D^*_0, U^*_0 and C_0 denote the angular frequency of the main component of the tidal wave, the average flow depth, a typical value of the cross sectional average flow velocity and a characteristic flow conductance, respectively, while L^*_0 is the longitudinal scale depending on the dynamic balance prevailing in the momentum equation for the particular tidal flow considered.

The resulting dimensionless form of the equations (2) and (3) reads:

$$\begin{cases} \dfrac{1}{\varepsilon}\dfrac{\partial D}{\partial t} + \mathrm{F}\dfrac{\partial (DU)}{\partial x} - \mathrm{K}UD = 0 \\ \mathrm{S}\dfrac{\partial U}{\partial t} + \varepsilon \mathrm{S}\mathrm{F}U\dfrac{\partial U}{\partial x} + \dfrac{1}{\varepsilon}\dfrac{\partial H}{\partial x} + \mathrm{R}\dfrac{U|U|}{c^2 D} = 0 \end{cases} \tag{5-6}$$

where the dimensionless parameters appearing in (5) and (6) are defined as follows:

$$\varepsilon = \frac{a_0^*}{D_0^*},\ \mathrm{F} = \frac{1}{\varepsilon}\frac{U_0^*}{\omega^* L_0^*},\ \mathrm{K} = \frac{1}{\varepsilon}\frac{U_0^*}{\omega^* L_b^*},\ \mathrm{S} = \frac{F_0^2}{\varepsilon}\frac{\omega^* L_0^*}{U_0^*},\ \mathrm{R} = \frac{F_0^2}{\varepsilon}\frac{L_0^*}{C_0^2 D_0^*} \tag{7}$$

Here F_0 denotes a tipical value of the Froude number and a^*_0 represents the wave amplitude of the tidal wave at the mouth.

The parameter K in the continuity equation (5) is a relative measure of the degree of convergence of the estuary; the parameters S and R weigh the relative importance of local inertia and friction with respect to gravity while F is related to the spatial variations of flow discharge associated with depth and velocity changes.

Depending on the values attained by the ratio R/S, estuaries can be classified as strongly ($R/S>>1$) or weakly dissipative ($R/S<<1$).

2.2. *The morphodynamic problem.*

The bottom of the estuary is assumed to consist of cohesionless, nearly uniform sediment which may be transported either as bedload or suspended load, depending on the value of the bottom shear stress. Neglecting the effects of the local variations of the cross sectionally averaged sediment concentration, the evolution equation of the bed interface, i.e. the one-dimensional equation of mass conservation of the solid phase (Exner, 1925) reads:

$$(1-p)B^*\frac{\partial \eta^*}{\partial t^*} + \frac{\partial (B^* q_s^*)}{\partial x^*} = 0 \tag{8}$$

where p is the sediment porosity, q^*_s is the sediment flux per unit width and η^* is the local and instantaneous value of the cross sectionally averaged bed elevation.

The relevant variables of the problem are made dimensionless as follows:

$$t^* = \mathrm{T}_0{}^*\tau, \qquad \eta^* = D_0^*\eta, \qquad q_s^* = \sqrt{\Delta g d_s^{*3}}\, q_s, \; \mathrm{T}_0{}^* = \frac{(1-p)D_0^* L_0^*}{\sqrt{\Delta g d_s^{*3}}} \quad (9)$$

where T^*_0 is a typical morphological time scale, Exner's sediment balance equation becomes:

$$\frac{\partial \eta}{\partial t} + \left(\frac{\partial q_s}{\partial x} - \frac{\mathrm{K}}{\mathrm{F}} q_s \right) = 0 \quad (10)$$

Finally a closure relation is needed to evaluate the total load q^*_s. Fairly established semi-empirical relationships are available in the fluvial literature which may be extended to tidal channels simply relating the total load to the instantaneous and local values of the Shields stress θ and of the particle Reynolds number R_p, respectively defined as follows:

$$\theta = \frac{\tau_0^*}{(\rho_s - \rho) g d_s^*}, \; R_p = \frac{\sqrt{(s-1) g d_s^3}}{\nu} \quad (11)$$

2.3. *Scaming rules of physical models in tudal morphodynamics.*

Physical models are based on scaling rules constructed by imposing that all the relevant dimensionless parameters governing the phenomenon keep the same value in the model and in the prototype. Scaling factors can be introduced as follows (the apex referring to the model):

$$\lambda = \frac{D_0^*}{D_0^{*'}}, \qquad \varphi = \frac{U_0^*}{U_0^{*'}}, \qquad \tau = \frac{t^*}{t^{*'}}, \qquad \delta = \frac{d_s^*}{d_s^{*'}}, \qquad \sigma = \frac{s-1}{s'-1}, \quad (12)$$

where λ, φ, τ represent the length, velocity and time scales respectively, δ is the scale of grain size, σ is the scale factor for relative density and χ is the scaling ratio for flow conductance. Let us determine the scaling rules applying in the case of strongly ($R/S >> 1$) and weakly ($R/S << 1$) dissipative estuaries.

2.3.1. *Weakly dissipative estuaries.*

Estuaries characterised by large flow depths and low friction coefficients, are often found in nature. This limiting behaviour is mathematically

described by the condition that $R<<S$, which implies that gravity, driving the tidal wave, must be dominantly balanced by local inertia, the effects of friction (and most often also of convective inertia) being negligible.

Since in eq. 6, the contribution of spatial variations of H is of order ε, we can set S=1 and express the F parameter as a function of S as follows:

$$\mathrm{F} = \frac{F_0^2}{\varepsilon^2} \cdot \frac{1}{\mathrm{S}} = \frac{F_0^2}{\varepsilon^2}. \tag{13}$$

Hydrodynamic and sediment transport similarity then requires:

$$\frac{\mathrm{F}}{\mathrm{F}'} = \frac{F_0^2}{F_0'^2} \cdot \frac{\varepsilon'^2}{\varepsilon^2} = \frac{\varphi}{\lambda e^2} = 1, \qquad \frac{\vartheta}{\vartheta'} = \frac{\varphi^2}{\chi^2 \sigma \delta} = 1, \qquad \frac{R_p}{R_p'} = \sigma^{1/2}\delta^{3/2} = 1. \tag{14}$$

Relations (13) can be alternatively expressed in the form:

$$e\sqrt{\lambda} = \chi\sigma^{1/3}, \qquad \varphi = \chi\sigma^{1/3}, \qquad \delta = \sigma^{-1/3}. \tag{15}$$

Finally, the exact reproduction of dissipative effects would require:

$$\frac{\mathrm{R/S}}{\mathrm{R}'/\mathrm{S}'} = \frac{\varphi\tau}{\lambda\chi^2} = 1, \qquad \text{i.e.} \qquad \tau = \frac{\lambda\chi^2}{\varphi} \tag{16}$$

Unfortunately, the periods employed in the model were constrained by the size of our generating system, hence we were forced to use periods lower than 180 *s* (τ=240).

In the first experiment, characterised by a straight channel with a constant width, a period of 180 *s* has been assumed, while in the second experiment, having introduced a convergence degree in the channel, the period adopted was 120 *s* (τ=360).

The reproduction of the convergence of the estuary, requires the following condition:

$$\frac{K}{K'} = 1, \qquad \text{i.e.} \qquad \lambda / \lambda_b = e\tau\sigma^{-1/3} \tag{17}$$

Using eq.17 the value of the convergent length characteristic of the model L'_b can be determined.

2.3.2. *Strongly dissipative estuaries.*

Space does not allow us to describe the case of strongly dissipative estuaries. It suffices here to state that the scaling rules become:

$$\tau = \frac{e^2 \lambda^2}{\chi \sigma}, \qquad \varphi = \chi \sigma^{1/3}, \qquad \delta = \sigma^{-1/3}. \tag{18}$$

Observations similar to those made at the end of sect. 2.3.1 can be made on the constraint concerning the need to reproduce the relative role of advection on the spatial and temporal distribution of the average concentration of suspended sediments.

Using (18) one readily shows that the ratio $(R/S)/(R'/S')$ is typically greater than one: hence, if the model is strongly dissipative, the prototype is also strongly dissipative.

2.4. *Experimental apparatus.*

Experiments were carried out in the laboratory of the Department of Environmental Engineering of the University of Genoa (Italy), on a large indoor platform.

A *24.14 m* long straight rectangular channel, closed at one end and connected to a basin (*2,3 m* wide and *2,23 m* long) representing the sea at the other end, was built over the platform (fig. 2.). The apparatus for tidal wave generation, installed in a feeding tank directly connected to the basin, consisted of a cylinder, characterised by a diameter of *1.1 m*, controlled by an oleo-dynamic mechanism driven by a control system which could generate the desired law of motion. The flume was filled with crushed hazelnut shells characterised by a density of 1480 Kg/m^3 and median grain size d^*_{50}=0.3 mm. Sediments were chosen light enough to be entrained into suspension throughout most of tidal cycle with the values of friction velocity typically generated in the experiments. For the first experiment the width of the flume was kept constant throughout the channel and chosen small enough (B*=0.3 m) to prevent the formation of tidal free bars. The crucial parameter controlling free bar formation is the aspect ratio β, defined as the ratio between half width of the channel and average flow depth. *Seminara & Tubino* (2001) have recently investigated the formation of tidal free bars in straight channels by means of a linear stability analysis and were able to find a critical stability curve below which bars are not expected to form. For the set of values of the relevant parameters corresponding to our experimental conditions, the latter theory suggests

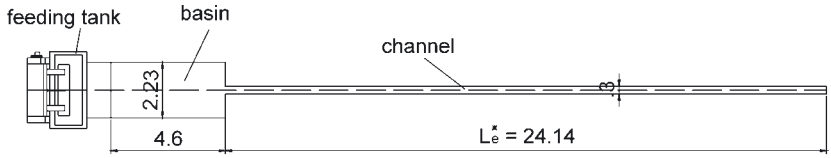

Fig. 2 - Sketch of the experimental apparatus (plan view).

that the critical value of β ranges about 5. Hence we do not expect bar formation for depths greater than few centimetres in this experiment. On the contrary, in the second experiment we have employed a convergent channel characterised by a width decreasing from 1 *m* at the inlet to 0.3 *m* at the landward end of the channel following an exponential law.

During the experiments the water surface elevation was continuously monitored in five cross sections along the channel by means of ultrasound probes. The bottom evolution was monitored along the channel centreline using a profile indicator while the bottom topography of the whole channel was scanned at different times by means of a laser system.

3. *Preliminary observations.*

Let us point out some relevant parameters which characterise the experiment:

Channel shape	**Not convergent**	**convergent**
Initial mean flow depth at the inlet $D^*_0(m)$	0.082	*0*.094
Initial bottom configuration	*Flat*	*flat*
Dimensionless tidal amplitude at the inlet ε	0.32	0.37
Tidal period (*s*)	180	120
Duration of the experiment (*tidal cycles*)	2000	12000

3.1. *Straight not convergent channel.*

Starting from an initial flat bottom configuration, sediments were found to be scoured by the tidal motion in the seaward portion of the channel, driven landward and deposited in the inner part of the channel.

The evolution of the bed profile is plotted in figure 3 at different times. Comparison between the bed profiles at 50 *h* and 100 *h* shows us that the latter pattern is quite close to equilibrium. Note that the weak upward concavity of the final bottom profile is consistent with field observations concerning both tidal estuaries and coastal lagoons and with the theoretical findings of *Lanzoni* & *Seminara* (2002).

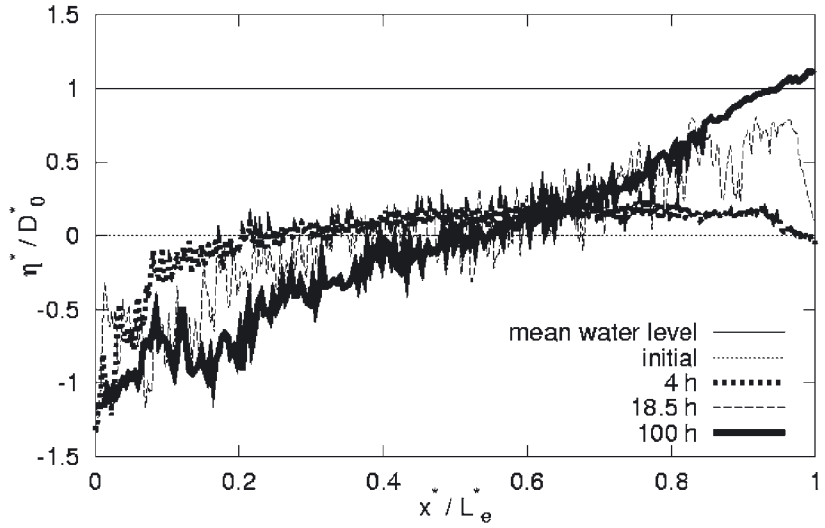

Fig. 3 - Evolution of the bottom profile at different times.

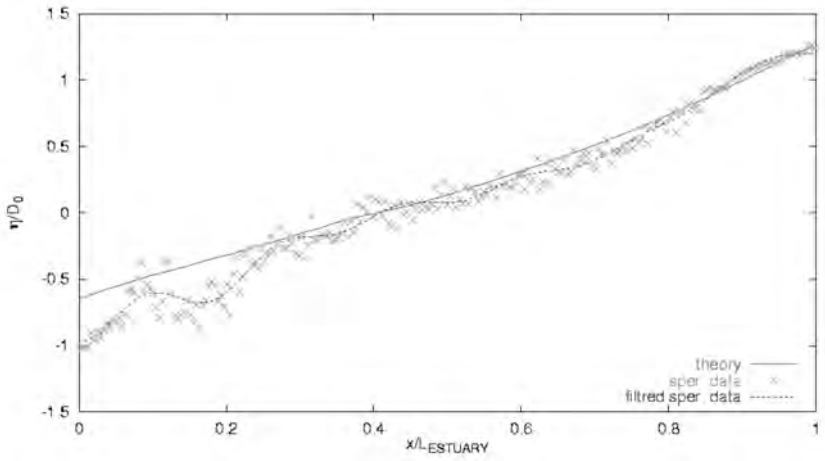

Fig. 4 - Comparison between the observed equilibrium profile in the experiments and the theoretical prediction of Lanzoni and Seminara (2002) after 2000 tidal cycles.

A detailed comparison between observations and theoretical predictions has been recently pursued and is shown in figure 4. It appears that the time scale of the evolutionary process observed in the experiment is

somewhat faster than the one predicted theoretically, a feature possibly related to the inability of the model to reproduce accurately the actual bedforms present in nature. However, the equilibrium profile eventually reached shows a very good agreement with theoretical predictions.

3.1.1. *Equilibrium of Tidal Inlets.*

The problem of maintaining tidal inlets in equilibrium is of major importance for its obvious implications on navigation and, in general, on the morphodynamic evolution of estuaries and lagoon.

The complexity of the problem is confirmed under the idealised conditions examined in the laboratory experiments. In fact, even in the absence of significant wave action in the flow field around the mouth of the channel the flow is highly asymmetric throughout the tidal cycle. At the initial stage of the experiment, with the 'sea' bottom flat, the near inlet flow field is nearly irrotational during the flood phase and behaves like an unsteady turbulent jet during the ebb phase. The hydrodynamics of such flow configuration was thoroughly investigated theoretically by *Blondeaux & al.*(1982) in the fixed bed case.

However, the problem turns out to be more complex as the evolution of the bed topography drives a modification of the hydrodynamics until a final equilibrium is reached.

The pattern of bottom topography in the near inlet region at the initial and final stages of the first experiment is reported in figures 5 and 6, while the cross sections plotted in figure 7 and figure 8 suggest that the eroding action of the jet flow excavates a submerged channel in the sea bottom, with depth decreasing in the seaward direction.

3.1.2. *Bedforms.*

The formation of ripples along the channel was observed since the very beginning of the experiment displaying a quasi 2-D pattern, wavelengths ranging between 2 and 5 times the local flow depth and amplitudes roughly 0.1 times the local flow depth (figure 9). The damping effect of suspended load on ripples development was clearly detected since, during the flood phase, ripples were washed out to form again during the ebb phase which was characterised by lower values of suspended sediment transport. Ripples migrated upstream during the flood phase and downstream during the ebb phase, displaying a net upstream migration in a tidal cycle due to the asymmetry of the velocity field. The flow was indeed flood dominated. The quasi two-dimensional ripple pattern was replaced

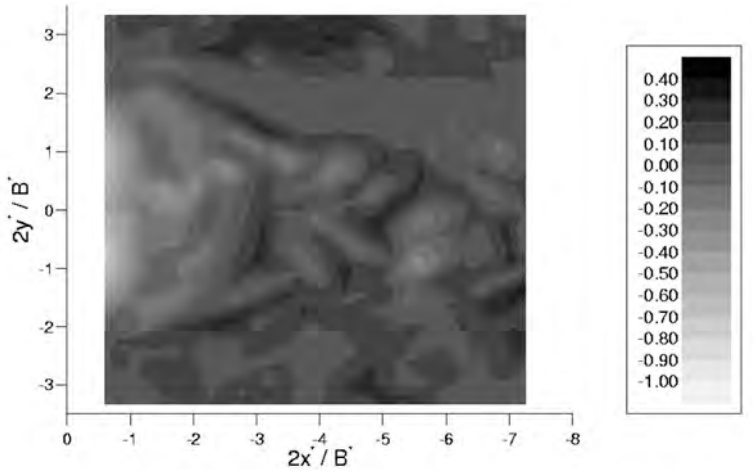

Fig. 5 - Near inlet region bottom topography after 1 *h*. The channel inlet is between $2y^*/B^*$=-1 and $2y^*/B^*$=1 at the transverse cross section $2x^*/B^*$=0.

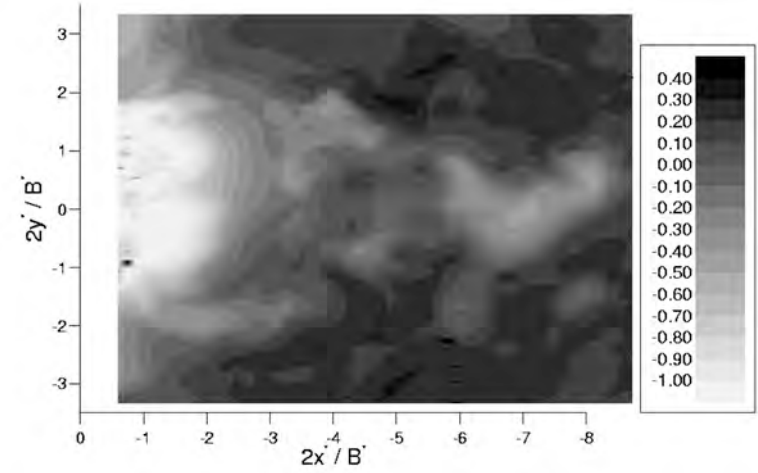

Fig. 6 - Near inlet region bottom topography after 100 *h*. The channel inlet is between $2y^*/B^*$=-1 and $2y^*/B^*$=1 at the transverse cross section $2x^*/B^*$=0.

by complex three-dimensional patterns all along the channel after the first hours of experiment.

In the later stages of the process, when the channel profile had attained quasi equilibrium conditions, ripples underwent very weak modifications throughout each tidal cycle. In other words, the picture emerging suggests that ripples are essentially imprinted in the channel at some initial stage.

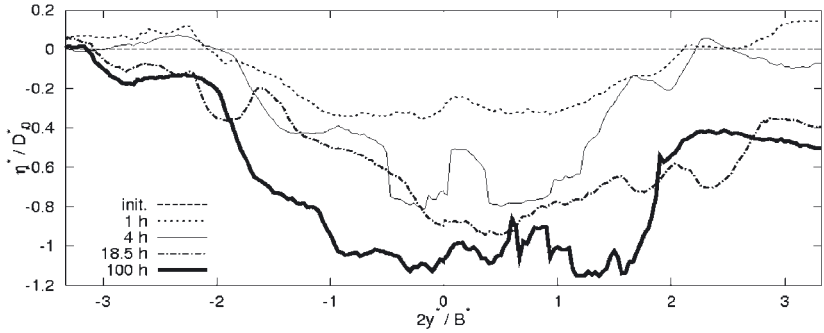

Fig. 7 - Cross section of the near inlet region at $2x^*/B^*$=-1.

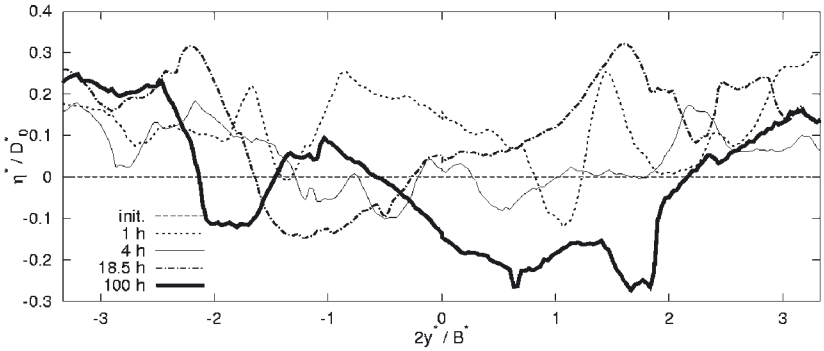

Fig. 8 - Cross section of the near inlet region at $2x^*/B^*$=-3.

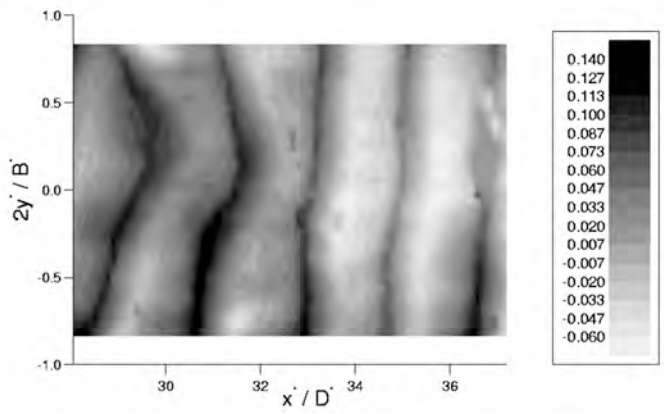

Fig. 9 - Two dimensional ripple pattern after 1 hour of experiment. Bed elevations are made dimensionless with the mean local flow depth D^*.

3.2. *Convergent channel.*

We now outline some significant observations performed during the second experiment characterised by channel convergence. This experiment is still in progress and a detailed comparison between the experimental results and the theory will be performed in the near future. The morphological effect associated with channel convergence leads to decreasing the tidal distortion and asymmetry which develop as the tidal wave propagates landwards.

Furthermore, in the previous experiment the tidal wave was invariantly flood dominated throughout the channel, higher flood velocities having shorter duration than ebb velocities. Conversely, in the present experiment a transition from ebb dominance to flood dominance occurs while the tidal wave propagates upstream.

Figure 10 shows the bottom evolution from an initial flat bed configuration. It clearly appears that the sediment scoured in the seaward reaches of the channel are flushed towards the inner portion of the estuary, leading to the formation of an emerged area in the inner portion of the flume. The longitudinal extension of this area fixes the length of the channel at the equilibrium. The longitudinal bed profile of the channel evolves towards a configuration characterised by an upward concavity and by a well defined depth at the inlet. A comparison with the first experiment shows that the upward concavity of the bottom profile increases as a result of channel convergence.

A limit of the present model is represented by width of the channel inlet being too large (1 m) compared with the basin width, as result, the latter affects the turbulent jet forming during the ebb phase. Further experiments employing lighter sediments have been planned in order to overcome the latter problem and will be performed in the near future.

3.2.1. *Bedforms.*

The second experiment was characterised by the presence of a variety of bedforms at different scales, namely bars with superimposed ripples. The formation of ripples along the channel was observed since the beginning of the experiment displaying a pattern similar to that observed in the previous experiment.

The presence of bars agrees with Seminara & Tubino's (2001) theory. The latter shows that the parameter controlling the formation of free bars is the ratio between the channel width and the average flow depth. Such parameter exceeded the critical value for bar formation predicted in the above theory.

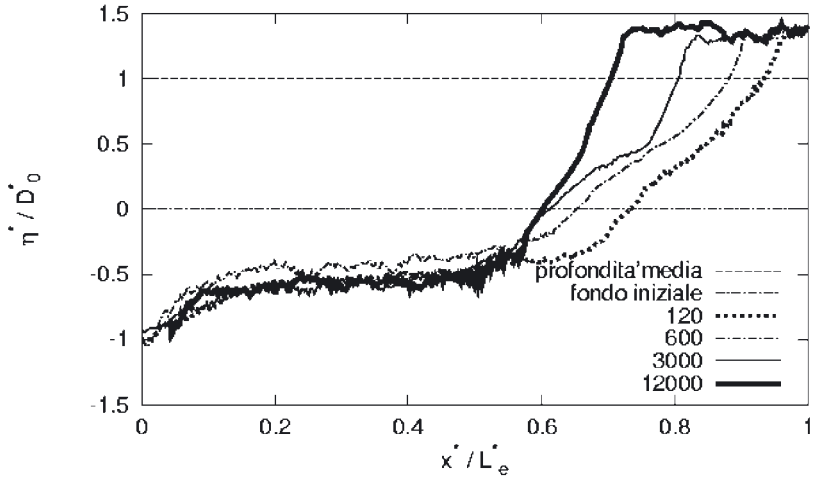

Fig. 10 - Evolution of the bottom profile at different time.

4. *Discussion and conclusion.*

A major observation emerged from the experiment is the fact that the bed elevation established close to the inlet at equilibrium results from the readjustment of the bed profile in the whole channel. In other words, except for the immediate neighbourhood of the inlet where the flow acceleration induced by streamline convergence during the flood phase gives rise to enhancement of local scour, the equilibrium cross section develops near the inlet as a result of non local effects. It will be of interest in the near future to investigate systematically whether a relationship can be established between the length of a tidal channel at equilibrium and the flow depth established at the entrance, for given values of the hydrodynamic parameters. Several questions will require attention in the near future:

- Can an equilibrium of the channel still persist in the presence of intertidal storage areas?
- What is the effect of the lateral exchange of sediments between channel and tidal flats on the morphodynamic evolution of tidal flats and salt marshes? What is the effect of wind waves in sediment re-suspension?
- What is the role played by the hydrodynamics and morphodynamics of tidal inlets on the exchange of sediments between channels and adjacent seas?

Some of the basic mechanisms underlying the latter questions will be investigated in the present experimental apparatus. Developments are in progress.

References.

Blondeaux P., Bernardinis B., Seminara G., 1982. Sulle correnti di marea in prossimità di imboccature e loro influenze sul ricambio lagunare. In Atti del XVIII Convegno di Idraulica e Costruzioni Idrauliche, Bologna.

Bolla Pittaluga M., Tambroni N., Zucca C., Solari L., Seminara G., 2001. Long term morphodynamic equilibrium of tidal channels: preliminary laboratory observations. In 2nd IAHR Symposium on River, Coastal and Estuarine Morphodynamics, Obihiro Japan, 10-14 Sept., 423-432.

Bolla Pittaluga M., Seminara G., 2002. Trasporto solido in moti lentamente variabili ed equilibrio morfodinamico di canali mareali. In Atti del 28° Convegno d'Idraulica e Costruzioni Idrauliche, Potenza.

Bolla Pittaluga M. e Seminara G., 2002. Long term equilibrium of tidal channels: effects of settling lag, sediment supply and overtides, (in preparazione).

Lanzoni S., Seminara G., 2002. Long-term evolution and morphodynamic equilibrium of tidal channels. J. Geophys. Res., Vol.107,C1, pp.1-13

Schuttelars H.M., De Swart H., 2000. Multiple morphodynamic equilibria in tidal embayment. J. Geoph. Res. 105 C10, 24105-24118

Seminara G., Tubino M., 2001. Sand bars in tidal channels. Part. 1. Free bars. J. Fluid Mech., 440, 49-74.

Tambroni N., Bolla Pittaluga M., Seminara G., 2002. Equilibrio morfodinamico di canali mareali: osservazioni sperimentali. Atti del 28° Convegno d'Idraulica e Costruzioni Idrauliche, Potenza.

AREA 4.
DATA MANAGEMENT AND DISTRIBUTION

RESEARCH LINE 4.1.
Distributed Information System

"METEOLAGUNA" GIS OF METEOMAREOGRAPHIC STATIONS IN VENICE LAGOON

P. Campostrini, S. De Zorzi, E. Rinaldi, C. Zago
CORILA, Venezia

1. *Introduction.*

Availability of meteomareographic data for the Venice lagoon and Northern Adriatic sea, is of doubtless, importante for scientific research, environmental management and policy decision making. The present paper represents a preliminary attempt to organize the meteomareographic information collected in the Lagoon in a flexible and interactive Geographical Information System.

The GIS application currently being developed, called "Meteolaguna", involves meteomareographic stations belonging to 8 different institutions, for a total of about 90 stations spread throughout the lagoon. A possible next step will be to include other stations located in the drainage basin and/or belonging to other institutions.

The "Meteolaguna" GIS includes as *metadata* general and detailed geospatially referenced information of the various stations and the meteomareographic parameters measured in each station.

This configuration, constitutes a flexible and effective structure for connecting the different databases of each station, historical series or real time measurements.

The GIS "Meteolaguna" will shortly be available via the www.corila.it site, and subsequently remote access to databases of the institutions governing of the meteomareographic stations will be provided.

2. *GIS elements: database and cartographic layers.*

The "Meteolaguna" GIS is composed by cartographic layers with different information levels and a further level representing the "station" object. The station object is characterized by information on measured

environmental parameters, which are in two distinct databases: the general attributes database and the measuring instrumentation database (Fig. 1). General attributes identify the station characteristics and the measured parameters, while the measurement mode concerns the frequency, mean, data availability, data transmission and data registration.

Information levels initially adopted for the cartographic layers are the minimum necessary to identify the elements in their station's context: land areas, lagoon channel network, road network, mainland hydrological network. These basic information levels were provided by Magistrato alle Acque, Consorzio Venezia Nuova, Servizio Informativo.

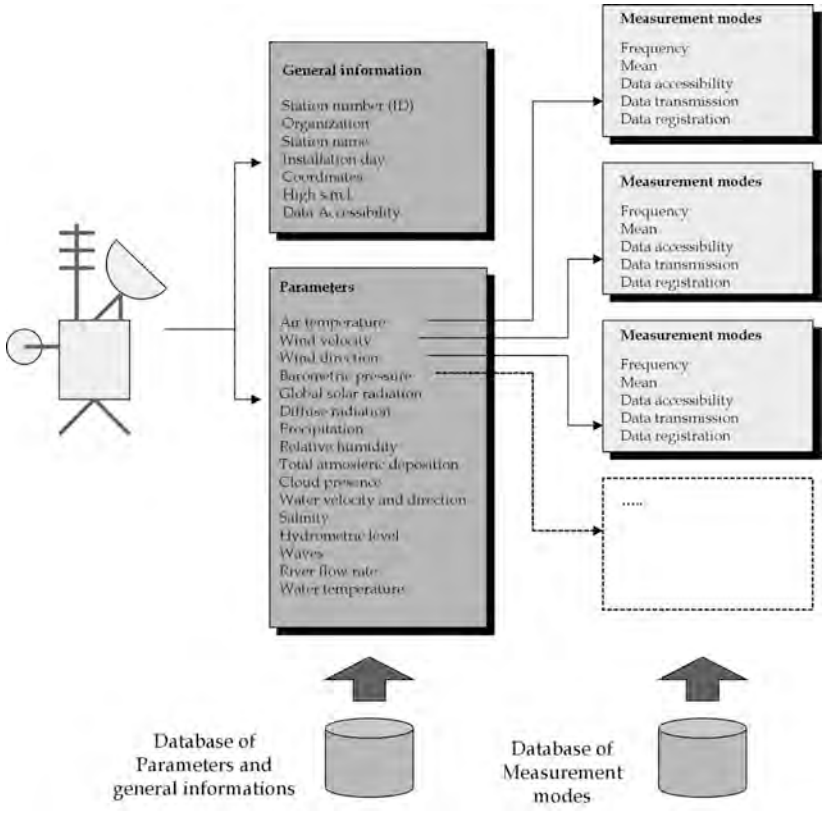

Fig. 1 - The GIS databases.

The ownens of the 87 meteomareographic stations: Comune di Venezia, ARPAV, ENEL, IBM-CNR, Ufficio Idrografico e Mareografico di Venezia, Magistrato alle Acque-CVN, Ente Zona Industriale, Istituto Cavanis.

The attributes of each station in the general attributes database include identification number, general information, and location (Fig. 2).

For each parameter measured, data acquisition mode is shown in Fig. 3.

Station number (ID)
Organization
Station name
Installation date
Longitude
Latitude
Coord. Gauss-Boaga Est
Coord. Gauss-Boaga Nord
Altitude s.m.l.
Data Accessibility

Fig. 2 - Station general information.

General information
Frequency
Mean
Data accessibility
Data transmission
Data registration

Fig. 3 - Measurement modes.

Various parameters and the number of stations measuring them are shown in the figure (Fig. 4).

HYDROMETEOROLOGICAL PARAMETERS MEASURED IN THE STATIONS	Number of stations
Air temperature	**20**
Wind velocity	**26**
Wind direction	**26**
Barometric pressure	**20**
Global solar radiation	**9**
Diffuse radiation	**2**
Precipitation	**20**
Relative humidity	**7**
Total atmosferic deposition	**2**
Cloud presence	**1**
Water velocity and direction	**20**
Salinity	**4**
Hydrometric level	**68**
Waves	**6**
River flow rate	**17**
Water temperature	**20**

Fig. 4 - Measurement parameters.

3. *Use of the GIS.*

In figure 5 all the stations are reported, as they appear in the GIS window. All usual GIS instruments are available.

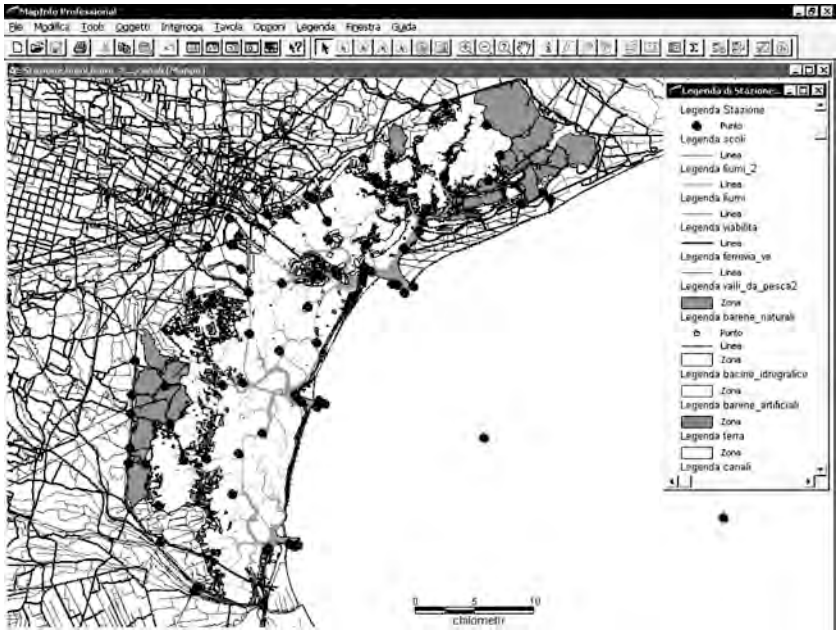

Fig. 5 - GIS window with the meteomaregraphic lagoon stations.

Moreover, via a specific query (SQL language with a dedicated editor) the database supplies information on the meteomareographic parameters and the specific station characteristics (Fig. 6).

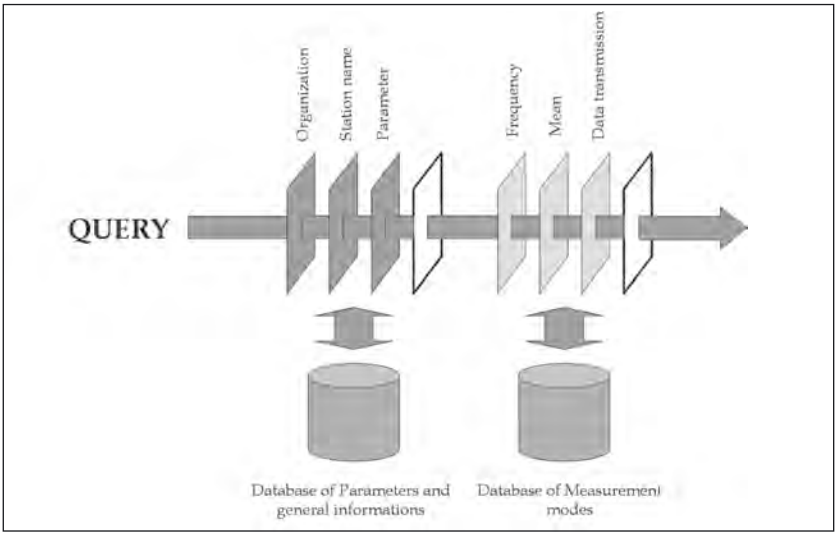

Fig. 6 - GIS query.

It is possible, for example, to find all stations measuring the same parameter and the data acquisition mode (Fig. 7).

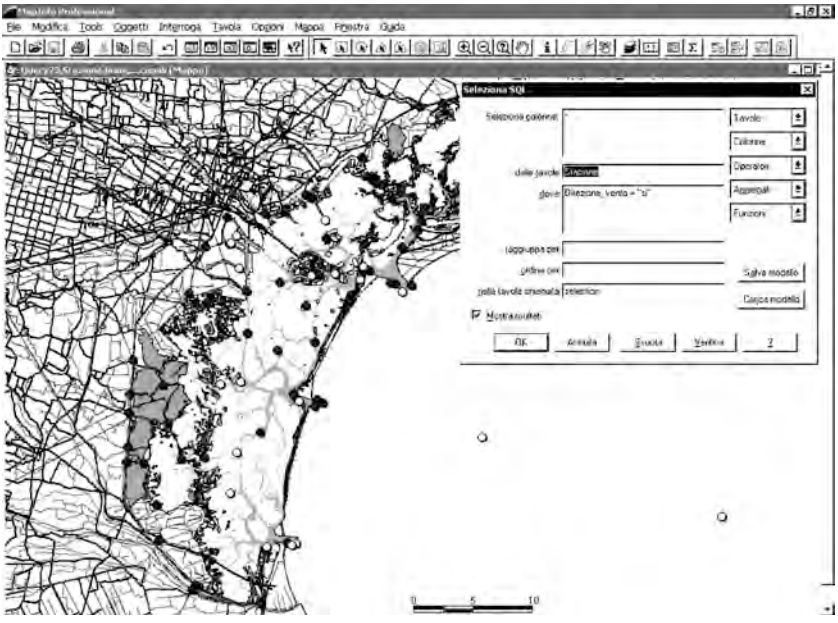

Fig. 7 - GIS selection of stations measuring wind direction (in light grey).

Furthermore, by connecting the general attributes database and the instrumentation database it is possible to have specific information on meteomareographic variables (Fig. 8).

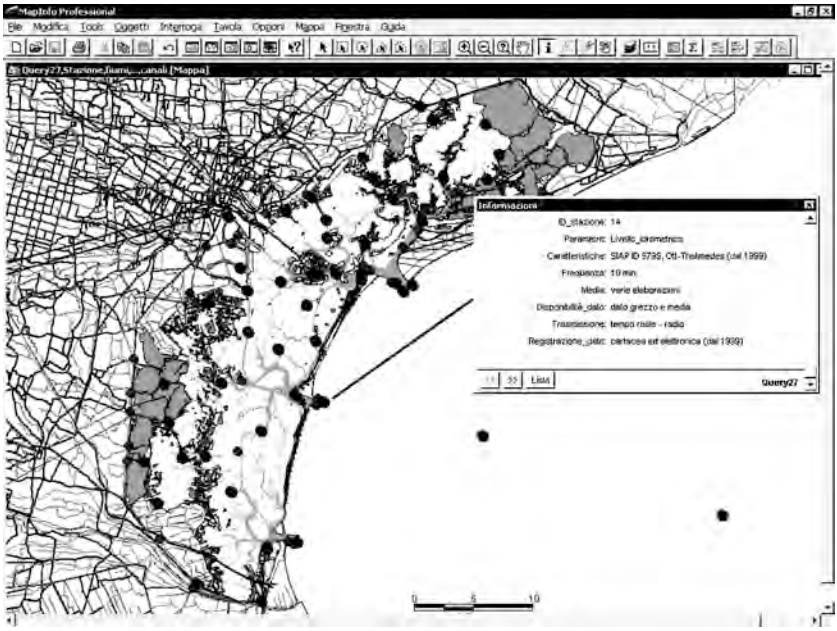

Fig. 8 - Join between the database of the station general information and the measuring instrumentation database.

RIVELA (DATABASE FOR THE RESEARCH ON VENICE AND THE LAGOON) AN INSTRUMENT FOR ENVIRONMENTAL RESEARCH

P. Campostrinil, C. Dabalà[1], S. De Zorzil, R. Orsini[2]
[1]*CORILA, Venezia*
[2]*Dipartimento di Informatica, Università Ca' Foscari, Venezia*

1. *Introduction.*

The integrated management of information across the disciplines in the first Research Programme constitutes an important goal of CORILA.

RIVELA is a relational and flexible database for storage and management of information, designed to facilitate the provision of the research results to scientific community, the decision makers and the general public. RIVELA allows the permanent and secure archival of results from research activities and the wide dissemination of the data, subject to an appropriate user authorisation. All interactions between users and RIVELA occur via Web.

The main problem in planning, structuring and organising an environmental database is the management of the mass of data which derive from different disciplines[1]. In fact, the complexity and the richness of the programme requires a carefully designed data management, both for long term archiving of data and for the immediate and interdisciplinary data usage by researchers. The environment, indeed, is a complex system, which is studied by many different sciences (such as geology, hydrology, biology, etc.). So, it is necessary to create one powerful tool which would permit, e.g., the interaction between chemical parameters, information about the biota and physical data [2,3].

The development of this inter-disciplinary database required, in the planning phase, the lengthy task of organisation of the existing knowledge, to obtain an accurate description of environmental matrices, sampling localities, parameters to be measured, types of sample, data acquisition

methodologies, and a lot of other ancillary information to be stored in the database in addition to the main data.

Thus, the classification of records in RIVELA is the result of a complex interaction with the Research Groups to collect and define, in a common structure, the different ways to store the relevant information.

2. *The database structure.*

The RIVELA database consists of two main components: a static part, relative to the results of auxiliary support data, and a dynamic part, relative to surveys performed in field or laboratory activities.

The static part contains the following information:

- Research Groups administrative data and performed activities list (Research Projects, Work Packages, Activity);
- geographical location of the data (Zones, Environmental Units, Localities);
- data type (Matrices, Types of Sample, Parameters);
- data acquisition methodologies (Method, Apparatus).

The dynamic part contains four interconnected fundamental entities: *Measurements, Samples, Stations* and *Sampling Activities*. A *measurement* is the value of a parameter deriving from a certain sample, which has a precise spatial location (*Station*) and temporal location. The samples are, in turn, classified according to type (*Sample type*), depending on the environmental matrix.

3. *RIVELA applications.*

A simple web application allows to visualize the static part and to suggest modifications/additions. Other three applications are available via Web: insertion of data from field activities, search and extraction of data with guided interrogations, data visualization within a GIS system.

The left part of the RIVELA's web pages is occupied by a set of links for a rapid visualisation of the list of the parameters, the list of all the entities, the return at the RIVELA's main page, and a link to send an e-mail query to CORILA.

3.1. *Visualization and updating of the static part.*

All information in the static part can be easily searched and visualized (Fig. 1).

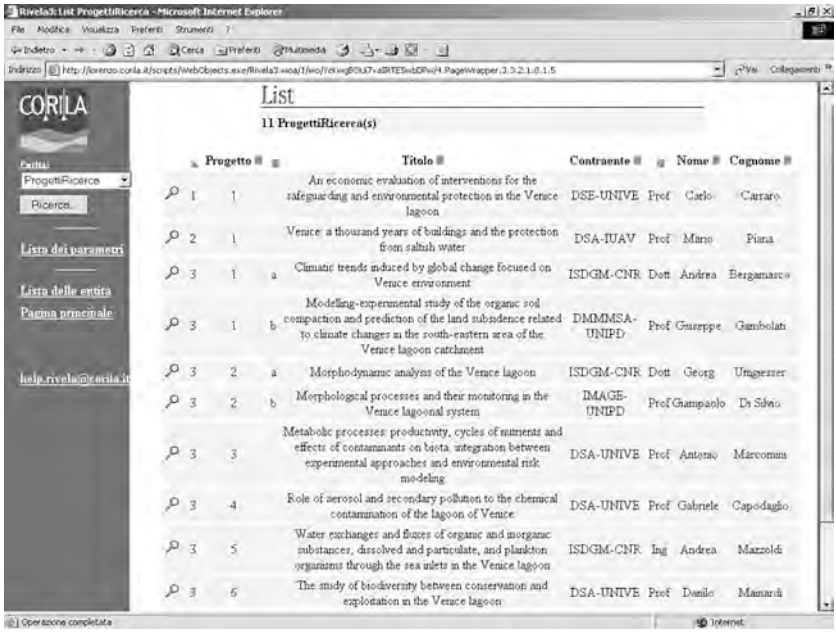

Fig. 1 - Sample page from the section “Research Projects”.

In Fig. 1, the result of a query about Research Projects is shown: each Research Project is identified by a code, a title, a Leader Institution and a Project Leader. On the left of each name, a link (magnifying glass) allows quick visualization of the other ancillary pieces of information.

Furthemore, users can suggest modifications and additions, via expressly prepared pages, to the following lists of static information: Parameters, Environmental Units, Localities, Substratum, Unit of Measurement. All proposals for modification will be considered by the data base administrator before being implemented.

In the case of a suggestion for a new locality, for example, the user must specify the name of the place, the appropriate environmental unit to which the locality refers (choosing between the ones already listed in the database); a free module enables the insertion of any notes. The bottom key, at the end, is for sending the proposal.

3.2 *Insertion of data.*

In order to simplify and automatize the insertion of data by each research unit, a web application has been provided. This approach, even

if largely suggested, presently it is not so frequently implemented in scientific data base [1, 3]

The scientific coordinator of a research unit (e.g. at the end of survey campaign) simply accesses an appropriate Web page containing both a series of fields to be filled manually, and buttons to send one or more files in CSV format, containing the data previously prepared on the user's computer.

Information relative to the methodologies used must also be inserted, and auxiliary data like bibliographies, images, etc., can be provided, too.

Three kinds of format for data file are foreseen, according to the following types of measurements:

1) A set of measures relative to a unique sample of a unique station in a unique sampling activity;
2) A set of measures relative to a set of samples and measurements related to a unique station via a unique sampling activity;
3) Data relative to a unique sampling activity, with many stations and many measurements.

As an example, the Web page of the second insertion format (Fig. 3) contains modules to insert information about the sampling activity (specific Activity in the Research Projects, start and end date of the sampling activity, Lead Institution and Activity Leader, other facultative modules) and about the specific station (spatial localization: Locality, geographic coordinates), and a link for sending the data file with the information about both the collected samples and the measured values.

In the data files, data are organized in tabular form, where, as a general rule, lines represent different values of a set of parameters measured in a specific sample and/ or at a particular time; the columns, represent all the values taken for each parameter during measurements of the samples or over time. So, the number of the columns is variable, as each of column contains all the measured values of each single parameter.

The file can be prepared with any program managing tables, like MS Excel or MS Access, or any text editor, and saved in the standard CSV format.

Each file sent to the database is processed by an automatic loading programme, which carries out a set controls of validity (presence of the coordinates in the correct reference frame, correct name of the parameters, etc.) and it indicates by e-mai) any errors, both to the user and to the administrator. This control is of importance to guarantee data quality [1, 4].

An important features of the input mechanism is that the CSV file containing the input data is also permanently stored in the database.

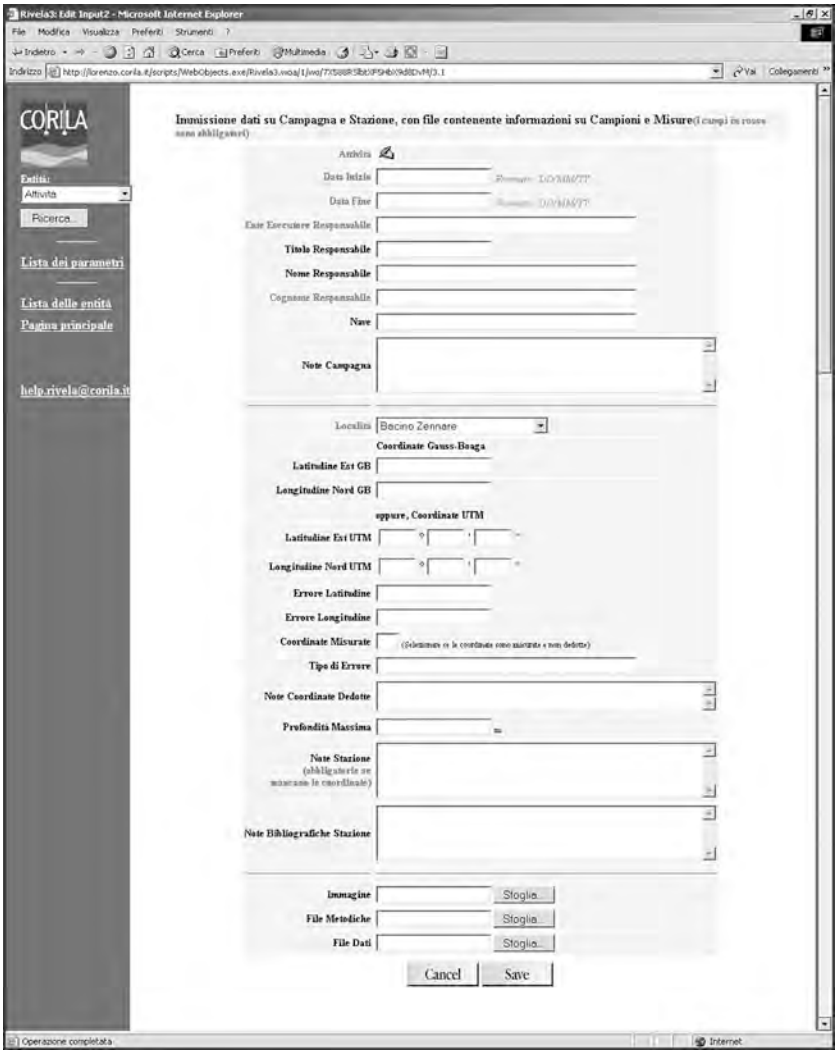

Fig. 3 - Example of a data input page.

Moreover, all data in the database can be traced back to the original input file. In this way, it is always possible to recover the initial dataset, when errors are discovered in an input data file.

4. *Guided queries.*

RIVELA is a relational database, and therefore all the usual modes of access to data are available to users: SQL, "individua) productivity" tools such as MS Excel and MS Access, used to extract sets of data in tabular format.

Moreover, two additional access and extraction modes have been provided: a guided interactive search and a CIS query instrument.

In formulating an interactive interrogation, the user could choose between different query mode:

- user can write a free test to select a parameter;
- all parameter type are listed and divided in different matrices;
- all parameter type are classified by the corresponding type of sample.

Then, the user is guided towards:

• Selection of time and location;
• Selection of attributes required to be shown on the report table.

The spatial location can be indicated either by selecting a locality, or by specifying directly the geographical coordinates of the area of interest.

The attribute selection page allows, by checking of boxes, an easy-to-read representation of the report table in the screen window.

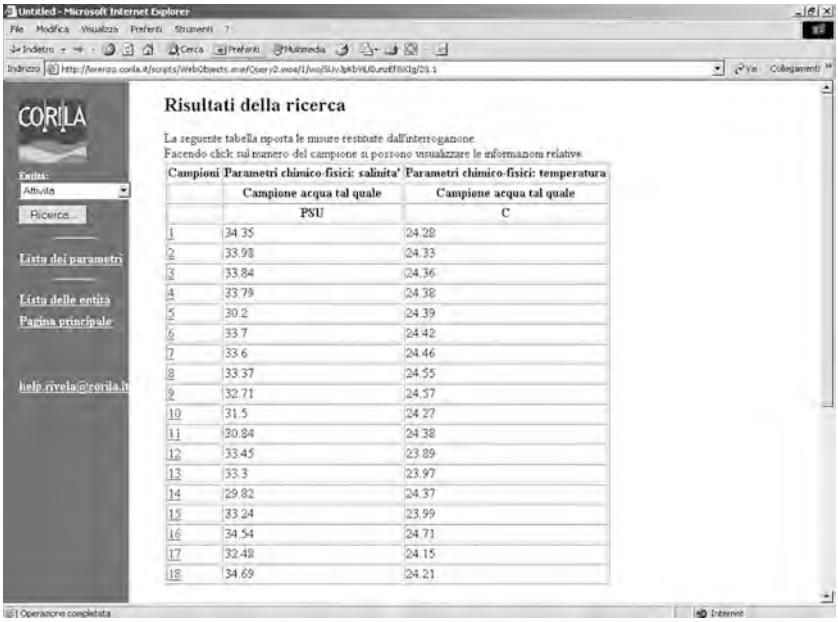

Fig. 4 - Guided queries: example of the results of an interrogation.

The interrogation result is a chart, which can also be downIoaded, in CVS format, for further elaborations. On the Web page, each record is always linked to its ancillary information.

5. *Integration with a Geographical Information System.*

The correlation between the environmental information, the landscape and the geographical representation is extremely important in RIVELA [5]: for each stored piece of information, a specific temporal and geographic location is retained. This allows the "database engine" to be used for a number of GIS applications.

A set of base maps is provided as the default layout: these are active maps and allow to select any geographical object. The Venice lagoon is displayed at different scales to allow user to find the information needed.

All information stored in the database is in principle displayable overlaid on the Venice lagoon maps.

Presently, RIVELA and GIS instruments are integrated in the local CORILA network, where the GIS applications run on specific workstation and make use of the data stored in the Data Base Server. Different sorts of data classifications and correlations are available on this client - server architecture.

Fig. 5 - GIS queries: acquisition sites of the CORILA research program.

The website interface, that will allow to display the RIVELA data base georeferenced maps, is under construction.

Different types of result visualisations, modelling and statistical analyses, will be available directly via Web.

6. *Conclusions and future work.*

RIVELA is a flexible and open data base, growing with the CORILA Research Program.

It is developed in strong connections with the final user, i.e. the CORILA researchers and the scientific community.

While the use of a relational structure allows the use of standard tools for managing the database, the Web interface allows scientists to remotely load and query the data in a very simple manner.

RIVELA aim is to become an open archive able to store, in a standard format, the information related to the scientific researches, developed on the Venice Lagoon.

RIVELA has two main goals: to avoid any data loss and to permit inter-disciplinary data comparison and analyses.

The researchers will find in RIVELA a data warehouse, able to give added value to one s own data, accessing larger data pools and using advanced instruments, both for analyses and visualization.

Next works will concentrate on the web GIS interface, on a data engine to search information into textual documents, and on an interface for statistical and spatial analyses.

Bibliography

[1] Willam K. Michener, James W. Brunt., 2002. Ecologica Data (Design, Management and Processing) -Blackwell Science Ltd.
[2] Ray Hilborn and Marc Mangel - The Ecological Detective (Confronting models with data) - Princeton University Press.
[3] Angelo R. Bobak - Database distribuiti e multi - database - Jackson Libri 2000.
[4] Michael H. Brackett - Data Resource Quality: turning Bad Habits into Good Practices - Addison - Wesley 2000.
[5] John Hof & Michael Bevers - Spatial Optimization in Ecological Applications - Columbia University Press 2002.

DEVELOPMENT AND MANAGEMENT OF A DISTRIBUTED INFORMATION SYSTEM FOR VENICE LAGOON

A. Marani, S. Fant, L. Macaluso, G. Scalvini, O. Zane
Istituto Veneto di Scienze, Lettere ed Arti, Venezia

Since the late Seventies, the "Istituto Veneto di Scienze, Lettere ed Arti" (IVSLA) began promoting, collecting, cataloguing and organizing publications related to the Venetian environment ("Rapporti e Studi", "Atti", and other publications). In the Nineties IVSLA began an internet *environmental database* and in the year 2000 started cooperating with CORILA to support its information system activities.

The "Istituto Veneto", in its effort to promote the transparency of studies on the Venice lagoon, and in consideration of the universal interest generated by the cultural and environmental uniqueness of Venice, adopted the opportunities offered by new technologies in informatics and telematics in the cataloguing and disseminating of data and documents within the wider scope of promoting scientific culture on the Venice environment. Therefore it acquired technology as needed to automating procedures, shortening document acquisition times, improving efficiency in data storage, and rescheduling some activities related to the studies carried out by "Consorzio Venezia Nuova", the concessionary of the Ministry for Infrastructure and Transport - Venice Water Authority, responsible for implementing the measures to safeguard Venice and its lagoon delegated by the law to the State.

Material and data collection has made available an unprecedented amount of knowledge, but presented problems related to organization, cataloguing and management, because highly fragmented data and dispersed researches have made their co-ordination difficult. During the process of data collection, it became clear that it would be necessary to extend the *database* objectives up to building a reference point for environmental researches and lagoon initiatives, that would be accessible to anyone - students, professionals, researchers. The recent overcoming of some limits in the previous *database* has allowed the development of an

hyper text environment able to produce formats that are suitable for the non-specialized user.

The current version of "Banca Dati Ambientale sulla Laguna di Venezia" is aimed at acting as an *environment portal* for the venetian territory whereby to collect, organize and publish data, information and documents regarding lagoon environment. Another one of its features is listing and connecting Agencies and Institutions that operate on and study the Venetian territory. The portal is in other words a scientific dissemination tool, as well as one instrument for environment education accessible to the various levels of schooling.

In particular, the *database* purposes are:

- to throw light on close-to unknown research fields and therefore encourage researchers to help filling in the more evident gaps;
- to promote standardization and dissemination of sampling and measurement methods;
- to encourage data dissemination, making them reusable and more directly comparable;
- to promote a wider circulation of researches results.

In addition to realizing a centre for documentation and scientific dissemination, IVSLA seeks to develop a structure that supports environmental education and training, because it is difficult to start up shared environmental actions without deep-rooted convincements.

The initiative is especially addressed to scientific dissemination professionals (science teachers and scientific journalists), but also to specialists in scientific subjects, technicians working on the territory and public managers in charge of land safeguarding.

The dissemination process also involves citizens, who have to be able to find specific and selected information that meets requirements ranging from answering questions to solving doubts and providing justifications to operational choices.

The "Istituto Veneto" is currently also committed to find internet sites containing subjects similar to the ones included in the different sections of the *database* under construction. Its main goal, however, is establishing a dialogue channel with institutions and agencies that collect data and have bibliographic materials.

The "Istituto Veneto" is also confronting itself with the school world to understand the needs of teachers and students, in order to tailor archive organization to their needs and also to offer the opportunity to provide *on line* material educational products developed by schools.

Particular attention is paid to keeping open channel with the authors, and convey to them certainty on the full respect of their copyright. The "Istituto Veneto" has no interest in taking advantage of someone else's credit.

For this reason, the "Istituto Veneto" *database* is and will be freely open to everyone and will keep the characteristics of a network promoting suppliers of data and other web sites.

Four researchers are currently employed full time to *database* organization, each devoted to one of the fields of action – informatics, environmental and didactic competences – necessary to develop and maintain the web site.

Regarding data, the partnership with "Consorzio Venezia Nuova", "Istituto Cavanis", "ENEL – Centrale Termoelettrica di Fusina", "Ente Zona Industriale di Porto Marghera", Civic Historical Science Museum of Venice, "Società Veneziana di Scienze Naturali", Central Institute for Scientific and Technological Research Applied to the Sea (ICRAM) – Chioggia, Italy have been especially useful, as well as with some researchers, experts and university professors.

All collected material is archived in a format that ensures completeness and, at the same time, allows *on line* publication. What cannot be published directly *on line* because of its size, is catalogued and book marked, so to make its existence and the ways to obtain it well-known.

The "Istituto Veneto" *database* is divided into sections that avail themselves of reference-marks to other web sites and manage both outgoing and incoming information.

These complementary links have been selected partly with the aim to increase general knowledge on specific arguments, and partly with the aim to show a general view on similar items already available *on line*.

There is also a *Forum*, with discussions on each subject. It was created to keep in touch with the public, to stimulate debate among users, and to meet the requirement for more in-depth investigation.

Regarding the work that has been carried out, the first phase consisted in the definition of organization methodology. The latter has to meet elasticity and versatility requirements, in order to allow the progressive adjustment of the structure to characteristics of the new materials becoming available. Another goal is of course making the updating of data processing and system management easier.

The web site (fig. 1) can be visited at www.istitutoveneto.it and has a simple structure that lets the visitor easily orientate himself and find immediately his field of interest: a few descriptive lines introduce each section, showing its contents.

Fig. 1 - Home page of the "Istituto Veneto di Scienze, Lettere ed Arti" environmental *database*.

The display has been optimised for 800x600 pixel screens so to make the access to the web site easy for the general public, that not always has high definition screens.

The web site has been structured in the following sections (fig. 2).

The *Data* section has been organized into five categories: one for each environmental areas (*Atmosphere*, *Biosphere*, *Hydrosphere*, *Lithosphere*), in which data belonging to each category are recorded, and another one that collects *Metadata*.

Actually, most of the available data regard the sub-section called *Atmosphere*, in which it is possible to find parameter values recorded at

Fig. 2 - Web site Map.

ENEL (from 1996 to present day), at "Ente Zona Industriale di Porto Marghera" (from 1993 to 2001) and at "Istituto Cavanis" (102 years, from 1900 to present day).

These data are accessible through a map of the territory or through *sources* and *parameters* items. To these data are added links to web sites that report measurements made by: CNR – Institute of Marine Biology, ARPAV (Province Agency for Environmental Protection) and the Venice Municipality.

The *Hydrosphere* subsection includes information on oceanographic stations in the Lagoon, while the *Biosphere* subsection includes links to taxonomic sites.

The *Models* section currently contains some simple examples regarding the coupled system Venice Lagoon – Adriatic Sea, but it is to be hoped that the producers' reticence will be overcome and that it will be possible to enrich it with other simulations.

The *Regulation* section refers to external links with institutional web sites that publish municipal, provincial and national laws and regulations (Municipality of Venice, Province of Veneto, ENEA).

The Documents section is a kind of library, in which are collected *Articles*, *Reports and Studies*, *Research works*, *Degree and PhD dissertations* and *Other works* - books, images, video.

The *Images* section is perhaps the richest, thanks to the material made available by the Information Service of "Consorzio Venezia Nuova". In this section are collected several images obtained from Landsat and Spot data (9 different typologies indicated as: *Vegetation Classes, Natural Colours, Rot, Lagoon Morphology, Risk of Erosion, Suspended Sediments, Temperature, Land Use, Other Images*); photos taken during two MIVIS flight campaigns (1996 and 1998) – that, like satellite images, are available in two different dimensional formats – and numerous maps, among which a mosaic of 202 maps, drawn from the Province Technical Map (CTR), that covers the entire lagoon area.

The achievement of this section required a lot of care, not only because of the amount of material to handle, but also because it has been necessary to select, between different ways of elaborating and organizing contents, the ones that could best satisfie two conditions that can't be given up: easy access, assured by the utilization of well spread software, and fast loading, without compromising clearness and functionality of images.

This has been obtained by using .jpg format for *on line* images; .tiff format for images that have to be downloaded by FTP and .pdf format for images that have to be furnished with zoom function.

The aim of this section is to set a standard to which every author will comply for future contribution that use illustrations. For this purpose images have been archived so to return prints mainly in A4 format copy.

The section dedicated to *Dissemination* is a recent realization that stems from the conviction that data and scientific knowledge collection become meaningful when made usable not only in terms of their availability, but also in terms of how they are accessible to the general public.

This section is divided into four chapters: *Descriptions*, with general information about the types of environments that can be found in the lagoon and their dynamics; *Cards*, with specific information about

objects, phenomena and categories; *Didactics*, offering *Training Experiences, Educational Course* and *Games and Simulations*; *Glossary*, with technical terms and idiomatic forms.

For the planning and compilation of the didactical section, secondary school teachers have been involved, in order to get a first hand understanding of their requirements and also tap from their on-the-field experience when it came to deciding contents organization. Agreement with teachers has been found on a report format allowing standard cataloguing of the environmental didactics and education activities carried out within the school.

The following items are now accessible: *Descriptions* – including an illustrative example of a peculiar lagoon environment (fishing valley), accompanied by cards about flora and fauna, *Didactics* – including examples of *Training Experiences, Educational Course*, *Games and Simulations* and a lot of *Links* (subdivided in *Documents*, *Hypertexts* and *Didactical Plans)* and a *Glossary.*

Regarding the amount of work carried out, the present *database* uses up nearly 630 MB of memory (equivalent to nearly 60.000 text pages) and includes more than 600 images[1], about 280.000 meteorological records[2] and several documents[3]. Besides this there are 149 glossary words and an illustrative example of a peculiar environment[4].

Web sites contents are largely made available by several Agencies that conduct work on the Venice environment. The *database* offers a list of these agencies although this is probably incomplete and its consultation is hostile due to often scarce cooperation.

---

[1] 404 (202 in 2 colours and 202 in 4 colours) maps of lagoon territory, drawn by The Province Technical Map Office (CTR) between 1994 and 1998, in .pdf format. Also available are 25 maps in .pdf format and 8 in .gif format; 98 aerial photos of the lagoon (in 1996 and 1998) and 108 satellite shots (mostly Landsat 5 and 7) recorded between 1984 and 2001, in .jpg format.

[2] 36.510 meteorological records surveyed in Venice e 242.130 surveyed in Marghera, in .txt format.

[3] 2 University Degree dissertations on the quality of air in Mestre, 2 about didactics and environmental education and 1 about halhophytae vegetation and salt marshes morphology - Catalogue of Magazines of the Civic Museum of Historical Science Library-; 5 papers published in the Museum's Bulletin, issue nr. 50, Flora and Vegetation of salt marshes magazine, 1 paper titled "Arsenic in the Venice Lagoon", 3 ICRAM research works regarding fish breeding and fishery in the lagoon; all published in .pdf format.

[4] Fishing Valley, accompanied by descriptive cards regarding its flora and fauna.

Descriptions and cards that will be included in the *Dissemination* section are the product of careful bibliographical research, later reviewed by experts in the different fields.

The English version of the web site has already been started, but currently limited to an introduction to the main sections.

Finally, the "Istituto Veneto", has satisfied the requests of CORILA, that is developing the database named RIVELA (RIcerche su VEnezia e la LAguna) whose aim is to make pooled research results readily available to the scientific community, politicians and citizens. Particularly, some sectors of the CORILA research can call for meteorological and other data that can be found at the "Istituto Veneto" *Banca Dati*. The latter has therefore developed an application converting data records stored in various formats (mostly Excel data), into records that are directly legible by CORILA. This application transfers all the meteorological records contained in the *environmental database* through a MySQL *database* able to convert the records to the CSV (Comma Separated Value) variable fields, then renamed by CORILA in accordance with its standards.

Work planning for the near future will be dedicated to enriching the contents of each section. This effort will require a particular diligence to establish co-operation links with those who study environment and operate on it. Only by doing so it will be possible to achieve the successful integration of materials coming from different agencies, ensure their rapid updating, and kindle comparison and discussion with the public through the *Forum*. On the other hand, the variety of the material to examine encourages one not only to improve acquired techniques but also to experiment newer ones. For the above, work to be done in the future will include functional character verifications on:

- available results;
- efficiency assessments of selected schemes;
- ability to consider different objects.

Data collection and related cataloguing, file arrangement, skills updating, and the testing of new solutions leading to a greater efficiency will continue. Particularly, there is a need to visit data suppliers very often, to encourage users, and to monitor the web site functioning. A successful strategy for *Forum* setting is also being devised, that will allow discussion monitoring in a way that selects the most interesting themes and enhance the general public's level of the comprehension of the issues discussed. The forum should also serve as an indicator of the site's shortcomings and at the same time the tool whereby to improve the way revisions and updates are done.

A further planned initiative is the realization of a tool for both *database* presentation and dissemination on CD-ROM, and of a DVD based implementation device that be complementary to the existing structure. The implementation tool should allow the trying out of new solutions, for example using elements like high resolution images, animations, films that are too large in size to be supported by telephone band extent.